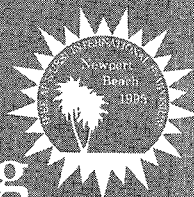




USNC/URSI Radio Science Meeting



Newport Beach Marriott Hotel
June 18-23, 1995
Newport Beach, California

W. STUTZMANN

URSI DIGEST

22

23

24

70

125

126

129

210

**National Academies of Science and Engineering
National Research Council of the
United States of America**

**United States National Committee
International Union of Radio Science**



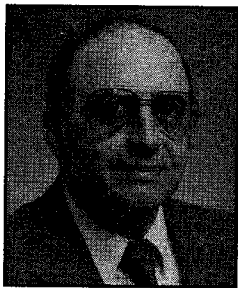
1995 Digest

USNC/URSI Radio Science Meeting

**June 18 - June 23, 1995
Newport Beach, California**

**Sponsored by USNC/URSI in conjunction with:
IEEE-APS International Symposium**

Chairman's Welcome



William Imbriale

On behalf of the Steering Committee, it is my pleasure to welcome you to the 1995 IEEE Antennas and Propagation Society International Symposium and URSI Radio Science Meeting. The Symposium is being held at the Newport Beach Marriott Hotel and Tennis Club in Newport Beach, California during the week of June 18-23, 1995. USNC/URSI Commissions A,B,D,E,F,G and K will be participating. An interesting and informative technical program has been assembled by the Technical Program Committee under the leadership of Dr. Ronald Pogorzelski. The technical program will be conducted in the Marriott Hotel, providing convenient access to all sessions. In

keeping with tradition, a number of Short Courses and Workshops are scheduled for Friday, June 23. A detailed listing of the course and workshop offerings can be found in the Final Program. You should also plan to visit the Industrial Exhibits, which will be open for three days from June 20-22, located adjacent to the technical sessions.

There are 104 technical sessions containing almost 900 papers. The title of the Plenary session, to be held on Wednesday morning, is "On to the Next Millennium". It will highlight how emerging technology and political change are going to affect the way antenna engineering will be practiced in the future. A student paper contest for university graduate students will also be a part of this conference. The finalists are listed in the Final Program and the winners will be announced at the Wednesday evening banquet.

The Newport Beach Marriott Hotel and Tennis Club has all the facilities and amenities required for what promises to be both a successful symposium and an enjoyable vacation. Newport Beach is a medium sized community with a charming and relaxing atmosphere. Located in Orange County, just south of Metropolitan Los Angeles, it is approximately fifteen minutes from the Orange County Airport and approximately one hour from the Los Angeles International Airport. The weather in June is extremely pleasant, and the area offers a variety of ways to enjoy the sun and the sea. Disneyland and other theme parks are located nearby, as are many museums, the California Angels and the Los Angeles Dodgers baseball teams, various movie and television studios, superb shopping centers, and countless fine restaurants.

This Digest was prepared by Aluizio Prata, Jr. with the help of his students and Robin Dumas.

Steering Committee

Chair

William Imbriale

Vice Chair & Exhibits

Michael Thorburn

Technical Program

Ron Pogorzelski

Tom Cwik

URSI Liaison

W. Ross Stone

Registration

S. Govind

Short Courses and Workshops

J. David Scholler

Digest Publications

Aluizio Prata, Jr.

Finance

Phillip Virga

Mark Romejko

Publicity and Calls for Papers

Sembiam Rengarajan

Allyson Yarbrough

Local Arrangements

Allan Love

John Wokurka

Michael Thorburn

Members at Large

Yahya Rahmat-Samii

William Moule

Meeting Planners

Three Dimensions Meeting Planners

Mary Ellen Vegter, Theodora Dirksen,

Bonnie Grosek

Technical Program Committee

D. Antsos	M. I. Herman	K. A. Michalski	W. R. Stone
C. A. Balaris	G. Hindman	E. K. Miller	W. L. Stutzman
W. Boerner, <i>ISF Liaison</i>	W. J. Hoefer	J. W. Mink	M. A. Thorburn
G. S. Brown	B. Houshmand	R. Mittra	V. K. Tripathi
C. M. Butler	J. Huang	B. A. Munk	L. Tsang
A. C. Cangellaris	Z. A. Hussein	K. Naishadham	A. Tulintseff
F. X. Canning	W. A. Imbriale	R. Nevels	K. R. Umashankar
A. Cha	A. Ishimaru	T. Y. Otoshi	P. L. E. Uslenghi
K.-M. Chen	M. F. Iskander	P. H. Pathak	M. L. VanBlaricum
Y. L. Chow	D. R. Jackson	L. W. Pearson	W. Vogel
C. Christodoulou	V. Jamnejad	R. J. Pogorzelski	J. L. Volakis
R. T. Compton	T. G. Jurgens	A. Prata	J. R. Wait
T. A. Cwik	L. B. Katehi	Y. Rahmat-Samii	D. R. Wilton
A. C. Densmore	S. J. Kubina	S. M. Rao	M. Wu
D. Dudley	Y. Kuga	S. Riad	B. Xu
S. L. Dvorak	S. R. Laxpati	E. J. Rothwell	A. D. Yaghjian
N. Engheta	S. A. Long	D. B. Rutledge	K. S. Yee
R. L. Gardner	R. J. Mailloux	T. B. A. Senior	R. A. York
W. P. Geren	A. Q. Martin	L. Shafai	A. I. Zaghoul
S. Govind	P. E. Mayes	G. S. Smith	R. W. Ziolkowski
T. M. Habashy	R. V. McGahan	H. K. Smith	C. Zuffada

Table of Contents

Monday

SESSION	TITLE	PAGE
URSI-B Session 1	Guided Waves	1
URSI-B Session 2	Transients	15
URSI-B Session 3	Antennas I	21
AP/URSI-B Session 1	Wavelets in Electromagnetics I	33
AP/URSI-B Session 2	Microstrip Antenna Design and Analysis	35
AP/URSI-E Session 3	Coupling and Shielding	37
URSI-B Session 4	Chiral Media	43
URSI-A Session 5	Antennas and EM Field Metrology	55
URSI-B Session 6	Antennas II	65
AP/URSI-B Session 4	<i>Special Session</i>	
	Higher Order Modeling in	77
	Computational Electromagnetics	

Tuesday

URSI-B Session 7	Finite Element Methods	85
URSI-B Session 8	<i>Special Session</i>	
	Tribute to Professor Irene Peden	99
URSI-B Session 9	Scattering	107
URSI-K Session 10	Electromagnetics in Biology and Medicine	119
URSI-B Session 11	<i>Special Session</i>	
	Antenna Applications of Photonics	129
URSI-F Session 12	Atmosphere and Propagation for Satellite	139
	and Terrestrial Communications	
AP/URSI-B Session 5	Microstrip Antenna Analysis Methods	147
AP/URSI-B Session 6	<i>Special Session</i>	
	Scattering by Wedges I	149
URSI-F Session 13	Remote Sensing of Terrestrial Media and	159
	Surfaces	
URSI-B Session 14	Hybrid Numerical Methods	171
URSI-B Session 15	High Frequency Techniques	185
URSI-A Session 16	Material Characterization	197
URSI-B Session 17	Microstrip I	205
AP/URSI-B Session 7	<i>Special Session</i>	
	Parallel and Distributed Computation	219
	in Electromagnetics	
AP/URSI-AB Session 8	<i>Special Session</i>	
	Image Reconstruction From Real Data	229
AP/URSI-B Session 9	Scattering by Wedges II	239

Wednesday

SESSION	TITLE	PAGE
URSI-B	Session 18	Theoretical Electromagnetics I 243
URSI-B	Session 19	Finite Difference Time Domain Methods 255
URSI-A	Session 20	Impulse Radar 265
URSI-B	Session 21	Microstrip II 275
URSI-G	Session 22	Propagation Phenomenology 287
AP/URSI-B	Session 10	<i>Special Session</i> In Honor of Victor Galindo-Israel 293

Thursday

URSI-B	Session 23	Integral Equation Techniques 297
URSI-F	Session 24	Propagation Modeling and Measurements 311 for Mobile/Personal Comm. Services
URSI-E	Session 25	Noise and Interference Control 321
URSI-B	Session 26	<i>Special Session</i> PML Absorbing Boundary Conditions for 331 Time and Frequency Domains
URSI-B	Session 27	Inverse Scattering 343
URSI-B	Session 28	Wavelets in Electromagnetics II 351
URSI-D	Session 29	Microwaves - Photonics - Electronics 357
URSI-B	Session 30	Numerical Methods 369
URSI-B	Session 31	Boundary Conditions 381
URSI-B	Session 32	<i>Special Session</i> Transient Electromagnetic Wave Propagation 391 in Dispersive Media
URSI-B	Session 33	Theoretical Electromagnetics II 397
AP/URSI-G	Session 11	<i>Special Session</i> Transionospheric Propagation 409
AP/URSI-G	Session 12	Rough Surfaces 419

Guided Waves**T. K. Sarkar and E. W. Lucas**

Page

- 8:20 Plane Wave to Coaxial Waveguide Coupling through 3
an Aperture, using modal expansions in the interior and
exterior domains
S. Marteau, B. L. Michielsen, ONERA*
- 8:40 Analysis of a Coaxial-line Probe Junction to Cylindrical Cavity 4
Filled with a Lossy Dielectric
Richard B. Kean, Adrian D. Green, The New Zealand Institute for
Industrial Research and Development*
- 9:00 An Analysis Approach for Large Planar Arrays Using a 5
Bound FDTD Model
Maria Gustavsson, John Sanford, Chalmers University,
Magnus Sundberg, Swedish Institute of Food Research*
- 9:20 Analysis and Design of Orthogonal Mode Couplers in 6
Rectangular Waveguides
*Luiz Costa da Silva, Pontificia Universidade Catolica de Rio de Janeiro,
Emilio Abud Filho, M. G. Castello Branco, CPqD/Telebras*
- 9:40 The Equivalent Circuit for the Junction between Curved 7
and Straight Waveguides
*Horacio Tertuliano, Federal University of Ceara, Pierre Jarry,
Bordeaux I University*
- 10:00 BREAK
- 10:20 Wave-Field Patterns on Electrically Large Networks 8
Ross A. Speciale, Redondo Beach, CA
- 10:40 Computer-Simulation of Isotropic, Two-Dimensional 9
Guided-Wave Propagation
Ross A. Speciale, Redondo Beach, CA
- 11:00 A New Edge Element Method for Dispersive Waveguiding 10
Structures
Guangwen Pan, Jilin Tan, University of Wisconsin, Milwaukee*
- 11:20 OHMIC Loss of Metal-Dielectric Waveguides with Ridges 11
Alexander Ye. Svezhentsev, Ukranian Academy of Sciences
- 11:40 Two-Channel Waveguide Modulator Based on the Surface 12
Eigenmode of the Semiconductor-Metal Interface
K. N. Ostrikov, N. A. Azarenkov, O. A. Osmayev, Kharkov State
University & Scientific Centre for Physical Technologies*

12:00 High-Q Disk Dielectric Resonators 13
V. S. Dobromyslov, V. I. Kalinichev, A. V. Krjukov, Moscow
Power Engineering Institute*

Plane wave to coaxial waveguide coupling through an aperture, using modal expansions in the interior and exterior domains

S.Marteau, B.L.Michielsen*
ONERA, France

We discuss the computation of the amplitudes of propagating waveguide modes induced in a coaxial waveguide by a plane electromagnetic wave incident on an aperture in the outer conductor. Two essentially different configurations are studied. Firstly, we consider the coaxial waveguide in free space. In this case the outside surface of the waveguide is taken with a finite conductivity to ensure the existence of at least one surface mode. Secondly, we consider the coaxial waveguide over a perfectly conducting ground. In this case all conductors are assumed to be perfectly conducting, because all essential phenomena are likely to show up already in this idealised case.

To obtain the waveguide mode amplitudes due to the incident wave, we solve in fact the reciprocal boundary value problem where a propagating waveguide mode excites the aperture. Then, the desired amplitudes are found as

$$A_p = j\omega\mu_0 e_p(\theta) \cdot E^{inc}$$

where $e_p(\theta)$ is the electric component of the far field in the direction θ due to the excitation with the p -th waveguide mode and E^{inc} is the incident electric field, defined as the field in absence of the complete conducting structure.

In order to calculate the exterior fields needed in the above expressions, we solve an integral equation for the aperture electric field

$$[Y^+ - Y^-]e_{tg,p} = (\nu \times h_p)|_{\mathcal{A}}$$

where \mathcal{A} is the aperture domain, h_p is the magnetic field of the p -th waveguide mode, $e_{tg,p}$ is the tangential electric field in the aperture due to the excitation by the p -th mode and Y^\pm are the interior and exterior admittance operators respectively of the aperture. We study these admittance operators in the modal expansions for the closed coaxial waveguide and the open waveguide representing the exterior domain.

The results of this study allow for a clear interpretation of the role of the continuous mode spectrum in waveguide coupling problems. The convergence of Green's function expansions in waveguide modes will be discussed in detail.

ANALYSIS OF A COAXIAL-LINE PROBE JUNCTION TO CYLINDRICAL CAVITY FILLED WITH A LOSSY DIELECTRIC

Dr Richard B. Keam* and Adrian D. Green.
Microwave Engineering Team,
The New Zealand Institute for Industrial Research and Development,
P.O. Box 2225,
Auckland, Ph: 64 9 303 4116
NEW ZEALAND Fax: 64 9 307 0618

November 1994

Abstract:

Junctions between coaxial-line and other waveguiding structures find wide application in a variety of microwave devices. Examples of such transitions include coaxial-line to rectangular waveguide, coaxial-line to radial-line, and coaxial-line to cylindrical cavity. A method has been developed (R. B. Keam & A. G. Williamson, *IEEE Trans.-MTT*, 41, 516-520, 1993) for modelling the input admittance and fields due to coaxial-line probe transitions for a wide range of different systems. The analysis models the coaxial excitation as a magnetic field "frill-ring" of assumed known field distribution, and so does not require empirical factors which have been relied upon in some earlier models.

Whilst the analysis of several specific junctions has been performed in the past, this technique has the desirable feature that the coaxial-line excitation region is treated as a functional block in a generic arbitrary junction. This enables the consideration of a wide range of environments external to the coaxial-line core.

In this paper the general coaxial-line to "radial-line environment" model is extended to the case where the external region is filled with some dielectric material of non-negligible loss. In particular the case where a coaxial-line enters through the flat face of a dielectric filled cylindrical cavity is considered. This case is of particular interest for developing a practical techniques for the measurement of dielectric permittivity of materials which do not require calibration with known permittivity standards, for use in on-line industrial and biological microwave applications.

A comparison of theoretical and experimental measurement for several lossy organic liquids is also presented which shows the theory to be very accurate over a wide frequency band.

Applicable Conference Topics for URSI:

- B5. Theoretical Electromagnetics
- B10. Guided Waves

An Analysis Approach for Large Planar Arrays Using a Bound FDTD Model

Maria Gustavsson, John Sanford* and Magnus Sundberg⁺

Department of Microwave Technology, Chalmers University, Gothenburg, Sweden

⁺Swedish Institute of Food Research, Gothenburg, Sweden

We use the finite difference time domain approach to model a waveguide simulator. The waveguide simulator mimics an element in the infinite array environment. Figure 1 shows the four types of simulators. Each of the simulators supports modes that can be decomposed into symmetric pairs of plane waves. The first of these simulators is the conventional waveguide structure commonly used in experimental models. It supports TE_{nm} modes and hence simulates H -polarised waves. The second is essentially the same as the first except the magnetic wall has the effect of doubling the waveguide width by reasons of symmetry. The third simulates normal incidence with a TEM mode. The fourth allows TM_{nm} modes to propagate simulating E -polarised waves.

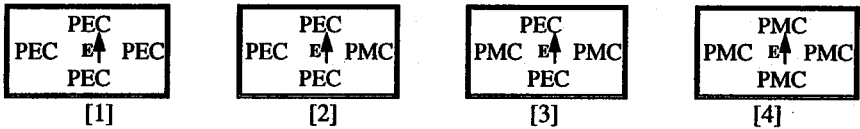


Figure 1 - Waveguide Simulator Types

The scattered field formulation of the FDTD algorithm is used to compute the amplitude of the reflected waveguide mode. The structure is discretized by first isolating one periodic cell and then subdividing this domain into Yee cells to form the FDTD mesh. We truncate the mesh with the four waveguide walls using the appropriate electric or magnetic boundary condition and at the two ends by with a Dispersive Boundary Condition or N th order. The absorbing boundary is calibrated to perfectly absorb the N propagating waveguide modes. Each of these modes equates to a plane wave reflected from the periodic surface. We space the absorbing boundary approximately two wavelengths from the periodic boundary. Broad band results are computed for normal incidence.

The method is applied to a number of periodic boundaries including a waveguide arrays and frequency selective surfaces. The results compare reasonable well with alternative methods and measurement but in some cases numerical difficulties limit the accuracy. The method provides quick and insightful solutions but not the accuracy available by some alternate techniques.

Analysis and Design of Orthogonal Mode Couplers in Rectangular Waveguides

Luiz Costa da Silva *

Pontificia Universidade Católica do Rio de Janeiro
Rua Marques de São Vicente 225, Gávea, RJ, Brazil
Emílio Abud Filho and M. G. Castello Branco
CPqD/Telebrás

Rodovia Campinas-Mogi Mirim , km 118.5, Campinas, SP, Brazil

A model for the analysis of orthogonal mode couplers in rectangular waveguides, as shown in Fig 1, based on the moment method, is developed. The model is incorporated into an optimization scheme, generating a design routine.

The main difficulty in the analysis model is the choice of an equivalent structure, composed by regions geometrically adequate to the analytical computation of electromagnetic fields. The more obvious solution is that indicated in Fig. 1, where metallic walls, and magnetic current densities, are placed on the surfaces indicated by traced and dotted lines (in this case, all the regions composing the equivalent structure are rectangular waveguide sections with short terminations). This choice of equivalent structure, however, results in finite magnetic currents (and infinite magnetic fields) at the junction between the traced and dotted surfaces of Fig.1, leading to instability and lack of convergence in the determination of the scattered fields. To circumvent such problem, metallic walls and magnetic current densities were placed only on the traced lines of Fig. 1. The resulting equivalent structure is composed by waveguide sections and a waveguide followed by a bifurcated waveguide. The dyadic Green's function for the waveguide-bifurcated waveguide was developed and the moment method used to the determination of the scattering matrix of the coupler, producing stable and accurate solutions. The model was applied to the optimization of the dimensions of couplers. Fig. 2 shows measured and theoretical results for the return loss of an optimized coupler, operating in the band of 3.625 to 4.2 GHz. The return loss is better then 30 dB in all the band.

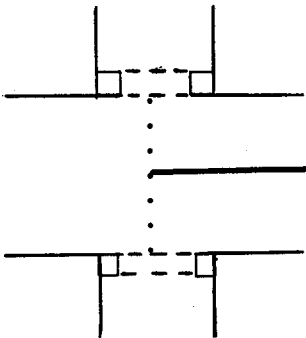


Fig. 1 Mode coupler and equivalent structure(longitudinal section)

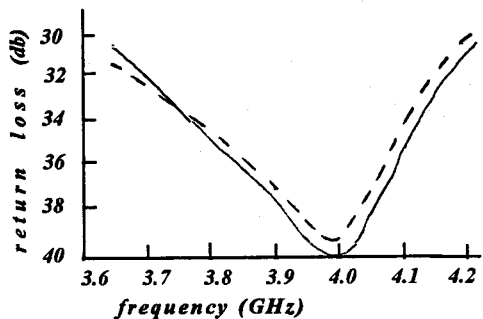


Fig. 2 Return loss for an optimized coupler (---- theory: ____ measurement)

The Equivalent Circuit for the Junction Between Curved and Straight Waveguides

Horacio TERTULIANO* and Pierre JARRY**

* Applied Tele-Data Computers Laboratory - LIA - Federal University of Ceara - Fortaleza - Brazil

** Telecommunications Laboratory - ENSERB - Bordeaux I University - Bordeaux - France

Abstract:

The curved and the straight waveguide discontinuities, can be analyzed using standard techniques like for instance the Mode Matching Technique, Time-Harmonic Electromagnetic Fields, Moments Method, Perturbation Technique and Variational Method. We used the Mode Matching Technique to make our electromagnetic study of the discontinuity and we found the matrix $[S]$ of the junctions: straight-curved and curved-straight discontinuities. It is assumed that both waveguides satisfy the single-mode condition and the TE and LM dominant-mode propagate along in the waveguide. After considering the concept of characteristic impedance and the wave and voltage formalisms equivalences, we have deduced the equivalent circuit for the discontinuities. The utilisation of this techniques lead us to developpe a computationally efficient method for analyzing waveguide discontinuity problems. The final proposed circuit for the discontinuity presented in Fig. 1, is show in the Fig. 2.

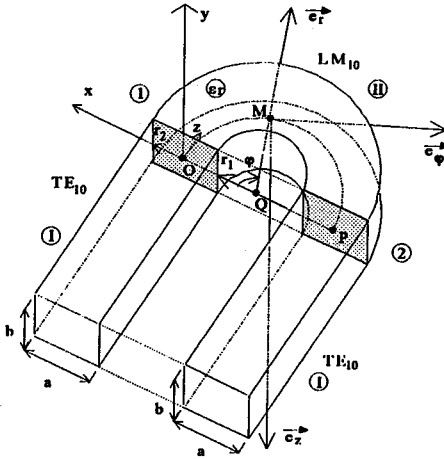


Fig. 1: junction between a straight and curved waveguide

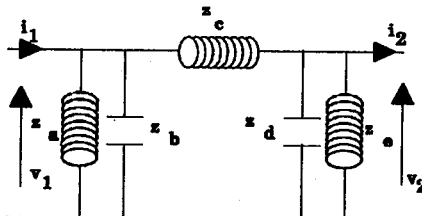


Fig. 2: equivalent circuit of the discontinuity

WAVE-FIELD PATTERNS ON ELECTRICALLY LARGE NETWORKS.

Ross A. Speciale

Redondo Beach, California

Recently formulated extensions of the old, classical concepts of *Image Impedance*, and of *Image Transfer Function*, from the basic theory of simple two-port networks to the broader context of large, complex systems of interconnected multiport networks, lead to new, and *far-reaching generalizations* of well known, elementary results.

The new, generalized results describe, in rigorous mathematical terms, the simultaneous propagation of multiple sets of *guided electromagnetic waves* through electrically large, *multi-dimensional delay-structures*, constructed by interconnecting large numbers of microwave multiport networks.

Closed form matrix expressions of new multidimensional quantities are given, that are conceptually equivalent to the classical *wave-impedance*, and *propagation-constant* of electrical transmission lines. All the given matrix expressions are cast in mutually complementary formulations, one set being suited to the *analysis* of wave-guiding system, the other set intended for system *synthesis* and *design*.

Numerous and varied applications of new analysis and synthesis methods, based on the here presented generalized theory of guided-wave propagation, have already been identified and studied in substantial depth. The most notable of these applications is perhaps the development of conceptually new, more affordable configurations for the *feed-networks* of large, two-dimensional, high directivity, low-sidelobe, electronically-steered *phased arrays* [1, 2].

The generalized theory of guided wave propagation presented here, applies to 2D and 3D wave-guiding systems of interconnected multiport microwave networks, that may physically span tens, hundreds, or even thousands of free-space wavelengths in all linear dimensions. Further, the considered network systems may be simultaneously excited by *any* arbitrarily large *number* of mutually coherent *sources*, connected to the network system at an equally large number of input ports. The input ports may be located in *any* arbitrary or prescribed *pattern*, and the sources may conform to *any* given arbitrary or prescribed amplitude and phase *distribution*.

The new generalized theory of guided wave propagation is applicable to the analysis and synthesis of *practical* microwave guiding structures, built by interconnecting well-known, established types of basic microwave devices such as coaxial lines, waveguides, resonant cavities, couplers, hybrid junctions, power splitters, power combiners, matching networks, and any other type of microwave device known to be *linear*, at least below some given level of power density. The emphasis of the new treatment is, however, on *periodic* structures having a substantial degree of *modularity*, as multi-atom molecules, or crystal lattices.

COMPUTER-SIMULATION OF ISOTROPIC, TWO-DIMENSIONAL GUIDED-WAVE PROPAGATION

Ross A. Speciale

Redondo Beach, California

A relatively simple computer-simulation method has been developed, for performing a first-approximation analysis of various two-dimensional guided-wave propagation processes. The method has been applied in two MATLAB programs. One of the programs synthesizes a phase-conjugated EM-field that approximates, with its amplitude-distribution, the shape of a two-dimensional Dirac impulse-function. The second program synthesizes any given two-dimensional, complex aperture distribution, in terms of local amplitude and phase.

The developed simulation method uses (as an initial, and qualitative first approximation) a square, two-dimensional wave-guiding medium (such as the well known parallel-plate waveguide !), a medium characterized by: a) total uniformity in any arbitrary azimuthal direction, b) mathematical linearity, reciprocity, and losslessness, and c) complete isotropy, as defined by an azimuth-independent propagation constant. The wave-propagation properties of the medium are thus characterized by total absence of internal scattering, of any wave-attenuation due to ohmic or radiation losses, and by a known azimuth-independent phase-constant. The developed method can be, however, easily modified to account for any known type of anisotropy of the wave-propagation medium, if such anisotropy can be defined by some functional azimuth-dependence of the propagation-constant. Further, any analytically-defined loss-mechanism can be easily accounted for.

A large number of different, two-dimensional guided-wave field-patterns of increasing complexity have already been analyzed and synthesized. All the two-dimensional wave-field patterns generated so far, have been obtained as weighted linear combinations of the individual, two-dimensional wave-field patterns of large numbers of mutually-coherent sources. The sources were mostly aligned along the outer perimeter of the square wave-propagation domain, although the geometric pattern of the source locations is quite arbitrary.

Many examples of sharp phase-conjugation focusing in two-dimensions have been synthesized, using either two or four sets of external sources, all aligned along two or all four outer sides of the square domain. The sources are assumed to have totally different, mutually independent, and arbitrary amplitudes and phases. An overwhelmingly large number of different, two-dimensional wave-field patterns can be obtained, simply by independently controlling the relative amplitudes and the relative phases of all the mutually-coherent external sources. Many of the generated wave-patterns resemble two-dimensional wave-caustics.

A New Edge Element Method for Dispersive Waveguiding Structures

Guangwen Pan*, Jilin Tan
University of Wisconsin, Milwaukee

Abstract

A new functional is rigorously derived for the edge element method to model the $2D\frac{1}{2}$ dispersive waveguiding structures. Moderate to heavy ohmic loss and dielectric loss are taken into account in a natural and consistent manner under the full-wave regime. As a result, finite cross section of arbitrary shape and finite conductivity can be handled without imposing the impedance boundary condition (IBC). In fact, the IBC may no longer be held for high-speed microelectronics applications, where the cross section dimension may have been in the same order of the skin depths for some frequency components. A new boundary condition of the third kind is derived and applied to the artificial boundaries to reduce the computational domain of opened structures with high accuracy. The propagation modes are obtained by solving the large scale (4000 X 4000) generalized eigenvalue and eigenvector equations employing the subspace iteration method. Spurious modes are completely suppressed in the whole frequency range of interest.

Numerical examples of dielectric waveguide, microstrip transmission lines with finite conductivity are computed and compared with previous publications of spectral domain method, volume integral equation method, mode matching method, etc. with good agreement.

References

- [1] B. Rahman, F. Fernandez and J. Davies, "Review of finite element methods for microwave and optical waveguides," *Proc., IEEE Trans.*, vol. 79, pp. 1442-1448, Oct. 1991.
- [2] J. Lee and et al, "Full-Wave Analysis of Dielectric Waveguides Using Tangential Vector Finite Elements" *IEEE Trans., Microwave Theory Tech.*, vol. MTT-39, No. 8, pp1262-1271, Aug. 1991.

OHMIC LOSS OF METAL-DIELECTRIC WAVEGUIDES WITH RIDGES

Alexander Ye. Svezhentsev
Institute of Radiophysics and Electronics
Ukrainian Academy of Sciences
12, Ac.Proskura st., Kharkov 85, 310085, Ukraine

When finding ohmic loss of metal-dielectric waveguides with ridges, the serious problems occur in integration of the square of longitudinal current density in the interval including a ridge edge. It is well known that for infinitely thin and ideally conducting walls the integral of current density squared diverges logarithmically. In this case, following (Lewin L., IEEE Trans. Microwave Theory and Tech., vol. MTT-32, 7, pp.717-719, 1984), the integration may be performed right up to the edge vicinity Δ specified from the static problem solution. The other difficulty in theory of complex metal-dielectric waveguides is that the current on a metal screen is formulated through slow converging Fourier series containing no singularity in explicit form. It is required to extract from there a singular piece containing the singularity explicitly. And finally, there exist waveguides which field formulation satisfies explicitly the edge condition. For them, the difficulties occur in the case of infinitely thin walls and may be alleviated by finding the mentioned Δ vicinity.

It is aimed to analyze the ohmic loss calculation results for three groups of waveguides. The first is represented by circular cylindrical strip and slot lines of infinitely long, ideally conducting strip. A rigorous solution to boundary value electromagnetic problem for such a structure is obtained with the Riemann-Hilbert problem technique. For loss calculation, both the Δ vicinity of an edge and a singular piece of longitudinal current on metal screen should be determined.

The next group consist of groove guides with rectangle-shaped grooves. Here both well-known axisymmetric groove guide and new central-symmetry one are considered. Boundary value problem is solved using the moment method technique, the basis functions are Gegenbauer polynomials with the proper weight. A singular piece of longitudinal current is deduced using the generalized Zeta-function of Riemann for vertical walls including edges, and represents some integral expression for horizontal ones.

For the third group, ohmic loss of wedge transmission lines in the form of a metal wedge with circular dielectric coating are discussed. Of interest is principal mode caused by the ridge edge. This mode field expression satisfies explicitly the edge condition. The analytical-numerical expression for ohmic loss of a wedge line with an arbitrary opening of the wedge was obtained. In the limiting case when a wedge changes to plane, some inaccuracies in the formula for attenuation factor were found in the work (D.D.King and S.P.Schlesinger, IRE Trans. on Microwave Theory and Techniques, vol. MTT-5, pp. 31-35, January, 1957). Some difficulties arise when a wedge changes to semi-plane. Then for loss calculation the edge Δ vicinity should be specified.

Frequency and geometry dependences of attenuation factor were carefully investigated for all the discussed types of waveguide structures.

TWO-CHANNEL WAVEGUIDE MODULATOR
BASED ON THE SURFACE EIGENMODE OF
THE SEMICONDUCTOR-METAL INTERFACE

K. N. Ostrikov, N. A. Azarenkov, O. A. Osmayev

Kharkov State University and Scientific Centre
For Physical Technologies, Novgorodskaya str. 2, #93
310145, Kharkov, UKRAINE.

The coupled waveguide structures such as the directional couplers and waveguide electrooptical modulators are the examples of very often used devices of the integrated optics and optoelectronics. There are a lot of different realizations of such directional devices which are usually served as electrooptical switches and modulators, power dividers, output and input coupling elements, e.t.c. The kind of the directional waveguiding device significantly depends on the number of coupled waveguide channels, on the material of the channel itself and of the plating as well as on the type of the used propagating waveguide mode. Here we deal with two-channel waveguide modulator based on the surface plasmon-polariton eigenmode (SM) of the semiconductor-metal interface propagating across an external magnetic field. The studied structure consists on two n-type semiconductor waveguide channels separated from each other by a dielectric gap and coated by a metal. In the transverse to the interface direction an external DC voltage is applied to the metal surface of one channel to provide a small phase shift between two propagating modes. The main peculiarity of these modes is their completely nonreciprocal character of propagation (M. Toda, J. Phys. Soc. Jpn, vol. 19(1964)1126). This fact allows one to avoid an unnecessary backward signal in directional devices and to use the SM in nonreciprocal elements. Moreover, the localization of the electromagnetic energy near the semiconductor-metal interface allows one to obtain relatively good coupling between two waveguide channels. In the coupled modes approximation two possible regimes of operation of the studied structure namely as a directional coupler and an electrooptical modulator are considered. The numerical results show that the characteristic length of electrooptical modulation increases with an increase of the dielectric gap thickness and an external magnetic field value and decreases with an increase of the free carries density in the semiconductor.

HIGH Q DISK DIELECTRIC RESONATORS

V.S. Dobromyslov*, V.I. Kalinichev, A.V. Krjukov
Moscow Power Engineering Institute, Department of Radioengineering

Disk dielectric resonators on azimuthal modes have been adopted in various microwave and millimeter-wave applications. Methods of dielectric parameters measurements using these resonators are very promising because they are characterized by a high degree of accuracy. The dielectric resonators can be applied for narrow-band filtration and frequency control.

The intrinsic property of such dielectric resonators is an opportunity to reach the extremely high Q-factor, which make it possible to use them for stabilization of generators with the extremely low level of phase noise. Indeed, at present the sapphire disk modes with Q-factor of $(1.3 \pm 0.2) \cdot 10^9$; $2.6 \cdot 10^5$ at $T = 4$ and 300 K respectively at $f = 10$ GHz have been realized. Such a level of Q-factor requires to solve the problem of protection of the dielectric resonator from external factors. Generally, application of a metal screen results in reducing a Q-factor. We can expect, however, that due to the dielectric effect there exists regimes characterized the very high Q-factor.

This work studies the properties of azimuthal resonant modes in open and shielded disk dielectric resonators. The electromagnetic analysis of the dielectric resonators has been carried out by making use of the presentation of the electromagnetic field as infinite series of the E- and H-cylindrical waves. This approach is especially effective in studying multilayer resonant structures. A homogeneous system of integral equations has been obtained regarding the axial components of the field at the boundary of partial regions. Programs for calculation the spectrum of the resonant modes and energy characteristics of the open and shielded dielectric resonators have been worked out on the basis of the suggested algorithm. Both the algorithms and the computer programs are highly universal and allow one to study variety of dielectric resonators made of isotropic and anisotropic materials with anisotropic axis oriented along geometrical axis. The accuracy of the spectrum calculations depends on number of the accounted harmonics. In order to obtain the satisfactory results we must take at least 5-6 radial harmonics.

By using of the developed programs we have obtained the family of resonance frequencies and a Q-factor of various modes as functions of the resonator parameters. We have also conducted the experimental investigation of the frequency spectrum and Q-factor of the open and shielded sapphire resonators. We have done comparison between our results and earlier obtained data of other works as well.

Our results demonstrate wide possibilities of using of open and shielded sapphire resonators on azimuthal resonant modes. The dimensions of the shielded sapphire disk can be made considerably smaller as compared with those of the open disk providing that a high Q-factor is preserved.

In practice, azimuthal modes with a small index $n = 5-6$ can be used in shielded resonators, while in open sapphire resonators modes with higher azimuthal index $n = 10-12$ have to be used. In turn, it leads to reduction of disk sizes. This is especially important at microwaves.

The obtained results can be successfully used for designing of various resonant devices, in particular, in some applications of superconducting electronics.

THIS PAGE INTENTIONALLY LEFT BLANK.

Transients**S. L. Dvorak and P. H. Pathak**

Page

- 8:20 Analytical Treatment of Transient Radiation from Pulse Excited 16
Parabolic Reflectors
H. T. Chou, P. H. Pathak, P. R. Rousseau, Ohio State University*
- 8:40 Antenna Parameterization in the Time Domain 17
Amir Shlivinski, Ehud Heyman, Raphael Kastner, Tel-Aviv University*
- 9:00 Transient Pulse Focusing by a Lens: Analytical and 18
Numerical Analyses
Steven L. Dvorak, Richard W. Ziolkowski, University of Arizona*
- 9:20 A New Method for the Wideband Protection of Ultra-fast 19
Pulse Generators Against Reflections From Unmatched Antennas
M. Piette, E. Schweicheir, Royal Military Academy Brussels,
A. Vander Vorst, Univ. Cath. de Louvain*
- 9:40 Design of Reflectionless Slabs for Obliquely Incident 20
Transient Plane Waves
Rasmus Hellberg, Royal Institute of Technology

ANALYTICAL TREATMENT OF TRANSIENT RADIATION FROM PULSE EXCITED PARABOLIC REFLECTORS

H. T. Chou, P. H. Pathak* and P. R. Rousseau

ElectroScience Laboratory

The Ohio State University, Department of Electrical Engineering
Columbus, Ohio 43212

Two different analytical approaches are presented to describe the transient radiation from parabolic reflector antennas which are pulse excited. Such an antenna could constitute an ultra-wide band radiator which can be used as a part of a ground penetrating radar system, as well as in some other remote sensing applications. In both approaches, the radiation by the reflector is found via an evaluation of the radiation integral over its equivalent aperture field distribution. The aperture field distribution is found by reflecting the fields of the feed from the parabolic surface according to geometrical optics. It is assumed that the feed is either a Huygen's source, or a more general source including an ultra-wide band slot line-bowtie feed antenna designed by Burnside and his coworkers at The Ohio State University which in its operating bandwidth has a stable phase center as well as feed pattern over the region illuminating the reflector (Lai et.al., IEEE Trans. AP, vol. 40, No. 7, July 1992, pp755-760). Such a feed essentially produces a ray optical field at the reflector over its bandwidth. The analysis presented here is different and somewhat more general than the pioneering one due to C.E. Baum and his coworkers who analyzed high power impulse radiating parabolic reflectors with step voltage excited transmission line feeds (C. E. Baum, Sensor & Simulation Note 321, 1989; Farr & Baum, Sensor & Simulation Note 358, June 1993). The feeds employed in the present development are primarily not meant for high power applications. The first analytical approach provides, to within the aperture field approximation, an exact closed form solution everywhere in the forward region for the transient radiation near or far from the reflector aperture when the feed radiation is a step function in time and it clearly shows how the impulse like response on the reflector axis broadens away from it. This approach provides a physical picture for the transient radiation from the aperture, but it requires one to find the response of the reflector to any other finite energy pulse radiation from the feed in terms of a convolution which must in general be done numerically. The second approach makes use of analytic (complex) time functions and provides a closed form solution for the transient radiation by the reflector at distances infinitely far when illuminated by a feed which behaves as a step function in time. Although it does not provide as much physical insight as the first approach, it allows one to do a convolution in closed form when the response due to a more general pulsed feed illumination is desired. Numerical results will be presented.

ANTENNA PARAMETERIZATION IN THE TIME DOMAIN

Amir Shlivinski, Ehud Heyman and Raphael Kastner*

Tel-Aviv University, Dept. of Electrical Engineering — Physical Electronics
Tel-Aviv 69978, Israel

With the trend toward increased bandwidth in radiating and detecting systems, there is a growing interest in the radiation, propagation and diffraction of ultra wideband, short-pulse fields. These fields provide high temporal-spatial resolution that cannot be ordinarily obtained by narrow band (quasi monochromatic) pulses.

This paper is concerned with developing a consistent time domain parameterization for a system comprising transmitting and receiving short pulse antennas. Emphasis is placed on modeling and interpretation directly in the time domain, where these fields are well localized. We consider time domain antenna concepts such as transient radiation pattern and gain, which lead to the formulation of a transmit- receive equation analogous to the time harmonic Frijs equation. Instead of the conventional frequency domain formulation which is phrased in terms of the gain and effective area the time domain formulation utilizes the effective length concept for both transmitting and receiving antennas. Rather than being algebraic quantities, as in the frequency domain, the time domain parameters constitute integro-differential operators. Physical insight is gained therefore by considering operator bounds that also lead to optimization procedures for an effective transient excitation. Further simplification is gained by considering single-shot pulsed fields for which closed-form approximations are obtained. Several examples for simple models of non-dispersive antennas will be considered

The concepts above are then extended to delay-arrays, which are the time-domain analog of time-harmonic phase arrays. Here we also explore the array kinematics as a function of the grid spacing, the pulse length and elements delay.

TRANSIENT PULSE FOCUSING BY A LENS:
ANALYTICAL AND NUMERICAL ANALYSES

Steven L. Dvorak and Richard W. Ziolkowski
Department of Electrical and Computer Engineering
University of Arizona
Tucson, AZ 85721

The standard procedure for finding transient fields focused by a lens involves: 1) representing the frequency-domain fields by the Kirchoff diffraction formula; 2) using either a two-dimensional (2d) spatial fast Fourier transform (FFT) or an asymptotic expression to compute the frequency-domain field for a number of frequencies; 3) employing a temporal FFT to transform the frequency-domain data to obtain the time-history of the pulse at the observation location. However, since the accurate computation of the frequency-domain field is challenging and computationally intensive, it is difficult to correctly compute the transient lens response. Purely numerical techniques such as the finite-difference time-domain technique can be employed (D. B. Davidson and R. W. Ziolkowski, *J. Opt. Soc. Am. A*, vol. 11(4), 1471-1490, 1994), but these techniques suffer from the problems of large memory and computation time requirements. In order to study the focusing of pulses with a lens in more detail without these numerically imposed constraints, we have developed a new technique which allows for the accurate and efficient computation of the transient fields focused by a lens.

In a previous paper (G. E. Evans and S. L. Dvorak, submitted to *J. Modern Optics*), it was demonstrated that the paraxial approximation allows the frequency-domain Fresnel-zone fields to be represented in closed form in terms of incomplete Lipschitz-Hankel integrals (ILHIs). In this presentation, we demonstrate that the transient Fresnel-zone fields can also be represented in closed form in terms of ILHIs. Convergent and asymptotic series expansions for the ILHIs are used to obtain accurate and efficient numerical results.

In order to demonstrate the usefulness of the new closed-form expressions and the corresponding numerical simulator, we have investigated the problem of the focusing of a pulsed Gaussian beam using a thin, non-dispersive lens. Both analytical and numerical results have been obtained for a variety of waveforms. The numerical FFT results have been validated with both double-exponential and continuous-wave time histories. More general incident pulses have been studied with the numerical approach. We have used our algorithm to investigate several parameters in the focal region. These include the shape of the transient pulses in the vicinity of the focus, the intensity and energy distributions in the focal region, and the dependence of these focus region quantities on the incident waveform parameters, such as the rise-time. We will present a variety of these results and will address further the enhancements in the intensity that can be obtained with focused pulsed-beams which were reported recently (R. W. Ziolkowski and D. B. Davidson, *Optics Letters*, Vol. 19(4), 284-286, 1994).

A New Method for the Wideband Protection of Ultra-fast Pulse Generators Against Reflections From Unmatched Antennas

M. PIETTE*, E. SCHWEICHEIR
Royal Military Academy Brussels
30, avenue de la Renaissance
1040 Brussels, Belgium

A. VANDER VORST
Univ. Cath. de Louvain
Bât. Maxwell.
1348 Louvain-la- Neuve

In the Transient Scattering Range of the Royal Military Academy Brussels, a long monocone antenna on ground plane is used as transmitting antenna for illuminating small-scale targets with pulses of duration as short as 50 ps. The antenna is coaxially fed by a transmission line connected to an ultra-fast step function generator (50V/50 ps). This type of antenna exhibits a purely real and frequency independent impedance during the time the transient current needs for travelling-up to the cone top. Moreover it is able to radiate without any waveform distortion and in the form of a TEM spherical wave the step voltage applied to its base. The cone flare angle has been kept small ($2\theta = 8^\circ$) to limit the amplitude of the higher order modes excited at the base of the antenna. So the antenna's input impedance is $(200 + 0 j)$ Ohms. Because the antenna is not matched to the generator's output impedance (50 Ohms), this one can not be directly connected to it. The large reflections coming from the antenna would damage its output stage.

The use of isolators is not possible with transient generators (insufficient bandwidth) and the insertion of attenuators to mitigate the reflections would also reduce considerably the amplitude of the voltage transmitted to the antenna.

Therefore a new method has been thought up, that requires only a broadband power splitter with a high degree of symmetry between its two outputs, a set of broadband coaxial mismatches of various VSWR and two coaxial cables of equal lengths. Even if no precision coaxial mismatch is available with the exact value of VSWR needed, one can still apply the method by replacing the mismatch by an attenuator and a fixed coaxial short set at the end of one of the cable. The method is reliable and powerful because it only requires a few passive components with which every microwaves' engineer is familiar. It enables to protect totally a transient generator against the reflections coming from unmatched resistive loads while transmitting the transient voltage of the generator without any waveform distortion and with very few losses: the only loss is the insertionloss of the power splitter.

Design of reflectionless slabs for obliquely incident transient plane waves

Rasmus Hellberg
Department of Electromagnetic Theory
Royal Institute of Technology
S-100 44 Stockholm, Sweden

This contribution concerns a method for designing reflectionless conductive dispersive slabs. The slabs are temporally dispersive where the dispersion in the time domain is modeled by the electric susceptibility kernel $\chi(z, t)$. The medium is characterised by the following constitutive relations:

$$\left\{ \begin{array}{l} \mathbf{D}(z, t) = \varepsilon_0 \varepsilon_r(z) \mathbf{E}(z, t) + \varepsilon_0 \int_{-\infty}^t \chi(z, t-t') \mathbf{E}(z, t') dt' \\ \mathbf{B}(z, t) = \mu_0 \mu_r(z) \mathbf{H}(z, t) \\ \mathbf{J}(z, t) = \sigma(z) \mathbf{E}(z, t) \end{array} \right.$$

The slabs have a spatially varying wave impedance, $Z(z) = \sqrt{\frac{\mu_0 \mu_r(z)}{\varepsilon_0 \varepsilon_r(z)}}$, and are impedance matched to the surrounding half-spaces. It is shown that the effects from the variation of the impedance can be matched by the temporal dispersive effects and the conductivity so that for a obliquely incident plane wave the slab does not reflect any field regardless of the shape of the incident transient field.

The problem of finding reflectionless media is formulated as an inverse problem where the constitutive relation is to be determined as a function of depth given a prescribed reflection kernel equal to zero. In general this problem has non-unique solutions. However, it may be reduced to a problem which is uniquely solvable, by assuming some of the parameters to be known. There are four suitable choices of the parameter to be determined, the impedance, the phase velocity, the conductivity, or the susceptibility kernel with a given time dependence. The inverse problem is solved by a time domain Green functions technique.

The present technique can also be used to design slabs with any prescribed reflection properties. The attractive feature is that clean data can be used in the solution of the inverse problem which then is well posed and well conditioned. The reflection data do not have to be prescribed, the basic theory and the algorithms can be applied also to measured data. In that case the inverse problem is ill-posed since the reflection kernel has to be obtained by deconvolution.

Several numerical examples of non-reflecting conducting dispersive slabs will be shown.

Antennas I**R. L. Fante and H. Steyskal**

Page

- 8:20 Analysis of a Diversity Antenna Using FDTD Method 22
Mark Douglas, Michal Okoniewski, Maria A. Stuchly,
University of Victoria*
- 8:40 Mobile SMM Antennas with Pattern-Diversity and Dual-Mode 23
Operations
J. J. H. Wang, J. K. Tillery, Wang-Tripp Corporation*
- 9:00 Numerical Modeling of an AM/FM Automotive Windshield 24
Slot Antenna
E. Walton, R. Abou-Jaoude, M. Pekar, The Ohio State University*
- 9:20 Array Pattern Synthesis in the Presence of a Near-Zone Scatterer 25
Hans Steyskal, Rome Laboratory/ERAA
- 9:40 Reducing the Off-Boresight Fields of a Broadband TEM Horn 26
*D. J. Wolstenholme, A. J. Terzuoli, G. C. Gerace, Air Force
Institute of Technology*
- 10:00 BREAK
- 10:20 Low Cost Steerable Beam HF Linear Array Antenna of 27
Subarrays for a Prototype Ground Wave Radar
S. A. Saoudy, R. Khan, R. Davis, Memorial University of Newfoundland*
- 10:40 Circularly Polarised Dielectric Resonator Antenna: Analysis of 28
near and Far Fields using FD-TD Method
Karu P. Esselle, Macquarie University
- 11:00 Extending a Neural Network Surface Error Compensation 29
Algorithm to Distorted Paraboloidal Reflector Antennas
W. T. Smith, S. Y. Cheah, University of Kentucky*
- 11:20 Beam Synthesis of Conformal Arrays 30
John P. Casey, Naval Undersea Warfare Center Detachment,
Roy L. Streit, Naval Undersea Warfare Center*
- 11:40 Adaptive Cancellation of Multiple Mainbeam Jammers 31
Ronald L. Fante, Richard M. Davis, Thomas P Guella,
The MITRE Corporation*
- 12:00 Superdirectivity in Statistical Antenna Theory 32
Y. S. Shifrin, V. V. Dolshykov, Kharkov State Technical
University of Radio Electronics*

Analysis of a Diversity Antenna Using FDTD Method

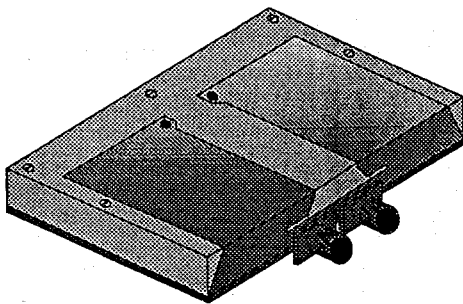
Mark Douglas*, Michal Okoniewski and Maria A. Stuchly

Department of Electrical and Computer Engineering
University of Victoria, Victoria, BC, Canada, V8W 3P6

Antennas for mobile communications must simultaneously be compact, account for the problem of signal fading in mobile communications environments and minimize the loss in performance due to the proximity of the user's body. They must also consider microwave energy deposited in the user's body, particularly in the head, and its possible harmful health effects. Given the complexity of dealing with all of the above problems simultaneously, an approach which uses a robust computer model to enhance experimental design and measurements is a natural choice.

This paper presents the results from a computer model of a microstrip diversity antenna held close to a human head. The computer model uses an FDTD technique developed at the University of Victoria. The antenna modelled was developed by the presenter (patents pending in the U.S.A. and Canada) and is shown below. This antenna performs two-way polarization diversity to minimize signal fading in mobile communications.

To model the human head, MRI scans are translated into the complex permittivity data representative of the following tissues: bone, brain, cerebral spinal fluid, muscle and blood. The voxel size is between three and five millimeters. The radiation pattern and input impedance of the antenna, as well as the Specific Absorption Rate (SAR) of microwave energy in the head are computed with the FDTD software. The radiation pattern and input impedance curves of the antenna model without the head are compared with experimental results. The effect of the head on antenna characteristics and the SAR data are then examined. These results are also compared with data for other types of antennas. The approach presented is novel, as it combines in one study the aspects of diversity to reduce signal fading, numerical techniques in antenna designs, the interaction between the antenna and the human body, and the absorption in the human body of microwave energy.



**Mobile SMM Antennas
with Pattern-Diversity and Dual-Mode Operations**

J. J. H. Wang* and J. K. Tillery
Wang-Tripp Corporation
1710 Cumberland Point Drive, Suite 17
Marietta, Georgia 30067

The use of two antennas with orthogonal or perpendicular radiation patterns to reduce the fading effect in mobile/personal antennas was demonstrated by using a monopole and a crossed slot (K. Itoh, et al, *IEEE Trans. Ant. Prop.*, 485-489, 1979) and a notch array (H. Arai, et al, *IEEE Trans. Veh. Tech.*, 483-486, 1991). The recently invented spiral-mode microstrip (SMM) antenna (J. J. H. Wang and V. K. Tripp, U.S. patent no. 5,313,216, also *IEEE Trans. Ant. Prop.*, 332-335, 1991) has inherent spiral modes of different radiation patterns over multioctave frequency bands, which make it uniquely suitable as a low-profile multifunction antenna.

Radiation patterns for spiral modes 0 and 1 are orthogonal, the former with a monopole (omnidirectional) pattern and the latter with a slot (unidirectional) pattern. These two modes can be used either by itself or in combination (with optional phasing between them) to reduce signal fading. This integrated approach of using diversity antennas in conjunction with propagation characteristics and diversity-control circuits constitutes an AIR INTERFACE™, which ensures good wireless transmission between a mobile terminal and a ground or satellite-based station. This antenna can also be used to function simultaneously for the cellular phone (824-894 MHz) and the GPS (Global Positioning System, 1.2-1.6 GHz).

The antenna is shaped like a disk 0.4" thick and 3.5" in diameter. Variation of these two dimensions is possible, and can be optimized on the basis of both technical and practical considerations. The antenna is mounted on the metallic rooftop of an automobile, which constitutes the ground plane of the SMM antenna. If a nonmetallic roof is used, a paste-on metallic foil of copper or aluminum with a diameter of 6" or larger can be used to serve as the ground plane.

Antenna pattern measurements were carried out in WTC's anechoic chamber. Field measurements were also conducted with the antenna mounted on the rooftop of a mockup vehicle made of metallic struts and wire mesh. The unique diversity and multifunction features of the SMM antenna are demonstrated in these applications.

Numerical Modeling of an AM/FM Automotive Windshield Slot Antenna

E. Walton*, R. Abou-Jaoude and M. Pekar

The Ohio State University
ElectroScience Laboratory
1320 Kinnear Road
Columbus, Ohio 43212-1191

The goal of the research described in this paper is to develop a conformal/hidden AM/FM automotive radio antenna. The antenna described here is an annular slot antenna created by imbedding a transparent metal film in the windshield between the two glass layers. Such metal films are becoming important as a means of controlling solar heat buildup in the vehicle by reflecting infrared light. They are transparent in the visible spectrum. A 2 to 3 cm gap is left around the circumference of the metal film to form the annular slot. The slot is driven by a coaxial cable where the shield of the cable is attached to the body of the vehicle and the center connector bridges the gap and is attached (directly or capacitively) to the internal metal film.

This paper will describe the design process, including impedance matching using a capacitive coupling patch on the outside of the glass (but inside the vehicle). Efficiency issues at both AM and FM frequencies will be discussed. Performance evaluation using measurements of gain patterns as well as on-road mobile measurements will be discussed.

A mathematical model of the antenna will be presented. In this case, the method of moments (MOM) technique will be developed for the case of the windshield film on the automobile. The Electromagnetic Surface Patch code (ESP IV) as developed at the Ohio State University ElectroScience Laboratory by Prof. E. Newman was used to model the film and the vehicle. This code was slightly modified to permit a RF current feed at the intersection of two plates. The entire body of the vehicle was modeled including the passenger compartment cavity. Gain patterns and impedance values were calculated and will be shown.

Comparisons between the theoretical results and the experimental measurements will be shown.

ARRAY PATTERN SYNTHESIS IN THE PRESENCE OF A NEAR-ZONE SCATTERER

Hans Steyskal

Rome Laboratory / ERAA

31 Grenier Street, Hanscom AFB, MA 01731, USA

We address the question to what extent the pattern perturbations caused by a scatterer in the proximity of an array antenna can be compensated by a suitably modified array excitation. This is a problem of practical interest, since for example masts or wing tips often are within the radiative near-zone of a ship or air borne antenna.

An earlier approach simply imposed a set of near-field nulls over the scatterer and used remaining degrees of freedom of the array excitation for a least-mean-square match to a desired pattern [Steyskal, Electronics Letters, Vol.30, 24th Nov. 1994]. This provided insight since it showed the resultant pattern to be the superposition of the original, desired pattern and cancellation beams focused on the null locations, and furthermore, that the pattern perturbations could be reduced over large sectors in many cases. Limitations of this solution are that it i) may impose a more severe field constraint than necessary and ii) does not allow direct sidelobe control.

A more general approach is to express the total perturbed far field pattern of a linear N-element array as

$$f(\vartheta) = \sum_{n=1}^N a_n e_n(\vartheta) + \sum_{n=1}^N a_n g_n(\vartheta)$$

where a_n denotes the array element excitation, $e_n(\vartheta)$ the array element pattern, and $g_n(\vartheta)$ the scatterer pattern when illuminated by element n , and then to determine the a_n 's by a suitable pattern synthesis method. We use both least-mean-square approximation, which is a direct method and alternating projections [Bucci et al, Proc. IEEE, Vol.137, Pt. H, No.6, Dec.1990], which is an iterative method and allows local sidelobe control. Results obtained for typical cases of pencil beams and sector beams demonstrate that the pattern perturbations caused by the near-zone scatterer can indeed be reduced still further.

Reducing the Off-Boresight Fields of a Broadband TEM Horn

*D. J. Wolstenholme, A. J. Terzuoli, Jr, G. C. Gerace
Air Force Institute of Technology*

Ultra-Wideband (UWB)/Short-Pulse (SP) radiation systems require broadband antennas with low dispersion characteristics. Unfortunately many broadband antennas do not have high directivity. In their effort to find a highly directive wideband antenna, many researchers have turned to the Transverse Electromagnetic Horn (TEM) horn. A TEM horn antenna meets many of the four criteria for a UWB/SP system: 1) a constant amplitude response, 2) a linear phase response, 3) no reflections or resonances, and 4) a wide bandwidth.

With proper selection of the length of the conductors, flare angle of the plates, and width at the aperture, the TEM horn meets the constant amplitude response, linear phase response, and bandwidth criteria; the problem occurs with reflections. The abrupt transition from conductive plates to free space causes part of the transmitted pulse to reflect back toward the source. This reflection also causes some of the field to diffract at the free space edge of the horn. The diffraction increases the off-boresight field levels and thereby decreases the directivity of the antenna.

Changing the impedance along the length of the horn is effective in reducing the diffraction at the free space end of the horn. One method of changing the impedance is to use a tapered periodic surface (TPS), which tapers the impedance in the same way a resistive card (R Card), tapers the impedance. The impedance increases from some Z_0 to an infinite imaginary impedance ($Z = \pm j\infty$). The gradual change of impedance from a low impedance (conductor) to a high impedance (free space) reduces the reflection from the end. Therefore, the taper reduces the off boresight field levels by decreasing the amount of diffraction at the free space end.

Using the Periodic Moment Method (PMM), and Finite Difference Time Domain (FDTD), two tapered periodic surfaces are designed (and later fabricated) to approximate known broadband impedance functions; they are a triangular function and an exponential function. The triangular impedance function maximizes bandwidth. The exponential taper function provides the smoothest transition. Conductive strips separated by a dielectric slab were chosen as the elements of the TPS. The top and bottom layers of conductive elements are the same with the bottom layer shifted back towards the source by 0.44 inches. The center-to-center spacing between the elements is kept at a constant value of 0.88 inches. Conductive strips are capacitive elements. As the gap width increases, the impedance increases. The gap widths are scaled so that the desired impedance function is approximated.

The TPS is attached to the ends of a TEM horn designed to operate from 300 MHz to 6 GHz. A probe is fixed on a rotating arm in order to sample the field levels at various elevation angles. A TEM horn without a TPS is used as a reference case for the measurement of the off boresight fields. The antennas are excited with a step. The probe records the time differentiated field, or impulse response.

The exponential taper outperformed the triangular taper. The peak field levels decrease as the elevation angle increases. At the greatest angle measured, 90°, the exponential taper reduced the diffracted fields by 10.048 dB. At the same test location, the triangular taper reduced the diffracted fields by 8.277 dB.

**Low Cost Steerable Beam HF Linear
Array Antenna of Subarrays for
a Prototype Ground Wave Radar**

S.A. Saoudy*, R. Khan and R. Davis

Centre for Cold Ocean Resources Engineering
Memorial University of Newfoundland
St. John's, Newfoundland, Canada A1B 3X5.

An over-the-horizon, High Frequency Ground Wave Radar (HF-GWR) has recently been built at Cape Race, Newfoundland. Within this HF-GWR, the receiver antenna is a 40 element linear array that extends 866 metres on top of a 100 foot-high cliff. Real time operation at substantially reduced cost can be achieved by employing only 10 receivers. The 40-element array is divided into 10 identical subarrays of 4 elements each where each subarray is connected to one of the ten receivers. These receivers are high dynamic range units with 16-bit digital outputs.

The electronic steering of the array's thin main lobe is done using both software (digital) as well as hardware (analog) phase shifting arrangements. The software steering is performed on the 10 digital signals from the receivers. The hardware (external) steering is done within each subarray using custom designed analog hardware beamformers.

Present work describes the structure of the receiver array antenna system with specific emphasis on the hardware steering mechanism.

The far field radiation patterns due to this elaborate system of steering will be illustrated at different design parameters. The hardware steering is achieved by using tens of lumped phase shift passive circuit elements whose operation is controlled using relays.

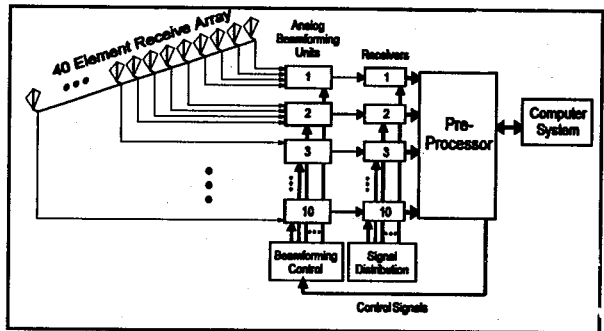


Fig.1: Simple block diagram of Cape Race GWR receiver antenna System

Efficient quantitative and qualitative techniques for *in situ* performance evaluation of the hardware phase shifters have been developed such that any operational deficiency is detected in the performance of the phase shifters, antenna elements and its transmission lines.

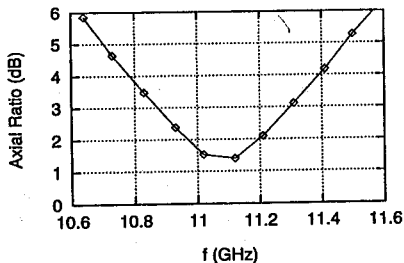
CIRCULARLY POLARISED DIELECTRIC RESONATOR ANTENNA: ANALYSIS OF NEAR AND FAR FIELDS USING FD-TD METHOD

Karu P. Esselle
Electronics Department
Macquarie University
Sydney, NSW 2109, Australia
Tel: 61 2 850 9141, Fax: 61 2 850 9128
Email: esselle@mpce.mq.edu.au

A circularly-polarised dielectric resonator antenna has been reported recently (A. Ittipiboon et al, ANTEM'94, Ottawa, Aug 2-5, 427-430). It has two rectangular dielectric resonators placed perpendicular to each other to form a cross. The antenna is fed from a microstripline through a single aperture. A good axial ratio (< 3 dB) has been achieved over a 4% frequency bandwidth or about 100° beamwidth at 11.2 GHz. However, the design of this antenna was based on design curves generated from various measurements. No rigorous theoretical analysis of the antenna is available yet.

This paper presents a theoretical analysis of the above antenna using the FD-TD method. This method has been successfully applied for the analysis of a rectangular dielectric resonator antenna previously (K.P. Esselle, URSI Meeting, Seattle, June 19-24, 420). It is based on Yee's FD-TD equations, Mur's absorbing boundary conditions, time-domain Field Equivalence Principle, Image Theory and FFT. The analysis takes into account the presence of the substrate, the aperture and the microstrip feed, and assumes an infinite ground plane. All computations were performed in a Cray YMP four-processor supercomputer.

Our theoretical results compare very well with the experimental results of Ittipiboon et al. As an example, the calculated axial ratio of the antenna in the boresite direction is shown in the figure. Theoretically, the best axial ratio of 1.18 (1.40 dB) is predicted at 11.1 GHz; the best experimental axial ratio is 1.12 (1.0 dB) at 11.2 GHz. The near and far fields obtained from this analysis lead to a better understanding of the antenna. This theoretical approach also facilitates the optimisation of the antenna without performing many experiments.



EXTENDING A NEURAL NETWORK SURFACE ERROR COMPENSATION ALGORITHM TO DISTORTED PARABOLOIDAL REFLECTOR ANTENNAS

W. T. Smith*, S. Y. Cheah
Department of Electrical Engineering
University of Kentucky
Lexington, Kentucky 40506-0046

This paper presents the steps involved in extending a neural network electromagnetic surface error compensation algorithm to include paraboloidal reflector antennas. The feasibility of using neural network computing for compensation algorithms had previously been demonstrated with the simplified problem of infinite cylindrical parabolic reflectors. The major steps involved in the extension to paraboloidal reflectors include increased complexity of the surface error expansion and a significant increase in the number of trained networks and feed array elements. The computational time for the neural network algorithm, however, is only negligibly increased.

Electromagnetic compensation for surface errors can be used to supplement mechanical techniques at frequencies where subtle residual errors in the reflector surface remain electrically significant. Electromagnetic compensation techniques are implemented with algorithms that control the amplitude and phase of array feed elements. In a previous study (Smith & Bastian, *AP Digest*, 1993), the use of neural network computing to perform electromagnetic surface error compensation was demonstrated for the case of infinite cylindrical parabolic reflector antennas. The major advantage of using the neural network approach is that, once trained, the large computational overhead often associated with EM compensation is overcome and real-time compensation is facilitated.

In the previous study, infinite cylindrical reflectors were chosen to simplify the physics and the math (the radiation equations are scalar). The simpler math allowed for easier insight into how the algorithm works. In addition, the required surface error expansion is implemented with univariate functions. For paraboloidal reflector compensation, however, the equations are vector and surface error expansion now involves bivariate orthogonal functions. The number of trained neural networks required corresponds to the number of surface expansion functions.

In this presentation, the steps involved in extending the neural network algorithm to paraboloidal reflectors are outlined. The surface error expansion will be discussed. Compensation results for distorted paraboloidal reflector antennas are presented and compared to algorithms not using neural network computing.

BEAM SYNTHESIS OF CONFORMAL ARRAYS

John P. Casey*

Submarine Electromagnetic Systems Department
Communications Antennas Branch, Code 3413
Naval Undersea Warfare Center Detachment
New London, CT 06320

Roy L. Streit

Combat Control Systems Department, Code 2214
Naval Undersea Warfare Center
Newport, RI 02841

For arrays conformal to nonplanar surfaces, the radiation patterns and polarizations of individual antenna elements are not identical because of their dissimilar orientations and because they couple differently with the host surface. Consequently, neither the principle of pattern multiplication nor conventional beam synthesis methods apply. Unfortunately, no proven synthesis technique is available for conformal antenna arrays (W. H. Kummer, *Proc. IEEE*, **80**, p. 137, Jan. 1992).

In this paper, an optimization procedure is applied in the determination of the complex excitations to produce a beam pattern which has high gain, desired polarization across the main beam, sufficiently low sidelobes, and which satisfies practical excitation restrictions. Optimization methods have been successfully applied to the synthesis of conformal sonar arrays (Streit and Nuttall, *J. Acoust. Soc. of Am.*, **72**, pp. 181-190, July 1982).

The optimization model is based on the minimization of the total radiated power in the sidelobe region S (defined by the designer) subject to the following constraints: (i) restrictions on the variations in magnitude and phase of the antenna excitation currents; (ii) the polarization loss factor (PLF), i.e., the loss associated with the mismatch between the array polarization and the desired polarization, must be less than or equal to a specified upper bound throughout the main beam region M (defined by the designer); (iii) the directive gain of the array must be greater than or equal to a specified lower bound. Sidelobe constraints may be added as needed. The effect of the individual element patterns and polarization in the presence of the host surface is incorporated.

The optimization model is carried out via a sequential quadratic programming (SQP) algorithm, in which the search direction is the solution of a quadratic programming subproblem. SQP algorithms are generally superior to gradient descent methods as they exhibit a higher rate of convergence in the vicinity of the solution. In addition, an SQP algorithm is well suited to this application since the objective and constraint functions are quadratic functions of the excitation variables. The algorithm is applied to the synthesis of an arbitrary phased array antenna conformal to a convex three-dimensional surface. However, the algorithm is potentially applicable to arbitrary volumetric arrays.

The optimization model is validated through comparison with conventional procedures for the synthesis of various linear and planar arrays. Results will be presented for the synthesis of phased arrays conformal to both cylindrical and spherical surfaces. Slot elements are considered in the conformal array examples.

Adaptive Cancellation of Multiple Mainbeam Jammers

**Ronald L. Fante
Richard M. Davis
Thomas P. Guella**

**The MITRE Corporation
Bedford, MA 01730**

Mainbeam jammers offer a serious challenge to a radar system. The usual solution is to place a strobe in the jammer direction, but this effectively blanks out two beamwidths of azimuth scan. Furthermore, if there is an array of jammers, with an azimuthal spacing of several radar beamwidths, detection can be denied over an entire azimuth sector. Thus, it is desirable to devise a technique to compensate for mainbeam jammers. We will show that this can be achieved by using auxiliary antennas that are separated from the main antenna by distances that are sufficiently large that the array can place narrow nulls on the mainbeam jammers while still maintaining peak gain on a target. In order to compensate over large bandwidths, adaptive tapped delay lines are required for each auxiliary.

We will present a design procedure for the required array, including the number of auxiliaries needed, their gain, spacing, number of taps, etc. Simulated results for the sum and difference beam performance will be presented for both the narrowband and wideband limits.

SUPERDIRECTIVITY IN STATISTICAL ANTENNA THEORY

Y.S.Shifrin*, V.V.Dolzhykov

Kharkov State Technical University of Radio Electronics

Sources fluctuations always present in the real antennas, change (sometimes cardinally) the results of the deterministic antenna theory (DAT). This manifests itself rather distinctly with reference to such an interesting phenomenon as superdirectivity (SD).

The analysis of this question is stimulated by the following factors.

- In general definite restrictions are imposed in the DAT on the nature of the sources amplitude-phase distribution (APD) being sought in synthesis to exclude the SD solutions with disadvantages inherent to them (narrow-band, low efficiency of radiation, bad efficiency, high sensitivity to the sources fluctuations). These restrictions are rather arbitrary and it remains vague whether it is possible practically to "advance" somehow in the SD domain.

- Development of antenna technique (in particular aircraft and short-wave antennas) push the designers steadily to attempts to use at least a "moderate" SD.

- In a number of cases the antennas narrow band and low efficiency of its radiation are insignificant and their efficiency can be improved if superconductive materials are used. In these cases the sources fluctuations prove to be the main obstacle on the way of the SD antennas construction.

The restrictions imposed by them on the SD can be elucidated if the presence of fluctuation is taken into account from the very beginning, at the stage of the synthesis problem statement. In this case it is also possible to define the maximum attainable antenna characteristics with known fluctuations statistics. Taking these as a guide the report treats solutions of the statistical synthesis problem of the linear continuous antenna with the sources phase fluctuations by the given radiation pattern (RP) or its integral parameters (gain, etc.) The choice of the linear antenna allows to obtain the solution in the analytical form, this facilitates analysis of the obtained regularities.

In all the cases the sought optimal APD $A(x)$ is presented as a series by eigenfunctions of the finite "Fourier transform operator" Ψ_n

$$A(x) = \sum_{n=0}^{\infty} a_n \Psi_n, \quad (1)$$

where a_n are the sought coefficients.

The terms of the series (1) can be treated as the APD spatial harmonics, its own partial RP corresponds to each of them. With $n \leq 2L/\lambda$ (λ is a wave length) the maximum of this RP is in the region of visibility, with $n > 2L/\lambda$ - in the region of imaginary angles. Respectively, it is possible to speak about active and reactive harmonics.

For every of the indicated problems of synthesis the expressions for the optimal APD and the attainable characteristics of the antennas are obtained. It is shown that the account of the sources fluctuations in the synthesis problems results in a diminution of the reactive harmonics contribution to the optimal APD, its smoothing and, respectively, in limiting the SD effects. The plots and tables, allowing to state the possibilities of the SD conditions implementation according to different antenna characteristics depending on dispersion α and correlation radius of the source fluctuations ρ , are given. It is shown that with small (as compared to the dimensions of the antenna L) values of ρ these possibilities are significantly limited even with rather small α . With the increase of ρ the SD realization possibilities are widening. In this case the optimal APD tends to the APD for the determined synthesis case. The plots, showing the dependence of the SD realization possibilities on the antenna dimensions, are also given. These possibilities are rather restricted for the antennas whose length is more than several λ .

Wavelets in Electromagnetics I

A. Chan and H. Ling

Page

- 8:20 Linear Frequency Modulated Signal Detection using Wavelet Packet, Ambiguity Function and Radon Transform
Minsheng Marshall Wang, Andrew K. Chan*, Charles K. Chui, Texas A&M University*
- 8:40 A Fast Multiresolution Moment Method Algorithm Using Wavelet Concepts
H. Kim, Hanyang University, H. Ling, The University of Texas, Austin*
- 9:00 Characterization of Microstrip Patch Antennas Based on the Two-Dimensional Wavelet Theory
Kazem F. Sabet, Linda P.B. Katehi, University of Michigan*
- 9:20 Super-Resolved Parameterization of Dispersive Scattering Mechanisms in the Time-Frequency Plane
L.C. Trintinalia, H. Ling, University of Texas, Austin*
- 9:40 Time-Frequency Representation of Wideband Radar Echo Using Adaptive Normalized Gaussian Functions
L.C. Trintinalia, H. Ling, University of Texas, Austin*
- 10:00 BREAK
- 10:20 Resolution Enhancement and Small Perturbation Analysis using Wavelet Transforms in Scattering Problems
Z. Baharav, Y. Leviatan, Technion - Israel Institute of Tech.*
- 10:40 On the Use of Wavelet-Like Basis Functions in the Finite Element34 Solution of Elliptic Problems
Richard K. Gordon, University of Mississippi, Jin-Fa-Lee, Worcester Polytechnic Institute*
- 11:00 New Wavelet-Like Basis Functions for the 2D Mode Analysis of Coupled Microstrips
K. Blomme, D. DeZutter, H. Devos, University of Ghent*
- 11:20 A Hybrid Wavelet Expansion and Boundary Element Method in Electromagnetic Scattering
Gaofeng Wang, Tanner Research, Inc. Jiechang Hou, Wuhan University*

On the Use of Wavelet-Like Basis Functions in the Finite Element Solution of Elliptic Problems

Richard K. Gordon*

Electrical Engineering Dept.
University of Mississippi
University, MS 38677

Jin-Fa Lee

Electrical Engineering Dept.
Worcester Polytechnic Institute
Worcester, MA 01609

In this paper, the use of wavelet-like basis functions in the finite element solution of elliptic equations over one dimensional and two dimensional domains is considered. Jaffard has recently shown that when such basis functions are employed in the finite element solution of elliptic problems, it is possible, using simple diagonal preconditioning, to obtain a global matrix the condition number of which is bounded by a constant as the number of points of discretization is increased (S. Jaffard, *SIAM J. Numer. Anal.*, pp. 965-986, August 1992). This contrasts sharply with the situation that arises when the traditional finite element basis functions are used; in this case the usual preconditioning methods make the condition number $O\left(\frac{1}{h}\right)$; and if simple diagonal preconditioning is used, the condition number will go to infinity as, at best, $\frac{C}{h|\log h|}$ as the number of points of discretization is increased, i.e., as h goes to zero. This is important because when iterative algorithms are employed, such ill conditioning can lead to numerical instabilities, slow convergence, or even failure to converge.

In this paper, the use of wavelet-like basis functions in the finite element solution of elliptic problems will be discussed in detail; both Dirichlet and Neumann boundary conditions will be considered. The construction of the wavelet-like basis functions will be illustrated for both of these cases. Comparisons with the use of the traditional finite element basis functions will be made. The global matrices arising in both of these analyses will be presented. The iterative solution of several problems using these methods will be discussed; a comparison of the rates of convergence observed and cpu times required in each case will be presented.

Microstrip Antenna Design and Analysis**L. Shafai and K. Chang**

Page

- 8:20 The Effect of Air-Bridges on the Mode Suppression of Asymmetrical CPW-FED Slot Antennas
*Chung-Yi Lee**, Tatsuo Itoh, University of California at Los Angeles
- 8:40 Tolerance Effects on Low-Cost Printed DBS Antennas
Manuel Sierra, Universidad Politecnica de Madrid, George Jankovic, Boulder Microwave Technologies, Inc.
- 9:00 Alternate Cutoff Radius Criterion for Probe-Fed, Circular Microstrip Patches
D. Chatterjee, R. G. Plumb, University of Kansas
- 9:20 Design of 24 GHz Microstrip Travelling Wave Antenna for Radar Application
*H. Moheb**, InfoMagnetics, L. Shafai, University of Manitoba, M. Barakat, InfoMagnetics
- 9:40 An Electromagnetically Coupled Microstrip Antenna with a Rotatable Patch
*Atsuya Ando**, Yasunobu Honma, Kenichi Kagoshima, NTT
- 10:00 BREAK
- 10:20 Ka-Band Aperture Coupled Microstrip Antenna with Image Line Feed
*Ming-yi Li, Sridhar Kanamaluru, Kai Chang**, Texas A&M University
- 10:40 Scattering and Radiation by Conformal Microstrip Antennas with36 Dielectric Overlay
*Leo C. Kempel**, Mission Research Corporation, James T. Aberle, Arizona State University
- 11:00 Design and Analysis of Slot Array Antennas on a Radial Feed Line
*M. Sierra**, J. Redoli, Universidad Politecnica de Madrid, M. Vera, A.G. Pino, Universidad de Vigo
- 11:20 Slotline Antenna with Non-Leaky Coplanar (NLC) Waveguide Feed
*Yaozhong Liu**, Chung-Yi Lee, Tatsuo Itoh, University of California, Los Angeles
- 11:40 Applications of Planar Multiple-Slot Antennas for Impedance Control, and Analysis Using FDTD with Berenger's PML Method
*H.S. Tsai**, R.A. York, University of California at Santa Barbara

Scattering and Radiation by Conformal Microstrip Antennas with Dielectric Overlay

Leo C. Kempel*
Mission Research Corporation
147 John Sims Parkway
Valparaiso, FL 32580

James T. Aberle
Electrical & Computer Engineering
Arizona State University
Tempe, AZ 85287

Conformal antenna arrays are becoming increasingly popular for use on aircraft. Microstrip patch antennas generally offer lower construction cost, lower drag and more flexibility over conventional protruding antenna elements. Various Computer Aided Design tools have been developed by academic, government, and industrial research and development teams over the past several years. These new, powerful design tools have exploited the vast increase in computational capability and reduction of cost which has occurred over the past ten years. Various numerical techniques have been applied to microstrip antenna design such as: the finite difference-time domain method, the integral equation method, and the finite element method. A particularly attractive technique involves a hybridization of the later two methods. This finite element-integral equation (FE-IE) method has been successfully applied to cavity-backed microstrip patches which are recessed in either a metallic ground plane or a metallic circular cylinder. A primary feature of both these configurations is their amenability to solution using the BiCG-FFT algorithm which greatly enhances the efficiency of the method in terms of both computational effort and memory demand.

In this paper, the FE-IE method will be extended to cavity-backed microstrip antennas with a dielectric superstrate. Figure 1 illustrates two typical configurations. The new formulation will utilize an appropriate dyadic Green's Function in the integral equation portion of the formulation. The discrete convolution property which permits a BiCG-FFT solver will be maintained. Examples of input impedance, radiation pattern, and scattering pattern calculations will be given at the meeting.

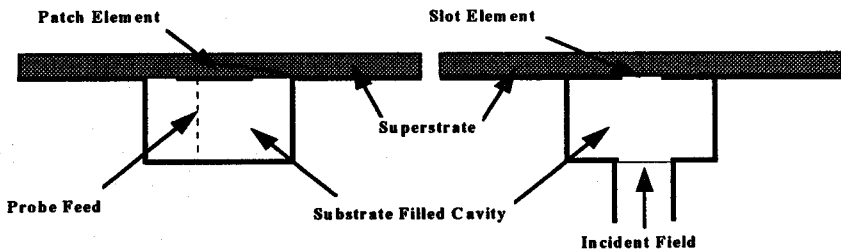


Figure 1. Typical Cavity-Backed Antenna Elements

Coupling and Shielding*J. L. Drewniak and W. P. Wheless*

Page

- 8:20 Development of Statistical Electromagnetics (STEM) Techniques38
W. P. Wheless, University of Alabama, C. B. Wallace, BDM Federal, Inc.,
W. E. Prather, Phillips Laboratory*
- 8:40 Analysis of Coupling Through Shielded Apertures39
Steven P. Castillo, New Mexico State University, Hector DeAguila,
Thomas Loughry, Phillips Laboratory*
- 9:00 On the Protection Against EM Leakage from ITE40
Fang Han, Linchang Zhang, Northern Jiaotong University*
- 9:20 Shielding Enclosure Radiation Enhancement Due to Attached41
Cables
D. M. Hockanson, J. L. Drewniak, T. H. Hubing, T. P. Van Doren,
University of Missouri-Rolla*
- 9:40 High Intensity Radiated Field (HIRF) Penetration in Helicopters
*Panayiotis A. Tirkas, Constantine A. Balanis, William V. Andrew, Arizona State
University, George C. Barber, NASA Langley Research Center*
- 10:20 Coupling Prediction of HF Antennas Mounted on Helicopter Structures
Using the NEC Code
Jian Peng, Constantine A. Balanis, Arizona State University

DEVELOPMENT OF STATISTICAL
ELECTROMAGNETICS (STEM) TECHNIQUES

W.P. Wheless, Jr. *

University of Alabama, Tuscaloosa, AL

C.B. Wallace

BDM Federal, Inc., Albuquerque, NM

W.D. Prather,

Phillips Laboratory, Kirtland AFB, NM

Understanding the electromagnetic (EM) response of complex systems is a key risk minimization activity for many programs. Confidence in the ability to explain, and predict, how complicated systems respond to EM radiation facilitates sound program management. Useful conclusions for decision makers, system planners, and design engineers can be extracted by the application of statistical techniques to this important class of applied EM problems.

Statistical methods are justified by two major difficulties. First, the non-integrable nature of many EM response problems renders analytic solutions intractable; the chaotic nature of the resulting eigenfunctions, eigenfrequencies, and EM energy flow (voltages and currents) is best described statistically. Second, statistical techniques are also effectively applicable to system susceptibility analysis when examining the effect of perturbations (topology, measurement location, source parameters, etc.) and incomplete target/source configuration information (which may cause large EM response changes).

The acronym STEM has been coined from Statistical ElectroMagnetics; STEM embraces the study of non-integrability and physics-based statistics as applied to EM response problems. STEM applications include problems associated with large complex system susceptibility, mode-stirred chamber validity and interpretation, development of calibrated measurement techniques, pre-test prediction, far-field EM scattering, target recognition, and problems in other areas of science and engineering such as space science and geophysics.

A program for the orderly discovery, development, and exploitation of STEM is discussed here. Problems of immediate interest include EM measurement and testing, fundamental EM interactions and coupling, and programmatic risk reduction.

ANALYSIS OF COUPLING THROUGH SHIELDED APERTURES

Steven P. Castillo*
Electrical and Computer Engineering Dept.
Dept. 3-O, Box 30001
New Mexico State University
Las Cruces, NM 88003

Hector DeAguila and Thomas Loughry
Phillips Laboratory
PL/WSM
Kirtland AFB, NM 87117-6008

Coupling of electromagnetic energy through apertures into shielded electronic systems is a problem of interest because of the need to quantify the electromagnetic vulnerability of such systems. Typically the aperture is required for optical viewing requirements. To reduce electromagnetic coupling through the aperture, a dielectric slab with an imbedded conductive mesh is used to effectively create a good shield over the aperture for the frequency range of interest.

In this paper we present an analysis for coupling into a conducting cavity through a general, dielectric-covered aperture with an imbedded conducting mesh. The transfer function for a composite wall with an imbedded conducting mesh given by Casey [K. F. Casey, "Electromagnetic shielding by advanced composite materials," AFWL IN 341, June 1977] is used to derive an integral equation for the unknown aperture electric field. For the transfer function used, it is assumed that the mesh spacing is small with respect to wavelength and that the dielectric slab is thin. The Galerkin Method-of-Moments technique is used to discretize the integral equation. Vector, roof-top basis functions are used to represent the aperture fields [S. M. Rao, D. R. Wilton, and A. W. Glisson, "Electromagnetic scattering by surfaces of arbitrary shape," IEEE Trans. Antennas Propagat., vol. AP-30, No. 3, pp. 409-418, May 1982].

In this paper, results will be given for coupling through a variety of mesh-covered apertures for several different plane-wave excitations. The effects of mesh spacing, dielectric constant and aperture size and geometry are examined. In addition, the extension of this analysis to coupling into conducting cavities will be given as well.

On the Protection against EM Leakage from ITE

Fang Han* and Linchang Zhang
Northern Jiaotong University, Beijing 100044, CHINA

Summary

The projective of this paper is to present a review on recent development of the mechanism of, and protective technique against, electromagnetic leakage of information from computer-based information technology equipment (ITE), emphasising on electromagnetic emission and information leakage from computer systems. It is recognised that electromagnetic leakage of computer information and computer virus are two major topics concerning information and computer security, which have aroused world wide concern and attention. However, many people remain ignorant of the hazards of electromagnetic leakage from computers and its related ITE.

Developments on theoretical models for radiated emission from electron beam in CRT, PCBs, and cables connecting various devices are presented and discussed. Numerical technique in both time domain and frequency domain are applied in the presentation of the models. On basis of these models, shielding theory for leakage protection, for several structure and active exciting sources are addressed. Comprehensive methods and techniques for suppression and protection against electromagnetic leakage of information, including shielding, filtering, bonding and grounding, deceptive leakage, enciphering, are finally discussed.

The methods and results presented in this paper can be utilised to solve the problem of information leakage via electromagnetic radiation, through a synthetic protection techniques against temperate electromagnetic emission from computer-based information technology equipment.

Shielding Enclosure Radiation Enhancement Due to Attached Cables

D. M. Hockanson, J. L. Drewniak*, T. H. Hubing, and T. P. Van Doren
Electromagnetic Compatibility Laboratory
Department of Electrical Engineering
University of Missouri-Rolla

Conducting enclosures are employed for minimizing EMI from high-speed digital systems as well as shielding from external electromagnetic radiation. However, the shield must be perforated with apertures and seams for moving air to cool the device, and cables penetrating the shield to supply power to the electronics and communicate with peripherals. Radiation from apertures in enclosures, and energy coupling through apertures to cables penetrating the enclosure is largely unstudied. In enclosure design, apertures are carefully specified to avoid resonances, however, energy may couple from a resonant cavity through a non-resonant aperture to a resonant or non-resonant cable located in proximity to the aperture. The Finite-Difference Time-Domain (FDTD) method is used to model enclosures (with and without external cables) and observe the emissions over a range of frequencies where a number of resonances are expected.

Cables are modeled with a quasi-static wire algorithm introduced by Taflov. The method was validated for near-field calculations relevant to EMI by modeling dipole and monopole antennas and comparing FDTD input impedance and near field results with existing moment method results. The comparison revealed an accuracy acceptable for EMC applications. The modeling errors resulted predominantly from modeling sources with finite lengths which appeared electrically long at higher frequencies.

A simple enclosure was modeled with perfectly conducting walls and an aperture in one face. A cable was attached to the shield face containing the aperture to investigate coupling through the aperture to the cable. The time-averaged power through the aperture as a function of frequency was calculated. In the vicinity of the TE_{301} cavity resonance, the aperture was of appreciable length ($\approx \frac{\lambda}{2}$) and the Q of the system was low in the absence of an attached cable. The addition of the cable "tuned" the system resulting in an increased Q . The system response to the addition of a cable was partially a function of cable location with respect to the aperture. The peak radiated power was increased by approximately 3 dB for the worst case. In addition, the cable could potentially increase the directivity of the radiated energy. FCC guidelines limit maximum field strength and, therefore, the addition of shielded and unshielded cables to the system may make the device fail emissions testing.

FDTD modeling is useful for determining appropriate placement of cables and apertures in shielding designs. Furthermore, FDTD may be employed to ascertain the most effective placement and thickness of internal lossy coatings for lowering the Q and EMI of the enclosure system. FDTD modeling methods will be used to further study the coupling mechanisms between apertures and cables. Internal ground planes may be added to the enclosure to model printed circuit boards and backplanes to contribute to a more realistic simulation.

THIS PAGE INTENTIONALLY LEFT BLANK.

Chiral Media

Page

D. L. Jaggard and I. V. Lindell

1:20	Some Possible Effective-Medium Descriptions for Bi-anisotropic Inclusions with Non-random Orientation <i>Ari Sihvola, Juha Juntunen, Helsinki University of Technology</i>	44
1:40	Source Decomposition Theory for Uniaxial Media <i>I. V. Lindell, Helsinki University of Technology</i>	45
2:00	Analysis of Wave Propagation in a Chiral-Filled Rectangular Waveguide <i>Abhay R. Samant, University of Illinois, Keith W. Whites*, University of Kentucky</i>	46
2:20	Scattering From a Chiral-Coated Conducting Cylinder of Arbitrary Cross Section <i>M. Al-Kanhal*, E. Arvas, Syracuse University</i>	47
2:40	Measured and Computed EM Scattering Comparison for Chiral-Material Slabs <i>Keith W. Whites, University of Kentucky</i>	48
3:00	BREAK	
3:20	Reflection and Transmission Characteristics of Chiral Panels <i>D. E. Jussaume*, Rockwell International, S. Singh, The University of Tulsa</i>	49
3:40	TE - TM Decoupling in Rectangular Coordinates for Guided Propagation in Bianisotropic Media <i>P. L. E. Uslenghi, University of Illinois at Chicago</i>	50
4:00	On The Brillouin Diagrams for Periodic Chiral Media <i>D. L. Jaggard, K. M. Flood, University of Pennsylvania</i>	51
4:20	Electromagnetic Fields in Open Chirostrip Structures Excited by Printed Dipoles <i>J. C. da S. Lacava, Instituto Tecnológico de Aeronautica, Feliciano Lumini, EMBRAER</i>	52
4:40	Chiral Absorbers: Effects of Chirality or of Inclusion Shape? <i>S. A. Tretyakov, A. A. Sochava, St. Petersburg State Technical University, C. R. Simovski, St. Petersburg Institute of Fine Mechanics and Optics</i>	53
5:00	Electromagnetic Scattering By Bi-Uniaxial Stratified Media <i>S. Shulga*, O. Charkina, Kharkov State University</i>	54

Some possible effective-medium descriptions for bi-anisotropic inclusions with non-random orientation

Ari Sihvola and Juha Juntunen
Helsinki University of Technology, Electromagnetics Laboratory
Otakaari 5 A, FIN-02150 Espoo, Finland

One of the present trends in random media modeling is to allow more complex material effects in the analysis. The present study is also oriented in this direction. The problem is to find effective material parameters of a continuum which is, in a small scale, composed of inclusions that have contrast to the background in their electric and magnetic properties.

In particular, the inclusions are allowed to be of general bi-anisotropic material, obeying the constitutive relations

$$\begin{aligned}\bar{D} &= \bar{\epsilon} \cdot \bar{E} + \bar{\xi} \cdot \bar{H} \\ \bar{B} &= \bar{\zeta} \cdot \bar{E} + \bar{\mu} \cdot \bar{H}\end{aligned}$$

where the electric field is denoted by \bar{E} , magnetic field by \bar{H} , electric displacement by \bar{D} , magnetic displacement by \bar{B} . The dyadic material parameters are, permittivity $\bar{\epsilon}$, permeability $\bar{\mu}$, and the two magnetoelectric parameters $\bar{\xi}$, $\bar{\zeta}$.

Isotropic material characterization requires two parameters, bi-isotropic needs four, and the full bi-anisotropic medium description contains 36 parameters. This makes effective medium modeling difficult in the general bi-anisotropic case. In the isotropic case, the ordinary macroscopic models — like for example, Maxwell Garnett and Bruggeman formulas — exploit local fields and other polarizations are scalar expressions that only contain electric quantities. Bi-isotropic magnetoelectric coupling mixes electric and magnetic quantities, and finally, the full anisotropy forces one to use dyadic analysis to keep the expressions compact.

This presentation introduces six-vector formalism for the effective-medium characterization. Six-vectors (Lindell, Sihvola, Suchy; *J. Electro. Waves Applic.*, submitted) combine electric and magnetic quantities into one six-dimensional quantity, and the material characterization is contained in the six-dyadic.

In heterogeneous media containing anisotropic and/or bi-anisotropic inclusions, regardless of their shape, the orientation of a single inclusion with respect to its neighbors is essential. Therefore for mixtures where the orientation distribution of the inclusions is not random (in other words, the homogenized mixture also contains preferred directions), one has to perform orientational averaging of the electric and magnetic dipole moments induced in the inclusions. The present study will also touch the question of combining the averaging process with the six-vector description, and how the final effective (bi-anisotropic) parameters will be calculated.

SOURCE DECOMPOSITION THEORY FOR UNIAXIAL MEDIA

I.V. Lindell

Electromagnetics Laboratory
Helsinki University of Technology
Otakaari 5A, Espoo 02150 FINLAND

It is well known that, in an isotropic medium, any electromagnetic field can be split in two parts, one of which is TE (transverse electric) and, the other one, TM (transverse magnetic) with respect to a given axis in space [see, e.g. Harrington, *Time-Harmonic Electromagnetic Fields*]. To perform the decomposition for fields arising from a physical source, the source itself can be decomposed in two parts. This method has been originally introduced for isotropic media [*IEEE Trans. Ant. Prop.* 36(10)1382-8] and it can be applied to solve electromagnetic problems with boundaries and interfaces parallel or perpendicular to the axis. Recently, the method has been applied to create an image theory for the perfect anisotropic surface, the so-called soft and hard surface. In the present paper, the source decomposition method is generalized to uniaxially anisotropic media which can involve axial chirality. Such a medium can be fabricated by inserting parallel similar metal helices in a base material. It was also recently shown that a slab of axially chiral uniaxial medium works as a rotatable polarization transformer which can be used to change the polarization of a plane wave from linear polarization to any elliptic polarization and conversely by rotating the slab.

The decomposition theories split a vector problem to two scalar problems, which for certain boundary and interface conditions appear uncoupled. The electromagnetic problem of a dielectric uniaxial medium was first considered by Clemmow in 1963 through Fourier transformation and scaling of the fields. By extending the TE/TM decomposition of sources to uniaxial media, the unnecessary Fourier transformation can be avoided and the resulting problems are reduced to those in isotropic media. When generalized to media with axial chirality, the decomposed fields appear no longer TE or TM but possess constant axial impedance, i.e., ratio of the axial electric and magnetic field components. In the case of vanishing chirality, the axial impedance becomes zero or infinite, which gives us the TE and TM decomposition as the limiting case.

It is further shown that each of the decomposed fields sees the uniaxial chiral medium as a nonchiral anisotropic medium of its own. The two anisotropic media in question are actually affine-isotropic. This means that, in terms of certain affine transformations, the anisotropy of the media can be reduced to isotropy, after which well-known solution methods can be applied to the two decomposed problems.

Analysis of Wave Propagation in a Chiral-Filled Rectangular Waveguide

Abhay R. Samant

Electromagnetic Communication Laboratory
University of Illinois
1406 W. Green Street
Urbana, IL 61801-2991

Keith W. Whites*

Department of Electrical Engineering
University of Kentucky
453 Anderson Hall
Lexington, KY 40506-0046

The topic of electromagnetic wave propagation in chiral material-filled guided wave structures has only recently entered the literature. The aim of this work is to add to this body of knowledge a detailed analysis of wave propagation in a chiral-filled *rectangular* waveguide. Since a simple solution based on the conventional analytical method (separation of variables) cannot be obtained for this problem, a numerical solution using the finite difference method together with Muller's root-finding algorithm is used to compute the longitudinal wavenumbers k_z . To provide a convincing argument for the validity of these numerical solutions, it has been found that the values of k_z for the zero-field (trivial) solution correspond to wavenumbers for the right- and the left-circularly polarized waves in an unbounded chiral medium. Hence, a novel scheme is developed whereby the validity of the numerical solution is established with analytical results.

Central to this work is the use of a technique known as "mode tracing" which is a very useful and reliable method for computing the wavenumbers and subsequently assigning the proper mode designation. The latter is important for a completely numerical procedure such as this where a countably infinite number of solutions are possible. Using this technique, $k_z - \beta$ traces, where β is the chirality parameter in the Drude-Born-Federov constitutive equations, for different modes can be constructed. These traces provide significant insight into some of the notable features of the rectangular chiral waveguide such as the existence of complex modes. Additionally, the information obtained from these plots provides starting points for dispersion ($k_z - \omega$) diagrams for the hybrid modes at any physically realizable value of β . Using the computed values of the modal wavenumbers, the longitudinal and transverse components of the electric and magnetic fields can then be determined.

In this talk, a brief overview of the theoretical formulation will be given with emphasis on the proper choice for the solution space and boundary conditions for each of the two coupled partial differential equations that govern the response of chiral-filled waveguides. Complete verification of the mathematical formulation and accuracy of the numerical methodology will be established using the trivial solution technique as mentioned above. We will present $k_z - \beta$ diagrams for a set of chiral waveguide modes and confirm the existence of complex modes in the rectangular chiral waveguide. Significant features of the dispersion diagrams such as mode bifurcation and low frequency effects of chirality will be discussed. Finally, the field patterns in the rectangular chiral waveguide will be presented and compared with approximate analytical solutions using a first-order simple normal mode expansion (SNME) technique.

SCATTERING FROM A CHIRAL-COATED CONDUCTING CYLINDER OF ARBITRARY CROSS SECTION

M. Al-Kanhal* and E. Arvas

Dept. of ECE, Syracuse University, Syracuse, NY 13244

A simple moment solution is presented to the problem of electromagnetic scattering from a perfectly conducting cylinder of arbitrary cross section which is coated by layers of homogeneous chiral material. The system is assumed to be illuminated by either a TE or a TM wave. The surface equivalence principle is used to replace the cylinders by equivalent electric and magnetic surface currents. These currents radiating in unbounded external medium produce the correct scattered field outside. When radiating in unbounded chiral medium, they produce the correct total internal field. By enforcing the continuity of the tangential components of the total electric field on the surface of the cylinders, a set of coupled integral equations is obtained for the equivalent surface currents. Unlike a regular dielectric coating, the chiral coating produces both co-polarized and cross-polarized scattered fields. Hence both electric and magnetic surface currents each have a longitudinal and a circumferential component. These components of the currents are obtained by using method of moments to solve the coupled set of integral equations. Pulses are used as expansion functions and point matching is used. The Green's dyads are used to develop explicit expressions for the electric field produced by two-dimensional surface currents radiating in an unbounded chiral medium. Some of the advantages and limitations of the method are briefly discussed. Computed results include the internal field and bistatic and monostatic echo widths. Results for circular cylinders are in very good agreement with exact eigenfunction solution.

Measured and Computed EM Scattering Comparison for Chiral-Material Slabs

Keith W. Whites
Department of Electrical Engineering
University of Kentucky
453 Anderson Hall
Lexington, KY 40506-0046

During the past few years, there has been an ongoing effort by a number of research groups to characterize the constitutive parameters for chiral materials. These efforts have included both numerical simulations and experimental measurement. As is the case with any material, the knowledge of these constitutive parameters allows for the computation of the electromagnetic scattering and the possibility of optimizing the material's performance in various applications.

One method for numerically computing the effective constitutive parameters for chiral materials has been developed by the author ("Full-wave computation of constitutive parameters for lossless composite chiral materials," to appear in *IEEE Trans. Antennas Propagat.*). This technique is based upon a combination Monte-Carlo/moment-method solution for thin-wire scatterers and completely accounts for all self- and mutual-coupling between the inclusions. The effects of loss in the inclusions and the effects of dielectric and/or magnetic hosts have also been incorporated into the simulation code (*Digest of the 1994 URSI Radio Science International Symposium*, Seattle, WA, pp. 428, June 1994; *Proceedings of Chiral'94*, Perigueux, France, pp. 77-82, May 1994).

This numerical simulation package has been subjected to a number of validating tests and the results have been encouraging. For example, the appearance of the Cotton effect in the optical rotatory dispersion (ORD), the pseudo-scalar behavior of the chirality parameter β , a linear dependence of the ORD as a function of the density of right- and left-handed chromophores and the effective electric susceptibility for a cloud of non-interacting rods all have been correctly predicted.

As a further validation of this simulation package, laboratory measurement of the scattering by chiral-material slabs has been undertaken and comparisons made with the numerical predictions. The objective of this talk is to present the methods and results of this latest work. As an overview of this presentation, a brief outline of the numerical simulation package will be given. This will be followed by a description of the construction of the chiral-material samples and the free-space measurement setup, both of which closely follow previously published work (T. Guire, *et. al.*, *IEEE Trans. Electromagn. Compat.*, vol. 32, no. 4, pp. 300-303, 1990). Finally, comparisons of the scattering by a number of slabs of varying inclusion density will be shown and the methods used to mitigate the effects of sample inhomogeneity will be described.

Reflection and Transmission Characteristics of Chiral Panels

D. E. Jussaume, Rockwell International, Tulsa, Ok
S. Singh, Department of Electrical Engineering
The University of Tulsa, Tulsa, Ok, 74104

This paper presents the results of an experimental study on composite chiral panels measured at microwave frequencies. The experimental data consisted of the reflected and transmitted power acquired for two helix orientations and densities, four material path lengths and two incident field polarizations. The chiral composite panels measured were constructed by embedding the helices into a low dielectric foam panel host. The helices were oriented with either their axis parallel or perpendicular to the panel face with one orientation direction per panel. The transmitted power magnitude and phase data was acquired over an 180 degree angular range. The reflected power magnitude and phase were also acquired for each configuration. The interaction of the incident linear electric field with the chiral panels resulted in the incident linear field becoming elliptical or circular polarized as the field traveled through the panels. The axial ratio and phase differential were extracted by matching the theoretical model to the transmitted power over a 180 degree angular range. The axial ratio and phase differential were then used to determine the composite chiral panels' intrinsic properties.

Past research, theoretical and experimental, centered on lossless composite chiral materials to study the degree of field rotation as a function of density and path length of helix elements. This study has extended the area of research by introducing lossy composite chiral materials. This paper will present the experimental data comparing the degree of rotation for each helix orientation and density, path length, and incident field polarization. Comparison between the lossy and lossless chiral materials will be made to demonstrate the effectiveness of introducing loss. A mathematical model will be presented which was developed to predict the characteristics of the chiral panel. A comparison of the predicted and experimental results will also be presented.

TE -TM DECOUPLING IN RECTANGULAR COORDINATES FOR GUIDED PROPAGATION IN BIANISOTROPIC MEDIA

P. L. E. Uslenghi

Department of Electrical Engineering and Computer Science
University of Illinois at Chicago

The most general bianisotropic, or magneto-electric, medium is considered in the frequency domain. Necessary and sufficient conditions are established in rectangular coordinates for guided propagation to be described in terms of superposition of TE and TM fields. An additional condition ensures TE - TM decoupling independently of the direction of propagation in the medium. The field components are given, and some guiding structures are discussed.

The medium is characterized by the constitutive relations

$$\underline{D} = \epsilon_0 \bar{\epsilon} \underline{E} + c_0^{-1} \bar{\xi} \underline{H}, \quad \underline{B} = \mu_0 \bar{\mu} \underline{H} - c_0^{-1} \bar{\eta} \underline{E},$$

where the field quantities are three-element column vectors in a rectangular coordinate system $[x,y,z]$, with z as the direction of propagation, and the four dimensionless tensors $\bar{\epsilon}$, $\bar{\mu}$, $\bar{\xi}$ and $\bar{\eta}$ are matrices of the type

$$\bar{\epsilon} = \begin{pmatrix} \epsilon_{xx} & \epsilon_{xy} & \epsilon_{xz} \\ \epsilon_{yx} & \epsilon_{yy} & \epsilon_{yz} \\ \epsilon_{zx} & \epsilon_{zy} & \epsilon_{zz} \end{pmatrix}$$

The electromagnetic field may be written as the superposition of a TE and a TM field if the five quantities ϵ_{xx} , ϵ_{yy} , μ_{xx} , μ_{yy} and $\epsilon_{xx}\epsilon_{yy} - \epsilon_{xy}\epsilon_{yx}$ are nonzero, and

$$\bar{\xi} + \bar{\xi}^T = 0, \quad \bar{\eta} + \bar{\eta}^T = 0, \quad \bar{\mu} = \alpha \begin{pmatrix} \epsilon_{xx} & \epsilon_{yx} & \epsilon_{zx} \\ \epsilon_{xy} & \epsilon_{yy} & \epsilon_{zy} \\ \epsilon_{xz} & \epsilon_{yz} & \mu_{zz}/\alpha \end{pmatrix}$$

where α is a constant. If the additional condition $\mu_{zz} = \alpha \epsilon_{zz}$ is imposed, the TE - TM decoupling remains valid after an arbitrary rotation of the medium.

The field components are determined, the boundary conditions are imposed, and the dispersion relations are studied for a variety of waveguiding structures.

ON THE BRILLOUIN DIAGRAMS FOR PERIODIC CHIRAL MEDIA

D. L. Jaggard and K. M. Flood

Complex Media Laboratory
 Moore School of Electrical Engineering
 University of Pennsylvania
 Philadelphia, PA 19104-6390

Here we consider the propagation and coupling of electromagnetic waves in a structure that is both chiral and periodic. The chirality is characterized by the constitutive relations $\underline{D} = \epsilon \underline{E} + i \xi_c \underline{B}$ and $\underline{H} = i \xi_c \underline{E} + \underline{B}/\mu$, where ϵ is the permittivity, μ is the permeability, and ξ_c is the chiral admittance. The periodicity is described by a sinusoidal perturbation of all three material parameters.

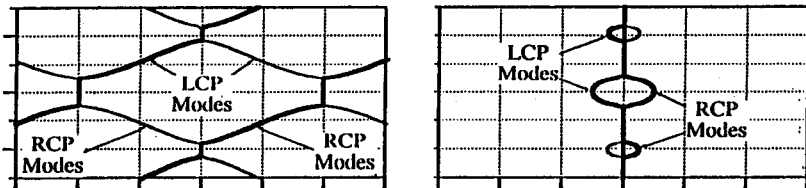
The vector coupled-mode equations are found to be

$$\underline{F}' - i \underline{\delta} \underline{F} = i \underline{\chi} \underline{B} \quad \text{and} \quad -\underline{B}' - i \underline{\delta} \underline{B} = i \underline{\chi} \underline{F}$$

where $\underline{\chi}$ denotes the coupling matrix, $\underline{\delta}$ is the phase mismatch matrix, the prime indicates differentiation with respect to the longitudinal coordinate, and \underline{F} and \underline{B} are forward and backward column vectors of RCP (+) and LCP (-) eigenmodes, respectively. These equations are of the same form as those for almost-periodic media [D. L. Jaggard and A. R. Mickelson, "The Reflection of Electromagnetic Waves from Almost Periodic Structures," *Appl. Phys.* 18, 405-412 (1979)] and can be used to determine the dispersion relation and the bandgap structure. The periodic chiral Riccati equation for the mode amplitudes can be written as

$$\underline{R}' = -i \underline{\chi}_- - \underline{R} \underline{\chi}_+ \underline{R} - i (\underline{\delta} \underline{R} + \underline{R} \underline{\delta}) \quad \text{for} \quad \underline{R} = \begin{bmatrix} r_{++} & r_{-+} \\ r_{+-} & r_{--} \end{bmatrix}$$

Below is shown one example of the bandgap structure in the vicinity of the Bragg condition for both LCP and RCP modes. The frequency as a function of the real part of the propagation constant (left) indicates three bandgaps. A similar plot involving the imaginary part of the propagation constant (right) indicates the strength of each characteristic coupling and confirms the bandgap width. Each circular eigenmode has its own resonant Bragg frequency with one bandgap in common. These results are useful in the design of finite length distributed feedback back devices [e.g., K. M. Flood and D. L. Jaggard, "Distributed Feedback Lasers in Chiral Media," *IEEE J. Quantum Electron.* 30, 339-345 (1994)].



ELECTROMAGNETIC FIELDS IN OPEN CHIROSTRIP STRUCTURES EXCITED
BY PRINTED DIPOLES

J.C. da S. LACAVA* and FELICIANO LUMINI**

* Division of Electronic Engineering, CTA-ITA, 12228-900, São José dos Campos, SP, Brazil (e.mail: lacava@ita.cta.br)

(Phone: 055 123412211 Ext.142) (Fax: 055 123417069)

** Division of System Engineering, EMBRAER S.A., 12227-901, São José dos Campos, SP, Brazil

INTRODUCTION: Chirostrip structures have become a topic of major interest in applied electromagnetism because of their potential applications in microwave printed circuits and integrated optics. Electromagnetic properties of rectangular microstrip antennas and printed dipoles on chiral substrates have recently been analyzed. Guided modes in chiral microstrip lines have also been discussed. However, there is not enough information about the characteristics of the guided electromagnetic fields when they are excited by printed antennas. The purpose of this work is to present the theoretical results of our investigation of the effects of chirality on the near field distributions excited by a short printed dipole and on the cross-polarization level (CPL) of radiated fields. The dispersion curves of surface wave modes are also analyzed.

THEORY: The calculation of electromagnetic fields excited by a short printed dipole is a problem that can be rigorously solved by means of the spectral domain analysis. As the calculation is carried out in the Fourier domain, we obtain the transformed Green's functions in compact and closed forms where only sine and cosine functions are present. This is a very convenient approach for the numerical calculation. The near fields in the space domain are obtained applying the inverse Fourier transform in the expressions of the transformed fields. This means that double integrals in the spectral variables k_x and k_y must be calculated. First of all, k_x and k_y are replaced by a set of new variables α and β such that $k_x = \beta \cos \alpha$ and $k_y = \beta \sin \alpha$. The integration in α is carried out analytically while in β , from 0 to $+\infty$, is evaluated numerically. The real part of the function to be integrated is different from zero only between 0 and k_0 and can be integrated straightforwardly. However, its imaginary part is not well behaved; it has one or more poles and a discontinuity in the first derivative at $\beta = k_0$. In addition, when $\beta \rightarrow +\infty$, the function's imaginary part has an oscillatory behavior and is divergent in the chiral/vacuum interface. Effects of the chiral admittance and antenna orientation on the near field patterns are then analyzed. On the other hand, the far electric field radiated by the printed dipole can be calculated using an asymptotic expression obtained by the application of the stationary phase method. A complete cross-polarization analysis is presented and considerable degradation of the CPL parameter is observed when chirality increases. Substrates with uniaxial anisotropy also show similar behavior. Enforcing the denominator of the transformed Green's function to be zero results in the eigenvalue equation for the chirostrip structure. Typical dispersion curves are presented. The results of this investigation confirm that all surface waves are hybrid waves and that bifurcated modes currently observed in other chirowaveguide structures are absent.

Chiral absorbers: effects of chirality or of inclusion shape?

S.A. Tretyakov¹, A.A. Sochava¹, C.R. Simovski²

¹St. Petersburg State Technical University, Radiophysics Department, 195251, St. Petersburg, Russia

²St. Petersburg Institute of Fine Mechanics and Optics, Physics Department, 197021, Sablinskaya 14, St. Petersburg, Russia

A novel concept of chiral absorbers was introduced in the eighties, and it was claimed that chirality of lossy composites can help to increase absorption and to reduce reflection. However, it has been recently shown that for the normal incidence of plane waves on chiral slabs, chirality of composites has little effect on reflection. This was demonstrated by Bohren et al. for dilute mixtures of small helices as compared to mixtures of nonchiral elements of otherwise same size. As to oblique incidence, more dense mixtures, and mixtures of more complex inclusions, the question seems to be still open.

The aim of this presentation is to clarify the influence of inclusion shape on reflection and absorption in chiral and nonchiral mixtures. We try to gain more understanding of why and when chirality of single inclusions produces little or strong effects on reflection, and what kind of influence can be expected. Unlike most of the previous work, we try to establish direct relations between the geometry of single inclusions and the reflective and absorptive properties of chiral composites.

The study is based on the analytical model for polarizabilities of conductive chiral particles, developed earlier by the present authors (in cooperation with F. Mariotte) and on the Maxwell Garnett model for bianisotropic composites.

There exists a relation between the components of the dyadic polarizabilities of chiral conductive particles, which is valid for small (compared to the wavelength) inclusions possessing certain symmetry properties. Provided that relation is satisfied, chirality of single particles (such as small helices) influences very little the permittivity and permeability of the averaged composite. The effect of this property is that the normal incidence reflection coefficient for chiral composite slab is nearly the same as from slabs of racemic mixtures of the same particles. This conforms to the earlier numerical results. For oblique incidence, however, effective averaged chirality affects absorption and reflection, and in the presentation we will give details which show this influence. The effect of chirality is usually quite small, and it is stronger in reflection from slabs in air as compared to metal-backed slabs.

Chirality enters the scene in mixtures of inclusions of more complex chiral shapes compared to the conventional helices. Chiral and racemic mixtures of such particles have different reflective properties also for the normal plane-wave excitation.

ELECTROMAGNETIC SCATTERING BY BI-UNIAXIAL STRATIFIED MEDIA

S. Shulga*, and O. Charkina

Chair of Theoretical Radiophysics, Kharkov State University,
Svobody Sq., 4, Kharkov 310077, Ukraine

The study of EM wave interaction with bi-anisotropic materials has now received considerable attention due to potential use of these materials in microwave circuit technology, optoelectronics, absorbing coating design etc. In most of these cases the spatial inhomogeneity and electromagnetic anisotropy of the material are also essential. In many areas of practical importance, the inhomogeneity can be approximated as occurring in only one direction, and the anisotropy takes the simplest form pertinent to uniaxial media. These assumptions lead to the basic model of a stratified bi-uniaxial medium.

The EM wave interaction with a stratified bi-uniaxial medium can be studied by approximately dividing the inhomogeneous region into thin homogeneous layers and subsequent use of the well known analytic technique referring to homogeneous regions. However, such approach requires the numerical treatment of the exponentially growing factors in each artificial layer which depict non-uniform plane waves. Besides, it may be unacceptably computationally intensive for certain profiles and sufficiently thick slabs. In view of these complexities a direct numerical solution of the respective EM problem may appear advantageous.

This contribution aims to describe an efficient computer-aided solution and the results of corresponding numerical experiments referring to a plane wave diffraction from an arbitrarily stratified bi-uniaxial non-reciprocal slab whose optic axis is parallel to the direction of stratification. Our methodology is an application of the finite difference scheme to a coupled system of second-order ordinary differential equations for two scalar potentials which determine the EM field within the slab. The equations are derived via proper generalization of the scalarization approach. The discontinuity of medium within the slab is incorporated into the FD equations via the "transition inhomogeneous layer" method. Special emphasis of the report is devoted to various means of validating the performance of the computer program, as well as the analysis of sample results obtained.

Antennas and EM Field Metrology

Page

B. Cown and Z. Hussein

- 1:20 Microwave Imaging and Holographic Diagnostic to Antennas in 56
 ylindrical Near-Field Measurement
 Ziad A. Hussein, Jet Propulsion Laboratory
- 1:40 Hybrid Near-Field Measurement/Analysis Technique for 57
 Predicting Installed Antenna Performance and Coupling
 *B. J. Cown, Satimo, Inc., J. Ch. Bolomey, D. Picard, SUPELEC,
 J. P. Estrada, Georgia Tech.*
- 2:00 A New Method for Phase Antenna Pattern Reconstruction from 58
 Amplitude Measurements Only
 Pavel Yu. Kostenko, Alexandr A. Adamenko, Yuri V. Bulka,
 Kharkov Aviation Institute*
- 2:20 EMF Near Passive Secondary Radiators 59
 Hubert Trzaska, Technical University of Wroclaw
- 2:40 A Method to Evaluate the Effectiveness Outside a 60
 Building of Electromagnetic Noise Countermeasures
 Yuji Maeda, Yoshiyuki Komatsu, Kazuo Murakawa, Hiroshi Yamane,
 NTT Telecommunication Networks Laboratories*
- 3:00 BREAK
- 3:20 On Modeling the Quantum Microscale Electromagnetic Probe 61
 Leon A. Steinert, Physical Synergetics Institute
- 3:40 Operative Testing of Antenna-Surface Thermic Distortions 62
 V. Khaikin, The Special Astrophysical Observatory
- 4:00 A Study of Reflecting Surface of Single RATAN-600 Panels 63
 V. Khaikin, The Special Astrophysical Observatory

MICROWAVE IMAGING AND HOLOGRAPHIC DIAGNOSTIC TO ANTENNAS IN CYLINDRICAL NEAR-FIELD MEASUREMENT¹

Ziad A. Hussein
Jet Propulsion Laboratory
California Institute of Technology
Pasadena, CA 91109

Abstract

In this paper, the issues pertaining to microwave imaging and holographic diagnostic to antennas in cylindrical near-field measurements are addressed. The theoretical approach is based on expanding the work in [1] and [2] where a cylindrical wave expansion of the field on a cylindrical near-field surface is given. The sampling probe is modeled by its equivalent aperture current (idealized circular aperture) and incorporated into the near-field to far-field transformation. The method of steepest descent is applied to obtain the far-field. In its implementation, however, one could specify directly the angular spectrum at which the far-field is desired to be calculated without resorting to interpolation. The microwave imaging and holographic diagnostic is based on back projection where a plane wave expansion of the far-field is obtained. This approach necessitates the knowledge of the far-field at exact angular spectrum resulting from application of 2-D FFT. Hence, we were able to construct simply the near-field on a plane not necessarily on the aperture plane of the test antenna but also on planes perpendicular to the aperture plane [3]. And a 3-D high resolution and high precision antenna imaging of the test antenna is obtained from cylindrical near-field simulated measurements. In addition microwave holographic diagnostic of large NASA scatterometer radar antenna obtained from measured near-field on a cylindrical surface will be given if time permits.

- [1] Z.A. Hussein, "Efficient And Fast Reconstruction Of The Far-Field From Measured Near-Field On A Cylindrical Near-Field Surface" *JPL D-9124, November 8, 1991.*
- [2] Z.A. Hussein and Y. Rahmat-Samii, "Probe Compensation Characterization In Cylindrical Near-Field Scanning" *1993 IEEE Digest AP-S International Symposium, Ann Arbor, Michigan, June 28, 1993.*
- [3] Z.A. Hussein "Microwave Imaging And Holographic Diagnostic To Antennas In Cylindrical Near-Field Measurement" *JPL Interoffice Memorandum 3361-94-108, June 8, 1994.*

¹The research work described in this paper was carried out by the Jet Propulsion Laboratory, California Institute of Technology, under contract with the National Aeronautics and Space Administration.

HYBRID NEAR-FIELD MEASUREMENT/ANALYSIS TECHNIQUE FOR PREDICTING INSTALLED ANTENNA PERFORMANCE AND COUPLING

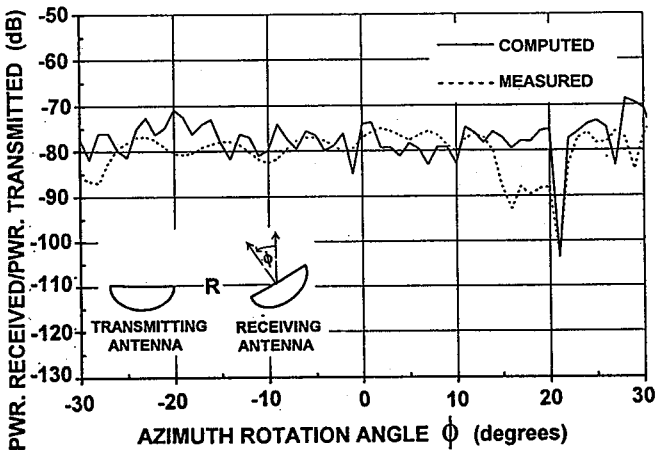
*B. J. Cown
 SATIMO, Inc.
 1318 Chandler Court
 Acworth, GA 30102

J. Ch. Bolomey
 SUPELEC
 Gif-Sur-Yvette
 France

D. Picard
 SUPELEC
 Gif-Sur-Yvette
 France

J. P. Estrada
 ATDD/SEAL/GTRI
 Georgia Tech
 Atlanta, GA 30332

This paper describes a hybrid measurement/analysis technique for predicting the antenna patterns and antenna-to-antenna coupling for antennas installed in their actual operating environments-- at earth-based field sites, on ship topsides, on space-borne platforms, etc. The *installed* antenna patterns can differ significantly from the "clear-site" antenna patterns, due to electromagnetic scattering from nearby scattering structures. Non-negligible amounts of electromagnetic coupling can occur between two or more co-sited antennas. However, the near-field antenna coupling coefficients and the installed antenna patterns can be predicted by using the measured or computed complex clear-site pattern data in specialized scattering and coupling computer codes based on the Spherical Angular Function (SAF) analysis technique (Cown and Estrada, "SAF Analysis of Shipboard Antenna Performance,....", Proc. of 1995 IEEE AP/URSI Symp., Newport Beach, CA.). Measured complex clear-site patterns can be obtained most efficiently via rapid near-field measurements based on the Modulated Scattering Technique (MST) (Bolomey, Cown, et. al., "Rapid NF Antenna Testing.....", IEEE Trans. AP-S, vol. 6, June 1988), or they can be obtained by classical near-field measurements or direct far-field measurements. Results of this hybrid approach for predicting the coupling coefficient between 3.6-foot diameter parabolic antennas are compared with measured data in the accompanying figure, for R=9.83 feet. Additional validations and simulations will be presented at the meeting.



A Method to Evaluate the Effectiveness Outside a Building of Electromagnetic Noise Countermeasures

Yuji Maeda*, Yoshiyuki Komatsu, Kazuo Murakawa, and Hiroshi Yamane
NTT Telecommunication Networks Laboratories
3-9-11 Midori-Cho, Musashino-Shi, Tokyo 180, Japan

Countermeasures against electromagnetic noise radiated from electrical equipment are usually implemented in a laboratory in an anechoic chamber or a shielded room. Methods to measure and evaluate electromagnetic noise in such a laboratory are specified by CISPR, FCC, VCCI, and so on. However, there are many cases where these countermeasures are implemented at the equipment installed in a building, but no method for evaluating countermeasure effectiveness has been clearly specified. Therefore, the evaluation of their effectiveness is highly subjective.

There are some applications in which countermeasures implemented inside a building need to have their effectiveness measured outside the building. This paper describes how we can do this. We used an electromagnetic shielding screen, which was partly installed in a building, as a noise countermeasure, and measured and calculated the shielding effectiveness of this screen at locations around the building. In the calculations, the building structure was modeled by a wire-grid representing the structural steel of the building and the shielding screen was modeled by a plane surface. Each wire element was divided into dipole segments and each plane surface into rectangular dipole segments. We evaluated the current distributions on all dipole segments and all rectangular dipole segments by Galerkin's method, which applies piecewise sinusoidal expansion functions.

The maximum deviation between calculated and measured data was about 5 dB, which shows the validity of this modeling technique and calculation. We calculated the shielding effectiveness over a wide area around the building shown in Fig. 1 and determined the characteristics of shielding effectiveness: shielding effectiveness is distributed sinusoidally about circles concentric with the center of the building, the interval between maximum and minimum effectiveness depends on the noise frequency and building size, and the radial distribution of shielding effectiveness does not change with distance from the building. We conclude that the effectiveness of countermeasures against electromagnetic noise should be measured on a line, whose length depends on the noise frequency and building size, on a concentric circle centered at the center of the building, as shown in Fig. 2. We should evaluate the maximum and minimum values of countermeasure effectiveness on this line.

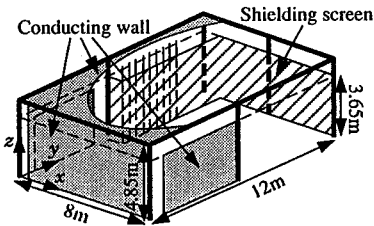


Fig. 1 Building structure.

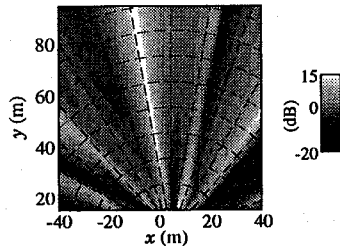


Fig. 2 Distribution of shielding effectiveness at 90 MHz and concentric circles centered at center of building.

On Modeling the Quantum Microscale Electromagnetic Probe

Leon A. Steinert
Physical Synergetics Institute
Riverside, California

This commentary addresses some theoretical factors underlying the real world performance attributes of quantum microscale technologies and sensor configurations. Emphasis is given particularly to the concept of quantum sensory phenomena, as epitomized in the context of some inherently nonlinear material properties of quantum-structured microsystems. One of the more immediate concerns is determining the internal electromagnetic sensitivities of quantum-scale sensor microsystems to low intensity electromagnetic field environments of external origin.

The electromagnetic phenomenological attributes of primary concern here are epitomized by a set of partial differential equations formulated within the mathematical framework of electromagnetic field theory with polarization sources. Appearing basically in the Helmholtz Equation motif, these formal relationships may be expressed also as antenna equations, by invoking the usual procedure for such functional transformations. In the present context, our interest relates primarily to the issues of characterizing the charge density profiles internal to the complex material microstructures, as well as the methodological problem of describing the quantum radiophysical attributes of the constitutive atomic structures underlying material physical configuration. Accordingly, the remainder of discussion here pertains to matters such as meaningful definition and derivation of spatio-temporally configured quantum probability distributions.

It is necessary at first to clarify just where the probabilistic nature of quantum-structured media enters into the picture, conceptually. The source functions which describe the material polarization and radiation effects are excerpted in the present context from the charge and current probability density functions appropriate to the material structure of interest. In their turn these probability density functions are characterized in terms of the quantum density of states operator, which contains embeddings of the mathematical forms inherent to the probability distributions. Extraction of this information for the purposes of mathematical modeling is discussed.

Operative Testing of Antenna Surface Thermic Distortions

V.Khaikin

The Special Astrophysical Observatory, N.Arkhыз, 357147,
Karachai-Cherkessia, Russia, e-mail: vkh@sao.stavropol.su

It is well known that the problem of reflector surface thermic distortions becomes urgent for large reflectors at MM wavelengths. The holographic equipment and technique developed at RATAN-600 radio telescope (V.Khaikin, Proceedings of IAU Colloquium 140 in Hakone, Japan, 1992) enables us to control phase-amplitude aperture distribution and its distortions in quasi-real time. This gives us a possibility to study the character of surface thermic distortions or remove them if it is necessary to form a precise antenna surface for short wavelength observations.

In the report the results are given of the testing of RATAN-600 surface thermic distortions during several 2-3 day cycles in conditions of various temperature overfalls in daytime and at night. Measurements were made from both Secondary and Primary radio telescope foci to separate thermic distortions of the Main and the Secondary mirror. Typical deviations of aperture phase at 1.35 cm are within $\pm(5-9 \text{ grad})$ at night and $\pm(8-17 \text{ grad})$ at daytime which corresponds to joint surface deformations $\pm(0.20-0.35 \text{ mm})$ and $\pm(0.30-0.65 \text{ mm})$. After antenna correction under computer control r.m.s. surface error falls from 0.60 mm to 0.10 - 0.15 mm. We estimate the accuracy of the method itself to be 20-30 μm .

The main reason for the visible large scale distortions of aperture field is deformations of the Secondary mirror and for small scale distortions it is deformations of reflecting surface of single elements. Distortions at several neighboring elements are usually correlated. The value of the surface thermic deformations and rate of their appearance are greatly influenced by overfalls of surrounding temperature and uneven heating by the Sun of the Main and Secondary mirrors.

A Study of Reflecting Surface of Single RATAN-600 Panels

V.Khaikin

The Special Astrophysical Observatory, Karachai-Cherkessia,
N.Arkhiz, 357147, Russia; e-mail:vkx@sao.stavropol.su

The holographic equipment and technique for measurements of integral surface profile and topography of RATAN-600 elements at 1.35 cm wavelength with accuracy of 100 mcm are described in (V.Khaikin, in Proceedings of 140 IAU Symposium in Hakone, Japan, 1992). This paper presents the results of the measurements and analysis of surface quality of single RATAN-600 elements.

Preliminary measurements have shown that RATAN-600 Secondary mirror situated in the near region of an element spoils the quality of reconstructed surface image. This requires substitution of Fresnel or more complicated transforms for Fourier transform in a process of holographic reconstruction. Besides Secondary mirror introduces its own errors and decreases the measurement accuracy as it is subject to thermic distortions. To eliminate the influence of Secondary mirror a special horn was applied to illuminate elements of Main mirror from Primary focus.

Using geodesic means (Yu. Zverev, S. Golosova, *Communications of SAO*, 63, 1989) and holography we inspected the state of single elements of Main mirror after 10 years of exploitation and found serious degradation of their reflecting surfaces. The reason of irreversible surface distortions induced by permanent thermic surface deformations was removed by hard fixing of adjusting screws at the reflecting surface of the single panel.

At present, the work has been started to readjust the reflecting surface of all the 1000 RATAN-600 single panels in the working position with the accuracy of 0.15-0.17 mm and to stabilize the obtained panel surface at this level.

THIS PAGE INTENTIONALLY LEFT BLANK.

Antennas II

S. R. Rengarajan and S. S. Stuchly

Page

- 1:20 The Dielectric Wedge Antenna Fed by a Slab Waveguide Using 66
Local Mode Theory and Equivalent Current Distributions: TE-Case
Felix Schwering, U. S. Army CECOM, Gerald M. Whitman,
Wan-Yu Chen, New Jersey Institute of Technology*
- 1:40 Modeling Antenna Performance with an Efficient Hybrid Finite 67
Element - Integral Equation - Waveguide Mode Matching Technique
Cinzia Zuffada, Tom Cwik, Vahraz Jamnejad, Jet Propulsion Laboratory*
- 2:00 Mutual Coupling Between Waveguide-Fed Transverse Slots 68
Radiating Between Baffles
Sembiam R. Rengarajan, California State University, Northridge
- 2:20 Millimeter-Wave Dielectric Resonator Antenna Array 69
M. G. Keller, M. B. Oliver, Y. M. M. Antar, Royal Military College
of Canada, D. Roscoe, R. K. Mongia, A. Ittipiboon, Communications
Research Centre*
- 2:40 Analysis of Equiangular Spiral Antennas 70
Stuart M. Wentworth, Sadasiva M. Rao, Auburn University*
- 3:00 BREAK
- 3:20 Equivalent Circuit of Long Dipole Antenna 71
M. Hamid, University of South Alabama
- 3:40 Impedance Bandwidth of Bent Wire Antennas 72
M. Ali, S. S. Stuchly, K Caputa, University of Victoria*
- 4:00 Active Antenna Phase Control using Subharmonic Locking 73
P. S. Hall, A. Zarroug, M. Cryan, The University of Birmingham
- 4:20 Below-Resonant Length Slot Radiators For Travelling Wave Array 74
Antennas
Klaus Solbach, Daimler-Benz Aerospace
- 4:40 Study of VLF Antennas Immersed into Seawater: Moment 75
Method Computations and Development of an Equivalent
Physical Model
ahia Benhabiles, Michel Pellet, DCN/CTSN/TIRN, Albert Papiernik,
Christian Pichot, Universite de Nice-Sophia Antipolis, Philippe Lacour,
TEUCHOS PACA*
- 5:00 Fast Data Weighting Algorithms for Equidistant Array 76
Digital Signal Processing
I. P. Anukhin, V. V. Lukin, Kharkov Aviation Institute*

ABSTRACT

THE DIELECTRIC WEDGE ANTENNA FED BY A SLAB WAVEGUIDE USING LOCAL MODE THEORY AND EQUIVALENT CURRENT DISTRIBUTIONS: TE-CASE

Felix Schwering, U.S. Army CECOM; Gerald M. Whitman, * Wan-Yu Chen, Anthony Triolo, N.J. Institute of Technology

The development of lowloss silicon and the availability of solid state energy sources has spurred interest in tapered dielectric radiators for use in millimeter and integrated optical devices. The structure studied here is the dielectric slab waveguide feeding the dielectric wedge antenna. Only recently has this integrated structure been accurately analyzed. The field solution was obtained for a dielectric slab feeding a wedge of the same material that is excited by the fundamental even TE mode of the slab. This was accomplished by modeling the tapered region by the well-known staircase approximation and using the step-transition method introduced by Marcuse, who applied it to step-tapered transitions between waveguides of different but uniform cross-sections. By making the steps of the staircase sufficiently small, the field of the dielectric wedge was obtained. For various slab/wedge geometries, the results verified that radiation patterns of directive gain monotonically decrease from a maximum in the endfire direction and in the forward region of interest shows no sidelobes. This method, however, is computationally quite intensive. To obtain quick design parameters for tapered dielectric radiators, an alternative and much simpler approach was developed and applied to the integrated dielectric slab-wedge configuration. It uses a local mode theory in conjunction with equivalent surface and volume current distributions. The waveguide section is assumed to support the lowest order even TE mode of the dielectric slab waveguide. The incident surface wave field is terminated by equivalent surface electric and magnetic current distributions in the interface plane separating the slab from the wedge. The far field is then found from the negative of these current distributions together with an electric volume current distribution. The later current distribution corresponds to the polarization current of the dielectric wedge. The directive gain is calculated and results are compared to data obtained from the more rigorous step-transition approach.

MODELING ANTENNA PERFORMANCE WITH AN EFFICIENT HYBRID FINITE ELEMENT - INTEGRAL EQUATION - WAVEGUIDE MODE MATCHING TECHNIQUE

Cinzia Zuffada*, Tom Cwik and Vahraz Jamnejad

*Jet Propulsion Laboratory
California Institute of Technology
Pasadena, CA 91109*

ABSTRACT

The finite element technique is very appealing for its ability to accurately model the physical features of an object to a scale much smaller than the wavelength of interest, particularly when one is concerned with the evaluation of near - zone fields or field related quantities inside a penetrable object, as is the case in antenna design and analysis.

To limit the computational domain in the case of open structures, an integral equation is set - up on a mathematical surface of revolution enveloping the true scatterer/radiator, thus enforcing an exact boundary condition. The surface of revolution needs not be in the far - field, thus reducing the problem size compared to alternative truncation methods employing absorbing boundary conditions. Moreover, the choice of a surface of revolution allows for a very efficient representation of the surface integral equation unknowns and resulting matrices.

To incorporate the treatment of radiation it is necessary to describe the source consistently with the finite element modeling technique. We propose here an approach which applies to antennas fed by waveguides or coaxial cables, but which are otherwise of general shape and material composition. In many practical cases an interface can be located which optimally separates the radiating structure from the feed. Such an interface is employed here as an additional surface which bounds the computational domain, thus allowing us to model only the antenna per se. At the interface, and looking toward the source, the representation of the EM fields is conveniently done via a waveguide mode decomposition, accounting for propagating and evanescent modes arising in the presence of geometric discontinuities at or near the interface. On the other hand, looking into the radiating structure, the finite element model completely describes the unknown field. By matching the two representations a constraint on the unknown field is found which allows for the correct truncation of the computational domain, without introducing additional unknowns, once the dominant waveguide mode is specified.

The formulation of this technique makes use of an integral form of the wave equation in the volume of computation, written for either the magnetic or the electric field, and of a combined electric field - magnetic field integral equation on the bounding surface of revolution, written for both electric and magnetic surface currents. A third equation is obtained by explicitly enforcing continuity of the tangential component of the unknown field at the surface of revolution, as expressed by the two representations. In the wave equation, matching of the waveguide modal representation to the finite element representation at the antenna interface is accomplished via a proper surface integral term, involving only the unknowns representing the tangential field at this surface.

First order, vector edge - elements are used in our finite element representation, and the unknowns are the field components along each edge of the tetrahedral elements meshing the computational domain. On the surface of revolution an additional set of surface currents unknowns is introduced for the integral equation; the surface currents are represented as linearly varying along the generator and having a Fourier series azimuthal variation. The problem of the radiation from an open - ended waveguide is presented here as an example, to validate the approach and to illustrate how to efficiently handle unbounded radiators. The issues of optimal mesh choice and related accuracy will be discussed.

Mutual Coupling Between Waveguide-Fed Transverse Slots Radiating Between Baffles

Sembiam R. Rengarajan

Department of Electrical and Computer Engineering
California State University
Northridge, CA 91330-8346

Transverse slots cut in the broad wall of a rectangular waveguide have found applications in array antennas requiring dual polarizations. In order to avoid grating lobes arising from one guide wavelength spaced slots in such a structure, it has been suggested that the slots radiate in a baffle region (Josefsson, *IEEE Trans. Antennas Propagat.*, 41, pp. 845-850, 1993). The impedance characteristics of isolated transverse slots radiating in an infinitely long parallel plate region have been obtained by Josefsson. We present mutual coupling computations between transverse slots radiating in an infinitely long parallel plate guide as well as finite length parallel plate region opening into a half space bounded by an infinite ground plane.

The method of analysis for the infinite parallel plate problem uses the parallel plate Green's functions in spectral domain. The required expressions are obtained for a number of discrete values of the longitudinal wavenumber k_z . These computed values are utilized during the inverse transform process to obtain the spatial domain values for the mutual impedance for a range of values of slot spacing in the longitudinal direction.

The analysis for the finite length parallel plate waveguide opening into a half space bounded by an infinite ground plane requires a solution to the aperture magnetic current in the ground plane. This has been accomplished for each k_z value by solving an integral equation by the method of moments by a manner similar to the analysis of self-admittance of a longitudinal slot in such a structure (Keyvan et al., *IEEE Trans Antennas Propagat.*, vol. 41, pp. 422-428, April 1993).

Numerical considerations on discretizing the k_z space, truncation and end-point evaluation, singularities, and interpolation techniques employed in this work will be discussed at the meeting. Results will be presented for a range of values of physical parameters.

Millimeter-Wave Dielectric Resonator Antenna Array

**+M.G. Keller*, +M.B. Oliver, ++D. Roscoe,
++R.K. Mongia, +Y.M.M. Antar, ++A. Ittipiboon**

+Royal Military College of Canada
Kingston, Ontario K7K 5L0, Canada

++Communications Research Centre
P.O. Box 11490, Station H, Ottawa, Ontario K2H 8S2 Canada

In the last several years the concept of using dielectric resonators as antennas has gained much popularity. The dielectric resonator antenna (DRA) has many attractive characteristics such as large bandwidth, high radiation efficiency, small physical size, and simple coupling schemes. Numerous papers have been published on dielectric resonators that operate at frequencies less than 20 GHz. For these antennas, topics such as: feed configurations; dielectric resonator shapes, and polarization states have been reported (R.K. Mongia & P. Bhartia, *International Journal of Microwave and Millimeter-Wave Computer-Aided Engineering*, Vol. 4. No. 3, pp. 230-247, 1994) In the millimeter-wave frequencies, only an array of non-resonant dielectric radiators excited by a dielectric guide has been reported (M.T. Birand & R.V. Gelsthorpe, *Elect. Lett.*, Vol. 17, Sept. 1981, pp. 633-635). To date, the concept of a millimeter-wave DRA has not been explored.

This paper investigates the feasibility of utilizing DRAs in the millimeter-wave frequency band. A rectangular resonator was placed on a metallic ground plane and an aperture-fed configuration was used to couple to a transmission line on a substrate below. This configuration utilizes the well documented electrical advantages of an aperture-coupling feed mechanism. The dimensions of the rectangular dielectric for millimeter-wave resonance were determined using the dielectric waveguide model as applied by Mongia (R.K. Mongia et. al., Conf. Proc. IEEE APS Int. Symp. 1994, pp 764-767). This configuration shows that the low microwave frequency designs are easily scaled to operate in the millimeter-wave region, and that fabrication and alignment tolerances are not nearly as critical as they are for millimeter-wave microstrip patch antenna design.

The results of a single element and four element H-plane array of aperture-coupled DRAs are presented. This paper shows that the use of dielectric resonators as antennas can be extended into the millimeter-wave spectrum.

ANALYSIS OF EQUIANGULAR SPIRAL ANTENNAS

Stuart M. Wentworth* and Sadasiva M. Rao
 Department of Electrical Engineering
 200 Broun Hall, Auburn University, AL 36849-5201

Equiangular spiral antennas are analyzed with the well known method of moments in conjunction with triangular patch modeling (see Fig. 1a). In particular, the analysis focuses on the validity of several generic guidelines hitherto available for designing such antennas. In our study, numerical results indicate that increasing the number of spiral arm turns broadens the radiation pattern (i.e. the axial ratio increases), but that tapering the outermost portion of the arms has little effect. Beam patterns are smoothest for spirals of 1.25 to 1.5 turns (see Fig. 1b). We also show that the useful frequency range of the spiral antenna depends not only on the spiral arm length and the inner radius near the spiral center, but also on the wrap tightness. While the more tightly wrapped spirals exhibited the highest boresight gain and the broadest radiation pattern, the axial ratio is minimized for spirals with tightness parameters ranging from $a = 0.2 - 0.3$.

One surprising aspect of this study is the impedance variation with respect to the various parameters of the spiral antenna. Until now, it was generally believed that these spiral antennas, being self-complementary, have an impedance of 188Ω . However, in our study the impedance varied from about 300Ω down to 220Ω . Further experimental and theoretical studies may be needed to resolve this problem. One possible area of study may be to develop a better model for the feed element to simulate the experimentally observed case.

We also found that placing a finite-sized conducting plane beneath the spiral results in a narrower radiation pattern, a reduced axial ratio, and an increased gain. Performance is analyzed with a conducting plane one-quarter and one-eighth wavelength below the spiral antenna.

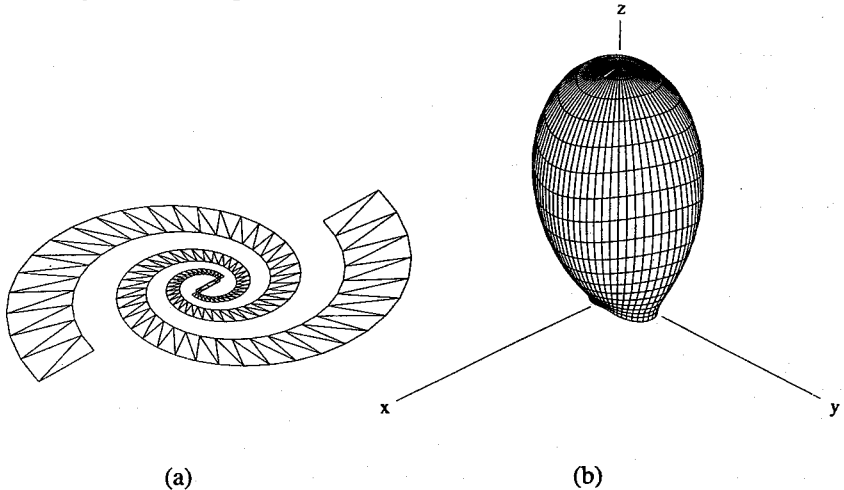


Figure 1: (a) Spiral antenna modeled using triangular patches, and (b) a typical 3-dimensional beam pattern.

EQUIVALENT CIRCUIT OF LONG DIPOLE ANTENNA

M. Hamid

Department of Electrical Engineering
University of South Alabama
Mobile, Alabama 36688

The input impedance Z_{in} (or $R_{in} + jX_{in}$) of a center-fed dipole is an important function of the frequency f (or radian frequency ω) or overall electrical length $2h/\lambda$ in wavelengths since it determines the efficiency of the antenna and facilitates the design of matching networks to the feedline. In a recent paper presented at the 1994 URSI Radio Science Meeting in June 1994, the author surveyed previous attempts to synthesize Z_{in} with two, three and four element equivalent circuits and presented a procedure to determine the components of a four-element equivalent circuit up to $2h/\lambda \approx 1$. The element values were optimized with the aid of standard computer software packages such as MICROCAP and MATHCAD.

The purpose of this paper is to describe the extension of the procedure to $2h/\lambda \approx 2$ and beyond and to compare Z_{in} vs f of the resulting equivalent circuit with published analytical and experimental data. The procedure employs three impedances (Z_0 , Z_1 and Z_2) in series. Z_0 is simply a capacitor to provide the high reactance at low frequencies and is determined from the condition $X_0 = -j/\omega C_0 = X_{in}(\omega = \omega_0)$, where ω_0 is conveniently selected to correspond to the range $0 < 2h/\lambda < 0.25$. Z_1 (or $R_1 + jX_1$) is a two-port parallel R_1, L_1, C_1 circuit, while Z_2 (or $R_2 + jX_2$) is similar except with parallel R_2, L_2, C_2 elements. In order to determine these six unknown values, it is postulated that the first two frequencies at which $X_{in} = 0$ are denoted by ω_{s1} and ω_{p1} (corresponding to $2h/\lambda \approx 0.5$ and 1 , respectively) and are the same frequencies at which $X_1 = 0$. Similarly it is postulated that ω_{s2} and ω_{p2} (corresponding to $2h/\lambda \approx 1.5$ and 2 , respectively) are also at which both X_{in} and X_2 vanish. On this basis the values of R_1 and R_2 are set equal to R_{in} at ω_{p1} and ω_{p2} , respectively. Furthermore, two relations to determine L_1 and C_1 are obtained by setting $X_1 = 0$ at ω_{s1} and ω_{p1} , while two similar relations to determine L_2 and C_2 are obtained by setting $X_2 = 0$ at ω_{s2} and ω_{p2} . Once these equations are solved simultaneously, Z_{in} vs f is plotted for the equivalent circuit using MATHCAD and minor adjustments are made to ensure a best fit with the original graph particularly at the two lower 3 dB points at which $R_{in} = X_{in}$. Examples are presented with and without these modifications to illustrate the accuracy and simplicity of the proposed method relative to previous results.

Impedance Bandwidth of Bent Wire Antennas

M. Ali, S. S. Stuchly* & K. Caputa,

Dept. of Electrical & Computer Eng.
University of Victoria, P.O.Box 3055, Victoria, BC, Canada.
V8W 3P6

Abstract

Wire antennas need not to be straight dipoles or monopoles. They can be bent. The main reason to deform a straight dipole or monopole is to shorten its resonant length. An important parameter of bent antennas is the *shortening ratio* (SR) which can be determined from the resonant lengths of the bent and the straight antennas. It has been reported by Nakano *et al.* and Rashed *et al* that whenever an antenna is bent, its resonant resistance (R_{res}) decreases, and if the antenna parameters are adjusted to achieve larger SR, its R_{res} decreases still further.

In this paper an attempt has been made to correlate the variation of *bandwidth's* (BW's) of bent antennas that occurs due to the change in their R_{res} 's, with the design variables. For this purpose, the sinusoidal and the meander configurations were selected and the BW's and the SR's of a number of such antennas were investigated experimentally. The design parameters of the sinusoidal antenna are its period P and amplitude A and that of the meander is its segment length e.

The SR, and the BW of the sinusoidal antennas, are listed in Table 1 as a function of P/A. From Table 1 it is clear that to achieve large SR, P/A has also to be large. But with increasing P/A, the BW narrows. Similarly, it is clear from Table 2 that with an increase in e, the SR increases and the BW narrows. In conclusion it can be said that, for both antennas, the SR is limited if certain BW is to be maintained.

Table 1: Wire sinusoidal antenna characteristics. Wire diameter=0.65 mm.

P/A	3.45	3.25	3.17	2.7	2.5	2.38	2.17	1.9	1.67	1.65
%BW	9.3	8.99	8.07	5.3	3.0	0.34	--	--	--	--
%SR	18.2	20.0	20.0	24.7	28.2	30.0	31.7	36.4	38.8	44.7

Table 2: Wire meander antenna characteristics. Wire diameter=0.65 mm.

e, cm	1.0	1.3	1.55	1.7	1.95	2.6
%BW	4.71	2.24	--	--	--	--
%SR	24.7	27.6	30	30	36.4	37.6

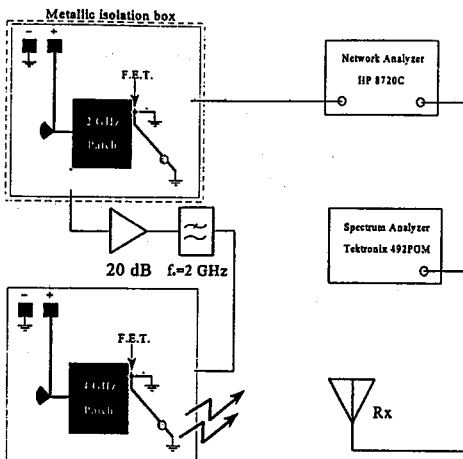
ACTIVE ANTENNA PHASE CONTROL USING SUBHARMONIC LOCKING

*Hall P S, Zarroug A, and Cryan M
The University of Birmingham, UK.

Radiated phase control in locked oscillator active array antennas is currently of interest as it can be used to provide the beam scanning necessary for many of the likely applications of the technology such as vehicular radar, personnel sensors and adaptive communications. We have previously shown that, in principle, a phase control range of 360° can be achieved with a microstrip patch element incorporating a pair of anti-phased oscillators, only one of which is used at any one time. The pair effectively double the 180° phase shift obtainable using fixed frequency locking and control of the oscillator free running frequency. However in practice much less than 360° is achieved due to mutual coupling between elements in the array and instabilities in the oscillator causing loss of lock at the locking band edges.

We are currently investigating the use of subharmonic locking to extend the phase range without the need to switch between a pair of oscillators. The figure shows a radiating patch locked by a oscillator operating at half the frequency which is itself externally locked. To date we have obtained over 360° phase shift by control of the bias of the two oscillators. One particular problem with this configuration is the need to prevent the harmonic of the first oscillator coupling directly to the second. Effective screening of the first oscillator and the use of a low pass filter is necessary.

We have demonstrated the promise of the subharmonic locking method for scanned active arrays. There are nevertheless some difficulties associated with a planar implementation and these will be discussed together with a description of measured results.

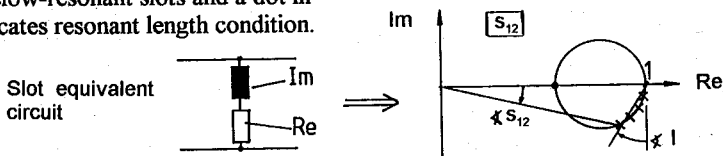


BELOW-RESONANT LENGTH SLOT RADIATORS FOR TRAVELING WAVE ARRAY ANTENNAS

Klaus Solbach
Daimler-Benz Aerospace, Sensorsystems, VS4FE4
89077 Ulm, Germany

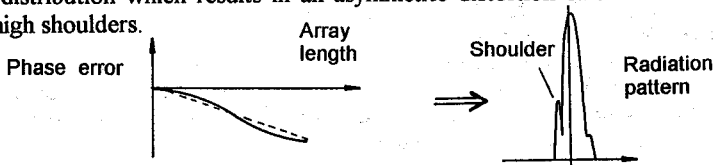
Conventional traveling wave slot array antennas employ resonant slots as radiating elements. Amplitude taper is provided by variation of slot offset (broad wall slots) or slot tilt (narrow wall slots), while phase is adjusted by correcting slot length for resonant condition. During the development of a frequency scanning waveguide antenna it became necessary to employ waveguide dimensions which did not allow full size slots to be implemented. Therefore, the characteristics of short, below-resonant slots as radiators were investigated and in due course were used successfully in several antenna designs using 40 to 180 slots in reduced size as well as full size waveguides at 10 GHz and 35 GHz.

The fundamental characteristics of narrow wall below-resonant slots were investigated by measurement of the scattering parameters of test sample slots in X-band waveguide, including conducting walls and a parallel plate section/horn transition on the radiating face to model the mutual coupling and radiation impedance conditions. It is found that the slots can be represented as complex shunt impedances with the capacitive reactive part increasing as the slot length is reduced to zero. The transmission coefficient s_{12} as a function of slot length thus maps onto a circle as shown in the drawing; crosses represent typical below-resonant slots and a dot indicates resonant length condition.



To allow the design of antenna arrays, the power loss per slot is calculated. In the special case of $\lambda/4$ -matched pairs of slots this is calculated from the transmission coefficient by $C \approx 1 - |s_{12}|^2$, which leads to an approximately linear relation $C \approx -74\text{dB} - 5.7\text{dB} \bullet L/\text{mm}$, where L is the slot length in an X-band realization and numbers are valid for dielectrically loaded cross slot pairs.

Thus, prescribed amplitude taper, e.g. for low sidelobe arrays, can be realized by simply tapering the slot length. However, at the same time the slot transmission phase varies nonlinearly along the array length, aggregating an S-shaped phase error distribution which results in an asymmetric distortion of the main beam, with high shoulders.



This effect can be compensated for by appropriate spacing of the slots. Yet, several low sidelobe designs produced so far have shown extremely satisfactory far-off sidelobe behaviour, even without compensation. Similar behaviour was observed also in Dielectric Image Line antennas using nonresonant radiators.

STUDY OF VLF ANTENNAS IMMERSED INTO SEAWATER : MOMENT METHOD COMPUTATIONS AND DEVELOPMENT OF AN EQUIVALENT PHYSICAL MODEL

Bahia BENHABILES*, Michel PELLET
DCN / CTSN / TIRN, BP 28, 83 800 Toulon Naval, France

Albert PAPIERNIK, Christian PICHOT
Laboratoire d'Electronique & Laboratoire Informatique, Signaux, Systèmes de Sophia-Antipolis,
CNRS / Université de Nice-Sophia Antipolis, Bât 4, 250 rue Albert Einstein
06 560 Valbonne, France

Philippe LACOUR
TEUCHOS PACA, rue G. Simenon, Centre Europe-'Le Palatin', 83 400 Hyères, France

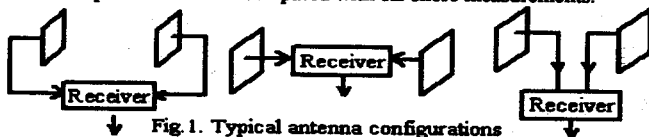
VLF E-field reception into seawater has been a problem of interest for many years. As it is well known, seawater is a lossy medium which causes a strong attenuation of the field, entails the presence of inhomogeneous plane waves and leads to a wavelength much smaller than in the air. Since the experimental measurements are difficult to conduct, the study of a receiving antenna immersed into the sea needs specific theoretical investigations. The antennas under investigation here are formed by a pair of metallic electrodes with wires connected to their centers (some examples are given in Fig. 1).

In the first part of the study, a computer model based on an EFIE with a method of moments (MoM) is used to investigate the scattering and radiation from an immersed antenna. Both the receiving case (an incident plane wave in the air) and the emitting case have been carried out. The conducting surface of each electrode is decomposed into triangular patches, and the induced surface current on the plate is expanded in triangular functions while other basis functions suitable for wire / surface junctions have been developed. The Galerkin method is applied for testing functions. The surface currents, the scattered field and the impedance are computed. This part of the study shows the important role played by the wires of the antenna.

In the second part, an equivalent circuit model of the antenna operating into seawater is developed, which focuses on two dominant antenna parameters : the impedance Z and the voltage V that can be measured through the wires. Z is calculated by the means of relevant approximations such as quasi-static and stationary wave solutions. V is computed with the MoM, using the circulation of the E-field along straight lines.

A comparison study has been made between computer simulations and the results using the equivalent model. These results show that the received voltage is only due to the presence of the wires while the electrodes, through the impedance, are related to the matching with the background medium (i.e. seawater).

Using this equivalent circuit model enables to investigate thoroughly the geometrical configurations of different antennas (shape and configuration of the electrodes, distance between the electrodes, wire position, ...), in order to optimize the intensity of the received signal. Calculations and computed results are compared with off-shore measurements.



FAST DATA WEIGHTING ALGORITHMS FOR EQUIDISTANT ARRAY DIGITAL SIGNAL PROCESSING

Anukhin I.P.* (Ph.D. Student), Lukin V.V. (Ph. Doctor)
Kharkov Aviation Institute, Dept. 507, Chkalova St., 17
310070, Kharkov, UKRAINE, Tel (0572) 442665,
Fax (0572) 441131

Time expenses required for data weighting performing in equidistant arrays with digital signal processing are often to be decreased. At the same time the directivity pattern of such array has to be characterized by low level of side lobes and narrow main lobe. Considered task can be solved by application of weighting functions (windows) for which sampled values are integer.

Corresponding approximation of well known weighting functions results in changing their response characteristics to worse, in the first order, to maximal side lobe level (MSLL) growth. That is why we investigated the other approach supposing from the very beginning that amplitude factors by which data samples must be multiplied can be only integer values, and the parameters of such windows were optimized using MSLL as the criterion and taking care over main lobe width.

Several families of such weighting functions are proposed. For the first one (called step-like) the amplitude factor can be only integer from 1 to N , maximal N is 6. For the second family the amplitude factors were supposed to be equal to n -th power of 2, n varies from 0 to $N-1$, N - the number of steps (Dirichlet window components); the step relative length was varied and optimized. At last the third family was obtained as the result of convolution of two identical or not identical step-like windows, these weighting functions can also be presented as an array of integer values but maximal values are usually greater than 6.

It was shown that MSLL of directivity pattern for arrays using proposed windows varied from -20.8 dB to -60 dB. Their response parameters were compared with corresponding characteristics of Dolph-Tchebishev's windows and patterns, in many cases the results were enough close. The approaches to data weighting procedure implementation in hardware (specialized digital devices and units) are discussed. Other applications of considered algorithms (in particular, in SAR or arrays operating in Fresnel zone) are presented.

Special Session

Higher Order Modeling in Computational Electromagnetics

<i>D. R. Wilton, A. F. Peterson and R. D. Graglia</i>		Page
1:20	Some Results on H(curl) Finite Elements <i>Jean-Claude Nedelec, CMAP Ecole Polytechnique</i>	78
1:40	Edge Elements, Nodal Elements and the Finite-element Modeling of Electromagnetic Fields <i>Gerrit Mur, Delft University of Technology</i>	79
2:00	Why Complete Continuity Constraints in Vector Basis Functions are Undesirable <i>A. F. Peterson, Georgia Institute of Technology, Donald R. Wilton*, University of Houston</i>	80
2:20	High-Order Finite Element Methods in Electromagnetic Field Computation <i>Zoltan Cendes, Carnegie Mellon University</i>	81
2:40	Application of Higher Order Vector Elements to the Coupled Finite Element-Combined Field Integral Equation (FE/CFIE) Technique <i>Vahraz Jamnejad*, Tom Cwik, Cinzia Zuffada, Jet Propulsion Laboratory</i>	82
3:00	BREAK	
3:20	Higher Order Edge Finite Elements in Electromagnetic Field Modelling <i>I. Bardi*, O. Biro, R. Dyczij-Edlinger, K. Preis and K. R. Richter, IGTE, Technical University of Graz</i>	83
3:40	Higher Order Divergence-Conforming and Curl-Conforming Bases on Curved Elements <i>R. D. Graglia*, Politecnico di Torino, A. F. Peterson, Georgia Institute of Technology, D. R. Wilton, University of Houston</i>	84
4:00	Higher-Order Discretization of Integral Equations with Singular Kernels <i>Stephen Wandzura, Hughes Research Lab.</i>	
4:20	Local Interpolatory Cardinal Spline (LICS) Method in Solving Linear and Nonlinear Schrodinger Equation <i>J. J. Chen, National Yunlin Polytechnic Institute, J. Zha, Valmet Automation Inc. M. Du, J. C. Goswami, A. K. Chan, C. K. Chui, Texas A&M University</i>	

Some Results on $H(\text{curl})$ Finite Elements

JEAN-CLAUDE NEDELEC
CMAP ECOLE POLYTECHNIQUE
91128 PALAISEAU CEDEX, FRANCE

We will present some results on low degrees $H(\text{curl})$ finite elements in R^3 for tetrahedrons cubes and prisms. We will indicate some links with finite difference schemes. We will also present some numerical results on some coupling of this technique with integral equations for electromagnetics problems.

Edge elements, nodal elements and the finite-element modeling of electromagnetic fields

Gerrit Mur

Laboratory of Electromagnetic Research, Faculty of Electrical Engineering,
Delft University of Technology, P.O. Box 5031, 2600GA Delft,
The Netherlands

When designing a finite element method for computing electromagnetic fields, it is necessary to decide what type(s) of finite element expansion will be used and what type of finite element formulation will be used. The combination of these two basic tools should be such that a) accurate and reliable results are obtained with a minimum of computational effort and that b) these results are free of spurious solutions.

The elements: Because of their supposed advantages edge elements have recently become a popular tool for modeling electromagnetic fields. Contrary to the expectations of many authors, however, edge elements *cannot* be used to enforce the divergence condition upon the solution (G.Mur, IEEE Trans. on Magn., vol. 30, pp. 3552 - 3557, 1994). The main reason for this is that edge elements allow surface charges at the interfaces between adjoining subdomains.

The formulation: The divergence condition, together with other properties of the electromagnetic field equations (that will together be referred to as the compatibility relations), can only be enforced by making them a part of the formulation of the problem (G.Mur, IEEE Trans. on Magn., vol. 30, pp. 2972 - 2975, 1994). Accurate finite element solutions are obtained by accurately modeling both the electromagnetic field equations and the appertaining electromagnetic compatibility relations.

In summary: Edge elements are very useful for modeling the conditions along interfaces between different media since they allow the normal component of the field strength to jump. An additional advantage of edge elements is that they can be used to relax the continuity requirements near singularities such as reentrant corners. Nodal elements, that enforce all components of the field strength to be continuous functions of the spatial variables, and that are more efficient than edge elements having the same degree of approximation, are preferred in homogeneous subdomains (G.Mur, IEEE Trans. on Magn., vol. 24, pp. 330 - 333, 1988).

We shall discuss the commonly used divergence-free "linear" edge elements, defined on tetrahedra, as well as the more accurate consistently linear edge elements and the consistently linear nodal elements. The relation between the choice of the type of finite element, the finite-element formulation that is used and the properties of the resulting finite-element method will be expounded.

Why Complete Continuity Constraints in Vector Basis Functions are Undesirable

A. F. PETERSON,[†] AND D. R. WILTON^{*}

[†] GEORGIA INSTITUTE OF TECHNOLOGY, ATLANTA, GA 30332-0250

^{*} UNIVERSITY OF HOUSTON, HOUSTON, TX 77204-4793

A long-standing problem in the calculation of cavity resonance and waveguide cutoff frequencies is the appearance of spurious modes, which often arise when the finite element method is used to solve the vector Helmholtz equation. For example, spurious modes appear when scalar Lagrange bases independently interpolate all the vector components on a finite element mesh. In contrast, the so-called edge elements, which have only continuous tangential components, appear to completely eliminate the spurious mode problem while retaining high accuracy. In this presentation we consider the properties required to extend simple, low order edge elements to higher order vector basis functions with similar desirable attributes.

The appearance of spurious modes has been variously attributed to the use of bases that cannot exactly model the null space of the curl operator (i.e., vectors of the form $\nabla\phi$), and to the existence of eigensolutions that do not satisfy the divergence condition, or more properly, Gauss' law. Our studies suggest that imposition of unneeded continuity constraints on normal field components is at the root of the problem and point out a connection between the two points of view. We present a simple example showing that imposition of normal continuity reduces the number of degrees of freedom needed to correctly model the $\omega = 0$ eigensolutions which are in the null space of the curl operator. Furthermore, for basis functions which do exactly model this null space, we find that Gauss' law in both point and boundary form is automatically satisfied in a weak sense. These results imply that normal field continuity conditions are natural conditions imposed by the Helmholtz equations, and should not be explicitly enforced. A dual argument similarly suggests that continuity of tangential components should not be enforced for surface currents appearing in electric field integral equations. Numerical results illustrating these points are presented, and the particular suitability of the higher order Nedelec bases is pointed out.

High-Order Finite Element Methods in Electromagnetic Field Computation

Zoltan Cendes

Department of Electrical and Computer Engineering
Carnegie Mellon University
Pittsburgh, PA 15213

One overriding goal of electromagnetic field computation is to obtain the greatest accuracy in computing electromagnetic field quantities with minimal computer time and resources. Towards this end, high-order methods have been developed to increase the speed of the computation. Although these high-order methods involve more complicated analyses and are harder to program than low order methods, the reward is often a several orders of magnitude speed-up in the time required to achieve a given accuracy.

High-order methods are currently used in three different ways to speed up finite element analysis. The first of these uses high-order polynomials to approximate the electromagnetic field. High-order scalar finite elements for the solution of homogeneous waveguide problems were introduced by Silvester twenty-six years ago (P. Silvester, IEEE Trans., MTT-17, 204-210, 1969). He showed that, for a given matrix size, high-order finite elements are not only more accurate than low-order elements, but that the rate of convergence of the high-order elements is faster. High-order vector finite elements were developed subsequently and provide the same benefits (Z. Cendes, IEEE Trans., MAG-27, 3958-3966, 1991). The second way to speed up finite element analysis is to use precise solid models to approximate the geometry. Finite element methods that use faceted models in which, say, a circle is approximated by an n-sided polygon introduce an error into the solution. With precise solid models, circles, spheres and other curved surfaces are represented exactly so that the geometric approximation is eliminated during mesh refinement. The third way to speed up finite element analysis is to use high-order polynomials to approximate the spectral response of the fields. By using high-order polynomials and a procedure called AWEfem, the spectral response of a device is obtained orders of magnitude faster than by computing the solution at many separate frequency points (X. Yuan & Z. Cendes, Proc. URSI Symposium, p. 196, June 1993).

This talk will explain the use of high-order methods in the finite element analysis of electromagnetic fields. It will examine the rate of convergence of the methods and show by using real-life examples that high-order methods result in more accurate solutions in a given computer time than is obtained by using low-order methods.

APPLICATION OF HIGHER ORDER VECTOR ELEMENTS TO THE COUPLED FINITE ELEMENT-COMBINED FIELD INTEGRAL EQUATION (FE/CFIE) TECHNIQUE

Vahraz Jamnejad*, Tom Cwik, and Cinzia Zuffada

Jet Propulsion Laboratory
California Institute of Technology
Pasadena, CA 91109

In the original formulation of the coupled Finite element-Integral equation method, first order vector tangential edge elements (Whitney elements) were used (T. Cwik, V. Jamnejad, and C. Zuffada, IEEE-APS Symposium, June 1993). Although excellent accuracy with relatively fast computation time is achieved, it is possible to obtain even better accuracy for the same mesh size and/or a smaller mesh size but with similar accuracy, by using higher order basis elements. These elements have been rigorously formulated by the French researcher Nedelec. The elements are formulated in terms of barycentric coordinates in a tetrahedron, which provides the simplest approach to solving the problem. The field inside the tetrahedron is then written as a sum over these basis functions. We will discuss three types of elements in a comparative investigation of these elements.

- i) The first order edge-based elements are composed of six(6) basis functions related to the six edges of a tetrahedral finite element. These elements have a constant value along the edges. This is the approach taken by most finite element researchers (e.g., Bossavit, et al). These basis functions preserve the continuity of tangential components of the fields across element interfaces, and are superior to node-based elements in a majority of cases, by avoiding spurious modes and easily handling material boundary edges, corners, etc.
- ii) The incomplete second order elements are composed of twelve (12) basis functions related to the six edges of a tetrahedral finite element, two per edge. These elements have a linear variation along the edges as opposed to the first elements which provide only a zero order along the edges. These twelve basis functions are only a part of a complete second order representation as proposed by Nedelec. This approach is similar to the one proposed by G. Mur and T. De Hoop. The total number of unknowns in this approach is twice that of the first but provides a higher accuracy for the same number of finite elements.
- iii) The complete second order Nedelec elements are composed of twelve (12) basis functions related to the six edges of a tetrahedral finite element, two per edge, as above, and eight additional basis functions related to the four facets of the tetrahedron, two per facet, for a total of 20 basis functions. The edge elements have a linear variation along the edges, while the face elements are constant vectors on their respective facets. The number of unknowns in this formulation is about six times that of the first order elements, but even higher accuracies can be achieved for the same number of elements.

Application of the above basis functions to the finite element equation for the EM field reduces to the evaluation of two element matrices for each tetrahedron element:

$$[S]_{mn} = \int_{tet} (\nabla \times \bar{\alpha}_m) \cdot (\nabla \times \bar{\alpha}_n) dv \quad \text{and} \quad [T]_{mn} = \int_{tet} \bar{\alpha}_m \cdot \bar{\alpha}_n dv$$

These matrices involve two types of integrals. Both types can be integrated analytically in terms of the barycentric coordinate system in the tetrahedron element, and reduce to terms involving only edge vectors and normal vectors to the facets. Application of all three methods to typical three-dimensional field problems and their pros and cons will be discussed. Some examples will be demonstrated and comparative results will be presented.

HIGHER ORDER EDGE FINITE ELEMENTS IN ELECTROMAGNETIC FIELD MODELLING

I. Bardi*, O. Biro, R. Dyczij-Edlinger, K. Preis and K.R. Richter
IGTE, Technical University of Graz
Kopernikusgasse 24, Graz, A-8010, Austria

The paper gives a brief summary of the edge finite elements applied in electromagnetic field modelling. The similarities and differences of the various edge elements like vector finite elements, tangential finite elements, projection elements, curl conform elements and edge elements with integral degrees of freedoms will be discussed. Whereas the properties of linear finite elements are thoroughly documented in the literature, little attention has been paid to higher order interpolation. The accuracy of the approximation can however be substantially improved using higher order edge elements of curvilinear shapes instead of the widely used linear edge finite elements. The aim of the paper is to discuss the properties and the way of construction of higher order edge elements. A new family of higher order curl conform edge finite elements will be presented built on triangles and tetrahedrons in 2D and 3D cases, respectively. A study will be included in order to compare the accuracy of the solution of linear and higher order elements.

The use of the edge finite element interpolation in electromagnetic field modelling has merits and demerits. The advantageous properties of the curl conform edge elements are that they do not support any spurious solutions and are superior to conventional nodal finite elements approximating the field singularities. Their main deficiency is the poor convergence rate of the iterative solvers when edge elements are used for the interpolation. The paper discusses ways of retaining the advantages while avoiding the shortcomings of the edge element applications both in static and high frequency cases. A survey of different descriptions and gauging methods will be presented to help choose the proper formulation fitting particular problem types and edge elements.

Several examples, mainly with quadrilateral and hexahedral higher order elements, will be presented to demonstrate the applicability and superiority of edge elements over nodal elements in certain electromagnetic field simulations (e.g. structures with sharp edges, eigenvalue problems, TEAM WORKSHOP problems).

Higher Order Divergence-Conforming and Curl-Conforming Bases on Curved Elements

R. D. GRAGLIA,* A. F. PETERSON,† AND D. R. WILTON‡

* DIPARTIMENTO DI ELETTRONICA, POLITECNICO DI TORINO, 10129 TORINO, ITALY

† GEORGIA INSTITUTE OF TECHNOLOGY, ATLANTA, GA 30332-0250.

‡ UNIVERSITY OF HOUSTON, HOUSTON, TX 77204-4793

A systematic development of p -th order divergence- and curl-conforming bases on curved elements is presented. In a numerical solution process, divergence- or curl-conforming bases are used to ensure the continuity of the normal or tangential components, respectively, of the vector unknown on the common boundary between adjacent 2D or 3D elements. Bases of the curl-conforming type are widely used in the finite element method for their ability to eliminate spurious solutions. Higher order divergence-conforming bases on curved 2D elements also appear promising for use with surface integral equations solved by the (subsectional) moment method, since current continuity conditions at the interfaces between adjacent subdomains are automatically satisfied by divergence-conforming bases.

Bases of p -th order on a curved element of the object space $\mathbf{r} \equiv (x, y, z)$ are defined by introducing a parent element (simplex) having a simple shape in the parent space (ξ_1, ξ_2, ξ_3) . The object element is obtained by parametric distortion of the parent element, though the vector basis ℓ_1, ℓ_2, ℓ_3 (with $\ell_i = \partial \mathbf{r} / \xi_i, i = 1, 2, 3$) used to represent a vector of the object space is, in general, not orthonormal and depends on the degree of distortion of the given element. The p -th order completeness of our bases is proved in the parent element, along with the p -th order completeness of the divergence of the divergence-conforming functions and of the curl of the curl-conforming functions, where in the latter case we mean completeness with respect to the representation of a p -th order vector having zero divergence.

Construction of the bases starts with knowledge of the zeroth order bases of the curved element. Multiplying these by p -th order complete polynomials in the parent variables generates the higher order functions. By eliminating linearly dependent functions obtained by this procedure, one obtains the independent basis functions, counts the number of degrees of freedom of the bases, and partitions the bases into face-based, volume-based and edge-based families. Examples of bases up to third order are given for the triangular and quadrilateral element and for the tetrahedron, hexahedron, and triangular prism.

Finite Element Methods

T. Cwik and T. P. Fontana

Page

- 8:20 A Functional That Eliminates Spurious Solutions and the 87
Finite Element Implementation
*C. F. Bunting**, *Old Dominion University, W. A. Davis, Virginia*
Polytechnic Institute and State University
- 8:40 Investigation of Numerical Dispersion in the Finite-Element 88
Method Using Three-Dimensional Edge Elements
*Gregory S. Warren**, *USAF Rome Laboratory, Waymond R. Scott, Jr.*
Georgia Institute of Technology
- 9:00 Finite Element Analysis of Conformal Antennas on 89
Doubly Curved Platforms
*Tayfun Ozdemir**, *John L. Volakis, University of Michigan*
- 9:20 The Treatment of Edge Singularities in Waveguiding Problems 90
Using a Finite Element Method Based on Edge Elements
*Z. Pantic-Tanner**, *San Francisco State University, D. R. Tanner,*
Lockheed Martin, J. S. Savage, A. F. Peterson,
Georgia Institute of Technology
- 9:40 Finite Element Analysis of Cavity Backed Apertures in Three 91
Dimensional Bodies
*C. J. Reddy**, *M. D. Deshpande, C. R. Cockrell, F. B. Beck,*
NASA-Langley Research Center
- 10:00 BREAK
- 10:20 Implementing Voltage and Current Gap Sources in Finite Elements 92
*Xingchao Yuan**, *Zoltan Cendes, Ansoft Corporation*
- 10:40 A 3-D Vector Finite Element Analysis for Modeling Lossy 93
Anisotropic Ferrite Devices
*Thomas P. Fontana**, *Eric W. Lucas, Westinghouse Electric Corporation*
- 11:00 Edge-based Vector Finite Element Method and its Application to 94
Aperture Coupling Between Rectangular Waveguides
*J. Zhou**, *J. J. Song, Y. Kang, R. L. Kustom, Argonne National Laboratory,*
T. T. Wong, Illinois Institute of Technology
- 11:20 An Infinite Element for the Finite Element Quasi-Static Analysis 95
of Open Waveguiding Structures
*Magdalena Salazar-Palma**, *Universidad Politecnica, Jose-Felix Hernandez-Gil,*
Telefonica Investigacion y Desarrollo

- 11:40 First and Second Order Curved Non-Standard Finite Elements96
for the Dynamic Analysis of Waveguiding Structures with
Curved Contours
*Fernando Blanc-Castillo, Magdalena Salazar-Palma,
Luis E. Garcia-CAstillo*, E.T.S.I. Telecomunicacion*
- 12:00 A Second Order Non-Standard Finite Element for the Dynamic97
Analysis of Generalized Waveguiding Structures
Fernando Blanc-Castillo, Magdalena Salazar-Palma,
Luis E. Garcia-Castillo, E.T.S.I. Telecomunicacion.
Universidad Politecnica*

A Functional That Eliminates Spurious Solutions and The Finite Element Implementation

by

C. F. Bunting*

Department of Engineering Technology
Old Dominion University, Norfolk Va. 23529
and

W. A. Davis

The Bradley Department of Electrical Engineering
Virginia Polytechnic Institute and State University, Blacksburg, Va. 24060

The introduction of a new functional is motivated by the failure of typical functional forms to properly enforce the divergence criterion on the problem to be solved. Most formulations begin with Maxwell's equations and then perform a substitution to obtain a representation that is either in terms of the electric field or the magnetic field. These approaches essentially constitute an application of the method of weighted residuals since the "functionals" used do not provide a mapping to the real line and do not provide a minimization. The purpose of this research is to introduce a new functional whose minimum corresponds to a solution of Maxwell's equations, eliminates spurious solutions, and that provides a mapping from the complex space to the real line. The Euler equation will be examined. A modal approach will be applied to the new functional. It will be shown that the new functional eliminates the gradient part of a general vector expansion function, thus eliminating divergent solutions.

The finite element implementation of the new functional will be examined. After presenting a detailed expression for the first variation in terms of a normalization that allows the wavenumber to be explicitly represented, the matrix representation will then be examined. A direct application of finite element techniques to the functional leads to difficulties in practical computation of the eigenvalues, so alternative representations are explored. A scalar analog of the matrix representation allows for a circular solution of the eigenvalues in the complex plane that will be suggestive of a grouping that satisfies the modal approach. Finally a least squares matrix approach will be employed that will yield results that are free from the spurious solutions that plague the full-field and penalty approaches as well as avoiding the difficulties arising due to the circle type solutions. This functional will be shown to eliminate spurious solutions in finite element applications and provide a solution which converges as the node density of the mesh used to discretize the domain is increased.

INVESTIGATION OF NUMERICAL DISPERSION IN THE FINITE-ELEMENT METHOD USING THREE-DIMENSIONAL EDGE ELEMENTS

Gregory S. Warren*
USAF Rome Laboratory
RL/ERAS
31 Grenier St.
Hanscom AFB, MA 01731-3010

Waymond R. Scott, Jr.
School of Electrical Engineering
Georgia Institute of Technology
Atlanta, Georgia 30332-0250

The finite-element method is used extensively to solve electromagnetic problems. There are basically two types of elements used with the method: the nodal element and the edge element. The edge element is studied in this work; it is the more recent of the two and was developed to overcome some of the drawbacks of the nodal element. Regardless of which element is used in the finite element modeling process, certain errors will occur. An error common to both types of element is the discretization error which arises from the inability of the polynomial basis functions to represent the fields exactly within an element. A wave propagating through a finite-element mesh will experience numerical dispersion as a result of this error.

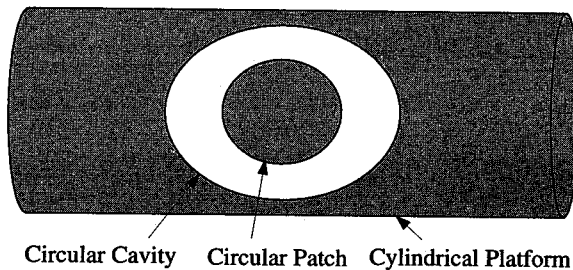
The discretization error of two-dimensional edge elements has been characterized in a previous work (G. Warren & W. Scott, IEEE Tran. Ant. & Prop. 11, 1502-1508, 1994). The dispersion of two-dimensional, edge elements gives some indication of the dispersion of three-dimensional, edge elements. However, the dispersion of the three-dimensional elements do exhibit some effects that are not present in the dispersion of the two-dimensional elements. In fact, preliminary results indicate that the dispersive behavior of tetrahedral edge elements is considerably more complicated than that of triangular, edge elements. As a result, the dispersion of three-dimensional, tetrahedral and hexahedral, edge elements is investigated. The dispersion is represented by the phase error in a plane wave propagating through an infinite, uniform, three-dimensional mesh. The phase error is determined as a function of the propagation direction, element size, and element order.

FINITE ELEMENT ANALYSIS OF CONFORMAL ANTENNAS ON DOUBLY CURVED PLATFORMS

Tayfun Özdemir* and John L. Volakis

Radiation Laboratory, Department of Electrical Engineering and Computer Science, University of Michigan, Ann Arbor, Michigan 48109-2122
tayfun@engin.umich.edu, volakis@engin.umich.edu

Characterization of radiation and scattering from doubly curved conformal antennas is important as they are commonplace on aircraft and other airborne vehicles. In this paper, we present a finite element analysis of conformal antennas on doubly curved platforms. Modeling such antennas requires only two dimensional geometric fidelity (over the surface) and this can be readily accomplished using prismatic meshes. To generate a prismatic mesh, one starts with an unstructured surface grid of triangular patches and the volumetric mesh is then grown by extending the surface grid along the surface normals. Generating such a mesh is rather simple (in comparison to the tetrahedral mesh) and the resulting tessellation element is the distorted triangular prism. The mesh is terminated using conformal absorbing boundary conditions (A. Chatterjee & J.L. Volakis, *Micr. Opt. Tech. Lett.* 6, 886-669, 1993). Also, artificial absorbers will be examined as an alternate means of truncating the mesh (T. Özdemir & J.L. Volakis, *Radio Sci.* 29, 1255-1263, 1994). Results will be presented concerning radiation, scattering and resonance characteristics of coated rectangular and circular patch antennas on cylindrical and other doubly curved platforms. Also the coupling between antenna array elements will be examined and some preliminary results pertaining to hybridization with high frequency techniques for pattern computation will be presented. Validation of the results will be carried out by comparison with the experimental data as well as finite element-boundary integral method solutions where available.



Geometry of a circular patch antenna on cylindrical platform

THE TREATMENT OF EDGE SINGULARITIES IN WAVEGUIDING PROBLEMS USING A FINITE ELEMENT METHOD BASED ON EDGE ELEMENTS

Z. Pantic-Tanner*
School of Engineering
San Francisco State University
San Francisco, CA 94132

D. R. Tanner
Lockheed Martin
1111 Lockheed Way B1076
Sunnyvale, CA 94088-3504

J. S. Savage, and A. F. Peterson
School of Electrical and Computer Engineering
Georgia Institute of Technology
Atlanta, GA 30332-0250

The finite element method (FEM) based on edge elements is a powerful numerical technique for solving a variety of waveguide problems. It is not only capable of handling waveguides of complicated cross-sections and with arbitrary fillings of inhomogeneous media, be they isotropic or anisotropic, but it also eliminates nonphysical, spurious modes from the numerical solution. In this paper we use edge elements derived from the Nedelec constraints (A. Peterson, T-AP, 43, 357-365, 1994). The use of high-order edge elements allows one to enhance the numerical accuracy of the solution without increasing the number of unknowns when the field inside the guide is well behaved. However, many waveguiding structures contain conducting or dielectric edges embedded in an inhomogeneous isotropic or anisotropic medium, and the field behavior can be singular in the vicinity of these edges. If polynomial edge elements are used to model these rapidly varying fields, it becomes necessary to use a fine mesh near the edge regions. The increase in the number of unknowns in the mesh has the effect of increasing the computational time as well as memory requirements. However, it has been shown that for both the quasi-static (Z. Pantic and R. Mittra, T-MTT, 34, 1096-1103, 1986) as well as the dynamic transmission line problems (Z. Pantic-Tanner, C. H. Chan, and R. Mittra, URSI Symp. Dig., 336, 1988), the number of unknown parameters necessary to model the fields can be significantly reduced by employing singular elements. While the ordinary edge elements represent the field components using polynomials, the singular elements are based on analytical solutions for the fields near the edges, and are designed to mimic the theoretically-predictable singular behavior of these fields as closely as possible (J. Van Bladel, T-AP, 33, 450-455, 1985). The basis functions used in this paper consist of a singular part derived as a gradient of a scalar function, and a nonsingular part. The continuity of the tangential field component is provided along all edges of the singular element as well as the compatibility with the neighboring ordinary edge elements. In this paper the FEM matrices for a singular element are derived with the necessary integrations evaluated in closed form.

In order to construct singular-element basis functions, *a priori* knowledge of the singularity parameter governing the field behavior at the edges is required. For that purpose a transcendental equation for the singularity parameter (C. H. Chan, Z. Pantic-Tanner, and R. Mittra, *Elect. Lett.*, 24, 355-356, 1988) is used.

Numerical results for some typical waveguiding structures containing sharp edges are presented in the paper.

FINITE ELEMENT ANALYSIS OF CAVITY BACKED APERTURES IN THREE DIMENSIONAL BODIES

C.J.Reddy*, M.D.Deshpande, C.R.Cockrell and F.B.Beck
NASA-Langley Research Center, Hampton VA 23681, USA

ABSTRACT

Radiation from cavity backed apertures in three dimensional bodies is of interest due to their applications in aerospace and automobile antennas. Analyses of such antennas are usually complicated due to the arbitrary shape of the three dimensional body. In this paper a Finite Element Method(FEM) approach is presented to analyze radiation from arbitrarily shaped apertures in a 3D body with an arbitrary shape. The FEM computational volume is terminated by either using the Method of Moments (MoM) or Absorbing Boundary Conditions (ABCs). The FEM/MoM approach results in a partly sparse and partly dense matrix, whereas the FEM/ABC approach results in a completely sparse and symmetric matrix. In figure 1, radiation patterns of a rectangular aperture in a three dimensional perfectly conducting(PEC) box excited by a rectangular waveguide is presented. The rectangular waveguide is assumed to have a TE_{10} mode as the incident field. Comparison of numerical data obtained from the FEM/MoM and FEM/ABC computation agree well. More numerical data and comparison of both methods will be presented at the conference.

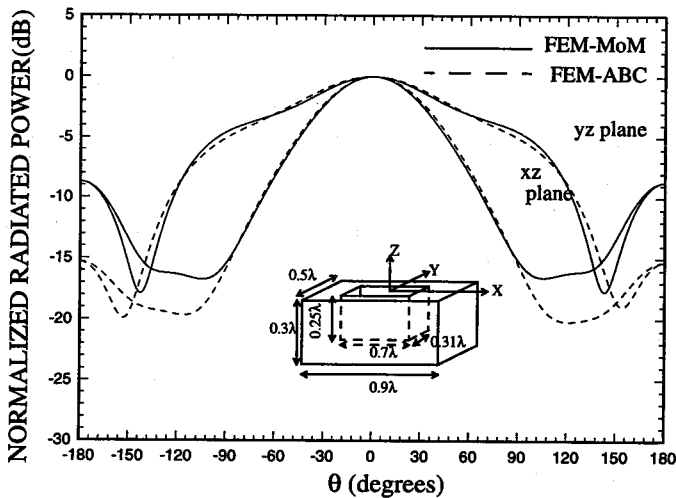


Figure 1

Implementing Voltage And Current Gap Sources In Finite Elements

Xingchao Yuan* and Zoltan Cendes
Ansoft Corporation
Pittsburgh, PA 15129

As the speed of electronic circuits continues to increase, there is greater need to minimize unwanted electromagnetic radiations. One way to achieve this goal is to employ computer aided design tools to model EMI/EMC effects early in the design process. A powerful way to solve such problems is by using a general finite element solver based on the transfinite element method (TFEM) (Z.J. Cendes and J.F. Lee, *IEEE Trans. on Microwave Theory and Techniques*, Vol.36, No.12 pp.1639-1649, Dec. 1988). Combined with the second order vector absorbing boundary condition, this procedure may be used to model high frequency structures such as connectors, waveguide transitions, resonators, antennas, and printed circuit boards. While this approach is versatile and accurate, it always requires ports or transmission lines to excite the structures under consideration. In modeling high speed circuits, this requirement becomes an unnecessary complication.

To address this problem, we introduce voltage and current gap sources in finite element analysis in this paper. When the size of sources compared to wavelength is very small, a voltage gap source may be modeled by a constant electric field and similarly a current gap source may be modeled by a constant surface current. The TFEM method is modified to accommodate both cases. In addition, we have introduced the gap sources in AWEfem (X.C. Yuan, D.K. Sun, and Z.J. Cendes, *1994 IEEE AP/URSI Joint Symposium, URSI Digest*, pp. 29) for extracting wide bandwidth frequency information rapidly. This technique predicts device resonances analytically and is orders of magnitude faster than conventional techniques.

Both the theory and application examples of voltage and current gap sources will be presented. The numerical results will be compared with results obtained by using either analytical or numerical methods.

A 3-D Vector Finite Element Analysis for Modeling Lossy Anisotropic Ferrite Devices

Thomas P. Fontana* and Eric W. Lucas
Antenna/Apertures and Integrated Sensors Department
Westinghouse Electric Corporation
P.O. Box 746
Baltimore, Maryland 21203

In this work, a vector finite element analysis has been applied to a general periodic 3-D cell that contains lossy anisotropic ferrite media. Other sources of loss have also been included such as dielectric loss and loss attributable to finite conductivity. The 3-D region can be connected to 2-D semi-infinite propagating structures of arbitrary cross section. Using calculated 2-D finite element $E_t - H_t$ eigenmodes, these "ports" may be used to drive or terminate the 3-D region via a vector-mode boundary element technique (E. W. Lucas and T. P. Fontana, IEEE AP/S Digest, 1994).

The lossy ferrite regions are modeled by a non-Hermitian Polder-type permeability tensor dependent upon the constitutive properties of the ferrite, and the arbitrarily orientated DC magnetostatic field. Both E-field as well as H-field variational formulations have been developed based upon the partial variational principle, PVP (S. J. Chung and C. H. Chen, IEEE, MTT-36, March 1988). The basis for the electromagnetic field consists of second order vector edge elements on a mesh of tetrahedra. Upon applying PVP, the resulting system of linear equations has a general, non-symmetric, non-Hermitian structure. Both the lossy ferrite regions and the BEM vector formulations for non-normal scattering result in this non-self-adjoint characteristic.

We have applied the analysis to a variety of devices including periodic scatterers and ferrite circulators. Comparisons of predictions to measurements are shown.

Edge-based Vector Finite Element Method and its Application to Aperture Coupling between Rectangular Waveguides

J. Zhou*, J.J. Song, Y. Kang and R. L. Kustom
Accelerator Systems Division, Argonne National Laboratory
9700 S. Cass Avenue, Argonne, IL 60439

T.T. Wong
Dept. of ECE, Illinois Institute of Technology, Chicago, IL 60616

Electromagnetic coupling through an arbitrarily-shaped aperture in the common wall of two rectangular waveguides is calculated by the edge-based vector finite element method. The electric and magnetic fields in the coupled waveguides are represented by the surface integral of dyadic Green functions and the tangential electric field in the aperture region. An integral equation is obtained by matching the tangential magnetic field in the aperture area. Galerkin's technique is applied to solve the integral equation for the electric field or the virtual magnetic current in the aperture. The aperture area is divided into a set of triangular elements, which could easily conform to complex geometries without any special treatment compared to quadrilateral meshes. Triangular elements are also more appropriate for automatic adaptive mesh generation, which is an important feature for efficient and accurate simulation of practical problems. The edge-based vector shape functions guarantee the tangential continuity of the electric field and the normal continuity of the virtual surface magnetic current. After expansion of the electric field by vector shape functions, the resulting equation is tested by the inner product with the same set of shape functions as test functions. The numerical integration is carried out using the four-point Gaussian-Legendre quadrature rule. Various circuit parameters such as scattering parameters, input impedance, and beam coupling impedances, can be readily evaluated from the aperture field distribution.

This general method can be applied to various kinds of rectangular waveguide coupling problems, such as capacitive and inductive diaphragm of arbitrary shape, transverse wall waveguide coupling, broad-wall to narrow-wall coupling, crossed coupling by offset apertures, coupling by aperture arrays, etc. The method can deal with arbitrarily shaped apertures located at any position on either the broad or the narrow wall of the waveguide.

AN INFINITE ELEMENT FOR THE FINITE ELEMENT QUASI-STATIC ANALYSIS OF OPEN WAVEGUIDING STRUCTURES

Magdalena Salazar-Palma^{}(1), José-Félix Hernández-Gil(2)*

(1) Dpto. de Señales, Sistemas y Radiocomunicaciones. E.T.S.I. Telecomunicación. Universidad Politécnica. C/ Ciudad Universitaria, s/n. Madrid 28040. SPAIN.

(2) Telefónica Investigación y Desarrollo. Emilio Vargas,6. 28034 Madrid. Spain.

Although open structures can be treated by the conventional FEM placing an artificial shielding far away from the near field region, the computation efficiency may be improved if infinite elements are used. Infinite elements should provide an approximation of the unknown so that its asymptotic behaviour would coincide with the real one. Different types of infinite elements may be derived depending on how the asymptotic behaviour is achieved (P. Bettess, J.A. Bettess, Eng. Comput., vol. 1, March 1984, pp. 4-15). The direct method uses an infinite master element (that will be transformed as usual into the infinite ones) and modified basis functions for the approximation of the unknown. This type of elements requires special quadrature techniques; the numerical integration must be performed in the infinite domain. Infinite elements based on the inverse method employ instead a finite master element and the ordinary basis functions for the approximation of the unknown; the asymptotic behaviour is obtained by means of an adequate geometrical transformation that maps the finite master element into the infinite real one. Numerical integration may be performed in the usual way and on the finite master element. This paper presents rectangular infinite elements of the inverse type providing asymptotic behaviour of type $(1/r)^n$, where r is the distance from the origin and n is any positive number. To the authors knowledge the concrete elements that are presented have not been used in the past in the electromagnetic area. The authors have applied them to the quasi-static analysis of open structures with one $(1/r)$ or two infinite ground planes $(1/r^2)$. The geometrical transformation functions for a master element with 6 geometrical points will be shown. From them, an infinite element of first order as well as subparametric infinite elements of second order may be obtained.

Several waveguiding structures have been analyzed in order to show the efficiency of the infinite elements. As an example, Table I shows results regarding the normalized capacitance of a single-wire transmission line (of diameter $2r$) over an infinite ground plane placed at a distance $h=2r$. A mesh with triangular elements for the near field region and rectangular elements for the far field one has been used. The rectangular elements have been treated as ordinary or infinite elements for comparison purposes.

Table I. Results for the normalized capacitance of a single-wire transmission line over an infinite ground plane

Second degree elements	Number of Unknowns	Error (%)
Using finite elements only	41	12.06
Using finite and infinite elements	41	-1.92

FIRST AND SECOND ORDER CURVED NON-STANDARD FINITE ELEMENTS FOR THE DYNAMIC ANALYSIS OF WAVEGUIDING STRUCTURES WITH CURVED CONTOURS

*Fernando Blanc-Castillo, Magdalena Salazar-Palma, Luis E. García-Castillo**
Dpto. de Señales, Sistemas y Radiocomunicaciones. E.T.S.I. Telecomunicación.
Universidad Politécnica. C/ Ciudad Universitaria, s/n. Madrid 28040. SPAIN.

The Finite Element Method (FEM) is a powerful numerical tool for solving electromagnetic problems. The analysis of waveguiding structures can be done in an accurate and efficient way by means of the so called non-standard triangular elements. A companion paper presents the second order one and references the first order one. These elements are a combination of a Lagrange element and an edge element in H(rot) of the Nedelec type.

When the waveguiding structure presents curved contours, if the domain of the problem is discretized using only straight elements the resulting discretization error will reduce the efficiency of the FEM. In order to recover the convergence rate of the method curved elements may be used to mesh the curved boundaries. Curved elements reduce the discretization error or even eliminate it.

This paper presents the curved version of the first and second order triangular elements. Curved and straight elements may be obtained from a same master element using adequate geometrical transformations. A geometrical transformation employing second order Lagrange polynomials has been used to obtain the curved version of both the first and second order non-standard elements. Thus, the curved first order non-standard element is a superparametric element, while the curved second order one is an isoparametric one. To the authors knowledge results employing curved edge elements or any other type of curved vector elements have not been presented up to date.

Curved and straight non-standard elements have been used for the analysis of several waveguiding structures with curved boundaries. As an example and in order to show the efficiency of curved elements, Table I compares de number of nodes required and the CPU time employed to obtain the same order of accuracy in the computation of the TE_{11} mode cut-off wave number of a circular waveguide, when using only straight elements or both straight and curved ones.

Table I. Results for the TE_{11} mode k_c value of a circular waveguide

	Number of Nodes	CPU time (Sun Sparc 10)(s)	Error (%)
Straight elements only (1 st order)	2113	145.2	0.21
Straight and curved elements (1 st order)	545	24.7	0.23

A SECOND ORDER NON-STANDARD FINITE ELEMENT FOR THE DYNAMIC ANALYSIS OF GENERALIZED WAVEGUIDING STRUCTURES

Fernando Blanc-Castillo, Magdalena Salazar-Palma, Luis E. García-Castillo
Dpto. de Señales, Sistemas y Radiocomunicaciones. E.T.S.I. Telecomunicación.
Universidad Politécnica. C/ Ciudad Universitaria, s/n. Madrid 28040. SPAIN.*

The Finite Element Method is a flexible numerical procedure capable of analyzing different geometries without the need of new analytical developments. The accuracy of the method depends on several issues like a well adapted mesh, the order of the approximation employed, etc. This paper presents a second order triangular element of the so called non-standard type consisting in a combination of a Lagrange interpolation and an edge type interpolation. In a waveguiding problem, the first one is employed for the discretization of the longitudinal component of the electric or magnetic field and the second one for that of the transverse component. These elements provide spurious free solutions belonging to $H^1(\Omega) \times H(\text{rot}, \Omega)$ space. The first order triangular element was presented previously (L.E. García-Castillo, M. Salazar-Palma, Proc. 1992 URSI Int. Symp. Electromag. Th., pp. 31-33, Sydney, Australia). The second order non-standard triangular element follows the same philosophy, combining a second order Lagrange element and a second order edge element in $H(\text{rot})$. The characteristics (number of nodes, degrees of freedom, basis functions) of this edge element may be derived directly from those of the second order edge element in $H(\text{div})$ presented previously (M. Salazar-Palma et al, 1991 Int. IEEE/AP-S Symp. Digest, pp.1232-1235, London, Ontario, Canada), taking into account the relations between edge elements in $H(\text{rot})$ and in $H(\text{div})$. It must be pointed out that this edge element of second order is different from those used in the past by other authors, having a different location of the nodes and a different definition of the degrees of freedom; the basis functions satisfy the Nedelec constraints (A.F. Peterson, IEEE Trans. Antennas Prop., Vol.43, March 1994, pp:357-365).

The resulting non-standard second order element has been applied to the analysis of several homogeneous and inhomogeneous waveguiding structures showing a higher efficiency than the first order one in terms of accuracy, CPU time and storage requirements. As an example Table I shows a comparison for the cutoff wave number computation of the TE_{10} mode of a $2axa$ rectangular waveguide; it can be seen that the same order of accuracy is obtained with only 73 nodes when using the second order element in comparison with 325 nodes for the first order one. Comparisons with other authors results will also be provided.

Table I. Results for the TE_{10} mode k_c value of a $2axa$ rectangular waveguide

	Number of Nodes	Error (%)
1 st order	325	0,2
2 nd order	73	0,24

THIS PAGE INTENTIONALLY LEFT BLANK.

Special Session

Tribute to Professor Irene Peden

A. Ishimaru

	Page
8:20 Irene Peden: Her Professional and Human Impact <i>Akira Ishimaru, University of Washington</i>	100
8:40 Reminiscences of Research in Antarctica: A Tribute to Professor Irene Peden <i>George E. Webber, HFS Inc.</i>	101
9:00 Dr. Irene Peden and the NSF <i>Lawrence S. Goldberg, National Science Foundation</i>	102
9:20 Engineering Education in the Nineties: Challenges and Opportunities <i>David C. Chang, Polytechnic University</i>	103
9:40 Irene Peden: A Lady for all Seasons <i>Gary S. Brown, Virginia Polytechnic Institute and State University</i>	104
10:00 BREAK	
10:20 The First Course in Electromagnetics <i>Donald G. Dudley, University of Arizona</i>	105
10:40 Vision, Persistence, Commitment, and Leadership: The Role of Irene in the Development of CAEME <i>Magdy F. Iskander, CAEME</i>	106

IRENE PEDEN: HER PROFESSIONAL AND HUMAN IMPACT

Akira Ishimaru
Department of Electrical Engineering
University of Washington
Seattle, Washington 98195

It has been my great privilege to have worked with Irene for the past 35 years. She came to the University of Washington in 1961 from the Stanford Research Institute where she had already conducted important microwave research. Soon she was involved in Antarctic research on the characteristics of long-buried antennas near Byrd Station which generate low-frequency radiation into the ionosphere. She was the first woman scientist to conduct research in the Antarctic. This was an unprecedented event requiring enormous perseverance. Her constant efforts to overcome many barriers have helped to create an atmosphere that is fair to all people including women and minorities in universities, professional organizations and government agencies. She has a strong sense of serving the profession and has made enormous contributions to universities, education, and government agencies by freely giving her time and her extraordinary talents in administration. She has had a keen sense of direction for our educational and research activities, which has helped us identify important future problems. She has always been generous and willing to share her time with anyone who needed help. We all remember her personal touch, understanding and concern for us as individual human beings. Many students have been motivated by her encouragement to do their best, and they look to her as their mentor and role model. The IEEE, URSI, universities, and the government have benefited greatly from her many contributions. But above all, we have benefited from and will cherish her most personal and human warmth.

REMINISCENCES OF RESEARCH IN ANTARCTICA: A TRIBUTE TO IRENE PEDEN

George E. Webber
HFS Inc.
7900 Westpark Drive
McLean, Virginia 22102-4299

This brief presentation will focus on several of the rewarding experiences that I have had with Irene Peden particularly during the period when I worked under her guidance as a graduate student at the University of Washington. In particular it will focus on several aspects of the research work that we did together relating to anomalies in VLF radio wave propagation in the polar regions of Antarctica. In conducting that work I actually had occasion to "winter-over" at Byrd Station during the 1966-67 season, and Irene made one of the first visits to Antarctica by a woman during the summer season of 1970. The presentation will attempt to highlight some of the interesting experiences we had during the course of that project and particularly some of the significant accomplishments made by Irene in helping to "open the doors" for women to do on-site research in Antarctica.

DR. IRENE PEDEN AND THE NSF

Lawrence S. Goldberg
Director, Division of Electrical and Communications Systems
National Science Foundation
Arlington, VA 22230

During her long and productive academic career, Irene Peden has maintained a close professional relationship with the National Science Foundation: as Division Director within the Directorate for Engineering, as member of Engineering's External Advisory Committee, as reviewer, and as grantee. It is my pleasure to recount some of Dr. Peden's special contributions to the NSF over the period that I have known and worked with her, including during her tenure as Division Director for Electrical and Communications Systems.

ENGINEERING EDUCATION IN THE NINETIES: CHALLENGES AND OPPORTUNITIES

**David C. Chang, President
Polytechnic University
6 Metro Tech
Brooklyn, NY 10201**

While dramatic restructuring and re-engineering continue to occur in industry, engineering colleges are facing serious challenges and exciting opportunities to redefine themselves to reflect the changes in the workplace. It is quite apparent that superb technology alone will not lead to commercial success for a high-tech based company: concurrence, agility, cost-performance ratio, total quality, diversity and customer-orientation are all becoming increasingly more critical in determining the competitiveness of a company in the market place. Equally apparent is that future engineers will be less involved in the design of individual components, and more in integrating components into systems. If the current trend continues, the need for engineers to design may decline, while the need for individuals with skills and technical know-how to manage complexity in both technical and non-technical fields, may increase. The changing requirements in the workplace necessitate a re-examination of today's engineering educational practices and thus provides us a rare opportunity to develop new paradigms and curricula to meet the new challenges. In this talk, I would briefly discuss my perception of the new reality and outline some of the new thinking being discussed or implemented in many engineering colleges across the nation.

IRENE PEDEN: A LADY FOR ALL SEASONS

Gary S. Brown
ElectroMagnetic Interactions Laboratory
Bradley Department of Electrical Engineering
Virginia Polytechnic Institute and State University
Blacksburg, Virginia 24061-0111

The norms by which we in academia are usually judged are derived from the three-fold mission of land grant universities - teaching, research, and service. Those individuals who excel in all three categories are extremely few in number and they are not always properly recognized by their peers. It is both fitting and proper that we in the profession of electrical engineering should pause and pay homage to Irene Peden for she is a leader not only in the areas of teaching, research, and service, but more importantly as a lady in a field that has not always been kind or supportive of women. The young women of today who choose electrical engineering as a vocation also owe a great debt of gratitude to Irene for she blazed the trails of acceptance and respect through competence, firmness, and kindness well before there were laws and programs to guarantee such treatment. With the calm forcefulness and dogged determination that is a consequence of her Scandinavian heritage, Irene has consistently shown us how to overcome the most vexing of problems in the kindest way possible. It is, therefore, the unique manner in which Irene combines expertise, forcefulness, and pure kindness and diplomacy which clearly qualify her as a "Lady For All Seasons."

My own personal experiences come primarily from dealing with Irene in the administration and leadership of the IEEE Antennas and Propagation Society. In particular, Irene was Vice President of the Society when I was President and she subsequently became the President. What is most vivid in my mind about this time period and especially just when she was assuming the Presidency are the problems she faced. Her beloved husband Leo was told that the simple act of walking would no longer be easy or routine for him. Irene, upon return from a trip, fell in the Seattle airport parking lot and literally shattered some of her major bones in one of her legs. Finally, and perhaps worst of all, Irene was faced with one of the worst tasks in the world - selecting a new editor of the *Transactions!* We make light of this now because her choice was an excellent one, but it certainly was far from easy for Irene. I distinctly remember worrying when Irene took over as a President because she had not been able to attend all of the IEEE HQ briefings and meetings to prepare one for such a Presidency. I should not have concerned myself with such trivial matters for Irene "hit the ground running" and I doubt that there are many Adcom members of that time who knew just how little formal preparation she really had.

When Irene became President of AP-S, she completed a number of tasks and initiated a number of ones which had a lasting impact on our Society. The most memorable of these is the idea she originated for what is now known as CAEME. As President, she put forth the idea, found someone to run the program, and was the advisory force behind that proposal to NSF for initial support.

Our society owes much to Irene; we owe much to her. Clearly, she is a "Lady For All Seasons."

THE FIRST COURSE IN ELECTROMAGNETICS

Donald G. Dudley
ECE, Bldg. 104
University of Arizona
Tucson, AZ 85721

Over a 35 year teaching career, the author has made an informal study of what motivates the student in a first course in electromagnetics and what does not. In this paper, we discuss the following factors: the preparation of the student; the attitude of the student; the attitude of the non-EM faculty; the role of the instructor; the use of a teaching assistant; the use of classroom demonstrations; the use of student projects; the emergence of computer visual aids; the importance of electromagnetic history; and the role of government.

We conclude the paper with some remarks concerning the influence that Professor Irene Peden has had and will continue to have on the first course in electromagnetics. We also comment on the future trends in first course instruction.

VISION, PERSISTENCE, COMMITMENT, AND LEADERSHIP: THE ROLE OF IRENE IN THE DEVELOPMENT OF CAEME

Magdy F. Iskander
CAEME Center
University of Utah
Salt Lake City, UT 84112

The purpose of this presentation is to acknowledge with thanks and appreciation the significant role of Prof. Irene Peden in the original vision, establishment, and guidance of the NSF/IEEE Center for Computer Applications in Electromagnetic Education (CAEME). With the publication of the Wiley journal, *Computer Applications in Engineering Education*, the establishment of the CAEME Center for Multimedia Education, and the organization of the CoLoS USA (Conceptual Learning of Science) Consortium, CAEME has now expanded its activities across the engineering, science, and math curricula. None of this would have been possible without Irene's original vision, her persuasion and persistence in obtaining support from the AP-S AdCom, her commitment to help organize and support the development of CAEME, and her leadership in guiding the Center in a highly productive and beneficial path.

The presentation will highlight the countless contributions Irene made in establishing the CAEME Center. Starting with her initial call to NSF, working with Prof. A. Adam and me on preparing the proposal, establishing the blue ribbon evaluation committee to satisfy NSF's guidelines, persuading the AP-S AdCom to sponsor the project, to literally cutting through the bureaucracy to get IEEE to sign off on the project on behalf of the Antennas and Propagation Society, Irene's efforts were tireless.

With the funding of the project, Irene was very much aware of the responsibility to IEEE, NSF, and above all, to education. She continued to work hard with all involved; and through her vision, persistence, and commitment to excellence, we owe to her the success of the CAEME project.

Scattering

<i>C. Torres-Verdin and R. H. MacPhie</i>		Page
8:20	Axial Scattering of a Coated Tubular Cylinder <i>H.-M. Lee, Naval Postgraduate School</i>	108
8:40	Plane Wave Scattering by Two Coalescing Spheres <i>R. H. MacPhie, T. Do-Nhat, University of Waterloo</i>	109
9:00	Methods for Evaluating the Performance of Electromagnetic Scattering Prediction Codes <i>J. P. Meyers, A. J. Terzuoli, Jr., G. C. Gerace, P. F. Auclair, Air Force Institute of Technology</i>	110
9:20	A Fast and Accurate Three-Dimensional Multiple Scattering Approach Involving Large Conductivity Contrasts <i>Tarek M. Habashy*, Carlos Torres-Verdin, Schlumberger-Doll Research</i>	111
9:40	Modeling Three-Dimensional Scattering Using TransFinite Elements <i>Xingchao Yuan*, Dinkow Sun, Zoltan Cendes, Ansoft Corporation</i>	112
10:00	BREAK	
10:20	Electromagnetic Scattering From a Cylindrical Inlet Using Combined Field Integral Equations <i>M. D. Deshpande*, C. J. Reddy, C. R. Cockrell, F. B. Beck, NASA-Langley Research Center</i>	113
10:40	Higher Order Statistics of Scattering from Small Clutter Cells <i>Lisa Mockapetris, Rome Laboratory, Hanscom AFB</i>	114
11:00	On the Rayleigh Approximation for Electromagnetic Scattering from a Small Scatterer <i>M. A. Karam*, A. Stogryn, Aerojet Electronic Systems Plant</i>	115
11:20	Electromagnetic Scattering from a Continuously Inhomogeneous Random Medium with Cylindrical Symmetry <i>Magali Jean, MOTHEM Society</i>	116
11:40	Parameter Estimation of Frequency Dependent Scatterers <i>JW Odendaal*, PA van Jaarsveld, University of Pretoria</i>	117
12:00	Iterative Minimum Discrepancy Method for Three-Dimensional Scattering Problems <i>Alexander B. Samokhin, Moscow Institute Radiotechnics</i>	118

AXIAL SCATTERING OF A COATED TUBULAR CYLINDER

H.-M. Lee

Naval Postgraduate School (EC/Lh), Monterey, CA 93943-5121, U. S. A.

Scattering of a circular, tubular cylinder of length $2h$ and radius a coated on the outside and inside surfaces with anisotropic normalized surface impedances $[Z^+]$ and $[Z^-]$ has been studied. In the cylindrical coordinates (ρ, ϕ, z) where z lies along the axis of the cylinder, the normalized $[Z]$ -matrices are defined in terms of the impedance boundary condition $[\mathbf{n} \times (\mathbf{E} \times \mathbf{n})] = (\mu_0/\epsilon_0)^{1/2} [Z][\mathbf{n} \times \mathbf{H}]$ where $[\mathbf{n} \times (\mathbf{E} \times \mathbf{n})]$ and $[\mathbf{n} \times \mathbf{H}]$ are considered as 2×1 matrices with their ϕ -components carrying the index 1 and their z -components carrying the index 2. The wave incident along the axis of the cylinder is polarized in the y -direction. With $kh=7$ and $ka=1.75$, the cross sections normalized to πa^2 in the backward direction (Figs. 1 and 2), the forward direction (Fig. 3) and along the x axis (Fig. 4) versus $[Z^+]_{11} + [Z^-]_{11}$ for three cases are presented. In all these cases, the $[Z]$ -matrices are assumed to be diagonal while the sum $[Z^+]_{11} + [Z^-]_{11} + [Z^+]_{22} + [Z^-]_{22}$ is held constant. In Case 1, $[Z^+] = [Z^-]$; in Case 2, $[Z^-] = 0$ and the inside surface is perfectly conducting; in Case 3, $[Z^+] = 0$. In each figure, Case 1 is plotted as a solid line, Case 2 as a dotted line while Case 3 is represented by a dashed line. Note that only Case 1 contains two null in the backscattering cross section when $\{[Z^+]_{11} + [Z^-]_{11}\} / 2 \times \{[Z^+]_{22} + [Z^-]_{22}\} / 2 = 1$, as predicted previously.

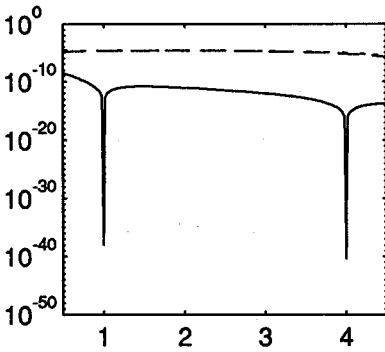


Fig. 1

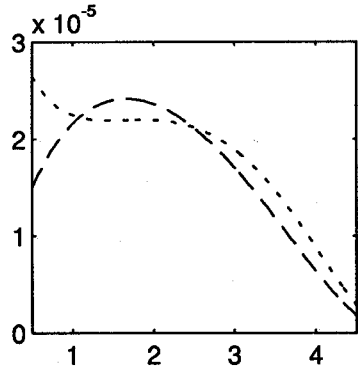


Fig. 2

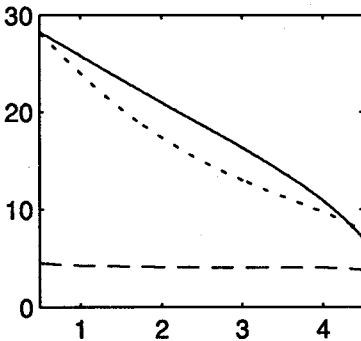


Fig. 3

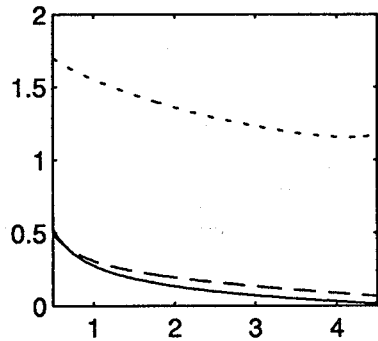


Fig. 4

PLANE WAVE SCATTERING BY TWO COALESCING SPHERES

R.H. MacPhie and T. Do-Nhat
Dept. of Elect. & Comp. Eng., University of Waterloo
Waterloo, Ontario, Canada N2L 3H1

In a classic paper (*IEEE Trans. on Antennas and Propagat.*, vol.AP-19, pp.391-400) Bruning and Lo treated the problem of electromagnetic plane wave scattering by two perfectly conducting spheres. Their formally exact solution used multipole field expansions for the waves scattered from the two spheres and the translational addition theorem for these multipole fields. However, in all cases the spheres were physically separated from each other, although the limiting case of two spheres in point contact was treated.

In this paper we consider the problem of two coalescing spheres A and B, as shown in Fig. 1. The plane wave is incident at the angle α with respect to the z axis and has a polarization angle γ between E and the projection of OO' on the incident wavefront. As did Bruning and Lo, we assume multipole expansions of the fields scattered from spheres A and B given in the spherical coordinate systems centered at O and O' respectively. Enforcing of the boundary conditions that $\vec{E} \times \hat{n} = 0$ on sphere A for $\theta_0 < \theta < \pi$ and on sphere B for $0 < \theta' < \theta'_0$, together with the use of the translational addition theorem (Bruning and Lo, AP-19, p.389) to express the scattered fields of sphere A in terms of the coordinates of sphere B, and vice versa, leads to a linear system of equations for the unknown amplitudes of the multipole fields scattered from each sphere. Due to the reduced ranges of θ and θ' , the orthogonality of the multipole vector fields (see Stratton, *Electromagnetic Theory*, McGraw-Hill, 1941, pp.417-418) no longer exists and complicates the resulting matrix elements associated with the E-field matching on the two partial spheres. Nevertheless, exact closed form expressions for the matrix elements are obtained.

Numerical results will be presented for a variety of configurations of the two coalescing conducting spheres.

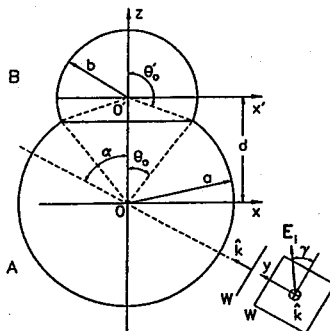


Fig 1. Plane wave incident on two coalescing spheres

Methods for Evaluating the Performance of Electromagnetic Scattering Prediction Codes

*J. P. Meyers, A. J. Terzuoli, Jr., G. C. Gerace, P. F. Auclair
Air Force Institute of Technology*

The ability to accurately predict electromagnetic scattering from arbitrary objects is of general interest within the electromagnetic community. Many computer codes exist that predict electromagnetic scattering from arbitrary objects. A code must be validated before it can be used to make useful predictions of Electromagnetic scattering from arbitrary objects. This typically involves making predictions of scattering from test objects for which the scattering pattern is known. These predictions are then compared with either measured data, exact analytical solutions, or results from other prediction codes.

Traditionally, only a qualitative comparison has been performed while validating prediction codes. These qualitative comparisons involve overlaying plots of measured and predicted data. This approach does not provide enough useful information about subtle differences between predicted and theoretical results. In addition, it does not provide a mechanism by which various predictions can be compared to each other.

This paper presents a quantitatively based method of analyzing prediction code accuracy. A high frequency based prediction code, XPATCH, is chosen as a sample code for which the method was demonstrated. Several validation issues are addressed. These issues include using measured data as a reference base, effects of geometry modeling errors, and comparing arbitrary, rapidly varying scattering patterns.

Once a quantitative set of metrics exist to measure a code's performance, it is possible to use these metrics to locate optimal input parameters for the prediction code. One such approach is the Response Surface Methodology (RSM). An RSM approach was used to model the prediction error as a function of the various input parameters used by the prediction code.

The methods presented in this study are independent of the specific prediction code being used to perform the predictions. Therefore, they are applicable to the entire set of prediction codes. They also provide a common method for comparing a group of prediction codes to each other.

A Fast and Accurate Three-Dimensional Multiple Scattering Approach Involving Large Conductivity Contrasts

Tarek M. Habashy* and Carlos Torres-Verdín

Schlumberger-Doll Research, Old Quarry Road, Ridgefield, CT 06877

Extending our previous work on a new nonlinear electromagnetic scattering approximation (Habashy et. al., *J. Geophys. Res.*, 98, 1759-1775, 1993; Torres-Verdín and Habashy, *Radio Sci.* 29, 1051-1079, 1994), we have developed a fast numerical scheme to efficiently simulate multiple scattering due to an arbitrary collection of 3-D objects. Unlike the method of moments, this procedure does not require the inversion of a full matrix to estimate the values of the electric field inside the scattering objects and yet remains accurate for a large range of conductivity contrasts, thereby allowing the fast simulation of scattering arising from geometrically complex models.

Our scattering formulation is based on the integral equation for the electric fields, which is first solved for observation points within the scatterers. In so doing, we take advantage of the knowledge that the Green tensor is singular at the observation point, hence allowing the internal electric field to be approximated by a Taylor series expansion around the observation point. This is justified by the assumption that the internal electric field is a smoothly varying function with respect to the Green tensor. The resulting expression is exactly equivalent to the one obtained by expressing the highly localized Green tensor in terms of a Dirac-delta function expansion.

The first term in the Taylor series expansion of the internal field gives rise to a simple analytical solution which we have termed the Localized Nonlinear Approximation. This first-order solution for the internal electric field is expressed as the projection of the background field onto a scattering tensor. The latter tensor is governed, in a nonlinear fashion, by the distribution of scattering objects, their geometries and conductivity contrasts, but is independent on the source of excitation. Moreover, the scattering tensor accounts for amplitude, phase, and polarization distortions of the background field which arise as a consequence of the interaction among scatterers.

The second term in the Taylor series expansion of the internal electric field accounts for gradients in the electric field. We have also developed a procedure whereby this term can be taken into account when producing a higher order approximation of the internal electric field. This results an expression that involves both the background electric field and its gradient projected onto a new scattering tensor which is determined by the Green tensor and its gradient. We present simulation results for the external electric field obtained with the new approximations assuming a collection of 3-D objects. These simulations results are compared against those obtained from a finite-difference code.

Modeling Three-Dimensional Scattering Using TransFinite Elements

Xingchao Yuan*, Dinkow Sun, and Zoltan Cendes
Ansoft Corporation
Pittsburgh, PA 15129

The transfinite element method (TFEM) (Z.J. Cendes and J.F. Lee, *IEEE Trans. on Microwave Theory and Techniques*, Vol.36, No.12 pp.1639-1649, Dec. 1988) has been applied successfully to solve the vector wave equation using tangential vector elements. The application of such procedure has predominantly been to model closed structures such as connectors, waveguide transitions, and resonators. Last year we reported adding second order vector absorbing boundary conditions to allow the TFEM to model radiating problems for EMI/EMC and antennas application (X.C. Yuan, D.K. Sun, and Z.J. Cendes, 1994 IEEE AP/URSI Joint Symposium, URSI Digest, pp. 29).

In this paper, the vector wave equation is solved by reformulating the transfinite element method to solve for the scattered field. The main feature of this new formulation are: (1) It retains all advantages of the previous TFEM such as modeling ports using eigenfunctions and extracting accurate S-parameters for radiating structures; (2) Radiating and scattering problems can be modeled at the same time; (3) Both bistatic and monostatic radar cross section may be extracted with a single matrix LU decomposition; and (4) The computer time required to model scattering problems is minimized by using second order vector ABCs and adaptive meshing techniques.

In this talk, the theory and selected application of the procedure will be presented. The numerical results will be compared with results obtained by either analytical or numerical methods.

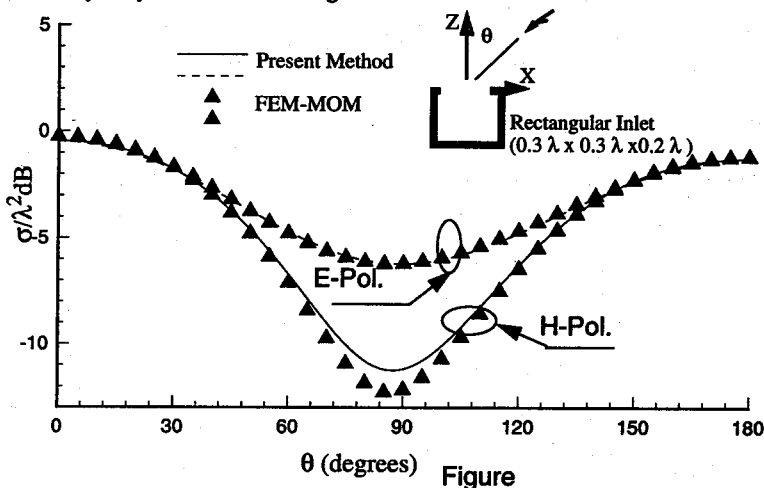
Electromagnetic Scattering From a Cylindrical Inlet Using Combined Field Integral Equations

M. D. Deshpande*, C. J. Reddy, C. R. Cockrell, & F. B. Beck, NASA LaRC,
Hampton, VA 23681

Summary

In the past electromagnetic characterization of a cylindrical inlet has been done using asymptotic techniques such as the geometrical optics ray method, the hybrid combination of asymptotic high frequency and modal methods, and the use of Gaussian beams (P. H. Pathak & R.J. Buckholder, IEEE Trans. APS-37, pp 635-647, 1989). However, these asymptotic techniques are applicable when the frequency is high or when the inlet is large in size compared to operating wavelength. For inlets with size comparable with wavelength, rigorous integral equation formulation such as those of earlier workers (Mitschang & Eftimiu, IEEE Trans. APS-30, pp.628-636, 1982) where entire domain expansion functions were used to represent the surface current density. The entire domain approach can be used to study regularly shaped cylinders. A need, therefore, exists to develop general analytical tools to determine low frequency electromagnetic characteristics of open ended waveguide cavities without a flange or open ended waveguide cavities recessed in a 3D conducting surface.

This presentation discusses an application of the combined field integral equation to determine EM scattering from a cylindrical inlet. EM fields outside the inlet required to setup equations are determined in terms of electric and magnetic surface current densities using free space Green's functions whereas EM fields inside the inlet are determined using waveguide modal expansion. The numerical results for a rectangular inlet are shown in Figure along with the results obtained by a hybrid method using FEM-MoM..



HIGHER ORDER STATISTICS OF SCATTERING FROM SMALL CLUTTER CELLS

Lisa Mockapetris
Applied Electromagnetics Division
Rome Laboratory
Hanscom AFB, MA 01731

For high resolution radars, the size of the illuminated clutter cell becomes small relative to the correlation distance. The study of the statistical variation of the scattering introduced by the physics of small clutter cells can lead to an understanding of how these changes will affect the performance of a radar system. For large clutter cells with many similar sized scatterers, the distribution is typically assumed to be Rayleigh. For small clutter cells the distribution deviates from Rayleigh. In particular, as the cell size decreases the variance of the scattered power increases. This effect was shown to become more prominent in the backscatter direction. Performance of a radar system can be severely affected by the changing distribution of the scattered power from small clutter cells.

Because the mean and variance do not completely specify the distribution of the scattering, calculation of the third moment will allow a better understanding of what the actual distribution is. The skewness will demonstrate how asymmetrical the distribution is and whether there are more returns above the mean value or below it. This information will further define what effects the clutter will have on a high resolution radar system. The distributions studied previously were completely specified by the mean and variance. Based on this, the skewness can be calculated for any of these two parameter distributions. If the scattering from the finite clutter cells follows any of these two parameter distributions, the calculated skewness for these small clutter cells will be the same as the skewness for that particular distribution. The skewness will then give us insight into which of these distributions, if any, best describes the scattering distribution of small cells.

In this paper a method for calculating the skewness of the scattered power from a finite clutter cell is developed. This skewness is then calculated for several different scattering parameters. Comparison of the calculated value of the skewness with the Rayleigh value of the skewness confirm that the scattering from small clutter cells is not Rayleigh, and this difference is more pronounced in the backscatter direction, which agrees with previous results from the variance calculations. The positive skewness for the non-Rayleigh distribution will have a negative effect on radar performance because more high energy values will result from the longer tails. Analyses are underway to determine the effect of parameters such as wavelength, rms surface height and cell size have on the skewness of the distribution. These results will then be used to determine what distribution functions most closely fit the distribution of the scattering from small clutter cells.

ON THE RAYLEIGH APPROXIMATION FOR ELECTROMAGNETIC SCATTERING FROM A SMALL SCATTERER

M. A. Karam*, A. Stogryn
Aerojet Electronic Systems Plant
1100 West Hollyvale Street
Azusa, CA 91702, USA.

ABSTRACT

For a small scatterer, the application of the optical (forward scattering) theorem on the scattered field obtained via the Rayleigh approximation leads to extinction loss value equal to the absorption loss only. To account for the scattering loss, it has been calculated by integrating the scattered field over a closed surface enclosing the scatterer. In this study numerical calculations over a spherical scatterer prove that such an approach for calculating the extinction loss under estimates the extinction loss values within the validity range of the Rayleigh approximation.

On the other hand, an improvement for the Rayleigh approximation is sought through approximating the Mie series solution of the field inside a spherical scatterer. Such an improvement is represented by an equivalent polarizability tensor relating the field inside the scatterer to the field exciting the scatterer. The extinction, scattering and absorption losses are formulated according to the developed polarizability tensor. Those losses are compared to each other to check if the extinction loss formulation conserve energy. The possibility of generalizing the developed polarizability tensor and the extinction loss formulations for non - spherical scatterers is investigated.

The results of this study can be used to give accurate representations for microwave interaction with rain drops and millimeter wave interaction with cloud particles. Such representations are of great interest for different scientific communities, e.g. remote sensing, communication, and meteorology.

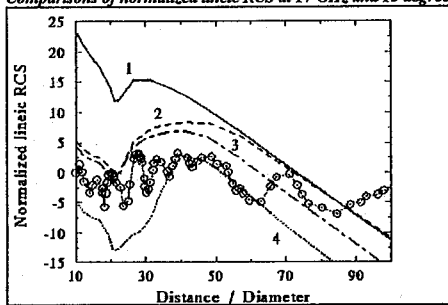
Electromagnetic Scattering from a Continuously Inhomogeneous Random Medium with Cylindrical Symmetry

Magali JEAN, MOTHEMIM Society
"La Boursidière" R.N. 186
92357 LE PLESSIS ROBINSON FRANCE
Tel : (1) 46 32 65 30
Fax : (1) 46 32 72 40

In the frame of the determination of the electromagnetic response of a recenter-vehicle, Born's approximation is used to determine the mean value of the turbulent Radar Cross Section (RCS) of an inhomogeneous cylindrical random medium, at oblique incidence. The mean medium is divided in a mean value and a fluctuating part. The novelty of the method is to take into account the mean medium by a renormalization procedure, in which the unperturbed solution is no longer the incident field in the vacuum but the field diffracted by the mean medium. Then only the diffraction due to the fluctuating part of the permittivity has to be considered. The fluctuations are approached by means of the turbulence spectrum given by Kolmogorov's theory. Our method is limited at the first order. It provides access to all single incoherent diffractions, i.e. including one diffraction by the fluctuating part of the medium and all multiple diffraction by the mean medium. Moreover all coherent diffractions are taken into account as they are solved exactly by the wave equation applied to the mean medium. Thus, we can determine the polarized as well as the depolarized diffracted fields, with only a first order or single scatter approximation.

Considering the mean medium, as the cylinder is in 2D geometry of revolution, it is split in concentric layers where the Gaussian profile of the permittivity is approached by a piecewise constant function. Thus using the properties of continuity and derivability of the Gaussian function, Maxwell's equations are solved in terms of modal tangential fields rather than electric and magnetic potentials, by making the steplength of the layers tend to zero. It leads us to a significant reduction of the linear system size which simplifies numerical calculations.

Comparisons of normalized lineic RCS at 17 GHz, and 15 degrees



Curve 1 : Born method. Curve 2 (and 3 : other spectrum) : renormalized method,
Curve 4 : Cross RCS and experiment (O).

It turns out that the fields which propagate in the mean medium are noticeably modified by the mean medium. Thus the renormalization affects considerably the assessment of the turbulent RCS of the wake. Moreover, the influence of the direction of incidence on the RCS levels is also analysed. In fact, it is even possible to define a critic angle for which there is a reflection area. For such angle, renormalized results are quite different from the classic Born results, but are close to experimental measurements. For this range of parameters, our method seems to be well adapted and relevant. But for various distances from the body, it overestimates the RCS levels. This may be due to incoherent multiple diffractions, which are not taken into account. Hence, we are interested in a renormalization with respect to the fluctuations, as we have performed with the mean medium. This would ensure a better compatibility with experimental results.

Parameter Estimation of Frequency Dependent Scatterers

JW Odendaal* and PA van Jaarsveld
Dept. of Electrical and Electronic Engineering
University of Pretoria
Pretoria, 0002, South Africa
E-mail: Wimpie.Odendaal@ee.up.ac.za

Super resolution algorithms are often modelling the backscattered field as a sum of non-dispersive scatterers (point-scatterers) in the presence of noise. For realistic microwave scattering, modelling errors are introduced by approximating the backscattered data as a sum of complex exponentials.

In this paper a super resolution radar imaging algorithm is presented to estimate the parameters of frequency dependent scattering centers. Previous algorithms apply an iterative approach to estimate the frequency dependence of each scattering center. The backscattered data are pre-multiplied by the inverse of an assumed frequency dependence. The pre-multiplication process is iteratively applied to estimate the frequency dependence of each scattering center contributing to the total backscattered field. This approach is computationally very intensive [A Moghaddar, Y Ogawa and EK Walton, *IEEE Trans. on Ant. and Propagat.*, 1412-1418, 1994].

In this paper the backscattered field is approximated by a sum of damped complex exponentials in noise. The computationally intensive iterative approach to estimate frequency dependence is overcome by deriving a relationship between the magnitude of the pole corresponding to the scatterer and the frequency dependence of the scatterer. The Matrix Pencil Method is applied to estimate the poles corresponding to the various scatterers. From the poles it is possible to estimate the positions and frequency dependence of the various scatterers contributing to the total backscattered field. The relative contribution from each scatterer can then be estimated using least squares solution.

The technique is applied to estimate the frequency dependence of scatterers using simulated and measured backscattered field data.

ITERATIVE MINIMUM DISCREPANCY METHOD FOR THREE-DIMENSIONAL SCATTERING PROBLEMS

Alexander B. Samokhin

Moscow Institute Radiotechnics, Electronics and Automatics,
78, Vernadsky av., 117454, Moscow, Russia

In this paper, we formulate iterative method of minimal discrepancies for solving some linear equations with non-self-adjoint operator and prove the theorem which determine the conditions for convergence of iterations. Further, based on volume integral equations (singular equations for electromagnetics problems and Fredholm equations of the 2nd kind for acoustics problems) we consider three-dimensional scattering problems by penetrable unhomogeneous bodies. By the help of energetic inequalities the feasibility of the iterative method to obtain a solution of the integral equations is demonstrated. For approximation of these equations the moment and collocation methods are applied. We prove that the approximate solution converges to the exact solution as number of basis functions or collocation points arises to infinity. To reduce the computing cost for calculating iterations, the direct and inverse discrete Fourier transformation are used. To accelerate the convergence of the iterations to the solution, the multistep method of minimal discrepancies which is a generalization of the above-mentioned iterative procedure is formulated. The efficiency of suggested algorithm for numerical solution of scattering problems in quasistatic and resonance ranges is investigated. The number of iterations required to obtain a specified accuracy versus the size of obstacle and permittivity is studied. The three-dimensional structures for which solutions with predicted precision could be obtained are determined. Numerical results are presented and discussed with the comparative data obtained by other numerical methods.

Electromagnetics in Biology and Medicine

C. M. Rappaport and K. M. Chen

Page

- 8:20 EM Wave Life-Detection System for Post Earthquake Rescue 120
Operations
K. M. Chen, Y. Huang, A. Norman, P. Ilavarasan,
Michigan State University*
- 8:40 FDTD Investigation of Electromagnetic Fields on Tumors 121
in the Head
*D. B. Dunn, A. J. Terzuoli, Jr., G. C. Gerace, Air Force Institute
of Technology, C. M. Rappaport, Northeastern University*
- 9:00 Mathematical Aspects of EEG Modeling by the Finite 122
Element Method
*Kassem A. Awada, David R. Jackson, Jeffery T. Williams,
Donald R. Wilton, University of Houston*
- 9:20 Currents Induced in a Person Standing Under or Near a 123
High-Voltage Power Line
Ronold W. P. King, Harvard University, Sheldon S. Sandler,
Northeastern University*
- 9:40 Modeling of Magnetic Field Stimulation of the Human Cortex 124
M. A. Abdeen, M. A. Stuchly, University of Victoria*
- 10:00 BREAK
- 10:20 Currents Induced in a Growing Monolayer of Biological Cells 125
in Low Frequency Magnetic Fields
A. El-Sayed, M. A. Stuchly, University of Victoria
- 10:40 Computation of the Response of a Realistic Human Body Model 126
to ELF Electric Fields
Trevor W. Dawson, Kris Caputa, Maria A. Stuchly, University of Victoria*
- 11:00 Magnetic Shielding of Cellular Phone Antennas 127
El-Badawy El-Sharawy, Craig Birtcher, Arizona State University*
- 11:20 Review and Recent Results for in-vivo Ocular Polarimetry 128
in the Presence of Biological Chiral Media
Sunghoon Jang, Laurence R. Welch, Martin D. Fox, Dan Censor,
University of Connecticut*

EM WAVE LIFE-DETECTION SYSTEM FOR POST EARTHQUAKE RESCUE OPERATIONS

K. M. Chen*, Y. Huang, A. Norman and P. Ilavarasan
Department of Electrical Engineering
Michigan State University, E. Lansing, MI 48824

A life-detection system utilizing electromagnetic wave at UHF range was constructed for the purpose of locating victims trapped under earthquake rubble. This system can also be used to detect small moving objects located behind a barrier.

The system operates on the principle that when an EM wave beam illuminates a trapped human subject, the reflected wave from him is modulated by the body movement which include heartbeat and breathing. Thus, when the reflected wave is received and properly demodulated, the heartbeat and breathing signals can be extracted. Since an EM wave at UHF range can penetrate walls and rubble to a great depth, it is possible to construct an EM wave life-detection system to locate passive victims trapped under a thick pile of rubble by measuring their heartbeat and breathing signals. Also from the recorded heartbeat and breathing signals, the physiological status of the victim can be determined.

The life-detection system consists of (1) a phase-locked generator which produces an EM wave at 450 MHz with a power of 100 mW, (2) a probing antenna which can penetrate into the rubble and a reflector antenna which can be placed on the rubble surface, (3) a microprocessor-controlled clutter cancellation unit, and (4) a signal processing and monitor system. The antenna is used to transmit the EM wave through the rubble and also to receive the reflected wave. The reflected wave received by the antenna consists of a large clutter signal reflected from the rubble and a weak signal reflected from the victim's body. The large clutter signal is cancelled by the automatic clutter cancellation unit which consists of a digitally controlled phase-shifter and attenuator. The uncanceled signal reflected from the victim's body is amplified and mixed with a reference signal so that low-frequency heartbeat and breathing signals can be extracted. The extracted signal is fed to a signal processing system to reduce background noise. The final output showing the heartbeat and breathing signals is displayed on a computer monitor.

Measured results showing the heartbeat and breathing signals from various human subjects lying under simulated earthquake rubble as well as the results from a field study test in a realistic earthquake environment will be presented in the meeting.

FDTD Investigation of Electromagnetic Fields on Tumors in the Head

*D. B. Dunn, A. J. Terzuoli, Jr, G. C. Gerace • Air Force Institute of Technology
C. M. Rappaport • Northeastern University*

Microwave hyperthermia as a means of treating cancer in humans has been explored for several years. The advantage of non-invasively focusing electromagnetic radiation within a volume of tissue may, without surgery, allow the preferential heating of tumors while sparing surrounding healthy tissue. Tumors in the brain are particularly well-suited for this treatment modality, since the head can be almost completely surrounded by an antenna applicator, yet the maximum required wave penetration depth is limited to about 10 cm. However, because of the complex structure of the head, the exact power distribution and heating profile due to a focused surface excitation is difficult to determine.

Rappaport and Morgenthaler (IEEE Trans. Micro. Thry. Tech., Dec. 1987) approached to the problem of irradiation of brain tumors by producing the optimal source distribution around a sphere of muscle tissue to realize maximum depth of heating. To do this they examined the solution to the spherical vector wave equation and optimized the odd-order spherical harmonics to distribute the power evenly around the surface of the sphere. This distribution of the power on the surface allowed for more power with lower surface maxima in the source distribution, thereby increasing the effective depth of muscle tissue through which a tumor could be treated.

This current paper looks at the optimal solution to radiating a deep-set brain tumor previously proposed and first duplicates the results with an FDTD computation at 9.15 MHz using 2.554 mm cubic cells, run on a 9.45 cm radius sphere. Exceptional correlation with only small errors found due to the dispersion and stair-stepping inherent in FDTD. The comparison showed a maximum error of 33%, and an average error of 2.446%.

Next, runs were performed on non-uniform concentric sphere tissue models. These runs were designed to simulate the skin, skull, and brain structure of a human head. As expected, considerable field spiking resulted at the two poles, but the spiking was confined to bone regions. Considering the low conductivity of bone this implies non critical power levels, even at these high field levels. In addition there was a small amount of spiking due to the stair step approximation of the spherical tissue boundaries. No spikes had power levels above that at the skin surface, and hence they are not critical.

These results were then extended by using a more accurate model of a human head within the sphere. The model was developed at Penn State University from a Microwave Resonance Image (MRI) of an actual human head, giving the locations of the different tissue types. Each location was then given the typical electrical characteristics for that tissue at 9.15 MHz. The model was assumed to be surrounded by a spherical liquid bolus, placed to allow the use of the same source distribution as that used around the homogeneous sphere model. The results for this run demonstrated considerable correlation to the concentric sphere model, which in turn fairly well duplicated the homogeneous sphere, except for high power levels at the top of the head. In addition, due to the inability to place a source in the neck region, anomalous results were found toward the bottom of the head. The head model produced higher power levels than the uniform model in the center due to the lower power dissipation through the bone tissue.

This study demonstrates the validity of spherical models for the head and showed that deeper penetration may be in fact possible. The tests were done on a small, approximate head model, but illustrate the application of FDTD analysis to an MRI scan of an actual human head, and show that even better results may be obtained in the realistic head model than the homogeneous model suggests.

MATHEMATICAL ASPECTS OF EEG MODELING BY THE FINITE ELEMENT METHOD

Kassem A. Awada, David R. Jackson, Jeffery T. Williams, and
Donald R. Wilton
Department of Electrical and Computer Engineering
University of Houston
Houston, TX 77204-4793

The finite element method (FEM) is one of the most versatile techniques for solving partial differential equations, such as Poisson's equation, when inhomogeneous medium is present. This method is becoming more important in the numerical solution of EEG problems because an accurate modeling of the conductivity variation within the brain and surrounding layers is necessary to achieve an accurate solution. In the FEM method the electric potential Φ is described by the Poisson equation,

$$\nabla \cdot (\sigma \nabla \Phi) = \nabla \cdot \mathbf{J}^p,$$

where $\sigma = \sigma(\mathbf{r})$ is an arbitrary conductivity profile and \mathbf{J}^p is the primary (dipole) current located at \mathbf{r}_0 . It is easy to directly implement the above equation in a standard FEM program. As an alternative, the potential Φ_0 from the source dipole in an infinite medium of conductivity $\sigma_0 = \sigma(\mathbf{r}_0)$ may be subtracted from the total potential Φ , and a new Poisson equation derived for the difference potential $\Phi_d = \Phi - \Phi_0$. This technique, which is denoted here as the subtraction method, results in a modified Poisson equation of the form

$$\nabla \cdot (\sigma \nabla \Phi_d) = -\nabla \cdot (\sigma_d \nabla \Phi_0),$$

where $\sigma_d = \sigma(\mathbf{r}) - \sigma_0$. The right-hand side of the above equation results in source contributions from the element boundaries in the FEM solution, requiring a flux integration for their computation.

One of the purposes of this presentation is to compare the above two implementations of the FEM method for solving the EEG problem. A 2-D transaxial MRI slice of the brain is used to provide realistic conductivity values for the study. It is shown that the subtraction method is usually more accurate, both for the forward and inverse problems, provided that the flux integrations are computed accurately. Even small errors in the flux contributions may be detrimental however, because the condition number of the FEM matrix is very high. The high condition number is a consequence of the Neumann boundary condition imposed at the outer boundary (the scalp). The physical reason for the high condition number is the existence of an eigenvector of the FEM matrix that corresponds to a very low eigenvalue. Numerical error in the computation of the flux integrations may result in an erroneously large excitation of this eigenvector, resulting in an inaccurate total solution. Results will be presented for both the forward and inverse solutions to help examine the physical consequences of the above conclusions.

CURRENTS INDUCED IN A PERSON STANDING UNDER OR NEAR A HIGH-VOLTAGE POWER LINE

Ronold W. P. King

Gordon McKay Laboratory, Harvard University, Cambridge, MA 02138

Sheldon S. Sandler*

Elect. & Comp. Engrg. Dept., Northeastern University, Boston, MA 02115

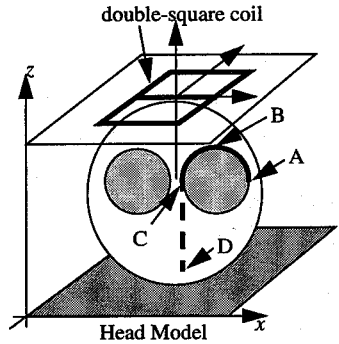
The six components of the electromagnetic field generated by a traveling wave in a three-phase, three-wire, high-voltage power line over a finitely conducting earth are determined analytically. The currents induced in the body of a man standing under or near such a power line consist of two parts. The first is the axial current induced by the transversely constant part of the vertical component of the electric field and the associated differential part of the transverse magnetic field. The second part is the circulating current induced by the vertically constant part of the horizontal magnetic field and the associated differential part of the vertical electric field. The axial current is determined from the integral equation for an electrically short parasitic antenna; the circulating current is obtained from an integral form of the Maxwell equation $\nabla \times \mathbf{E} = i\omega\mathbf{B}$. The analytically determined currents are shown to be in good agreement with those obtained by Gandhi and Chen (Bioelectromagnetics Suppl. 1, 43-60, 1992) using the FDTD method. From the total axial current, the current and power densities in different organs in the body can be determined if the shapes, sizes, and conductivities of these are known in each cross section.

MODELING OF MAGNETIC FIELD STIMULATION OF THE HUMAN CORTEX

M. A. Abdeen* and M. A. Stuchly. Electrical and Computer Engineering Department, University of Victoria, Victoria, B. C. V8W 3P6, Canada

Magnetic field stimulation of the human cortex has gained an acceptance in the clinical practice as a diagnostic tool for various neural disorders. The parameters of importance in this application are the magnitude of the activating function (the stimulus), the location of the stimulation, and the coil type, position, and orientation. In the previously published work the following models were analyzed: straight neurons in a semi-infinite, cylindrical, and spherical volume conductors, and neurons with bends in a semi-infinite volume conductor. In this work, we consider a bent neuron in an inhomogeneous spherical volume conductor. This model is suitable for study of magnetic field stimulation of the human cortex. The

human head is modeled by three spheres, as illustrated: a larger sphere represents the head, and the two smaller spheres represent the two halves of the human brain. Different conductivities are assigned to the small spheres from that of the remaining part of the large sphere. The neuron consists of two parts: a semi-circle ABC, and a straight part CD leading to the spinal cord. The neuron is located in a plane parallel to the x - z plane. Two stimulating coils are considered: a double-circular and a double-square each of two sections of 5 cm diameter or a side, respectively. Both coil shapes were previously analyzed and showed advantages compared with other shapes, except for a four-section (quadrupole) coil. The coil is positioned above the head in a plane parallel to the x - y plane in such a way that its longer dimension is perpendicular to the nerve.



The activating function is the spatial derivative of the electric field along the neuron. For bent neurons it depends on both the electric field and its derivative along the straight part of the neuron. In this problem, only the x and z -components of the induced electric field contribute to the neuron stimulation. The electric field within the problem space is obtained using the 3-D impedance method. A two-dimensional interpolation (linear) with a spline method is also used to obtain smooth field components and their derivatives along the neuron. The analysis shows that, the spatial derivative of the x -component of the electric field in the x -direction, i.e. $\partial E / \partial x$, contributes the most to the neuron stimulation. On the other hand, the x -derivative of the z -component of the electric field, i.e. $\partial E_z / \partial x$, decreases the activating function. For both coil configurations, the location of the stimulation is on the bent part of the neuron and is in the vicinity of point B (the highest point on the nerve). The optimum coil position is such that the coil centre is directly over the point B on the nerve, but the stimulation point is shifted towards C. The analysis also shows that the double-square coil produces stronger stimulus than the double-circular coil. This result agrees with that obtained for straight neurons, however, it is contrary to those obtained for bent neurons analyzed in a semi-infinite volume conductor. Although the model is simplified when compared to the anatomy of the brain, it is believed to be useful in clinical practice and as a start point for more complicated geometries of the neurons as well as the human head.

CURRENTS INDUCED IN A GROWING MONOLAYER OF BIOLOGICAL CELLS IN LOW FREQUENCY MAGNETIC FIELDS

A. El-Sayed and M. A. Stuchly
University of Victoria
Department of Electrical & Computer Engineering
Box # 3055, MS 8610
Victoria, B.C. V8W 3P6

In recent years there has been a considerable amount of research into biological effects of low frequency magnetic fields. Both experiments with animals and cell preparations in-vitro have been performed. Some of the in-vitro experiments have indicated interactions of fields with the cells, while other experiments have failed to observe any effects. Exposure conditions have frequently been poorly characterized. Furthermore, even similar exposure conditions can result in significantly different induced currents in the preparation. This was underscored in an earlier modeling (M. A. Stuchly and W. Xi, Phys. Med. Biol., Vol. 39, pp. 1319-1330, 1994).

In this study, we consider growing monolayer of cells in a petri dish. We investigate how the induced current density and pattern vary as the cells proliferate, forming clusters of increasing size, and culminating in a confluent monolayer. The cell diameter is 100 μm , and the dish diameter is 2.5cm. The conductivity of the medium is 1 S/m. The cell membrane conductivity is 10^{-7} S/m. The magnetic field is uniform and perpendicular to the axis of the petri dish.

The main challenge of the problem is due to the small dimensions of the biological cells as compared to the total computational space, leading to the need for a large number of computational elements. The finite element method (FEM) was selected to solve the problem, as the FEM elements (tetrahedrons) are naturally better conforming to the surface of a sphere or hemi-sphere that represent biological cells and their clusters than cubic elements used in finite difference methods. A commercially available package MSC/EMAS with an automatic mesher ARIES was used. A parametric study was performed to select the optimal mesh size, type of elements and location of the boundary conditions. The results for one of the cell configurations were also verified by a comparison with an analytical solution (for a low density of cells at the start of biological cell proliferation). The optimization considered the accuracy of results and computational resources required. These analysis indicated that the boundaries can be placed as close as 0.5 cm from the petri dish. The mesh size is different for the biological cells, the solute, and the surrounding space. The linear elements provide only marginally less accurate results compared to the quadratic ones, but with a very significant reduction of the CPU time. Typically, there were 2000 - 3000 nodes, CPU of 2-4 minutes and about 200 iterations.

Computation of the Response of a Realistic Human Body Model to ELF Electric Fields

Trevor W. Dawson*, Kris Caputa and Maria A. Stuchly
Department of Electrical & Computer Engineering
University of Victoria, Victoria, B.C., Canada

The Boundary Integral Equation and Impedance Methods are combined to compute the distributions of surface charge and current induced in a realistic model of the human body under the influence of arbitrary (uniform or non-uniform) applied ELF electric fields.

The process of computing the internal current distribution involves two stages. In the first stage, Laplace's Equation is solved for the electric potential exterior to the body model, treating it as a perfect conductor. The use of a Green's function appropriate to the exterior domain reduces the problem to the solution of an integral equation for the surface charge density over the body surface (K.-M. Chen, H.-R. Chuang & C.-J. Lin, IEEE Trans. Biomed. Eng., BME-33(8), 746-756, 1986). Incorporation of an image term in the Green's function readily allows for the inclusion a ground plane in the model. The source term is essentially the applied potential of the external field in the absence of the body, and so can be quite general. For example, both line charges, and compact charge distributions which can be well-described by a few multipole expansion coefficients, are particularly easy to implement. The integral equation is solved by both the point-matching (with one equation per element) and full Galerkin (with one equation per node) methods. Although the latter is more computer-intensive in that the matrix elements are defined by two double integrals, the fact that the inner integrals can be evaluated analytically greatly simplifies the task. This feature also means that setting up the coefficient matrix for the point-matching method is very quick in that all the matrix elements can be computed analytically, although the resulting system of equations is larger.

In the second stage of solution, the surface charge distribution is used as the forcing terms in the solution for the interior currents by the impedance method. At this stage, the full heterogeneous internal conductivity distribution of the model can be employed. The details of the internal conductivity distribution can have a significant influence on the resulting current flow, when compared to homogeneous or layer-averaged models (W. Xi, M.A. Stuchly and O.P. Gandhi, IEEE Trans. Biomed. Eng., 41(11),1-5,1994).

The human body model is essentially one that has been described earlier (O. P. Gandhi & J.-Y. Chen, Bioelectromagnetics Supplement 1, 43-60, 1992), based on published cross-sectional slices through human cadavers. However, the various cross-sections have been recently scanned into computer files, to allow curve fitting to the body and organ outlines. This process allows for flexibility in choosing the resolution used in solving the integral equation. The outline data for each slice are sampled by a discrete set of nodes, and the nodes on adjacent slices are connected to form a set triangular elements covering the body.

Resulting surface charge distributions and internal current flow patterns are presented for a variety of source configurations relative to the body model.

Magnetic Shielding of Cellular Telephone Antennas

El-Badawy El-Sharawy and Craig Birtcher
Department of Electrical Engineering
Telecommunication Research Center
Arizona State University
Tempe, AZ 85287

This paper presents a novel approach of shielding cellular phone antennas. The magnetic shield is comprised of a metallic shield loaded with a ferrite absorbing material. The metallic shield blocks most of the radiation from reaching the head of the human user. Adding ferrite layers to the metallic shield increases its impedance seen by the antenna. Since the dimensions of the shield is physically limited by the phone dimensions, the use of ferrite is imperative to avoid excessive loading of the cellular antenna due to close proximity to the metallic shield. Overall, the design objectives of this shield are:

- 1-Minimize radiation toward the human user to reduce potential health hazards that may be associated with exposure to EM signals.
- 2-To achieve the above goal without adversely altering the electrical performance of the antenna and the range of the cellular phone.
- 3-To keep the size of the antenna as small as possible to follow the trend in today user's electronics.

The measurements performed to date resulted in a) the "proof of concept" that the radiation pattern of cell phone antennas can be significantly modified through the application of ferrite-loaded elastomeric absorbing material (magram) in concert with a small metallic shield, b) some quantitative measure of the relative gains and reductions in the radiated power of the modified antenna compared to those of the unmodified antenna and compared to those of the antenna in the presence of the shield only, and c) some guidelines concerning the most effective placement of magram on the shield. The present configuration resulted in an increase in the far-field radiation pattern in the "desired" direction (away from the user) and a reduction in the far-field radiation pattern in the "undesired" direction (the human user).

Review and Recent Results for *in-vivo* Ocular Polarimetry in the Presence of Biological Chiral Media

Sunghoon Jang, Laurence R. Welch, *Martin D. Fox and (*) Dan Censor
Department of Electrical and Systems Engineering,
University of Connecticut, Storrs, CT 06269.

(*) on leave from the Department of Electrical and Computer Engineering,
Ben Gurion University of the Negev, Beer Sheva, Israel.

The idea of non-invasive optical measurements using animal and human eyes is presently scrutinized in the literature (e.g., G.X. Zhou et al., *Rev. Sci. Instrum.*, 1993; T.W. King et al., *Optical Eng.*, 1994). The prospect of non-invasive ocular polarimetry, for measurement of chiral media, exploiting transparent components of the eye, is especially important for glucose concentration monitoring in *diabetes mellitus* patients. Inasmuch as glucose is a chiral medium, polarized light passing through the aqueous humor behind the cornea is expected to show a change in the direction of polarization, and thus indicate the blood glucose concentration.

We will review a few approaches and discuss their problematics: Laterally directed corneal beams, Brewster angle reflection from the lens, and what seems at the moment the most promising approach--retinal retro-directed light. The electromagnetic theory for each approach is well understood, however, the meeting point of the theory, the biological components and the optical and electronic instrumentation involved raises grave questions regarding the feasibility of various methods. Through-the-cornea ray tracing seems to be impractical, if not altogether impossible, especially for the human cranial morphology. Reflections off the lens will be discussed, and results obtained by computing the relevant Jones matrices will be given. However, with the refractive index of the lens being only slightly different from the surrounding medium, the signal to noise level is expected to be low. We have experimented with light reflected from the retina, passing through the cornea, the aqueous humor, the lens and the vitreous humor. The sensitivity and signal to noise are very promising. The question of multispectral polarimetry, because of confounding chiral agents along the path, have not been addressed to date, but the outlook is optimistic.

One of the main points of interest involves the round trip of light travelling through a chiral medium and being returned from it by some mechanism. In the case of light returned by a perfect reflector, it is well known that the polarization rotation will be cancelled on the way back. In the case of reflection in the vicinity of the Brewster angle, it can be shown that under certain circumstances the rotation will be enhanced. The theory predicts that retrodirected light, as in the case of light returned by a corner reflector, can actually enhance the polarization rotation. Experiments carried out in our lab suggest that this is happening to light returned by the goat's eye retina used in our experiments.

Special Session

Page

Antenna Applications of Photonics

M. L. VanBlaricum and J. Moellers

8:20	Broadband Photonic Links for Shipboard Antenna Applications	130
	<i>S. A. Pappert*, C. K. Sun, R. J. Orazi, M. H. Berry, NCCOSC</i>	
8:40	Fiber-Optic Links for the VHF and UHF Antenna Manifolds	131
	<i>Drew E. Flechsig*, Irwin Abramovitz, Westinghouse Electric Corporation</i>	
9:00	Optical Analog Links using Linearized Modulators for Antenna	132
	Remoting <i>G. E. Betts*, F. J. O'Donnell, K. G. Ray, Lincoln Laboratories</i>	
9:20	Array Antenna Time-Steered by a Fiber-Optic Beamformer	133
	<i>Michael Y. Frankel*, Ronald D. Esman, Naval Research Laboratory</i>	
9:40	Wavelength-multiplexed fiberoptic true time delay steering system ..	134
	<i>A. Goutzoulis*, D. Davies, J. Zomp, P. Hrycak, A. Johnson, J. Moellers, Westinghouse</i>	
10:00	BREAK	
10:20	Remote Optical control and Tuning of Antenna Elements	135
	<i>Michael L. VanBlaricum*, Catherine J. Swann, Thomas L. Larry, Toyon Research Corporation</i>	
10:40	Digitally Reconfigurable Antenna	136
	<i>Kris W. Turk, California Microwave, Inc.</i>	
11:00	A Review of the Photonic Reconfigurable Antenna Technologies	137
	Study <i>Rosemary N. Edwards*, William C. Nunnally, University of Texas at Arlington, Bryan C. Miller, Robert B. Liechty, L. Keith Robinette, E-Systems</i>	
11:20	Optical Control of Scanning Oscillator Arrays	138
	<i>H. C. Chang, R. A. York*, University of California at Santa Barbara</i>	

Broadband Photonic Links for Shipboard Antenna Applications

S. A. Pappert*, C. K. Sun, R. J. Orazi, and M. H. Berry
NCCOSC RDT&E DIV 555
San Diego, CA 92152-5000
(619) 553-5704

The performance of microwave photonic links have progressed to the point where they are seriously being considered for analog transmission of shipboard antenna signals. Optical fiber transmission offers advantages in size, weight, bandwidth, EMI immunity, and receiver site flexibility over conventional coaxial or waveguide electrical transmission lines which are important issues for Navy surface ships.

In this paper, photonic links and modulation techniques to handle both broadband and narrowband antenna signals out to 50 GHz are described. Shipboard systems employing direct current modulation of laser diodes and external voltage modulation of integrated optic modulators will be described. Broadband semiconductor electroabsorption and lithium niobate Mach-Zehnder waveguide modulators are compared for shipboard use. The potential for each of these modulators to achieve RF link transparency with high dynamic range will be discussed. Shipboard results of an 18 GHz externally modulated photonic link used for topside electromagnetic environment (EME) monitoring will be presented. Results for a 2 GHz direct modulation photonic link for a multiband RF distribution system will also be described. For higher frequencies where efficient broadband modulators are not presently available, an optical RF mixing technique capable of efficiently translating microwave signals into and out of the millimeter wave range is also discussed. Conversion losses as low as 6 dB have been measured using this optical heterodyne technique.

FIBER-OPTIC LINKS FOR THE VHF AND UHF ANTENNA MANIFOLDS

Drew E. Flechsig* and Irwin Abramovitz
Westinghouse Electric Corporation
Electronic Systems
Advanced Technology Laboratory
Baltimore, Maryland 21203

Recent advances in laser and modulator technology are facilitating the development of high dynamic range optical links with performance levels that are suitable for phased array antenna applications. These high fidelity fiber-optic (FO) links offer the potential of supplanting conventional metallic waveguides and greatly reducing the weight of existing RF antenna manifolds. The light-weight fiber manifolds also provide immunity to EMI and support large signal bandwidths necessary for advanced radar systems. External and direct-modulation FO links have been demonstrated with large spurious-free dynamic range for potential application in antenna manifolds. In general, these links have been developed to extend the state-of-the-art and demonstrate the capability of the technology to satisfy one or more of the system requirements.

In this paper, we present the results of FO links developed to simultaneously satisfy a set of system flow-down requirements for VHF and UHF antennas. The link requirements are specified in terms of the link gain, bandwidth, noise figure, spurious-free dynamic range and maximum signal-to-noise ratio. The components which comprise these links are selected to satisfy the system requirements consistent with need to minimize the power, cost, weight and volume. We present the results of an external-modulation link in the VHF band with large dynamic range over the full operational bandwidth while maintaining low noise figure. In the UHF band, a direct-modulation link with improved dynamic range performance is reported. In order to achieve the low noise figure so that system sensitivity is not compromised, a low-noise amplifier is inserted at the RF input of the links. A summary of the link performance, with and without the LNA, is presented and compared to the system flow-down requirements.

Optical Analog Links using Linearized Modulators for Antenna Remoting

G.E. Betts*, F.J. O'Donnell, and K.G. Ray
Lincoln Laboratory, Massachusetts Institute of Technology
Lexington, MA 02173-9108
(617) 981-4429 fax (617) 981-5793 email betts@LL.mit.edu

Optical analog links for antenna remoting applications often require large third-order-intermodulation-free dynamic range and low noise figure together, and most need less than one octave bandwidth because most antennas are bandpass devices. We have developed a simple modulator, consisting of two standard Mach-Zehnder interferometric modulators (MZs) in series, optimized for exactly these criteria [1]. At frequencies <1 GHz, this modulator can be further simplified, with an increase in performance, by cutting it in the middle and adding a mirror: light passes through the modulator twice, effectively duplicating the series MZ structure but requiring only a single RF drive. We have constructed several links using both reflective and series linearized modulators, at center frequencies from 150 MHz to 4 GHz, and measured their performance.

The lowest noise figures were achieved at VHF frequencies by links with the reflective modulator configuration. We fabricated the modulator using Ti-indiffused lithium niobate and attached a mirror to one end. We tested the modulator in an analog link by using an optical circulator with the modulator on port 2, a 1321nm diode-pumped Nd:YLF laser on port 1, and a 300- μm -diameter InGaAs *pin* detector on port 3. The modulator bias point was set for minimum third-order distortion (second-order distortion, while present, is out of band). A noise figure of 6.0 dB (the lowest ever reported for a linearized link without a preamplifier!) was achieved at 150 MHz with a resonant impedance-matching circuit connected to the modulator electrodes. In a two-tone intermodulation test, the third-order intermodulation signal fell as the fifth degree of the input power, as expected for a linearized modulator. The intermodulation-free dynamic range was 85.5 dB for a 1-MHz noise bandwidth; for modulation depths where the fifth degree slope held, the bandwidth-normalized dynamic range was $134 \text{ dB}\cdot\text{Hz}^{4/5}$.

We tested links at frequencies up to 4 GHz, including links at the 900 MHz and 2 GHz cellular telephone bands, by using two of our 10-GHz-bandwidth modulators in series. These links had noise figures of 27 to 35 dB, and dynamic ranges of 75 to 88 dB. These modulators were not fully optimized to produce low noise figure links, but even if they were, the link noise figures would still be high enough that a preamplifier would be required for most applications. These links do, however, demonstrate a key advantage of external modulators: the dynamic range does not fall as the frequency increases into the microwave range.

These links operate over a wide temperature range and are practical solutions to applications requiring optical links with maximum dynamic range.

This work was supported by the Department of the Air Force.

1. G.E. Betts, *IEEE Trans. Microwave Theory Tech.*, vol. 42, p. 2642-2649, 1994.

Array Antenna Time-Steered by a Fiber-Optic Beamformer

Michael Y. Frankel* and Ronald D. Esman

Naval Research Laboratory, CODE 5672, Washington, DC 20375

We describe the implementation and characterization of a true time-delay fiber-optic beamforming network feeding an eight-element time-steered array (TSA) antenna in both transmit and receive modes. The beamformer requires only one wavelength-tunable laser for each steering dimension, provides feeds to each TSA element or subarray, is based on all commercially-available components, and has potentially high reliability and stability. The sparsely-populated TSA has an instantaneous bandwidth of 2 to 18 GHz in the transmit mode and shows squint-free steering over a $>100^\circ$ azimuth. In the receive mode, the antenna is microwave component limited to two elements, and shows a squint-free steering over $>70^\circ$ azimuth across a 6 to 16 GHz frequency range.

The optical source is a tunable fiber-optic σ -laser, which is amplitude-modulated, amplified, and fed to an 8-channel fiber-optic dispersive prism. Each channel of the prism feeds an individual InGaAs pin photodiode and a corresponding antenna elements. The active elements were separated by 7.5, 7.5, 7.5, 10., 10., 17.5, 12.5 cm to form a sparsely-populated array with a narrow main lobe and suppressed grating lobes at the expense of increased side lobe amplitudes. The lengths of the high-dispersion fiber ($D \sim 70$ ps/nm km) that were used were nominally 0, 138, 276, 414, 598, 782, 1104, 1334 m in each channel, with the overall nominal lengths equalized with zero dispersion fiber to 1350 m.

Array patterns were obtained as a function of the azimuth angle, and were corrected by an equivalent single-element pattern. Figure 1 shows the comparison between corrected measured and the ideal calculated transmit patterns with the array steered to -24° off broadside by a -10 nm laser wavelength detuning. Figure 2 shows the corrected measured receive patterns with the TSA steered to $+35^\circ$ by a -2 nm laser wavelength detuning. Both the transmit and receive patterns show no observable squint in the measured frequency range.

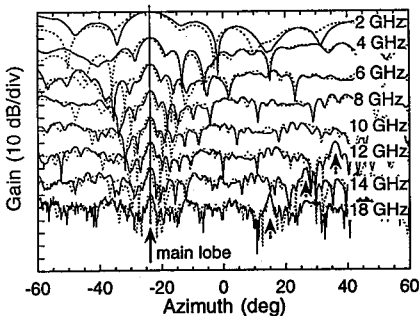


Figure 1. TSA transmit patterns steered to -24° off broadside. Solid-measured; dashed-calculated.

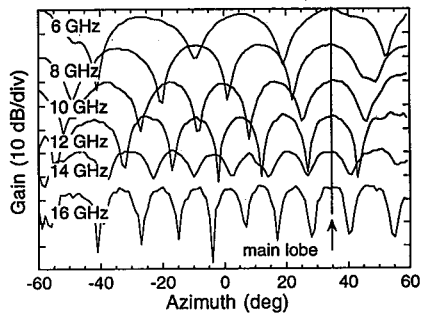


Figure 2. TSA receive patterns steered to $+35^\circ$ off broadside.

Wavelength-multiplexed fiberoptic true time delay steering system

A. Goutzoulis, D. Davies, J. Zomp, P. Hrycak^{*}, A. Johnson^{*} and J. Moellers^{*+}

Westinghouse STC
1310 Beulah Rd,
Pittsburgh, PA 15235

^{*} Westinghouse ESG
P. O. Box 1693,
Baltimore, MD 21203

ABSTRACT: During the last 3 years the Westinghouse Science and Technology Center in Pittsburgh has been developing fiberoptic TTD technology for broadband UHF and L-band high-performance radar applications. The TTD steering system is based on a unique architecture which employs both electronic and fiberoptic programmable delay lines in conjunction with optical λ -MUX to dramatically reduce system complexity, weight, volume, and cost. During September 1993 the first phase of the overall program (transmit) was completed, and the system was thoroughly evaluated in the laboratory. Following this evaluation, the prototype system was successfully demonstrated at the Westinghouse antenna range in Baltimore using a 2x16 element broadband antenna developed for future, high-performance surveillance applications. Squint-free photonic TTD beam steering over $\pm 45^\circ$ was demonstrated with a resolution of 1.8° over the full antenna-limited 0.6-1.5 GHz band. The range demonstration also showed satisfactory sidelobe level performance which was within 1.5 dB of theoretical expectations. We are now modifying the prototype system to demonstrate the receive operation. To this point we have developed broadband fiberoptic links operating over the 0.7-1.4 GHz with 0.5 dB ripple and $\pm 1.7^\circ$ of phase error, 4.7 dB of noise figure and about 68 dB-MHz spurious free dynamic range. In addition, we have identified optimum transmit-receive integrated TTD architectures and component requirements for low noise figure high dynamic range TTD systems.

Remote Optical Control and Tuning of Antenna Elements

Michael L. VanBlaricum*, Catherine J. Swann, and Thomas L. Larry
Toyon Research Corporation
75 Aero Camino, Suite A
Goleta, CA 93117
805-968-6787

Future generations of military platforms will require radar and communication systems with strict performance requirements: bandwidth of an octave or more; dramatic reduction in size and weight; low observability; and greater isolation from electromagnetic interference and crosstalk among hundreds to thousands of modules, subarray feeds, and elements. These requirements will drive innovative antenna element and matching network designs, antenna feeds, and control interfaces. The use of photonic-based antenna feeds, links, and controls opens the possibility of unique, very high performance antenna systems while meeting future stringent requirements.

In this paper we present the concept of using an optically controlled reactive element which can be placed either in the arms of an antenna element itself or in the antenna's tuning / matching network. In the case of using the reactive impedance as a control device in the arms of the antenna element, it will be shown that the antenna's pattern can be steered by varying the reactive value. Theoretical examples will be presented for broadband antennas such as spirals and helices. The optical feed will minimize the effect of the control lines on the antenna characteristics.

For receive only antennas there are many techniques that have been presented for optically bringing the RF signal from the antenna element back to the receiver. Hence, the antenna is optically isolated. However, if the antenna needs to be tuned or the matching network needs to be controlled then it is desirable to perform that function optically as well. An electrically small loop antenna is a good example. An electrically small loop can be tuned to have a very high Q which gives it a very narrow passband. We will show that a small loop can be tuned over almost an octave of bandwidth by using remote optical control via an optically variable reactance. Both theoretical and experimental results will be presented.

Digitally Reconfigurable Antenna

Kris W. Turk
California Microwave, Inc.
6022 Variel Avenue
Woodland Hills, CA 91367
Phone (818)712-4506 / FAX (818)712-4496

1.0 Abstract

This paper describes a lightweight, high gain, digitally reconfigurable antenna that utilizes Synaptic¹ antenna technology and Photistor^{TM2} device technology. We fabricated and tested a demonstration unit with switching junctions (Synapses) that change the type and size of the antenna in order to optimize its performance. The Synapses contain a number of optoelectronic switches (PhotistorsTM) controlled by light from a laser source. Optical energy is applied to the active area of a PhotistorTM by an optical fiber causing it to become conductive. This activates a particular portion of the radiating structure. Removal of the optical energy from a Synapse deactivates that particular portion of the radiating structure. The Synapses are switched by a microprocessor located at the base of the antenna that receives digital frequency information from a receiver and reconfigures the antenna in real-time to achieve the desired pattern and impedance match. A number of Synapses are used to achieve a multi-octave operational bandwidth.

First, I will present a brief history of this technology. Second, I will discuss the system design, fabrication techniques, and performance test results. Finally, I will present future recommendations.

¹ Patent Number - 4,728,805

² Trademark - California Microwave, Inc.

A Review of the Photonic Reconfigurable Antenna Technologies Study[†]

Rosemary N. Edwards* and William C. Nunnally
Applied Physical Electronics Research Center, The University of Texas at Arlington
PO Box 19380, Arlington, TX 76019
Phone: (817) 794-5100 FAX: (817) 794-5105

Bryan C. Miller, Robert B. Liechty and L. Keith Robinette
E-Systems Greenville Division, PO Box 6056, Greenville, TX 75403
Phone: (903) 457-5534 FAX: (903) 457-4413

A reconfigurable antenna element whose size, shape, and polarization can be dynamically modified is a desirable component for communications, radar, and surveillance systems deployed from airborne, seaborne, or space-based platforms. To date, most proposed reconfigurable antenna concepts have used a matrix of conducting elements connected by electronic/optoelectronic switches with the on-off pattern of the switches defining the size or shape of the antenna. For the past two years the Reconfigurable Antenna Technologies Study has been evaluating the potential of photonically excited silicon as a reconfigurable antenna aperture. As illustrated below, the photo antenna is produced by illuminating selected regions of a high resistivity silicon wafer with an antenna-shaped optical pattern. The impinging RF signal is received by the highly conducting region within the wafer and transmitted through metallized contacts to a standard RF balun and coax. The antenna geometry can be reconfigured to any shape consistent with the contact pattern by merely changing the optical pattern. This paper will briefly review the initial proof-of-concept results, the doped silicon antenna studies which examined RF performance as a function of conductivity, and the engineering development model that is currently being designed and fabricated.

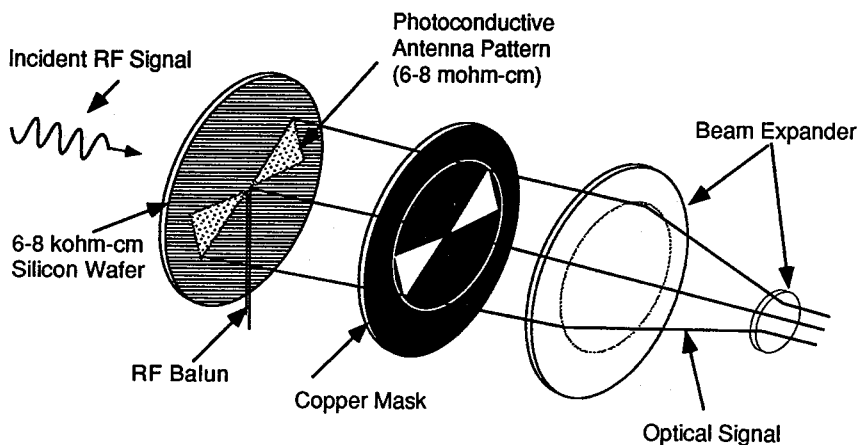


Figure 1. Reconfigurable Photonic Bowtie Antenna

[†]This work is sponsored by E-Systems Greenville and ARPA/Rome Labs.

Optical Control of Scanning Oscillator Arrays

H. C. Chang and R. A. York*

Department of Electrical and Computer Engineering
University of California at Santa Barbara

Santa Barbara, CA 93106

Tel: (805) 893-7113 FAX: (805) 893-3262

Abstract — Coupled-oscillator techniques show great promise for providing compact and inexpensive scanning transmit/receive systems for commercial applications such as collision avoidance radar and wireless communications [1,2]. These circuits are well suited to optical control, which allows the arrays to be manipulated remotely and also provides desirable isolation in electrically noisy ambients. Due to the simplicity and inherent efficiency of scanning oscillator configurations, it may also be possible to optically bias these arrays for low-power applications. This paper explores optical control of the scanning oscillator array using a small linear X-band prototype.

Scanning oscillators exploit the nonlinear injection-locking phenomenon. A set of standard voltage-controlled oscillators are coupled together by sections of transmission line, allowing the array to achieve coherence by mutual injection-locking. Each oscillator feeds a planar antenna. Simple models of the coupled oscillator interactions show that the phase relationships are a strong function of the oscillator tunings. If the inner elements are tuned to a common frequency, a linear phase progression can be synthesized by detuning the end-elements of the array in opposite directions. Optical control of this scanning process then amounts to optically controlling the peripheral VCOs. Thus only two control fibers are required in a linear scanning array. The information to be transmitted is provided by a third fiber which modulates the center element in the array. Since the oscillators are mutually synchronized, this is sufficient to modulate the entire array.

In this preliminary investigation, a simple optical detection scheme (Avalanche PhotoDiode and amplifier) is used. The VCO's are standard MESFET designs operating at 4 GHz, using an abrupt-junction varactor for frequency control. The optical detector circuit controls the varactor bias. The VCOs are followed by frequency doublers, which in turn feed a set of 8 GHz patch antennas. The frequency doublers are FET-based providing 2 dB conversion gain, and are utilized to double the phase-shift between the elements and hence extend the scanning range of the system.

- [1] R.A. York and P. Liao, "A new phase-shifterless beam-scanning technique using arrays of coupled oscillators", *IEEE Trans. Microwave Theory Tech., special issue on quasi-optical techniques*, vol. MTT-41, pp. 1810-1815, October 1993.
- [2] P. Liao and R.A. York, "Beam scanning with coupled VCO's", *IEEE Antennas and Propagation Society Symp. Dig.* (Seattle), pp. 836-839, June 1994.

Atmosphere and Propagation for Satellite and Terrestrial Communications

Page

J. Neves and A. Webster

- 8:20 Propagation Channel Characterization at 20 GHz and XPD 140
Frequency Scaling
A. Rocha, J. Neves, University of Aveiro
- 8:40 Estimation of Rain Structure and Ice Anisotropy by 141
Means of a Multipolarization Radiowave Beacon
*Aldo Paraboni, Centro Studi Telecomunicazioni Spaziali Piazza,
Antonio Martellucci*, Alberto Aresu, Fondazione Ugo Bordoni,
Rolf Jakoby, Deutsche Bundespost Telekom*
- 9:00 Attenuation and Noise Temperature of Non-Rainy Atmosphere 142
for Satellite Communication Systems
Francesco Barbaliscia, Marina Boumis, Antonio Martellucci,
Fondazione Ugo Bordoni*
- 9:20 Modelling of Attenuation Dynamic Measured by Radiometers 143
of the Colorado Research Network
Ed. R. Westwater, NOAA/ERL/ETL, Ermanno Fionda,
Antonio Martellucci, Fondazione Ugo Bordoni*
- 9:40 Extended Observations of Fading on Microwave Communications ... 144
Links
Alan R. Webster, The University of Western Ontario
- 10:00 BREAK
- 10:20 Lidar Atmospheric Measurements of Tropospheric Refractivity 145
during Developing Santa Ana Winds
D. W. Blood, C. R. Philbrick, Penn State University*
- 10:40 Detection and Physical Description of Clouds Making use of 146
Laser-Diode Ceilometer, and Upper Air and Surface
Meteorological Data
Francesco Barbaliscia, Marina Boumis, Ermanno Fionda,
Fondazione Ugo Bordoni*

Propagation Channel Characterisation at 20 GHz and XPD Frequency Scaling

A. Rocha

University of Aveiro, Aveiro, Portugal

J. Neves

University of Aveiro, Aveiro, Portugal

Abstract

The Olympus satellite offered an excellent opportunity to collect slant path propagation data over a wide frequency range. The propagation package consisted of three linearly polarised beacons: Bo, B1 and B2 at 12.5, 20 and 30 GHz respectively. Bo and B2 beacons had vertical polarisation while B1 was a dual polarised one making it possible to measure the full transfer propagation matrix.

A propagation receiver, able to receive all beacons and detect in phase and quadrature components for both copolar and crosspolar signals, was developed and operated at the University of Aveiro.

We made a model oriented data analysis on an event set with up to 35 events in order to study the properties of the propagation channel. Anisotropy, canting angle (real and imaginary part) and longitudinal homogeneity index were calculated after converting the event transfer matrix to circular polarisation and some joint statistics performed. Anisotropy and canting angle parameters are strongly related with the physical properties of the meteorological phenomena so they can be compared with data measured at other places and enabling possibly a better integration of meteorological data for developing future prediction methods.

Some conclusions about the rain and ice propagation medium behaviour, derived both from the event based analysis and statistical results, are presented.

As rain and ice XPD frequency scaling rules are different, prediction using physical parameters requires that a possible existing ice population and the underlying rain population can be separated and characterised. A model, recently suggested, was used to derive anisotropy and canting angle for both populations [A. Paraboni, A. Martelluci, 2^o Workshop-OPEX, Vol.2, 13-18, 1994]. The first order approach used gives the same results for cascaded or mixed medium however it can be easily shown that XPD amplitude for both cases is very similar unless population misalignment produce an high degree of cancellation (XPD too small to be measured with high accuracy or to be important). This model could describe very well our events even with mixed rain and ice. For a few events both populations anisotropy measured at 20 GHz were scaled to 12 and 30 GHz (using a MP drop size distribution, Rayleigh scattering for ice and frequency independent canting angle) and predicted XPD vector compared with the measured one giving promising results.

Some comments are given on the issue of the estimation of population parameters, their impact on XPD predictions and as a consequence how simultaneous B0 and B2 vector XPD measurements can contribute to fine tune the description of the propagation channel.

ESTIMATION OF RAIN STRUCTURE AND ICE ANISOTROPY BY MEANS OF A MULTIPOLARIZATION RADIOWAVE BEACON

Aldo Paraboni

Centro Studi Telecomunicazioni Spaziali Piazza L. Da Vinci 32, 20133, Milano, Italy

Antonio Martellucci*, Alberto Aresu

Fondazione Ugo Bordoni, Viale Europa 190, 00144, Roma, Italy

Rolf Jakoby,

Deutsche Bundespost Telekom, FTZ, Postfach 10 00 03, D-64276, Darmstadt, Germany

The OLYMPUS and ITALSAT satellites have been equipped with multipolarization radiowave beacons, at the frequency of 19.77 GHz and 50 GHz respectively, that permits the full assessment of the atmospheric transmission matrix, which is degraded by the presence in the atmosphere of non-spherical particles, like raindrops and ice crystals. Moreover these satellites have been designed with single polarization beacons, at 12, 30 GHz on the OLYMPUS and 20, 40 GHz on the ITALSAT satellite, that allow the measurement of attenuation and cross-polar discrimination ratio of the transmitted polarization. The measured atmospheric matrix can be used primarily to determine the cross-polar discrimination ratio of whichever polarization. Moreover the measurement of the transfer matrix permits the estimation of quasi-physical complex parameters, anisotropy and canting angle, which assume a physical meaning in various conditions and can be related to the microphysical properties of atmospheric hydrometeors. The development of a model that describes the dispersion of hydrometeors as formed by two families of moderately depolarizing particles (e.g. rain and ice) mixed or cascaded, permits the evaluation of the depolarizing properties of each family. This assessment is based on the assumption that the first family is formed by rain, whose microphysical properties are well known, while the second family is formed by ice and acts as a pure phase shifter. The concurrent presence of rain and ice can be revealed and their respective microphysical and depolarising properties evaluated by means of this approach, giving an accurate description of precipitation structure along the slant path. The accuracy of this estimation can be verified by comparing the cross-polar discrimination ratio predicted by this technique, using frequency scaling, with that measured using the single polarised beacon. The effect of ice on depolarization at various frequencies can be also assessed on a physical basis.

In this work the described technique has been applied to data measured in Italy, near Milano, using ITALSAT and OLYMPUS receiving stations, near Roma, using an ITALSAT station and Germany, near Darmstadt using an OLYMPUS station. The experimental results, obtained in different meteorological sites and using different experimental setup, confirm the assumptions done in the modelling and give a concordant description of precipitation structure aloft.

ATTENUATION AND NOISE TEMPERATURE OF NON-RAINY ATMOSPHERE FOR SATELLITE COMMUNICATION SYSTEMS.

Francesco Barbaliscia*, Marina Boumis, Antonio Martellucci
Fondazione Ugo Bordonis, Viale Europa 190, 00144, Roma, Italy

The design of satellite communication systems, working in the 20/30, 40/50 and 80/90 GHz frequency bands, requires an accurate evaluation of the impact of atmospheric propagation effects on system design parameters. Technology and regulation trends drive for the development of user oriented systems that are intended to work as low availability systems to complement existing terrestrial networks. Therefore the analysis of propagation factors is to be focussed on the effect of those atmospheric components like gases, clouds and light rains, which occur for larger percentages of time with respect to stronger rainfalls, the attenuation characteristics of which are at present better understood. A key parameter is the noise figure of the satellite communication system which can be affected by the noise collected through the earth-looking antenna. The noise collected by the antenna is characterised by random, regional and seasonal fluctuations of atmospheric parameters. In addition, the ground reflectivity can cause variations of the observed atmospheric brightness temperature.

In this work the analysis of attenuation and brightness temperature, as observed by a downlooking satellite antenna, due to oxygen, water vapour and cloud liquid water is performed. The brightness temperature is computed taking into account the ground reflectivity. The computation of propagation parameters is done in the atmospheric transmission windows contained in the frequency bands 20/50 GHz and 70/110 GHz, using the MPM93 model developed by H.J. Liebe and employing a meteorological database that has been collected and processed in the framework of the ESA/ESTEC Contract 10195/92/NL/GS. This database contains upper air (radiosonde) and surface meteorological data covering an observation period of 10 years and 320 geographical sites. The database has been enriched with data obtained via the application of models concerning tropopause profiles, ground reflectivity, cloud liquid water and atmospheric aerosols. The availability of a large meteorological database permits a full assessment of the statistical properties of propagation parameters. For example, the joint distribution of attenuation and atmospheric brightness temperature can be evaluated. The geographical and seasonal variability of propagation parameters can be also evaluated using averages of atmospheric profiles, determined for each site of the meteorological database on a monthly basis.

MODELLING OF ATTENUATION DYNAMIC MEASURED BY RADIOMETERS OF THE COLORADO RESEARCH NETWORK

Ed R. Westwater

NOAA/ERL/JETL, 325 Broadway, Boulder, Colorado, USA

Ermanno Fionda*, Antonio Martellucci

Fondazione Ugo Bordoni, Viale Europa 190, 00144, Roma, Italy

The assessment of dynamic properties of propagation parameters is relevant for the design of future satellite communication systems. This topic is the subject of a long term activity to study strong rain events which makes use of propagation experimental results, like that obtained using the COMSTAR, SIRIO and OTS satellites. The trend towards higher frequency bands, such as those that are employed in OLYMPUS, ITALSAT and ACTS satellites, and the development of Very Small Aperture Terminals (VSAT) requires to study also the dynamical properties of attenuation due to other atmospheric components such as gases, clouds and light rains. The total attenuation due to these components can be accurately determined by making use of multi-channel radiometric instruments, with frequencies selected taking into account the water vapour and liquid absorption spectra.

The data analysed in this paper were collected by a network of four zenith-viewing microwave radiometers, with frequencies of 20.6 and 31.65 GHz, covering the period from November 1987 to October 1988 and located in Denver, Platteville, Fleming and Flagler, Colorado, USA, with a spatial separation ranging from 50 to 190 Km. The sampling interval of the instruments was of 2 minutes. The measured sky noise temperature are used to derive attenuation up to about 12 dB with a good accuracy. The derived attenuation values are employed to perform statistical analysis of event duration by determining the number of occurrences and the duration of fades with thresholds ranging from 0.25 to 10 dB. The statistics of occurrences and duration are determined for each site and considering the data from all the sites as a single pool, in order to increase statistical stability of the analysis. The fade duration statistics of joint events, between couple of stations, are also determined. The duration values range from 3 minutes to several hours. This spread of duration is due to the different behaviour of atmospheric components like clouds and water vapour. The results of statistical analysis is used to perform the parameter estimation of a fade duration probabilistic model which is an evolution of that used in the COST 205. The statistics of occurrences and duration can be adequately modelled using a log-normal distribution, with parameters that change at different attenuation thresholds.

Extended Observations of Fading on Microwave Communications Links.

Alan R. Webster,
Department of Electrical Engineering,
The University of western Ontario,
London Ontario, CANADA. N6A 5B9.

Several years of observations have been made during the summer fading season on microwave communications links in Southern Ontario aimed at establishing the underlying causes of the signal fading and the associated statistics. The prime experimental tool has been a vertical wide-aperture array designed to measure the angle-of-arrival (AOA) and amplitude of individual rays in a multipath situation. Operating a frequency of 16.65 GHz, for practical reasons, the system is capable of a resolution approaching 0.1° in AOA over an unambiguous range of $\pm 0.7^\circ$. Samples of the complex amplitude across this array, together with the amplitude of a reference channel taken from a separate antenna, are taken once per second on a continuous basis. In order to enhance these experimental data, and to give better insight into the processes involved, acoustic sounding has been used recently to provide some information on atmospheric layering effects in the region of interest.

The bulk of the data has been accumulated on a 51 km link between Kemptville and Avonmore, Ontario, and the main system has been in operation on this link from 1989 through 1994. Previous observations had been made with the same equipment on two shorter links and data from these are presented for comparison where appropriate. One of the main features to date is the remarkable consistency of the statistical data from year to year. The distribution in AOA of the most significant ray paths under fading conditions indicate consistently elevated values for the strongest and the statistically reproducible occurrence of low amplitude ground reflected rays. This point is of some importance if counter-measures such as tailored antenna patterns are used in the design of such communications systems.

The fading itself arises from two clearly identifiable distinct processes involving defocussing effects in the first instance and atmospheric multipath in the second. The amplitude fading distribution in each case is significantly different, and similar overall effects are observed from year to year. The effects of these two distinct fading mechanisms on wide-band digital systems is likely to be different and comment is made on this point.

LIDAR ATMOSPHERIC MEASUREMENTS OF TROPOSPHERIC REFRACTIVITY DURING DEVELOPING SANTA ANA WINDS

D. W. Blood* and C. R. Philbrick
Applied Research Laboratory/Penn State University
P.O. Box 30, State College, PA 16804
(814) 863-7089, Fax (814) 863-8783

ABSTRACT

A multi-wavelength Raman lidar was used to measure profiles of water vapor, temperature and other atmospheric properties in the troposphere during the beginnings of the 1993 Los Angeles fire storm period with developing high velocity Santa Ana wind conditions. The PSU/LAMP lidar instrument was being used to make measurements at Point Mugu, CA for an observational campaign called VOCAR (Variability of Coastal Atmospheric Refractivity). The Raman technique provides an accurate way to measure the profiles of water vapor from the ratio of the Raman vibrational backscatter signal from water vapor to that of nitrogen. The lidar has been used both to obtain water vapor profiles from molecular Raman vibrational scattering at several wavelengths, and temperature profiles from Raman rotational scattering at 528 and 530 nm. The water vapor measurements have been made using the vibrational Raman backscatter intensity from the 660/607 ratio from the 532 nm, 407/387 ratio from 355 nm, or the 294/285 ratio from 266 nm laser radiation.

The measurements of the atmospheric refractive environment on October 26 and 27th, 1993 at Point Mugu, CA during the developing wind storm, produced an intense temperature inversion and gradient further producing an RF ducting condition in the lower troposphere. The lidar temperature and water vapor data were used to compute profiles of refractivity, N , and modified refractivity, M , at 75 m height intervals in the lower tropospheric region (surface to 5000 m). The lidar data, stored at one minute intervals, is examined with integration times of several minutes. The time history of these profiles shows a dramatic low altitude drying effect in the maritime boundary layer. This changes the atmospheric refractive condition from a strong refractive surface based duct to the complete absence of any ducting over a 5 hour period. Atmospheric variability decreases as the moisture is driven entirely out of the surface air layer. This anomalous type of refractive ducting is entirely different from the usual ducting conditions produced during more quiescent conditions, where an elevated or surface duct is frequently formed by a significant drop in water vapor near a temperature inversion. The time history of this rare developing atmospheric condition is shown and the corresponding physical parameters contributing to the refractivity effects are analyzed.

DETECTION AND PHYSICAL DESCRIPTION OF CLOUDS MAKING
USE OF LASER-DIODE CEILOMETER, AND UPPER AIR AND
SURFACE METEOROLOGICAL DATA

Francesco Barbaliscia, Marina Boumis*, Ermanno Fionda
Fondazione Ugo Bordoni
Viale Europa 190, 00144, Roma, Italy

ABSTRACT

In the development of the present communication systems operating at frequencies above 30 GHz, the presence of clouds, in particular in the lower part of the Earth's atmosphere, plays an important role being source of attenuation and affecting the quality of Earth-satellite links. Various techniques can be employed to investigate the physical features of clouds, including the use of the laser-diode ceilometer, that in addition to surface and upper air meteorological data, can be used to improve the present knowledge about the cloud features. In this paper the statistical evaluation of the cloud bottom height and of the fractional cloudiness, in addition to the estimation of the integrated liquid water content and water vapour content associated to different types of clouds, are presented. The analysis is based on the data of cloud bottom height, cloud coverage and vertical profiles of pressure, temperature and relative humidity, concurrently acquired by a laser-diode ceilometer, upper air soundings and ground-based measurements, for an observation period of 2 years, in the zone of Roma, Italy. In particular, to describe the statistical behaviour of cloud bottom height and of the fractional cloudiness, seasonal, daily and hourly statistical bases have been analyzed. Moreover, in a few particular events the evaluation of the cloud thickness and of the associated integrated water vapour and liquid water content has been performed, making use of thermodynamic models present in literature. For a more complete and accurate analysis of the results, a comparison with the concurrent meteorological ground observations has been done, as well.

Microstrip Antenna Analysis Methods

R. G. Rojas and D. De Zutter

Page

- 10:20 Analysis and Treatment of Edge Effects on the Radiation Pattern of a Microstrip Patch Antenna
Michael F. Otero, Roberto G. Rojas, The Ohio State University*
- 10:40 Extension of the Compression Approach to Include Device Metalizations in Electromagnetic Simulations
S. Ooms, D. De Zutter, University of Gent*
- 11:00 On The Space Domain Green's Function for Microstrip Geometries
S. Marchetti, J. M. Laheurte, Universite Nice-Sophia Antipolis*
- 11:20 A Full-Wave Analysis of Active Uniplanar Structures
E. Vourch, M. Drissi, J. Citerne, INSA/LCST*
- 11:40 A Moment-Method Analysis Technique for Microstrip Antennas 148
S. Adeniyi Adekola, A. Ike Mowete, University of Lagos*

A MOMENT-METHOD ANALYSIS TECHNIQUE FOR MICROSTRIP ANTENNAS

S. ADENIYI ADEKOLA*, Professor of Electrical Engineering
and

A. IKE MOWETE, Senior Lecturer in Electrical Engineering
Department of Electrical Engineering
University of Lagos
Akoka, Yaba, Lagos, Nigeria

Abstract

The main objective of this presentation is the development of a new analytical foundation for the electromagnetic characteristics of microstrip antennas. It is shown therein that when use is made of surface equivalent currents for the conducting patch and volume equivalent currents for the dielectric substrate, the problem reduces to that of evaluating the electric field in the substrate region. Based on the assumption that this electric field is related to the distribution of current on the conducting patch, it is further shown that the effects of the dielectric substrate can be accounted for by a perturbation of the generalized impedance matrix obtained for a corresponding "air-dielectric" microstrip antenna. Closed-form expressions are obtained for this additional generalized impedance sub-matrix, and representative results for the antenna parameters of current distribution and associated far-zone electric field obtained from a moment-method solution are given.

* To present the paper.

Special Session

Scattering by Wedges I

E. Marx and P. L. E. Uslenghi

Page

- 8:20 Electromagnetic Scattering by Wedges 150
Egon Marx, National Institute of Standards and Technology
- 8:40 A Formulation of Self-Similar Dielectric Wedge Diffraction
G. L. Wojcik, Weidlinger Associates
- 9:00 Scattering by a Dielectric Wedge: Oblique Incidence
Egon Marx, National Institute of Standards and Technology
- 9:20 Scattering by a Composite Wedge of Metal and Dielectric
Huen-Tae Ha, Jung-Woong Ra, Korea Advanced Insitiute of Science and Technology*
- 9:40 Geometrical Optics Exact and Approximate Solutions for 151
Metal-Dielectric Wedge Structures
P. L. E. Uslenghi, University of Illinois at Chicago, N. J. Damaskos, Damaskos, Inc.*
- 10:00 BREAK
- 10:20 Diffraction by a Second Order Impedance Wedge 152
Thomas B. A. Senior, The University of Michigan
- 10:40 Oblique-Incidence Scattering from Impedance and Coated 153
Wedges by the Method of Virtual Rays
N. G. Alexopoulos, University of California at Los Angeles, D. R. Jackson, University of Houston, P. Ya. Ufimtsev, J. A. Castaneda, Phraxos Research and Development, Inc.*
- 11:00 Diffraction at an Edge of a Truncated, Grounded Dielectric Slab 154
L. Borselli, S. Maci, L. Rossi, University of Siena, R. Tiberio, University of Florence
- 11:20 Scattering of a Plane Wave by a Dielectric Wedge 155
D. Bogy, University of California, Berkeley, B. Budaev, Steklov Mathematical Institute
- 11:40 Eigenfunctions of Wedge-Shaped Regions 156
Bair Budaev, Steklov Mathematical Institute
- 12:00 Towards Applied Adaptation of the Malyuzhinets' Solution 157
A. V. Osipov, St. Petersburg State University

ELECTROMAGNETIC SCATTERING BY WEDGES

Egon Marx
National Institute of Standards and Technology
Gaithersburg, MD 20899

The scattering of electromagnetic waves by wedges is a problem that has been addressed at least as far back as the end of the 19th century. In addition to the intrinsic challenges presented by these types of solutions of the Helmholtz equation, the presence of edges in finite or cylindrical scatterers provides an added incentive to the study of scattering by wedges. Similar problems occur in related fields such as those of heat transfer, acoustics, and fluid dynamics.

Monochromatic fields scattered by infinite perfectly conducting wedges have been determined rigorously. Some of the components of these fields diverge near the edge of the wedge, although the energy flow remains finite. Results of numerical calculations agree with the expected behavior of the fields. Edges in perfect conductors also have to be singled out for special treatment in approximations such as the geometric theory of diffraction.

The scattering of electromagnetic waves by dielectric wedges is less well understood. Simple power series expansions have been shown to be invalid for wedge angles that are rational multiples of π because coefficients of higher-order terms diverge. Terms with powers of $\log \rho$, where ρ is the distance of the field point to the edge of the wedge, have been added to avoid this problem. These power series expansions indicate that the behavior of the fields near the edge of the wedge is that of static fields that satisfy the Laplace equation. Nevertheless, numerical solutions of scattering problems show a different behavior. (The difference between rational and irrational multiples of π is not significant in numerical calculations. The forms of the solutions for these kinds of wedge angles also differs for perfectly conducting wedges.) Numerous other solutions of the exact and approximate scattering problems can be found in the literature.

The peculiar behavior of the fields near the edge of the wedge occurs at distances that are a small fraction of the wavelength, where the model of an infinite sharp wedge may have no physical significance. Nevertheless, the theoretical problem continues to draw attention and numerical solutions can be affected by these divergences. For instance, divergent unknown surface fields occur in the computation via integral equations of far fields scattered by bodies with sharp edges. Rounding off the edges is not helpful if three different media meet, as in multiple wedges. Similar problems occur in the scattering by three-dimensional bodies such as cones and bodies with curved edges or indentations. The remaining papers in this session give a taste of the lively interest of mathematicians, scientists, and engineers in problems related to wedge geometries in many different fields.

GEOMETRICAL OPTICS EXACT AND APPROXIMATE SOLUTIONS FOR METAL-DIELECTRIC WEDGE STRUCTURES

P.L.E. Uslenghi *

Department of Electrical Engineering and Computer Science
University of Illinois at Chicago, Chicago, IL 60607-7053

N.J. Damaskos

Damaskos, Inc., P.O. Box 469, Concordville, PA 19331

This work describes some exact and approximate geometrical optics solutions to the two-dimensional scattering by metal-dielectric wedge structures.

The exact solutions involve wedge configurations for which the edge of the wedge does not scatter under plane wave incidence in a direction perpendicular to the edge with the magnetic field parallel to the edge. Since the results obtained are based on the total transmission associated with Brewster's angle, they are valid for one direction of incidence only. Several different topologies involving single and multiple metal-dielectric wedges are examined, and the allowed combinations of wedge angles and dielectric constants are determined. A distinction is made between structures for which the geometrical optics exact solution is insensitive to frequency and frequency-dependent structures. For either category, two-dimensional metal-dielectric lattices are constructed and discussed. The results obtained are important for two reasons; first, they represent simple exact solutions for complex two-dimensional structures; second, they serve as benchmarks to validate other analytical and numerical techniques.

The approximate solutions are for the two-dimensional scattering of a plane wave of arbitrary polarization by a structure composed of a metallic wedge in contact with a penetrable wedge; the two wedges have arbitrary angles and a common edge. The primary wave may be incident either from air or from inside the penetrable wedge region; the geometrical optics field is determined in both regions. Formulas are given which allow the complete determination of the discrete spectrum of plane waves in both media. This geometrical optics solution is expected to provide a good approximation to the exact solution provided that the observation point is at a distance of several free-space wavelengths from the edge of the structure and is not near an optical boundary. Considerations are given to improving the solution by smoothing the transitions across optical boundaries via Fresnel-type integrals.

DIFFRACTION BY A SECOND ORDER IMPEDANCE WEDGE

Thomas B. A. Senior
Radiation Laboratory, University of Michigan
Ann Arbor, MI 48109-2122

Approximate boundary conditions have proved effective as a means of simplifying the analytical and numerical solution of electromagnetic problems. The standard (first order) impedance condition has been widely used to model the geometric and/or material properties of a surface, but the need to improve the accuracy has led to the consideration of higher order conditions whose order is determined by the highest field derivative present. In recent years, solutions have been developed for a plane wave incident on a half plane or wedge subject to second (and higher) order boundary conditions, but many of these are in error because of a failure to impose the additional constraints (or "contact conditions") at the edge necessary to ensure a unique solution of the boundary value problem. The constraints are additional to the standard edge condition. They are required for all boundary conditions of higher order than the first, and it is shown how they can be obtained from the standard uniqueness theorem for electromagnetic fields.

To illustrate their use, we consider the problem of the H-polarized plane wave

$$\mathbf{H}^i = \hat{z} e^{jk\rho \cos(\phi - \phi_0)}$$

incident on a right-angled wedge subject to the same second order boundary conditions

$$\prod_{m=1}^2 \left(\Gamma_m \pm \frac{1}{jk\rho} \frac{\partial}{\partial \phi} \right) H_z = 0$$

on the two faces $\phi = \pm 3\pi/4$, where ρ, ϕ, z are cylindrical polar coordinates and Γ_m are constants specified by the material properties of the wedge. Application of Maliuzhinets' method then leads to an *inhomogeneous* first order difference equation for the spectral function. It is shown that the most general solution consistent with the singularity and order requirements contains one arbitrary constant which is specified by the contact condition. The resulting solution is presented, and this is believed to be the first complete solution of a second order wedge problem.

Oblique-Incidence Scattering from Impedance and Coated Wedges by the Method of Virtual Rays

N. G. Alexopoulos
Department of Electrical Engineering
University of California at Los Angeles
Los Angeles, CA 90034-1594

D. R. Jackson*
Department of Electrical and Computer Engineering
University of Houston
Houston, TX 77204-4793

P. Ya. Ufimtsev and J. A. Castaneda
Phraxos Research and Development, Inc.
2716 Ocean Park Blvd., Suite 1020
Santa Monica, CA 90405
Houston, TX 77204-4793

The method of virtual rays is a novel technique for obtaining high-frequency scattering from canonical structures such as wedges. Originally introduced by Orlov, it was developed by Vainshtein and Ufimtsev, and applied to the problem of scattering from conducting wedges. A review of this method, including an extension to the case of impedance wedges and perfectly conducting wedges coated with thin material layers, is given in [J. Opt. Soc. Am. A, pp. 1513-1527, Vol. 11, April 1994]. The method of virtual rays for an infinite wedge starts by recasting the free-space Green's function $\psi(\mathbf{r}_1, \mathbf{r}_2)$ for the field at (r_2, ϕ_2) from a line source at an arbitrary position (r_1, ϕ_1) as an infinite sum of cylindrical waves centered at the origin, using the addition theorem. The Poisson summation formula is then used to convert this sum into one where the summand consists of an integral over the Bessel function order parameter ν . Each integral term in the sum is then geometrically interpreted as a set of "virtual rays" that initially propagates radially from the source until becoming tangent to a circle of electrical radius $\nu = k_0 r$. The rays then propagate around the circle a certain number of times (depending on the summation index) until shedding off and propagating towards the observation point. Scattering from a wedge is obtained by generalizing the summation by allowing for the virtual rays to reflect from the wedge faces as they propagate around the virtual circle. In the case of an impedance wedge or a coated wedge, the Fresnel reflection coefficients are used to determine the ray reflection at each wedge face.

In the previous formulation for wedge scattering, the formulation was for normal incidence, in which case the scalar function ψ represents either the A_z or F_z vector potential. For the case of oblique incidence, the polarization is not purely TE or TM, since cross-coupling occurs during reflection from the wedge faces. In this presentation, the method of virtual rays will be extended to the oblique-incidence case by accounting for such cross-polarization in the ray reflection. This is done by introducing reflection matrices that generalize the simple reflection coefficients in the normal-incidence case. Results are obtained for scattering from impedance and coated wedges. A comparison with measured RCS results is also given for a particular case of a wedge coated with a RAM material.

DIFFRACTION AT AN EDGE OF A TRUNCATED, GROUNDED DIELECTRIC SLAB.

L. Borselli¹, S. Maci¹, L. Rossi¹, R. Tiberio²

¹College of Engineering, Univ. of Siena, Via Roma 77, 53100, Siena, Italy

²Dep. of Electronic Engineering, Univ. of Florence, Via S.Marta 3, 50139, Florence, Italy

At high frequency, the description of diffraction mechanisms at edges in a grounded dielectric slab is of importance in several engineering applications. In particular, the need for taking into account such effects may arise when considering actual patch antennas on finite substrates; also, it may occur in predicting radar cross section of object with a dielectric coating. UTD diffraction coefficients from such canonical configurations may provide efficient engineering tool. Diffraction coefficients have rigorously been derived from the exact solution of a half-plane with surface impedance boundary conditions (b.c.) on one face and perfectly conducting b.c. on the other [1]. However, this solution fails for increasing substrate thickness, when the impedance b.c. approximation is no longer applicable. A more general solution of the canonical problem was obtained by the Wiener-Hopf technique in [2], where generalized impedance b.c. have been employed to model the slab. This latter solution allows to relax, but not to remove the condition of thin coating.

In this paper, the case of an electric dipole placed at the interface of a truncated, semi-infinite grounded dielectric slab is considered. In order to provide a practical tool for patch antenna application, a Physical Optics (PO) estimate is adopted for both the volumetric currents in the slab and the surface currents on the ground plane. In particular, the analysis consists of four steps. i) First, by applying the equivalence theorem the half-slab and the half-ground plane are replaced by polarization and surface currents, respectively, radiating in free space; ii) next, according to PO approximation, these currents are estimated from those existing in an infinite grounded slab, and their plane-wave, spectral representation is adopted; iii) then, the far field is obtained by end-point evaluation of the radiation integral of such currents; iv) finally, the spectral integral which is obtained at the previous step is asymptotically evaluated by the Van Der Waerden method of the steepest descent, taking also into account the presence of surface and leaky wave poles.

This procedure leads to uniform diffraction coefficients that provide an approximate but effective high-frequency description of the diffraction of surface and space waves. Within the expected limitations of a PO approximation, the present formulation is applicable to most substrate thickness of practical interest.

In order to improve the formulation, a more accurate description of the diffraction effects is attempted by introducing into the radiation integral of the polarisation currents the Green's function of a perfectly conducting half-plane or wedge.

[1] R.G. Rojas, "Electromagnetic diffraction of an obliquely incident plane wave field by a wedge with impedance faces," *IEEE Trans. Antennas Propagat.*, Vol. AP-36, No. 7, pp. 956-970, July 1988.

[2] H. C. Ly, G. Rojas, P. H. Pathak "EM plane wave diffraction by a planar junction of two thin material half-plane - oblique incidence" *IEEE Trans. on Antennas and Propagat.*, Vol. AP-41, No. 4, pp 429-441 1993.

SCATTERING OF A PLANE WAVE BY A DIELECTRIC WEDGE

D. Bogy and B. Budaev

Dept. Mech. Eng., University of California, Berkeley, CA 94720

Math. Institute, Fontanka 27, St. Petersburg, 191011, Russia

A classic problem of electromagnetic wave scattering by a dielectric wedge consists of solving the Helmholtz equations

$$\nabla^2 \phi_n + k_n^2 \phi_n^2 = 0, \quad n = 1, 2,$$

whose solutions are defined and bounded in contacted infinite sectors

$$I_1 = \{r > 0, -\alpha < \theta < \alpha\} \quad \text{and} \quad I_2 = \{r > 0, \alpha < \theta < 2\pi - \alpha\};$$

satisfy boundary value conditions

$$\phi_1|_{\theta=\pm\alpha} = \phi_2|_{\theta=\pm\alpha}, \quad \frac{\partial}{\partial\theta}\phi_1\Big|_{\theta=\pm\alpha} = \frac{\partial}{\partial\theta}\phi_2\Big|_{\theta=\pm\alpha},$$

and have a structure

$$\phi_1 = e^{ik_1 r \cos(\theta - \theta_0)} + \tilde{\phi}_1; \quad \phi_2 = \tilde{\phi}_2, \quad |\theta_0| < \alpha,$$

with terms $\tilde{\phi}_n$ satisfying radiation conditions at infinity.

The solutions ϕ_n are represented by Sommerfeld integrals

$$\phi_n = \int_C [\Phi_n(\omega + \theta - \epsilon_n) - [\Phi_n(-\omega + \theta - \epsilon_n)] e^{ik_n r \cos \omega} d\omega, \quad \epsilon_1 = 0, \quad \epsilon_2 = \pi,$$

along the standard contour C running from $-\pi/2 + i\infty$ to $3\pi/2 + i\infty$.

By use of an original analytic technique we locate all basic singularities of $\Phi_n(\omega)$ and obtain decompositions

$$\Phi_n(\omega) = \Phi_n^0(\omega) + \tilde{\Phi}_n(\omega),$$

where the singular components $\Phi_n^0(\omega)$ are predefined in explicit form and $\tilde{\Phi}_n^0(\omega)$ are given by explicit quadratures involving auxiliary functions

$$X_n(\omega) = \tilde{\Phi}_n(\omega + \alpha - \epsilon_n) + \tilde{\Phi}_n(\omega - \alpha + \epsilon_n),$$

which are proved to satisfy some canonical singular integral equations.

We already applied this approach to a similar problem of elastodynamics and calculated Rayleigh wave reflection and transmission coefficients in a traction-free elastic wedge. The numbers obtained in this way were in a good agreement with experimental data.

EIGENFUNCTIONS OF WEDGE-SHAPED REGIONS

Bair Budaev

Math. Institute, Fontanka 27, St. Petersburg, 191011, Russia

Consider a p -parameter family of series

$$\phi_p(r, \theta) = \sum_{\nu=-1}^{\infty} a_{\nu}(p) J_{p+\nu}(kr) \cos(p + \nu)\theta, \quad (1)$$

and a differential boundary operator T :

$$T\phi = \left\{ \mp \frac{2}{kr} \frac{\partial \phi}{\partial \theta} + \mu \phi \right\} \Big|_{\theta=\pm\alpha}, \quad \mu = \text{const.} \quad (2)$$

By use of the elementary properties of Bessel functions one can easily see that

$$T\phi_p = \sum_{\nu=-1}^{\infty} b_{\nu}(p) J_{p+\nu}(kr),$$

where

$$a_{\nu+1}(p) = \frac{b_{\nu}(p) - \mu a_{\nu}(p) \cos(p + \nu)\alpha - a_{\nu-1}(p) \sin(p + \nu - 1)\alpha}{\sin(p + \nu + 1)\alpha}, \quad (3)$$

and $b_{-1}(p) = 0, b_{-2}(p) = 0$.

Let a contour l together with the functions $b_{\nu}(p)$ provide a relation

$$\int_l \sum_{\nu=-1}^{\infty} b_{\nu}(p) J_{p+\nu}(kr) dp = 0.$$

Then the function

$$\phi(r, \theta) = \int_l \sum_{\nu=0}^{\infty} a_{\nu}(p) J_{p+\nu}(kr) \cos(p + \nu)\theta dp = 0$$

calculated in accordance with (3) satisfies the boundary conditions $T\phi = 0$ and the Helmholtz equation $\nabla^2 \phi + k^2 \phi = 0$, i. e., $\phi(r, \theta)$ is an eigenfunction of the wedge $\{r > 0, |\theta| < \alpha\}$.

By a special choice of the contour l and of the functions $b_{\nu}(p)$ we may obtain all already known kinds of Meixner's (power) series, of the generalized Meixner's series (with logarithmic factors), and to get exact representations of a complete sets of eigenfunctions for arbitrary parameters α and μ .

This approach may be equally applied to study wave fields in general wedge-shaped structures with arbitrary linear differential boundary conditions.

TOWARDS APPLIED ADAPTATION OF THE MALYUZHINETS' SOLUTION

A.V.Osipov

*Radio Physics Dept., Inst. of Physics, St. Petersburg State Univ.
Uljanovskaya 1 - 1, Petrodvorets, 198904 St. Petersburg, Russia*

There is no question that one of the most remarkable achievements in theoretical electromagnetics of 20-th century consists in obtaining a closed-form analytical solution for the diffraction of a plane wave in an angular region with impedance faces given by famous Russian scientist G.D.Malyuzhinets (*Dokl.Akad.Nauk SSSR* 121, 436-9, 1958). This model which according to the vertex angle value covers a broad variety of canonical structures, from an imperfect half-plane and an impedance wedge to a flat surface with an impedance step and a wedge-like hollow in an imperfectly conducting substratum, can serve as a universal basis for treating problems of electromagnetic scattering from complex objects, radio wave propagation over terrain features and in urban environments, as well as those of antenna designing and measurements. Nevertheless, the external complexity of the solution caused many researchers to use different mathematical methods (Wiener-Hopf, for example) which seem simpler and clearer but prove to be fundamentally restricted to rectangular geometries.

This report is intended to give an overview of author's recent results in the area of applied adaptation of the Malyuzhinets' solution, including its theoretical investigation, derivation of useful approximative formulas, and its generalization to more complicated cases in which the faces of the configuration are coated with an absorbing material. In particular, special attention will be focused on new algorithms for calculating Malyuzhinets' functions (A.V.Osipov, *Sov.Phys.-Acoust.* 36, 63-6, 1990), high-frequency asymptotic expansions of the solution for both exterior and interior wedges (A.V.Osipov, *ibid.*, 180-3; 287-90), series representations to evaluate the wave field in the near and intermediate zones (A.V.Osipov, *Sov.Phys.-Acoust.* 37, 733-40, 1991), derivation of the Green's function from the plane wave solutions (A.V.Osipov, *Proc. Int. Symp. on Antennas, JINA '94*, 270-3, 1994). Moreover, the report will present a promising generalization of the Malyuzhinets' technique to higher-order boundary conditions (A.V.Osipov, *J.Phys.A: Math.Gen.* 27, 27-32, 1994).

THIS PAGE INTENTIONALLY LEFT BLANK.

Remote Sensing of Terrestrial Media and Surfaces

K. Sarabandi and R. A. Simpson

Page

- 1:20 A Coherent Scattering Model for Tree Canopies Based on 161
the Fractal Theory
Yi-Cheng Lin, Kamal Sarabandi, University of Michigan*
- 1:40 Analysis and Application of Backscattered Frequency Correlation 162
Function
Kamal Sarabandi, Adib Nashashibi, University of Michigan
- 2:00 Effective Permittivity of a Two-Dimensional Dense Random 163
Medium: Comparison Between QCA and the Method
of Moments
Paul Siqueira, Kamal Sarabandi, University of Michigan*
- 2:20 High Resolution Radar Rain Backscatter Measurements 164
at NRL - Preliminary Report
William B. Gordon, Naval Research Laboratory
- 2:40 Application of Theoretical Models to Experimental Studies of 165
Hydrometeors by Dual-Polarization Radars
*A. B. Shupiatsky, S. V. Antipovsky, V. R. Megalinsky,
Central Aerological Observatory*
- 3:00 BREAK
- 3:20 Sensing of Ice Particles in Wintertime Thunderclouds Using 166
C-Band Dual Polarization Radar
Yasuyuki Maekawa Osaka Electro-Communication University,
Shoichiro Fukao, Kyoto University, Yasuo Sonoj, Kansai Electric
Power Company, Katsunari Masukura, Ministry of Construction*
- 3:40 Experimental/Numerical Evaluation of Sky-Wave Directed 167
Field for a Number of HF Antennas in the Vicinity of a Cliff
S. Saoudy, F. Hartery, D. Power, K. Hickey, Memorial University
of Newfoundland*
- 4:00 FDTD Simulation of Scattering from Objects near a Dielectric 168
Interface
J. E. Baron, G. L. Tyler, R. A. Simpson, Stanford University*
- 4:20 Coherent Multiple Scattering and Effective Polarization 169
Anisotropy of a Grass Layer
*S. K. Kamzolov, V. L. Kouznetsov, The Moscow State Technical University of
Civil Aviation*

4:40	Radar Determination of Ocean State Parameters with 170
	Microwave Signal Doppler Spectrum (Quasispecular Backscattering)
	<i>M. B. Kanevsky*, V. Yu. Karaev, Institute of Applied Physics,</i>
	<i>Russian Academy of Sciences</i>

A Coherent Scattering Model For Tree Canopies Based On The Fractal Theory

Yi-Cheng Lin* and Kamal Sarabandi

Radiation Laboratory

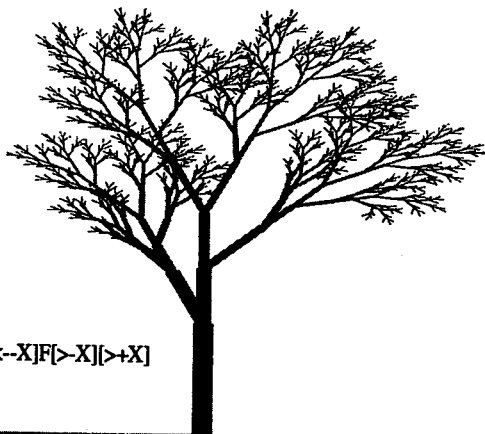
Department of Electrical Engineering and Computer Science

The University of Michigan, Ann Arbor, MI 48109-2122

Tel : (313) 936-1575

e-mail : yclin@engin.umich.edu and saraband@eecs.umich.edu

Vegetation canopies are usually represented by a three-layer (crown, trunk, and ground) random medium containing a mixture of random scatterers. However, the natural complex structures of trees follow certain patterns. The Lindenmayer systems (L-systems) is used to construct a tree with a more realistic branching structure using only a few parameters and simple algorithms (an example is shown below). Once the tree structure is formed scattering models for the constituent scatterers (branches and leaves) are used to find the scattering contribution from all the individual particles. In this model branches and tree trunks are modeled by straight cylinders with possible variability in radial permittivity and leaves are modeled by resistive sheets. The polarimetric bistatic scattering response of the tree is computed while the relative phases of the scattering components are preserved. In the computation of the scattered field, multiple scattering from the constituent particles are ignored. The statistics of the scattered field is obtained using a Monte Carlo simulation by generating many independent tree structures constructed from a stochastic L-systems algorithm. The backscattering coefficients and phase difference statistics are compared with other first order models such as radiative transfer. Also variations of the backscattering coefficients with the radar parameters, such as the incidence angle and frequency, and the physical parameters, such as biomass, soil moisture, and the ground plane tilt angle, are studied.



$n = 6$

$w : X$

$p1 : X \rightarrow FF[<+X]F[<-X]F[>-X][>+X]$

$p2 : F \rightarrow FF$

Analysis And Applications of Backscattered Frequency Correlation Function

Kamal Sarabandi and Adib Nashashibi
Radiation Laboratory

Department of Electrical Engineering and Computer Science
The University of Michigan, Ann Arbor, MI 48109-2122

Tel : (313) 936-1575

Email: saraband@eecs.umich.edu

In this paper a novel application of radar backscatter data to the classification and inversion of biophysical parameters of terrestrial targets is proposed. Traditionally in radar remote sensing, the backscattering coefficients and the backscatter phase difference statistics of a distributed target are used to estimate the biophysical parameters of interest. However, because of the complex nature of random media scattering problems, target classification and parameter inversion algorithms are very convoluted. One obvious way of enhancing the success and the accuracy of an inversion algorithm is to expand the dimension of the input vector space. In this paper some applications of a new measurable, namely the target frequency correlation function (FCF), for radar classification and inversion of biophysical parameters is proposed. Imaging radars and advanced scatterometers use a wideband signal as a means for measuring the range or enhancing the range resolution. In this process the frequency response of the target is measured over the chirp bandwidth which can be used directly to calculate the frequency correlation function. Depending on the radar parameters such as foot print (pixel) size, incidence angle and the target attribute (physical parameters) the backscatter signal decorrelate as function of frequency. In this paper, the frequency correlation function of random media is studied for the purpose of establishing a relationship between the physical parameters of the target and the measured correlation functions. Two classes of distributed targets are considered: (1) rough surfaces, and (2) random media. Analytical expressions for the frequency correlation function are derived and it is shown that the effect of radar parameters can be expressed explicitly and thus removed from the measured correlation function. The University of Michigan wideband polarimetric scatterometer systems are used to verify the theoretical models and algorithms developed in this study.

Effective Permittivity of a Two-Dimensional Dense Random Medium: Comparison Between QCA and the Method of Moments

Paul Siqueira* and Kamal Sarabandi

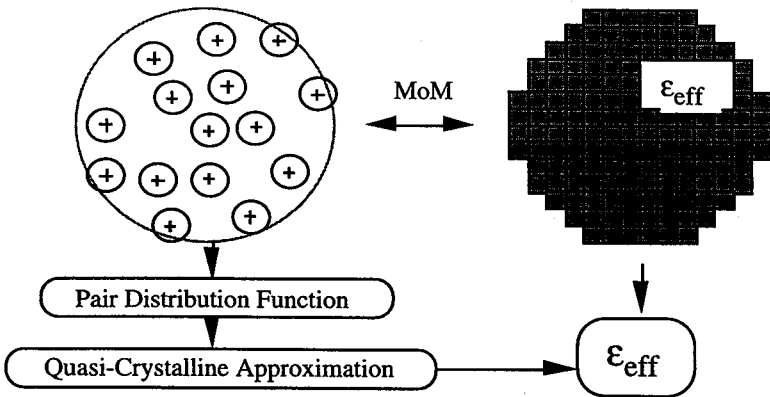
Radiation Laboratory, Department of Electrical Engineering and Computer Science,
University of Michigan, Ann Arbor, MI 48109-2122

Tel: (313)936-1575.

Email: siqueira@eecs.umich.edu, sarabandi@eecs.umich.edu

Effective permittivity in a dense, random medium characterizes the manner in which a coherent field propagates through the medium. When the medium consists of a dense (volume fraction $> 10\%$) arrangement of discrete scatterers, interactions between neighboring scatterers must be taken into account. Theoretically, this is accomplished by applying the Quasi-Crystalline Approximation (QCA: Tsang, Kong and Shin, Theory of Microwave Remote Sensing, John Wiley & Sons, 1985) where it is shown that the effective permittivity is dependent on the pair distribution function of scatterer centers. A common form of this function is given by Percus and Yevick (Physical Review, 1958) for hard disks; other pair distribution functions may be found by numerical simulation. Thus, given the pair distribution function, we may determine the effective permittivity via QCA. Alternatively, the effective permittivity may be found through the use of the Method of Moments by comparing the mean scattered field (coherent field) of a random distribution of scatterers confined in a known geometrical boundary with that of a uniform dielectric with the same geometrical boundary as the random distribution. By minimizing the differences between the mean scattered field from the random distribution and the scattered field from the uniform dielectric for a number of scattering directions, an effective complex permittivity can be found for the random distribution. This has been accomplished for both TM and TE polarizations in two dimensions.

An independent, integral equation based method has thus been developed that can be used to compare with theoretical results derived using QCA. This paper will offer a comparison between the two methods and thus provide a basis by which to test the range of validity of QCA.



Alternative routes for determining the effective permittivity

High Resolution Radar Rain Backscatter Measurements at NRL - Preliminary Report

William B. Gordon
Radar Division
Code 5311
Naval Research Laboratory
Washington, D.C. 20375

ABSTRACT

Rain backscatter measurements are currently being taken at the Naval Research Laboratory's Chesapeake Bay facility with an experimental high resolution X-band radar whose pulse widths can be varied between 10 and 700 ns. One of our main concerns is to relate properties of the Doppler power spectra to radar and environmental parameters. In standard models of stratiform rain the dominating factors producing spectral spread are expected to be differential raindrop fall rate for vertically pointing radars, wind shear for horizontally pointing radars, and it is anticipated that there should be a smooth transition from one case to the other as the elevation angle is scanned from 0 to 90°. In measurements so far obtained at vertical incidence we find that the reflectivity, mean Doppler velocity, and Doppler spectral spread vs. height profiles conform to a model proposed by Ekpenyong and Srivastava (1970) for precipitation falling through and below the melting layer. We have also taken low elevation angle data at heights well below the melting layer, but at present our low elevation data base is not sufficient to test the standard model. However, we have found that bimodal spectra are fairly common at low elevation angles, and we believe that these bimodal spectra at low elevation angles are produced by wind shear acting on inhomogeneities in the raindrop spatial distribution.

In our measurements of mean Doppler velocity and spectral spread we are careful to remove the effects of receiver noise. The spectra are thresholded by zero-ing out Doppler components that fall below a certain threshold ϵ whose value is set by specifying a value for the ratio (ϵ/Π) , where Π is the measured peak spectral value. More specifically, we set the ratio (ϵ/Π) for each radar dwell. Each dwell contains data from hundreds of radar range resolution cells, and since the value of Π varies from cell to cell, so does the value of ϵ . The ratio (ϵ/Π) must be made large enough to avoid noise generated errors, but not so large as to result in large deterministic errors which are produced by the thresholding itself. However, it turns out that the deterministic errors vary as the square of the ratio (ϵ/Π) ; hence the technique is simple, accurate, and robust.

Application of Theoretical Models to Experimental Studies of Hydrometeors by Dual-Polarization Radars

A. B. Shupiatsky, S. V. Antipovsky, V. R. Megalinsky

Central Aerological Observatory
Dolgoprudny, Moscow Region, 141700, Russia
Fax: (095) 576-33-27 or 200-42-10; Tel: (095) 408-77-14
E-mail: vvcao@sovam.com

Techniques which are currently used in weather modification—in particular, to suppress hail—are essentially aimed at modifying the microphysical processes occurring in clouds. In this connection, to detect the seeding effects when clouds are treated with nucleating material (ice-forming agents), the use of polarized radars appears to be promising, as they do allow determination of the microphysical state of clouds and precipitation from the measurements of echo parameters.

Theoretical models of polarization characteristics of radar signals from different kinds of clouds and precipitation are presented. Algorithms of the detection of a variety of hydrometeors are discussed. These algorithms were realized on the basis of air-borne and ground dual-polarization weather radars. These diversity-polarization radars are described.

Experiments have been carried out for studying the evolution of the microstructure of clouds and precipitation during their natural development and weather modification. The results of these studies have shown that polarimetric characteristics of radar signals make it possible to distinguish the microstructure and development stages of cumulonimbus.

In particular, from polarimetric characteristics a hail-fall region can be determined, and zones of large supercooled parts of the cloud are connected with the updraft regions. This serves as additional information for determining the seeding region in hail-suppression and intended precipitation-enhancement operations.

Typical vertical and horizontal sections of polarimetric characteristics and evolution of clouds during their natural development and weather modification are presented.

Sensing of Ice Particles in Wintertime Thunderclouds using C-band Dual Polarization Radar

Yasuyuki Maekawa*, Osaka Electro-Commun. Univ., Neyagawa, Osaka 572, Japan
Shoichiro Fukao, Radio Atmospheric Science Center, Kyoto Univ., Uji, Kyoto 611, Japan
Yasuo Sonoji, Kansai Electric Power Company, Amagasaki, Hyogo 661, Japan
Katsunari Masukura, Ministry of Construction, Tsukuba, Ibaraki 305, Japan

Along the coast of the Sea of Japan, thunderstorms frequently occur even in wintertime, as the northerly cold seasonal winds (monsoon) and convective motions due to the warm ocean current are increased. The wintertime thunderclouds are characterized by their low cloud top of 5-6 km and their oblique structure with the cloud top sloped leeward. These clouds often form a band-like structure associated with a cold front, and this makes it more difficult to predict lightning locations than those of isolated summertime thunderclouds. Also, very little is yet known about this type of thunderclouds and their mechanism for producing lightnings. This study uses the dual polarization radar technique to observe ice particles in the wintertime thunderclouds. The polarimetric information (ZH , ZDR) obtained from the dual polarization radar observation is then discussed in view of prediction of lightning time and location.

The C-band dual polarization radar used in this experiment is named the DND (Dobokuken-Nijuhenna-Doppler) radar of the Ministry of Construction. In the winter season, the DND radar was located at Sakata, Yamagata ($38^{\circ}55'32''N$, $130^{\circ}51'47''E$) in 1990-1991 and at Arai, Niigata ($37^{\circ}00'49''N$, $138^{\circ}14'32''E$) in 1992-1993. This radar has the operational frequency of 5280 MHz and the peak output power of 75 kW. The antenna beam width is 1.8° for both polarizations. The pulse repetition frequency (PRF) is 280 Hz and the pulse width is $2 \mu s$. The minimum detectable signal power of the low noise amplifier (LNA) is -107.5 dBm. In this experiment, the thunderclouds are primarily observed by scanning the antenna in azimuth at a rate of 6 rpm, and the four elevation angles of $3, 5, 7, 9^{\circ}$ or $4, 7, 10, 13^{\circ}$ are used to depict so-called CAPPI displays. A vertical section of cloud is then presented in the east-west of north-south direction to see the height distribution of ice particles.

Graupel and ice crystals are discriminated by their extremely low- and high- ZDR values, respectively. The observational results show that the graupel is lifted up to 5 km well above -10° level around the lightning location and approaches the ice crystals near the cloud top. Furthermore, compared with thunderclouds at the previous observational time, the graupel tends to descend to the cloud base, whereas the ice crystals tend to ascend to the cloud top. This situation just satisfies the recent thunderstorm electrification theories due to contact and mixing between these two kinds of ice particles. The height distribution of these ice particles is also confirmed by *in-site* measurements using radiosondes. Also, electric charge distribution of each ice particles obtained from the radiosondes indicates evidence of charge separation between graupel and ice crystals.

**Experimental/Numerical Evaluation of
Sky-Wave Directed Field for a number of
HF antennas in the vicinity of a Cliff**

S. Saoudy*, F. Hartery, D. Power and K. Hickey

Centre for Cold Ocean Resources Engineering
Memorial University of Newfoundland
St. John's, Newfoundland, Canada A1B 3X5.

The prototype High Frequency Ground Wave Radar (HF-GWR) which is located at Cape Race, Newfoundland, employs vertically-polarized antennas; a log periodic dipole array (LPDA) as a transmitter and a forty-element linear array (LA) as a receiver. The GWR lies on top of a 100-foot high cliff. The GWR vertically directed signals scatter from the ionosphere. Acting as a self-generated interference source, this sky wave mode contaminates the desired ground wave propagation mode returns. This leads to reduction in both the reception quality and the radar's maximum detection range, especially during daytime.

Since the level of the self-generated interference depends on the radiation characteristics of the *in situ* HF antennas, the need arises to evaluate their vertically directed field strengths using experimental and numerical techniques. Using the GWR system, the vertically-directed field strength of these antennas can be determined through measuring the self-generated ionospheric interference levels from the radar data. This is done by comparing the interference levels resulting from

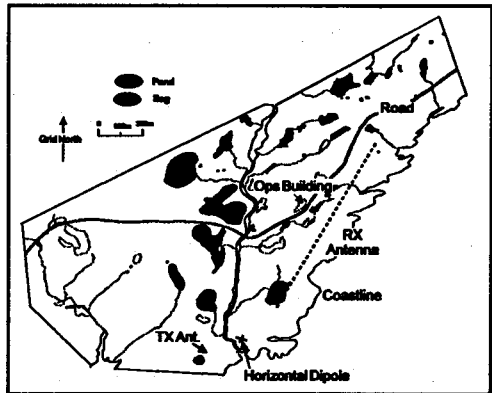


Fig 1: Cape Race GWR Geography

different antenna pairs with assorted radiation characteristics. These pairs are composed of three antennas, LPDA, LA and a half-wavelength horizontal reference dipole. The numerical results are obtained using both the Numerical Electromagnetics Code (NEC)- based on the moment method and Basic Scattering Code (BSC)-based on Geometrical Theory of Diffraction (GTD). The BSC code is used to account for diffraction effects at the cliff edge.

The measured ionospheric interference levels are correlated to respective cases of the numerically calculated vertically-directed field strengths. This correlation has produced a quantitative relation between antenna numerical modelling and self-generated interference levels in GWR systems. These specifications are needed to design optimal antennas for GWR applications.

FD-TD Simulation of Scattering from Objects near a Dielectric Interface

J.E. Baron*, G.L. Tyler, and R.A. Simpson
Center for Radar Astronomy
Stanford University
Stanford, CA 94305-4055

Interpretation of radar backscatter observations from geophysical surfaces is limited by the theoretical models available. Assuming a well-behaved, gently undulating surface and incidence angles near nadir, the primary contribution to the backscattered field is due to mirror-like reflection from suitably oriented surface facets. Under these conditions, quasi-specular models can be used to determine geophysical parameters such as dielectric constant and rms surface slope. At more oblique incidence angles, however, where the diffuse scattering contribution becomes important, these models no longer accurately predict the observed scattering behavior. The effects of small-scale surface structure, irregularities, and inhomogeneities, such as rocks, fractures, and pits, which are difficult to incorporate into theoretical models, can be studied using numerical methods. A combination of experimental data, theoretical models, and numerical simulations may provide a basis for improved geologic interpretation of radar backscatter observations.

Finite-difference time-domain (FD-TD) techniques have been used to study scattering from random rough surfaces in two dimensions [F.D. Hastings *et al.*, *URSI Digest*, p. 372, 1994 APS/URSI Symposium] and three dimensions [Fung *et al.*, *IEEE Trans. Geosci. Remote Sensing*, 986-994, Sept. 1994]. In order to study diffuse scattering mechanisms more closely, we have performed FD-TD simulations of scattering from discrete wavelength-scale objects in the presence of a lossless dielectric half-space (representing a "surface"), the primary difference between our implementation and those cited above being the manner in which the computation space is divided into total field and scattered field regions [Wong *et al.*, *Bull. Am. Astro. Soc.*, p. 1086, 1993].

Two-dimensional simulations indicate that the power backscattered from a wavelength-diameter dielectric cylinder (representing a "rock") resting on a surface decreases roughly by a factor of ten when the cylinder is buried tangential to the surface, for typical values of the constitutive parameters. Electromagnetic coupling between wavelength-scale rocks on the surface appears to be significant only for center-to-center separations less than approximately four wavelengths. Three-dimensional simulations, currently in progress, are expected to produce similarly informative results for more realistic cases, as well as additional polarization effects. By investigating the response of ensembles of scatterers, it may be possible to determine a statistical distribution of small-scale structure on a gently undulating surface that accounts for the discrepancy between backscatter observations and theoretical backscatter predictions at oblique angles.

COGERENT MULTIPLE SCATTERING AND EFFECTIVE
POLARIZATION ANISOTROPY OF A GRASS LAYER

S. K. Kamzolov & V. L. Kouznetsov

The Moscow State Technical University of Civil Aviation
Kronstadtsky Bld., 20, 125838, Moscou, Russia

A wave backscatter from earthly cover (by remote sensing) contain information from both vegetation and the ground. However the separation of this information is difficult as the canopy and ground effects on a wavefield are not additive. In this work we consider a scattering aspect isolated under limited conditions the information from vegetation. A grass layer is simulated as an assemblage of a randomly disposed finite-length dielectric cylinders normally oriented to ground. The multiple forward-scattering effects by such canopy slab are analysed. Essentially, this approach reduces to spectral-domain method developed for analyzing wave propagation in discrete and continuous random media (C. L. Rino, IEEE Trans. Ant. Prop. 36(8), 114, 1988; V. L. Kouznetsov & V. G. Budanov, Radiofizika, 31(4), 493, 1988, in Russian). We extend that method to vector wavefields propagating in discribed model of random media. A modification of the method concerns the revision of the averaging procedure of stochastic equations and its result is analogous to Novikov-Furutsu theorem. The results show that the phase speed of the wavefield by propagation along an oblique path is polarization-dependent. Thus two cross-linearly polarized waves propagate in the grass layer at different speeds. The difference between these speeds depends on grass spacing, relative permittivity of canopy and incidence angel of wavefield. The phase shift $\Delta\phi$ depends also on thickness of the grass layer. If the ground may be considered as a polarization-isotropic target, then the intensity of a target echo by exploiting circularly polarized waves is given by $I_c = 2 \cdot I_1 \cdot \cos^2(\Delta\phi)$, where I_1 is the intensity of a target echo by exploiting the linear polarization. The measurements of phase shift $\Delta\phi$ determine a bond of grass layer parameters.

RADAR DETERMINATION OF OCEAN STATE PARAMETERS
WITH MICROWAVE SIGNAL DOPPLER SPECTRUM
(QUASISPECULAR BACKSCATTERING)

M. B. Kanevsky* and V. Yu. Karaev
Institute of Applied Physics, Russian Academy of Sciences
46, Uljanov Str., 603600, Nizhny Novgorod, Russia
Tel: (8312)384528, Fax: (8312)365745,
E-mail: volody@hydro.nnov.su

Unlike the backscattering cross section the Doppler spectrum of microwave radar echo is not influenced by such ocean surface parameters as water temperature and salinity. At small incidence angles the Doppler spectrum depends on large ocean waves but not on the fast changing spatio-temporal field of ripple, i.e. on the ocean state parameters only.

Theoretical study of the microwave radar ocean echo Doppler spectrum at small incidence angles was carried out on the basis of the Kirchhoff method. The calculations were performed for the X-band radar signal and JONSWAP ocean wave spectrum model. The Doppler spectrum width and shift dependence on the radar beamwidth and radar platform velocity were also investigated.

It was shown that if the Doppler spectrum width and shift as well as the significant wave height are available (the latter from the simultaneous altimeter measurements) then one can determine the near surface wind speed, dominant wave length & direction and to find whether the ocean wave is wind generated or swell and its maturity (if windsea).

The nomogram allowing to find wind speed and fetch for wind generated waves as well as wavelength for swell is presented.

Also, it was shown that the area of the intermediate incidence angles where both the specular and Braggovian signals are present is very sensitive to the presence of oil slicks on the ocean surface because the Doppler spectrum abruptly changes in form when the slick appears.

Evidently, joint use of the Doppler spectrum and backscattering cross section for remote sensing of the ocean will allow one to improve the precision of wind speed determination and obtain additional information about the sea state parameters.

Hybrid Numerical Methods

X.-B. Xu and E. Heyman

Page

1:20	Hybrid Ray-FDTD Moving Window Solution for Long Distance 173 Modeling of Space-Time Wavepackets <i>B. Fidel, E. Heyman, R. Kastner, Tel-Aviv University, R. W. Ziolkowski, University of Arizona</i>	173
1:40	An Investigation on the Electromagnetic Shielding of Sources 174 Within a Ferromagnetic Pipe by a Hybrid Finite-Element and Unimoment Method Formulation Approach <i>Xiao-Bang Xu*, Xiaomei Yang, Clemson University</i>	174
2:00	Using the Integral Form of Maxwell's Equations to Modify and 175 Improve the FD-TD (2,4) Scheme <i>Mohammed F Hadi*, Melinda Piket-May, University of Colorado at Boulder</i>	175
2:20	Study of Numerical Dispersion and Stability of the Discrete 176 Surface Integral FDTD Method <i>H. Shi, J. L. Drewniak, University of Missouri-Rolla</i>	176
2:40	Waveguide Coupler Modeling with the Discrete Surface 177 Integral-FDTD Method <i>H. Shi, J. L. Drewniak, University of Missouri-Rolla</i>	177
3:00	BREAK	
3:20	A Modal Analysis Approach - An Exact Approach for the 178 Investigation of the Causes of Spurious Solutions in Finite Element Techniques <i>C. F. Bunting*, Old Dominion University, W. A. Davis, Virginia Polytechnic Institute and State University</i>	178
3:40	An Hybrid Finite Difference - Finite Volume Method for Solving 179 Maxwell Equations in Time Domain <i>A. D. Kalfon*, P. H. Klotz, Centre d'Etudes et de Recherches de Toulouse-ONERA</i>	179
4:00	Full-Wave Analysis and Design of Circular Waveguide 180 Dual-Mode Filters by an Hybrid Technique Finite-Element Mode-Matching <i>J. R. Montejo Garai*, J. Zapata, E. T. S. I. Telecomunicacion</i>	180
4:20	Computation of Wave Propagation on Microstrip Structures of 181 Arbitrary Shape Using TLM and FEM <i>Jun Wei Lu, Derek Gray, David V. Thiel*, Steven O'Keefe, Griffith University</i>	181
4:40	Method of Higher Order Basis Functions Applied to the MOM 182 Portion of the SWITCH Code <i>Y. C. Ma, M. I. Sancer, G. E. Antilla, Northrop Corporation</i>	182

5:00	Antenna Pattern Evaluations using a Hybridization of the 183
	Finite Element and High Frequency Methods
	<i>R. Kipp*, S. W. Lee, DEMACO, T. Ozdemir, J. L. Volakis,</i>
	<i>University of Michigan, L. Kempel, J. Berrie, Mission Research Corporation</i>

HYBRID RAY-FDTD MOVING WINDOW SOLUTION FOR LONG DISTANCE MODELING OF SPACE-TIME WAVEPACKETS

B. Fidel[†], E. Heyman[†], R. Kastner[†], and R.W. Ziolkowski[‡]

[†]Tel-Aviv University,
Department of Electrical Engineering - Physical Electronics
Tel-Aviv 69978, Israel

[‡]University of Arizona,
Department of Electrical and Computer Engineering
Tucson, AZ 85721

A hybrid ray-FDTD moving window scheme has been presented recently for the one dimensional propagation of electromagnetic pulses in homogeneous and inhomogeneous media [Fidel, Heyman, Kastner and Ziolkowski, 1994 AP symposium, pp. 1414-1417]. This paper describes further developments of this moving window method, including extensions to higher spatial dimensions. This method provides an efficient and accurate numerical approach for modeling the propagation of localized three dimensional space-time wavepackets in complex environments over large distances. The major difficulties in modeling such long distance propagation problems with an explicit, discrete numerical approach are the vast computer resources needed to discretize the entire region of interest and the accumulation of numerical dispersion error. The moving window FDTD method overcomes these difficulties because the discretization window is constructed only where the wavepacket is located and is progressively propagated together with the wavepacket. In inhomogeneous medium, the propagation trajectory of the wavepacket, and hence of the window, can be determined *á priori* by solving the corresponding ray equation subject to the appropriate initial conditions. The gross features of the discretization grid, i.e., its spatial and temporal support or the discretization cell, can also be determined *á priori* from the analytic equations of the wavepacket dynamics. The moving window FDTD approach is therefore naturally tailored into a Lagrange formulation of the wave equation involving the wavepacket local (or eigen) moving coordinates. Furthermore, this numerical scheme becomes dispersion-free for the forward propagating spectral components.

In this paper we shall present numerical results for wavepacket propagation in homogeneous and smoothly stratified medium. The boundary condition around the grid is a modified 1st order Mur that accounts for the movement of the coordinate frame. In homogeneous medium the results obtained are in agreement with known closed form wavepacket solutions.

An Investigation on the Electromagnetic Shielding of Sources Within a Ferromagnetic Pipe by a Hybrid Finite-Element and Unimoment Method Formulation Approach

Xiao-Bang Xu* and Xiaomei Yang
Department of Electrical and Computer Engineering
Clemson University
Clemson, SC 29634-0915

In this paper is presented the development of a numerical technique for investigating the electromagnetic shielding of sources within a ferromagnetic pipe. The structure is buried in the earth and is assumed to be infinitely long. There may be several current-carrying conductors, in arbitrary configuration, enclosed by the pipe. This numerical technique is developed based on a hybrid finite-element and unimoment method formulation (L.W. Pearson, A.F. Peterson, L.J. Bahrmassel, and R.A. Whitaker, IEEE Transactions on Antennas and Propagation, Vol. 40, No. 6, pp. 714-729, June 1992). The finite element method part is employed to analyze the region interior to the tube, and the unimoment method part is for treating the exterior regions. These two parts are coupled at the bounding surfaces of the pipe and coupled matrix equations for the unknown equivalent surface currents are formulated. In the development of the numerical technique, special attention is paid to the nonlinear B-H characteristic of the ferromagnetic pipe. An iterative solution procedure (D. Labridis and P. Dokopoulos, IEEE Transactions on Power Delivery, Vol. 7, No. 3, pp. 1060-1067, July 1992) is developed for determining the relative permeability in each element of the ferromagnetic pipe. The knowledge of the varying permeability in the pipe is then used to solve the matrix equations for the unknown equivalent surface currents, and subsequently, to calculate the electromagnetic fields at points of interest. Sample numerical results for the magnetic flux density observed outside the pipe are presented. They are compared with measurement data for validating the numerical technique.

Using the Integral Form of Maxwell's Equations to Modify and Improve the FD-TD (2,4) Scheme

Mohammed F. Hadi*
 Prof. Melinda Piket-May
 Department of Electrical Engineering
 University of Colorado at Boulder
 Boulder, CO 80309-0425

We have observed that applying finite-difference time-domain analysis to the integral forms of Maxwell's equations provides a more accurate model than with the differential forms. This is especially true when we encounter sub-cell material variations.

Based on this observation we succeeded in starting with the standard (2,4) scheme (second-order finite differences in time and fourth-order finite differences in space) which was derived using the differential Maxwell's equations, and modifying it to provide a more accurate representation of the integral Maxwell's equations. The end result being a marked improvement in the spatial dispersion behavior over the standard (2,4) scheme as shown in Fig. 1.

Fig. 1a compares the dispersion error-grid resolution relation of our modified (2,4) scheme with the standard (2,2) and (2,4) schemes. In Fig. 1, ν is the courant number which is defined as $\Delta t_{\max}/\Delta t$. For the standard (2,4) scheme, $\nu = 1$ is no longer the optimum value, an unpleasant computational drawback which is eliminated by the modified (2,4) scheme.

Fig. 1b shows the needed grid resolutions by the different schemes to provide a maximum specified dispersion error. Note that for the standard (2,4) scheme, having a resolution of $\lambda/16$ with an optimum $\nu = 5.826$ is equivalent (from a computational point of view) to a resolution of $\lambda/(16\sqrt{5.826}) \simeq \lambda/39$.

Fig. 1a: Dispersion Error Comparison with Optimum ν , error = $\frac{2}{\pi} \int_0^{\pi/2} \left[\frac{k(\alpha) - k}{k} \right]^2 d\alpha$

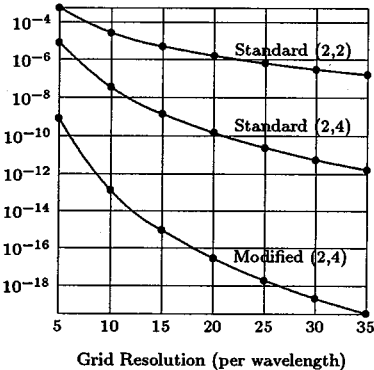
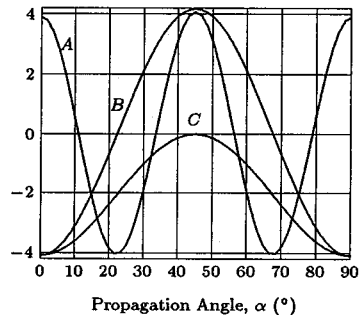


Fig. 1b: An Error Envelope of ± 4 parts per 100,000, error = $\frac{k-k}{k}$

- A. Modified (2,4), $\lambda/5$, $\nu = 1$
- B. Standard (2,4), $\lambda/16$, $\nu = 5.826$
- C. Standard (2,2), $\lambda/142$, $\nu = 1$



A Study of Numerical Dispersion and Stability of the Discrete Surface Integral FDTD Method

H. Shi and J. L. Drewniak
 Department of Electrical Engineering
 University of Missouri-Rolla
 Rolla, MO 65401

The Discrete Surface Integral (DSI) is a time domain solver of Maxwell's curl equations for non-orthogonal mesh developed by Madsen [Niel K. Madsen, "Divergence preserving discrete surface integral methods for Maxwell's curl equation using non-orthogonal unstructured grids," RIACS Tech. Report 92.04, NASA Ames Research Center, CA, Feb. 1992]. In the present study, a generalized FDTD algorithm is formulated based on the principles of DSI. An analytical form for the vector reconstruction and projection operations has been derived for hexahedral and wedge elements that results in a simple updating equation for the electric and magnetic fields. For example, the updating equation for electric field is $E_{\alpha}^{n+1} A_{\alpha}^s = \frac{1}{1 + \frac{\sigma_{\alpha}}{2\epsilon_{\alpha}\Delta t}} \times \left[\left(1 - \frac{\sigma_{\alpha}}{2\epsilon_{\alpha}\Delta t} \right) E_{\alpha}^n A_{\alpha}^s - \frac{\Delta t}{\epsilon_{\alpha}} J_{\alpha}^{n+1/2} A_{\alpha}^s + \frac{\Delta t}{\epsilon_{\alpha}} \sum_{\beta=1}^{\beta_{\max}} t_{\alpha\beta} H_{\alpha\beta}^{n+1/2} l_{\alpha\beta}^s \right]$, where α is the index of field location; A_{α}^s is the area of the face in the secondary mesh; σ_{α} and ϵ_{α} are the average values of conductivity and permeability, respectively; β is the running index for neighboring edges in secondary mesh; β_{\max} is 20 for a general hexahedral mesh, and 4 for the orthogonal case; $l_{\alpha\beta}^s$ is the length of the neighboring edge in the secondary mesh; and, $t_{\alpha\beta}$ are the coefficients representing contributions from all the surrounding H-field locations. The coefficients $t_{\alpha\beta}$ can be extracted from the geometry of any given mesh that consists of hexahedral or wedge cells. The explicit FDTD-DSI formulation allows for the study of numerical dispersion and stability of the DSI method. A special mesh is considered which is translationally invariant in the z-direction and composed of parallelogram cells in the x-y plane. Using Von Neumann's approach, the eigenmode solution of a generic field component is written as $u_{i,j,k}^n = u_0 e^{J\omega n\Delta t - J\vec{\beta} \cdot \vec{r}} = u_0 e^{J\omega n\Delta t - J[i\Delta l_1\beta_1 + j\Delta l_2\beta_2 + k\Delta l_3\beta_3 + (i\Delta l_1\beta_2 + j\Delta l_2\beta_1)\cos\theta_{12}]}$ where $J = \sqrt{-1}$, $\vec{r} = i\hat{r}_1\Delta l_1 + j\hat{r}_2\Delta l_2 + k\hat{r}_3\Delta l_3$, $\vec{\beta} = \beta_1\hat{r}_1 + \beta_2\hat{r}_2 + \beta_3\hat{r}_3$, $\hat{r}_1 \cdot \hat{r}_2 = \cos\theta_{12}$, $\hat{r}_2 \cdot \hat{r}_3 = 0$, and $\hat{r}_3 \cdot \hat{r}_1 = 0$. Upon substituting the above solutions into the six update equations for $(E_1, E_2, E_3, H_1, H_2, H_3)$, a system of simultaneous linear equations are obtained for $(E_{10}, E_{20}, E_{30}, H_{10}, H_{20}, H_{30})$. When setting the secular determinant to zero, a dispersion relation is obtained as $\sin^2\left(\frac{\omega\Delta t}{2}\right) = \left(\frac{c\Delta t}{\sin\theta_{12}}\right)^2 \left\{ \frac{1}{\Delta l_1^2} \sin^2\left[\frac{\Delta l_1(\beta_1 + \beta_2 \cos\theta_{12})}{2}\right] + \frac{1}{\Delta l_2^2} \sin^2\left[\frac{\Delta l_2(\beta_2 + \beta_1 \cos\theta_{12})}{2}\right] \right\}$. Since the value $\frac{\omega\Delta t}{2}$ must be real, the right-hand side of the above equation is no greater than unity. For arbitrary β_1, β_2 , this condition is ensured only when $\left(\frac{c\Delta t}{\sin\theta_{12}}\right)^2 [(\Delta l_1)^{-2} + (\Delta l_2)^{-2}] \leq 1$ which leads to the stability criterion $c\Delta t \leq \frac{\sin\theta_{12}}{\sqrt{(\Delta l_1)^{-2} + (\Delta l_2)^{-2}}}$. Thus, in practical simulations, it must be observed that angles between neighboring cell-edges should be kept as close to 90 degrees as possible. Very skewed mesh could result in instability. In this paper, the developed dispersion and stability relations will be presented, as well as detailed dispersion and grid anisotropy results for the FDTD-DSI method.

Waveguide coupler modeling with the Discrete Surface Integral-FDTD Method

H. Shi and J. L. Drewniak

Electromagnetic Compatibility Laboratory

Department of Electrical Engineering

University of Missouri-Rolla, Rolla, MO 65401

A generalized FDTD algorithm has been developed based on the Discrete Surface Integral (DSI) technique described by Madsen *et al* [Niel K. Madsen "Divergence preserving discrete surface integral methods for Maxwell's curl equation using non-orthogonal unstructured grids", RIACS Tech. Report 92.04, NASA Ames Research Center, CA, Feb. 1992.] In the current study, an analytical form for the vector reconstruction and projection operations has been derived for hexahedral and wedge elements that results in a simple updating equation for the electric and magnetic fields. For example, the updating equation for electric field is: $E_{\alpha}^{n+1} A_{\alpha}^s = \frac{1}{1 + \frac{\sigma_{\alpha}}{2\epsilon_{\alpha}\Delta t}} \times \left[\left(1 - \frac{\sigma_{\alpha}}{2\epsilon_{\alpha}\Delta t} \right) E_{\alpha}^n A_{\alpha}^s - \frac{\Delta t}{\epsilon_{\alpha}} J_{\alpha}^{n+1/2} A_{\alpha}^s + \frac{\Delta t}{\epsilon_{\alpha}} \sum_{\beta=1}^{\beta_{\max}} t_{\alpha\beta} H_{\alpha\beta}^{n+1/2} l_{\alpha\beta}^s \right]$, where α is the index of field location; A_{α}^s is the area of the face in the secondary mesh; σ_{α} and ϵ_{α} are the average values of conductivity and permeability, respectively; β is the running index for neighboring edges in secondary mesh; β_{\max} is 20 for a general hexahedral mesh, and 4 for the orthogonal case; $l_{\alpha\beta}^s$ is the length of the neighboring edge in the secondary mesh; and, $t_{\alpha\beta}$ are the coefficients representing contributions from all the surrounding H-field locations. The coefficients $t_{\alpha\beta}$ can be extracted from the geometry of any given mesh that consists of hexahedral or wedge cells. A validation test is conducted by analyzing a rectangular waveguide. The source excitation is applied at the left wall ($z=0$) with $E_y|_{z=0} = f(t)\sin\left(\pi\frac{x}{x_{\max}}\right)$. In the frequency domain, $f(t)$ is band-limited between the cutoff frequencies of the TE_{10} and TE_{20} modes. First order Mur ABCs are applied at the far end ($z=L$). When L is very large, an analytical solution has been obtained for the transient response of E_y at any point inside the waveguide as $E_y(x, y, z; t) = \{f(t - \tau) - f(t) * [u(t - \tau) \frac{\omega\tau}{\sqrt{t^2 - \tau^2}} J_1(\omega\sqrt{t^2 - \tau^2})]\} \sin\left(\pi\frac{x}{x_{\max}}\right)$ where $J_1(\cdot)$ is the Bessel function of order one. Two meshes are created to model the same waveguide problem with one orthogonal and the other non-orthogonal. A sinusoidally modulated smooth pseudo-Gaussian $f(t) = \sin(2\pi f_0 t) \frac{e^{-\beta(f_0 t - 1)^2} - e^{-\beta}}{1 - e^{-\beta}}$ is employed for the temporal variation of the source, with $f_0 = 12\text{GHz}$ and $\beta = 1$. The simulations in both cases agree well with the analytical solution. Finally, the FDTD-DSI technique is used to study a waveguide coupler with broadwall coupling holes. Each waveguide has a broad wall of 22.86 mm, and ratio $a:b = 2:1$. Along the longitudinal direction, $L = 79.52$ mm. In the common broad wall, two circular holes are arranged symmetrically about the centerline with diameters of 7.16 mm and inter-center distance of 12.8 mm. A 2D mesh is generated to conform to the geometry of the coupling wall. The mesh is extended invariantly along the third dimension from the 2D mesh. The coupler is excited in the TE_{10} mode using the temporal variation given above, with the excitation plane located at the left end of the lower waveguide. Other open ends are truncated by first order Mur ABCs. The time increment is 0.40 ps. The computed forward coupling parameter agrees reasonably well with experimental data published in the literature.

A Modal Analysis Approach- An Exact Approach for the Investigation of the Causes of Spurious Solutions in Finite Element Techniques

by

C. F. Bunting*

Department of Engineering Technology
Old Dominion University, Norfolk Va. 23529
and

W. A. Davis

The Bradley Department of Electrical Engineering
Virginia Polytechnic Institute and State University, Blacksburg, Va. 24060

Finite element techniques have been applied to a wide variety of problems in electromagnetics, but are often handicapped by the appearance of spurious solutions. A method is developed that focuses on the functional form as the fundamental cause underlying the difficulties with spurious solutions. By using analytical rather than numerical means, it is shown that the functional form allows for the existence of an improper gradient behavior in a general field expansion.

Finite element analysis applied to a simple waveguide example experiences fundamental difficulty in that unwanted or spurious solutions are typically generated. The waveguide example is used as a vehicle for exploring finite elements. The emphasis of this research is to establish a methodology for evaluating the "functional" representations and to lay the groundwork for a new functional based on the insights gained. The method to be developed directs the focus to the functional representation; thus identifying the fundamental cause underlying the difficulties with spurious solutions. By using entire domain expansion functions that satisfy the boundary conditions, the difficulties that may be introduced by discretizing the domain for finite elements are completely avoided. This approach yields significant insight into the nature of a given functional and provides answers regarding the true source of spurious solutions. This modal approach will be applied to the commonly used weighted residual form used in the penalty method, with a special case being the generic full-field "functional". By using analytical rather than numerical means, it will be shown that the solution form allows for the existence of an improper gradient behavior in a general expansion function. It will be shown that the linear behavior of the parameter in the penalty method found in numerical solutions is predicted by the exact modal approach.

"An hybrid Finite Difference - Finite Volume Method for solving Maxwell equations in time domain"

A.D. Kalfon* and P.H. Klotz

Centre d'Etudes et de Recherches de Toulouse-ONERA
B.P. 4025, 31055 - TOULOUSE CEDEX (FRANCE)

The techniques for computing electromagnetic solutions in the time domain rely on finite differences with structured mesh (FDTD) or on finite elements (FEM). All absorbing boundary conditions used on the artificial boundary for open problems have been studied and essentially developed with the FDTD approach. Therefore, when the computational domain is complex, which is the case for problems requiring extreme local refinement of zones, unstructured grid is a reasonable approach. Unfortunately FEM is very costly in computational time.

The object of this work is to hybridise the FDTD method and a Finite Volume Method (FVM) which uses unstructured meshes with no coincidence of nodes. The FVM used here is based on the Flux splitting approach of the PDE of first order and the unknowns are cell centred in each cell. The method is second order accurate as the Yee scheme. The time integration scheme is locally implicit in the refined zones and explicit anywhere else. The explicit FVM time step is smaller than the FDTD time step so the local time step technique is used. Moreover to minimise the computational cost the FVM is only applied around the object. To absorb the outgoing waves we use the Perfectly Matched Layer method proposed by J.P. Berenger (Journal of computational Physics to appear). We present some numerical results in 2D and 3D for steady (RCS) and unsteady cases (cavity).

Full-Wave Analysis and Design of Circular Waveguide Dual-Mode Filters by an Hybrid Technique Finite-Element Mode-Matching

J. R. Montejo Garai*, J.Zapata

Departamento de Electromagnetismo y Teoría de Circuitos

E.T.S.I. Telecomunicación. U.P.M.

Ciudad Universitaria S/N

Madrid 28040 Spain

Tel 91-5495700 Ext 480 Fax 91-3367348

e-mail: jr@gauss.etc.upm.es

Advanced satellite communications systems aspire to optimal utilization of the available frequency bands. The sophisticated responses that can be implemented by dual mode filters constitute one of the most important arguments to carry out such spectral optimization. In addition, the dual-mode configuration has led to a reduction of 50 per cent in mass and volume with respect to traditional single mode filters (Butterworth of Chebyshev responses). However, in spite of the progress made in multimode filters during the last years, some design troubles have not been solved yet. For example, to obtain the coupling value of slots and cross-irises between cavities it is necessary to resort to approximate models. Equally important, the coupling between the degenerate modes in the same cavity provided by the screw inserted at a 45° angle, will also be considered.

In this paper, a new full-wave method for the design and the realization of dual-mode circular waveguide filters (DMCWF) is presented. The procedure is a combination of full-wave methods and circuital models. This mixture joins the power of full-wave techniques and the information provided by simplified circuits. As a result, an efficiency CAD has been developed.

The rigorous CAD is a combination of the mode-matching and the finite-element techniques (MM-FEM) which permits obtaining the Generalized Scattering Matrix (GSM) for all the blocks that compose the structure (rectangular slots, cross-irises and screws). The finite thickness of the irises, the higher order mode interaction as well as the coupling and tuning screws are rigorously taken into account. A systematic design process for the different elements will be described. Due to the possibility of full-wave analysis only one tuning screw per cavity is employed, therefore the losses are decreased.

As a consequence of this new process, the manufacturing cost is lowered and the final adjustment and tuning time is also reduced. A full prediction of resonant out-of-band spurious has been accomplished prior to the filter construction. In order to verify the proposed method a four-pole elliptic circular waveguide cavity filter in X band has been designed and constructed. The experimental filter results show excellent agreement with theory.

COMPUTATION OF WAVE PROPAGATION ON MICROSTRIP STRUCTURES OF ARBITRARY SHAPE USING TLM AND FEM

Jun Wei LU, Derek GRAY, David V. THIEL* and Steven O'KEEFE
School of Microelectronic Engineering, Faculty of Science & Technology,
Griffith University, Nathan, Qld 4111, AUSTRALIA

In this paper a transmission line model combined with the finite element method (TLM-FEM) is used to solve electromagnetic field problems. The TLM-FEM method is a suitable method for the study of wave propagation in transmission line systems in both time domain and frequency domain. In particular, wave propagation on microstrip structures of arbitrary shape were modelled.

The TLM method is a numerical approach in which the discretization of a field involves the replacement of a continuous system by a network or array of lumped circuit elements. Since FEM techniques have been well established especially for problems with arbitrary shape, inhomogeneity and nonlinear characteristics, the TLM model can be solved by FEM techniques. This is due to the equivalence between the physical discretization approach of the TLM and the mathematical discretization approach of the FEM in the spatial domain.

Several practical planar structures such as MMIC striplines have been modelled by TLM-FEM. Figure 1 shows the time harmonic EM field of two different structures. Case (a) is a two wavelength long microstrip line section with open termination, and (b) is a model of half of a shunt radial stub matching element.

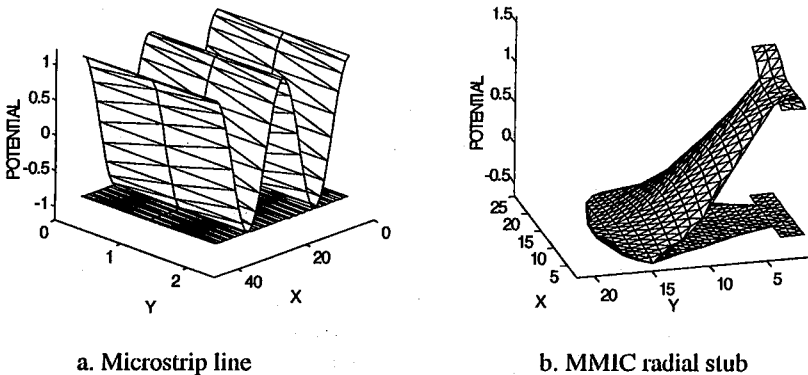


Fig. 1 Wave propagation on transmission line structures

Method of Higher Order Basis Functions Applied to the MOM portion of the SWITCH code

**Y. C. Ma, M. I. Sancer, G. E. Antilla
Northrop Grumman Corporation, B-2 Division
Pico Rivera, California 90660**

ABSTRACT: The SWITCH code is a fully curvilinear hybrid finite element - method of moments code. This paper only deals with the MOM portion of SWITCH using higher order geometry description and higher order basis functions. The full hybrid aspect of SWITCH has been used to compute all Electromagnetic Code Consortium (EMCC) targets yielding excellent agreement.

This curvilinear higher order MOM code uses Lagrange interpolation polynomials in two different ways. It uses them to create geometry from a limited number of geometry control points. Secondly, it uses these polynomials as the basis functions for the surface currents that are computed. It reduces to standard curvilinear rooftop functions if first order Lagrange polynomials were used. These first order polynomial basis functions are referred to as subdomain basis functions.

To explain the benefit of the method of higher order basis functions over subdomain basis functions, two sets of results will be shown. The first is a square flat plate at grazing incidence. Topics that will be discussed are (1) the increase in matrix build time, (2) the increase in accuracy and therefore the decrease in the number of unknowns, (3) the required quadratures for accurate numerical integration. Comparisons of results from the two methods will be addressed. The second scatterer is a lossy or non-lossy dielectric sphere. The method of higher order basis functions is applied to both electric and magnetic field integral operators. Comparisons to exact solutions will be shown.

Recent calculations for the EMCC VFY218 benchmark using SWITCH show excellent agreement with measured data and this comparison is shown. The success of the runs together with the gridding of the model point to an appropriate role for higher order basis functions. The gridding near rapidly changing geometry is unavoidably dense in order to describe the geometry with sufficient accuracy. In this region it makes sense to use subdomain basis functions. When the geometry is smooth higher order basis functions reduce the number of unknowns. It appears that the most efficient code would have a mixture of various orders of basis functions including subdomain.

ANTENNA PATTERN EVALUATIONS USING A HYBRIDIZATION OF THE FINITE ELEMENT AND HIGH FREQUENCY METHODS

R. Kipp*, S.W. Lee*, T. Ozdemir⁺, J.L. Volakis⁺, L. Kempel** and J. Berrie**

*DEMACO
100 Trade Centre Dr.
Champaign, IL 61820

⁺Radiation Laboratory
EECS Dept.
University of Michigan
Ann Arbor, MI 48109-2122

**Mission Research Corp
3975 Research Blvd
Dayton, OH 45430

When an antenna is mounted on an airborne platform, there is certain pattern deformation due to interactions between the radiator and the platform's components. These interactions can often be treated by high frequency techniques and this has been demonstrated by Burnside, et. al.(IEEE Trans. Ant. Propag., 1975) who employed the GTD to model these interactions. With the goal of retaining a high degree of geometry fidelity and accuracy, in this paper we employ a hybridization of the finite element method(FEM), the physical theory of diffraction(PTD) and the shooting-bouncing ray(SBR) method. This hybridization is implemented as follows. First the FEM is used for calculating the printed antenna or array aperture fields. Next, equivalent currents are computed which are then used as sources in a general-purpose PTD/SBR high frequency code. The first order interactions with the platform are computed using the PTD formalism while incorporating appropriate shadowing as dictated by the radiator's location and the platform structure. Higher order interactions can be included using the shooting the bouncing ray method(Baldauf, et. al., IEEE Trans., Ant. Propagat. 1991)

At the conference we will present the details relating to the hybridization and the high frequency implementation. Comparison of measured and calculated data will be also presented. Of particular interest is the treatment of the near zone field interactions and prediction of the printed antenna pattern in the shadow region.

THIS PAGE INTENTIONALLY LEFT BLANK.

High Frequency Techniques

A. F. Peterson and G. Pelosi

Page

- 1:20 Extension of the Integral Equation - Asymptotic Phase Method to 186
 Three-dimensional Scattering
 Kieth R. Aberegg, Andrew R. Peterson, Georgia Institute of Technology*
- 1:40 Scattering Matrix networks for the solution of high- 187
 frequency electromagnetic interaction problems with large structures
 B. L. Michielsen, V. Gobin, ONERA*
- 2:00 Methods to Increase the Efficiency of a Planar Reflector 188
 J. Shaker, L. Shafai, University of Manitoba*
- 2:20 Application of the Generalized Multipole Technique (GMT) 189
 to High-Frequency Electromagnetic Scattering from 3-D
 Perfectly Conducting and Dielectric Homogeneous Bodies of Revolution
 J. M. Tranquilla, H. M. Al-Rizzo, University of New Brunswick*
- 2:40 TD-UTD Analysis of the Scattering from a Perfectly Conducting 190
 Finite Cylinder
 Paul R. Rousseau, Prabhakar H. Pathak, The Ohio State University*
- 3:00 BREAK
- 3:20 Improving the Capabilities of High-Frequency Techniques 191
 with FEM
 *G. Pelosi, R. Coccioli, M. T. Suadoni, University of Florence,
 G. Manara*, University of Pisa*
- 3:40 High Frequency Analysis of EM Scattering by Masts and Towers 192
 Present in Certain Propagation Environments
 C. W. Chuang, P. H. Pathak, R. J. Burkholder, Ohio State University
- 4:00 Generalization of the Rubinowicz Ray Theory 193
 P. Ya. Ufimtsev, Phraxos Research & Development, Inc.,
 N. G. Alexopoulos, University of California at Los Angeles,
 J. A. Castaneda, Phraxos Research & Development, Inc.*
- 4:20 Diffraction Principles in Design and Detection of Invisible Objects 194
 P. Ya. Ufimtsev, Phraxos Research & Development, Inc.
- 4:40 Uniform Asymptotic Solutions for Whispering Gallery Mode 195
 Radiation from Smooth Concave-To-Convex Boundary
 T. Ishihara, K. Goto, National Defense Academy, Japan*
- 5:00 Asymptotics of Creeping Waves in a Vicinity of the Surface 196
 Discontinuity
 Ivan V. Andronov, University of St. Petersburg

Extension of the Integral Equation – Asymptotic Phase Method to Three-dimensional Scattering

Keith R. Aberegg and Andrew F. Peterson
School of Electrical & Computer Engineering
Georgia Institute of Technology
Atlanta, GA 30332-0250*

A hybrid numerical/asymptotic procedure called the integral equation – asymptotic phase (IE–AP) method was previously developed for scattering from perfectly conducting two-dimensional cylinders (K. R. Aberegg and A. F. Peterson, "Formulation and application of a hybrid numerical – asymptotic integral equation technique," *1993 URSI Radio Science Meeting*, Ann Arbor, MI, p. 160, June 1993). The IE–AP approach employs an asymptotic solution to predict the relatively rapid phase dependence of the unknown current distribution, in order to leave a slowly-varying residual function that can be represented by a coarse density of unknowns. Results suggest that the use of the physical optics approximation as the asymptotic solution can often reduce the required density of unknowns to as few as one per wavelength on average without a significant loss of accuracy, even for scatterers with edges.

In the present investigation, the IE–AP formulation is extended to treat three-dimensional conducting bodies. The surface current density appearing within the combined-field integral equation is replaced by a product of the physical optics current and an unknown residual function. In order to increase the electrical size of the cells without incurring unnecessary error, the residual function is represented by novel mixed-order vector basis functions defined on curved triangular patches. The specific basis functions we employ provide a linear normal component and a quadratic tangential component of the vector surface current along the patch edges, and maintain normal continuity between patches in order to produce a finite surface divergence (A. F. Peterson, "Higher-order surface patch basis functions for EFIE formulations," *1994 IEEE Antennas and Propagation Society International Symposium*, Seattle, WA, pp. 2162-2165, June 1994.). They can be thought of as an extension of the Rao, Wilton, and Glisson triangular rooftop basis functions to a higher polynomial order. The basis functions can also be modified to incorporate the singular behavior of the current density at a geometrical edge.

The three-dimensional IE–AP formulation will be described in detail, and results for simple three-dimensional scatterers will be presented to illustrate the approach.

Scattering matrix networks for the solution of high-frequency electromagnetic interaction problems with large structures

B.L.Michielsen*, V.Gobin
ONERA, France

In order to be able to deal with scattering geometries which are very large compared to the wavelength of the incident field, we study a domain decomposition technique where each subdomain is characterised by a scattering matrix relating locally incoming waves into the subdomain to outgoing waves. The subdomain scattering matrices can be computed independently for the various subdomains, with some numerical technique adapted to the peculiarities of the subdomain at hand. For a subdomain which continues to be too large to be handled with a straightforward discretisation technique, we do a second level domain decomposition on its boundary surface. Each surface patch again receives a surface scattering matrix, which is computed (analytically) using approximate canonical geometries.

On each decomposition level, we have a master equation describing the true problem in terms of the partial (i.e. subdomain- or surface patch-)scattering matrices. This master equation can be relatively sparse, depending on the global geometrical properties of the structure. In order to solve the master equation as efficiently as possible, an optimised multi-front algorithm is developed.

The following estimate allows for a comparison between a straightforward computation and one using the above indicated decomposition method (not accounting for the accelerations due to the optimised multi-front method)

$$OC \sim M(N/M)^3 + 2(MRP)^3$$

here, OC is the asymptotic operation count, N is the number of unknowns of the entire original problem, M is the number of subdomains, R is the average number of neighbouring subdomains per subdomain and P is the additional number of unknowns, introduced on each of the interfaces in order to be able to perform the separation. The second term on the RHS represents the additional effort necessary for the separation of the subdomains and the resolution of the master equation and is completely determined by the subdomain discretisations. Hence, as soon as $MRP < N/M$ the first term begins to dominate and we begin to obtain computation time reductions attaining factors of upto $1/M^2$. Typically we have: $N = 10^5$, $M = 10$, $R = 4$, $P = 100$ giving $OC \approx 10^{13}$ which should be compared to $OC \approx 10^{15}$ for a straightforward computation.

We discuss some examples where the exterior domain is treated with the surface decomposition technique, and a number of interior subdomains with an electric field surface integral equation.

Methods to increase the efficiency of a planar reflector

J. Shaker*, L. Shafai

*Department of Electrical and Computer engineering
University of Manitoba, Winnipeg, Manitoba, R3T 2N2*

Planar reflectors (F. S. Johnason, *IEEE Trans. Antennas & Propag.*, Vol. 38, No. 9, Nov. 1990, pp. 1491–1495) are flat semi-periodic structures of strip gratings and their focusing capability is the result of conversion of incoming wave into $(0,-1)$ Floquet's mode. Due to the excitation of Floquet's modes other than the desired $(0,-1)$ mode, the conversion process is often not perfect and results in a reduction of antenna efficiency. This is an important restriction for the application of planar reflectors. In this presentation, we propose two methods for overcoming this problem.

One method of reducing the conversion loss is by increasing the focal length. This is due to the fact that the illuminating wave approaches a plane wave as the source moves away from the planar reflector. Another way of reducing the conversion loss, was found to be the realignment of gratings so that they match the polarization of the illuminating wave.

In order to perform the numerical simulation of the structure, the surface of the planar reflector was divided into zones and conversion loss was calculated for each zone. A zone is defined to be a region on the planar reflector throughout which the periodicity is almost uniform. In order to calculate the conversion loss for a zone, that specific region of reflector was approximated with an infinite periodic structure that is illuminated by a plane wave in the same direction and has the same uniform periodicity as the zone. The intensity of each of the Floquet modes that are generated by the respective infinite periodic surface were obtained using the Green's function methodology.

**APPLICATION OF THE GENERALIZED MULTIPOLE TECHNIQUE (GMT) TO
HIGH-FREQUENCY ELECTROMAGNETIC SCATTERING FROM 3-D PERFECTLY
CONDUCTING AND DIELECTRIC HOMOGENEOUS BODIES OF REVOLUTION**

J. M. Tranquilla
*H. M. Al-Rizzo

ABSTRACT

In this paper the GMT technique is utilized for accurately predicting the electromagnetic (EM) fields scattered from electrically large, 3-D, perfectly conducting (PC) or dielectric bodies of revolution of smooth but otherwise arbitrary geometry, arbitrarily oriented with respect to the direction of propagation of a generally polarized plane-wave incident field. In this approach, analytical tractable, multiple spherical multipole (MSM) equivalent sources, involving spherical Hankel functions (SHFs) of the first kind with their origins suitably located along the axis of rotational symmetry of the object, are employed as basis functions for the series expansions of the unknown fields in the exterior domain of the scattering problem.

The underlying principle of the proposed formalism is that the induced electric and magnetic field vectors in the interior volume of dielectric objects are simulated by equivalent multiple spherical vector wavefunctions involving spherical Bessel functions (SBFs) of the first kind and located in the interior of the object to be treated. A salient feature of the proposed technique is that a self-validation procedure can be easily implemented whereby the accuracy of the boundary-field match between the matching points can be utilized to some extent to ascertain the precision of the computed results. Numerical results for the differential scattering cross-section (DSCS) patterns, extinction, scattering and backscattering efficiencies are presented for a wide range of 3-D electrically extended geometries which have not been hitherto considered by either existing analytical solutions or any other integral, differential and hybrid numerical methods. As yet, our GMT code has been successfully applied for dielectric prolate spheroids with $k_1 a = 529.2889$, where

a is the length of the semi-major axis, $k_1 = \frac{2\pi\sqrt{\epsilon_r}}{\lambda_0}$ is the wave number inside the dielectric object and ϵ_r is the relative permittivity.

Finally, due to the paucity of information on scattering from electrically large objects, it is hoped that the comprehensive set of numerical results provided in this paper may provide a useful reference for comparison purposes with other numerical techniques.

TD-UTD ANALYSIS OF THE SCATTERING FROM A PERFECTLY CONDUCTING FINITE CYLINDER

Paul R. Rousseau* and Prabhakar H. Pathak

ElectroScience Laboratory

The Ohio State University, Department of Electrical Engineering
Columbus, Ohio 43212

The transient bistatic far zone field scattered from a finite cylinder as predicted by the time domain uniform geometrical theory of diffraction (TD-UTD) when the excitation is an impulsive plane wave will be presented. The "far zone" for the time domain impulse response is simply defined as being infinitely far from the target. A finite far zone distance only makes sense after the impulse response is convolved with an excitation which has a frequency response with a finite bandwidth. When the observation and incident direction are located in the plane containing the axis of the cylinder the first order TD-UTD includes just three diffracted ray field contributions. Although this decomposition is not strictly valid for an impulsive time pulse excitation (since the UTD is not valid at low frequencies in the frequency domain), an approximate impulse response of the target can be calculated using the TD-UTD which will be valid for short to intermediate times with respect to the arrival times of the various ray fields. This approximate impulse response can then be convolved with any chosen excitation and very accurate results are obtained when the excitation frequency response does not contain low frequencies. Special care must be taken when the observer is close to the specular direction with respect to the flat end caps of the cylinder, because the TD-UTD has an erroneous singularity in the specular direction due to the caustic created by the circular rim of the cylinder, just as in the frequency domain UTD. A modified TD-UTD diffraction coefficient will be presented which will cause the scattered field to converge to a TD physical optics (TD-PO) solution at specular and smoothly transition from the TD-PO solution to the TD-UTD away from specular.

Several interesting numerical results will be presented including the TD-UTD impulse response. The TD-UTD impulse response will also be convolved with a finite energy excitation pulse and this solution will be compared with a reference solution to verify the accuracy of the TD-UTD for short pulse excitations. It will be shown that the TD-UTD not only provides an approximate impulse response which characterizes the target, but also offers an efficient alternative analysis method for scattering problems in the time domain when the excitation is a short finite energy pulse.

IMPROVING THE CAPABILITIES OF HIGH-FREQUENCY TECHNIQUES WITH FEM

G. Pelosi, R. Coccioli, M.T. Suadoni
Department of Electrical Engineering, University of Florence
Via C. Lombroso 6/17, I-50134 Florence, Italy

G. Manara*
Department of Information Engineering, University of Pisa
Via Diotisalvi 2, I-56126 Pisa, Italy

When the dimensions of scatterers are large with respect to the operating wavelength both in antenna and scattering problems, suitable high-frequency techniques must be employed. In practice, a simplified model is defined approximating the outer surface of the scatterer by canonical geometrical shapes and imposing on them suitable boundary conditions (b.c.). In most cases, to simplify the problem the boundary condition for a perfect electric conductor is chosen, although impedance b.c. are sometimes used to approximately consider the material properties of the body. However, this procedure is in principle not able to account for significant contributions to the scattered field, which may arise from localized material inhomogeneities and geometrical irregularities of the structure.

The aim of this paper is to present a hybrid technique, based on a particular formulation of the equivalence principle and the Finite Element Method (FEM) [P.P. Silvester, G. Pelosi, *IEEE Press*, 1994], which allows to systematically include field contributions associated with localized irregular parts of the scatterer in the general solution. This parts can be identified for instance with cavity-backed apertures, truncated wedges, wedges with a blunt tip [G. Pelosi *et al.*, Int. Symp. on Antennas (JINA '94), Nice, France, 1994].

The method consists in dividing the original issue into an open problem and a set of interior problems. This is done by applying the equivalence principle, in a form that implies metallizing the actual or fictitious surfaces separating the exterior and the interior problems. Interior problems, which may be characterized by a strongly inhomogeneous material constitution and irregular geometrical configurations, are analyzed by FEM. The exterior problem is solved by the most suitable technique (ray method, eigenfunction expansions, etc.). The coupling among problems is imposed through integro-differential equations, that are solved by the Moment Method. This procedure allows to extend the class of problems that can be analyzed by standard high-frequency codes.

HIGH FREQUENCY ANALYSIS OF EM SCATTERING BY MASTS AND TOWERS PRESENT IN CERTAIN PROPAGATION ENVIRONMENTS

C.W. Chuang, P.H. Pathak, and R.J. Burkholder*

The Ohio State University ElectroScience Laboratory

Department of Electrical Engineering

1320 Kinnear Road, Columbus, Ohio 43212

In the analysis of certain types of EM propagation environments, such as those involving the presence of TV antenna towers and similar large towers for communication networks in the propagation path, or those involving the radiation from a microwave radar antenna on a ship topside containing masts/towers, it becomes necessary to include the effects of the scattering by such masts/towers. An approximate high frequency solution is developed for analyzing the near or far zone scattering by masts/towers illuminated by plane or spherical EM waves. In this approximation, the mast can be modeled by a single circular cylindrical geometry; whereas, a tower can be built up by connecting finite length circular cylinders in a given zig-zag pattern. Furthermore, the scattered field is considered as being comprised of two components. The first is the field scattered by each individual finite cylinder making up the tower (in the case of a solid cylindrical mast there is only one such cylinder) with all others absent. The second component accounts for the multiple scattering between cylinders. The method ignores the effects of the actual junction or contacts between cylinders. As long as each finite cylinder is a few wavelengths in extent, the scattered field is generally most significant in the specular direction associated with each individual cylinder, and the junction point and multiple scattering effects are of secondary importance. Since the specular scattering can be found accurately, the method is expected to yield reasonably good results. The singly scattered fields from each cylindrical section induces additional currents on the other cylinders which in turn produce the multiply scattered fields. The singly scattered fields are produced by forced wave currents (due to primary illumination) and surface wave currents (launched from the ends); these forced and surface wave currents as well as their radiation, which constitute an important part of this development, are found in an approximate but reasonably accurate fashion valid for angles not near grazing on the cylinder. The inaccuracy of scattering from one cylinder at grazing is not serious since in that direction the scattering is dominated by other cylinders which are not near grazing incidence. Numerical results based on this approach are shown to compare well with a rigorous integral equation based moment method reference solution which can be implemented easily for some simple geometries built up of thin wire connections. This analysis is then extended to predict the scattering by a more realistic tower illuminated by a nearby AN/SPS-48E shipboard air-search radar antenna.

GENERALIZATION OF THE RUBINOWICZ RAY THEORY

P.Ya. Ufimtsev *

Phraxos Research & Development, Inc.
2716 Ocean Park Blvd. Suite 1020
Santa Monica, California 90405, USA
Also with the Electrical Engineering Department
University of California at Los Angeles
Los Angeles, California 90024-1594, USA

N.G. Alexopoulos

Electrical Engineering Department
University of California at Los Angeles
Los Angeles, California 90024-1594, USA

J.A. Castaneda

Phraxos Research & Development, Inc.
2716 Ocean Park Blvd., Suite 1020
Santa Monica, California 90405, USA

Abstract

The ray properties of diffraction fields have attracted a great deal of attention for a long time. Sommerfeld (1896) discovered theoretically the edge wave in the field scattered by a straight wedge. He pointed out that the edge wave can be interpreted as a set of rays diverging from the edge. The term "diffracted rays" was introduced by the Russian scientist Kalashnikov (1912). He also was the first to present an objective experimental proof of the existence of these rays which was appreciated by Sommerfeld. The next important step in the development of the diffracted ray concept was done by the Polish scientist Rubinowicz (1924). He investigated the asymptotic properties of the Kirchhoff integral and discovered the diffracted rays diverging from the edge of an aperture in an opaque screen. His paper predicted some basic elements of modern asymptotic theories. Surface diffracted rays arising in the vicinity of a cylinder and sphere were studied by Deppermann, Franz, and Imai (1954). All the above results can be considered as the foundation for the general theory of diffracted rays, the Geometrical Theory of Diffraction, suggested by Keller (1953 -1962). He developed this theory in an axiomatic way.

The goal of this talk is to show how the Keller theory of edge rays can be constructed as a natural generalization of the Rubinowicz results which were found using the Kirchhoff approximation. This generalization consists of two stages. First, the transition is done from the Rubinowicz scalar asymptotics which are independent of the boundary conditions on a scattering screen to the asymptotic solution satisfying these conditions. The next stage is the transition from the asymptotic solution of the three-dimensional scalar problem to the asymptotic solution of the three-dimensional vector problem.

DIFFRACTION PRINCIPLES
IN DESIGN AND DETECTION OF INVISIBLE OBJECTS

P.Ya.Ufimtsev
Phraxos Research & Development, Inc.
2716 Ocean Park Blvd., Suite 1020
Santa Monica, California 90405, USA
Also with the Electrical Engineering Department
University of California at Los Angeles
Los Angeles, California 90095-15945, USA

Abstract

The problem of target radar cross section (RCS) reduction exists since radar was invented. Until recently only radar absorbing coatings were used. However, this approach is not sufficient for complete reduction. The present talk addresses the basic physical restrictions of this methodology. The essential role of the shape of scattering objects is emphasized and the necessity of transition to flat surface elements is discussed. Positive and negative consequences of such type of shaping are considered from the detection point of view.

It is shown that this shaping leads to the reduction of monostatic backscattering RCS and simultaneously to the increase of bistatic RCS, especially in the specular directions. The latter can be partially reduced by using of absorbing coatings. An important restriction in reduction of bistatic RCS is the black body scattering, i.e. shadow radiation.

The black body is defined as an object which completely absorbs the whole power of the intercepted part of the incident radar beam. Basic features of this phenomenon are considered. The physical nature of this phenomenon consists of the transversal diffusion of the wave field in the vicinity of the shadow boundary. In the case of an object with sharp edges this phenomenon creates edge waves. It is noted that connection exists between shadow radiation, creeping waves, and surface diffraction rays. An estimation of the level of the bistatic RCS caused by shadow radiation is presented for objects with flat facets. These examples make clear the possibility of the detection of invisible (stealth) objects by bistatic radars.

UNIFORM ASYMPTOTIC SOLUTIONS FOR WHISPERING GALLERY
MODE RADIATION FROM SMOOTH CONCAVE-TO-CONVEX BOUNDARY

T. Ishihara* and K. Goto
Dept. of Electrical Engineering
National Defense Academy
Hashirimizu, Yokosuka, 239, Japan

High-frequency asymptotic field solutions for a perfectly conducting smooth boundary whose curvature changes from concave to convex are of interest for a variety of applications involving propagation along, and (or) scattering from, the surface contour[S. Ohta and T. Ishihara, Japanese Journal of Applied Physics, Vol.30, pp.92-94(1990)]. The focusing concave, and the defocusing convex, portions are connected by a transition region surrounding the inflection point.

When the source is far from the boundary, the ray method can be employed to approximate the surface currents on the illuminated portion, and asymptotic treatment of the physical optics(PO) integral containing these currents can then provide information about the inflection-induced transition behavior[P. H. Pathak and M. C. Liang, IEEE Trans. Antennas & Propagat., Vol.38, pp.1192-1203(1990); L.C. Kempel, J.L. Volakis, T.B.A. Senior, S.S. Locus, and K.M. Mitzner, IEEE Trans. Antennas & Propagat., Vol. 41, pp.701-708(1993)]. This does not account, however, for trapped whispering gallery(WG) modes and their conversion to the radiating beam fields and creeping waves, which is relevant when the source is located near the surface on the concave side.

In this work, we examine the beam fields over the concave-to-convex boundary excited by the adiabatic WG mode which is incident on an inflection point from the concave side[K.Goto and T.Ishihara, IEICE Transactions, Vol. J77-B-II, No.10, pp.539-547(1994)]. The modal ray congruences of the WG mode are converted into the geometrical rays in the free space and construct the beam fields at large distances from the radiation point. The beam fields may be represented by applying the uniform PO (UPO) and uniform GTD (UTD) solutions. The UPO solution may be applied to evaluate the beam fields near the caustic formed by the geometrical rays, which are converted from the ray congruences of the incident WG modes. The remaining parts of the beam fields including the transition region near the shadow boundary of the geometrical ray, incident on the convex portion of the concave-to-convex boundary, may be calculated by applying the UTD solution.

Numerical comparisons with the reference solution calculated from the hybrid parabolic equation method and Fresnel-Kirchhoff diffraction formula[K. Goto, T. Ishihara, and K. Kitamura, Proc. of ISAP'92, Sapporo, Japan, pp.617-620(1992)] reveal the validity and the utility of the uniform asymptotic representations proposed in the present study.

Asymptotics of Creeping Waves in a Vicinity of the Surface Discontinuity

Ivan V. Andronov

*Institute in Physics, University of St. Petersburg
Ulianovskaja 1-1, 198904 St. Petersburg, Russia
E-mail: andronov@niif.spb.su*

In high frequency diffraction the shadowed side of a body is reached by creeping waves. The standard asymptotics of the creeping waves field (V.M. BABIČ, N.Y. KIRPIČNIKOVA *The Boundary-Layer Method in Diffraction Problems* Springer-Verlag, Berlin Heidelberg New York 1979) is not valid close to lines or points of discontinuity of the surface or of boundary condition. In this paper the effects caused by such discontinuity upon the field of creeping waves are examined.

If a creeping wave is incident on the line of discontinuity at finite (not small) angle the description of the effects of its transformation can be drawn from the paper (V.B. PHILIPPOV *Wave Motion* 3, 1981, pp. 71-80), where the two-dimensional problem of diffraction by a nonplanar screen is considered. The case of asymptotically small angles of incidence has its specific effects and needs special examination. The two problems are considered in the paper: the field of electromagnetic creeping waves near an edge of a curvilinear screen and the field near the line of contact of superconductor and dielectric. In both cases the line of discontinuity is assumed to be a geodesics of the surface. This permits to find the asymptotics of the electromagnetic field explicitly.

First the existence of "edge" waves connected with the edge and "discontinuity" waves connected with the line of discontinuity in the boundary condition is established and the principal term of the asymptotic expansions in both cases are found. These asymptotics are given in terms of Fourier integrals with transformants containing results of the factorization by μ of symbols $w_1(\xi + \mu^2)/w_1'(\xi + \mu^2)$ and $v(\xi + \mu^2)w_1(\xi + \mu^2)$ respectively. (The Fock notations for the Airy functions are used.) It is discovered that the main effects are concentrated in a narrow of order $k^{-2/3}$ boundary-layer near the discontinuity.

Then the two kinds of excitation are examined. If the incident field is some ordinary creeping wave running to the edge (discontinuity) the coefficients of the "edge" ("discontinuity") waves generation are determined by the procedure of matching of asymptotics. In the case of spatial incident wave the asymptotics in the Fock zone should be considered. The examination of the field in the Fock zone shows that a tangentially incident on an edge of a screen spatial wave generates not only creeping waves on its external side, but waves of the whispering gallery type on the internal side as well. The latter form nondecreasing field along the edge.

Material Characterization

S. Riad and K. M. Chen

Page

- 1:20 Intercomparison of Magnetic Material Characterization 198
 using the Transmission/Reflection Method in 7-MM and 14-MM
 Coaxial Air Lines
 Claude M. Weil, Eric J. Vanzura, National Institute of Standards and
 Technology*

- 1:40 Determination of EM Parameters of Anisotropic Materials 199
 Using a Waveguide Probe System
 C. W. Chang, K. M. Chen, J. Qian, D. P. Nyquist,
 Michigan State University*

- 2:00 Dielectric Characterization Using a Shorted Circular Waveguide 200
 Fed By a Coaxial Line
 Mohammad A. Saed

- 2:20 Measurement of Complex Dielectric Permittivity using 201
 Microstrip Transmission Line
 Richard B. Keam, W. S. Holmes, Industrial Research Ltd.

- 2:40 Field Analysis of High TC Superconducting Strip Transmission 202
 Lines
 Jeffrey S. Herd, Rome Laboratory

- 3:00 BREAK

- 3:20 Time Domain Analysis of Skin Effect Losses in Transmission Lines ... 203
 Sedki M. Riad, Mohammed Abd-el Rahman, Iman M. Salama,
 Virginia Polytechnic Institute*

- 3:40 Variable-Temperature Microwave Dielectric Properties of 204
 Isotropic and Anisotropic Materials
 Richard G. Geyer, NIST, Jerzy Krupka, Instytut Mikroelektroniki
 i Optoelektroniki*

INTERCOMPARISON OF MAGNETIC MATERIAL CHARACTERIZATION
USING THE TRANSMISSION/REFLECTION METHOD IN 7-MM AND 14-
MM COAXIAL AIR LINES

Claude M. Weil* and Eric J. Vanzura
Electromagnetic Fields Division (813.08)
National Institute of Standards and Technology
Boulder, CO 80303-3328

In an attempt to assess the quality of RF material characterization being performed by industrial and government laboratories, NIST organized a national measurement intercomparison of dielectric permittivity, ϵ' in the 0.05-18 GHz frequency range (E.J. Vanzura et al, IEEE Trans. MTT, 42, 2063-2070, 1994). Four samples of different low-loss dielectric materials with ϵ' in the range 5-20 were circulated amongst some 12 participating laboratories, who measured the samples using a standardized Transmission/Reflection (T/R) method in 7-mm diameter coaxial air line. Considerable interlaboratory variation was apparent in the measured data due to differences in the data-reduction algorithms used and in the methods of correcting for the presence of air gaps.

This talk discusses a follow-on intercomparison involving measurements of both complex permeability and permittivity of magnetic materials. Four samples of different ferrites were circulated amongst about 12 participating laboratories (many identical to those that participated in the earlier study). Most of these materials exhibit much larger magnetic and dielectric loss and are therefore generally better suited to the T/R method, which has poor sensitivity for measuring low-loss materials. Two sample kits were circulated. One, containing samples suitable for placement in a 7-mm diameter coaxial air line, was sent to most participants for characterization over the range 0.05-18 GHz. The other, containing samples suitable for a 14-mm diameter line, was sent to selected participants having such measurement capabilities for characterization over a lower frequency range of 1-8000 MHz. Preliminary conclusions derived from the data so far returned indicate that, in general, there is good interlaboratory agreement in magnetic permeability measurements, but that, as before, wide variations in the dielectric permittivity data are evident. Intercomparison measurements will be completed this year and the data compiled and published.

DETERMINATION OF EM PARAMETERS OF ANISOTROPIC MATERIALS USING A WAVEGUIDE PROBE SYSTEM

C. W. Chang, K. M. Chen*, J. Qian and D. P. Nyquist
Department of Electrical Engineering
Michigan State University, E. Lansing, MI 48824

A study was conducted to measure non-destructively the electromagnetic parameters of anisotropic materials using a waveguide probe system. The system consists of an open-ended rectangular waveguide with a large conducting flange which can be placed against a material layer to be measured, and a network analyzer (HP 8720B). In this study a forward algorithm and an inverse algorithm were developed.

In the forward algorithm, the EM field inside the waveguide near the waveguide aperture is expressed as the sum of incident and reflected dominant modes plus higher-order waveguide modes. The EM field inside the material layer is expressed in terms of eigenmodes of the spectrum-domain transverse EM fields which are derived directly from Maxwell's equations. When the tangential components of electric and magnetic fields in the waveguide and the material layer are matched at the waveguide aperture, two coupled electric field integral equations (EFIEs) with transverse components of the aperture electric field as unknowns can be derived. These coupled EFIEs are solved numerically by Galerkin's method, and the reflection coefficient of the dominant mode is determined as an implicit function of the tensor permittivity of the anisotropic material.

In the inverse algorithm, the tensor permittivity of the anisotropic material is inversely determined using the Newton's rootfinding algorithm when the reflection coefficient of the waveguide dominant mode is measured experimentally. An experimental setup was constructed with an open-ended rectangular waveguide terminated on a large conducting flange which was placed against a material layer to be measured. The reflection coefficient or the input impedance of the dominant mode of the waveguide terminated on a material layer was measured at the X-band using a network analyzer. The measured reflection coefficient was then used to inversely determine the EM parameters of the anisotropic material.

DIELECTRIC CHARACTERIZATION USING A SHORTED CIRCULAR WAVEGUIDE FED BY A COAXIAL LINE

Mohammad A. Saed
Electrical Engineering Department
State University of New York at New Paltz
New Paltz, New York 12561

This paper presents the concept, method of analysis, and experimental results for a new technique for measuring the complex permittivity of dielectric materials. The proposed technique uses a circular waveguide shorted at one end while the other is fed by a coaxial line. The dielectric sample to be characterized must fit precisely in the shorted waveguide so that air gaps between the waveguide wall and the sample are not present. The method allows for inhomogeneous filling of the waveguide using two (or more) layers of dielectric materials. However, the complex permittivity can be measured for only one layer, the other layers must have known permittivities. This makes the proposed technique suitable for characterizing liquid dielectrics where the dielectric sample does not have to be in contact with the feed line. It is also convenient for characterizing dielectric thin films and thick films since the film must be attached to a dielectric substrate with known material properties. The proposed technique can be used for dielectric characterization for a very broad frequency range, from low frequencies to microwave frequencies.

The proposed geometry is analyzed using a finite difference method since it is easy to implement for multilayer configurations. First, the forward problem is analyzed where the reflection coefficient is computed assuming that dielectric properties for all layers are known. This will allow us to investigate the sensitivity of the reflection coefficient to various parameters. Then, the inverse problem, the computation of the complex permittivity of one layer assuming known reflection coefficient and known permittivities for the other layers, is implemented using iterative techniques. Several experiments are carried out to investigate the accuracy of the method and its limitations.

Measurement of Complex Dielectric Permittivity using Microstrip Transmission Line

Submission for 1995 IEEE/AP-S International Symposium and USNC/URSI Radio Science Meeting at Newport Beach, CA.

Dr Richard B. Keam and W. S. Holmes
Microwave Engineering Team,
Industrial Research Ltd,
P.O. Box 2225, Auckland,
NEW ZEALAND

Ph: +64 9 303 4116
Fax: +64 9 307 0618
Email: R.KEAM@IRL.CRI.NZ

APPLICABLE CONFERENCE TOPICS:

- A1 Microwave to submillimeter measurements
- A9 Materials
- B2 Microstrips

ABSTRACT:

A new type of broadband antenna, the spiral microstrip antenna, has been suggested for use in communication applications. As a first step in the development of such a transducer for use in dielectric permittivity measurement an uncertainty analysis is performed on the change in effective permittivity, characteristic impedance and propagation constant of a microstrip transmission line brought into contact with an unknown dielectric sample. A comparison of the method presented here with existing measurement techniques for several known dielectric materials is given.

Whilst there is a great interest in the measurement of dielectric permittivity of materials for use in industrial and biological microwave applications, many of the existing measurement techniques either produce only single frequency measurements (such as resonant cavity methods), or require complicated calibration with known permittivity standards (such as the coaxial-line probe method). Also many microwave measurements are performed on solid materials that are not suited to machining for cavity measurements. These solids often exhibit significant variations in the permittivity over quite small physical distances.

To overcome effects caused by structural inhomogeneity, microwave transducers must have field patterns that are large enough to "average" the microwave properties of the material. Given that the response of the sensor is normally a strong function of frequency and interacts adversely with any periodicity in the spatial frequency components of the inhomogeneity of the material, it is not sufficient in most cases merely to average the permittivities obtained from several measurements as if they were independent data points.

As a first step in the development of a spiral microstrip antenna for measurement of complex dielectric permittivity, a study is presented which investigates the sensitivity of parameters such as characteristic impedance of microstrip transmission line to changes in the permittivity of the external medium (see Figure 1). It is assumed that the frequency of operation and the permittivity of both the substrate and unknown material are such that the only propagating mode is quasi-TEM.

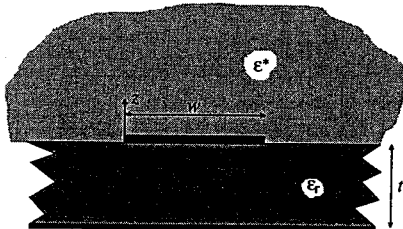


Figure 1: Cross-section of a microstrip transmission line embedded in a material of unknown permittivity ϵ^* .

Field Analysis of High T_c Superconducting Strip Transmission Lines

Jeffrey S. Herd
USAF Rome Laboratory
Hanscom AFB, MA 01969

The new high T_c thin film superconducting materials are currently being utilized in a variety of low loss microwave circuit applications including very high Q resonators, low loss delay line filters, matching networks, and large antenna array power dividing networks. Nonlinear effects have been observed at power levels near one watt, and are believed to be due to weak link defects inherent to certain materials and growth processes. These nonlinearities are detrimental to the performance of the devices, and manifest themselves in the form of intermodulation products, harmonics, and increased insertion loss.

In order to study and understand these effects, it is useful to know the field and current distributions for various thin film transmission line geometries such as stripline, microstrip, and coplanar waveguide. For that purpose, a two dimensional finite difference field solver has been developed which analyses the time harmonic eigenmodes of general high T_c wave guiding structures. Use of transverse field components avoids the spurious mode problem, and a non-uniform mesh is employed to make efficient use of sample points. Special steps have been taken to allow for very general cross-sectional geometries, and the numerical modeling is carried out in an efficient fashion that minimizes storage and execution time. The model is also capable of including uniaxial anisotropy in the superconductor, and efforts are currently under way to incorporate a phenomenological nonlinear field dependence of the superconductivity.

The high T_c electromagnetic field solver will be described, and computed results shown for several geometries. Comparisons will be made with experimentally measured results.

TIME DOMAIN ANALYSIS OF SKIN EFFECT LOSSES IN TRANSMISSION LINES

Sedki. M. Riad,

Mohammed Abd-el Rahman, Iman M. Salama

The Bradley Department of Electrical Engineering

Virginia Polytechnic Institute and State University

Blacksburg, Virginia 24061-0111

Phone: 703-231-4463 Fax: 703-231-3362

The skin effect phenomena encountered in transmission lines can seriously affect signal transmission. The phenomena are due to the fact that at relatively high frequencies, the distributed internal inductance and resistance of the conductors become frequency dependent. This results in dispersion of transmitted signals and sets bandwidth limitations on the properties of the line. In this paper, it is intended to study the skin effect from a time domain perspective. A transmission line can generally be modeled by the four parameters $L, C, G, (R_i, L_i)$. Where L is a series inductance per unit length of the transmission line accounting for the magnetic flux external to the conductor, C is a shunt capacitance, G is a shunt conductance representing losses of the dielectric and R_i and L_i denote the internal resistance and inductance of the conductors (internal impedance of the conductors).

The internal impedance of the conductors is expected to be frequency dependent and consequently, so is the characteristic impedance of the line. If the characteristic impedance of the line is treated as having a constant nominal value plus a frequency dependent term, the load and generator resistance can be considered matched to this nominal value. The frequency dependence of the characteristic impedance of the line will result in mismatches between the line and both the load and generator and consequently, successive reflections from the load and generator. The contribution of each of these reflections can be studied. The IFFT algorithm can be used to study these effects in the time domain. Alternatively, it is proposed to study the possibility of deriving an analytical expression for the step response in time domain with some approximations. The effect of the permeability and conductivity as well as the dimensions of the conductors on the skin effect can also be discussed. Finally a comparison can be made with the analytical expressions introduced in previous work.

VARIABLE-TEMPERATURE MICROWAVE DIELECTRIC PROPERTIES OF ISOTROPIC AND ANISOTROPIC MATERIALS

Richard G. Geyer*

National Institute of Standards and Technology
Electromagnetic Fields Division, 813.08
325 Broadway, Boulder, CO 80303, U.S.A.

Jerzy Krupka

Instytut Mikroelektroniki i Optoelektroniki, Politechniki Warszawskiej
Koszykowa 75, 00-662 Warszawa, Poland

Dielectric resonator techniques are commonly used for measurement of permittivity and the dielectric loss tangent of low-loss dielectric materials. Measurements on isotropic materials are usually performed using the TE_{011} (or TE_{0nl}) mode. Generally, if dielectric characterization is required at various frequencies, more than one sample of the material under test must be provided. In the measurements reported here, we use, in addition to the TE_{0nl} mode, higher-order $TE_{0,\nu\delta}$ modes. These higher-order modes are tuned by changing the distance between the conductor ground planes of the dielectric resonator, which allows the dielectric properties of a single sample to be measured at several contiguous frequency subbands. Use of several cylindrical samples of the material under test allows properties to be determined over a broad frequency spectrum. Dielectric loss tangents on the order of 10^{-5} to 5×10^{-3} can be measured with this technique. Accurate measurements of losses as low as 10^{-5} are not achievable with transmission line or free-space methods.

The same circularly symmetric modes are also used for measurements of the relative permittivity tensor component that is perpendicular to the anisotropy axis of uniaxially anisotropic substrates. For anisotropic materials, determination of the parallel permittivity tensor component requires additional experiments with one of the hybrid or TM modes. We use the HE_{111} and the HE_{211} modes since they can be easily excited.

Applications of this dielectric resonator technique for characterizing isotropic and uniaxially anisotropic materials as a function of temperature are presented. Changes in dielectric loss characteristics with temperature can be particularly significant. When dielectric losses in substrates are important in microwave device application, they should be measured and specified at the operating temperature and frequency.

Microstrip I

A. C. Cangellaris and L. Shafai

Page

1:20	Series Fed Microstrip Array Antenna	207
	<i>Babau R. Vishvakarma, Banaras Hindu University, Milind B. Mahajan, Indian Space Research Organization</i>	
1:40	High Gain Cavity Back Microstrip Antenna as Active	208
	Array Element <i>L. Shafai*, A. Asi, University of Manitoba, D. J. Roscoe, Communications Research Centre</i>	
2:00	Effect of Superstrate Thickness and Permittivity on Stacked	209
	Electromagnetic Coupled Patch Antennas <i>Kai-Fong Lee*, Wei Chen, University of Toledo, R. Q. Lee, NASA Lewis Research Center</i>	
2:20	A Microstrip Phased Array Antenna with Low Q Elements for	210
	Southern Coverage Using MSAT <i>Radha Telikepalli*, Tim Musclow, Peter Strickland, CAL Corporation</i>	
2:40	Time Domain Analysis of Microstrip Networks using a Rational	211
	Function Approach <i>Thomas Karle, Tapan K. Sarkar, Syracuse University</i>	
3:00	BREAK	
3:20	Resonance Properties of Rectangular Patch in the Presence of	212
	Laminated Ground Plane <i>Jean-Fu Kiang*, Chung-Yuan Kung, National Chung-Hsing University</i>	
3:40	Double-Layer Circularly Polarized Microstrip Antenna with a	213
	Single Coaxial Feed <i>Choon Sae Lee, Southern Methodist University, Vahakn Nalbandian*, Felix Schwering, US Army CECOM</i>	
4:00	Numerical Analysis of a Waveguide Simulation of A Microstrip	214
	Phased Array Antenna on a Normally Biased Ferrite Substrate <i>Kang H. Lee, Sharad R. Laxpati*, University of Illinois at Chicago</i>	
4:20	Application of the PML Grid Truncation Scheme for the FDTD	215
	Analysis of Microstrip Patch Arrays <i>M. Pasik*, Sandia National Laboratories, G. Aguirre, A. C. Cangellaris, University of Arizona</i>	
4:40	A Time-Domain Iterative Method for Microstrip Antennas	216
	<i>I. Baracco, Ch. Pichot*, A. Papiernik, M. Scotto, CNRS/Universite de Nice-Sophia Antipolis</i>	

5:00 Improved Design of a Quadrature Hybrid Using an Elliptic Patch
K. L. Chan*, F. A. Alhargan, S. R. Judah, *University of Hull*

SERIES FED MICROSTRIP ARRAY ANTENNA

Babau R. Vishvakarma
Centre of Advanced Study
Electronics Engineering Department
Institute of Technology
Banaras Hindu University
Varanasi-221 005(INDIA)

And

Milind B. Mahajan
Indian Space Research Organization
Space Application Centre
Ahmedabad (INDIA)

Abstract:

The operation of radar generally needs cyclic modification of the radiation beam to suit the practical requirements. Further the growing needs for faster data rates and low reaction could be achieved with electronic scanning. The microstrip frequency scanning array antenna provides potential alternative to the existing conventional system because of its numerous inherent advantages like low weight, low cost, low profile, planar configuration, and compatibility with microwave integrated circuits and its versatile applications in aircraft, missiles, satellites, tanks, and artillery shell etc.

In view of the above some experimental investigations were conducted to examine the radiation and scanning characteristics of indigenously developed frequency scanning microstrip array antenna. Three antennas with 6 element, 12 element, and 18 element were fabricated and experimentally tested. It has been found that there is beam steering of 50° ($Q_m = \pm 25^\circ$) when the frequency deviation of ± 200 MHz is effected. The sidelobe level for 6 element, 12 element, and 18 element array is found to be -14dB, -12dB, and -10dB respectively. The scanning is found to improve with increasing number of elements in the array. The scan rate of 0.125 deg/MHz has been obtained which is much better than the earlier reported data. It has been noticed that apart from the off set error in the centre frequency due to 3% error in the lay out, the measured and calculated values of the main beam direction are in good agreement. At the centre frequency the beam is observed to be quite sharp as compared to the frequencies ^{at} off resonance, which indicates the degradations of beam during the course of scanning. However, the predicted values of 3dB beam width are found to be 10% larger than the experimentally observed values which is attributed to the overestimated values of transmission coefficient and element to element attenuation factor. From the observations recorded for the return loss, 2:1 VSWR band width were found to be 660 MHz, 1100 MHz, and 1200 MHz for 6, 12, and 18 element array respectively. This reveals that increasing number of elements in the array increases the bandwidth.

High Gain Cavity Back Microstrip Antenna as Active Array Element

L. Shafai* and A. Asi

Antenna Laboratory

Department of Electrical and Computer Engineering

University of Manitoba

Winnipeg, Canada, R3T 5V6

D.J. Roscoe

Antennas and Integrated Electronics

Communications Research Centre

Ottawa, Canada, K2H 8S2

Microstrip arrays are attractive antenna candidates for low cost satellite communication terminals. The feed line loss, however has limited their use in high gain applications and successful designs have been limited to low to moderate gain arrays. Two separate issues have restricted their use. At the low frequency end, around the L and C Bands, the resistive losses are moderate, but the practical arrays, with gains around 30dB or higher, are physically large. Since high quality substrate materials are still relatively expensive, the resulting antennas become too costly for practical applications. At the high frequency end, on the other hand, the resistive losses become excessive and limit the array gain, while deteriorating its G/T. Consequently, most microstrip arrays have been limited to moderate gains and for applications around the Ku-band.

Here, we consider an array design in the EHF-band, for both 20 and 30 GHz applications. An active array configuration is of interest to distribute the active elements in the array, to improve the efficiency or G/T, by minimizing the resistive losses. Naturally, the array cost is influenced by the number of the active elements, but may be controlled by using subarrays of microstrip patches. In such a case the resistive losses at the subarray level will limit the array performance. To remedy this problem the subarray is replaced here by a high gain microstrip element. This is achieved by using the microstrip patch to feed a moderate size cavity that radiates through its aperture to yield gains around 15dBi at the array broadside. Such a design eliminates the subarray and its lossy feed network and improves the array performance. The size of the cavity, however, is an important parameter that should be optimized for a given array configuration. The performance data will be presented for various practical configurations.

EFFECT OF SUPERSTRATE THICKNESS AND PERMITTIVITY ON STACKED ELECTROMAGNETIC COUPLED PATCH ANTENNAS

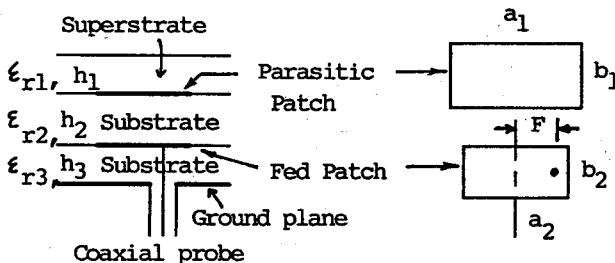
Kai-Fong Lee* and Wei Chen

Dept. of Electrical Engineering, University of Toledo, Toledo, Ohio

R. Q. Lee

NASA Lewis Research Center, Cleveland, Ohio

The geometry of the stacked two-layer electromagnetic coupled patch antenna is shown. In this paper, we study theoretically the effects of superstrate thickness and superstrate permittivity on the input impedance and half-power beamwidths of the antenna, using a model developed previously [K. F. Lee, W. Chen, R. Q. Lee, Microwave and Optical Technology Letters, March 1995]. As an example, we consider an antenna with the following parameters: $a_1=2.198$ cm, $b_1=1.465$ cm, $a_2=2.027$ cm, $b_2=1.351$ cm, $F=0.94$ cm, $h_2=3.63$ mm, $h_3=0.486$ mm, $\epsilon_{r2}=1.2$, $\epsilon_{r3}=2.2$. To study the effect of superstrate permittivity, h_1 is set at 0.26 mm and five values of ϵ_{r1} are used: 2.2, 4.0, 6.0, 8.0, 10.0. For $\epsilon_{r1}=2.2$, a double loop impedance locus with a bandwidth (VSWR=2) of 12% is obtained, centered around 5 GHz. As ϵ_{r1} increases from 2.2 to 10.0, the double loop characteristic of the impedance loci gradually degenerates into a single loop. The HPBW in the E plane decreases from 70° to 61° while that in the H plane remains unchanged at 85° . To study the effect of superstrate thickness, ϵ_{r2} is set at 2.2 and four values of h_1 are used: 0.26 mm, 1.0 mm, 3.0 mm, and 5.0 mm. As h_1 increases from 0.26 mm to 5.0 mm, the double loop characteristic of the impedance loci again gradually degenerates into a single loop. The HPBW in the E plane decreases from 70° to 57° while the HPBW in the H plane increases from 85° to 98° . This example shows the importance of a proper combination of thickness and permittivity if a dielectric cover is used in the two-layer electromagnetically coupled patch antenna. Other examples will be presented in the meeting.



A MICROSTRIP PHASED ARRAY ANTENNA WITH LOW Q ELEMENTS FOR SOUTHERN COVERAGE USING MSAT

Radha Telikepalli*, Tim Musclow and Peter Strickland
CAL Corporation
1050 Morrison Drive
Ottawa, ON CANADA K2H 8K7

A microstrip phased array has been designed and developed to satisfy the requirements for southern coverage using MSAT. Required bandwidth of the array was 8.5% to cover a frequency range of 1530 - 1660 MHz which was achieved with the help of the element used in the array. The developed array consists of nine elements, each of which was built over a substrate which is a combination of 1" air core honey comb and 0.010" FR - 4 which facilitates the fabrication of the patch. This combination gives a low dielectric constant and a low unloaded quality factor which increases the impedance bandwidth of the element. Developed element has an input impedance of 400 Ohms which was transformed to 190 Ohms with the help of stubs at two sides of the patch as shown in Figure 1.

Developed array was to satisfy the envelope requirements shown in Figure 2 to give a beam around 43° above the horizon. Design requirements include right hand circular polarization, a maximum gain of 11 dBic. Right hand circular polarization was provided by feeding the patch at two ports with an equal power and 90° out of phase. The array consisted of nine elements within a circle of 11.5", had a minimum return loss of -20 dB, a beam peak at 43° above horizon and a maximum gain of 11 dBic. This paper presents the design, development and measured characteristics of the element and array.

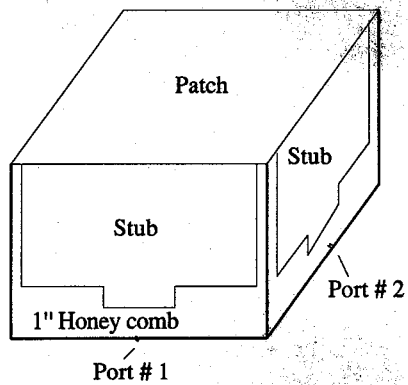


Figure 1 Configuration of the patch used in the array development

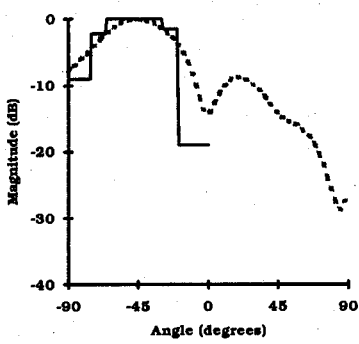


Figure 2 Measured radiation pattern (- -) and the required envelope

TIME DOMAIN ANALYSIS OF MICROSTRIP NETWORKS USING A RATIONAL FUNCTION APPROACH

Thomas Karle
Tapan K. Sarkar

Department of Electrical Engineering
Syracuse University
Syracuse, NY 13244-1240, USA

Abstract

Conventional FFT techniques are frequently used to estimate the time domain response of microwave networks. These techniques require a large bandwidth of frequency domain data in order to resolve two or more reflections from closely spaced discontinuities. The need for large bandwidth is also a concern in determining the time domain response of more complicated networks which contain tapered discontinuities. This restriction of the FFT can be avoided by using a parametric technique.

This paper discusses a parametric technique which is based on modeling the Z-transform of the frequency data samples as an overdetermined rational function and transforming the result into the time domain. The rational function approach is advantageous in that broadband information can be obtained from narrowband input data. Thus, the requirement for large bandwidth of the frequency data samples is diminished with this parametric technique.

The development of the overdetermined rational function requires a solution to a matrix system whose unknowns are the coefficients of the rational function. The singular value decomposition of the matrix provides insight in choosing the appropriate orders of the polynomials which comprise the rational function. Upon determining an appropriate matrix order, the matrix system is solved by using the Total Least Squares method.

The new parametric technique is evaluated on several microstrip networks which contain different degrees of tapered discontinuities. The experimental time domain results are compared to measured results using an HP8510B network analyzer and a TEK7854 oscilloscope with TDR capability.

Resonance Properties of Rectangular Patch in the Presence of Laminated Ground Plane

Jean-Fu Kiang* and Chung-Yuan Kung
Department of Electrical Engineering
National Chung-Hsing University
Taichung, Taiwan, ROC

Conventionally, the ground plane of a patch resonator is modeled as a perfect electric conductor. In modern aircraft and vehicle surface designs, composite materials have been widely used to reduce weight or radar cross section. An example of composite is made of graphite fibers embedded in an epoxy resin. The conductivity along the fiber orientation is much higher than that in the perpendicular orientations. If a resonator is built on such composite, the resonance properties will be different from that of a perfect conductor ground plane.

We assume that the fiber spacing in each lamina of the composite is much smaller than a wavelength, hence each lamina can be modeled as an anisotropic layer with a conductivity tensor. A transition matrix in the spectral domain is then formulated to relate the tangential field components in different laminae. By imposing boundary conditions, we derive an integral equation in terms of the electric surface current on the rectangular patch. Next, we choose a set of basis functions to represent the patch surface current, then apply the Galerkin's method to calculate the resonance frequencies. We also derive a perturbation approach to compare with Galerkin's method.

We calculate the resonance frequency of a rectangular patch in the presence of a two-lamina G/E composite ground plane. The real part of resonance frequency decreases significantly when the substrate thickness d approaches zero, especially with high substrate dielectric constant. We also observe that higher substrate dielectric constant gives higher imaginary part. As d gets smaller, the field beneath the patch tends to leak through the laminated ground plane. The results with solid copper ground plane are obtained for comparison. Next, we vary the conductivity in the fiber direction, σ'_{xx} , from 10^4 to 10^7 U/m. We observe that higher substrate dielectric constant gives higher imaginary frequency shift at low σ'_{xx} .

In summary, the imaginary frequency shift increases when the substrate gets thinner and when the lamina conductivity decreases. It is caused by power leakage through the laminated ground plane, which is more significant at higher substrate dielectric constant.

DOUBLE-LAYER CIRCULARLY POLARIZED MICROSTRIP ANTENNA WITH A SINGLE COAXIAL FEED

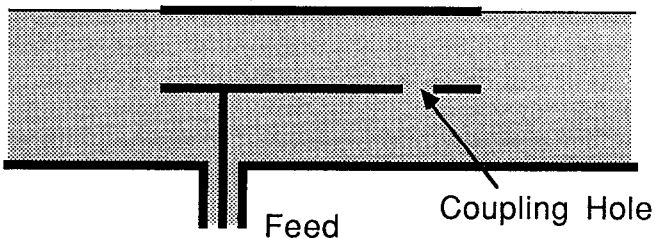
Choon Sae Lee
Electrical Engineering Department
Southern Methodist University
Dallas, Texas 75275

Vahakn Nalbandian* and Felix Schwering
US Army CECOM
Fort Monmouth, New Jersey 07703

In many applications, antennas are required to have a circularly polarized (CP) radiation. Even though single-feed CP microstrip antennas are available, the CP bandwidth is too small to be useful in some applications. Presently for a CP microstrip antenna, two feeds with a 90° phase difference are usually used to provide a sufficient CP bandwidth. In this presentation, a novel CP microstrip antenna with a single coaxial feed is described.

The proposed CP antenna consists of two layers and two patches as shown below. The top patch is a radiating element and the middle patch is a microstrip dividing the upper and the lower layers. The lower layer is fed by a coaxial transmission line and the upper layer is coupled with the lower layer through small circular holes on the middle patch. The coupling apertures should be small enough to provide field excitations in those two layers 90° out of phase, but large enough to give substantial coupling between the upper and lower resonant cavities (R. E. Collin, *Field Theory of Guided Waves*, 2nd Ed. New York: IEEE Press, Ch. 7). Also those holes are arranged in order that the radiation at the zenith from the lower layer be perpendicular to that from the upper layer.

The proposed antenna is simple and inexpensive to fabricate. The CP quality is excellent over a wide range of radiation angle and the design procedure is relatively simple. Both theoretical and experimental results for optimum designs will be presented.



Numerical Analysis of A Waveguide Simulation of A Microstrip Phased Array Antenna on A Normally Biased Ferrite Substrate

Kang H. Lee and Sharad R. Laxpati*

Department of Electrical Engineering and Computer Science (M/C 154)
University of Illinois at Chicago
851 South Morgan Street
Chicago, IL 60607-7053

Several analytical studies of the microstrip patch antennas on ferrite substrates with or without layers of dielectric material have been reported in the literature over the past few years. Almost all of these works utilize spectral domain moment method analysis. This requires determination of an appropriate Green's function which for antennas with complex geometries has to be evaluated numerically. Recently, McGrath and Pyati [1994 IEEE AP-S Symposium Digest] presented a study using finite element method and using Floquet's theorem to analyze an infinite phased array microstrip patch antenna.

Waveguide simulators have been used for many years [Gregorwich, Hessel and Knittel, Microwave J., 1971; Pozar and Schaubert, IEEE Trans. Antennas Propagat., 1984] for experimental verification of the radiation characteristics of an infinite phased array at a discrete set of radiation directions. There are limitations placed on the kind of substrate materials that may be used in such an experimental study. However, such limitations can be relaxed, if a computer simulation of such a waveguide simulator is undertaken.

In this study, numerical analysis of a two dimensional, infinite array of microstrip patches is carried out using a waveguide simulator. A single substrate of either dielectric or normally biased ferrite is included. This waveguide geometry is analyzed numerically using the FDTD technique. Mur's 2nd order radiation boundary condition is imposed on the patch side of the waveguide. The patch is fed with a probe where the excitation is modeled as a delta-gap voltage source near the ground plane. The voltage source is a unit amplitude sine modulated Gaussian pulse. The biased ferrite substrate is characterized via appropriate first order magnetization equation. The FDTD technique is used to solve the coupled set of Maxwell's and magnetization equations. The current on the probe is obtained from the magnetic field. The input impedance of the probe is determined from the ratio of the Fourier transform of the source voltage and the probe current. The results of input impedance are found to compare favorably with the available spectral domain method of moment results. The effect of the dc biasing of the substrate on the radiation and resonance characteristic of an array of microstrip patches is discussed.

APPLICATION OF THE PML GRID TRUNCATION SCHEME FOR THE FDTD ANALYSIS OF MICROSTRIP PATCH ARRAYS

*M. Pasik**, *G. Aguirre†*, and *A.C. Cangellaris†*

* Computational EM & Plasma Physics Department
Sandia National Laboratories

Albuquerque, NM 87185-5800, USA

phone: 505-845-7261; FAX: 505-845-7890

† Center for Electronic Packaging Research

Department of Electrical and Computer Engineering

University of Arizona, Tucson, AZ 85721, USA

phone: 602-621-4521; FAX: 602-621-2999

e-mail: jaguir@helios.ccc.arizona.edu

This paper examines the issues associated with the application of the Perfect Latched Layer (PML) numerical grid truncation scheme to the FDTD analysis of planar integrated circuits that involve both waveguiding structures and radiating elements, of the type encountered in one- and two-dimensional patch antenna arrays.

Despite its modeling versatility and computational simplicity, applications of the FDTD method to the electromagnetic modeling of open planar microwave integrated circuits with strong radiation characteristics have been hindered by the lack of robust absorbing boundary conditions capable of handling the propagating, radiating, and evanescent character of the electromagnetic fields in such structures. The PML numerical grid truncation scheme, recently proposed by J.-P. Berenger, appears to be a very promising alternative to earlier, rather cumbersome absorbing boundary conditions, constructed specifically for the FDTD analysis of integrated planar microwave circuits.

The focus of this presentation is on the performance of the PML as it is brought very close to the planar waveguiding and radiating elements (essentially in the near field of the structure). From a computational efficiency point of view, this is highly desirable since it reduces both memory and CPU requirements. It is shown that placement of the PMLs very close to the planar structures perturbs their electromagnetic properties. To alleviate this difficulty, a modification to the standard PML model is proposed that allows placement of the PMLs only a few cells away from the planar structures without perturbing the electromagnetic behavior of the circuit and the radiating properties of the patches. Numerical examples of radiation from patch antenna arrays are used to examine the accuracy and computational efficiency of the resulting FDTD algorithm.

I. Baracco[†], Ch. Pichot^{‡*}, A. Papiernik[†], M. Scotto[†]

[†]Laboratoire d'Electronique, Antennes et Télécommunications,
[‡]Laboratoire Informatique, Signaux et Systèmes de Sophia Antipolis,
 CNRS/Université de Nice-Sophia Antipolis,
 250 rue A. Einstein, 06560 Valbonne, France.

This paper deals with a new time-domain iterative method for the study of printed antennas. Until now, various numerical methods have been used for studying printed antennas. They can be classified in two different groups : frequency and time-domain approaches. Among these two, FD-TD, finite-element and the integral equation methods are very well known. In the frequency domain, either spatial or spectral domain approaches have been used. For time-domain and to our knowledge, only spatial approaches have been used. Consequently, it seems interesting to investigate and develop a time-domain method based on a spectral-domain approach by carrying the analytical calculations as far as possible.

To illustrate the method, a printed antenna with square shape patch and fed by coaxial probe with $\delta(t)$ dependence for impressed current has been considered. The layer is the vacuum and the ground plane is assumed to be infinite. Applying a 2D spatial-Fourier transform to time-dependent Maxwell's equations, one can derive a partial differential equation for the vector potential in terms of the unknown surface current. The corresponding dyadic Green's function is calculated. The tangential components of the electric field are exhibited. One makes use of an integral equation based on the reaction concept. A method of moments is applied via a spatial Galerkin's procedure with sinus basis functions, the time-dependence being arbitrary :

$$\tilde{j}_s = \sum_{n=1}^N a_n(t) \cdot \tilde{f}_n(\alpha, \beta)$$

where the overtilde indicates the 2D-Fourier transform.

The goal is the determination of coefficients $a_n(t)$ with an iterative procedure.

In order to simplify the calculations and estimate the performance of the method, some assumptions have been made. First, the spatial dependence of the surface current is assumed to be along one axis only (x axis) and the summation is restricted to $n=1$ (fundamental mode). Under these assumptions, it is possible to find a relation allowing to express the coefficient $a_1(t)$ at any time t in function of the coefficient values at previous time steps.

After investigating the performance of this new method in this simple case configuration, more complicated cases will be studied with less assumptions on the surface current. The spatial dependence of the surface current will be decomposed along the two axes (x axis and y axis) and the summation will be extended beyond $n=1$ (multimode configuration). The case of time-dependence arbitrary $S(t)$ for impressed current will be also investigated.

Improved Design of a Quadrature Hybrid Using an Elliptic Patch

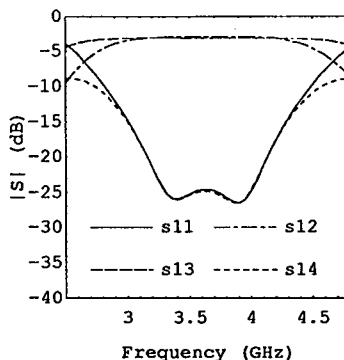
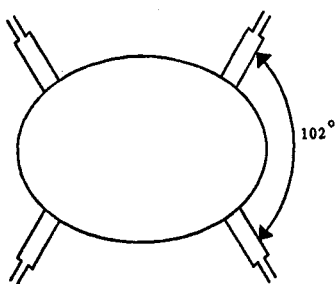
K.L. Chan*, F.A. Alhargan† and S.R. Judah

Department of Electronic Engineering, University of Hull, U.K.

Quadrature hybrids are one of the key components in microwave systems. These generally are of TEM mode transmission line type; they have the disadvantage of being difficult to implement at very high frequencies. To overcome this difficulty, a circular patch configuration was used (M.J. Page and S.R. Judah, IEEE MTT-38, 1733-1736). This though has limited bandwidth and to improve this, dummy ports have been introduced by (M.E. Bialkowschi and S.T. Jellett IEEE MTT-42 1437-1442). The short length of lines at the dummy ports are subject to additional junction effects and increased manufacturing difficulty.

An elliptic patch provides more design flexibility by offering two variables, namely eccentricity and port position, which one can vary at will to obtain a desired response. The analysis of the elliptic disk is carried out using the cavity model Green's function (F.A. Alhargan and S.R. Judah, IEEE MTT-40, 1726-1730). This approach is sufficiently accurate and computationally efficient, allowing an interactive optimisation to be performed. Fringing fields are accounted for by using effective permittivity and effective dimensions of the elliptic patch.

A quadrature hybrid using an elliptic patch with an eccentricity of 0.62 and focal length of 12.09 mm has been designed on RT/Duroid 5880 with relative permittivity 2.2 and substrate thickness of 0.508mm. Ports are located at circumferential angles of 51 degrees with respect to the major axis of the elliptic patch and are connected to microstrip lines with characteristic impedance of 23.4 ohms and lengths of 10.8mm. This configuration exhibits a flat coupling response over a relatively wide frequency band giving an operational bandwidth of approximately 26%.



† now with King Abdulaziz City for Science and Technology, Saudi Arabia

THIS PAGE INTENTIONALLY LEFT BLANK.

Special Session

Parallel and Distributed Computation in Electromagnetics

T. Cwik and R. Mittra

Page

- 1:20 Parallel Solution of Unstructured Sparse Finite Element Equations
*N. Kapadia, B. Lichtenberg, J. A. B. Fortes, J. L. Gray, H. J. Siegel,
K. J. Webb, Purdue University*
- 1:40 Large Scale Finite Element Modeling Using Scalable Parallel 220
Processing
*Tom Cwik, JPL, Daniel Katz, Cray Research, Cinzia Zuffada,
Vahraz Jamnejad, JPL*
- 2:00 The Performance of Linear Algebra Routines on a Distributed 221
Memory Massively Parallel Computer
Steven Castillo, Jay Martinez, William Dearholt,
New Mexico State University*
- 2:20 Distributed Parallel Finite Difference Time Domain Calculations 222
using Parallel Virtual Machine 3.2
V. Varadarajan, D. Oh, R. Mittra, University of Illinois at Urbana-Champaign*
- 2:40 Implementation of Advanced FDTD Methods on Parallel and 223
Distributed Computers
Stephen D. Gedney, University of Kentucky, Faiza Lansing,
Jet Propulsion Laboratory*
- 3:00 BREAK
- 3:20 Large Scale Integral Equation Modeling Using Scalable Parallel 224
Processing
Tom Cwik, Jet Propulsion Laboratory, Daniel Katz,
Cray Research, Inc. Jean Patterson, Jet Propulsion Laboratory*
- 3:40 Parallel Performance of the CARLOS-3D Method of 225
Moments Code
*J. M. Putnam, D. D. Car, McDonnell Douglas Corp., J. D. Kotulski, Sandia
National Laboratories*
- 4:00 Massive Parallelism is the Solution: Are We Kidding Ourselves? 226
Adrian S. King, Kent Lusted, Intel Corporation
- 4:20 Time and Space Parallel Solution of Maxwell's Equations on 227
Massively Parallel MIMD Architectures
Michael A. Jensen, Brigham Young University, Amir Fijany,
Jet Propulsion Laboratory, Yahya Rahmat-Samii, University of California at Los
Angeles*

Large Scale Finite Element Modeling Using Scalable Parallel Processing

Tom Cwik*, Daniel Katz†, Cinzia Zuffada, Vahraz Jamnejad

Jet Propulsion Laboratory
California Institute of Technology
Pasadena, CA 91109

†Cray Research Inc.
El Segundo, CA 90245

Finite element modeling has proven useful for accurately simulating scattered or radiated electromagnetic fields from complex three-dimensional objects whose geometry varies on the scale of a fraction of an electrical wavelength. An unstructured finite element model of realistic objects leads to a large, sparse, system of equations that needs to be solved efficiently with regard to machine memory and execution time. Different solvers can be used to produce solutions to these systems of equations including both factorization methods and iterative ones. Factorization methods lead to high memory requirements that limit the electrical problem size of three-dimensional objects that can be modeled. An iterative solver can be used to efficiently solve the system without excessive memory use, and in a minimal amount of time if the convergence rate is controlled.

In this work an iterative solver for use with our finite element codes was developed for the Cray T3D massively parallel processor located at the Jet Propulsion Laboratory. This development was completed in two stages. First, a matrix decomposition algorithm was constructed, properly decomposing the sparse *matrix entries* into data sets that were read by the T3D processing elements (PEs). It is noted that this is a different strategy than the usual *mesh* decomposition algorithms developed in the past. The second stage was the construction of an scalable iterative solver on the T3D that efficiently computes a solution of the sparse system. The initial sparse matrix decomposition algorithm was originally developed for a YMP processor and then ported to the T3D.

In this talk we will present an overview of sparse matrix methods for distributed memory machines, as well as the specific implementation of the iterative solver. Example solutions have been obtained for systems with over one-half million unknowns.

THE PERFORMANCE OF LINEAR ALGEBRA ROUTINES ON A DISTRIBUTED MEMORY MASSIVELY PARALLEL COMPUTER

Steven Castillo*, Jay Martinez, and William Dearholt
Electrical and Computer Engineering Dept.
Dept. 3-O, Box 30001
New Mexico State University
Las Cruces, NM 88003

A large class of numerical solutions applied to complex electromagnetic problems result in a large, sparse system of algebraic equations which must be solved. The solution is found either by a Gaussian elimination procedure such as LU or Choleski factorization or by using one of the many iterative procedures which belong to the family of Krylov subspace methods. The application of an implicit finite-difference method on an orthogonal grid results in a coefficient matrix with a regular sparsity structure while a finite-element procedure will result in a coefficient matrix with an irregular sparsity structure. In all cases, the memory size and CPU speed of the most advanced conventional scalar or vector processors limit the size of problems that can be solved. Additionally, the rate of increase in CPU speed for conventional processors is beginning to level off because of physical limitations.

In this paper, we examine the use of a massively parallel supercomputer for solving large sparse systems of equations. The particular computer used for this research is the Cray T3D which uses DEC 21064 'Alpha' microprocessors arranged in a three-dimensional wrapped torus topology. The T3D requires a Cray YMP front end for managing I/O, compiling, and directing the processing on the parallel machine. While the actual computer can be considered to be a distributed-memory parallel processor, programming is done using the Cray CRAFT programming model which uses shared memory constructs. Explicit message passing can be used but is not considered here.

Examples of problems for both irregular and regular problems using direct solvers and Krylov subspace solvers will be given. The complexity of using the CRAFT programming model for linear algebra routines will be discussed in detail as well as timings and efficiencies for several different problem types and sizes from the areas of electromagnetic scattering, electrostatics and semiconductors. Specific routines affecting the overall performance of a given solver such as vector-vector products, matrix-vector products, outer and inner factorization schemes and gather-scatterer operations will be examined in detail.

Distributed Parallel Finite Difference Time Domain Calculations using Parallel Virtual Machine 3.2

V. Varadarajan, D. Oh and R. Mittra*
Electromagnetic Communication Laboratory
Department of Electrical and Computer Engineering
University of Illinois at Urbana-Champaign, IL 61801

Distributed parallel implementation of the Finite Difference Time Domain (FDTD) algorithm for the solution of Maxwell's equations has the potential to solve problems involving large data sets on a workstation cluster, as well on distributed memory machines. This presentation describes an implementation of the FDTD calculations using the Parallel Virtual Machine [PVM] 3.2 algorithm, for a test problem involving a three-dimensional rectangular cavity and an FDTD code called PTAP. An optimum decomposition of the computational volume can also be achieved for microstrip problems by localizing the volume around the material regions. Optimization issues such as regulated communications, and minimization of task idle times are discussed, and performance factors for representative large problem sizes are given. It is found that the speedup factors can approach the maximum values for large problem sizes if the computation-to-communication ratios are maintained at values significantly greater than unity. It is also found that, in order to achieve linear speedups, it becomes necessary to increase the problem sizes with the increase in the number of processors so that an adequate computation-to-communication ratios can be maintained on individual processors in a workstation cluster, or on a distributed memory machine. As an example, Fig. 1 below indicates the speedups achieved for several large size FDTD problems on an HP workstation cluster, and presents the speedups for two fixed-size problems (75x75x150 cells and 75x75x300 cells) and one variable size problem (100x100x800 cells per processor). In the presentation, the performance improvement due to faster communication modes available in the distributed memory machines will be illustrated with the results obtained on an IBM-SP1, and a mixed group of workstations. The paper will demonstrate that the PVM 3.2 can provide a low-cost approach to the solution of large FDTD problems without recourse to expensive parallel computers.

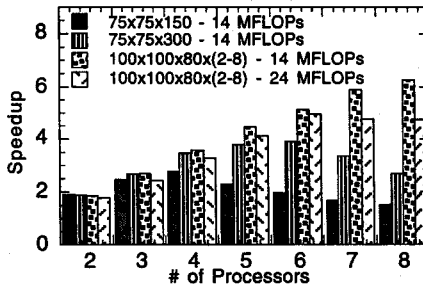


Fig. 1. Speedup for several problem sizes: 75x75x150 cells (total), 75x75x300 cells(total), and 100x100x80 cells (per processor) at 14 and 24 MFLOps.

Implementation of Advanced FDTD methods on Parallel and Distributed Computers

Stephen D. Gedney*
Electromagnetic Laboratory
Department of Electrical Engineering
University of Kentucky
Lexington, KY 40506

Faiza Lansing
Spacecraft Telecommunications
Equipment Section
Jet Propulsion Laboratory
Pasadena, CA 91109

The efficiency and versatility of finite-difference time-domain (FDTD) based algorithms has enabled the accurate computational analysis of a wide range of practical engineering problems. Problems with highly irregular geometries and boundaries have also been readily treated through recent development of advanced FDTD algorithms based on non-uniform orthogonal grids [P. Monk, *IEEE Trans. Magnetics*, vol. 30, pp. 3200-3203, September 1994] and unstructured non-orthogonal grids, such as the planar generalized-Yee (PGY) algorithm [S. Gedney and F. Lansing, *IEEE Antennas Prop. Symposium Dig.* Ann Arbor, MI: 1993].

The analysis of relatively modest-sized problems using FDTD based algorithms can usually be simulated on conventional sequential workstations quite efficiently. On the other hand, the analysis of very large problems often require much greater resources, such as that provided by high performance parallel computers. By exploiting the architecture's of such computers, the sizes of problems that can currently be solved are orders of magnitudes larger than problems that could have been treated only two or three years ago.

FDTD based algorithms are ideally suited for massively parallel computers and highly scalable algorithms have been developed for them [S. Gedney, et. al, *Int. J. Numerical Modeling (Electronic Networks, Devices and Fields)*, in press]. It is the intent of this paper to present an overview of efficient parallel algorithms for the implementation of non-uniform grid and unstructured grid based FDTD methods on a variety of platforms, such as the Intel Paragon, the Cray T3D, and the Convex Exemplar. Specific focus will be on methodologies used to optimize the parallel efficiencies and overall computational speeds of the parallel computations. Techniques such as interleaving computation with communication and other secondary tasks such as field updates on absorbing boundaries are shown to result in improved speedups. Methods to reduce interprocessor communication and load imbalances will also be presented. Finally, it will be demonstrated, that efficient parallel algorithms for FDTD based methods can be easily developed for high performance parallel computers resulting in highly effective computational tools for the analysis of challenging engineering problems.

Large Scale Integral Equation Modeling Using Scalable Parallel Processing

*Tom Cwik**, *Daniel Katz*[†], *Jean Patterson*

Jet Propulsion Laboratory
California Institute of Technology
Pasadena, CA 91109

[†]Cray Research Inc.
El Segundo, CA 90245

The evolution of computing hardware and software continues to allow the solution of electromagnetic problems of ever increasing electrical size. This advancement has been a partial stimulus to the development of partial differential techniques such as finite difference or finite element methods, as well as permitting the use of existing integral equation techniques to solve larger problems in shorter amounts of time. Integral equation solutions generally involve geometry description via a computer aided geometry package, matrix fill algorithms which involve the basis functions and all electromagnetic parameters of the scatterer or antenna, matrix equation solution, and finally calculation and display of the observables. For electrically large structures, the matrix equation solution algorithm typically becomes the dominant component of the calculation, both in execution time and needed memory.

Dense matrix solution algorithms are written to optimize both computational speed and storage. Traditional factorization algorithms are used to decompose the general complex-valued, impedance matrix resulting from the integral equation solution into factors that are used to solve for field solutions due to different excitations. The factorization algorithms can use the in-core memory attached to the machine—therefore problem size is limited by this parameter—or out-of-core algorithms which use the associated disk to hold the impedance matrix and its factors. The out-of-core methods therefore allow the solution of much larger problems if the disk space is available. Current developments in non-factorization solution methods use preconditioned iterative algorithms, or low-rank approximations to the linear system, to extend the problem size or reduce the solution time.

In this talk, we will discuss the development of in-core and out-of-core dense matrix solvers, and their integration into existing integral equation codes on distributed memory, scalable parallel processors. Problem sizes exceeding 60,000 unknowns modeling the fields or currents are capable of being solved in less than 100 minutes time for the factorization using an in-core algorithm on a 1024 processor Cray T3D. Out-of-core algorithms have been developed that run at nearly the same execution rate as the in-core algorithms, extending the problem size limit past this number. The current development in preconditioned iterative algorithms and low-rank approximations will also be discussed as applied to distributed memory, scalable parallel processing.

Parallel Performance of the CARLOS-3D Method of Moments Code

J.M. Putnam and D.D. Car
McDonnell Douglas Corporation
PO Box 516
MC 064-2263
St. Louis, MO 63166-0516

J. D. Kotulski
Sandia National Laboratories
Radiation and Electromagnetic Analysis Department
MS 1166
PO Box 5800
Albuquerque, NM 87185-1166

CARLOS-3D is a three-dimensional electromagnetic scattering code based on a Galerkin method of moments formulation employing roof-top basis functions developed by Rao, Wilton, and Glisson to model arbitrary geometries composed of multiple conducting and homogeneous dielectric regions. Various boundary conditions including conducting, dielectric, resistive, and impedance can be specified on surfaces composing the target. This presentation will begin with an overview of the basic features of the implementation of the method of moments formulation in CARLOS-3D.

The presentation will then discuss the changes to the serial code to allow porting to the Intel Paragon. The key steps in the parallelization process will be discussed focusing on the matrix fill, right-hand-side fill, and the far-field computation. The solution for the surface currents depends on the available parallel solver packages. Three will be discussed including the Intel Pro-Solver DES package for out-of-core solutions, and in-core and out-of-core solvers developed at Sandia.

Results will be presented demonstrating the performance of the code for large scattering problems. The performance of the solvers will also be discussed along with other issues related to the parallel implementation.

Massive Parallelism is the Solution: Are We Kidding Ourselves?

**Adrian S. King
Kent Lusted**

**Intel Supercomputer System Division
CO6-10, Zone 8
14924 NW Greenbrier Pkwy
Beaverton, OR 97006**

The solution of large scale electromagnetic problems can be very computationally intensive. Furthermore, many problems of critical importance are not currently tractable. One method of addressing this problem is by "brute forcing" traditional algorithms onto larger and larger computational platforms such as massively parallel processors. Brute force methodologies are often limited by overwhelming operation counts that degrade accuracy and require unacceptable compute times. Furthermore, memory costs of brute force solutions are too expensive. This presentation will examine the effectiveness of simply depending on increases in computational power to solve problems of interest. Alternative formulations and the inter-relationships between the computer architecture, physics, and algorithms will be shown. The factors presented will clearly demonstrate the need for significant advances in computer platform capabilities as well as algorithms.

Time and Space Parallel Solution of Maxwell's Equations on Massively Parallel MIMD Architectures

Michael A. Jensen*[†], Amir Fijany[‡], and Yahya Rahmat-Samii^{††}

[†]Dept. of Comp. and Elec. Eng., BYU, Provo, UT 84602

[‡]JPL, California Institute of Technology, Pasadena, CA, 91109

^{††}Dept. of Elec. Eng., UCLA, Los Angeles, CA 90024-1594

Recently, considerable effort has been devoted to the massively parallel solution of finite-difference time-domain (FDTD) approximations to Maxwell's equations. Traditionally, these implementations exploit spatial domain decompositions or "spatial parallelism" in which each processor performs the differencing in a given spatial region at each time step. For many of these schemes, however, communication and synchronization requirements tend to limit the computational speed-up enabled. In response to these communication bottlenecks, a new approach, known as the time-parallel algorithm, was recently introduced which represents a drastic departure from traditional techniques (M. Jensen et al, 1994 IEEE AP-S Intl. Symposium Digest, pp. 380-383). This new algorithm uses the eigenvalue-eigenvector (EE) decomposition of the FDTD matrix to diagonalize the time-stepping matrix equation. This diagonal linear recurrence can then be efficiently solved on massively parallel multiple instruction multiple data (MIMD) computer architectures with minimal communication and synchronization requirements.

Since the algorithm's original introduction, several issues associated with its theoretical basis as well as its practical implementation have been explored. From a theoretical standpoint, the algorithm has been expanded to use time and space parallelism to incorporate absorbing boundary conditions on the outer domain boundary and to allow modeling of materials with some degree of inhomogeneity. From a more practical standpoint, different algorithms for parallelizing the EE decomposition of the FDTD matrix and the solution of the diagonal linear recurrence have been compared and evaluated. Additionally, the computational implications of solving a given geometry for several different source configurations has been investigated. For these scenarios, excellent computational speed-up has been achieved using practical implementations.

The presentation will expand upon the theoretical and computational bases for the time-parallel algorithm and will detail its application to the Crank-Nicolson solution of the time-domain scalar wave equation. Results of practical implementations of the algorithm on the Intel Touchstone Delta and Paragon supercomputers will be provided for several representative configurations. Additionally, comparisons of the different parallel implementations of the EE decomposition computation and the linear recurrence solution will be demonstrated.

THIS PAGE INTENTIONALLY LEFT BLANK.

Special Session

Page

Image Reconstruction From Real Data

R. V. McGahan, R. Kleinman and M. Fiddy

- 1:20 Image Reconstruction from Ipswich Data 231
*P. M. van den Berg**, Delft University of Technology, R. E. Kleinman,
University of Delaware
- 1:40 Two-Dimensional Tomography Algorithms applied to the 232
Ipswich Data
*K. Belkebir, J. M. Elissalt, J. M. Geffrin, Laboratoire des Signaux
et Systemes*
- 2:00 Object Reconstruction from Far-Field Data Using Gradient 233
and Gauss-Newton Type Methods
*P. Lobel, CNRS/Université de Nice-Sophia Antipolis, R. Kleinman,
University of Delaware, Ch. Pichot*, L. Blanc-Feraud, M. Barlaud,
CNRS/Université de Nice-Sophia Antipolis*
- 2:20 Microwave Tomography: Problems Related to Reconstructions 234
from Experimental Data
J. Joachimowicz, J. Ch. Bolomey, A. Joisel, A. Franchois, M. Geleoc,
SUPELEC/LSS*
- 2:40 On Modified Gradient Solution Methods Using the Binary 235
Aspect of the Unknown Electromagnetic Parameters and
Their Application to the Ipswich Data
B. Duchene, D. Lesselier, Laboratoire des Signaux et Systemes*
- 3:00 BREAK
- 3:20 Diffraction Tomography Reconstructions from Real Data 236
J. J. Stamnes, University of Bergen, L.-J. Gelius, Norwave Development
AT, T. C. Wedberg, Norwegian Institute of Fisheries & Aquaculture*
- 3:40 Processing Experimental Data with Local Shape Function 237
Method and Distorted Born Iterative Method
C. C. Lu, W. C. Chew, University of Illinois*
- 4:00 Imaging of Unknown Targets from Measured Scattering Data 238
*J. B. Morris, Rome Laboratory, D. A. Pommet, University of
Massachusetts-Lowell, R. V. McGahan, Rome Laboratory, M. A. Fiddy,
University of Massachusetts-Lowell*
- 4:20 Application of Holographic Synthetic Aperture Radar Techniques to
Monochromatic Swept-Angle Bistatic Data
Brian D. Jersak, Marc J. Byrd, Andrew J. Blanchard, Houston Advanced
Research Center*

- 4:40 Three Dimensional Time Harmonic Electromagnetic Inverse Scattering:
The Reconstruction of the Shape and the Impedance of an Obstacle
*P. Maponi, Universita di Camerino, M.C. Recchioni, Universita di Ancona, F.
Zirilli*, Univesita di Roma "La Sapienza"*
- 5:00 An Improved MUSIC Algorithm for High Resolution Image Reconstruction
Fumie Kasahara, Hiroshi Shimotahira, ATR Optical and Radio Communications
Research Laboratories*

Image Reconstruction from Ipswich Data

P. M. van den Berg*
Delft University of Technology
Department of Electrical Engineering
Laboratory of Electromagnetic Research
P.O. Box 5031, 2600 GA Delft
The Netherlands

R. E. Kleinman
Center for the Mathematical of Waves
Department of Mathematical Sciences
University of Delaware
Newark, Delaware 19716, USA

In this paper we describe the results obtained by using the modified gradient algorithm developed earlier (e.g. R. E. Kleinman and P. M. van den Berg, *J. Comp. and Appl. Math.*, **42**, 17-35, 1992) together with some of the Ipswich data sets to reconstruct the shape, location, and/or index of refraction of the unknown scattering object.

This method has already been applied to one Ipswich data set (P.M. van den Berg, M. G. coté, and R. E. Kleinman, PIERS '94, Noordwijk, The Netherlands) and the same procedure is followed with the new sets. One important step is the preconditioning or renormalization of the data which is accomplished as follows. The measured data from a known scatterer (circular cylinder) is multiplied by an unknown complex constant and this constant is determined by minimizing the L_2 difference with the exact data as computed using the representation in cylindrical wave functions. This constant, which is essentially a phase correction, is then used as a multiplier of the measured data for all other cases.

The conditioned data is then used in the reconstruction algorithm which consists of constructing two sequences of functions, one representing the unknown field and one representing the unknown contrast by linearly updating the previous term. The direction of the updates are taken either as gradient or conjugate gradient directions for a functional consisting of the normalized errors in both the domain integral equation and the error in matching the measured data. The magnitude of the correction step is determined by minimizing the functional at each step. Any a priori information about the contrast is incorporated into the functional. The starting values for the contrast and field are obtained by back propagating the measured data.

The results obtained using this method on at least two of the Ipswich data sets will be presented.

K. Belkebir, J. M. Elissalt and J. M. Geffrin

Division Ondes - Laboratoire des Signaux et Systèmes (CNRS-ESE)

ESE - Plateau de Moulon, 91192 Gif-sur-Yvette Cedex - France

The present paper considers the application of Newton solutions (J. M. Geffrin *et al.*, *PIERS'94*, Noordwijk, 142) and of modified gradient ones (R. Kleinman and P. M. van den Berg, *Radio Science*, vol. 28, No 5, 877-884, 1993) to the Ipswich Data.

The object is taken to be an infinite cylinder of unknown cross-section and unknown dielectric constants (which can vary spatially) illuminated by a set plane waves. The scattered field is measured in the exterior object domain. Both inverse scattering methods are based on domain integral representations of the field in the object. The Newton technique builds up the solution by solving successively the forward problem and a linear inverse problem. This method needs a regularization. We use the gradient regularization where the Tikhonov parameter is determined by generalized cross-validation. The modified gradient method is iterative, like the Newton algorithm, but it does not involve a linearization of the non-linear relationship between the scattered field and the contrast. The modified gradient method builds up two sequences, the complex permittivity the contrast and the total field inside the explored region, by minimizing an adequate cost function.

These techniques have been first developed for a biomedical application where data are scattered near-field measured on a circle surrounding the object at a single frequency and multiple incidence. The object is placed in a metallic cylinder and the Green's functions are not the free space ones. Here the configuration is different since the scatterer is in free space and the scattered field measurements are in the far-field. Moreover the contrast corresponding to the impenetrable target has a high imaginary part that is not encountered in the biomedical case.

Results of inversions with both methods on known and mystery targets are discussed.

OBJECT RECONSTRUCTION FROM FAR-FIELD DATA[†] USING GRADIENT AND GAUSS-NEWTON TYPE METHODS

P. Lobel¹, R. Kleinman², Ch. Pichot^{1*}, L. Blanc-Féraud¹, M. Barlaud¹

¹ Laboratoire Informatique, Signaux et Systèmes de Sophia Antipolis,
CNRS/Université de Nice-Sophia Antipolis,
250 rue Albert Einstein, 06560 Valbonne, France.

² Center for the Mathematics of Waves,
University of Delaware, Newark, DE19716, USA.

This paper deals with the reconstruction of 2D-TM objects using scattered far-field data. Two iterative methods have been used. The first one is based on a Levenberg-Marquardt method which is a variant of a Gauss-Newton type or Newton-Kantorovich algorithm. The second one is a Gradient method. They are applied both to the complete non linear inverse scattering problem discretized using the method of moments with pulse basis functions and point matching. Iterative solutions are determined by minimizing the residual error between the measured scattered data and the computed ones.

For the Gauss-Newton, a standard Tikhonov regularization with identity operator is used. Different strategies have been utilized for finding the regularization parameters (an empirical formula and the Generalized Cross Validation method). For the Gradient method, first order and second order approximations were taken into account in the algorithm. Various correction directions (standard gradient direction and Polak-Ribière conjugate gradient direction) were also employed.

The computation of an appropriate initial guess can improve the efficiency of the algorithms in terms of stability and convergence. Investigations on computing initial guess have been made using a backpropagation scheme by means of the adjoint operator which allows to provide an estimate of the induced current on the object surface (conductor) or inside the object (penetrable target). Influence of the initial guess (without a priori information and using the backpropagation scheme) has been studied.

Different objects such as a perfectly electrically conducting target (PEC), a coated PEC and a penetrable target have been investigated using these two methods.

[†] Measured data provided courtesy of Rome Laboratory, RL/ER, 31 Grenier St., Hanscom AFB, MA 01731-3010.

**MICROWAVE TOMOGRAPHY: PROBLEMS RELATED TO
RECONSTRUCTIONS FROM EXPERIMENTAL DATA**

**N.Joachimowicz, J.Ch.Bolomey, A.Joisel, A.Franchois, M.Geleoc
SUPÉLEC/LSS, Plateau de Moulon, 91190 Gif-sur-Yvette, France**

The SUPÉLEC/LSS Group is involved in active microwave imaging for now ten years, developing several microwave imaging equipments and gaining practical experience in facing with true experimental situations (Bolomey J.Ch. & Pichot C., *Int.Journ. Imag. Syst. Techn.*, 2,144-156,1990). In 1989, a joint research effort with Institut d'Optique (Orsay, France) has been devoted to non-linear quantitative reconstruction algorithms of 2D and 3D inhomogeneous penetrable objects (Joachimowicz N., Pichot C., Hugonin J.P., *IEEE Trans. AP-39*,1742-1752, 1991). As well known in solving such inverse problems, a key point concerns the stability of the reconstruction process with respect to noise. In Newton-Kantorovitch approaches, which have been used, the noise includes both thermal noise and model noise. Thermal noise is present in any physical measurement, while model noise results from the comparison, at each step of the iterative reconstruction process, between the measured and the estimated scattered field, the later being calculated from a numerical model. Usually, thermal noise can be quite conveniently taken into account by means of a random additive gaussian signal for corrupting synthetic data. On the contrary, model noise cannot be realistically introduced in synthetic data and the analysis of its effects requires experimental data and the knowledge of the related experimental setup. The reconstruction algorithms have been used to process the experimental data provided by two kinds of equipment, a planar microwave camera (Bolomey J.Ch., Pichot C. and Gaboriaud G., *Radio Science*,26,541-549,1991) and a circular scanner (A.Broquetas, J.Romeu, A.R.Elias Fuste, A.Cardama, L.Jofre, *IEEE Trans. MTT-39*,836-844,1991), developed, respectively, by the SUPÉLEC/LSS Group and the Polytechnic University of Catalunya. Both equipments can provide multiview data around 2.45 GHz. This paper 1) identifies the major reasons for possible discrepancies between true and reconstructed targets, 2) analyses the difficulties encountered when dealing with experimental data, and 3) comments the role of the a priori information used to initiate the iterative process. As a conclusion, suggestions are provided to guide future assessments of newly developed or future reconstruction algorithms.

ECOLE SUPERIEURE D'ELECTRICITE

Plateau de Moulon, 91192 Gif-sur-Yvette, France; Tel 33 (1) 69 85 12 12 Fax 33 (1) 69 85 12 34

On modified gradient solution methods using the binary aspect of the unknown electromagnetic parameters and their application to the Ipswich Data

B. Duchêne and D. Lesselier*

Division Ondes - Laboratoire des Signaux et Systèmes (CNRS-ESE)

ESE - Plateau de Moulon, 91192 Gif-sur-Yvette Cedex - France

The present paper considers the application of modified gradient solution methods to the Ipswich Data. Here emphasis is on those which account for the binary aspect of the unknown scatterers (PEC or homogeneous penetrable objects).

Nonlinearized modified gradient methods attempt to solve both the observation equation, which relates the scattered field data to the sources induced inside the unknown object, and the coupling equation, which links these sources to themselves, for a given excitation. They are now well-known inversion tools (R. E. Kleinman and P. M. van den Berg, *J. Comp. Appl. Math.*, 42, 17-35, 1992) but extensions capable to tackle the inversion of "binary" structures where the unknown electromagnetic or acoustic contrast function is allowed to take only two values, are just being developed (R. Kleinman *et al.*, *Proc. PIERS'94*, Noordwijk, 408).

These extensions appear to be successful in a variety of electromagnetic and acoustic scalar scattering cases when an object is embedded in a known half-space which is illuminated from the above (data are aspect-limited and frequency-diversity is used so as to make up for the loss of information). Effectiveness is related to the choice of a cooling parameter α introduced so as to transform the binary inversion into one where a new contrast function varies continuously between the two limiting values at every space point. To do so provides differentiability with respect to this function, and a modified gradient method – where the field inside the object and the contrast are both considered as unknowns and updated separately – can be applied. When a stable contrast function is reached, suitably decreasing α pushes its values towards the known limits, and the inversion is started again, this being done a number of times until convergence.

Here the configurations at hand are quite different from the previously investigated ones. They are in some respect easier to deal with, since scatterers are now placed in free space and are seen from any direction of interest at fixed frequency. But they are also more complicated due to the introduction of both E and H polarizations, perfectly conducting boundaries (whereas observation and coupling equations are domain-integral formulations) and the absence of near-field data (only RCS are available).

Derivation of methods tailored for such cases, numerical implementations, and results of inversions on both known and mystery targets are discussed.

Diffraction Tomography Reconstructions from Real Data

J.J. Stamnes^{1) 2)*}, L.-J. Gelius²⁾, and T.C. Wedberg³⁾

¹⁾Physics Department, University of Bergen, Norway

²⁾Norwave Development AS, Oslo, Norway

³⁾Norwegian Institute of Fisheries and Aquaculture, Tromsø, Norway

We present reconstructions of scattering objects from real data using three different methods based on diffraction tomography, namely a modified version of the filtered backprojection algorithm, a modified version of the filtered backpropagation algorithm, and a generalized diffraction tomography algorithm.

The modification of the first two algorithms consists of using exact backpropagation of the measured field from the measurement line to the reconstruction area before forming Rytov data and applying the standard filtered backprojection or filtered backpropagation algorithm. These two algorithms are based on the weak-scattering approximation, while the third, generalized algorithm is based on a distorted-wave Born approximation. Thus, it can accommodate scattering objects embedded in a nonuniform background.

The real data come from scattering experiments using ultrasound, laser light or microwaves. From experimental data obtained with ultrasound, we present quantitative reconstructions of objects embedded in a homogeneous background or in biological tissue. The long term goal of this work is to develop an ultrasound tomography instrument for imaging of tumors in the female breast.

From experimental data obtained with laser light, we present quantitative reconstructions of objects having either a uniform, real anisotropic index of refraction or a nonuniform, complex or real refractive index distribution. Some of these reconstructions were obtained using both the modified filtered backprojection and the modified filtered backpropagation algorithm. From comparisons of these reconstructions, we conclude that both algorithms give very good results provided the weak-scattering approximation is fulfilled. The objective of this work is to develop a new tomography instrument for quantitative phase microscopy.

To test the generalized diffraction tomography algorithm, we have carried out a number of model tank experiments (employing conical dipole antennas) and field experiments (employing a frequency-swept georadar), in which the test objects were known a priori. We obtained good results in these tests, which included monitoring of dynamic changes in a reservoir, monitoring of leakage from a buried drum, and imaging of an underground tunnel. The potential application areas are many, i.e. prospecting geophysics, geotechnical surveying, and environmental geophysics.

Processing Experimental Data with Local Shape Function Method and Distorted Born Iterative Method

C. C. LU* AND W. C. CHEW

ELECTROMAGNETICS LABORATORY

DEPARTMENT OF ELECTRICAL AND COMPUTER ENGINEERING

UNIVERSITY OF ILLINOIS

URBANA, IL 61801

Abstract

We have developed two inverse scattering algorithms in our group: the local shape function (LSF) method and the distorted Born iterative method (DBIM). These methods have been used to process both synthetic and experimental data in the past. In this paper, we will show the use of these algorithms to process the experimental data provided by Rome Laboratory.

The aforementioned methods are useful when multiply scattered field is an important component of the scattered field data. Multiple scattering causes the scattered field to be nonlinearly related to the scattering object. However, when multiple scattering is unimportant, simpler algorithm based on first-order Born approximation, such as diffraction tomography, is sufficient for processing the data. The disadvantage of LSF and DBIM is that they are usually more computationally intensive compared to the simpler diffraction tomographic method.

In the LSF method, we characterize a scatterer by its shape or T matrix, rather than the conductivity or the permittivity of the object. This maps a nonlinear problem into a more linear one, allowing for the ease of applying an optimization approach. In the distorted Born iterative method, a distorted Born approximation is made at each stage, using the previously constructed permittivity profile as the background. A linear inverse problem ensues from such an approximation, and the inverse problem is solved by an optimization approach. The DBIM is equivalent to Newton's method, and hence, has second order convergence.

IMAGING OF UNKNOWN TARGETS FROM MEASURED SCATTERING DATA

J. B. Morris*, D. A. Pommet, R. V. McGahan* and M. A. Fiddy
Department of Electrical Engineering, University of
Massachusetts-Lowell, Lowell, MA 01854

*Rome Laboratory, Hanscom AFB, MA 01731

Using data provided, we employ several inverse scattering methods to recover and estimate an image of the permittivity distribution responsible for the scattering. Using linearized approximations such as the Born approximation for diffraction tomography, requires that the object either be weakly scattering or small in size compared with the illuminating wavelength. While usually inappropriate for most scattering targets of interest, these linearizing approximations lead to simple Fourier inversion procedures.

In this paper, we present extensions of these Fourier-based methods and apply them to real microwave scattering measurements taken from a penetrable target. The first approach used is a distorted wave method, which assumes some *a priori* knowledge of the support of the target and incorporates this into the inversion step. This *a priori* knowledge can also be incorporated into a spectral extrapolation method, which can be implemented simultaneously, and which alleviates the problems associated with only limited view data being measured. A second and novel approach, using a differential cepstral filtering technique, is also applied to the data. This technique remains computationally simple and straightforward. It is based on the recognition that the image recovered for each illumination direction, when adopting the Born approximation, is the product of the target's permittivity distribution and the (unknown) internal field. In the cepstral domain, spectral information about the sum of these functions is available. By filtering backpropagated images in the differential cepstral domain, one can remove the contribution from the internal field and recover the target distribution.

Scattering by Wedges II**E. Marx and P. L. E. Uslenghi**

Page

- 3:20 Scattering by a Wedge with Variable Impedance Faces
G. Pelosi, Univ of Florence, G. Manara, P. Nepa, Univ. of Pisa*
- 3:40 A UTD Solution for the Diffraction of an Inhomogeneous 240
Plane Wave Obliquely Incident on a Wedge
G. Manara, P. Nepa, University of Pisa, R. G. Kouyoumjian,
The Ohio State University*
- 4:00 Solution for a DC Anomaly Caused by a Wedge in Conducting 241
Ground
Keijo Nikoskinen, Mikko Flykt, Helsinki University of Technology*
- 4:20 Double Diffraction Coefficients for Source and Observation
at Finite Distance for a Pair of Wedges
M. Albani, F. Capolino, S. Maci, Univ. of Florence, R. Tiberio,
Univ. of Siena*
- 4:40 Diffraction at the Junction of a Two-Impedance Half-Plane
A.H. Serbest, Cukurova University, E. Luneburg,
German Aerospace Research Establishment*
- 5:00 Further Notes on Electromagnetic Field Behavior Near
Homogeneous Anisotropic Wedges
Yuad S. Brisker, Carey M. Rappaport,
Northeastern University*

A UTD SOLUTION FOR THE DIFFRACTION OF AN INHOMOGENEOUS PLANE WAVE OBLIQUELY INCIDENT ON A WEDGE

G. Manara*, P. Nepa

Dept. of Information Engineering, University of Pisa, Italy

R. G. Kouyoumjian

Dept. of Electrical Engineering, The Ohio State University, USA

A uniform, high-frequency solution has been presented for the scattering of a scalar inhomogeneous plane wave obliquely incident on a wedge with either soft or hard boundary conditions (G. Manara *et al.*, URSI Radio Science Meeting, Seattle, 1994). In this paper the solution is extended to the three-dimensional vector problem where an electromagnetic inhomogeneous plane wave is diffracted by a perfectly-conducting wedge. The case of a lossy medium surrounding the wedge is also treated.

All field components are expressed in terms of those parallel to the edge (E_z, H_z). Both principal polarizations are treated, i.e., the incident electric field may be either parallel or perpendicular to the edge-fixed plane of incidence. An exact integral representation is obtained for each component of the field. Then, these representations are asymptotically evaluated to provide uniform high-frequency expressions for the total field. The solution is interpreted in terms of the uniform GTD (UTD), so that it can be applied to calculate the scattering from objects with edge geometries. The diffracted field properly compensates the discontinuities in the incident and reflected fields at their respective shadow boundaries. The displacement of these boundaries from their conventional locations, which occur in the case of homogeneous plane wave incidence, is described. The dependence of these displacements on losses in the medium surrounding the wedge is also discussed. The expression for the diffracted field contains the UTD transition function with a complex argument. Away from the shadow boundaries the UTD diffracted field reduces to the GTD approximation, as expected. Outside the transition regions it is seen that the diffracted field can be interpreted as a locally inhomogeneous plane wave. By referring to the ray-fixed coordinate system, a dyadic diffraction coefficient is determined, which can be written in the form of a 2×2 matrix. In the limit of an incident homogeneous plane wave, the off diagonal terms in this matrix vanish, and the resulting expression reduces to the standard UTD dyadic diffraction coefficient.

To demonstrate the accuracy of the UTD solution, numerical comparisons are made with results calculated from the eigenfunction solution. The numerical results also show that the UTD solution is smooth and continuous at the shadow and reflection boundaries.

SOLUTION FOR A DC ANOMALY CAUSED BY A WEDGE IN CONDUCTING GROUND

Keijo Nikoskinen, Mikko Flykt
Electromagnetics Laboratory
Helsinki University of Technology
Otakaari 5, FIN-02150 Espoo
Finland

The electrostatic potential of a point current source, located on the surface of the earth above a dipping conducting wedge, is solved exactly. The edge of the wedge is restricted to situate at the surface but its opening angle and orientation can be arbitrary. Hence, the model of the earth actually consists of three wedges that form the ground region. The conductivity is assumed to be finite everywhere in the ground. Once the potential is known at the top of the ground, it enables one to calculate the apparent resistivity that is commonly used when interpreting the dc measurement data in terms of the geological structure. Thus, the present analysis provides a point of comparison that can be used in certain limited way when geological interpretations are based on dc measurements.

The unknown potential field can be solved mathematically from Poisson's equation with continuous potential and normal current density as boundary conditions. The application of the Fourier transform and eigenfunction expansion leads to a simple differential equation for the transformed unknown potential than can be solved analytically. Instead of trying to compute the inverse Fourier transform of the potential, the contribution of the primary current source in the transformed potential corresponding the air region is extracted and the remaining part is interpreted as originating from an image current distribution. The image contains all information about the geometry and the media conductivities and it can be solved through an integral equation. Its expression consists of a set of point sources and a continuous line source whose position is in complex space, i.e. its coordinates are complex numbers. Once the image is known the total potential above the ground can be computed easily by convolving the Green's function with the primary source and its image. The anomalous part of the potential due to the wedge can be obtained by extracting the primary potential and the effect of the homogeneous earth.

The limitation of the developed analysis is that there can be only one electrode that lies on the surface of the ground and the potential cannot be computed below the surface. However, the approach could be generalised for several electrodes whose positions can be freely chosen. Furthermore, if the information about the potential field in the ground or inside the wedge is needed, it is possible to derive proper images applicable to these domains.

THIS PAGE INTENTIONALLY LEFT BLANK.

Theoretical Electromagnetics I

A. A. Oliner and N. Engheta

Page

1:20	Can One "Hear" the Handedness or Topology of A Knot?	244
	<i>D. L. Jaggard, O. Manuar, University of Pennsylvania</i>	
1:40	Fractional Derivatives, Fractional Integrals and Electrostatic Image Methods	245
	<i>Nader Engheta, University of Pennsylvania</i>	
2:00	Applications of Fractional Calculus to Fields of Finite-Size Sources	246
	<i>Nader Engheta, University of Pennsylvania</i>	
2:20	Puzzles Relating to Radiation Fields Within the Spectral Gap Between Surface Waves and Leaky Waves	247
	<i>A. A. Oliner*, Polytechnic University, D. R. Jackson, University of Houston, H. Ostner, Technische Universitat Munchen</i>	
2:40	A Derivation of Recursion Relations of the Translational Theorems for Scalar and Vector Spherical Harmonics	248
	<i>Kristopher T. Kim, Rome Laboratory</i>	
3:00	BREAK	
3:20	Field Penetration and Charge Distribution in a Polarized Semiconductor Sphere	249
	<i>Thomas Wong*, Xinhua Hu, Illinois Institute of Technology</i>	
3:40	Solution for Radiation Characteristics of a Thin Truncated Dielectric Disk Antenna by the Method of Steepest Descent and Weinner-Hoff Technique	250
	<i>Chinmoy Das Gupta*, A. C. Trivedi, Indian Institute of Technology, Anup Gogoi, Assam Engg. College</i>	
4:00	Total Surface Current on a PEC Angular Sector	251
	<i>W. J. Koh*, R. J. Marhefka, The Ohio State University ElectroScience Laboratory</i>	
4:20	Rigorous Solution to the Problem of Dielectric Slab Natural Modes ... Scattering from Compound Resonant Cylindrical Inhomogeneity	252
	<i>Andrey S. Andrenko, Ukrainian Academy of Sciences</i>	
4:40	Free Electromagnetic Oscillations and Waves of Gratings and Scattering Anomalous Regimes	253
	<i>Vasily V. Yatsik, Institute of Radiophysics & Electronics of the National Academy of Sciences of Ukraine</i>	
5:00	Normal Modes in Open Waveguides with Non-compact Boundaries	254
	<i>Youri V. Shestopalov*, Vadim V. Lozhechko, Moscow State University</i>	

CAN ONE "HEAR" THE HANDEDNESS OR TOPOLOGY OF A KNOT?

D. L. Jaggard and O. Manuar[†]

Complex Media Laboratory
Moore School of Electrical Engineering
University of Pennsylvania
Philadelphia, PA 19104-6390

[†]Also Department of Biochemistry and Biophysics
University of Pennsylvania
Philadelphia, PA 19104-6059

In a classic paper by Kac [M. Kac, "Can One Hear the Shape of a Drum?" *Am. Math. Month.* 73, 1 - 24 (1966)] the question was posed regarding finding the shape of a drum through listening to its sounds. Here we examine the electromagnetic counterpart in which we wish to determine the geometric descriptors of a knot by "striking" it with an incident electromagnetic wave. In particular, we are interested in finding information regarding the handedness and topology of knots from their electromagnetic signature.

Although the blending of knot theory and electromagnetic theory first occurred in considering flux linkages in the nineteenth century, today there is interest in knotted structures in DNA plasmids and in optical wave interactions with complex structures. We are interested in electromagnetic wave scattering from and propagation in knotted media. This study is a first step in our investigation.

In the figure below are shown two simple knots denoted *trefoils*. We examine in this presentation the characteristic electromagnetic signatures of trefoils and their associated *unknots*. The latter are topologically equivalent to a loop and are formed by changing one of the crossings of the trefoil.

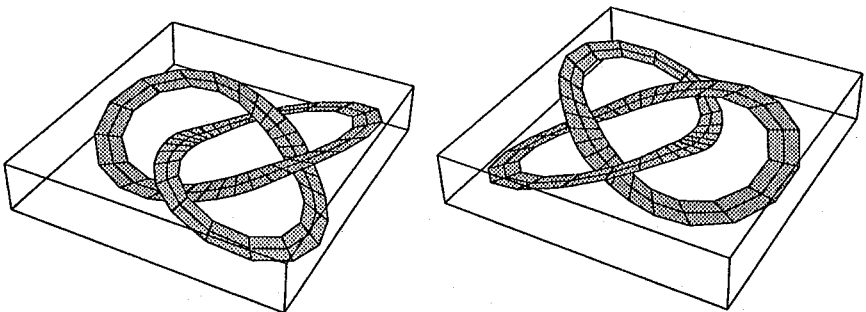


Figure. Three-fold rotationally symmetric trefoil knot (left) and its enantiomorph or mirror image (right).

We examine the electromagnetic differences between trefoils and their associated unknots. We also investigate the electromagnetic properties of knots and their enantiomorphs. This study is carried out through a calculation of induced secondary sources and differential scattering cross-sections.

FRACTIONAL DERIVATIVES, FRACTIONAL INTEGRALS AND ELECTROSTATIC IMAGE METHODS

Nader Engheta

Moore School of Electrical Engineering
University of Pennsylvania
Philadelphia, Pennsylvania 19104, U.S.A.

Fractional derivatives/integrals are generalization of well-known differentiation and integration to arbitrary general orders--orders that can be fractional or even complex. This area of calculus, known as fractional calculus, has been the subject of interest for many researchers in pure and applied mathematics. [K. B. Oldham and J. Spanier, *The Fractional Calculus*, Academic Press, New York, 1974.]

It is of interest to bring this area of mathematics into electromagnetic theory and to explore possible applications and physical implications of its use in electromagnetic problems. One such application is in treatment of certain electrostatic problems using the image methods. As one case, consider the two-dimensional electrostatic potential distribution of a uniform line charge located in front of a perfectly conducting wedge with arbitrary wedge angle β . It is well known that for certain values of β , namely, when π/β is an integer value, one can express the total electrostatic potential in front of the wedge in terms of potential of the original line charge plus potential of $(2\pi/\beta-1)$ image line charges. However, when π/β is not an integer, what would happen to the images? We attempt to answer this question using the concept of fractional derivatives/integrals. We show that the order of such fractional operators depends on the geometry of the wedge, namely, its angle. In the past, we showed that the idea of fractional calculus could be used to describe certain aspects of electrostatic fields near sharp edges [N. Engheta, On the role of non-integral (fractional) calculus in electrodynamics," a talk given at 1992 IEEE AP-SI/URSI Symposium, Chicago, Illinois, July 17-20, 1992, Abstract in URSI Digest, p. 163.]

Another case of possible application of fractional derivatives in electrostatic problems to consider here, is the use of fractional calculus in providing alternative way of expressing electrostatic image charges for dielectric spheres. The classic problem of electrostatic image charge for a perfectly conducting sphere was solved by Lord Kelvin in 1848, and the corresponding problem for a dielectric sphere was solved elegantly by Lindell in 1992. [I. V. Lindell, *Radio Science*, 27, 1-8, 1992]. We show that the distributions of image charges for the dielectric sphere (Lindell's solution) and the image charges for the perfectly conducting spheres (Lord Kelvin's solution) can be related by way of fractional calculus, and that the order of such fractional operators is dependent on the sphere's dielectric constant.

In this talk, we will present and discuss some of these applications of fractional derivatives in electrostatic image problems, we will address their novel and interesting aspects and physical insights.

APPLICATIONS OF FRACTIONAL CALCULUS TO FIELDS OF FINITE-SIZE SOURCES

Nader Engheta

Moore School of Electrical Engineering
University of Pennsylvania
Philadelphia, Pennsylvania 19104, U.S.A.

In this talk, we will present some of the novel applications of fractional calculus to a class of electromagnetic problems, namely, fields of finite-size sources. Fractional calculus is an area in mathematics that treats the problem of generalization of differential and integral operators to general arbitrary orders (e.g., differentiation to non-integer order such as $d^{1/2}f(x)/dx^{1/2}$) [K. B. Oldham and J. Spanier, *The Fractional Calculus*, Academic Press, New York, 1974.] It has been used in such areas of mathematics as partial differential equations (PDE), complex analysis, integral equations, Mellin transforms, and generalized functions [see, e.g., A. C. McBride and G. F. Roach (eds.), *Fractional Calculus*, research Notes in Mathematics, Pitman Advanced Pub., Boston, 1985.]

We have been studying potential applications of fractional derivatives and fractional integrals in electromagnetism. One of these applications is the effect of fractional differentiation of fields of a finite-size source. Let us consider a finite-size source distributed in some bounded region. Electromagnetic fields of this current source at any given observation point can obviously be described by the standard Green's function method. Let us pick an observation point and evaluate the fractional derivative/integral (with respect to space) of the electric field at that point. What is the result of this fractional differentiation/integration of the field at any given point? Can this result be equivalently related to fractional derivatives/integrals of the source? Would the resulting source be limited to a bounded region in space? We have studied these issues and have obtained interesting results for such fractional differentiation/integration of the fields. We will show that, using this technique, one would be able to describe source distributions that are effectively "intermediate" distributions between multipoles, e.g., sources that are effectively acting as distributions between dipoles and quadrupoles, or between monopoles and dipoles, etc.

We will first present a brief review of definitions and properties of fractional calculus, and then will present results of our analysis of fractional operators on fields of finite-size sources. Physical justification and insights into mathematical results will be addressed.

PUZZLES RELATING TO RADIATION FIELDS WITHIN THE SPECTRAL GAP BETWEEN SURFACE WAVES AND LEAKY WAVES

A. A. Oliner*

Polytechnic University, Brooklyn, NY, 11201

D. R. Jackson

University of Houston, Houston, TX 77204-4793

H. Ostner

Technische Universität München, 80290 München, Germany

At the transition between surface waves and leaky waves on dielectric layers, there exists a range in frequency over which the guided mode is *nonphysical*. This frequency range is called a *spectral gap*, and it consists of two regions, one in which the modal solution is *improper real*, and is therefore clearly nonphysical, and another in which the solution is *leaky*, but which contains several puzzling features concerning its physical reality. This talk addresses these puzzling aspects.

When the properties of the *near field* of the leaky wave within the spectral gap are examined, it is found that the leaky-wave pole is *not* captured in the steepest-descent plane, but that this field does actually leak *real power* at a small but *real angle* into the air region. On the other hand, the field at all angles and even along the surface is *slow*. Since the pole is not captured, and the phase velocity associated with this leaking power is slow, not fast, can this leaking power actually radiate into the far field? Conventional first-order reasoning suggests it should not. Since the pole is near to the steepest-descent path, however, it should continue to influence the far-field pattern even in this region.

Exact *radiation fields* both within and outside of the spectral gap were then calculated for a specific structure and compared with the corresponding radiation fields derived from the leaky-wave near fields. The *pattern shapes* agreed remarkably well whenever the mode was leaky, both within and outside of the spectral gap, but the *amplitudes* did not. The leaky-wave amplitudes were then multiplied by a transition function T , which is equal to the ratio of the real power radiated in the transverse direction to the magnitude of the complex power in that direction. The agreement between the exact and the leaky-wave radiation fields then became surprisingly good in *both* amplitude and pattern shape at all frequencies over which leakage occurs, both within and outside of the spectral gap.

This talk will summarize the understanding to date with respect to the extent of physical reality associated with the leaky portion of the spectral gap, and indicate what steps would be desirable to take in the future to clarify the remaining unclear aspects.

A DERIVATION OF RECURSION RELATIONS OF THE TRANSLATIONAL THEOREMS FOR SCALAR AND VECTOR SPHERICAL HARMONICS

Kristopher T. Kim
USAF Rome Laboratory
RL/ERCT
31 Grenier Street
Hanscom AFB, MA 10731-3010

The translational theorems for scalar and vector spherical harmonics have been useful analytic tool in many areas of acoustic and electromagnetic research, such as the theoretical study of scattering from multiple spheres and probe correction in the spherical near-field to far-field transformation. Recently, several fast scattering algorithms (W.C. Chew, C.C. Liu & Y.M Wang, *J. Opt. Soc. Am.*, Vol.11A, 1528-1537, 1994) were proposed that use the translational theorems to reduce computational complexity. These fast scattering algorithms have in turn brought about renewed interest in the translational theorems (K.T. Kim, *ANTEM94 Proceedings*, 655-658, 1994, W.C. Chew, *Microwave Opt. Tech. Lett.*, Vol.37 No.7, 256-260, 1990), and efficient ways to compute coefficients of the scalar (W.C. Chew, *J. Electromag. Waves Appl.*, Vol. 6, NO.2 133-142, 1992) and vector (W.C. Chew & Y.M. Wang, *J. Electromag, Waves Appl.*, Vol. 7, No. 5, 651-665, 1993) translational theorems.

An earlier paper (K.T. Kim, *op. cit.*) showed that the translational theorem for vector spherical harmonics can be derived in a very simple and straightforward manner by judiciously coupling and decoupling angular quantities using the spherical tensor formalism. In this paper the spherical tensor formalism is used to derive the recursion relations satisfied by the translational coefficients of the scalar and vector spherical harmonics. The derivation is concise and general, and the resulting recursion relations are somewhat more general than the ones reported recently (W.C. Chew, *op. cit.*). These recursion relations can be used to compute the translational coefficients efficiently.

FIELD PENETRATION AND CHARGE DISTRIBUTION IN A POLARIZED SEMICONDUCTOR SPHERE

Thomas Wong * and Xinhua Hu
Department of Electrical and Computer Engineering
Illinois Institute of Technology
Chicago, Illinois 60616

The presence of mobile charges in an object can significantly influence its interaction with an electromagnetic field. In addition to energy dissipation, mobile charges give rise to the screening effect, which prevents an external field from reaching the interior of a conducting object.

In this work, we studied the results of calculation on a semiconductor sphere immersed in an originally uniform static electric field. The Poisson's equation with Boltzmann statistics for the charge density was solved by a finite-difference method and compared with a linearized model, valid for weak-field conditions and amenable to closed form solutions in terms of spherical harmonics. It was observed that the weak-field approximation gave results that agreed with those of the finite-difference method up to field strength of quite substantial magnitude.

At the interior of the sphere, the electric field becomes insignificant beyond a few Debye lengths from the surface. To an outside observer, the charge distribution leads to a dipole field. Accordingly, one may define an equivalent dielectric constant for a given semiconductor sphere to account for the external field. Numerical results on internal field, external field, charge distribution, total dipole moment and equivalent dielectric constant will be presented.

SOLUTION FOR RADIATION CHARACTERISTICS OF A THIN TRUNCATED DIELECTRIC DISK ANTENNA BY THE METHOD OF STEEPEST DESCENT AND WEINER-HOFF TECHNIQUE.

Chinmoy Das Gupta, Senior Member IEEE, A.C. Trivedi, Research Engineer,

Department of Electrical Engineering, Indian Institute of Technology, Kanpur, India

Anup Gogoi, Professor, Dept. of Electronics Engg., Assam Engg. College, Guwahati.

Abstract

Successful experimental simulation of ferroelectric rod antenna down upto UHF range of frequency has been reported by the author at ANTEM, 86 and 1988 IEEE-APS Symposium of [1,2] this at Syracuse University. In order to improve directivity a modified structure of thin truncated disk is proposed. No readymade solution for radiation characteristics of this structure is available in contrast to that of dielectric rod antenna.

Theoretical solution for radiation characteristics is worked out by the method of Steepest Descent and [3] Weiner-Hoff technique. In order to avoid machining difficulty of the ferroelectric material PZT experimental verifications of the theoretical model is done with RTDuroid at scaled up microwave frequency of S band.

It is proposed to enhance directivity of the unit by incorporating artificial dielectric structure.

References:

1. C. Das Gupta: Ferroelectric Antenna for Mobile Communication System, Proceedings ANTEM, University of Manitoba, 1986.
2. C. Das Gupta: Proceedings IEEE-URSI International Symposium on A&P, University of Syracuse, 1988.
3. Anup Kr. Gogoi: Effect of Dielectric Substrate on Radiation from Microstrip Antennas, M.Tech Thesis (guide, K.C. Gupta) IIT Kanpur, 1981.

Total Surface Current on a PEC Angular Sector

W. J. Koh and R. J. Marhefka

The Ohio State University ElectroScience Laboratory

Department of Electrical Engineering

1320 Kinnear Rd.

Columbus, Ohio 43212-1191

Electromagnetic scattering from large perfectly conducting flat plate with straight edges illuminated by plane wave has been investigated for many years. Several high frequency techniques were developed which includes Uniform Geometrical Theory of Diffraction (UTD), Physical Theory of Diffraction (PTD), Michaeli's Equivalent Edge Current (MEC), Tiberio's Incremental Theory of Diffraction (ITD) etc. However, none of these could accurately predict the scattered field in nonspecular regions, especially those for plates with small vertex angle such as the 3 wavelength 30 degree isosceles triangle (Sikta's triangle).

Recently, Brinkley combines the Physical Optic (PO) current, the UTD 1st order edge diffracted currents and a vertex current as the total surface current on the flat angular sector. He was able to predict much more accurately the far zone backscattered field from the Sikta's triangle. This vertex current is obtained by subtracting the PO current and the 1st order edge diffracted currents from the exact surface current on an angular sector using Satterwhite's eigenfunction solution. However, he gives no formula for this vertex current and it has to be obtained by computing the eigenfunction solution for every observation point on the surface of the plate, thus making the computation very tedious and time consuming.

Using the similar approach used by Brinkley, but instead of the UTD edge diffracted current, the ITD edge diffracted current is chosen. ITD edge diffracted current is preferred because it produces smooth, continuous and accurate field at or near the vertex shadow boundary. Subsequently, a formula was developed for the vertex current, and an edge correction current is also obtained to correct for the inaccuracy near the edges of the angular sector as a result of asymptotic approximation used in deriving the ITD edge diffracted current. Combining the vertex current and edge correction currents with the PO current and the 1st order ITD edge diffracted currents, the total surface current shows good agreement with the exact eigenfunction solution for flat angular sectors. Applying this total surface current on the Sikta's triangle, a much more accurate far zone field is obtained compared with moment method solution.

Rigorous Solution to the Problem of Dielectric Slab Natural Modes Scattering from Compound Resonant Cylindrical Inhomogeneity

Andrey S. Andrenko
Institute of Radiophysics and Electronics
Ukrainian Academy of Sciences
12 Acad. Proskura st., Kharkov 85, 310085, Ukraine

As it is well known, the further progress in modern theory of diffraction is connected with the development of the rigorous methods allowing to take into account the real environment of the scatterers. As a matter of fact, most scattering objects of practical importance are usually placed in inhomogeneous medium. That is why the next step in correct analysis of the prospective electrodynamic devices should be directed to the new approaches describing the interaction of local scatterers with real environment.

The purpose of this study is the further development of the rigorous method to the solution of two-dimensional problems of wave scattering by localized obstacles in plane-parallel layered medium. This method combines the Green's function approach and the idea of regularization of initial operator based on the classical Riemann-Hilbert Problem (RHP) technique. As for the analyzed structure, the dielectric slab natural modes scattering by combined resonant inhomogeneity is considered. The scatterer has been formed as the dielectric cylinder with permittivity different from that of slab partially covered by perfectly conducting unclosed screen.

The main idea of treatment is to derive the Green's function of layered medium containing the dielectric inhomogeneity but except the unclosed screen, i.e. dielectric slab with embedded dielectric cylinder, and then apply the generalized potential theory and RHP technique for the calculation of current density induced on the screen. In contrast to scattering by single unclosed screen in homogeneous or layered medium, the Green's functions of two types have been derived. The first type corresponds to the line current source's location outside the dielectric rod but inside the slab while the Green's function of second type describes the inner location of the source. Analytical expressions for the Green's functions include the singular term involving the location of the source, Fourier-type integral representation of regular dielectric slab and Fourier-series terms indicating the cylindrical waves due to insertion of dielectric rod into the slab. To find the scattered field outside the compound inhomogeneity, the corresponding part of second type Green's function should be taken, however, the first type Green's function is used for the inner field calculation.

Finally, the Fredholm system of linear algebraic equations for the numerical calculation of current density is obtained using the RHP technique. The slab's natural mode conversion coefficients as well as the radiation field pattern function are derived. It is shown that the created numerical algorithm allows us to model the effects of mode conversion and wave rejection in dielectric slab guide due to the scattering from compound resonant inhomogeneity.

**FREE ELECTROMAGNETIC OSCILLATIONS AND WAVES
OF GRATINGS AND SCATTERING
ANOMALOUS REGIMES**

Vasily V. Yatsik

*Institute of Radiophysics and Electronics of the National Academy of Sciences
of Ukraine, 12, Ac. Proskury st., Kharkov, 310085, Ukraine
Phone: (7-0572)-44-85-57 Fax: (7-0572)-44-11-05
E-mail: yura@ire.kharkov.ua*

This report deals with a detailed analysis of the features of analytical prolongation of the solutions of stationary boundary problems of the electromagnetic grating theory to the range of complex values of parameters. The spectral of gratings as open periodic resonator and waveguides are studied. Their role in the formation of resonance response of structures on the external excitation.

Quantitative characteristics of the point spectrum of the waveguide-type gratings are investigated and an algorithm is constructed for calculating free oscillations in such structures.

The intertype oscillations and waves have been revealed and investigated on the base of the rigorous spectral theory of gratings by numerical methods. The existence of which (oscillations and waves) has been caused by the "interaction" of natural fields in open periodic structures. The nature of a number of anomalous regimes of wave scattering by one-dimensional-periodical gratings (Wood anomalies, effects of full passing and reflection) has been studied. They appeared to be caused by excitation of field oscillations in the structure close to the free ones.

It is shown that an analysis of solution of problems on natural oscillations and waves of one-dimensional-periodic structures is essentially simplified when using the results of the theory of features of smooth mappings. It is also shown that the Morse critical points are applied to effectively restore spectral characteristics connected with manifestation of the effects of intertype coupling and to study degenerate states of free electromagnetic fields of gratings.

A qualitatively new method for detecting and analysing the phenomenon of total transformation of plane waves (wave packets) by the open periodic resonators is suggested and illustrated by same numerical examples. The solution of the corresponding spectral boundary problems opens a direct approach to investigation of transformation conditions for the Floke channel.

Normal modes in open waveguides with non-compact boundaries

Youri V. Shestopalov* and Vadim V. Lozhechko

Department of Computational Mathematics and Cybernetics
Moscow State University
119 899 Moscow, RUSSIA

Waves propagation in a rather general family of open cylindrical waveguides formed by infinitely conducting plane screens with arbitrary local multi-connected perturbations of the (rectilinear) non-compact boundaries and piece-wise constant dielectric filling is considered. For example, the transversal cross-section of such a waveguide may be formed by an open domain (whose boundary differs from the straight line on a finite interval) containing a finite number of finite domains bounded by closed piece-wise smooth curves and closed and (or) unclosed non-intersecting finite piece-wise smooth curves (cross-sections of dielectric inclusions and perfectly conducting strips, respectively). The general demand is that the cross-sections differ from the half-plane only inside a finite ball and all dielectric inclusions lie inside this ball.

Determination of the longitudinal wavenumbers of normal waves is much more complicated than the problem on fundamental frequencies in such cylindrical structures (considered as open resonators) recently studied by the authors. The former is stated as the mixed boundary eigenvalue problem for the system of Helmholtz equations with piece-wise constant coefficients and the Reichardt-Sveshnikov radiation conditions in infinity. The spectral parameter enters both the boundary conditions and radiation conditions in a nonlinear way.

In the considered case of arbitrary cross-sections it is not possible to apply the known methods (variables separation, boundary integral equations, summation-type equations, partial domains, etc.) and the spectral problem considered is equivalently reduced in the generalized statement to the one for operator-valued pencils. The Fredholm property is proved. Discreteness and general properties of the normal waves spectra are established.

For the particular case of an image slot line formed by a rectangular domain and half-plane connected by a slot existence of the normal modes with strictly negative imaginary part of the transversal wavenumbers is shown. Asymptotical representations for the longitudinal wavenumbers with respect to the slotwidth taken as a small parameter are obtained.

Finite Difference Time Domain Methods

R. W. Ziolkowski and R. Janaswamy

Page

1:20	An Investigation of Arbitrary Grid Finite Difference Time Domain Algorithms <i>A. M. Davidson*, J. LoVetri, The University of Western Ontario, N. R. S. Simons, Communications Research Centre</i>	256
1:40	3D FDTD Treatment of Perfect Electric Conductors <i>J. Anderson*, M. Okoniewski, S. S. Stuchly, University of Victoria</i>	257
2:00	An Optimized Finite Difference Scheme for Time Domain Maxwell's Equations <i>Ramakrishna Janaswamy*, Naval Postgraduate School, Yen Liu, NASA Ames Research Center</i>	258
2:20	SVD Based Prony Hildebrand Technique for CFDTD Processing <i>Ali Asi*, Lotfollah Shafai, University of Manitoba</i>	259
2:40	Simulation and Measurement of High Speed Digital Test Modules <i>M. Piket-May, J. Mix*, D. Barnhart, University of Colorado at Boulder, Roger Gravrok, Kevin Thomas, Cray Research Inc.</i>	260
3:00	BREAK	
3:20	An FDTD Simulator for Ground-Probing Radars <i>Zhubo Huang*, Kenneth Demarest, Richard Plumb, Pawan Chaturvedi, The University of Kansas</i>	261
3:40	An Explicit Finite Element Time Domain Method Using Whitney Forms <i>Jin-Fa Lee*, Zachary Sacks, Worcester Polytechnic Institute</i>	262
4:00	A Non-Dissipative Upstream Biased Scheme for Time Domain Computational Electromagnetics <i>Brian T. Nguyen*, Philip L. Roe, University of Michigan</i>	263
4:20	An Accelerated Algorithm for the Time Domain Analysis of Guided Wave Problems Involving Ferrites <i>M. Okoniewski *, University of Victoria, M. Mrozowski, Technical University of Gdansk</i>	264

AN INVESTIGATION OF ARBITRARY GRID FINITE DIFFERENCE TIME DOMAIN ALGORITHMS

A. M. Davidson*, J. LoVetri
Department of Electrical Engineering
The University of Western Ontario
London, Ontario, Canada, N6A 5B9

N. R. S. Simons
Directorate of Antennas and Integrated Electronics
Communications Research Centre
P.O. Box 11490, Station H
Ottawa, Ontario, Canada, K2H 8S2

The purpose of this work is to make a comparative investigation of arbitrary grid finite difference time domain algorithms. Recently, various algorithms have been proposed, such as Holland's modification of Yee's FDTD algorithm (R. Holland, *IEEE Trans. Nucl. Sci.*, vol. NS-30, no. 6, 4589-4591, Dec. 1983), Shankar's application of the finite volume technique (V. Shankar, W. F. Hall, A. H. Mohommadian, *Proc. IEEE*, vol. 77, no. 5, 709-721, 1989), and Taflove's contour finite difference time domain technique (T. G. Jurgens, A. Taflove, K. Umanshankar, T. G. Moore, *IEEE Trans. Antennas Propagat.*, vol. 40, no. 4, 357-366, Apr. 1992). The main advantage of using arbitrary discretization of complex shaped objects is increased accuracy over stair stepped approximations. The disadvantage of arbitrary discretization is added algorithm complexity.

Two problems are used to compare the various algorithms. The first problem uses a two dimensional waveguide structure that is discretized with a skewed grid. The amount of grid skew is varied, and the affect on the accuracy of the results is compared. The second problem uses the same two dimensional waveguide structure discretized with a uniform rectangular grid and one node (i.e., the intersection of two orthogonal grid lines) is displaced from its original position. (Note that with a uniform rectangular grid some of the algorithms reduce to the well known Yee algorithm.) The numerical results indicate the presence of numerical artifacts.

The numerical artifacts due to grid distortion are compared for each scheme as a function of grid distortion. A general comparison of the numerical results obtained from these algorithms is presented for both problems described.

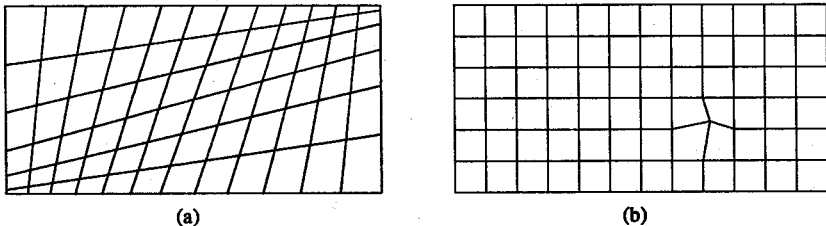


Figure 1: Waveguide structure with (a) skewed grid and (b) uniform rectangular grid with one node displaced from its original position.

3D FDTD Treatment of Perfect Electric Conductors

J. Anderson*, M. Okoniewski, and S.S. Stuchly
 University of Victoria, Department of Electrical and Computer Engineering
 P.O. Box 3055, Victoria, B.C. V8W 3P6

Perfect electric conductors of arbitrary shape are usually represented in FDTD with a 'staircase' technique, in which each Yee cell is classified as either entirely inside or outside metal. The technique shifts the metal surface until it coincides exactly with tangential electric fields, and maps a variety of physical objects into a single FDTD representation. Successful 2D algorithms accurately treating metal boundaries have been reported by several authors (W.K. Gwarek, IEEE-MTT, No. 10, 1067-1072, 1985; A.C. Cangellaris et al, IEEE-AP, No. 10, 1160-1173, 1987), but are not easily extended to the 3D case.

Modified update formulas for cells containing metal boundaries are obtained by considering the curl equations in integral form, replacing part of the integration path with a contour running along the metal boundary, and incorporating the known variation of tangential and normal field components near metal. The resulting formulas are implemented in a straightforward manner in a standard FDTD mesh, if the following information is known for cells containing metal boundaries: (i) the fraction of each integration path outside metal, (ii) the fraction of the cell's area outside metal, and (iii) the angle of the metal boundary relative to the cell. The 3D nature of the problem space need only be considered in the preprocessing stage, as (i) to (iii) are computed. It is important to note that once the preprocessing is complete, the modified formulas differ from the standard formulas only in the presence of a constant coefficient associated with each field quantity.

Numerical experiments indicated that the formulas are stable for cells less than half filled with metal. For cells more than half filled with metal, stability can be achieved using either update formulas based on multi-cell clusters or extrapolation from neighboring fields. The addition of a small amount of numerical dissipation to the cells in question was also sufficient to prevent instability in almost all cases, while having a negligible effect on accuracy.

A program incorporating the modified formulas was tested by computing the resonant frequencies of flat rectangular and cylindrical cavities, (TE_{101} and TM_{010} modes) in which the widths and diameters were varied between 1.0 and 1.1 m in an FDTD mesh with $\Delta x = \Delta z = 0.05$ m, and $\Delta y = 0.02$ m. The results were compared with theory, and computations made using the staircase method (Table 1). Both codes had the same execution time, and the code using the modified update formulas tracked the resonant frequencies more accurately.

Table 1: Rectangular and Cylindrical Cavity Resonant Frequencies (MHz, Dim. in m)

Dim.	Box (dim. is length and width)					Cylinder (dim. is diameter)				
	Theory	Strcse.	% Err.	New	% Err.	Theory	Strcse.	% Err.	New	% Err.
1.00	211.99	211.8	-0.087	211.80	-0.087	229.49	235.3	+2.53	229.27	-0.097
1.01	209.87	211.8	+0.091	209.71	-0.084	227.22	235.3	+3.55	227.04	-0.079
1.03	205.81	211.8	+2.900	205.62	-0.093	222.81	228.1	+2.38	222.72	-0.039
1.05	201.89	211.8	+4.900	201.71	-0.089	218.56	228.1	+4.36	218.50	-0.029
1.07	198.12	192.6	-2.800	197.99	-0.064	214.48	221.3	+3.18	214.34	-0.065
1.09	194.48	192.6	-0.970	194.37	-0.058	210.54	215.4	+2.31	210.38	-0.077
1.10	192.71	192.6	-0.059	192.62	-0.049	208.63	212.7	+1.95	208.49	-0.067

An Optimized Finite Difference Scheme for Time Domain Maxwell's Equations

Ramakrishna Janaswamy^{1,*}

Yen Liu²

¹Code EC/Js, Naval Postgraduate School, Monterey, CA 93943

²NASA Ames Research Center, Moffet Field, CA 94035

Finite methods in time domain have evolved as powerful techniques for solving electromagnetic problems. A method well known to the electrical engineering community is the Finite Difference Time Domain (FDTD) method first introduced by Yee and later refined by many authors. Errors introduced as a result of finite differencing include dispersion and dissipation errors. Generally, the accuracy of the finite methods increases as the grid size decreases relative to the wavelength, λ , of operation. For example, in the FDTD method, a spatial resolution of $\lambda/10$ to $\lambda/20$ appears to lead to acceptable results for moderately sized bodies (Taflove and Umashankar, *Proc. IEEE*, (77), 682-699, 1989). Computer resource limitations force the problem size to be small at higher frequencies. There is an ever increasing demand to devise efficient numerical schemes to handle electrically large problems.

In the present method, we consider an unstaggered, colocated, finite difference scheme for solving time-domain Maxwell's equations. A four-point, dissipation-free, one-sided, anti-symmetric stencil is considered to represent the spatial derivatives. A staggered leapfrog integration in time is used for the temporal derivative. The coefficients for the differences are chosen by minimizing the discretization error over all the numerical wavenumbers and Courant numbers of interest. This is in contrast to merely making the scheme higher order for a given stencil. We will choose the coefficients so that the error is minimized upto 4 points per wavelength. This will be very attractive for large bodies. Several test geometries will be considered and results compared with those available in the literature.

SVD Based Prony Hildebrand Technique for CFDTD Processing

Ali Asi* and Lotfollah Shafai

Department of Electrical and Computer Engineering

University of Manitoba, Winnipeg, Manitoba, Canada R3T-5V6

Ali_Asi@UManitoba.CA, shafai@ee.umanitoba.ca

Finite Difference Time Domain method has proved to be one of the most versatile techniques in dealing with applied electromagnetic problems. Several special modifications to this method have been made to enhance its performance in dealing with a particular category of problems. Compact FDTD, i.e. CFDTD (A. Asi, L. Shafai, **IEEE AP-S symposium digest**, vol.1, pp. 360-363, 1993) is among the methods which was derived from the original FDTD method. This method has shown promising results in providing accurate results efficiently. The domain of applicability of this method is restricted to resonant waveguide structures with no discontinuity along the z direction.

Usually, the raw information generated by a time domain technique, by itself, is not very informative. In most cases, another post-processing stage is required to transform this data from time to frequency domain. FFT is mostly the common choice for this stage of analysis. It is the objective of this article to present a new spectral estimation technique which is more efficient and convenient for resonant structures.

The Classical Prony method has already been implemented by researchers of the field for the calculation of the S-parameters of a three dimensional structure using conventional FDTD. The main distinctions between this work and earlier ones are twofold. First, SVD technique has been implemented to generate an overestimate system of equations. In the standard Prony method, only data arrays of the dimension equal to three times the number of assumed harmonics are used. This results in either deletion part of the time domain data, or considering a very large number of harmonics, which in turn renders the method inefficient. In the present method, we calculate the number of harmonics by counting the number of nonzero singular values, not just a blind guess. The second distinction is the use of conjugate harmonics. As it was mentioned, in earlier works, the main concern was calculating the characteristics, i.e. amplitude and exponent, of exponential functions. This was the natural choice for non-resonating structures. In the present work, the problem is a two dimensional resonator and hence can be formulated in terms of conjugate exponentials, i.e. sinusoids. The results and complete algorithm will be presented.

SIMULATION AND MEASUREMENT OF HIGH SPEED DIGITAL TEST MODULES

Prof. M. Piket-May, J. Mix *, and D. Barnhart
Department of Electrical Engineering
University of Colorado at Boulder
Boulder, CO 80309-0425

Roger Gravrok
Cray Research Inc.
Development Building
Chippewa Falls, WI 54729

Kevin Thomas
Cray Research Inc.
655E Lone Oak Drive
Eagan, MN 55121

In an effort to validate various measurement and computational methods, simple circuit board test modules were developed at Cray Research. These modules are meant to help us understand some of the fundamental physics involved in high speed digital circuit design. Measurements of the test modules were made using a time domain reflectometer (TDR). It has been shown (B.M. Oliver, "Time Domain Reflectometry" Hewlett Packard Journal, Vol. 15, No. 6, Feb. 1964: hp, Palo Alto, CA) that the area of a reflection in a TDR waveform is related to the impedance of the corresponding discontinuity. Specifically, a study is being done on a circuit board trace that runs over a solid ground plane with the exception of a slot in the ground plane located approximately at one quarter of the trace's length. Models of the TDR measurements using lumped elements in HSPICE were constructed in an attempt to replicate the waveforms produced by the measurements, and validate the relation between the area of the reflection in the TDR waveform and the theoretical values of the impedance of each discontinuity. However, the method of extracting the lumped element values of the signal lines were hindered by a relatively large capacitance produced by the pad that is the interface between the signal trace and the probe. Therefore, a more accurate computational technique is being investigated; the Finite Difference Time Domain technique (FDTD) is being used to provide a model of the physical structure instead of the lumped elements. We hope to reproduce the TDR waveform using a new FDTD simulation tool being developed at Cray Research in conjunction with the University of Colorado. A comparison between the TDR measurements and FDTD simulations will be made.

An FDTD Simulator for Ground-Probing Radars

Zhubo Huang*, Kenneth Demarest, Richard Plumb, Pawan Chaturvedi
Radar Systems and Remote Sensing Laboratory

Electrical Engineering and Computer Science, the University of Kansas
2291 Irving Hill Road, Lawrence, Kansas 66045-2969

Phone: (913)864-7739, Fax: (913)864-7789, e-mail: huang@iroquois.rsl.ukans.edu

Detecting objects buried in a ground by using a ground-probing radar is a subject that has received considerable interest in recent years. However, in order to process the returns obtained from these systems, electromagnetic numerical techniques are needed to simulate the returns of arbitrary targets. The Finite-Difference Time-Domain (FDTD) technique is well suited for modeling a wide variety of objects, sources and grounds. This technique has been implemented successfully by many investigators to evaluate the fields scattered by buried objects when the source of the incident fields is close the air-ground interface. In this paper, we discuss how the FDTD technique can be extended to evaluate the fields when the source is located far away from the interface.

As is well known, the standard FDTD technique can be well applied to evaluate the scattered fields from objects in a homogeneous medium when the incident field is a plane wave. However, difficulties arise when a stratified, half-space ground is introduced, since the incident field in the ground is actually the transmitted field. In a previous paper (Demarest, et al., 1994 URSI Symposium, Seattle WA), we presented a technique whereby the transmitted field can be calculated and subtracted from the total fields in the solution space, yielding only scattered fields at the outer boundary. These outward-propagating scattered fields are easily handled by standard absorbing boundary conditions. This technique yields accurate scattered fields throughout the solution space.

An important tool that is often used in the FDTD methods is the near-to-far field transformation. Again, modifications must be made to this technique in order for it to work when the scattering object is buried. In this paper, we present a technique to implement the near-to-far field transformation of the scattered fields for objects buried in an stratified, lossy ground. This is achieved by using Schelkunoff-Huygen's principle in conjunction with the reciprocity theorem and the stratified medium model.

The concepts developed in this paper are applied to model several types of targets buried in a stratified ground. These extensions are numerically efficient and applicable for both two- and three-dimensional cases. Several numerical examples are presented to demonstrate the accuracy and efficiency of these techniques.

An Explicit Finite Element Time Domain Method Using Whitney Forms

Jin-Fa Lee,^{*} *Member IEEE*

Zachary Sacks

The finite difference time domain (FDTD) algorithm has been used widely in solving transient responses of electromagnetic problems. However, using FDTD in its original form, it is difficult to model complex EM problems with curved surfaces. Many variants have been proposed in the past with the aim to circumvent this difficulty with varying degrees of success. Almost all of these approaches are based upon, one form or the other, the use of finite difference approximation in both spatial and temporal domains. It is the purpose of this paper to formulate, using Whitney forms, In this way, the proposed FETD methods can be used on a tetrahedral finite element mesh and consequently, they impose no geometric limitations.

It will be shown in the presentation that the current implementation of the finite element time domain method results in an explicit time marching scheme. The final time-stepping equations employed to update flux values within the computational domain are

$$\begin{aligned} B^{n+1/2} &= B^{n-1/2} - \Delta t [\mathcal{P}] [\mathcal{A}^e] D^n \\ D^{n+1} &= D^n + \Delta t [\mathcal{P}] [\mathcal{A}^h] B^{n+1/2} \end{aligned} \quad (1)$$

where B and D are coefficient vectors for magnetic and electric fluxes, respectively. The matrices $[\mathcal{P}]$, $[\mathcal{A}^e]$, $[\mathcal{A}^h]$ will be derived in detail in the presentation. Furthermore, in this presentation, we will show the stability condition for this FETD algorithm as

$$\Delta t \leq \frac{2}{\sqrt{\rho_{\max} ([C^e] [C^h])}}, \quad [C^e] = [\mathcal{P}] [\mathcal{A}^e], [C^h] = [\mathcal{P}] [\mathcal{A}^h] \quad (2)$$

where ρ denotes the spectral radius.

A Non-Dissipative Upstream Biased Scheme for Time Domain Computational Electromagnetics

Brian T. Nguyen and Philip L. Roe
Department of Aerospace Engineering
University of Michigan

January 19, 1995

Over the last decade, the use of upstream biased schemes have been decidedly favored in time domain solutions of complex hyperbolic systems of equations—and for many reasons. But for Maxwell's equations, the venerable Yee's scheme have been used almost exclusively, mainly because it is non-dissipative whereas all implementations of upstream biased schemes have been dissipative. However these features are neither necessary nor exclusive to non-dissipative discretizations or upstream formulations. We propose that a form of Maxwell's equations can be combined with a modified leapfrog scheme to devise a non-dissipative, upstream biased numerical scheme. This paper will describe the upwind-leapfrog scheme, the bicharacteristic form of Maxwell's equations and their combination to achieve this. We will demonstrate this upwind-leapfrog scheme, in one- two- and three-dimensional problems.

The modified leapfrog scheme implements the upstream biasing while the bicharacteristic forms discriminate information by their direction of travel. In combination, they also provide a straight forward extension to multiple dimensions while avoiding the pitfalls of using dimensional splitting. Schemes using bicharacteristic equations have been unsuccessful in the past due to the use of interpolation schemes that contaminate upstream information with downstream information. The upwind leapfrog scheme requires no such interpolation even in multiple dimensions and thus preserves the advantages of the bicharacteristic equations.

In addition to a more proper treatment of information propagation, our implementations have several further advantages over a central differencing scheme. With an appropriate implementation on a finite difference grid, this includes more compact non-overlapping stencil, preservation of accuracy up to the boundary, ease of the application of boundary conditions, ease of treatment of material interfaces, stability on locally refined meshes, and lower overhead on parallel message passing computers. An upstream biased scheme can use a more compact stencil because the support is limited to the side where information is taken. Central difference stencils must cover a wider support to get the same data and in so doing, also gets unnecessary and inappropriate data. Central difference stencils cannot be used at grid boundaries due to the absence of grid points on the other side, but upstream biased stencils can and should be jugged up to the grid boundary, providing normal accuracy up to the boundary. The application of boundary condition is easier in the context of an upstream biased scheme, because boundary conditions are simply statements on the relationship between outgoing and incoming waves. Material interfaces can be treated as normal since the stencil can be kept entirely within one material. On parallel message passing computers, the non-overlapping stencils allow partitionings that never cuts across a stencil, reducing the amount of data that must be shared through communication.

An Accelerated Algorithm for the Time Domain Analysis of Guided Wave Problems Involving Ferrites.

M.Okoniewski^{*†}, M.Mrozowski[‡]

[†]University of Victoria, Dept. of Electrical and Computer Engineering
P.O.Box 3055, MS 8610, Victoria, BC, V8W-3P6, Canada

[‡]Technical University of Gdańsk, Dept. of Electronics,
80-956 Gdańsk, Poland

In MMIC transmission lines the largest gradient of fields occurs in the small area of computational space in the vicinity of the slots or strips. In most practical cases this is the only region with inhomogeneous continuity conditions. This sets great demands on computer resources if typical FDTD or TLM schemes are applied, since a dense discretization has to be used throughout the structure.

Recently, a new accelerated method was introduced for the analysis of guided wave problems (M.Mrozowski, IEEE-MGWL, No 10, 323-325, 1994) which alleviates this problem. In this method different algorithms are used in different regions of the structure:

- FDTD method is applied in a region where high inhomogeneity of the structure occurs
- 1D discretization and function expansion is applied in homogeneous regions of the structure.

The two algorithms are combined via continuity conditions which must be fulfilled on the boundaries between the regions. Since the function expansion part of the method involves discretization in one dimension only, dramatic savings in both computer memory and time are achieved.

This approach is now extended to allow for magnetized ferrites in the structure. An FDTD method of analysis of structures comprising magnetized ferrites (M.Okoniewski, IEEE-MGWL, No 6, 169-171, 1994) is introduced to the algorithm.

Note, that a Yee mesh based FDTD for ferrite structures requires substantially more operations and memory than corresponding FDTD for isotropic structures. More field components have to be stored, and additional equations solved. In the new approach, the fine FDTD discretization is applied only in the cross section area comprising ferrites, while the remaining part is treated with function expansion and 1D discretization.

The resulting technique is a powerful simulation tool. Initial tests indicate that the method is 10-30 times faster and requires a fraction of the memory typically used by ferrite FDTD itself, while providing the same accuracy.

Impulse Radar

J. P. Hansen and L. Peters

Page

1:20	Ground Penetrating Radar Antennas	266
	<i>Leon Peters, Jr.*</i> , <i>Chi-Chih Chen</i> , <i>Frank Paynter</i> , <i>The Ohio State University</i>	
1:40	Time-Domain Imaging of Radar Targets using Ultra-Wideband267 or Short Pulse Radars	
	<i>Y. Dai</i> , <i>E. J. Rothwell*</i> , <i>D. P. Nyquist</i> , <i>K. M. Chen</i> , <i>Michigan State University</i>	
2:00	Calibration of an Impulse Radar Scattering Range with268 Conducting and Dielectric Canonical Targets: Sphere, Cube and Knife Edge	
	<i>M. Piette*</i> , <i>E. Schweicheir</i> , <i>Royal Military Academy Brussels</i> , <i>A. Vander Vorst</i> , <i>Univ. Cath. de Louvain</i>	
2:20	Aspect Angle Sensitivity of Backscatter Measured by an269 Ultrawideband Synthetic Aperture Radar for Detection of Obscured Targets	
	<i>Ravinder Kapoor*</i> , <i>U. S. Army Research Laboratory</i> , <i>N. Nandhakumar</i> , <i>University of Virginia</i>	
2:40	Ultrawideband, Impulse Driven X-Band Clutter Measurement270 Radar	
	<i>J. P. Hansen*</i> , <i>M. Sletten</i> , <i>K. Scheff</i> , <i>Naval Research Laboratory</i>	
3:00	BREAK	
3:20	Enhanced Detection of Radar Targets in a Realistic Sea Clutter271 Environment Using E-Pulse Clutter Cancellation	
	<i>G. Wallinga</i> , <i>E. J. Rothwell*</i> , <i>D. P. Nyquist</i> , <i>K. M. Chen</i> , <i>A. Norman</i> , <i>Michigan State University</i>	
3:40	On a New Family of E-Pulses for UWB Radar Target272 Discrimination	
	<i>Sergey Primak*</i> , <i>Ben-Gurion University of the Negev</i> , <i>Margarita Horenian*</i> , <i>Library of the Russian Academy of the Science</i>	
4:00	Matching Score Properties Between Range Profiles of273 High Resolution Radar Targets	
	<i>Hsueh-Jyh Li*</i> , <i>Yung-Deh Wang</i> , <i>National Taiwan University</i>	

Ground Penetrating Radar Antennas

Leon Peters Jr.*, Chi-Chih Chen and Frank Paynter
ElectroScience Laboratory
Dept. of Electrical Engineering
The Ohio State University
1320 Kinnear Road
Columbus, Ohio 43212

Abstract

Ground Penetrating Radar (GPR) antennas used to detect finite obstacles are to be discussed. In addition to reflector antennas and crossed bowtie configurations, the dipole monopulse represents a relatively new antenna for this application and the slot-dipole configuration has not been reported previously. Since GPR systems are usually excited by a band limited impulse, bandwidth is an important factor. Since the obstacle to be detected is usually close to the antenna, direct coupling from the transmitter to the receiver is also an important factor. Size and mobility are also important in many applications since the GPR system may be used to scan large areas in a relatively short time. Since the electrical parameters of the earth also require that the operational frequency band lies in the VHF-UHF bands, most antenna systems in use are some form of monostatic or bistatic dipole (or bowtie) antennas operated just above the ground.

The reflector antenna with a slotline strip line feed or the transmission line feed satisfies the bandwidth and coupling conditions but mobility limits its use to detecting small near-surface targets.

The monostatic dipole antenna has often been replaced by the bistatic system which uses separate antennas for transmit and receive to reduce the direct coupling. The crossed dipole was introduced to further reduce this coupling as was the dipole monopulse antenna whose performance showed further improvement.

Recently the slot dipole geometry used in conjunction with a tapered resistive sheet has been introduced which shows substantial improvement. The direct coupling from transmitter to receiver is as low as the dipole monopulse system. It is expected that this antenna will show substantial further improvement when operated in a monopulse mode.

In addition to a brief discussion of the antenna properties the results obtained with these antenna systems for Unexploded Ordnance (UXO's) targets in a lossy clay medium where clutter is an important factor are to be reviewed.

TIME-DOMAIN IMAGING OF RADAR TARGETS USING ULTRA-WIDEBAND OR SHORT PULSE RADARS

Y. Dai, E.J. Rothwell*, D.P. Nyquist and K.M. Chen
Department of Electrical Engineering
Michigan State University
East Lansing, MI 48824

The development of viable short-pulse radar systems has renewed the interest in target imaging performed directly in the time domain with temporally measured signals. It is well known that the time-domain field scattered by a radar target consists of a complicated combination of higher frequency specular reflections and lower frequency natural resonances. A simple time-domain imaging technique based upon the specular nature of the target, and using the physical optics approximation, gives good results when the lower frequency components of the signal are ignored, but is hampered by the shadowing limitations of physical optics. To utilize the low-frequency information, or to eliminate the shortcoming of physical optics, a more rigorous scattering model is required.

Researchers such as C.L. Bennet (IEEE Trans. Ant. Prop., vol. AP-29, no. 2, pp. 213-219) and W.-M. Boerner, et al. (IEEE Trans. Ant. Prop., vol. AP-29, no. 2, pp. 336-341) have shown how the ramp response of a target can be used to determine the target's projected area and characteristic function, using rigorous time-domain scattering theory. This paper will expand that approach to the case of more realizable, band-limited, transmitting waveforms. It will also consider the effects of a bistatic configuration and restricted-aperture scattered-field data. Finally, the relationship between the imaging identity and the physical optics identity will be examined.

Examples will be generated using scattered field data measured in the Michigan State University scattering laboratory. The time-domain responses of several aircraft targets will be synthesized from ultra-wideband measurements (0.2-18 GHz) using the inverse Fourier transform. Measurements will be made within a plane for varying azimuthal aspect angle, producing images corresponding to the thickness of the target.

Calibration Of An Impulse Radar Scattering Range With Conducting And Dielectric Canonical Targets : Sphere, Cube and Knife Edge

M. PIETTE*, E. SCHWEICHEIR
Royal Military Academy Brussels
30, avenue de la Renaissance
1040 Brussels, Belgium

A. VANDER VORST
Univ. Cath. de Louvain
Bât. Maxwell
1348 Louvain-la-Neuve

The Royal Military Academy Brussels has developed an Impulse Radar Scattering Range. The purpose is to measure *directly in the time-domain* the impulse response (monostatic and bistatic) of complex targets and to analyse the scattering mechanisms. The system consists at the transmitting side of a long monocone antenna on ground plane coaxially fed by a fast step function generator (50 V/50 ps) and, at the receiving side, of a broadband e-sensor connected to a 20 GHz digitizing oscilloscope. The target under test is put on the ground plane. By taking into account the spherical character of the TEM wave radiated by the antenna, the far-field conditions and the reflections occurring at the end of the monocone and the groundplane, one can determine geometrically the best location of the target on the groundplane.

To validate the developed Scattering Range as measuring instrument and to quantify its global accuracy and precision, the impulse backscattering of canonical targets have been measured and compared to their theoretical responses. The targets consist of smooth shapes like spheres of various diameters and materials and of sharp bodies like the cube and the knife edge. Fig. 1 shows the impulse backscattering of a conducting sphere, where the specular reflection and the first creeping wave are clearly visible. In the impulse response of the lossless dielectric sphere shown in Fig. 2, one can see the series of doublets succeeding the specular reflection, due to the multiple reflections of some rays refracted in the sphere.

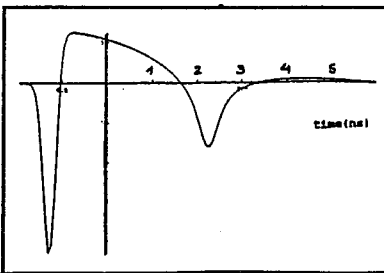


Fig.1 Response of the conducting sphere

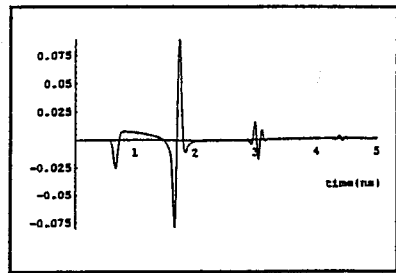


Fig. 2 Response of the dielectric sphere

Aspect Angle Sensitivity of Backscatter Measured by an Ultrawideband Synthetic Aperture Radar for Detection of Obscured Targets

Ravinder Kapoor *
U.S. Army Research Laboratory
Adelphi, MD 20783-1197
Attn: AMSRL-SS-SG

N. Nandhakumar
University of Virginia
Dept. of Electrical Engineering
Charlottesville, VA 22903-2442

A fully polarimetric ultra-wideband (50 Mhz to 1 Ghz) impulse radar is used in a synthetic aperture configuration for detecting man-made objects obscured by a forest canopy. The radar is situated on the roof of a four-story building where it collects the impulse backscatter of an image area at discrete points along the synthetic aperture. Each point has a different aspect angle to the image area but, unfortunately, the aspect-angle sensitivity information is inherently integrated out when forming the SAR image. This information is important when discriminating between objects in the image which have distinct aspect-angle sensitivity such as between man-made objects (targets) and natural objects (clutter). Although it has been shown that both the early- and late-time portion of the backscatter is sensitive to aspect angle (K.M. Chen, E.J. Rothwell, et. al., IEEE AP-S/ URSI conference 1994, URSI-A, p. 252), in our analysis, emphasis is placed on the early-time for discrimination since it is (a) more sensitive to aspect angle and (b) has a higher signal-to-noise ratio than the late-time.

Angular dependence information is extracted by integration of the radar returns from the object over smaller subapertures of the full synthetic aperture. This approach provides important aspect angle information while sacrificing some azimuth resolution provided by the full synthetic aperture. However, subaperture sizes are chosen such that target-to-clutter noise ratio remains at detectable levels. The backscatter energy in the early-time portion versus subaperture position (aspect angle) for both co- and cross-polarized channels are measured. This information is subsequently used to generate a feature vector which discriminates targets from clutter. Figure 1 below shows the full polarimetric response of a broadside vehicle and natural clutter (i.e. tree) with the associated feature vector, $R = (r_{xx_yy} \ r_{xx_xy} \ r_{yy_xy})$, where X and Y are orthogonal polarizations; r_{xx_yy} is the correlation coefficient for XX and YY channels and similarly for r_{xx_xy} , r_{yy_xy} . The feature vector is robust enough to detect vehicles with no specular return along the synthetic aperture (i.e. nonbroadside) as well as to reject clutter that appears to be dependent on aspect angle. Details of the radar system and experimental results are presented.

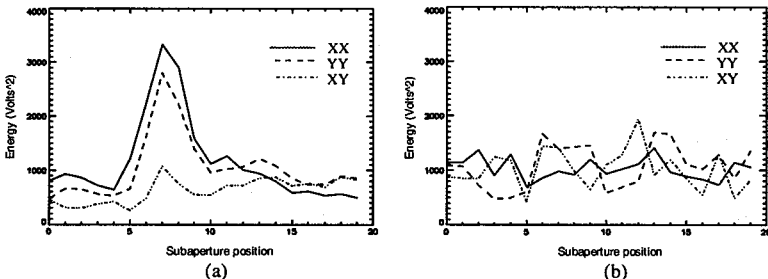


Fig. 1: Response of (a) vehicle with $R = (0.93 \ 0.57 \ 0.25)$ (b) clutter with $R = (0.01 \ 0.04 \ -0.04)$.

Ultrawideband, Impulse Driven X-band Clutter Measurement Radar

*P. Hansen, M. Sletten, K. Scheff
Radar Division
Code 5340
Naval Research Laboratory
Washington, D.C. 20735

ABSTRACT

A field deployable, ultra high resolution radar system for performing X-band sea scatter measurements is described. The dual linear polarized system employs two impulse excited traveling wave tube (TWT) amplifiers to produce alternate vertical and horizontal polarized transmit pulses with 1 KW peak power and a 3 dB power envelope of less than 250 picoseconds in duration. The RF transmitted waveform presents a nominal 4 GHz instantaneous bandwidth centered at 10 GHz. The driving function for the TWT amplifiers is a 5 volt video pulse with a 15 picosecond risetime. With this excitation, pulse-to-pulse transmit waveform variations are minimal. Separate transmit and receive antennas are employed to maintain receiver isolation.

The video driving pulse is also used as the master timing source for the receiver electronics. The receive system detects signals in coherent baseband quadrature form with a unique direct sampling detector based on a multiple sampling head, eight bit digital oscilloscope and analog transversal filters. The multiple sampling heads and analog filters utilize a real sample spacing of 25 picoseconds over a time limited sample window. Overall receiver bandwidth is in excess of 6 GHz centered at 10 GHz with a digitized dynamic range of 40 DB. For target ranges up to 200 meters, system timing jitter is within 3 picoseconds.

System parameters include pulse repetition rates as high as 100 KHz and consecutive pulse recordings of 5000 pulses. Variable data recording modes can be supported. Two examples are a 5 second dwell at a 1 millisecond frame rate on a 20 cm wide range window supporting five 4 cm wide range cells or a single frame mode producing one 25 meter range sweep of contiguous 4 cm range cells within a time period of 10 milliseconds.

ENHANCED DETECTION OF RADAR TARGETS IN A REALISTIC SEA CLUTTER ENVIRONMENT USING E-PULSE CLUTTER CANCELLATION

G. Wallinga, E.J. Rothwell*, D.P. Nyquist, K.M. Chen and A. Norman
Department of Electrical Engineering
Michigan State University
East Lansing, MI 48824

When a conventional radar is used to detect an airborne target flying close to a disturbed sea, the strong sea clutter signal is highly influenced by the specular scatter from the fine structure on the ocean waves (chop). This is due to the comparable sizes of the chop and the wavelengths of the radar. A similar phenomenon is seen in short-pulse (baseband) radars, when the pulse width is on the order of a transit time of the chop. However, if the pulse width is large compared to the fine structure, the time-domain clutter return is dominated primarily by the specular reflections from the periodic swell. Thus, the time-domain sea clutter signal measured by a short-pulse radar consists of a dominant periodic set of specular signals, superposed with a wide spatial-frequency band surface roughness signal.

It has been shown (E. Rothwell, et al., IEEE Trans. Ant. Prop., vol. 42, no. 9, 1336-1341) that both frequency-domain and time-domain E pulses can be created to annihilate a signal consisting of a train of specular reflections. This paper will present a theoretical study of the cancellation of sea clutter produced by realistic surfaces using these E-pulse techniques. Specifically, the effect of the wide spatial-frequency band component of the clutter on the cancellation process will be considered.

Simulation of the short-pulse radar clutter signal will be accomplished by using a method of moments analysis of both perfectly conducting and sea-water two-dimensional surfaces. The sea-wave profile will be obtained from models proposed by Pierson and Moskowitz (J. Geophysical Res., vol. 69, pp. 5181-5190, 1964) and by Donelan and Pierson (J. Geophysical Res., vol. 92 (C5), pp. 4971-5029, 1987).

ON A NEW FAMILY OF E-PULSES FOR UWB RADAR TARGET DISCRIMINATION

Sergey Primak*, *Department of Electrical and Computer Engineering, Ben-Gurion University of the Negev, POB 653, Beer Sheva, 84105, Israel.*

Margarita Horenian*, *Library of the Russian Academy of the Science, Birzhevaya Liniya 1, St. Petersburg, Russia.*

In recent years, many radar-target discrimination methods using the time-domain response of a target to a transient incident waveform have simulated growing interest. The singularity-expansion method (SEM) (C.E. Baum, E.J. Rothwell, K.M. Chen, and D.P. Nyquist, *Proc. IEEE*, vol.79, #10, pp. 1481-1492, 1991.) provides the necessary mathematical formulation for describing the transient behavior of conducting targets. The late-time response of the target can be represented as a sum of natural modes with aspect-independent natural complex frequencies:

$$r(t) = \sum_{n=1}^N a_n e^{\sigma_n t} \cos(\omega_n t + \phi_n), \quad t > T_l$$

where $s_n = \sigma_n + j\omega_n$ are aspect-independent natural frequencies of the targets, a_n and ϕ_n are the aspect-dependent amplitude and phase of the n 'th mode, T_l describes the beginning of the late time, and only N nodes are assumed to be excited by the incident field waveform. One of the most important techniques in radar-target discrimination based on the SEM involves the so-called E-pulse (C.E. Baum, E.J. Rothwell, K.M. Chen, and D.P. Nyquist, *Proc. IEEE*, vol.79, #10, pp. 1481-1492, 1991)

We regard on E-pulses as a filtering approach and construct a new family of such pulses with analytically known transfer function, which has the form:

$$H(j\omega) = \prod_{i=1}^N \exp\left(-\sigma_i \frac{\pi}{\omega_i}\right) \left(1 + \exp\left(\frac{\pi}{\omega_i} s_i\right)\right)$$

Let us point out the following advantages of the new approach:

- 1) It is possible to directly calculate of the filter parameters, not using the solution of the system of the equations as in (C.E. Baum, E.J. Rothwell, K.M. Chen, and D.P. Nyquist, *Proc. IEEE*, vol.79, #10, pp. 1481-1492, 1991.). It can simplify the adaptive filtering approach to target discrimination.
- 2) The analytical expression for the transfer function can be obtained. This opportunity allows us to analytically investigate such characteristics of the filter as sensitivity of poles, probabilistic characteristics and so on.

The model is validated by numerical simulations for data obtained for F-104, F-4, MIG-19 aircraft in presence of the noise

MATCHING SCORE PROPERTIES BETWEEN RANGE PROFILES OF HIGH RESOLUTION RADAR TARGETS

Hsueh-Jyh Li and Yung-Deh Wang
Department of Electrical Engineering
National Taiwan University
Taipci, Taiwan, R. O. C.

ABSTRACT

For a low resolution radar, a whole target is usually covered by one or two pulses. A slight variation in frequency or aspect can cause a drastic variation in the received field when the object size is large compared with a wavelength. For a high resolution radar, target echoes can be distributed in many range bins. Patterns of the target echoes are referred to as range profiles. The RCS properties of complex targets for a low resolution radar have been extensively studied. However, properties of range profiles for high resolution radar targets are rarely reported. Range profiles have been utilized as feature vectors for automatic target identification. A matching score has been defined to measure the similarity between two range profiles or feature vectors. The matching scores between range profiles of known and unknown targets are then used as the decision parameter. In that application one may have the following questions: How to determine the aspect increment in both elevation and azimuthal directions in order to establish a useful but not wasteful database? Will the feature vectors stored be still valid for identification when the testing range profiles are measured at shifted carrier frequencies? How to determine a threshold for the matching score in order to obtain a given percentage of correct identification?

In this paper how the statistical properties of the matching scores are affected by the carrier frequency, the aspect variation, the range resolution, and the target complexity are studied. The statistical parameters, mean and standard deviation, of the matching scores among range profiles of independent objects are derived, and their values are used as references to determine the threshold values for target identification. It is found that the range profile obtained at a certain carrier frequency can also be used as the feature vector for radars operated at shifted frequencies if the range resolution is fine enough or the target is simple. It is also found that a radar with higher range resolution can tolerate more aspect variation, yielding a significant advantage in saving memory space for establishing the data base. The results obtained can have several applications such as target identification, data association in multiple target tracking, and target direction determination when widely-spaced high resolution radars are employed.

THIS PAGE INTENTIONALLY LEFT BLANK.

Microstrip II

C. G. Christodoulou and J. L. Volakis

Page

1:20	FD-TD Analysis of Microstrip Antennas with Ferrite Substrates	276
	<i>T. Spreckic-Zugec*, C. G. Christodoulou, University of Central Florida</i>	
1:40	Radiation Patterns of Microstrip Antennas on Very Small	277
	Ground Planes	
	<i>W. Zhou, P. F. Wahid*, C. G. Christodoulou, University of Central Florida</i>	
2:00	Input Impedance of a Microstrip Wrap-Around Antenna	278
	on a Conical Surface	
	<i>D. N. Meeks, P. F. Wahid*, University of Central Florida</i>	
2:20	Computation of Radiation Pattern of Microstrip Patch Antennas	279
	on Complex Bodies	
	<i>Sean Ni*, Jian-Ming Jin, Shung-Wu Lee, University of Illinois at Urbana-Champaign</i>	
2:40	An Efficient Hybrid FEM Formulation for Analysis of Cavity-Backed	280
	Thin Spiral Slot Antenna	
	<i>Jian Gong*, John L Volakis, University of Michigan</i>	
3:00	BREAK	
3:20	The Sinusoidal Microstrip Patch Antenna	281
	<i>Mohammad A. Saed, State University of New York at New Paltz</i>	
3:40	Gain Calculations for Large Microstrip Antenna Arrays using	282
	Different Feed Networks	
	<i>Mohammad Shahid*, Alakananda Paul, Howard University</i>	
4:00	Wire-Grid Modeling of Single- and Double- Layered Perforated	283
	Microstrip Antenna	
	<i>H. Moheb*, InfoMagnetics Technologies Corp., L. Shafai, University of Manitoba</i>	
4:20	A Study of Microstrip Antennas on Very High Permittivity	284
	Substrate and Very Small Ground Plane	
	<i>Alessandro Perrotta*, Motorola, Ahmad Hoorfar, Villanova University</i>	
4:40	Analysis of Cylindrical Patch Microstrip Antenna with Circular	285
	Polarization by FD TD Method	
	<i>Yasuhiro Kazama*, Tamotu Suda, Japan Radio Co., Ltd., Nagayoshi Morita, Chiba Institute of Technology</i>	
5:00	A Radiation Mode Expansion Formulation of Radiated	286
	Fields From Microstrip Line Discontinuities	
	<i>Nagayoshi Morita, Chiba Institute of Technology</i>	

FD-TD ANALYSIS OF MICROSTRIP ANTENNAS WITH FERRITE SUBSTRATES

T. Spreckic-Zugec* and C. G. Christodoulou
Electrical and Computer Engineering Department
University of Central Florida
Orlando, FL. 32816

Abstract

At microwave frequencies, ferrite materials offer unique design capabilities because some of their properties depend on the dc magnetic field applied to them. (N.E. Buris, T. B. Funk, & R. S. Silverstein, *IEEE Trans. Antennas Propagat.*, vol 41, Feb. 1993.)

Since the FD-TD method has been proven to be a very powerful tool for the calculation of the frequency dependent characteristics of microstrip components and antennas, it is also used in this paper to analyze the radiation properties of microstrip antennas with ferrite substrates.

One of the advantages of the FD-TD approach is that a description of the transient radiation from the antenna can be obtained (J.G. Maloney, G. S. Smith, & W. R. Scott, Jr., *IEEE Trans. Antennas and Propagat.*, vol. 38, July 1990.). Transient radiation provides a physical insight in the radiation process of microstrip antennas with ferrite substrates and the effects of the applied dc bias on the radiation characteristics of this type of antennas.

In this paper, modifications are made to the classical Yee algorithm in order to incorporate the effects of the ferrite substrate. Several computed results, in both, the time domain and frequency domain are compared with experimental data and data obtained with other methods (D. M. Pozar D. M, *IEEE Trans. Antennas Propagat.*, vol 40, Sept. 1992).

These results are functions of the ferrite slab thickness, and the magnitude of the applied dc bias. Moreover, the results cover both normal and in-plane dc bias of the ferrite substrate.

RADIATION PATTERNS OF MICROSTRIP ANTENNAS ON VERY SMALL GROUND PLANES

by

W. Zhou, P. F. Wahid* and C. G. Christodoulou
Electrical and Computer Engineering Department
University of Central Florida, Orlando, FL 32816

ABSTRACT

Microstrip antennas on small ground planes are used in various portable communication systems. These antennas need to be sensitive to both vertically and horizontally polarized waves with radiation patterns that are essentially isotropic. Much of the reported work on microstrip antennas deals with these antennas or arrays on infinite ground planes. This paper will investigate the radiation patterns of microstrip antennas where the patch and the ground plane are of the same size. Image theory is used to account for the finite size ground plane. The current distribution on the patch is obtained by the moment method and the radiation pattern is determined through the use of Green's function. The edge radiation between patch and ground plane is included by the cavity model approach and the total radiation formula is developed. Radiation patterns for patches on finite ground planes are presented for various geometries and compared with available published results.

INPUT IMPEDANCE OF A MICROSTRIP WRAP-AROUND ANTENNA ON A CONICAL SURFACE

by

D. N. Meeks and P. F. Wahid*

**Electrical and Computer Engineering Department
University of Central Florida, Orlando, FL 32816**

ABSTRACT

Microstrip antennas on cylindrical and conical surfaces are of importance due to their applications in air and space vehicles. The radiation characteristics of these antennas have already been investigated in detail by the authors. This paper is an extension of this study to determine the input impedance of the conical wrap-around microstrip antenna. The input impedance is determined from a knowledge of the radiation fields calculated through the use of the cavity model. The conductors are assumed to be negligibly thin and ideal. Various cases of dielectric substrates and loss tangents are considered. Several feeding mechanisms are discussed. The input impedance is derived as a function of the number, placement and type of feed mechanism used.

COMPUTATION OF RADIATION PATTERN OF MICROSTRIP PATCH ANTENNAS ON COMPLEX BODIES

Sean Ni*, Jian-Ming Jin, and Shung-Wu Lee
Electromagnetics Laboratory
Department of Electrical and Computer Engineering
University of Illinois at Urbana-Champaign
Urbana, Illinois 61801-2991

Recently, a robust hybrid technique was presented for an evaluation of electromagnetic scattering by large bodies with cracks and cavities on their surfaces. This technique employed the high-frequency shooting-and-bouncing-ray (SBR) method to compute the scattering from the large bodies with the cracks and cavities filled with perfect conductors, and the low-frequency finite-element boundary-integral (FE-BI) method to characterize the cracks and cavities whose openings are covered with perfect conductors. The two methods were coupled by the equivalence principle which includes all significant effects of the complexity of the large body.

In a similar scheme, the radiation patterns of microstrip patch antennas on complex bodies can be evaluated. For this problem, the FE-BI method is first used to analyze the microstrip patch antennas whose geometry is modeled with a collection of small volume elements and whose fields are represented by edge-based vector basis functions. With this method, an equivalent magnetic current can be accurately found on the surface opening of the microstrip patch antennas.

Once the equivalent surface magnetic current is obtained, the radiated field in the presence of the complex body can be evaluated using the SBR method, and for this evaluation, two approaches can be employed. The first approach is to start from the computed magnetic current and trace the field propagation using the SBR tracer. At the last hit point or at each and every hit point, a physical-optics-type integration is performed to determine the ray contribution to the radiated field. For this approach to be accurate, many rays must be traced and the ray divergence must be considered. The second approach is to launch a dense grid of rays from the observation direction toward the complex body and find the magnetic field over the surface opening of the microstrip patch antennas using the SBR method. A reciprocity theorem is then employed to compute the radiated field in the observation direction. To be more specific, the radiated field can be evaluated using

$$E_{\theta}^{\text{rad}}(\vec{r}) = \frac{jk_0 e^{jk_0 r}}{2\pi r} \iint_S \vec{M} \cdot \vec{H}_v^{\text{sbr}} dS, \quad E_{\phi}^{\text{rad}}(\vec{r}) = \frac{jk_0 e^{jk_0 r}}{2\pi r} \iint_S \vec{M} \cdot \vec{H}_h^{\text{sbr}} dS$$

where \vec{M} denotes the equivalent magnetic current over the opening of the microstrip patch antennas, computed using the FE-BI method, and $\vec{H}_{h,v}^{\text{sbr}}(\vec{r})$ denotes the magnetic field due to the horizontally and vertically polarized incident fields, respectively, computed using the SBR method in the presence of the complex body with the patch antennas filled with perfect conductors. Since the SBR method includes multiple bounces and first-order edge diffraction, all significant interactions caused by the complex environment are included in this evaluation of the radiated field.

An Efficient Hybrid FEM Formulation For Analysis of Cavity-Backed Thin Spiral Slot Antenna

Jian Gong* and John L. Volakis

Radiation Laboratory

Department of Electrical Engineering and Computer Science

University of Michigan

Ann Arbor, MI 48109-2122

jxgum@engin.umich.edu, volakis@engin.umich.edu

It has been reported that the finite element - boundary integral (FE-BI) technique is quite versatile in modeling microstrip patch antennas of any shape, printed on a layered planar structure or cylindrical platform and fed with a coaxial cable or a microstripline network. However, direct application of the hybrid FE-BI technique to thin slot spirals requires excessive sampling rates to accurately simulate the geometry and this is particularly so when edge elements are used to tessellate the cavity volume. Although the edge elements are better suited for modeling metallic edges and corners, they cause major meshing difficulties because of the presence of thin slots in a metallic plane, in which case the edge elements must be specifically designed to have one of their edges perpendicular to the slot. This places severe restriction on the volume mesh in addition to increasing the computational requirements. Moreover, the FEM computational domain beneath the slot spiral antenna may contain a feeding circuitry or dielectric substrate whose structure can have significant geometrical differences than the slot spiral and this could lead to ill-conditioned systems.

To alleviate the meshing/modeling difficulties encountered with cavity-backed slot antennas, in this paper we describe a hybrid finite element-boundary integral formulation using mixed set of elements. As in the past, the boundary integral is used to describe the radiation of the slot above the cavity, however the cavity is now modeled using a suitable mix of edge- and node-based elements. The latter are used only at the aperture of the thin slot so that the nodes follow the center line of the slot(s). In this manner, regular size elements can be used regardless of the slot's width and any meshing restrictions are substantially relaxed. The proposed mixed-element FE-BI formulation introduces three different computational regions and as expected this complicates the generation of the discrete system. At the meeting, we will describe the proposed mixed-element FE-BI formulation and the development of the final discrete system by imposing field continuity at the interfaces of the computational regions. Computational results and validations with reference data and measurements will be also presented.

THE SINUSOIDAL MICROSTRIP PATCH ANTENNA

Mohammad A. Saed
Electrical Engineering Department
State University of New York at New Paltz
New Paltz, New York 12561

The most popular shapes for microstrip antennas are rectangular and circular patches. Those patches are treated extensively in the literature. Their main disadvantage is that they exhibit narrow impedance bandwidth. This paper is concerned with the analysis, design, and testing of a novel patch shape. We will refer to the proposed patch antenna as "The Sinusoidal Microstrip Patch Antenna". The borders of the proposed patch are formed on one side of the substrate by using a full period of a sinusoidal function and its image. A ground plane is placed on the other side of the substrate. The feeding techniques for the sinusoidal patch are similar to those for conventional patches, mainly using a microstrip line on the same side of the substrate, using a probe through the ground plane, or aperture coupling in a two layer configuration.

In this paper, the sinusoidal microstrip patch antenna with various coupling mechanisms is analyzed using the Finite-Difference Time-Domain method. A staircase approximation for the sinusoidal shape is used. Results for input impedance, bandwidth, antenna gain, as well as radiation patterns will be presented. Comparisons will be made to the conventional rectangular and circular patch antennas. The various versions of the antenna are fabricated using photolithographic etching. The numerical results are verified experimentally in the microwave frequency range.

SYNOPSIS

GAIN CALCULATIONS FOR LARGE MICROSTRIP ANTENNA ARRAYS USING DIFFERENT FEED NETWORKS

MOHAMMAD SHAHID* AND ALAKANANDA PAUL

Electrical Engg. Department, Howard University

High gain microstrip antennas are needed for satellite communications. To obtain higher gains, antennas made up of relatively large number of elements are required. For large antenna arrays, the feeding arrangement becomes more complicated and it becomes necessary to use numerical methods and efficient computer softwares to predict radiation pattern and the gain of the antenna. Transmission line and cavity models are often used to do the analysis of microstrip antennas, but more rigorous models are needed for better accuracy. For the precise determination of the electromagnetic fields radiated from a microstrip antenna, full wave analysis method is often used.

This paper presents a numerical solution for the analysis and design of rectangular patch microstrip antenna arrays. A computer software is developed to predict the radiated far field pattern, different types of losses in the antenna and the feeding network and thereby to calculate the directivity and the gain of a microstrip antenna array. The method used for the calculation of radiated field patterns is a generalization of the Green's function approach proposed by Mosig and Gardiol. Each patch is subdivided into a number of Hertz dipoles which are assumed to be excited by a unit step current. The vector and scalar potentials of these dipoles are found by solving corresponding wave equations. The calculated fields of Hertz dipoles yield Green's functions which in turn can be solved using network techniques to give far field radiation patterns of a microstrip antenna. The directivity is calculated from the radiation pattern. The losses occurring in the antenna and the feed lines are computed and the gain of the antenna array is determined. Numerical results are presented for 4x4, 8x8, 16x16, and 32x32 arrays. For example, directivity and gain for a 16x16 element microstrip antenna array using Duroid substrate operating at 13.5 GHz are 24.0 dB and 21.6 dB respectively. At least two types of feed networks have been considered.

WIRE-GRID MODELING OF SINGLE- AND DOUBLE-LAYERED PERFORATED MICROSTRIP ANTENNA

H. Moheb*, L. Shafai¹

InfoMagnetics Technologies Corps. Winnipeg, MB, Canada R2J-3T4

1-University of Manitoba, Winnipeg, MB, Canada R3T-2N2

The conventional microstrip patch radiators resonate at a single frequency and operate only over a very narrowband, in order of 3% bandwidth. The bandwidth can be easily increased by using parasitic element or stacked element configuration using probe or aperture coupling feeds[F. Croq, A. Pozar, *IEEE Trans. Antennas & Propagat*, vol. 39, no. 12, pp. 1770-1776, 1991]. As the operating frequency of antenna decreases, the size of patch radiator increases where at the lower Microwave frequency the patch size become significantly large. To miniaturize the patch size a simple technique is to use high dielectric substrate material. On the other hand, larger dielectric constant reduces the antenna bandwidth. An alternative is to use perforated strip mesh antenna to replace the continuous patch surface. The stacked perforated meshes can then be designed to obtain wideband performance.

In order to analyze these structures, the conventional approach is to use the Moment method based surface patch techniques to model the continuous metallic surfaces. The time-domain based numerical technique have also been used to model microstrip patch antennas[R. L. Chen, K.K. Mei, *IEEE APS Conf. London, Ontario, Canada*, pp. 645-649, June 1991]. These techniques usually requires either an extensive computer memory or computing time. Approximate numerical technique such as wire grid modeling is often used to model the solid patch metallic surfaces. In this technique [J. H. Richmond, *IEEE Trans. Antennas & Propagat*, vol. 14, pp.782-786, Nov. 1966] the continuous metallic surface is replaced by a set of straight wire segments. As the grid size becomes smaller relative to the wavelength, the grid supports an electric current distribution which approximates that of the solid patch antenna. Accordingly, one can model the patch antenna with a wire-grid model rather than continuous metallic patch. Such a solution is approximate, however, it provides the capability of studying the patch and also the perforated mesh element antennas.

In this paper, the wire grid modeling technique is applied to model a single- and double-layered perforated mesh antennas. The electrical characteristics of the antennas, i.e., input impedance, bandwidth, and the radiation patterns are studied for various wire grid radii, grid sizes, height of the antenna over the ground plane, and proximity effect of the double-layered for the stacked patches.

A STUDY OF MICROSTRIP ANTENNAS ON VERY HIGH PERMITIVITY SUBSTRATE AND VERY SMALL GROUND PLANE

Alessandro Perrotta*
MIRS Subscriber Division
Motorola Land Mobile Products Sector
Plantation, FL 33322

Ahmad Hoorfar
Dept. of Elec. & Comp. Eng.
Villanova University
Villanova, PA 19085

In recent years there has been a considerable amount of interest in the future mobile-telephone satellite systems. These systems require very small, light weight and low cost antenna elements. While these requirements can easily be achieved at high frequency bands by using microstrip patch antennas, due to the smaller resonant length of the patch, they could become a problem at frequencies in L-band or lower. The most direct way of reducing the dimensions of a microstrip patch radiator is the use of a high dielectric constant, $\epsilon_r > 10$, material together with a small ground plane. The antenna bandwidth and efficiency, however, reduce as ϵ_r is increased. There are certain receive-only mobile applications such as in satellite pagers where a bandwidth of a few tenth of a percent can be tolerated. To achieve a good design in these applications, however, such issues as the combined effects of very high ϵ_r and a very small ground plane on the radiation characteristics of the antenna, as well as possible methods of improving the bandwidth should be addressed.

In this work we have used a combination of CAD simulations and experiments to investigate the design feasibility and performance of a rectangular microstrip antenna, at 1.6 GHz, on substrates with dielectric constants as high as 37, and with ground planes as small as 1" x 1". An accurate cavity model is used to optimize the coaxial feed point on the patch assuming an infinite ground plane. Uniform theory of diffraction (UTD) is then applied to include the edge diffraction and determine the theoretical far fields. Several patch elements on various substrate materials are fabricated and in each case the effect of reducing the ground plane size on VSWR, input impedance, resonant frequency, bandwidth and radiation pattern are measured. In particular, it is observed that as the dimensions of the ground plane reduce, the input reactance varies significantly resulting in a small shift in the resonant frequency, f_r . Since the impedance bandwidth is very small, any shift in f_r should be considered in the design process. For the case of a ceramic Barium-Titanate (BaTi) substrate with $\epsilon_r \approx 37$ and a 2" x 2" ground plane, we found the measured pattern to be acceptable with a smooth small back-lobe. As the ground plane size is reduced further to 1" x 1", however, the back-lobe radiation increases significantly indicating a large edge-diffracted field. The pattern in this case resembles the one due to a horizontal dipole in free-space with two nearly identical lobes in the forward and backward directions. We note that the UTD results are not valid for such electrically small ground-planes. Finally, for a patch on a 50 mil BaTi substrate, the impedance bandwidth is measured to be about 2.4 MHz. To enhance the bandwidth, different techniques have been numerically studied using a moment-method based simulation code. In particular, we have found that the bandwidth can be improved to 4.2 MHz by cutting two parallel slots in the rectangular patch and optimizing their locations. Detailed results on this improved geometry as well as extensive experimental results on the effects of reducing the ground-plane size on various radiation parameters of a patch antenna will be presented.

Analysis of Cylindrical Patch Microstrip Antenna with Circular Polarization by FD-TD method

Yasuhiro Kazama* and Tamotu Suda

Laboratory, Japan Radio Co., Ltd.
Shimorenjaku, Mitaka, Tokyo 181, JAPAN

Nagayoshi Morita

Chiba Institute of Technology
Tsudanuma, Narashino, Chiba 275, JAPAN

Abstract

The finite-difference time-domain (FD-TD) method formulated for solving electromagnetic problems by Yee has been applied to a variety of antenna problems. Examples include linearly polarized microstrip patch antenna, radiating waveguide and horn antennas, and two-dimensional monopole and conical antennas. Impedance, radiation patterns, antenna gain and efficiency calculated by this method have been reported to agree very well with the experimental results.

Recently circularly polarized microstrip patch antennas with high dielectric constant have been widely used for GPS use, because of their pertinent properties of having a very broad beamwidth. Actually, the high dielectric constant microstrip antennas produce a very broad beamwidth with relatively good axial ratio characteristics over a wide angular range.

In this paper, a circularly polarized cylindrical patch microstrip antenna with high dielectric constant substrate is analyzed by using the FD-TD method. The antenna is made of a notched circular disk, cylindrical ceramic substrate with a dielectric constant of 8.84, and circular ground conductor. The notches in the disk are formed to produce right-handed circularly polarized wave. This type of antennas is expected to become widespread for mobile communication antennas.

A sinusoidal wave modulated by a Gaussian shape is supplied at a feed point, and Fast Fourier Transform is used to obtain the input impedance of the antenna. Radiation patterns and circular polarization properties are also investigated. Experimental results are presented for the purpose of comparison.

A RADIATION MODE EXPANSION FORMULATION OF RADIATED FIELDS FROM MICROSTRIP LINE DISCONTINUITIES

Nagayoshi Morita, Chiba Institute of Technology
Narashino, Chiba, 275 Japan

Abstract

In microwave and millimeter wave integrated circuits, and monolithic integrated circuits, various circuit elements are often closely placed each other, interconnected by microstrip-type lines. Therefore, in those circuits, careful attention should be paid to the problem of interelement coupling. Radiation from discontinuities in interconnecting waveguide lines also causes similar problems. Thus, it is very important to estimate the amount of fields radiated from each circuit element and discontinuity existing in the designed circuits. To the author's knowledge, however, almost no methods have been developed until now for dealing with this sort of problems.

This paper presents a method for calculating fields radiated from discontinuities in microstrip lines; circuit elements connected to microstrip lines can be included in the same category as discontinuities. As an example, consider Fig.1, which shows a typical discontinuity of a microstrip line. In the present method, the fields in the inside region surrounded by a closed surface S_c are calculated first by invoking the FD-TD technique, with one-way-travelling sinusoidal wave excitation given at a transverse plane of the microstrip line. Next, the fields on another closed surface S_0 taken inside S_c are expanded in terms of the radiation modes that are defined for the half-space region partitioned by a dielectric substrate backed with ground conductor (N. Morita, IEICE Trans. Electron., E77-C, 11, pp.1795-1801, 1994).

Radiation modes defined here consist of substrate modes and space modes. The former represent the fields propagated along dielectric layer and the latter the fields radiated into the air region. Both radiation modes satisfy boundary conditions at the interface between the dielectric substrate and the air region as well as the conductor surface, and also satisfy the orthogonality properties. The fields coming out from the closed surface S_0 are expressed in the form of spectral integral of radiation modes. However, practically important information on the radiated fields can be obtained from the relative magnitude distribution in the direction of radiation, i.e., radiation patterns. If so, spectral integrals can be performed analytically by means of the usual saddle point technique, and then it follows that far field patterns are calculated from only the surface integration of fields on surface S_0 . In this calculation, the fields accompanying the waveguide line mode propagated along the microstrip line should be eliminated from the fields on S_0 . This microstrip line mode field is obtained in the course of the FD-TD calculation process.

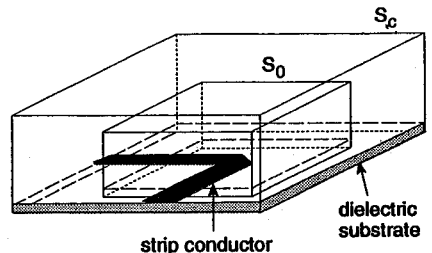


Fig.1 A typical discontinuity of microstrip lines

Propagation Phenomenology

F. T. Djuth

Page

- 1:20 The Polar Cap Ionosphere Above 80 Degrees Invariant Latitude288
L. E. Montbriand, Communications Research Centre

- 1:40 An Investigation of Lightning-Induced Ionospheric Effect289
Using RF Diagnostics
K. M. Groves, J. V. Rodriguez, PL/GPIA, J. C. Foster, MIT Haystack
Observatory, J. M. Quinn, PL/GPIA*

- 2:00 Measurements of Sprites and Blue Jets with High-Frequency290
Diagnostics
Frank T. Djuth, Geospace Research, Inc.

- 2:20 Formation and Relaxation of a Stratified Structure in the291
Ionospheric Plasma During its Heating (Theoretical and
Experimental Investigations)
*N. Blaunstein, Ben Gurion University of the Negev, G. S. Bochkarev,
IZMIRAN*

- 2:40 Spatial and Dynamical Properties of the Ionospheric Plasma292
Response to Processes Arising Due to the Nonlinear
Interaction of Two UHF Waves
V. V. Yevstafiev, Institute of Solar-Terrestrial Physics

The Polar Cap Ionosphere Above 80 Degrees Invariant Latitude

L.E. Montbriand
Communications Research Centre
P.O. Box 11490, Station "H",
Ottawa, Ontario, Canada,
K2H 8S2.

Abstract

Radio signals received by an HF receiving array were used to investigate ionospheric structures over the polar cap. Based on data recorded at a time when the F2 MUF was below the frequency of the intended transmissions, it was found that the "noise and interference" received was a valuable source of other signals. It was established that at least 15 useful signals-of-opportunity (SOPs) could be identified. These SOPs were blocked into time-bearing-elevation windows, and their mean bearings and elevations converted to the geographical location of their ionospheric reflection points. It was found that the time histories of the reflection points yielded a continuous monitor at enough points in the polar ionosphere to provide a time history of the polar ionosphere above 80 deg Invariant latitude. For the 8 hour interval studied in detail, most of the identified reflection points lay within localized 'patches' which appeared to be narrow parallel bands, somewhat sun directed and exhibiting a slow sideways drift. A technique was developed for determining the orientation, velocity and time of overhead passage of the front and then the back edge of these patches. The role of these patches in magneto-ionospheric theory is discussed.

An Investigation of Lightning-Induced Ionospheric Effects Using RF Diagnostics

K. M. Groves^{1*}, J. V. Rodriguez¹, J. C. Foster², and J. M. Quinn¹

¹PL/GPIA, 29 Randolph Road, Hanscom AFB, MA 01731

²MIT Haystack Observatory, Route 40, Westford, MA 01886

It has been known for decades that lightning causes significant local effects in the earth's lower atmosphere and generates intense very low frequency (VLF) radiation which can penetrate the ionosphere as whistler waves and subsequently induce energetic electron precipitation through wave-particle interactions in the magnetosphere. Recently, however, investigators have noted evidence for more direct interactions between phenomena associated with thunderstorms (e.g., lightning and sprites) and the earth's upper atmosphere. This evidence includes perturbations of electron density and temperature [Inan *et al.*, *GRL*, 20, 2355, 1993], excitation of electrostatic wave turbulence [Kelley *et al.*, *GRL*, 17, 2221, 1990] and the sprites themselves [Sentman and Wescott, *GRL*, 20, 2857, 1993]. Numerous theoretical efforts have attempted to explain these effects, but the virtual absence of quantitative observations makes it difficult to assess the merits of the various theories. Thus, we plan to conduct an extensive multi-diagnostic experimental campaign in mid-summer 1995 designed to provide quantitative data on ionospheric heating, ionization, and plasma wave turbulence induced by lightning and upward discharges. The primary diagnostic for the investigation is the MIT Millstone Hill incoherent scatter radar located in Westford, Massachusetts. The radar provides quantitative observations of stimulated ionization, enhanced wave turbulence and electron gas temperatures, particularly in the ionospheric E and F regions; instrument configuration and operation to permit detection of both transient and persistent perturbations are planned. A sensitive diagnostic of the impact of individual discharges on the D-region will be obtained from a narrow-band VLF receiver sited nearby. The system utilizes available VLF transmitters to detect conductivity changes in the earth-ionosphere waveguide along the propagation path. Potential electric field-driven F region structuring above thunderstorms will also be monitored by observations of amplitude scintillations of transionospheric UHF radio signals received from satellite beacons. While the effort emphasizes RF diagnostics for quantitative data, low-light B&W video cameras will be employed to determine the presence of sprites and other optical phenomena. The combined data set can be compared with lightning activity recorded by the National Lightning Detection Network to identify correlations of observed effects with individual lightning strikes. Anticipated signatures of specific lightning-induced effects, appropriate diagnostic measurement techniques and scientific issues related to the campaign will be discussed.

Measurements of Sprites and Blue Jets with High-Frequency Diagnostics

Frank T. Djuth, Geospace Research, Inc., 550 N. Continental Blvd., Suite 110,
El Segundo, CA 90245

Recently, a multi-disciplinary field has emerged with the quantitative detection of spectacular "lightning" flashes above thunderstorms in the Midwest [e.g., Sentman and Wescott, *GRL*, 20, 2857, 1993; Lyons, *GRL*, 21, 875, 1994.] The flashes extend from the tops of anvil clouds into the stratosphere and mesosphere. Because the physical processes involved are totally unknown, non-judgmental terms such as "sprites" and "blue jets" have been adopted to describe the phenomena. Sprites are blood red flashes that appear with bluish tendrils dangling from the bottom. These flashes last a few milliseconds and extend into the mesosphere (as high as 100 km altitude). The blue jets are flashes that appear in narrow beams, sprays, fans, or cones of light which give off a blue or purple hue. They appear to originate at the top of the storm clouds and travel to altitudes of about 35 km; their speeds range from 30 - 100 km/s.

To date, the principal diagnostics have been optical imagers, although similar events may also have been detected with VLF links. In this presentation, we describe experiments aimed at determining the effectiveness of HF radio diagnostics in measuring ionization created by flashes in the upper atmosphere. Two bi-static links having frequencies near 2.66 MHz and 27.80 MHz are used to detect ionization from flashes. The bi-static links are simultaneously operated in a continuous wave mode along a path ~ 800 km in length. The transmitter site is located in northeast Colorado, and the receiver site is near Kansas City, Missouri. Results from the Midwest campaign of Spring 1995 will be included in this presentation. In future experiments, radio interferometers will be used to establish the exact location of echoes and reference them to optical events above storm clouds.

In general, the sprites and blue jets may allow the upper troposphere (~10-15 km altitude) to directly couple to the stratosphere and mesosphere. This, in turn, may alter the chemistry and dynamics of both regions. Obviously, it is premature to judge the magnitude, extent, and nature of the coupling. However, this phenomenon could, in principle, have an impact on O₃ chemistry, which involves temperature-dependent interactions among trace species (e.g., Cl_x, NO_x, and HO_x). Moreover, the direct coupling between the troposphere and the mesosphere could alter global temperatures in the upper mesosphere. If this were the case, the interpretation of variations in mesospheric temperature/neutral density in terms of global change could become more difficult.

**FORMATION AND RELAXATION OF A STRATIFIED STRUCTURE IN
THE IONOSPHERIC PLASMA DURING ITS HEATING
(THEORETICAL AND EXPERIMENTAL INVESTIGATIONS)**

N. Blaunstein
Ben Gurion University of the Negev, P.O. Box 653
Beer Sheva 84105, Israel
G.S. Bochkarev
IZMIRAN, Troitsk, Moscow region, Russia

Abstract

A non-stationary problem of plasma concentration redistribution during a thermal heating of the F-layer of the ionosphere by powerful radiation from the ground-based facilities is investigated theoretically, taking account of quasi-regular gradients of the concentration of background plasma, ambient geophysical factors (electric and magnetic fields, neutral wind, gravity etc.) as well as altitudinal dependence of transport coefficients of plasma charged particles. The results of calculations are compared with experimental data obtained from measurements of the reflection of pulsed radio waves scattered from artificially induced plasma irregularities in the ionosphere for vertical incidence of HF-waves. The possibility of formation of a quasi-periodical structure in the disturbed plasma region during local heating of the ionosphere is shown both theoretically and experimentally.

The formation and further spatial and temporal evolution of striated plasma density structure obtained from numerical simulations [1] can be understood from experimentally found distance-frequency characteristics of backscattered signals from the disturbed ionospheric F-region [2].

The time of relaxation of such a plasma structure in the region of local heating and its dependence upon the initial transverse scales of artificially induced irregularities estimated from the theoretical model are in good agreement with experimentally found values as is the non-linear dependence of the life-time of a quasi-periodical plasma structure created in the field of powerful radio beam.

References

1. Blaunstein, N. Sh. and G.S. Bochkarev, *Geomagn. and Aeronom.*, 1993, vol. 33, No. 2, pp. 84-91.
2. Bochkarev, G.S., V.A. Erëmenko, and Yu. N. Cherkashin, *Adv. Space Res.*, vol. 8, No. 1, pp. (1)255-(1)260.

Spatial and Dynamical Properties of the Ionospheric
Plasma Response to Processes Arising Due to the Nonlinear
Interaction of Two UHF Waves

V. V. Yevstafiev

Institute of Solar-Terrestrial Physics (ISTP), P. O. Box 4026, Irkutsk 664033, Russia

Presented are the research results on widening the diagnostic scope of the ISTP-operated incoherent scatter radiowave (ISR) station, with the purpose of using it under conditions of a strongly disturbed ionosphere. The disturbance source is provided by the process of nonlinear interaction of two parallel beams of pulsed UHF radio waves, whose frequencies (f_1, f_2) are chosen such that the value of their difference (Δf) coincides with the plasma oscillation frequency. A choice of the source is dictated both by the importance of the problem of studying nonlinear effects and by technical capabilities of the ISR station, $f_1, f_2 > 150$ MHz, $\Delta f = 2-4$ MHz, and $\tau < 1$ msec, which make it possible to realize an experimental verification of results obtained. Here, τ is the length of emitted pulses.

The theoretical model for the process of nonlinear interaction of radio waves under development is based on a system of kinetic equations for a three-component collisional plasma residing within a constant gravity field and a constant magnetic field. By analyzing the expression for current of frequency Δf , obtained using an asymptotic method of multitime approximations, it is shown that with sufficient intensities of the incoming radiation a parametric decay-type instability develops, which ensures an effective (resonance) energy transfer from radio waves to Langmuir waves being produced. In the early stage of instability development, a growth of the Langmuir wave amplitude is ahead of the process of its decrease due to ordinary dissipative processes. At reasonably large values of the amplitude, a nonlinear absorption mechanism comes into play. The instability reaches a saturation stage, and the energy transferred to the Langmuir waves is now expended for an intense heating of the ambient medium. It should be noted that these processes are all evolving throughout the length of one pulse. Since electrons travel largely along external magnetic field lines, the resulting thermal irregularities of plasma density will also be aligned along this direction. In this paper it is shown that the typical size and dynamical properties of these irregularities depend primarily on the intensity and duration of the emitted pulses, next on the number of pulses emitted per unit time and, finally, on a total duration of the process of modifications.

For diagnostic purposes, of importance is the fact that among these irregularities are also such whose transverse size is comparable with the wavelength of the emitted pulses which are also used as sounding pulses simultaneously. This must lead to the appearance (in the ion spectrum of the incoherently scattered wave) of a coherent component, thereby causing the total power of the received signal to increase abruptly. Furthermore, the motion of charged particles under the action of a thermal pressure gradient implies the presence of an electric current in the scattered region and hence the asymmetry of the ion spectrum of the IS-signal. Indeed, the preliminary experiments conducted at the ISR station have confirmed the presence of these two effects in measured power spectra.

Special Session

In Honor of Victor Galindo-Israel

Yahya Rahmat-Samii and Raj Mittra

Page

- 1:20 Opening Remarks
Yahya Rahmat-Samii, UCLA, Raj Mittra, University of Illinois
- 1:40 Many-Faceted Contributions of Victor Galindo to the Analysis and ...294
Synthesis Problems Related to Reflector Antennas
Raj Mittra, University of Illinois*
- 2:00 High Performance, Low Cost Reflector Antennas
Warren L. Stutzman, Marco A.B. Terada, Virginia Polytechnic
Institute and State University*
- 2:20 Examples of Shaped Reflectors from a New Shaping Method
Lynn Baker, Cornell University
- 2:40 Compensation of Gravity-Induced Structural Deformations
on a Beam-Waveguide Antenna Using a Deformable Mirror
W. A. Imbriale, M. Moore, D. J. Rochblatt, W. Veruttipong,
Jet Propulsion Laboratory*
- 3:00 BREAK
- 3:20 MBA versus Phased Array for Electronic Beamsteering
William C. Wong, TRW Electronics Systems & Technology Division
- 3:40 A Comparison of Two Spherical Wave Expansion Techniques
Using the Circular Aperture as an Illustrative Example
R.G. Yaccarino, Hughes Aircraft, Sembiam R. Rengarajan, CSUN*
- 4:00 Modified Jacobi Polynomials in Analysis, Synthesis and295
Measurements of Antennas
Y. Rahmat-Samii, UCLA
- 4:20 Closing Remarks

Many-Faceted Contributions of Victor Galindo to the Analysis and Synthesis Problems Related to Reflector Antennas

Raj Mittra*

*Electromagnetic Communication Laboratory
Department of Electrical and Computer Engineering
University of Illinois, Urbana, IL 61801*

Victor Galindo is well recognized by his peer group as a giant in his field, who has made many fundamental and significant contributions in the areas of analysis and synthesis of reflector antennas. His paper on the synthesis of circularly-symmetric dual reflector antennas, published in the mid-sixties and now a recognized classic, laid the foundation of a series of other publications to follow on the subject of shaped dual-reflector antenna synthesis.

It is obvious that to analyze the synthesized reflectors, one needs a sophisticated software package that is accurate, and yet general enough to be capable of handling dual-shaped, Cassegrainian or Gregorian surfaces, illuminated by an arbitrary feed system. Here, too, Galindo has made many significant contributions in the field, by developing a number of techniques for reflector analysis that are highly numerically efficient, and are suitable for pattern computation of not only dual but multiple and shaped reflector antennas as well.

A brief survey of many-faceted contributions of Victor Galindo to the areas of analysis and synthesis of reflector antennas will be presented in the paper. Some of the selected references to Galindo's contributions, which he has authored or co-authored are:

- (i) V. Galindo-Israel and R. Mittra, "A new series representation for the radiation integral with application to reflector antennas," *IEEE Trans. on Antennas and Propagation*, pp. 631-641, September 1977;
- (ii) R. Mittra, Y. Rahmat-Samii, V. Galindo-Israel, and R. Norman, "An efficient technique for the computation of vector secondary patterns of offset paraboloid reflectors," *IEEE Trans. on Antennas & Propagation*, May 1979;
- (iii) V. Galindo-Israel, W. A. Imbriale, and R. Mittra, "On the theory of the synthesis of single and dual offset shaped reflector antennas," *IEEE Trans. on Antennas & Propagation*, pp. 887-96, August 1987;
- (iv) V. Galindo-Israel, W. A. Imbriale, R. Mittra, and K. Shogen, "On the theory of the synthesis of offset dual-shaped reflectors - Case examples," *IEEE Trans. on Antennas and Propagation*, pp. 620-626, May 1991;
- (v) V. Galindo-Israel, S. R. Rengarajan, W. A. Imbriale, and R. Mittra, "Offset dual-shaped reflectors for dual chamber compact ranges," *IEEE Trans. Antennas & Propagation*, pp. 1007-1013, July 1991; and,
- (vi) W. Imbriale, V. Galindo-Israel and R. Mittra, "Subreflector and feed scattering effects in dual-shaped reflector compact ranges," *Proceedings of ISAP '92*, pp. 993-996, held in Sapporo, Japan on September 22-25, 1992.

MODIFIED JACOBI POLYNOMIALS IN ANALYSIS, SYNTHESIS AND MEASUREMENTS OF ANTENNAS

Y. Rahmat-Samii
Electrical Engineering Department
University of California Los Angeles
Los Angeles, CA 90024-1594

This paper focuses on recent applications of the modified Jacobi polynomials as applied to the analysis, synthesis and measurements of antennas. The modified Jacobi polynomials are closely related to the circle polynomials of Zernike which have been used in optics. In antenna applications, the usage of the modified Jacobi polynomials was strengthened in one of Galindo's paper published in 1977. Since that publication, the modified Jacobi polynomials have been extensively used in modern analysis, synthesis and measurements of antennas.

In reflector antenna analysis, the Jacobi-Bessel expansion is used to present the antenna far field in terms of summation of Airy disk functions. This summation converges very rapidly for single or multi-reflector antennas using physical optics integration. The expansion technique has proven to be quite powerful in the analysis of contoured beam antennas utilizing large number of array feeds.

In applying optimization techniques for reflector antenna shaping, one needs to first parameterize the antenna surface before applying optimization technique. In the parameterization, the reflector surface is presented by a global orthogonal Jacobi-Fourier series expansion. The expansion coefficients are the parameters that characterize the reflector shape. Reflector shaping is achieved by adjusting (optimizing) these expansion coefficients. The global representation results in reflector configurations which are characterized by smooth surfaces, well defined circumferences, and continuous surface derivatives. The methodology has been applied to diverse category of applications such as, single-feed contoured-beam satellite antennas, reflector surface distortion compensation, etc.

In antenna near field measurements, the plane-polar and bi-polar techniques have found many applications. In implementing these techniques, one first measures the antenna near field in a planar circularly distributed grid. The objective is then to obtain the far field from these measured near-field data. A standard way to construct the far field is to use interpolation/FFT. The Jacobi-Bessel expansion allows one to directly utilize the circularly distributed measured data and construct the far field without any need for interpolation.

THIS PAGE INTENTIONALLY LEFT BLANK.

Integral Equation Techniques

D. R. Wilton and S. M. Rao

Page

8:20 An Efficient Preconditioner for Iterative Solution of Dense299
 Matrices in Electromagnetics
V. Varadarajan, Raj Mittra, University of Illinois, John Murphy,
 Nick Jennings, British Aerospace Ltd.*

8:40 Extrapolation Technique for Solving Large Body Scattering300
 Problems and Its Application to Bodies of Revolution
Zwi Altman, Raj Mittra, University of Illinois, Daniel Bouche, CEA*

9:00 Fast Integral Equation Solver Using Plane-Wave Basis301
 Representation Along the Steepest Descent Path
E. Michielssen, W. C. Chew, University of Illinois*

9:20 A New Technique to Generate Sparse Matrix Using the Method302
 of Moments - Application to Two-Dimensional Problems
G. K. Gzohard, S. M. Rao, Auburn University*

9:40 A New Technique to Generate Sparse Matrix Using the Method303
 of Moments - Wire Scattering Problems
Sadesiva M Rao, Griffin K. Gothard, Auburn University*

10:00 BREAK

10:20 Surface Integral Formulation for Calculating Conductor and304
 Dielectric Losses of Dielectric Filled Waveguides
Tanmoy Roy, Tapan K. Sarkar, Syracuse University, Madhavan
 Swaminathan, IBM*

10:40 New Uncoupled Integral Equations for the Radially-Graded305
 Dielectric Sphere
M. S. Viola, University of Akron

11:00 Electrostatic Solution for Three-Dimensional Arbitrarily-306
 Shaped Inhomogeneous Bodies in an Impressed Field
 Using FIT/MEI
John H. Henderson, S. M. Rao, Auburn University*

11:20 Effects of Laminated Ground Plane on Resonance307
 Frequencies of Wraparound Patch Resonator
Jean-Fu Kiang, Chung-Yuan Kung, National Chung-Hsing University*

11:40 Implementation of a Parallel Processing Computational308
 Electromagnetic Code Based on a Method of Moments Approach
D. I. Kaklamani, V. Kouloulis, A. Marsh, N. K. Uzunoglu, National Technical
 University of Athens*

12:00	Approximate Method of Solution of the Input Impedance of309
	Wideband Chopped Conical Dipole by Means of Moment Method
	<i>Chinmoy Das Gupta*, P. C. Das, A. C. Trivedi, Indian Institute</i>
	<i>of Technology</i>

An Efficient Preconditioner for Iterative Solution of Dense Matrices in Electromagnetics

*V. Varadarajan and Raj Mittra**
Electromagnetic Communication Laboratory
University of Illinois, Urbana, IL 61801

John Murphy and Nick Jennings
British Aerospace Ltd.
Sowerby Research Center, UK

It is shown in this paper that an efficient solution of the dense complex-symmetric linear system of equations, arising in the Method of Moments (MoM) formulation of electromagnetic problems, can be obtained by employing a combination of preconditioned QMR algorithm and matrix compression. The method presented herein can be used to solve large MoM problems generated by many 'legacy' codes, and can also be implemented efficiently on massively parallel computers. The preconditioner employed to speed up the iteration process is the L factor in the LL^T factorization of a banded diagonal part of the complex-symmetric MoM impedance matrix. The matrix-vector multiplications in the QMR iterations are speeded up by employing a compression procedure on the matrix sub-blocks via a rank-reducing, partial-QR decomposition.

The problem of scattering by a square plate was chosen as the test case, and the discretization of the E-field integral equation formulation of this problem was achieved by using triangular patches. Matrices with various sizes were generated by increasing the plate size in terms of the wavelength in a progressive manner. In general, the codes were written in FORTRAN 77 and C, and the standard BLAS and LINPACK/LAPACK subroutine calls were used to obtain optimum run times. The vectorization and parallelization were obtained automatically by using well-structured codes and by exercising compiler options. The parallelization and message passing in a distributed memory computer was achieved by writing the codes in PVM 3.2.

It was found that the preconditioned-QMR method, without matrix compression, was 2 to 10 times faster than the direct approach based on the LU decomposition. For very large problem sizes (rank > 20000), it is estimated that the preconditioned-QMR method alone would result in run-time reduction by a factor of 10 or more. In addition, the matrix compression could further reduce the time required for the matrix-vector multiplications by a factor of 3 or more for very large problems, and the resulting run time reduction factors with the new serial solution procedure could be substantial, possibly on the order of 20-40, over a solution method based on a direct LU decomposition. It is also useful to note that the preconditioner density has been found to be much less than 10% for very large problem sizes, and this is attributable to the fact that the MoM matrix has a tendency to be localized near the diagonal. Several numerical results on serial and parallel platforms (such as the Convex, SGI Power Challenge and IBM-SP1) will be provided to illustrate the potential of the new solution procedure for efficient solution of dense, complex-symmetric, linear systems.

Extrapolation Technique for Solving Large Body Scattering Problems and its Application to Bodies of Revolution

Zwi Altman and Raj Mittra*
Electromagnetic Communication Laboratory
Department of Electrical and Computer Engineering
University of Illinois, Urbana, IL 61801

Daniel Bouche
CEA
Limeil-Valenton
France

The objective of this work is to combine an extrapolation technique with the Method of Moments (MoM) to solve scattering problems involving large bodies. The proposed technique attempts to increase the capacity of the MoM to handle large scatterers by alleviating the memory and CPU time limitations imposed by present computers. The reduction in the burden on the CPU is achieved by reducing the number of unknowns in the MoM solution in a manner explained below.

We begin by using the MoM with subdomain basis functions to solve the scattering problem for only a part of the scatterer so that the number of unknowns is still manageable. We then use the Generalized Pencil of Function (GPOF) method to represent the current distribution on the smooth portion of the scatterer, away from the tips and edges, in terms of a summation of a small number of complex exponential functions. These complex exponents are then employed as entire domain basis functions on the smooth portion of the body, and they are complemented by subdomain basis functions near the edges and discontinuities. Next, the size of the scatterer is progressively increased in a series of steps, and the complex exponents are extrapolated and modified at each step to span a larger portion of the smooth part of the scatterer while leaving the subdomain basis function region unchanged. A key feature of the solution procedure is that the total number of basis functions is held constant, and this enables us to handle large scatterers with a relatively small number of unknowns.

To illustrate the application of the method we consider the problem of scattering from bodies of revolution (BORs), because the azimuthal symmetry of these geometries makes it possible for us to generate numerically rigorous MoM solutions for large scatterers with relative ease. First, we solve for the current distribution in the Fourier domain along the azimuthal direction, and in the spatial domain along the generating arc. Next, we apply the proposed extrapolation technique separately for each of the azimuthal harmonics to solve for the current distribution on the scatterer, and to calculate the RCS from this distribution.

Extensive numerical studies have been carried out with several different BOR geometries, e.g. cylinders, cones and barrel-shapes scatterers, and the results will be included in the presentation.

Fast Integral Equation Solver Using Plane-Wave Basis Representation Along the Steepest Descent Path

E. MICHELSEN* AND W. C. CHEW

DEPARTMENT OF ELECTRICAL AND COMPUTER ENGINEERING

UNIVERSITY OF ILLINOIS

URBANA, IL 61801

Abstract

The solution of integral equations for surface scatterers has been accelerated in the past by using iterative methods and ways to expedite the matrix-vector multiply. The matrix-vector multiply has been accelerated by diagonalizing the Green's operator, and using it in a two-level or multilevel algorithm. Two methods of diagonalizing the Green's operator have emerged in the past, notably, the fast multipole method (FMM) [Rokhlin, *J. Comp. Phys.*, 86:414-439, 1990] and the matrix-decomposition approach (MDA) [Michielssen and Boag, *Micro. Opt. Tech. Lett.*, in press]. In this paper, we will present a third way of diagonalizing the Green's operator using an inhomogeneous plane-wave basis along the steepest-descent path. Such a method for diagonalizing the Green's operator has been used in the context of a direct solver [Chew and Lu, *J. Comp. Phys.*, 107: 378-387, 1993], but not yet in an iterative solver.

This diagonalization allows interactions between far-groups to be calculated efficiently using a reduced set of inhomogeneous plane-waves along the steepest descent path. By using a two-level algorithm, the matrix-vector multiply can be effected in $O(N^{1.5})$ operations.

However, the construction of an interpolator that extrapolate the inhomogeneous plane wave basis along the steepest-descent path from the plane-wave basis on the real axis, allows for the recycling of the calculated aggregated field, and the computational complexity can be reduced to $O(N^{4/3})$. Moreover, since the inhomogeneous plane waves can be easily calculated, they could be calculated as needed, and the memory requirement of the method can be reduced to $O(N)$. This method will hold promise in solving scattering problems of dimensions that are large compared to wavelength.

A New Technique to Generate Sparse Matrix Using the Method of Moments - Application to Two-Dimensional Problems

G. K. Gothard * and S. M. Rao
Department of Electrical Engineering
Auburn University, Auburn, AL 36849

In this work, we present a new numerical method to solve the electromagnetic scattering problems for electrically large two-dimensional cylinders, while applying the well-known method of moments (MoM). The novelty of the present approach is the generation of a sparse moment matrix as compared to a full matrix usually obtained by the MoM method.

The basic concept utilized in the new approach, known as generalized sparse matrix reduction (GSMR) technique, may be qualitatively illustrated as follows. Following similar procedures of the MoM, a moment matrix is also generated in the GSMR method. However, in contrast to the conventional moment method where interaction is computed from each and every cell on other cells, only the interaction from the self-cell is computed in the GSMR technique. This implies that the moment matrix for the GSMR technique is essentially diagonal. Further, the effect of non-self terms is taken into account by defining a set of linearly independent functions over the entire contour of the cylinder. These entire functions are appropriately utilized to obtain a sparse matrix which accounts for all the interaction.

In this work, we present the scattering problem in terms of the electric field integral equation (EFIE) which is applicable to open/closed cylinders. Further, we consider both the transverse magnetic (TM) and transverse electric (TE) cases. For both cases, we utilize the two-dimensional Green's function which has the advantage of the built-in radiation condition. The contour of the cylinder is approximated by linear segments. Further, the usual pulse expansion and finite difference testing scheme is employed to obtain the moment matrix in the GSMR solution.

Finally, we present several numerical examples involving two-dimensional cylinders to demonstrate the validity of this new method.

A New Technique to Generate Sparse Matrix Using the Method of Moments - Wire Scattering Problems

*
Sadasiva M. Rao and Griffin K. Gothard, Department of Electrical
Engineering, Auburn University, Auburn, Alabama 36849-5201

In this work, we present a novel numerical method to solve the electromagnetic scattering/radiation problems, in particular for electrically large wire-structures, while applying the well-known method of moments (MoM). Although there exist several techniques to deal with the electromagnetic scattering problem involving large structures, all of them require substantial computer resources thereby limiting the applicability of these methods to structures of only a few wavelengths.

In this work, we present the scattering problem in terms of the electric field integral equation (EFIE) which has the advantage of the built-in radiation condition. The most popular technique to solve the EFIE equation is the MoM. However, the disadvantage of the MoM is that it generates a dense matrix and as the size of the structure increases, the method demands excessive computer resources. However, in the present work, we propose an alternate scheme known as the generalized sparse matrix reduction (GSMR) technique which effectively overcomes this disadvantage.

The basic concept utilized in the GSMR technique may be qualitatively illustrated as follows. Following similar procedures of the MoM, a moment matrix is also generated in the GSMR method. However, in contrast to the conventional moment method where interaction is computed from each and every cell on other cells, only the interaction from the self-cell is computed in the GSMR technique. This implies that the moment matrix for the GSMR technique is essentially diagonal. Further, the effect of non-self terms is taken into account by defining a set of linearly independent functions over the entire structure. These entire functions are appropriately utilized to generate a sparse matrix which accounts for all the interaction.

Finally, we present several numerical examples involving wire geometries to demonstrate the validity of this new method.

SURFACE INTEGRAL FORMULATION FOR CALCULATING CONDUCTOR AND DIELECTRIC LOSSES OF DIELECTRIC FILLED WAVEGUIDES

**Tanmoy Roy
Tapan K. Sarkar***

Department of Electrical Engineering
Syracuse University
Syracuse, NY 13244-1240, USA

Madhavan Swaminathan
IBM, E. Fishkill
Hopewell Junction, NY 12533-0999, USA

Abstract

The power-loss method along with a surface integral formulation has been used to compute the attenuation constant in dielectric filled waveguides of arbitrary cross-section. This method can be used for the analysis of both open and closed structures. Using the surface equivalence principle the waveguide walls are replaced by equivalent electric surface currents and dielectric surfaces are replaced by equivalent electric and magnetic surface currents. Enforcing the appropriate boundary condition an E-field integral equation (EFIE) is developed for these currents. Method of moments with pulse expansion and point matching testing procedure is used to transform the integral equation into a matrix one. The next step in the calculation of the attenuation constant is to obtain a relationship between the propagation constant and frequency. The relationship between the propagation constant and frequency is found from the minimum eigenvalue of the moment matrix. The eigenvector pertaining to the minimum eigenvalue gives the unknown electric and magnetic surface currents. Using these unknown electric and magnetic surface currents the fields inside and on the surface of the waveguide are calculated, which are used subsequently to compute the attenuation constant.

New Uncoupled Integral Equations for the Radially-Graded Dielectric Sphere

M.S. Viola
Department of Electrical Engineering
University of Akron
Akron, Ohio 44325-3904

Solution to the problem of the scattering of a plane wave by a homogeneous dielectric sphere was reported as early as 1890 by Lorenz. Since that time, numerous investigations have been conducted on scattering by dielectric spheres of both homogeneous and layered, piecewise-homogeneous composition. However, it appears that studies of electromagnetic interactions with spheres having general radial permittivity grading have been far less prevalent, despite such potential applications as the Luneburg lens and the spherical resonant antenna.

It is well known that for problems involving spherical symmetry, the electromagnetic fields can be decomposed into TE and TM modes. Furthermore, each mode is completely characterized by a single scalar potential from which the five non-zero field components may be generated. For example, either Debye potentials or radial electric and magnetic field components may serve as generating functions for these modal types. These generating functions are solutions to the governing partial differential equations and satisfy appropriate boundary conditions. Spherical harmonic expansions of the generating functions reduce that formulation to a set of uncoupled ordinary differential equations, the solutions of which are radially-dependent coefficients in spherical harmonic expansions.

In this paper, an integral equation description is adopted as an alternative to the differential approach discussed above. This description is valid for general bodies of revolution, and in it the azimuthal field component has been eliminated in favor of the transverse components. First, this integral equation is specialized to the case of a structure having purely radial grading. By decomposing the fields into TE and TM modes, an uncoupled pair of integral equations is obtained, the solutions of which serve as generating functions for the two modal types. Then, using spherical harmonic expansions for both the field components and the kernels appearing in the integral equations, it is found that these integral equations reduce to uncoupled, one-dimensional, domain-boundary type integral equations. The solutions of these integral equations are radially-dependent coefficients in spherical harmonic expansions of the TE and TM mode generating functions.

An attractive feature of this development is that it provides a pure integral equation description in which no term involving a derivative on an unknown appears. Additionally, all of the kernels within these integral equations are non-singular. Application of this model to the case of the homogeneous sphere yields both the expected characteristic equations for the resonant frequencies of the sphere, and the expected Mie series. Applications to more general problems are also presented.

Electrostatic Solution for Three-Dimensional, Arbitrarily-Shaped Inhomogeneous Bodies in an Impressed Field Using FIT/MEI

John H. Henderson* and S. M. Rao
Department of Electrical Engineering
200 Broun Hall
Auburn University, AL 36849-5201

The Finite Integral Technique (FIT), when used for modelling three-dimensional, arbitrarily-shaped inhomogeneous bodies, uses tetrahedral discretization of the object and explicit basis functions for the electric field and magnetic flux density. Edge-based basis functions are used for the electric field, and face-based functions are used for the magnetic flux density. The integral form of Maxwell's equations are applied to paths surrounding faces and edges, resulting in a sparse system matrix relating the electric field at each edge to the edges forming the tetrahedrons that share that edge. The constitutive parameters are considered constant throughout each tetrahedron, but may be different for each individual tetrahedron, allowing the modelling of inhomogeneous objects. The advantages of this method are that the tetrahedral modelling easily conforms to the shape of arbitrarily-shaped objects, and the resulting sparse system matrix requires less space for storage and shorter CPU time for inversion than full-matrix methods such as Method of Moments.

The disadvantage of FIT, as in Finite Element (FE) or Finite Difference (FD), is that for open-region problems, the space surrounding the object must be divided into a tetrahedral mesh, and realistically, this mesh must be truncated. Previous mesh-truncation techniques and absorbing boundary conditions either applied integral equations to the boundary, or assumed the form of the field at a distance away from the object. The disadvantage of the first technique is that it eliminates the sparsity of the matrix. The second technique typically must be applied at a large distance from the object for good results, requiring a large mesh. The Measured Equation of Invariance (MEI) is a mesh-truncation technique that is not hindered by either of these disadvantages.

In this work, FIT is augmented with MEI resulting in a technique to solve the electrostatic problem involving a three-dimensional, arbitrarily-shaped inhomogeneous body in an impressed field that maintains matrix sparsity, thus maintaining low storage and execution time requirements. Numerical results are presented that demonstrate the effectiveness of this technique.

Effects of Laminated Ground Plane on Resonance Frequencies of Wraparound Patch Resonator

Jean-Fu Kiang* and Chung-Yuan Kung
Department of Electrical Engineering
National Chung-Hsing University
Taichung, Taiwan, ROC

Due to the wide application of composite materials in modern aircraft and vehicle surface designs, the resonance characteristics of patch resonators flush-mounted on cylindrical composite structures such as space vehicles, missiles, or airplanes need to be studied. A patch resonator built on such surfaces will perform differently from those built on conductive ground plane.

Take for example, a G/E composite is made of several laminae of epoxy resin with conductive graphite fibers embedded in specific directions. The fiber spacing in each lamina is typically much smaller than a wavelength, hence each lamina can be modeled as an anisotropic layer with a conductivity tensor. Layers of different fiber orientations are stacked to form the composite. Planar laminates can be wrapped to form a cylindrical structure. A wraparound resonator is formed by printing a metal strip on the outer surface of the cylindrical structure, and coating a perfect conductor layer on the inner surface.

We first formulate a cascaded transition matrix in the spectral domain to relate tangential field components among different laminae of the composite. An integral equation is derived in terms of the electric surface current on the conducting patch. Then, Galerkin's method is applied to solve the integral equation for the resonance frequencies.

We first study the effect of substrate thickness and substrate dielectric constant on the resonance frequencies of various modes with a composite ground plane. The results with perfect conductor ground plane are also calculated for comparison. Next, we study the effect of changing the conductivity along the fiber orientation, $\sigma'_{\phi\phi}$, of each lamina. We observe that the real part of the resonance frequency increases with $\sigma'_{\phi\phi}$. At low $\sigma'_{\phi\phi}$, fields tend to penetrate into the laminate, and the perfect conductor underneath the laminate works as the ground plane. As $\sigma'_{\phi\phi}$ increases, Ohmic loss incurred in the laminate raises the imaginary part of resonance frequency. As $\sigma'_{\phi\phi}$ is increased further, the laminated ground plane becomes a better conductor for grounding, and the imaginary part decreases.

Implementation of a Parallel Processing Computational Electromagnetic Code Based on a Method of Moments Approach

D.Kaklamani, V.Kouloulis, A. Marsh and N.K. Uzunoglu
Department of Electrical and Computer Engineering
National Technical University of Athens
Athens 10682, Greece

Abstract

Electromagnetic structures consisting of arbitrary shaped perfectly conductive surfaces and dielectric media of arbitrary composition are analysed by using a method of moments technique based on a free space Green's function integral equation. Boundary conditions on the conductor surfaces and inside the dielectric media are employed to derive the corresponding integral equation. The involved unknown functions are the conduction currents on surfaces and polarizations currents within the dielectric media volume. The surface currents are expressed in terms of a superposition of local describing functions of roof top type while the polarization currents are expressed with similar three dimensional functions. Care is taken to insure the validity of boundary conditions between interface of dielectric media and edge conditions on conductor surfaces.

In order to insure numerical stability a Galerkin's approach is implemented deriving a linear system of equation. The system matrix is composed of terms expressing the interaction between the "cells" on the surface of conductors and dielectric media. These terms are calculated accurately by taking into account the behaviour of integrand function. For the closely spaced "cells" semi-numerical techniques are implemented while controlled approximation techniques are used to calculate the matrix elements with large distant. Emphasis is given to "self term" contribution and again semi-numerical techniques one employed.

A conjugate gradient matrix inversion algorithm is used to invert the linear system on a shared memory parallel processing system. In order to develop a user friendly interface both pre-processing and visualization techniques are used. Numerical computations are being carried out for structures has been solved by alternative method of moments technique to verify the accuracy of the method. Open resonators loaded with dielectric media are being analyzed and will be presented.

APPROXIMATE METHOD OF SOLUTION OF THE INPUT IMPEDANCE OF WIDEBAND
CHOPPED CONICAL DIPOLE BY MEANS OF MOMENT METHOD

Chinmoy Das Gupta* Senior Member IEEE, P.C. Das**, A.C. Trivedi†

Abstract

Harrington & Pozar [1,2] have done extensive work for calculating input impedance of dipoles by means of moment method. In Pozar's work problem of 'sensitive' feed point has taken by means of rigorous integral technique. In the present work of the authors calculation of input impedance by means of moment method more intricate 'sensitive' feed point could not be taken care exactly by the method adopted by Pozar.

In the work of Pozar selection of the basis function is somewhat arbitrary. In our work we are adopting more rigorous basis functions with prior experimental results as the safe control points for analytical basis.

Calculations of input impedance of the conical dipoles as per Shelkunoff's equation are giving disagreement with experimental results even upto 25%.

After comparative study of calculations by Shelkunoff's[3] equation and by Moment Method through rigorous control of the results with simultaneous interfacing the experimental results derived from HP Sweep Generator & Network Analyser through A/D card with HP Unix system; and subsequent exploration of the validity desegmentation technique will be a problem of Academic interest.

Optimal calculations of wideband chopped conical dipole will be presented at the time of oral presentation of the paper.

References:

1. R.F. Harrington:Field Computations by Moment Method, Macmillan, 1968.
2. David M.Pozar:Antenna Design Using Personal Computer, Artech house 85.
3. S.A. Schelkunoff, H.T. Friis:Antenna Theory & Practice, Wiley, 1952.

* Professor, Dept of Electrical Engg., Indian Institute of Technology, Kanpur-208016.

** Professor, Dept of Mathematics, IIT Kanpur

† Research Engineer, Computer Maintenance Div, IIT Kanpur.

THIS PAGE INTENTIONALLY LEFT BLANK.

**Propagation Modeling and Measurements for Mobile/
Personal Comm. Services**

J. C. Webster and E. R. Westwater

Page

- 8:20 L-band Propagation Measurement at Very Low Altitude and 312
Comparison to SEKE Propagation Model
Sean W. Gilmore, John C. Eidson, MIT Lincoln Laboratory*
- 8:40 A Comparison of the Longley-Rice and SEKE Propagation Models 313
John C. Eidson, M.I.T. Lincoln Laboratory
- 9:00 Prediction of VHF/L-Band Radio Wave Propagation in Urban and ... 314
Suburban Environment
*N. Blaunstein, Ben Gurion University of the Negev, M. Levin,
Tadiran Ltd.*
- 9:20 Near Range Radio Wave Propagation Prediction in Urban Area 315
Hing-On Ngai, Wong-Hing Lam, The University of Hong Kong*
- 9:40 Harmonic Signal's Level and Phase Cross Correlation Analytical 316
Description by Electromagnetic Ground Wave Propagation
Valery V. Pechenin, Alexey A. Andrejev, Kharkov Aviation Institute*
- 10:00 BREAK
- 10:20 PCS System Design Issues in the Presence of Microwave POFS 317
Solyman Ashrafi, Tom Tran, A. Richard Burke, Moffet,
Larson & Johnson, Inc.*
- 10:40 Field Simulator for Reproduction of Propagation Environment 318
Hiroyuki Arai, Yokohama National University
- 11:00 Dipole Antenna Radiation Patterns in a Concrete Building 319
at 800 to 2900 MHz for Indoor Wireless Communications
Hsing-Yi Chen, Yeou-Jou Hwang, Yuan-Ze Institute of Technology*
- 11:20 Modeling of 3D In-Building Propagation by Ray Tracing 320
Technique
Gong Ke, Xu Rui, Tsinghua University

L-band Propagation Measurement at Very Low Altitude and Comparison to SEKE Propagation Model

Sean W. Gilmore*
MIT Lincoln Laboratory
244 Wood Street
Lexington, MA 02173
and
John C. Eidson
affiliated with MIT Lincoln Laboratory

Abstract

The propagation of *L*-band radio waves (1–2 GHz) close to the ground is explored in this talk. Measurements were taken at three sites in central Massachusetts as part of a larger *L*-band Clutter Experiment (LCE). Because the propagation measurements were “piggy-backed” onto a radar clutter measurement, the test set-up included the use of an *L*-band radar at a central location on Wachusset Mountain with a signal repeater located on a truck stationed at several sites 20 to 30 km away from the radar. The repeater received the radar pulse and then transmitted a constant 2 W peak power delayed in time 13 μ s (to separate the desired signal from the radar return due to scattering from the remote truck) and shifted in frequency by one half the pulse repetition frequency (to remove the desired signal from the ground clutter return). Sites were chosen particularly to measure knife edge to ground interactions and compare results to Lincoln Laboratory’s terrain specific SEKE (Spherical Earth Knife Edge) propagation model. For heights 1 to 40 m above the ground, findings indicate the importance of accurately modeling the local terrain features in predicting propagation loss. Knife edge location as well as accurate Digital Terrain Elevation Data (DTED) were found to be particularly important to the modeling effort. However, with accurate placement of knife edges to account for tree lines (edges of forests) and improved DTED from actual site surveys, excellent results were obtained from the modeling as compared to the measurements. The modeling results are of interest to the personal communication industry in understanding and predicting the effects of terrain specific propagation phenomenon on mobile radio links.

A Comparison of the Longley-Rice and SEKE Propagation Models

**John C. Eidson
M.I.T. Lincoln Laboratory**

The Longley-Rice point-to-point propagation model, developed by the Institute for Telecommunication Sciences, has been chosen by the FCC as the basic model for use in calculating interference levels for personal communications services (PCS). The SEKE propagation model, developed by M.I.T. Lincoln Laboratory, is widely used in the defense industry for radar systems analysis. Both models require site-specific terrain path profiles as input, and produce estimates of propagation loss over these paths. Furthermore, both models can be automated to access digital elevation data and create these path profiles, using elevation data such as that provided by the U.S. Geological Survey (USGS). In this paper, we describe the algorithms and phenomenology underlying each model, and compare their relative strengths and weaknesses. In addition, recent upgrades to the SEKE algorithms for multipath propagation, multiple knife-edge diffraction, and spherical earth diffraction will be described.

Results for both models are evaluated against propagation data measured by Lincoln Laboratory at several sites and at various frequencies ranging from VHF to L-band. The database consists of measured propagation loss vs receiver height, with receiver heights ranging from ground level to over 0.5 km. The accuracy of each model as a function of the input parameters will be presented. In particular, the sensitivity of the results to the level of accuracy of the digital terrain elevation data will be examined in detail, based on elevation data provided by the USGS, the Defense Mapping Agency, and site surveys conducted by Lincoln Laboratory. The additional effect of tree cover and tree lines on modeling accuracy will be presented.

We have found that SEKE is an accurate tool for the prediction of propagation loss to low-altitude receivers. Suggestions for utilizing the predictions of SEKE as a diagnostic for the Longley-Rice model in estimating PCS interference levels will be given.

PREDICTION OF VHF/L-BAND RADIO WAVE PROPAGATION IN URBAN AND SUBURBAN ENVIRONMENT

N. Blaunstein
Ben Gurion University of the Negev, P.O. Box 653
Beer Sheva 84105, Israel
M. Levin
Tadiran Ltd., P.O.Box 500, Petach-Tikva 49104, Israel

Abstract

A theoretical and experimental investigations carried out by the communication group of Tadiran Ltd. to analyse VHF/L-band radio wave propagation in the urban and suburban environment with regularly planned buildings is presented for the purpose of Tadiran MultiGain Wireless Services prediction. The effectiveness of a wireless local loop system is examined in two different propagation conditions: of line-of-sight along the street level, when both radio ports are below the rooftop level, and of the "clutter" conditions, when one (or both) of the radio ports is below the rooftops. In the first case when a city area is constructed as a grid with regularly planned buildings, a three-dimensional multislit waveguide model is developed. The average intensity and path loss at the street level taking into account the reflection from the ground, multi-reflection and diffraction from the walls and building edges are examined. This model give good agreement with an experimentally found transformation of the law of attenuation from r^{-2} to exponential at distances about 200-350 m from the source and further exponential attenuation at the street level in the conditions of direct visibility for a street plan with high and low building density up to 1-2 km from the base station.

In the second case, when the buildings are regularly distributed as rows in a crossing-street grid, the 2D-model of multi-diffraction from the building roofs [1, 2] is used in conjunction with actual variations of building heights, the distances between them and the actual base station antenna height variations. The influence of multi-diffraction from the edges and roofs of buildings, taking into account the reflection from the ground surface and second diffraction from the roofs is examined. Comparison between theoretical calculations and real experimental data makes it possible to explain the coverage effects and to predict the cell shape for such Wireless Local Loop system in suburban and urban areas with regularly distributed rows of buildings.

References

1. L.R. Maciel, H.L. Bertoni, and H.H. Xia, "Unified approach to prediction of propagation over buildings for all ranges of base station antenna height", IEEE Trans. Vehic. Technol., vol. 42, no. 1, pp. 41-45, Feb. 1993.
2. J. Walfisch and H.L. Bertoni, "A theoretical model of UHF propagation in urban environments", IEEE Trans. Anten. Propag., vol. 36, no. 12, pp. 1788-1796, Dec. 1988.

Near range radio wave propagation prediction in urban area

*NGAI Hing-On and LAM Wong-Hing

Mobile Radio Communication R&D Group, The University of Hong Kong

Abstract

A deterministic radio wave propagation model is proposed to predict the mean signal strength for the radius less than 500m from the transmitter in the highly urbanised area of Hong Kong. The area is characterised by closely packed high-rise buildings with non-uniformly distributed height. In the model, the multipath propagation along the vertical plane between the transmitter and receiver is considered. Each obstructing building along the plane is modelled as the absorbing screen which is perpendicular to the incident ray. The effective height of the screen is equal to the average height of the closely packed buildings in the neighbourhood of the obstructing building. The separation of neighbouring building is usually less than the road width of 25m. The resultant screens are classified into primary and secondary. Severe diffraction loss are mainly due to the primary screens. Multiple diffraction loss due to screens are calculated by using the modified uniform theory of diffraction (UTD) for finite conductivity. Single reflected rays due to both the screen behind the receiver and the ground in front of the receiver are also included. Reflection and multiple diffraction loss due to secondary screens are neglected in the model. Therefore, the received signal strength is the complex sum of all the individual rays along the plane, as shown in equation (1). Figure 1 shows a typical ray path profile over the obstructing screens along the vertical plane of the model. Measurement field trials had been carried out along the urban city streets in Hong Kong. The omni-directional transmitting antenna of 2.8m with radiation power of 10 watts at carrier frequency of 938 MHz was mounted on the roof top of a 54m high building. The receiving antenna was mounted on the rear window of a standard sedan which is about 1.5m high above the ground. The measurement was conducted along a test route within a radius of 500m from the transmitter in Wanchai. By applying the propagation environment of the measurement to the proposed model, the predicted signal strength achieved a good approximation of the trend of the mean received signal over a travelling distance of 400m with an rms error of 4.1dB as shown in figure 2.

- PS_i : ith primary screen
- SS_{ij} : jth secondary screen of ith primary screen
- RS : reflection screen

- Diffacted ray by primary screen
- ⋯ Diffacted ray by secondary screen

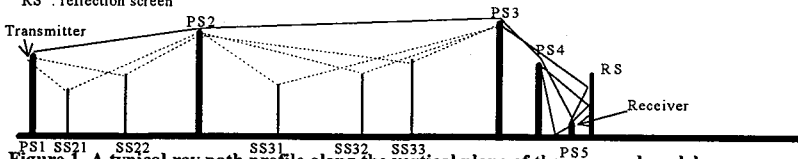


Figure 1. A typical ray path profile along the vertical plane of the proposed model

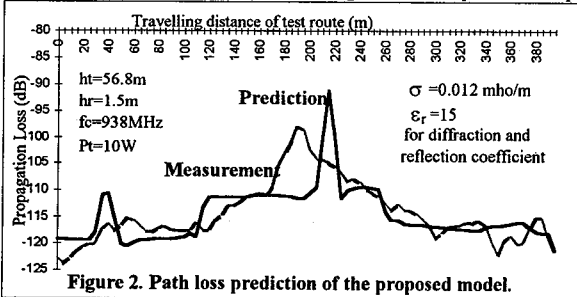


Figure 2. Path loss prediction of the proposed model.

$$\hat{E}_T = \sum_{i=1}^N \hat{E}_{DRi} \dots (1)$$

- where
- E_T : total E field strength at the receiver
- E_{DRi} : ith diffracted-reflected E field strength from transmitter to receiver
- \hat{E} : complex E field strength

HARMONIC SIGNAL'S LEVEL AND PHASE
CROSS CORRELATION ANALYTICAL DESCRIPTION
BY ELECTROMAGNETIC GROUND WAVE PROPAGATION

Valery V. Pechenin*, Prof.,
Alexey A. Andrejev

Kharkov Aviation Institute
Kharkov, Ukraine

Radiotechnical systems with directed radiation and detection of electromagnetic waves has large usage for information transmission, remote probing of space and atmospheric environment. Development and wide utilization of this systems, improvement their technical and exploration characteristics demand to account many factors. Such on usage of superhigh frequency band electromagnetic radiation it's necessary to account the radiophysical effects of propagation environment influence on radiation parameters.

Electromagnetic superhigh frequency band ground wave propagation is accompanied by level and phase chance distortions, which are evoked by random media of troposphere. On certain meteorological conditions and ground surface influence level and phase chance distortions may be cross correlated. Sufficiently high value of cross correlation coefficient allows to decide the task of phase distortions decreasing by information extracted from level distortions of harmonic signal. Practical usage of level and phase cross correlation analytical description is, e.g., accuracy increasing of phasemeter measuring system.

In this report we have theoretical investigations results of level and phase fluctuations correlation analytical model on output of ground signal channel. It was supposed that phase distortions may be introduce by line differential equation of first range, and level fluctuations model was described by Reley and normal distributing laws.

The analysis of graphic dependences of cross correlation coefficient are carried out with different intervals of correlation and different combinations of distributing laws. So, for normal phase and Reley level fluctuations normalized cross correlation function has oscillation character. In this case the speed of oscillation attenuation the more the less phase distortion autocorrelation interval, and the frequency of oscillation increases. In the case of normal level and phase fluctuations normalized cross correlation function changes by law of attenuate exponent. The specific values of base and level fluctuation correlation intervals are taken from results of experimental investigation which had been carried out by authors during some years.

PCS System Design Issues in the Presence of Microwave POFS

Solyman Ashrafi*¹, Tom Tran², A. Richard Burke³

Moffet, Larson & Johnson, Inc.

5203 Leesburg Pike

Suite 800

Falls Church, VA 22041

Telephone: (703) 824-5660

Fax: (703) 824-5672

There are many important issues concerning the design of the next generation personal communication services (PCS) systems such as microcell and macrocell propagation prediction models, multiple access technology, interference among PCS users and POFS users, traffic capacity, service quality, and deployment costs. This paper presents microcell/macrocell propagation modeling, PCS/POFS field measurement techniques, analysis and results, and interference studies between the POFS and PCS users. The paper focuses on how to deploy PCS sites without removing microwaves but working around them. The propagation model is a combination of the deterministic and statistical approaches which is based on geometrical theory of diffraction (GTD) and the path loss exponential law. The models use terrain and morphology data for macrocell and microcell predictions. PCS measurement data are used to validate the propagation models and to optimize the model accuracy. Also, POFS roof tops measurement data are collected, analyzed, and used to compute the interference power from PCS base stations to the POFS users. Depending on the locations of the base stations and the capacity demands, certain frequencies cannot be used by the PCS base station unless the offending POFS is relocated. This is the unexpected costs and should be minimized for initial PCS system deployment.

1. Director of Advanced Technologies

2. Scientist

3. President

Field Simulator for Reproduction of Propagation Environment

Hiroyuki ARAI

Division of Electrical and Computer Engineering, Faculty of Engineering,
Yokohama National University, Hodogaya-ku, Yokohama-shi, Kanagawa 240, Japan

This paper proposes a field simulator to reproduce propagation environment as indoor facilities, simulating outdoor and indoor multi-path fading environment. The propagation measurements are important to analyze propagation characteristics and to examine performance of base stations and mobile terminals. Since propagation measurements require transmitting and receiving equipment setting at a specific location to obtain valuable measurement data and a lot of examining time, we need compact facilities to simulate propagation environment. The field simulator is required to reproduce Rayleigh or Nakagami-Rice fading, hand over simulation in cellular system, arbitrary time delay spread, frequency selective fading, and Doppler fading.

To satisfy the above requirements, this paper proposes field simulator consisting of a few pair of transmitting antennas installed inside a cavity covered with finite resistivity walls. The cavity is an oversized waveguide to excite many higher order modes disturbing field distributions inside, and phases of antennas are controlled as a time depending function to change the fields at a specific position in the simulator. This simulator configuration gives Rayleigh or Nakagami-Rice field distributions inside the simulator as reproduced propagation environment. The excited fields in the simulator attenuated by lossy walls are decay field profile, which simulates cell edge in the cellular system. Since the decay profile can be controlled by the phase difference between antennas, two sets of transmitting antennas on both sides of the cavity provides an environment for hand over simulation. Since the maximum time delay spread depends on the simulator size, long time delay signals are produced by a delay line in the feeding circuits like as a fading simulator. These configurations are simple, low cost, and are appropriate for the field simulator.

The characteristics of the field simulator are calculated by ray tracing method and mode matching method. The numerical results show that three pairs of dipole antenna installed inside the cavity satisfy the requirements of the field simulator by selecting the location of antennas and phase varying function.

DIPOLE ANTENNA RADIATION PATTERNS IN A CONCRETE BUILDING AT 800 TO 2900 MHz FOR INDOOR WIRELESS COMMUNICATIONS

Hsing-Yi Chen* and Yeou-Jou Hwang

Department of Electrical Engineering
Yuan-Ze Institute of Technology
Nei-Li, Taoyuan Shian, Taiwan 32026

Measurements of the characteristics of indoor wireless communications have been reported by many researchers. However, theoretical studies about the characteristics of radio signals propagating in a building are not quite easy due to the difficulty in implementing general modeling techniques that require three-dimensional computational capabilities. In this study, the Geometric Theory of Diffraction (GTD) method was used for the calculations of radiation patterns in a concrete building at the frequencies in the range of 800 to 2900 MHz. A new but empty building having seven floors was constructed of reinforced concrete slabs, wooden doors at the front and back of the building, glass windows on each floor. To simplify calculations and make reasonable assumptions, the other floors of the building, except three successive floors, were excluded for the simulations. All the measurements were made with two identical dipole antennas located inside the building. The transmitter antenna was placed at the center of the horizontal plane with a height of 1.5m above the 5th floor. The transmitter power was +20 dBm into the antenna. The receiver antenna was moved along a circle of radius of 1.5 meter centered at the center of the horizontal planes with a height of 1.5 meter above the 5th, 6th, and 7th floor, respectively. The vertical polarization was chosen for both antennas when the receiver was in the 5th floor. As the receiver was in the 6th and 7th floors, it was taken the horizontal polarization. The simulation results of radiation patterns were compared with those obtained from the experimental measurements. It was found that the simulation results made good agreement with the measurement data. Fig. 1 shows the comparison of radiation pattern between the simulation results and the measurement data for waves propagating from the 5th floor through a reinforced concrete slab to the 6th floor at 800 MHz.

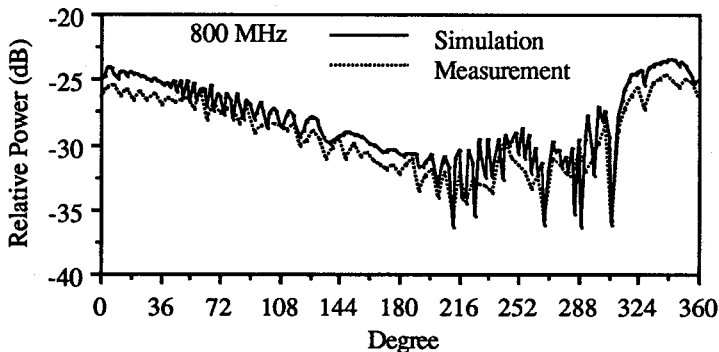


Fig.1 Comparisons of radiation pattern. Zero dB is based on 20 dBm (0.1Watts)

MODELING OF 3D IN-BUILDING PROPAGATION BY RAY TRACING TECHNIQUE

Gong Ke and Xu Rui

State Key Laboratory of Microwave and Digital Communications
Tsinghua University, 100084 Beijing, China

ABSTRACT

Implementation of wireless communication system, such as WPAX, WLAN, etc., requests the knowledge of indoor propagation. Though many investigations have been made and published, however, the results drawn from certain building can hardly be used to predict the radio coverage in another building. By using of ray tracing technique, therefor, the efforts have been made in Tsinghua Univ. to work out a general planning tool for indoor wireless systems.

This paper introduces the author's preliminary study of applying ray tracing technique to characterize path loss and delay spread of radio propagation within building. Differing from the image approach, which is most frequently used by geometrical optics to treat multi reflections but it is found that such treatment would become rather cumbersome if specific transmitted rays and multiple reflections in a complicated circumstance are taken into account, this paper models the transmitter by a number of source rays in different directions, each of them occupies the similar solid angle, so that each wave front has an identical shape and size on a unit sphere. By making use of the theory of geodesic dome, the direction of each source ray can be determined, and tracing every source ray, all possible propagation path leads to receiving point could be found out. Further, a power delay profile could be turn out from the rays reaching the receiver, and the path loss and rms. delay spread could then be obtained. To do all of these works, a computer program is developed and described in the paper.

To prove the validity of the above mentioned simulation approach, comparison has been made between the results to those derived from traditional image approach in a simple propagation environment, where only two walls, floor and ceiling are considered. Moreover, the simulated results are compared to experiment made in the corridor of a typical university building. Fairly good agreements of both comparisons are shown in the paper.

At last, some comments are made on the effects of different shape of the wave front of relevant source rays, for the author have found that would rather affect the accuracy of the predictions.

Noise and Interference Control

J. L. Drewniak and E. Asari

Page

8:20	EMI Sources Resulting from Finite Impedance Reference Structures <i>J. L. Drewniak*, T. H. Hubing, T. P. Van Doren, University of Missouri-Rolla, J. D. Shaw, Allison Transmission - Division of General Motors</i>	322
8:40	Modelling and Simulation of Weibull Distributed Radar Clutter by ... Means of Stochastic Differential Equation <i>Valerii Kontorovich, Centro de Investigacion y de Estudios Avanzados del I. P. N., Vladimir Lyandres, Sergey Primak*, Ben-Gurion University of the Negev, Margarita Horenian*, Library of the Russian Academy of the Science</i>	323
9:00	Modelling and Simulation of K-Distributed Radar Clutter by ... Means of Stochastic Differential Equation <i>Valerii Kontorovich, Centro de Investigacion y de Estudios Avanzados del I. P. N., Vladimir Lyandres, Sergey Primak *, Ben-Gurion University of the Negev, Margarita Horenian*, Library of the Russian Academy of the Science</i>	324
9:20	Enhanced Skynoise Mitigation via Adaptive Beamforming <i>Gary A. Somers*, Allan-O. Steinhardt, Lincoln Laboratory, Massachusetts Institute of Technology</i>	325
9:40	Detecting Technologies and Characteristics of Meteorological Noises Related with Weather <i>Eikichi Asari, Hokkaido College of Arts and Sciences</i>	326
10:00	BREAK	
10:20	Receiving Communication Signals in the Presence of Man-Made Noises with Nonlinear Blind Spatial Separation <i>P. V. Gorev, The Joint Laboratory of NPP "Polyot" and Radiophysical Research Institute</i>	327
10:40	Fast Adaptive Algorithms for Compensation of Time-Varying Interferences in Arrays <i>Boris B. Pospelov*, Alexander Yu. Zaitsev, Kharkov Aviation Institute</i>	328
11:00	A Combined Reference Method for Adaptive Spatial Processing of Communication Signals in the Presence of Man-Made and Noisy Interferences <i>P. V. Gorev, The Joint Laboratory of NPP "Polyot" and Radiophysical Research Institute</i>	329

EMI Sources Resulting from Finite Impedance Reference Structures

J. L. Drewniak*, T. H. Hubing, T. P. Van Doren, and J. D. Shaw †

Electromagnetic Compatibility Laboratory

Department of Electrical Engineering

University of Missouri-Rolla

Rolla, MO 65401

and

†Allison Transmission - Division of General Motors

Indianapolis, IN

Meeting FCC limits on radiated emissions from high-speed digital designs is becoming more difficult as technologies become faster, and designs become more dense. Further, these advances also make anticipating EMI problems at the design stage more difficult. Design maxims based on previous generations of technology and simplified problems for which analytical solutions are known are proving inadequate for current and emerging digital designs. While full-wave numerical electromagnetic modeling methods can model gross features well, modeling a full printed circuit board is currently not achievable. The challenge then is to model only the features necessary to predict EMI with engineering accuracy. At the hardware stage, EMI antennas can usually be identified with only a modest effort. For current clock speeds and edge rates, the majority of EMI antennas are either "wire type", i.e., two distinct conductors driven by an RF potential difference, or radiation through a slot or aperture for shielded digital designs. By selective and creative disabling of portions of the design, the particular IC device sourcing the emissions in a given region of the spectrum can also be determined. However, among the most challenging problems currently in modeling and predicting EMI, is determining the coupling mechanisms between the IC source and the antenna.

Two fundamental noise-source mechanisms have previously been identified that drive "wire-type" antennas. Often one part of the antenna is a cable attached to the PCB. The common-mode current induced on this cable will result in radiated emissions. One of the identified mechanisms that serves as a driving source for "wire-type" antennas results from finite impedances in ground or reference structures. Numerical and experimental examples of this mechanism will be presented. The FDTD method and NEC are employed for demonstrating the concept on simple perfectly conducting structures. The mechanisms are also demonstrated with two-port measurements on simple passive circuit geometries representative of printed circuit layouts. Finally, experimental results from production hardware will be presented. Equivalent circuit models for the source coupling paths have been developed and will be given, as well as EMI solutions.

MODELLING AND SIMULATION OF WEIBULL DISTRIBUTED RADAR CLUTTER BY MEANS OF STOCHASTIC DIFFERENTIAL EQUATION.

Valerii Kontorovich, *Centro de Investigacion y de Estudios Avanzados del I.P.N., Apartado Postal 14-740, Mexico 07000. D.F.*

Vladimir Lyandres & Sergey Primak*, *Department of Electrical and Computer Engineering, Ben-Gurion University of the Negev, POB 653, Beer Sheva, 84105, Israel.*

Margarita Horenian*, *Library of the Russian Academy of the Science, Birzhevaya Liniya 1, St. Petersburg, Russia.*

We consider the mathematical modelling of the undesired return from a radar environment (clutter) as the solution of proper stochastic differential equation. Such modelling can be useful for cases where computer or hardware simulation is required, that clutter patterns conforming to the given model be easily generated by algorithmic procedures. At the same time the hardware realization of such algorithms can be easily achieved.

The amplitude distribution of the clutter is most often assumed to be a Rayleigh distribution. Starting from the experimental evidence that in many situations of practical interest the clutter returns no longer exhibit Rayleigh distributed amplitude, a general agreement has been reached that in most cases the clutter envelope R may be approximated by Weibull distribution (E. Conte, M. Longo, and M. Lops, IEE Proc, F, 1991, 138, (2), pp.121-130).

$$w(A) = acA^{c-1} \exp(-aA^c), \quad A \geq 0 \quad (1)$$

where c is a positive shape parameter and a is related with average power as $2\sigma^2 = a^{-2/c} \Gamma(1 + 2/c)$.

We present the random process with Weibull distributed envelope as the reaction to fluctuation excitation of some dynamic system. The mathematical model of the process under investigation is presented as the solution of the appropriate (non-linear for non-Gaussian processes) system of the stochastic differential equation (SDE):

$$\ddot{x} + f(x, \dot{x})\dot{x} + \omega_0^2 x = \xi(t) \quad (2)$$

where $\xi(t)$ is the delta-correlated White Gaussian Noise with spectral density $0.5N_0$. It can be shown that

$$f(x, \dot{x}) = Cx^{c-2} \quad (3)$$

where C is the properly defined constant.

Relations between the clutter parameters and the parameters in equation (2) are found and model is numerically validated.

MODELLING AND SIMULATION OF K-DISTRIBUTED RADAR CLUTTER BY MEANS OF STOCHASTIC DIFFERENTIAL EQUATION.

Valerii Kontorovich, *Centro de Investigacion y de Estudios Avanzados del I.P.N., Apartado Postal 14-740, Mexico 07000. D.F.*

Vladimir Lyandres & Sergey Primak*, *Department of Electrical and Computer Engineering, Ben-Gurion University of the Negev, POB 653, Beer Sheva, 84105, Israel.*

Margarita Horenian*, *Library of the Russian Academy of the Science, Birzhevaya Liniya 1, St. Petersburg, Russia.*

We consider the mathematical modelling of the undesired return from a radar environment (clutter) as the solution of proper stochastic differential equation. Such modelling can be useful for cases where computer or hardware simulation is required, that clutter patterns conforming to the given model be easily generated by algorithmic procedures. At the same time the hardware realization of such algorithms can be easily achieved.

The amplitude distribution of the clutter is most often assumed to be a Rayleigh distribution. Starting from the experimental evidence that in many situations of practical interest the clutter returns no longer exhibit Rayleigh distributed amplitude, a general agreement has been reached that in most cases the clutter envelope R may be approximated by K -distribution (K.D. Ward, C.J. Baker & S. Watta, IEE Proc, F, 1990, 137, (2), pp.51-62).

$$w(A) = b^{\nu+1} 2^{1-\nu} A^{\nu} K_{\nu-1}(bA) / \Gamma(\nu), \quad A \geq 0 \quad (1)$$

where $\Gamma(\bullet)$ is the Eulerian gamma function, ν is a positive shape parameter, $K_{\nu}(\bullet)$ is the modified second-kind Bessel function of order ν , and b is related with average power as $b^2 = 2\nu / \sigma^2$

We present the random process with K -distributed envelope as the reaction to fluctuation excitation of some dynamic system. The mathematical model of the process under investigation is presented as the solution of the appropriate (non-linear for non-Gaussian processes) system of the stochastic differential equation (SDE):

$$\ddot{x} + 2\alpha\dot{x} + \omega_0^2 f(x) = \xi(t) \quad (2)$$

where $\xi(t)$ is the delta-correlated White Gaussian Noise with spectral density $0.5N_0$. It can be shown that

$$f(x) = N_0 b K_{\nu-3/2}(b|x|) / 8\alpha K_{\nu-1/2}(b|x|) \quad (3)$$

Relations between the clutter parameters and the parameters in equation (2) are found and model is numerically validated.

Enhanced Skynoise Mitigation via Adaptive Beamforming

Gary A. Somers* and Allan O. Steinhardt
Lincoln Laboratory, Massachusetts Institute of Technology
244 Wood Street
Lexington, Massachusetts 02173-9108

Adaptive array processing by means of sample matrix inversion beamforming has been widespread for suppressing clutter and jamming in active sonar and radar systems. The adaptive beam is formed by modifying a given quiescent pattern to optimally suppress the localized jamming and clutter. If the noise is purely uncorrelated between elements the quiescent pattern is already optimal and nothing is gained (in terms of SNR) by adaptive techniques. Sky noise will produce uncorrelated elements if the array is half-wavelength spaced, and the elements are isotropic.

In this paper we show that if the antenna deviates from isotropic, half wavelength spaced elements within the array then sky noise produces correlation amongst elements, even if the sky noise is uniformly distributed spatially. One concludes that even in the absence of clutter and jamming there are benefits in sensitivity ensuing from adaptive processing. Therefore for general arrays sky noise power level is *not* the fundamental limit on reception sensitivity.

We derive the array covariance matrix for sky noise as a function of element pattern and spacing. We then show how the range of improvement in sensitivity is bounded by the eigenspread of this matrix. (The exact improvement is also function of the look direction dictated by the quiescent pattern.)

We will show some examples of linear and rectangular array lattices, with several interelement spacings, quantifying the amount of improvement associated with adaptation. In realistic scenarios we found several dB of enhancement.

Our analysis assumed only sky noise. In general the presence of a few narrowband sidelobe jammers (undersaturating ECCM) has negligible effect on sensitivity. We will present simulations indicating that even with jamming, we can obtain a level of adaptive suppression below that of the average sky noise power level.

DETECTING TECHNOLOGIES AND CHARACTERISTICS OF METEOROLOGICAL NOISES RELATED WITH WEATHER

Eikichi Asari

Department of Management and Information science,
Hokkaido College of Arts and Sciences

Bunkyoudai-Midori-machi 582, Ebets, Hokkaido, 069 JAPAN

Tel. +81-11-386-1111 Fax +81-11-387-5848 (Home: Tel./Fax +81-11-761-8856)

ABSTRACT

Of detecting of meteorological noises, we have to solve four problems as follows: Finding out sensitive place to the noises, avoidance from obstructions of artificial noises, decrease of the internal noise of receiver and separation of characteristic parts of meteorological noises from a mixture of internal noise and meteorological noises in the receiver. Most interesting matter of them is last one. Author developed a receiver system for detecting of meteorological noises by addition of non-linear sensitivity to usual AM receiver and injection of a CW wave into the receiver. The CW wave useful to separation of characteristic parts of meteorological noises from the mixture in the receiver. Decrease of internal noise of receiver is solved by basic electronic circuits technologies such as making of Hi-Q resonance circuits and using of Hi-gm FET.

Until now, the official method of noise's analysis executed as the observation of noise's waveforms appear at output stage of demodulator in receivers. Author payed attention to characteristics at output of AF stage in receivers because the analysis is easy and watchable by sensuous inspections, for example, we can discriminate by sounds and observing to waveforms by oscilloscopes. And we can use many kinds of electric meters and analysing equipments. Thus, since 1974, author observed and analysed to meteorological noises at LF, MF, HF, and VHF frequency bands, and classified as fourteen types of AF noises which related to weather conditions.

Even at suburban districts of cities, the finding of nice places for receiving of weak meteorological noises is a difficult problem. We have to receive the aimed noises avoid obstructions of artificial noises, communication waves and broadcasting waves. Author used some guide object for receiving strengthened meteorological noises. The receiving technology of meteorological noises is not so much an engineering as an art.

The technologies are useful not only local and instant weather forecast but also research of other kinds of atmospheric electro-magnetic phenomena. For example, we may apply above mentioned technologies to observations and research for volcanic activities and short range forecasts of earthquakes and so on.

RECEIVING COMMUNICATION SIGNALS IN THE PRESENCE OF MAN-MADE NOISES WITH NONLINEAR BLIND SPATIAL SEPARATION

P. V. GOREV, The Joint Laboratory of NPP "Polyot" and Radiophysical Research Institute,
603600 Nizhny Novgorod, RUSSIA.

In the submitted paper a nonlinear sliding iterative algorithm is proposed for blind spatial separation of independent non-Gaussian signals received with a set of sensors, both antenna array and other type. This algorithm is very useful for recovering the desired signal in communication systems in the presence of man-made signal-like interference. Desired and undesired signals may be of a very similar structure, for example, frequency manipulated with the same baud rates and carrier frequencies, which case presents difficulties for the signal separation with many other methods.

The main merit of this approach is its universality - the possibility of processing arbitrary types of signals without any a priori information about them. In this case the least mean squares criterion is replaced by the criterion of mutual statistical independence of all output signals. Both numerical simulations and results of processing real radio-communications signals show the possibility of successful separation of one or more desired signals.

For example, if the antenna system consists of two H-field crossed loops and an E-field monopole, all responsive to Transversal Magnetic waves, and receives three signals with the identical signal-to- (thermal noise) ratio (SNR) 30 dB and the probability density function corresponding to "arcsin" law from the azimuths 0, 30, and 60 degrees, then the method recovers each signal separately in its own output channel with the output desired signal - to - (undesired signals + thermal noise) ratios (SINR) 16, 10 and 15 dB. Another numerical experiment is performed for the antenna system consisted of two magnetic loops without the monopole and two signals with input SNRs = 30 and 30 dB and azimuths = 0 and 30 degrees. In this case the signals have been recovered with the output SINRs 18 and 25 dB. Other examples are: if input SNRs = 15 and 15 dB and azimuths = 0 and 30 degrees, then output SINRs are 9 and 9 dB; if input SNRs = 30 and 30 dB and azimuths = 0 and 5 degrees, then output SINRs are 9 and 9 dB.

These results may be provided no longer than after processing 50 independent samples from the sensors. The algorithm proposed improves the convergence performance, in comparison with the algorithms derived by applying the neural networks approach. By selecting an appropriate iteration number one may rich the compromise between the convergence speed and implementation complexity.

FAST ADAPTIVE ALGORITHMS FOR COMPENSATION OF TIME-VARYING INTERFERENCES IN ARRAYS

Boris B. Pospelov[†] Ph.D.,
and Alexander Yu. Zaitsev

Kharkov Aviation Institute
Kharkov, Ukraine

Real conditions of arrays operating are characterized by a quite high power of non-stationarity variables of signal-interference situation and, in some cases, by uneven varying of these variables. Considered conditions, for example, occurs for organizing of communication with mobile and high mobile objects with essential space dynamics or for using of the mode of programmable varying of operation frequency in the communication systems. One should emphasize that this mode is mainly used in the communication systems with the mobile objects. For that reason the conditions of mobile arrays operating are characterized with essential non-stationarity of signals and interferences.

Available arrays interferences compensation algorithms (B. Widrow and S.P. Appelbaum) possess unacceptable speed and, because of this reason, gives unsatisfactory results for the time-varying environment. In this paper the authors propose a new approach to problems solution of enhancing of the speed of arrays time-varying interferences compensation adaptive algorithms.

Considered approach is based on an analogous idea of using of varying adaptation parameter. In apposite to approach described above, our parameter is considered as some parametric function (matrix) of definite variety of variables, values of which are determined by specific characteristics of non-stationarity. Next, the principles of selection of these specific variables of variety, as well as a method of definition of a concrete type of multiparametric dependence are presented.

It is shown that by appropriate selection of specific variables variety of non-stationarity, as well as the definition of type of the functional dependence of the adaptation factor (matrix) from mentioned variables, it is accessible to ensure a new capability of effective operating in time-varying conditions as well as in conditions of the uneven varying of interference for the available algorithms of interference compensation. In this paper it the concrete list of basic specific variables of non-stationarity yielded by space mobiling of objects has been shown, allowing the programmable varying operation frequency mode in the system of communication is given. The concrete fast adaptive algorithms for compensation of time-varying interferences in arrays, realizing the criterion of RMS error-minimum has been suggested. The results of array numeric modeling, which realizes the proposed algorithms are represented. These results has shown a sufficient effectivity of their operating in the communication systems with considered type of non-stationarity.

A COMBINED REFERENCE METHOD FOR ADAPTIVE SPATIAL PROCESSING OF COMMUNICATION SIGNALS IN THE PRESENCE OF MAN-MADE AND NOISY INTERFERENCES

P. V. GOREV, The Joint Laboratory of NPP "Polyot" and Radiophysical Research Institute, 603600 Nyzhny Novgorod, RUSSIA.

Most existing methods for adaptive spatial filtering via the least squares (LS) criterion require using known reference signals for their realization. This is rather restrictive condition for the communication applications where the signals contain unknown desired manipulation. At the same time, the spectral self-coherence restoral method exists which requires knowledge of only a cycle frequency of the desired signal, e.g. a baud rate, which is more available information for the receiver.

This paper concerns the intermediate situation in radio-communications when not only the baud rate of the manipulated signal is known, but almost the full information about it is available, excluding the manipulating sequence itself.

The method proposed is to solve the LS problem where the system of equations right-hand side contains a reference signal expressed as a linear combination of the known signals with unknown coefficients. These coefficients are adaptively tuned simultaneously with the weights on the left-hand side. This approach may be used for the intersymbol interference cancellation in multipath channels as well as in the case of the noisy interference.

To illustrate the applicability of the principle proposed in various interference environments some numerical experiments were carry out. They concern frequency manipulated desired signal, received with the narrow-band communication system using two antenna elements. Two kinds of the interference were analyzed: a narrow-band noisy interference and a signal-like one being the shifted copy of the signal. The last case is typical for multipath channels.

Simulations have shown that for the narrow-band noisy interference the degradation of output signal - to - (interference + thermal noise) ratio (SINR) of the proposed combined reference method from that of the optimal adaptation scheme with the fully known desired signal not exceeds 0.1 dB. Similar results have been obtained for the signal-like interference in the case when the antenna system resolution is high enough to spatially resolve the signal and the interference.

As a result, the conclusion have been made that the output SINR yielded by the proposed method is close to that provided by the optimal LS decision in the adaptive spatial processing scheme with the same antenna configuration and with the fully known desired signal.

THIS PAGE INTENTIONALLY LEFT BLANK.

Special Session

PML Absorbing Boundary Conditions for Time and Frequency Domains

K. S. Yee and R. Mittra

Page

- 8:20 Opening Remarks
Kane Yee, Lockheed Palo Alto Research Laboratory, Raj Mittra, University of Illinois
- 8:40 Extension of FD-TD Simulation Capabilities using the Berenger333
PML ABC
Daniel S. Katz, Cray Research, Inc., Christopher E. Reuter, Rome Laboratory/ERST, Eric T. Thiele, University of Colorado, Rose M. Joseph, Allen Taflove, Northwestern University
- 9:00 Applying Berenger's Perfectly Matched Layer (PML) Boundary334
Condition to Non-Orthogonal FDTD Analyses of Planar Microwave Circuits
Stephen D. Gedney, Alan Roden, University of Kentucky*
- 9:20 Numerical Investigations of the PML Layer for Mesh Truncation335
in FDTD
Jonathon C. Veihl, Raj Mittra, University of Illinois*
- 9:40 Experiments on the Perfectly Matched Layer Boundary336
Condition in Modeling Wave Propagation in Waveguide Components
Zhonghua Wu, Jiayuan Fang, State University of New York at Binghamton*
- 10:00 BREAK
- 10:20 FDTD/PML Modeling of HIRF Interactions with Embedded337
Cavity-Backed Apertures
Richard W. Ziolkowski, David C. Wittwer, The University of Arizona*
- 10:40 Analysis of Perfectly-Matched Layers Using Lattice EM338
Theory in a Discretized World
W. C. Chew, J. M. Jin, University of Illinois*
- 11:00 Performance Characterization of a Perfectly Matched Anisotropic339
Absorber for Frequency Domain FEM Applications
D. Kingsland, R. Dyczij-Edlinger, J. F. Lee, R. Lee, Worcester Polytechnic Institute*

- 11:20 A Finite Element Frequency Domain (FEFD) Formulation with 340
Perfectly Matched Layer (PML) for Mesh Truncation
U. Pekel, R. Mittra, University of Illinois*
- 11:40 Improving the PML Absorbing Boundary Condition with Optimal ...341
Complex Mapping of the Normal Coordinate
Carey M. Rappaport, Northeastern University
- 12:00 Discussion

Extension of FD-TD Simulation Capabilities using the Berenger PML ABC

Daniel S. Katz^{*1}, Christopher E. Reuter², Eric T. Thiele³, Rose M. Joseph⁴, Allen Taflove⁴

¹Cray Research, Inc., 222 N. Sepulveda Blvd., Ste. 1406, El Segundo, CA 90245

²Rome Laboratory / ERST, 525 Brooks Road, Griffiss AFB, NY 13441-4505

³University of Colorado, ECE Department, Boulder, CO 80309

⁴Northwestern University, EECS Department, Evanston, IL 60208

In 1994 Berenger published a novel absorbing boundary condition (ABC) for FD-TD meshes in two dimensions with substantially improved performance relative to any earlier technique (J. P. Berenger, *Jour. Comp. Phys.* 114, 185-200, 1994). This method is based on a decomposition of fields in the boundary region into split fields, in order to assign differing losses to individual directional components of the finite difference used to update these fields. Following this paper many extensions have been studied, including three dimensional application (D. S. Katz, et al., *IEEE MGWL* 4, 268-270, 1994, J. P. Berenger, *Annales des Telecom.*, 1994), the use of the ABC for waveguide termination (C. E. Reuter, et al., *IEEE MGWL* 4, 344-346, 1994), etc... Many groups are now trying to apply the concepts of the Perfectly Matched Layer (PML) ABC to finite element techniques. The majority of the work to date has been on extending this ABC or examining the parameters of the ABC in order to further reduce the reflection beyond the 40-70 dB of the first papers.

The primary focus of this paper will be on results that have been obtained by use of the PML ABC, with comparison to results obtained from similar problems using the Mur RBC. We will show how the PML ABC enables both more accurate solutions of some problems that have been attempted using other ABCs and solution of problems that were not possible without the PML ABC. Examples will include radar cross section calculations for the NASA Almond and microstrip analysis. Additionally, we will briefly highlight some recent attempts at extension of the PML ABC to problems such as waveguiding structures. We will also include a discussion of the relationship between the conductivity profile in the PML, the thickness of the PML, and the amount of reflection.

Applying Berenger's Perfectly Matched Layer (PML) Boundary Condition to Non-Orthogonal FDTD Analyses of Planar Microwave Circuits

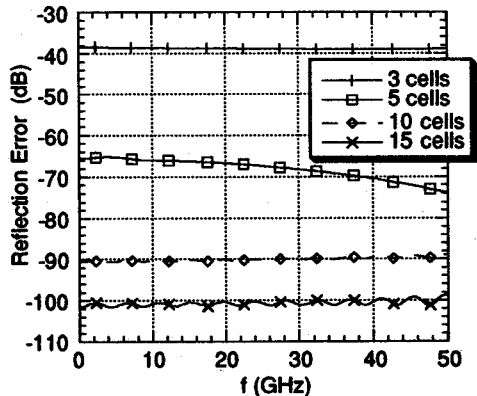
Stephen D. Gedney* and Alan Roden

Electromagnetic Laboratory, Department of Electrical Engineering
University of Kentucky, Lexington, KY 40506-0046

Explicit time-domain methods such as the finite-difference time-domain (FDTD) method and the planar generalized Yee (PGY) algorithm have been highly effective for the analysis of practical microwave circuit devices and antennas. One of the most challenging aspects of these methods is implementing absorbing boundary conditions to accurately truncate the mesh over broad frequency bands. Recently, J.-P. Berenger introduced an absorbing material boundary condition [J. of Comp. Phys., 1994] which in the continuous space absorbs electromagnetic waves for all angles of incidence and frequencies. This is achieved by a coordinate stretching and the introduction of additional degrees of freedom for the vector electric and magnetic fields. With the use of this *perfectly matched layer* (PML), reflections on the order of -60 to -70 dB were demonstrated for open region scattering problems by Berenger in two-dimensions, and in three-dimensions by Katz and Taflove [IEEE Microwave Guided Wave Let., 1994], and Chew and Weedon [Microwave Optical Tech. Let., 1994].

In this paper, the PML boundary condition is extended to the application of printed microwave circuit devices. When modeling infinite dielectric substrates and ground planes, this application offers additional challenges over the previous studies since the material medium in the PML region is inhomogeneous. Secondly, the PML boundary condition is extended to the use of non-uniform and non-orthogonal based FDTD methods. Classically, for stability of the absorbing boundary condition, these methods require that the non-orthogonal mesh must be uniform and orthogonal in the near vicinity of the absorbing boundary, posing additional constraints on mesh generation. It is shown that the PML boundary condition can be used as an efficient and accurate absorbing boundary condition without the need of a uniform orthogonal grid.

To illustrate the capability of the PML boundary condition, the reflection loss of a PML boundary used to terminate a 50 Ω microstrip line printed on a 10 mil dielectric substrate ($\epsilon_r = 9.8$) versus frequency for various PML thicknesses is illustrated in the accompanying figure. Reflection losses on the order up to -100 dB are observed using this technique. Finally, techniques will be presented that lead to effective and accurate implementations of the PML boundary condition for the FDTD analysis microwave circuit devices.



NUMERICAL INVESTIGATIONS OF THE PML LAYER FOR MESH TRUNCATION IN FDTD

Jonathon C. Veihl and Raj Mittra*
Electromagnetic Communication Laboratory
University of Illinois, Urbana, IL 61801

The perfectly matched layer (PML), proposed by Berenger [*J. Comput. Phys.*, 114:185-200, 1994] as a reflectionless termination in FDTD appears to have the potential to be major breakthrough in mesh truncation for PDE/FDTD simulations. It has been shown to reduce reflection errors by more than 40 dB when compared to second order Mur ABC for free space radiation problems [Katz et al., *IEEE/MGWL*, 4:268-270, 1994]. Reflection coefficients on the order of -70 dB have been reported for wideband terminations in two-dimensional waveguide problems [Reuter et al., *IEEE/MGWL*, 4:344-346, 1994]. The principal objective of this paper is to carry out a critical examination of the numerical aspects of the PML layer termination in FDTD. In particular, we will examine the issues pertaining to stability and computational efficiency for two- and three-dimensional open region as well as guided wave problems.

To verify our implementation of the PML for inhomogeneous environments, the problem of a point source radiating above an infinite dielectric slab was studied. Use of the PML layer allows one to greatly reduce the white space between the source and the truncation plane that is normally required with the Mur ABC, without an undue sacrifice in numerical accuracy. It was found that the selection of the maximum conductivity for a PML region, in which the permittivity or permeability varies from unity, can have a profound effect on late-time stability, with three-dimensional cases being more sensitive than two-dimensional ones. Also, a modification of the wave velocity from the speed of light in dielectric or magnetic media often leads to instability. A separate stability issue arises due to the special exponential differencing method used in the PML update equations. As an illustration, an empty PEC cavity was simulated using the PML update equations, giving results identical to the regular Yee update equations. However, when uniform electrical and magnetic conductivity satisfying the perfectly matched condition were applied everywhere, the simulation with PML medium quickly became unstable, while the regular update equations with the same discretization and time step behaved normally. This implies that care must be taken when attempting to apply the PML absorber to a problem with non-zero loss, such as a lossy earth.

The usefulness of the PML layer as reflectionless terminations for guided wave problems containing dielectric or PEC discontinuities was also examined and compared with other ABCs, such as the Mur and the dispersive boundary condition. Preliminary results for the PML show unacceptable reflections in microstrip simulations and for waveguide modes exactly at cut-off. Further work must be done to determine if the added memory and CPU expense of a multi-layer PML is outweighed by the prospective benefits of decreased buffer zones and wide angle and wideband absorption without loss of accuracy.

Experiments on the Perfectly Matched Layer Boundary Condition in Modeling Wave Propagation in Waveguide Components

Zhonghua Wu* and Jiayuan Fang

Department of Electrical Engineering

State University of New York at Binghamton, Binghamton, NY 13902

This talk presents the investigation of the performance of the Perfectly Matched Layer (PML) boundary condition in the modeling of wave propagation in metal waveguide and microstrip line components.

In typical practice of implementing PML, PML is terminated by a perfect electric wall. An electromagnetic wave entered into PML is attenuated as it propagates to the electric wall, and is further decayed as it propagates back from the electric wall. With a proper selection of the conductivity and the thickness of PML, the amplitude of the wave in PML can be attenuated to a sufficiently small value.

It will be shown that, for waveguide components, PML is very effective in absorbing outgoing waves somewhat above cutoff frequencies. On the other hand, it is found that PML is actually ineffective in absorbing waves near cutoff frequencies and fields of evanescent nature. Total reflections appear at cutoff frequencies, and PML does not accelerate the attenuation of evanescent waves. Theoretical analysis as well as numerical tests will be presented to demonstrate the performance of PML for propagating and evanescent waves.

Comparisons are made between the performance of PML and high order Higdon's type of boundary conditions. Pros and cons of using the PML and Higdon's type of absorbing boundary conditions are discussed.

This talk also presents the experiments of replacing the electrical wall used to terminate the PML by a regular absorbing boundary condition. The degree of improvements that can be made by using an absorbing boundary condition with PML will be analyzed and demonstrated with numerical tests.

FDTD/PML MODELING OF HIRF INTERACTIONS WITH EMBEDDED CAVITY-BACKED APERTURES

Richard W. Ziolkowski and David C. Wittwer*
Electromagnetics Laboratory
Department of Electrical and Computer Engineering
The University of Arizona
Tucson, AZ 85721

The interaction of high intensity radio frequency fields (HIRF) with civilian and military aircraft continues to be a prominent EMC/EMI issue. Current and future generation fly-by-wire or fly-by-light aircraft may have flight-critical subsystems or components that are susceptible to HIRF upsets. There is a strong need for enhanced simulation capabilities to model these HIRF environments; these tools would provide engineers with the capability to design adequate hardening protocols for these systems.

Full-wave vector Maxwell's equations solvers, such as the finite difference time domain (FDTD) approach, are rapidly becoming mainstream computational electromagnetics modeling tools. FDTD codes have been used and validated in a wide range of applications including radar cross section, HPM aperture coupling, and electronic interconnects. Recently the Berenger perfectly-matched-layer (PML) absorbing boundary condition (ABC) has provided another potential enhancement for the FDTD approach. It could permit modeling of the interactions of electromagnetic fields with electrically-large structures with higher accuracies than is currently possible with traditional ABC's. However, its behavior for high-Q resonance problems has not been established to date.

We have incorporated the PML ABC into our FDTD simulator and have considered several cavity-backed aperture coupling geometries. These configurations present high-Q cavities to incident pulsed radar beams. We have made direct comparisons for these high-Q systems between an FDTD/PML-based simulator and one constructed with the standard second-order Mur ABC. The results of our comparisons will be presented. Of particular interest, because of its potential for enhanced hardening, is an embedded, double-walled structure. Simulations will be shown that demonstrate extremely high coupling levels into the interior of the structure despite the additional layer of shielding. The coupling occurs at frequencies that are characteristic of the compound structure rather than each layer separately. Direct comparisons of the amplitudes of the interior fields and the locations of the resonances with both simulators will be given. Results indicate that the PML ABC may be particularly well-suited to this class of aperture coupling problems.

Analysis of Perfectly-Matched Layers Using Lattice EM Theory in a Discretized World

W. C. CHEW* AND J. M. JIN

ELECTROMAGNETICS LABORATORY

DEPARTMENT OF ELECTRICAL AND COMPUTER ENGINEERING

UNIVERSITY OF ILLINOIS

URBANA, IL 61801

Abstract

A perfectly matching layer (PML) medium has been proposed [Berenger, *J. Comp. Phys.*, 114:185-200, 1994]. This medium is capable of forming a lossy-lossless media interface with no reflection for all incident angles and all frequencies. An analysis has been performed in three dimensions [Chew and Weedon, *Micro. Opt. Tech. Lett.*, 7:559-604, 1994] using a stretched coordinates analysis in the continuum world. The dispersion relations and the reflection coefficients are both derived in the continuum world.

However, the practical use of PML is as an absorbing boundary condition for a finite-difference time-domain (FDTD) simulation in a discretized world. Hence, the analysis in the continuum world need not hold true in the discretized world. In this paper, we will use the tools developed in lattice electromagnetic theory [Chew, *J. Appl. Phys.*, 75:4843-4850, 1994] to analyze the concept of a perfectly matched layer in the discretized world. In this analysis, first, the coordinate stretching is performed in the discretized world as was done in the continuum world. Next, we derive the dispersion relation, matching condition, and stability criterion for a PML medium in the discretized world. Then we study the one interface problem and derive the reflection coefficients for both TE and TM polarization when a plane wave is incident on this interface. The N -interface problem can be similarly studied. It is shown that even though a PML interface is perfectly absorbing in the continuum world, it is not a perfectly absorbing interface in the discretized world.

Performance Characterization of a Perfectly Matched Anisotropic Absorber for Frequency Domain FEM Applications

D. Kingsland, R. Dyczij-Edlinger^{*}, J. F. Lee, R. Lee

Traditionally, the truncation of finite element solution domains has been accomplished through the application of local or global boundary operators to the outer surface of the finite element mesh. There is a tradeoff involved between the accuracy of global operators (boundary integral solutions) and the efficiency of local operators (ABC's). Alternative methods of truncation based on placing a layer of absorbing material at the outer boundary of the solution domain have been widely investigated in the past. These absorbers possess the same desirable property as local boundary operators: they preserve the sparse structure of the system matrix generated by the finite element method. Unfortunately, their accuracy is also similar to that of local boundary operators.

Recently, J.P. Berenger (J. P. Berenger, J. Comp. Physics 114, 185-200, 1994) introduced a high performance absorbing layer for FDTD simulations based on a non-physical generalization of Maxwell's equations. By splitting cartesian field components into two subcomponents (i.e. $H_z = H_{zx} + H_{zy}$), this "Perfectly Matched Layer" (PML) approach yields a reflectionless interface between free space and the absorbing material. Berenger and others (W. C. Chew & W. H. Weedon, Microwave & Optical Technology Letters 7, 599-604, 1994) have demonstrated that PML provides a much more accurate truncation scheme for FDTD grids.

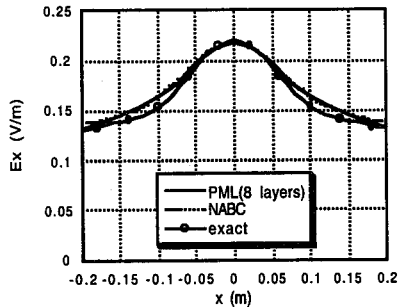
A reflectionless interface between free space and a lossy material absorber can also be achieved when the bulk properties of the material, ϵ and μ , are anisotropic. Specifically, if ϵ and μ are appropriately chosen complex diagonal tensors, the impedance of the medium will be independent of the frequency, polarization, and incident angle of the wave at the interface. In this paper, we characterize the performance of an absorber of this type when applied to 3-D finite element analysis of open domain problems.

A Finite Element Frequency Domain (FEFD) Formulation with Perfectly Matched Layer (PML) for Mesh Truncation

Ü. Pekel* and R. Mittra

Electromagnetic Communication Laboratory
University of Illinois, Urbana, Illinois 61801

The recently-introduced concept of Perfectly Matched layer (PML) of Berenger has engendered considerable interest in the EM/PDE community, because it exhibits the potential of being an almost ideal approach to mesh truncation in PDE solution of Maxwell's equations. The objectives of this paper are to critically examine the viability of using PML absorbers in FEM, and to present the results of numerical experimentation with of a test problem to evaluate the PML approach for frequency domain applications. We begin by revisiting the twelve *split* equations in the time domain, referred to herein as the PML-I equations, originally introduced by Berenger to replace the six, conventional, FDTD curl equations for the electric and magnetic fields. We find that these equations are not well-suited for FEM applications and we manipulate them into six *unsplit* equations, which may be viewed as the curl equations for an active medium with *dependent sources*, and which will be referred to here as the PML-II equations. We show that the stretched-coordinate version of PML equations proposed by Chew and Weedon, and by Rappaport, that utilize longitudinal co-ordinate scaling in the PML medium, can be derived from the PML-II equations, as can the Maxwellian form of equations of Sacks et al. for a PML medium with negative conductivities. However, the longitudinally-stretched equations are found to contain surface integral terms in the weak form of FEM formulation at the interface between free space and the PML layer, that render them undesirable for our purposes. This prompts us to seek yet another form of PML-II that circumvents this difficulty, and we derive such a form, called PML-III, by scaling the *transverse* co-ordinates in the PML medium instead, which serves to eradicate the surface integral term in the weak form. We then carry out extensive numerical experimentation with PML-III on a canonical test problem, viz., an x-directed dipole in free space (for representative results see Figure in inset) and draw the following preliminary conclusions: (i) A minimum of eight or more layers are required to obtain reasonably accurate results using a PML medium, and the optimal conductivity profile must be determined by numerical experiments; (ii) increasing the number of layers to sixteen or more would improve the accuracy, and make the design of the PML region more robust, but at a considerable increase in cost in terms of memory and CPU time; (iii) reducing the number of layers to 4 or less lead to unacceptably inaccurate results, regardless of whether a PEC or other type of termination is used; (iv) the NABC uses less memory and is considerably more robust than the 8-layer PML, and yet their accuracies are comparable; and, (v) the NABC does generate an asymmetric FEM global matrix, albeit smaller, while its PML counterpart is symmetric.



Improving the PML Absorbing Boundary Condition with Optimal Complex Mapping of the Normal Coordinate

Carey M. Rappaport
Center for Electromagnetics Research
Northeastern University
Boston, MA 02115

The Berenger Perfectly Matched Layer (PML) numerical electromagnetic absorbing boundary condition (Berenger, *J. Comp. Phys.*, Oct. 94) can be interpreted in the frequency domain as an anisotropic mapping of space (Rappaport, *Micro. Guide. Wave Let.*, Feb. 1995). If the coordinate normal to the matched layer boundary is given by x , the PML equations differ from Maxwell's Equations by the simple mapping: $x \rightarrow x^{PML} = (1 - j\sigma/\omega\epsilon_0)x$, which leads to the normally directed wave number in the PML: $k_x^{PML} = (1 - j/\omega\tau)k_x$, with $\tau = \epsilon_0/\sigma$ being the frequency independent dielectric relaxation constant. The transverse impedance in the PML is given by E_y/H_z (or some equivalent rotation about the x -axis), and these field components are related by Ampere's Law by the operation $-\partial/\partial x^{PML}/j\omega\mu_0 = k_x/\omega\mu_0$, which is identical to the impedance of any incident wave. Thus, the layer is matched to free space for all frequencies and incident angles, yet since it is lossy, waves will attenuate in it as $e^{(-k_x/\omega\tau)x}$ (or $e^{-t/\tau}$ in the time domain). This angle and frequency independence is particularly useful in FDTD computations where scattered wave having many frequencies and incident directions must be absorbed at the ABC. The space mapping concept is quite efficient for the FDFD method since the usual equations can be used with the complex coefficients pre-computed. The major disadvantage of the PML is that the attenuation rate depends on incidence angle, with grazing waves decaying slowly than normally incident waves.

The basic PML can be augmented, however, by altering the anisotropic mapping. By increasing the real part of the mapping, the propagation *direction* can be altered, refracting with a smaller transmitted angle. That is, let $x \rightarrow x^{PML'} = (\epsilon' - j\sigma/\omega\epsilon_0)x$ for $\epsilon' > 1$. Although this layer is still perfectly matched, frequency independent, and mathematically as simple to state as usual, the wave transmitted into this new PML will propagate more closely toward the x -direction, thereby increasing its decay rate. Also, any evanescent waves incident on this augmented PML—with entirely imaginary k_x —will experience increased attenuation, with a rate increase proportional to ϵ' .

This new formulation is realized in the time domain by simply replacing (ϵ_0, μ_0) in those PML equations which have conduction current terms with $(\epsilon'\epsilon_0, \epsilon'\mu_0)$. As with the standard PML where σ varies parabolically, ϵ' can also be gradually increased with layer depth.

One further advantage of the new PML is that if a lossy first-order, one-way (Engquist-Majda type) ABC (Rappaport *IEEE Trans. Mag.*, May 1995) is used to terminate the PML, having the propagation direction more nearly normal increases the annihilation effect. Using this lossy termination to an augmented PML improves the absorption performance over the standard PML by almost an order of magnitude.

THIS PAGE INTENTIONALLY LEFT BLANK.

Inverse Scattering

T. M. Habashy and W. C. Chew

Page

8:20	Different Spatial Iterative Methods for Microwave Inverse Scattering <i>P. Lobel, CNRS/Universite de Nice-Sophia Antipolis, R. Kleinman, University of Delaware, Ch. Pichot*, L. Blanc-Feraud, M. Barlaud, CNRS/Universite de Nice-Sophia Antipolis</i>	344
8:40	The Reconstruction of Scattering Potentials from Incomplete Data: A New Look at the Fundamental Theorem of Diffraction Tomography <i>Tarek Habashy*, Schlumberger-Doll Research, Emil Wolf, University of Rochester</i>	345
9:00	Processing of Ultrasonic Data with Electromagnetic Inverse Algorithm <i>W. C. Chew*, C. C. Lu, University of Illinois, G. P. Otto, ThermoTrex Corporation</i>	346
9:20	Processing Experimental Data with Local Shape Function Method and Distorted Born Iterative Method <i>C. C. Lu*, W. C. Chew, University of Illinois</i>	347
9:40	Bistatic Polarimetric Extension of GO/PO and GTD/PTD Inverse Scattering Theories to Aerial RCS Analyses in Wideband POL-SAR Image Interpretation <i>Wolfgang-M. Boerner, University of Illinois at Chicago, Frederic A. Molinet Societe Mothesim</i>	348
10:00	BREAK	
10:20	A Modified Approach in Input Waveform Shaping for Target Identification <i>Gonul Turhan Sayan*, Kemal Leblebicioglu, Serhat Inan, Middle East Technical University</i>	349
10:40	Simulation of Inverse Scattering by Clouds and Precipitation for 10 GHz Pulse Airborne Radar <i>Felix J. Yanovsky, Kiev International University of Civil Aviation</i>	350

DIFFERENT SPATIAL ITERATIVE METHODS FOR MICROWAVE INVERSE SCATTERING

P. Lobel¹, R. Kleinman², Ch. Pichot^{1*}, L. Blanc-Féraud¹, M. Barlaud¹

¹ Laboratoire Informatique, Signaux et Systèmes de Sophia Antipolis,
CNRS/Université de Nice-Sophia Antipolis,
250 rue Albert Einstein, 06560 Valbonne, France.

² Center for the Mathematics of Waves,
University of Delaware, Newark, DE19716, USA.

This paper deals with a comparative study between different iterative methods for reconstruction of 2D-TM objects using scattered near-field data in the microwave domain. Quantitative reconstruction of the complex permittivity of an inhomogeneous lossy dielectric embedded in homogeneous background is considered here for various configurations of practical interest: microwave imaging in the air and microwave tomography for biomedical applications.

Quantitative reconstruction of complex permittivity is an inverse scattering problem strongly non linear and ill-posed. We make use of the integral representation of the forward problem discretized using the method of moments with pulse basis functions and point matching. The formulation of the inverse scattering problem is given in terms of the minimization of a cost functional. This functional is the normalized error in the least squares sense matching the measured scattered data with the computed ones of the forward problem.

For this comparative study, the first iterative algorithm is based on a Levenberg-Marquardt method which is a modified Gauss-Newton or Newton-Kantorovich method. A standard Tikhonov regularization with identity operator is used. Different strategies have been utilized for finding the regularization parameters such as an empirical formula and the Generalized Cross Validation method.

A second iterative approach is based on a Gradient method. First order as well as second order approximations were taken into account successively in the algorithm. Various correction directions (standard gradient direction and Polak-Ribière conjugate gradient direction) were employed.

Performance of the different methods used in this comparative study convergence depends on the initial guess. Investigations on computing the initial guess have been made. We use a backpropagation scheme by means of the adjoint operator which allows to provide an estimate of the induced current inside the inhomogeneous object. Influence of the initial guess (without a priori information and using the backpropagation scheme) on the results has been also studied.

The Reconstruction of Scattering Potentials from Incomplete Data: A New Look at the Fundamental Theorem of Diffraction Tomography

Tarek Habashy* and Emil Wolf[†]

*Schlumberger-Doll Research, Old-Quarry Road, Ridgefield, CT 06877-4108

[†]Department of Physics and Astronomy, University of Rochester, Rochester, NY 14627

Inversion techniques utilizing X-ray, light waves, ultrasonic waves and electron beams have been remarkably successful in recent years and have led to major advances in fields such as condensed matter physics, medicine, non-destructive testing and astronomy. All the available reconstruction methods have, of course, been limited not only by the wavelength of the radiation used, but also by the fact that usually only some and not all the Fourier components of the unknown scattering object can be experimentally determined.

In this paper, we first show that within the accuracy of the first-order Born approximation there are no bodies that are invisible for all directions of incidence, i.e. that there are neither deterministic nor random non-scattering scatterers.

Next, we present an integral equation which, in principle, makes it possible to completely reconstruct the structure of weak scatterers of finite support whose scattering potentials are square-integrable. The reconstruction utilizes measurements of the scattered field in the far zone. The scattering is assumed to be due to monochromatic waves and is within the accuracy of the first-order Born approximation. The possibility of such an extrapolation is generally based on the fact that the Fourier transform of a band-limited function of N real variables is a boundary value in real space of an entire analytic function of N variables. Our procedure for solving the integral equation is closely related to the three-dimensional version of an extrapolation technique for band-limited functions, introduced by Slepian and Pollak in a well known investigation related to signal processing.

We give examples which illustrate how such an extrapolation method can be used to improve the resolution of diffraction tomography enabling the reconstruction of details of the scatterer beyond the usual resolution limit. In the language of the theory of crystal structure determination from X-ray diffraction experiments, these examples show how one can obtain information about Fourier components of the scatterer which lie outside the Ewald limiting sphere. We finally note some of the limitations of the method and discuss its performance with noisy data.

Processing of Ultrasonic Data with Electromagnetic Inverse Algorithm

W. C. CHEW* AND C. C. LU
ELECTROMAGNETICS LABORATORY

DEPARTMENT OF ELECTRICAL AND COMPUTER ENGINEERING
UNIVERSITY OF ILLINOIS
URBANA, IL-61801

G. P. OTTO
THERMO TREX CORPORATION
9550 DISTRIBUTION AVE.
SAN DIEGO, CA 92121-2306

Abstract

Electromagnetic waves and ultrasonic waves satisfy the same partial differential equation in the linear regime. Therefore, inverse algorithms developed for electromagnetic waves can be used to process ultrasonic data in principle. Assuming nonmagnetic materials, for instance, the E_z polarization in 2D electromagnetic scattering problem maps into the variable velocity acoustic wave equation. On the other hand, the H_z polarization in 2D electromagnetic scattering problem maps into the variable density acoustic wave equation.

In the past, we have developed a number of nonlinear electromagnetic inverse algorithm that accounts for multiple scattering within the scatterer. The multiple scattering effect makes the inverse problem a nonlinear problem. We will demonstrate the inversion of some ultrasonic data using electromagnetic inverse algorithms we have developed in our group. We will also discuss the use of multiple frequencies to process the data. We will compare the inverse image with linear inversion algorithm like diffraction tomography.

The principal difference between ultrasonic imaging and electromagnetic imaging is that the velocity contrast of soft tissues in ultrasound is small while that for electromagnetic waves is usually larger. Also, ultrasonic wavelengths are shorter compared to electromagnetic wavelengths, and hence, the sizes of objects are usually larger compared to wavelength in ultrasound as oppose to the electromagnetic case.

These inverse algorithms are driven by a forward solvers. Various fast ways of solving the forward scattering problem, like RATMA, NEPAL, and CG-FFT, will be discussed.

Processing Experimental Data with Local Shape Function Method and Distorted Born Iterative Method

C. C. LU* AND W. C. CHEW

ELECTROMAGNETICS LABORATORY

DEPARTMENT OF ELECTRICAL AND COMPUTER ENGINEERING

UNIVERSITY OF ILLINOIS

URBANA, IL 61801

Abstract

We have developed two inverse scattering algorithms in our group: the local shape function (LSF) method and the distorted Born iterative method (DBIM). These methods have been used to process both synthetic and experimental data in the past. In this paper, we will show the use of these algorithms to process the experimental data provided by Rome Laboratory.

The aforementioned methods are useful when multiply scattered field is an important component of the scattered field data. Multiple scattering causes the scattered field to be nonlinearly related to the scattering object. However, when multiple scattering is unimportant, simpler algorithm based on first-order Born approximation, such as diffraction tomography, is sufficient for processing the data. The disadvantage of LSF and DBIM is that they are usually more computationally intensive compared to the simpler diffraction tomographic method.

In the LSF method, we characterize a scatterer by its shape or T matrix, rather than the conductivity or the permittivity of the object. This maps a nonlinear problem into a more linear one, allowing for the ease of applying an optimization approach. In the distorted Born iterative method, a distorted Born approximation is made at each stage, using the previously constructed permittivity profile as the background. A linear inverse problem ensues from such an approximation, and the inverse problem is solved by an optimization approach. The DBIM is equivalent to Newton's method, and hence, has second order convergence.

**BISTATIC POLARIMETRIC EXTENSION OF GO/PO AND GTD/PTD INVERSE SCATTERING THEORIES
TO AERIAL RCS ANALYSES IN WIDEBAND POL-SAR IMAGE INTERPRETATION**

Wolfgang-M. Boerner
University of Illinois at Chicago
Communications, Sensing and
Navigation Laboratory
840 W. Taylor St., SEL-4210
CHICAGO, IL / USA 60607-7018
T&F: +{1}(312)996-5480

Frédéric A. Molinet
Société Mothesim
Modélisation Optimisation THEorie
Simulation Mathématique
La Boursidière-R.N. 186
F-92357 LE PLESSIS ROBINSON, FRANCE
T/F: +{33}(1)4632-6530/7240

In order to correlate high resolution/precision interferometric POL-SAR images with the underlying ground truth, it is essential to develop the RCS matrix expressions for simple, canonical shapes in closed analytic form and to provide numerical algorithm verification analyses. This is achieved by extending the common geometrical optics (GO) and physical optics (PO) scalar RCS closed form solutions via the Geometrical Theory of Diffraction (GTD) of J.B. Keller and the Physical Theory of Diffraction (PTD) of P. Ya. Ufimtsev to the full polarimetric, slightly bistatic cases as required for proper implementation in modern wideband (multispectral and impulse) POL-SAR Systems Calibration and Image Normalization procedures.

First, the PO current approximation, corrected by the second order term of the Lüneburg-Kline expansion of specular reflections from an arbitrary convex three-dimensional, perfectly conducting surface, is transformed in the time domain and injected in the time-domain Kirchhoff formula. Employing Kennaugh's bistatic correction approach of the transient ramp response formula, the expressions for the first-order and second-order corrections to the scattered far-field vector (polarization) wave interrogation are obtained for both the monostatic and the bistatic cases. The resulting expressions force the scattering matrix to become asymmetrical due to the local curvature difference as expressed in terms of the derivatives of the Kennaugh-Cosgriff silhouette area function. In a next step, canonical closed form solutions for the truncated cylinder, the wedge, the truncated cone and the cone-tip are found by employing GTD for the respective scattering matrices. Also, the polarimetric bistatic creeping wave solutions for the sphere, the prolate and oblate as well as for the generalized ellipsoidal perfectly conducting scatterers are provided by implementation Fock's theory of vector diffraction and Ufimtsev's Physical Theory of Diffraction. This brief analytical review analysis is then concluded, with a preliminary analysis of Huynen's doubly skewed asymmetric curved phylotaxic surfaces which requires the future extension of the vector PTD methods currently advanced by Pathak, Ufimtsev, Molinet, et al.

Some computer-numerical and experimental data results are provided for comparison using recent measurement-model corroborative results of Molinet who implemented the excellent UWB multispectral POL-RAD data sets collected at CELAR, Bruz in France.

A Modified Approach in Input Waveform Shaping for Target Identification

Gönül Turhan Sayan*, Kemal Leblebicioğlu and Serhat İnan
Electrical and Electronic Engineering Department
Middle East Technical University, 06531 Ankara, Turkey

A recent approach in electromagnetic target identification is based on input waveform shaping as utilized in the K-Pulse and the E-Pulse techniques. It is well known that an electromagnetic scatterer is uniquely characterized by its aspect and polarization independent system poles. Therefore, a unique time-limited input waveform whose Laplace transform zeroes coincide with these system poles theoretically leads to a time-limited response waveform via pole-zero cancellation. As the available methods to extract the system poles from measurement data are extremely noise sensitive, the input waveform shaping problem almost always utilizes an optimization approach. The input waveform to be estimated is expanded in terms of a suitable set of orthogonal basis functions whose expansion coefficients are the optimization variables. The energy content of the resulting system response is minimized after a properly determined late-time which is directly related to the time duration of the input waveform.

It is known from experience that the input waveform duration is the most critical parameter of this inverse problem. There are some rules of thumb to pre-estimate this parameter prior to optimization for simple target geometries. However, in the applications where the target geometry is complicated and/or the available measurement data is incomplete, the input waveform duration needs to be determined as a part of the optimization process.

In this paper, we will demonstrate the use of various basis function sets and optimization techniques when the input waveform duration is an additional optimization variable. The approach will be applied to several target geometries of varying complexity. The advantages of this modified technique will be discussed through comparisons of the new results with the previous results obtained by rough pre-estimation of the input waveform duration.

**SIMULATION OF INVERSE SCATTERING BY CLOUDS AND PRECIPITATION
FOR 10 GHZ PULSE AIRBORNE RADAR**

Felix J. Yanovsky

Kiev International University of Civil Aviation
1, Cosmonavta Komarova Prospect, Kiev, 252058, Ukraine
Telephone: (044) 484-9445, Facsimile: (044) 488-3027
e-mail: fvs%kiiga.kiev.ua@relay.UA.NET

Theory of forming radar signals during inverse scattering is being looked into. Generalised theoretical scheme of forming such signals is being proposed on the basis of internal models conception (B.E.Fishman & F.J.Yanovsky, Radiotekhnika (Moscow), 11, 56-58, 1983). This proposal allows for the consideration of different meteorological (physical nature of the scatterers, their shapes and size-distribution, turbulence, wind etc) and instrumental factors.

Chosen approach to the modelling is not connected with formation of radar signals having aprior-determined statistical characteristics but with modelling of processes of forming the signals actually. For each fraction of the scatterers with a given average size, the reflecting volume is conditionally divided into specified number of spatial cells whose size is being defined by the minimum spatial lengthscale of air vortices which set particles of a given diameter into motion.

We were able to get expressions for the partial components and general expression for the complex received signals. Amplitude and phase of the resultant signal (narrow band random process) are functions of the microphysical and dynamic characteristics of the scatterers in radar volume.

Adoption of the scheme allows for radar signal modelling in different meteorological situations. This way, receiving new information is possible in those cases when there are absent reliable experimental data.

Experimental operation allowed us to receive statistics of the amplitude and phase of the echo-signals for different values of turbulence intensity and different microphysical structure of meteoobjects. Good coincidence with experimental data was recorded.

The proposed model as a subsystem can be build into any system that simulates radiation, reception and processing of signals.

Some applications of the proposed approach in solving inverse problems of remote atmospheric sensing are given. It is shown that adoption of internal models allows for forecasting the behaviour of reflecting object and leads to a class of adaptation forecasting procedures which include operations of models' formation, specification of their parameters, predicting the object's behaviour, measurement of the object's parameters, estimating the reliability of the forecast, adequacy verification of the models and when necessary their correction.

Wavelets in Electromagnetics II

R. D. Nevels and F. X. Canning

Page

- 8:20 A Wavelet Multilevel Formulation for Electromagnetic Scattering352
Gaofeng Wang, Tanner Research, Inc.
- 8:40 Wavelet Basis Allows Diagonal Preconditioners for the EFIE 353
Francis X. Canning, James Scholl, Rockwell Science Center
- 9:00 A Comparison of Several Method of Moments Wavelet Basis354
Sets for Electromagnetic Scattering
R. D. Nevels, J. C. Goswami, A. K. Chan, C. K. Chui,*
Texas A&M University
- 9:20 A Computationally Efficient Method Using Intervallic Wavelets355
for the Solution of Surface Integral Equations
Guangwen Pan, University of Wisconsin, Milwaukee
- 9:40 Analysis of Coplanar Waveguide Using Wavelet-Like Basis 356
Functions
Subba R. Kunasani, Cam Nguyen, Texas A&M University*

A Wavelet Multilevel Formulation for Electromagnetic Scattering

Gaofeng Wang

Tanner Research, Inc., 180 N. Vinedo Avenue, Pasadena, CA 91107, U.S. A.

The integral equation formulation, which reduces the solution domain to a finite and often small region with the boundary conditions implicitly contained, is usually preferred in the numerical solution of an unbounded electromagnetic problem. However, the intensive computational cost of solving matrix equation via direct methods limits the application of the integral equation approaches. An alternative way is the use of iterative methods to reduce the computational complexity of solving matrix equations. Unfortunately, the matrices generated from integral equation formulations of electromagnetic problems usually lack both positive definiteness and sparsity, thus are generally not amenable to iterative procedures.

Recently, the wavelet expansion methods were introduced to solve the integral equations of electromagnetic problems (B. Z. Steinberg & Y. Leviatan, *IEEE Trans.*, AP-41(5), 610-619, 1993) (G. Wang, *IEEE Trans.*, AP-43(2), 1995). It was found that the matrices obtained from the integral equation formulations by using the wavelet expansion methods were rendered sparsely populated. Furthermore, the multi-resolution analysis implemented by the wavelet expansion methods naturally provides a multigrid (multilevel) scheme. By using more than one level of discretization and operating on both coarse and fine grids, the multilevel schemes can improve convergence of iterative methods by reducing both high and low frequency errors in contrast to the traditional way of operating only on the fine grid to reduce the high frequency error. A multilevel formulation of the conventional moment methods was introduced (K. Kalbasi & K. R. Demarest, *IEEE Trans.*, AP-41(5), 589-599, 1993). It was reported that, although additional computational effort was required to construct the operator representations at coarse levels, accurate solutions can be obtained with far less overall computation effort by using the multilevel methods

Here, a multilevel formulation inherent in the wavelet expansion methods in electromagnetic scattering is presented. The wavelet expansion methods decompose unknown functions into a series of wavelet basis functions in different scales, which lead to the so-called multiresolution analysis. The multilevel formulation is naturally derived from the multiresolution analysis implemented by the wavelet expansions. In this multilevel formulation, the coarse representations of operators are identified as sub-matrices of the fine representations of operators and thus no additional computational efforts are required for constructions of the coarse representations of operators. As an iterative method, this multilevel formulation allows the full use of the sparsity of the linear systems generated by the wavelet expansion methods. Numerical examples show that this multilevel formulation offers a stable and fast technique for electromagnetic scattering problems.

WAVELET BASIS ALLOWS DIAGONAL PRECONDITIONERS FOR THE EFIE

Francis X. Canning
James Scholl
Rockwell Science Center
1049 Camino Dos Rios
Thousand Oaks, CA 91360

The Electric Field Integral Equation (EFIE) is discretized using localized expansion and testing functions giving a matrix Z . An orthogonal wavelet transform W then gives:

$$T = WZW^h; \quad \text{where } WW^h = I \quad (1)$$

Because W is orthogonal, the eigenvalues of T are identical to those of Z . Several recent papers have observed that T may have many small elements which may reasonably be approximated by zero. We note, however, that T will always have at least as many remaining elements as would Z if two expansion functions and two testing functions per wavelength had been used.

Consider the condition number of Z as a function of the number of expansion and testing functions per wavelength, n . It is known that for a given physical problem, as $n \rightarrow \infty$, $Z(n) \rightarrow \text{Constant}$ for the MFIE and $Z(n) \rightarrow \infty$ for the EFIE. This behavior may be understood as due to the behavior of the eigenvalues as expansion functions oscillate more rapidly. We introduce a diagonal matrix D , whose diagonal elements are proportional to the rate of oscillation of the associated elements of T . For the EFIE with TM and TE radiation we define:

$$P = DTD \quad (\text{TM}); \quad P = D^{-1}TD^{-1} \quad (\text{TE}) \quad (2)$$

P is a preconditioned matrix. Numerical results show it has a much better condition number than T . Furthermore, these results also suggest that now as $n \rightarrow \infty$, $P(n) \rightarrow \text{Constant}$, as is known to be true for the Z of the MFIE.

A Comparison of Several Method of Moments Wavelet Basis Sets for Electromagnetic Scattering

R. D. Nevels*, J. C. Goswami, A. K. Chan and C. K. Chui

Department of Electrical Engineering

Texas A&M University

College Station, Texas 77843

In electromagnetic scattering analysis method of moments (MoM) integral equation formulations containing conventional subdomain basis sets result in an impedance matrix that is dense. If the scattering object is large in terms of wavelengths the associated dense matrix often becomes intractable due to excessively large computer memory requirements and the computation time necessary to determine the current amplitudes. To overcome these difficulties, wavelet-bases have been used recently which, primarily because of their local support and vanishing moment properties, lead to a sparse matrix. Two types of wavelet basis functions have been used to solve boundary integral equations. These are: (1) orthogonal wavelets and (2) compactly supported semi-orthogonal spline wavelets. The choice between these two wavelet types is an important issue not only in electromagnetic scattering analysis but also in signal processing where the value of wavelets has been firmly established.

In this paper we will present a comparison between several orthogonal bases, including Daubechies and Battle-Lemarie wavelets, and semi-orthogonal spline wavelets applied to solve for the current distribution on a two-dimensional perfectly conducting cylinder illuminated by a transverse magnetic plane wave. The current distribution produced by a conventional spline basis function will be included as a standard of comparison. The basis for our comparison will be the error in the surface current for different values of the threshold parameter δ , which determines the sparsity of the wavelet matrix, the computation time for each method and a subjective estimate of the formulation and numerical routine setup time. The following properties of these two types of wavelets will be emphasized in our presentation:

- Unlike most of the continuous orthogonal wavelets, compactly supported semi-orthogonal wavelets have closed-form expressions.
- Semi-orthogonal wavelets are symmetric and hence have generalized linear phase, an important factor for reconstructing the function.
- The greater the smoothness of a wavelet, the larger is its support in space. Spline wavelets approach the optimal "uncertainty principle" value of 0.5 very rapidly with increasing order of smoothness. For example a cubic spline wavelet has an uncertainty product of 0.505. This product approaches ∞ for orthogonal wavelets.
- Because of the "total positivity" properties of splines, they have certain very desirable properties from an approximation point of view.
- The dual of a semi-orthogonal wavelet does not have compact support. To overcome this problem the use of dual wavelets and scaling functions is avoided by introducing a change-of-bases sequence.

A Computationally Efficient Method Using Intervallic Wavelets for the Solution of Surface Integral Equations

Guangwen Pan

University of Wisconsin, Milwaukee

Abstract

A new topic in electromagnetics (EM) is the use of wavelets as the basis and testing functions in integral equation methods [1], [2]. Due to the orthogonality, vanishing moments, localization property, etc. of the wavelets, sparse matrices have been obtained. However, there have been concerns that the computational cost required to generate the matrix outweighs the benefits of having a sparse matrix. Generation of the matrix has generally been considered more expensive when using Galerkin's Method with wavelets, as opposed to traditional Method of Moments (MoM) using piecewise sinusoidal basis and testing functions.

In contrast to this argument we present a technique for generating a well structured sparse matrix employing wavelet basis which has a computation time superior to that of traditional MoM with pulse expansion and point matching. The zero value entries of the sparse matrix are directly identified using the vanishing moment properties of the wavelets, thus avoiding numerical evaluation of the double integrals. In addition, the computation of many non-zero entries are reduced to a direct evaluation of the integrand at a single point. The use of the intervallic wavelets provides a better treatment of the edges of the interval, on which the unknown is defined. Numerical examples for scattering of EM waves from 2D olive shaped objects and for waveguide structures are presented. The computational efficiency is tabulated and comparisons with the MoM is provided.

References

- [1] G. Wang and G. Pan, "Full-Wave Analysis of Microstrip Floating Line Structures by Wavelet Expansion Method," *IEEE Trans. Microwave Theory Tech.*, to appear in Jan. 1995.
- [2] X. Zhu and G. Pan, "A Fast Adaptive Algorithm Using Lemarie-Meyer Wavelet to Solve Boundary Integral Equations," resubmitted for publication, *IEEE Trans. Microwave Theory Tech.* Nov. 1994.

ANALYSIS OF COPLANAR WAVEGUIDE USING WAVELET-LIKE BASIS FUNCTIONS

SUBBA R. KUNASANI* AND CAM NGUYEN

Department of Electrical Engineering
Texas A&M University
College Station, Texas 77843-3128
(409) 845-7469
(409) 845-6259 (FAX)

ABSTRACT

Coplanar waveguide (CPW) appears extensively in microwave hybrid (MIC) and monolithic (MMIC) integrated circuits due to many appealing properties. Its characteristics have been investigated using various methods such as the spectral-domain approach (SDA).

In this paper, we report an analysis for the CPW through solving coupled integral equations in the space domain using wavelet-like basis functions. The use of wavelets in analyzing electromagnetic problems has recently received significant attention due to the resultant fast computations. The main advantage of our approach is that it allows the integral equations to be solved entirely in the space domain and still achieve extremely fast numerical results. This is due to the fact that the resultant matrix of the coupled integral equations, transformed under a two-dimensional wavelet transform, becomes sparse in the wavelet basis.

We begin the analysis by enforcing the boundary conditions along the CPW interfaces to obtain coupled integral equations. We then transform the equations using the wavelet basis. As the operator compresses under the two-dimensional wavelet transform, with a large fraction of its wavelet coefficients being negligibly small, the wavelet-transformed integral equation become a sparse system in the wavelet basis, which can be efficiently solved. Now by setting the matrix determinant to zero, we can solve for the propagation constant, and then the effective dielectric constant and characteristic impedance. The calculated results of the effective dielectric constant and characteristic impedance agree well with those computed by the SDA, but with less computational time.

Microwaves - Photonics - Electronics

L. P. B. Katehi and M. Shur

Page

1:20	Optical Beam Forming and Steering for Phased-Array Antenna	358
	<i>Dilip K. Paul*, Brian J. Markey, Rajender Razdan, COMSAT Laboratories</i>	
1:40	Time-Domain Numerical Analysis of Passive and Active	359
	Optical Microstructures <i>Rose M. Joseph*, Susan C. Hagness, Allen Taflove, Northwestern University</i>	
2:00	Photonic Bandgap Materials: New FDTD Analysis and	360
	Antenna Applications <i>James G. Maloney, Morris P. Kesler*, Brian L. Shirley, Denver J. York, Georgia Tech Research Institute, Glenn S. Smith, Georgia Institute of Technology</i>	
2:20	Macromodeling of Circuit Components for High Frequency	361
	Applications <i>Kavita Goverdhanam*, Emmanouil Tentzeris, Linda P. B. Katehi, The University of Michigan</i>	
2:40	An All Optical Millimeter-Microwave Generator	362
	<i>K. Daneshvar*, University of North Carolina, L. Hales, Redstone Arsenal</i>	
3:00	BREAK	
3:20	Band-Pass Filters Mounted with Cube Dielectric Resonators in	363
	Cut-Off Waveguide <i>Sachihito Toyoda, Takashi Murakami, Osaka Institute of Technology</i>	
3:40	A Novel Method for Suppressing Spurious Resonance Responses	364
	of the Coaxial-Resonator Bandpass Filters <i>Kouji Wada, Yasumasa Noguchi, Hideaki Fujimoto, Junya Ishii, Kinki University</i>	
4:00	A Power Amplifier Based on an Extended Resonance Technique	365
	<i>Adam Martin*, Amir Mortazawi, Bernard C. De Loach, Jr., University of Central Florida</i>	
4:20	An Active Ka-Band Antenna Element Amenable to Device	366
	Integration <i>D. J. Roscoe*, Communications Research Centre, L. Shafai, University of Manitoba, M. Cuhaci, A. Ittipiboon, Communications Research Centre</i>	
4:40	A Dynamical Analysis of the CMOS Circuit	367
	<i>Jilin Tan*, Guangwen Pan, University of Wisconsin, Milwaukee</i>	
5:00	Optical Temperature Sensor Using Surface Plasmon Resonance	368
	Technique <i>Sahin Kaya Ozdemir*, Gonul Turhan-Sayan, Middle East Technical University</i>	

Optical Beam Forming and Steering for Phased-Array Antenna

DILIP K. PAUL*, BRIAN J. MARKEY, and RAJENDER RAZDAN
COMSAT Laboratories, Clarksburg, Maryland, U.S.A. 20871

Abstract

Developing relevant photonics for insertion in communications satellites and other commercial and military avionics is very attractive because optical technology has the potential for a large bandwidth, complex functionality, and EMI/EMP free operation in a compact light-weight payload, and thus savings in prime power requirement and cost of service. These advantages can be further enhanced by using integrated photonics which promises high reliability and device yield. Several industry and government programs are currently pursued worldwide to develop on-board photonics technology (D. Paul, et. al., 15th AIAA Conf. Proc., 3, 1332-41, 1994).

In this paper, several optical beam forming network (BFN) architectures that are deemed viable for on-board satellite phased-array antenna applications are assessed for functional capability and technology feasibility: Specifically discussed are the implementation issues, reliability and long-term performance, and maintainability of four major BFN architectures: (a) Microwave true-time delay (TTD) using fixed length non-dispersive fibers to create fixed delays; (b) Microwave TTD using dispersive optical fibers and tunable optical transmitter; (c) BFNs using optical-to-microwave phase conversion with coherent detection at either RF or optical frequencies (both baseband, frequency-shifted single-sideband modulation and amplitude modulation); and (d) Coherent optical signal processor using 2-D Fourier transform method. The mass, prime power, and volume requirements of an optical BFN feeding an M-beam, N-element phased-array antenna at Ka-band have been estimated and various trade-off in BFN architecture and technology selection processes and critical long lead time technical areas such as RF-optical-RF power conversion efficiency and environmental qualifications that must be developed before its successful deployment on-board communications satellite identified. Also included are the results of recently demonstrated proof-of-concept BFNs which employ fiber optic TTD elements and coherent optical processor (COP) based approaches to phased-array antenna beam forming and steering. Amplitude and phase distributions measured in the 2-dimensional Fourier Transform plane of a COP-based BFN feeding a 462-element phased-array have adequate signal quality for frequency-agile space-borne transmit phased-array. An injection-locked, tunable frequency-offset dual-frequency optical transmitter consisting of a 5-mW and a 25-mW lasers provided the frequency-agile RF carrier. The phase front is found planar within 2° rms variation across the entire scanned aperture (1 cm x 1 cm) with ~ 120 pixels within ~3-dB signal power contour which can be increased by using tapered fiber bundles. The details of the trade-off study results and relevant POC hardware developed will be presented in the conference to demonstrate the advantage of light weight and large bandwidth capability of photonic beamforming which are at premium in large antenna arrays. Coherent optical processor using Fourier transform appears to be the best method.

D. Paul/ 1995 USNC/URSI Radio Science Meeting, Newport Beach, CA, June 18-23.
Category: Commission B (Fields and Waves); Sub-category - B8 Antennas or Commission D
(Electronics and Photonics); Sub-category - D1 or D3

Time-Domain Numerical Analysis of Passive and Active Optical Microstructures

Rose M. Joseph*, Susan C. Hagness, and Allen Taflove
EECS Department
McCormick School of Engineering
Northwestern University
Evanston, IL 60208

With the increasing availability of powerful workstations and supercomputers, it is now possible to numerically analyze a wide range of optical microstructures using time-domain techniques, directly from the Maxwell's equations. Finite-difference time-domain (FD-TD) models can incorporate the physics of dispersion, nonlinearity, and frequency-dependent loss and gain for geometrically complex heterostructures. Reflection and transmission characteristics, resonance frequencies, and coupling coefficients can be determined in a straightforward manner. The method also allows designers to quantify and minimize non-paraxial scattering losses.

Here, the FD-TD method is applied to selected linear and nonlinear periodic structures including optical mirrors and filters, as well as resonant cavities. FD-TD computed simulation results are compared to coupled mode theory and perturbative analyses. For the case of high-Q cavities, where the time-domain nature of the FD-TD method can lead to unacceptably long computer run times, linear predictive post-processing steps can be applied to FD-TD generated time waveforms to obtain cavity characteristics.

In addition, results are presented for a recently-developed FD-TD model for optical materials exhibiting frequency-dependent gain. To illustrate the capabilities of this method, we report results for a generic heterostructure laser. A lasing mode builds up from spontaneous emission, which is modeled as a noise current inside the device. The operating characteristics of the laser, including the gain threshold, turn-on delay, and L-I curve, are obtained from the FD-TD model.

PHOTONIC BANDGAP MATERIALS: NEW FDTD ANALYSIS AND ANTENNA APPLICATIONS

James G. Maloney, Morris P. Kesler*, Brian L. Shirley, Denver J. York
Signature Technology Lab, Georgia Tech Research Institute
Atlanta, GA 30332-0800

Glenn S. Smith
School of Electrical and Computer Engineering
Georgia Institute of Technology, Atlanta, GA 30332-0250

Photonic bandgap structures have received much attention in recent years because of their novel electromagnetic characteristics. Photonic bandgap materials are a class of periodic dielectric structures exhibiting frequency regions in which electromagnetic propagation is prohibited (i.e. bandgaps). The existence and characteristics of the bandgaps are dependent on the lattice type (triangular, simple cubic, face-centered cubic, etc.), element shape (spherical, cylindrical, etc.), and dielectric contrast between the element and the host material. Most techniques used to model these structures are only applicable to infinite structures; thus, they are not capable of determining the effects of boundaries. Last year we presented results of modeling a finite, two-dimensional photonic bandgap structure (circular dielectric rods on a square lattice) using the finite-difference time-domain (FDTD) technique (Kelly, et. al., *Proc. IEEE AP-S Symp.*, June 1994). The calculated results were in good agreement with laboratory measurements.

We now extend these results to finite, three-dimensional photonic bandgap structures, such as the "woodpile" structure (Sozuer, *J. of Modern Optics*, vol. 41, pp. 231-239, Feb. 1994), the new Lincoln Lab fcc crystal (Brown, *Microwave and Opt. Tech. Lett.*, vol. 7, pp. 777-779, Dec. 1994) and others. These 3D structures exhibit bandgaps in all directions, whereas the 2D structures only have bandgaps for the component of the wavevector in the principal plane. The structures we have investigated have bandgaps either in the 8-10 GHz or 17-19 GHz frequency regions. We will present details of the FDTD modeling effort and will use experimental measurements to validate the model.

The use of these materials with antennas has been proposed (Brown, *J. Opt. Soc. Am. B.*, vol. 10, pp. 404-407, Feb. 1993). However, there is little information showing how they can be used to tailor antenna performance. We are actively involved in applying our FDTD models to study the properties of antennas placed on or near the surface of photonic bandgap materials. We will present model results (plots and animations) that illustrate the interaction of the antenna and the photonic material. We will also discuss some new configurations utilizing photonic bandgap materials which show interesting antenna performance.

Macromodeling of Circuit Components for High Frequency Applications

Kavita Goverdhanam*, Emmanouil Tentzeris and Linda P.B. Katehi

The Radiation Laboratory
Department of Electrical Engineering and Computer Science
The University of Michigan, Ann Arbor, MI 48109, USA

With the advent of monolithic and millimeter-wave Integrated Circuits (M3ICs) and application specific Integrated Circuit (ASIC) technology, multichip module (MCM) applications in modern radar are broadening. Development of the transmit/receive (T/R) module in the 1980s using advanced MMICs and ASICs enabled the use of active elements within the antenna itself, reducing power loss levels typically associated with the antenna front. In modern radar systems digital and mixed mode multichip modules are extensively used, where microwave and millimeter-wave MCMs combine GaAs MMICs and silicon control devices to perform a desired function. In such a mixed mode environment with analog and digital functions performing in close proximity, advanced circuit design tools play a key role.

During the last twenty-year period, a number of full wave formulations were developed and explored intensively to provide a variety of approaches. All these techniques result in numerical treatments which are based on a direct or indirect solution of Maxwell's equations and involve an extensive discretization of part or whole volume of interest. The development of these techniques has resulted in very sophisticated circuit analysis tools which are capable of characterizing high-frequency effects very accurately. The result of a high-frequency circuit analysis may be expressed in the form of scattering parameters or equivalent circuits which represent the response of the circuit very accurately. However in view of the highly mathematical methodologies involved in such an analysis effort, computational times become prohibitively long even for medium size circuits and issues of numerical convergence and stability overwhelm circuit designers. While accurate high frequency circuit analysis has become possible at the expense of time, high frequency circuit design has remained a challenge. The highly advanced high frequency modeling techniques are not capable of providing means for design and, even today high frequency circuit design relies on low-frequency approaches.

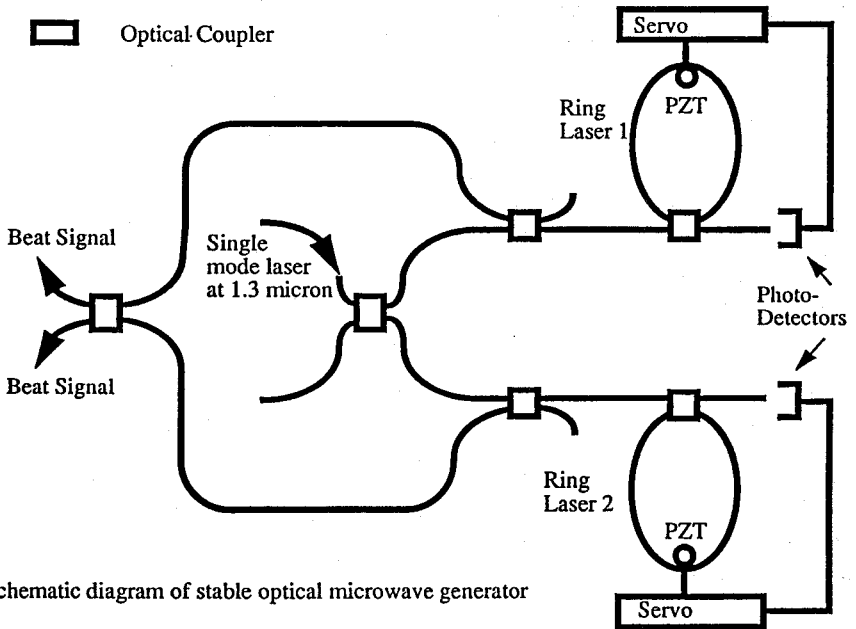
The disadvantages of high frequency modeling techniques which prevent their use from real time analysis or design of circuits can be overcome by means of appropriate macromodels. The concept of macromodeling has been used extensively in VLSI circuits for design and signal integrity evaluation, but it is rather unknown to high-frequency modeling. Macromodeling is based on the very simple concept of independent circuit component partition and the use of design rules. Any circuit is divided into independent components. These components are categorized by geometry and/or electrical function into groups and constitute the basis for any high-frequency circuit topology. The circuit components which belong to the previously identified groups are analyzed in advance using appropriate high-frequency techniques and the information on their performance is stored in the form of an equivalent circuit the complexity of which depends on the frequency range of interest. For this given frequency range, the elements of the equivalent circuit can be parametrized and can be put in the form of continuous functions using dimensional analysis. The macromodel functions derived through this approach are then used to compute accurate frequency-dependent equivalent circuits which can then be incorporated in a SPICE-like environment to analyze the complex circuit geometry under investigation. This presentation will discuss the details of macromodeling as it applies to a variety of circuit components.

An all Optical Millimeter-Microwave Generator

K. Daneshvar, Electrical Engineering Department, University of North Carolina, Charlotte, NC 28223 and L. Hales, Weapons Sciences Directorate, Redstone Arsenal, AL 35898-5248

Recently an optical microwave generator based upon Stimulated Brillouin Scattering (SBS) has been described by (D. Culverhouse, Electronics Letters, Vol.25, pp.915 (1989)). In their experiment, an Argon ion laser was used to launch optical power into two spools of fibers with approximate length of 500m each, while the power level was maintained above the SBS threshold. The combined back-scattered signals from two fibers resulted in a beat signal. It was observed that the beat frequency is in the microwave region, relatively unstable, and temperature dependent, therefore tunable.

We have design and constructed a highly stable millimeter-microwave generator using SBS method. The basic configuration consists of a single mode laser which is used to simultaneously illuminate two single mode fiber ring resonators. These resonators are locked in a way that stimulated Brillouin signals are generated in each ring resonator producing two highly stable SBS lasers. The frequency of each ring laser depends upon the optical length of its corresponding cavity. By selecting the order of fringe, and locking the cavity on a desired position, the frequency of the laser ring can be tuned. The two SBS signals are then beat at the output, fiber coupler generating waves with a highly stable frequency. The output frequency can be tuned over a large range of millimeters to microwave region.



Schematic diagram of stable optical microwave generator

Band-Pass Filters Mounted with Cube Dielectric Resonators in Cut-off Waveguide

Sachihiro Toyoda and Takashi Murakami

Department of Electrical Engineering

Osaka Institute of Technology

5-16-1 Asahiku, Omiya, Osaka 535 JAPAN

1. Introduction

In this paper, new band-pass filters mounted with cube dielectric resonators in the cut-off waveguide are proposed and tested. The height of the cut-off waveguide is 5 mm. The input and output sides of this cut-off waveguide are connected to a waveguide which tapers gradually from the rectangular waveguide of standard dimensions.

2. Experiment

Two types of filters are considered. For the first filter, the width and length of the cut off waveguide are 7mm and 8 mm, respectively. A resonant circuit mounted with a cube dielectric resonator was constructed in the center of this cut-off waveguide. The output side of this resonant circuit was connected to a rectangular waveguide 4 mm in length. An other similar resonant circuit was connected on the other side of this rectangular waveguide to make the first filter. When TE_{10} mode is incident, the mode of the cube dielectric resonator mounting in the cut off waveguide is TE_{100} . The experiments were carried out at the 10 GHz band. The center frequency of this

filter was 9.95 GHz. The band-width and insertion loss were obtained 0.5 GHz and 1 dB, respectively.

The attenuation characteristics of this filter was obtained a steep slope.

For the second filter, a brass plate is placed at a position of $a/2$ of the rectangular waveguide and the rectangular waveguide consists of two cut-off waveguides. The length and thickness of the brass plate are 7 and 5 mm, respectively. Two resonant circuits mounted with a cube dielectric resonator was placed in the center of each cut-off waveguide were constructed, and a rectangular waveguide was connected behind these resonant circuits, another similar circuit was connected on the other side of the rectangular waveguide to make the second band pass filter. This filter consists of four resonant circuits. The construction of the filter is shown in Fig. 1. The frequency characteristics are shown in Fig. 2. The center frequency is 9.7 GHz. The band-width and insertion loss were obtained 0.96 GHz and 0.4 dB, respectively.

3. Conclusion

This paper describes new band-pass filters mounted with cube dielectric resonators in the cut-off waveguide for 10 GHz band. The frequency characteristics of these filters are obtained comparatively good characteristics.

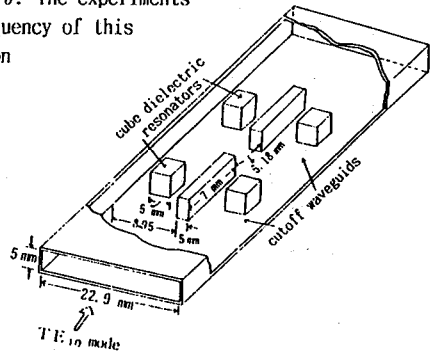


Fig. 1. Construction of bandpass filter

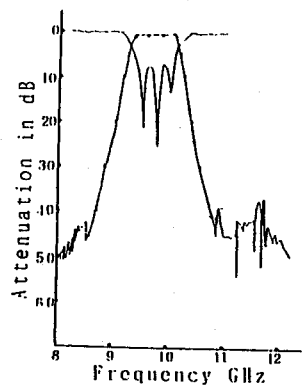


Fig. 2 Frequency characteristic of filter show in Fig. 1

A Novel Method for Suppressing Spurious Resonance Responses of the Coaxial-Resonator Bandpass Filters

Kouji Wada, Yasumasa Noguchi, Hidetaki Fujimoto and Junya Ishii

KINKI UNIVERSITY

Department of Electronic Engineering, 3-4-1 Kowakae,
Higashi-Osaka City, Osaka 577, Japan, FAX: +81-6-727-2024

Abstract

Recently, mobile communication systems are changing from analog systems to digital systems. Then, the microwave filters are required very severer specifications such as the lower insertion losses, the suppressing spurious resonance responses over the wide frequency range and the getting finite attenuation poles near by the passband. One of the recent trends in those apparatus is to adopt the new materials which have the high dielectric constant and almost independent on the variation of temperature. In these equipments, the dielectric coaxial-resonator filters are widely used.

We present a novel method for suppressing spurious resonance responses over the wide frequency range for the bandpass filters (BPFs) that are constructed by the $\lambda_{g0}/2$ coaxial-resonators with the tapped-line feed (Fig. 2). Furthermore, the transmission characteristics of the new type coaxial-resonator BPFs have the finite attenuation poles at the lower and/or the upper sides of the passband. In the simulation, the new type coaxial-resonator BPFs were suppressed more than -60.0dB between 4.0 and 20.0 GHz at the center frequency of the passband f_0 is equal to 2.0 GHz, because we take the tapped-line feed instead of the capacitor-feed and the coaxial-resonators were attached to the lumped-capacitors in ground and adjusted the length shorter (around $\lambda_{g0}/10$) than the original length (Fig. 4). We found that the transmission characteristics of the new type coaxial-resonator BPFs have the finite attenuation poles at the lower and/or the higher sides of the passband by conditions for the tapping positions on the coaxial-resonators and the spurious resonance responses are suppressed over the wide frequency range.

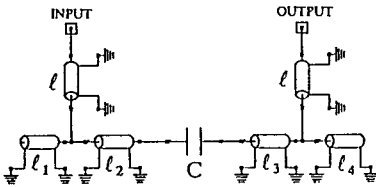


Fig. 1 $\lambda_{g0}/2$ Coaxial-Resonator BPF

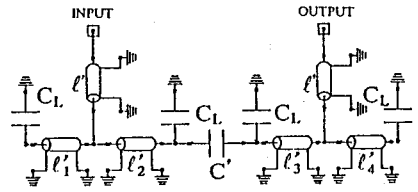


Fig. 2 Spurious Suppression Type Coaxial-Resonator BPF

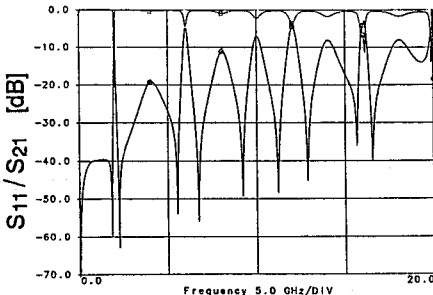


Fig. 3 Transmission Characteristics of $\lambda_{g0}/2$ Coaxial-Resonator BPF

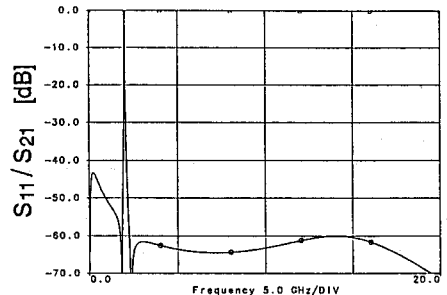


Fig. 4 Transmission Characteristics of Spurious Suppression Type Coaxial-Resonator BPF

A Power Amplifier Based on an Extended Resonance Technique

Adam Martin*, Amir Mortazawi and Bernard C. De Loach Jr.

Department of Electrical and Computer Engineering
University of Central Florida
Orlando, FL 32816-2450

A power combining oscillator based on an extended resonance method was introduced (A. Mortazawi and B. C. De Loach Jr., IEEE Trans. Microwave Theory Tech., vol. MTT-40, 2397-2402, December 1992). Here a new power amplifier is presented which is based on an extended resonance technique. High power amplification is achieved using this technique which essentially places many transistors in parallel, and consequently multiplies the power handling capability of a single device by the number of devices employed while maintaining the gain of a single device amplifier. It does not require matching circuits for individual devices, and based on simulations performed it is less susceptible to transmission line losses than Wilkinson type combiners. This technique can yield very compact circuits and biasing the circuits is very simple.

To demonstrate the extended resonance power combining amplifier, a 10 GHz four device power amplifier was designed and fabricated. The active devices used were Alpha power GaAs MESFET chips AF035P1-00 having a gate length of 0.25 μm and a total gate periphery of 400 μm . Devices were biased at 5 volts with the drain current of 70 mA. The amplifiers were fabricated on a 31 mil thick Duroid™ substrate with $\epsilon_r = 2.3$. The small signal gain was measured to be 11.5 dB and maximum of 480 mW was obtained at 9.57 GHz with a power added efficiency of 30.8 %. When compared to a single device amplifier the results indicate that a combining efficiency of better than 90% was achieved.

An Active Ka-Band Antenna Element Amenable to Device Integration

D.J. Roscoe*, L. Shafai[^], M. Cuhaci, and A. Ittipiboon

Communications Research Centre
3701 Carling Ave., Ottawa, Ontario, K2H 8S2

[^]Antenna Laboratory
Department of Electrical and Computer Engineering
University of Manitoba, Winnipeg, Manitoba, R3T 5V6

Several antenna technologies and architectures have been proposed for the portable communications terminal operating at 20/30 GHz for receive and transmit, respectively. Microstrip technology is a preferred candidate because the overall array architecture is well suited to the portability aspect of the terminal. However, to overcome the effects of the losses within a microstrip feed network, and to improve the overall efficiency, it is preferred to distribute amplifiers throughout the array. Within a corporate type feed network, issues such as device integration and thermal properties become critical. From a cost perspective, a preferred array architecture would have modular active devices which can easily be removed for repair or replacement if required. This implies that the devices should be on carriers which can be secured to the ground plane without solder. The array architecture should also utilize aperture coupling as the feed mechanism for the antenna elements. This reduces the amount of physical intervention with the array (as compared with probe feeding).

This paper presents an element which addresses the issues identified above. To fasten the carrier housing the amplifiers, a thick ground plane is required. However, as identified in (P.R. Haddad and D.M. Pozar, *Elect. Let.*, Vol. 30, No. 14, pp. 1106-1107, July 1994), efficient coupling to a standard microstrip patch antenna through a thick ground plane has yet to be resolved. Thus a novel element was developed. The resulting antenna structure is a cavity type microstrip element. The cavity is formed from a thick ground plane where a microstrip element is used to feed the cavity. Hence, coupling from the feed line occurs through a thin ground plane within the cavity, while device integration can be done using the thick ground plane outside the cavity. The passive antenna element is designed to yield gains of approximately 15 dBi. In addition to the mechanical advantages, the high gain obtained from this element is well suited for the application of an array for the personal communications terminal since fewer elements are required in comparison to an array using solely microstrip patches. This in turn reduces the size of the feed network and the required electronics. The measured results and mechanical aspects will be presented.

A Dynamical Analysis of the CMOS Circuit

Jilin Tan* and Guangwen Pan
University of Wisconsin, Milwaukee

Abstract

Recently, extremely lossy dielectrics have found applications in electronic systems. In CMOS circuits, the gate regions of the MOS transistors are usually doped heavily. The metal interconnects are deposited above these heavily doped substrates, resulting in a high capacitance from the metal lines to the substrate. It is difficult, however, to compute the design parameters, including the characteristic impedance, propagation delay, and cross talk, for the heavily lossy dielectrics, for which the loss tangents can be 10^5 or higher.

Beginning with the rederived dyadic Green's function for multilayered media, the integral equation of the first kind for the unknown current is formulated. This integral equation is then solved by the method of moments using Galerkin's procedure. The results of the field solutions are transformed into the equivalent circuit parameters of R, L, C, G, so that they can be directly utilized by digital electronic engineers in the design work. The mutual capacitance of the buried microstrip lines above a lossy layered substrate has been evaluated and compared with laboratory measurements with good agreement. It is not surprising that the results of many other software packages fail to predict correct mutual capacitances for the test coupons, since the quasi-static and small perturbation assumptions are no longer applicable to such lossy dielectrics.

References

- [1] W. Chew, *Waves and Fields in Inhomogeneous Media*, Van Nostrand Reinhold, New York, 1990.
- [2] Chih-Wen Kuo and Tatsuo Itoh, "Characterization of shielded Coplanar Type Transmission Line Junction Discontinuities Incorporating the Finite Metallization Thickness Effect," *IEEE Trans., Microwave Theory Tech.*, vol. MTT-40, no. 1, pp73-80, Jan. 1992.

Optical Temperature Sensor Using Surface Plasmon Resonance Technique

Şahin Kaya Özdemir * and Gönül Turhan-Sayan
Middle East Technical University
Department of Electrical and Electronic Engineering
06531 Ankara, Turkey

Various optical phenomena (absorption, fluorescence, reflection, etc.) have been used for chemical, physical and biomedical sensing. Surface Plasmon Resonance (SPR), a resonance condition in which surface plasmon waves (SPWs) propagate along the interface between two media having dielectric constants of opposite sign - a metal and a non-metal - is yet another optical phenomenon that can be used for sensor applications. As a surface wave the characteristics of SPW are very sensitive to the changes in the refractive indices of bulk and thin-film layers and to the thicknesses of thin films.

The objective of this paper is to briefly describe a novel application of SPR technique in temperature sensing. The stimulated temperature sensor employs the excitation of SP in Kretschmann's geometry with a sensing layer whose refractive index is strongly temperature dependent. The changes in the refractive index of the sensing layer will cause a shift in the resonance angle and it will also cause a change in full width at half maximum of the resonance curve. By measuring the SPR curve parameters (resonance angle, θ_{sp} , full width at half maximum, $\Delta\theta$ and the intensity of the reflected light at resonance angle, R_{min}) one can compute the refractive index of the sensing layer using multilayer dispersion equation. Consequently, the temperature of the environment can be calculated by using the relation between temperature and the refractive index of the sensing layer. The sensor geometry is composed of a prism, a metal layer and a sensing layer. As recent studies on temperature sensors have shown that refractive indices of polymers show a strong dependence on temperature, the sensing layer in this study is chosen to be a polymer thin film. In the meantime, the effect of temperature variation on the refractive index of the metal film and the the bulk will also be taken into consideration.

Optimization of the sensor geometry (metal and polymer type to be used and the thicknesses of these films, wavelength of the incident light), sensitivity considerations and the comparison of this sensor with the traditionally used optical temperature sensors will also be discussed.

Numerical Methods

K. K. Mei and V. Jamnejad

Page

- 1:20 A 3D High-Order Unstructured Finite-Volume Algorithm for370
Solving Maxwell's Equations
Yen Liu, NASA Ames Research Center
- 1:40 Three-Dimensional Calculations Using Impedance Matrix 371
Localization
Francis X. Canning, Rockwell Science Center, Erik Rosen, SFA, Inc.,
Luise Schuetz Couchman, Naval Research Laboratory*
- 2:00 Confirming the Invariance of the Measured Equation of Invariance ...372
Kenneth K. Mei, Yaowu Liu, City University of Hong Kong*
- 2:20 Finite-Difference Analysis of Circular Dielectric-Loaded373
Waveguides
Jenn-Ming Guan, Private China Junior College of Technology,
Da-Chiang Chang, National Tsinghua University*
- 2:40 Implementation of an Infinite Ground Plane in a 2-D 374
TLM Network
John B. Erwin, Stuart M. Wentworth, Auburn University*
- 3:00 BREAK
- 3:20 High-Frequency Asymptotic Reduction of the Fast Multipole375
Method
Robert J. Burkholder, Do-Hoon Kwon, Ohio State University*
- 3:40 Resource Management in Time-Domain Maxwell Solvers376
A. H. Mohammadian, W. F. Hall, V. Shankar, Rockwell International
Science Center*
- 4:00 Et-Ht FEM Modal Analysis of Transversely Periodic Waveguides377
Eric W. Lucas, Thomas P. Fontana, Westinghouse Electric Corporation*
- 4:20 Degeneration of Rectangular and Triangular Rooftop Functions378
in the Discretisation of Planar Structures
*Jeannick Sercu, University of Ghent, Niels Fache, HP-Belgium,
Paul Lagasse, University of Ghent*
- 4:40 An Unstaggered, Colocated Scheme for Solving Maxwell's379
Equations in Curvilinear Coordinates
Ramakrishna Janaswamy, Naval Postgraduate School, Yen Liu,
NASA Ames Research Center*
- 5:00 Fast-Multipole-Method Solution of Two-Dimensional380
Conductor Geometries
Levent Gurel, Bilkent University

A 3D High-Order Unstructured Finite-Volume Algorithm for Solving Maxwell's Equations

Yen Liu

NASA Ames Research Center
Moffett Field, CA 94035

A three-dimensional finite-volume algorithm based on arbitrary basis functions for time-dependent problems on general unstructured grids is developed. The method is applied to the time-domain Maxwell equations. Discrete unknowns are volume integrals or cell averages of the electric and magnetic field variables. Spatial terms are converted to surface integrals using the Gauss curl theorem. Polynomial basis functions are introduced in constructing local representations of the fields and evaluating the volume and surface integrals. Electric and magnetic fields are approximated by linear combinations of these basis functions. Unlike other unstructured formulations used in Computational Fluid Dynamics, the new formulation actually does not reconstruct the field variables at each time step. Instead, the spatial terms are calculated in terms of unknowns by precomputing weights at the beginning of the computation as functions of cell geometry and basis functions to retain efficiency. Since no assumption is made for cell geometry, this new formulation is suitable for arbitrarily defined grids, either smooth or unsmooth. However, to facilitate the volume and surface integrations, arbitrary polyhedral cells with polygonal faces are used in constructing grids. Both centered and upwind schemes are formulated. It is shown that conventional schemes (second order in Cartesian grids) are equivalent to the new schemes using first degree polynomials as the basis functions and the mid-point quadrature for the integrations. In the new formulation, higher orders of accuracy are achieved by using higher degree polynomial basis functions. Furthermore, all the surface and volume integrations are carried out exactly.

Several model electromagnetic scattering problems are calculated and compared with analytical solutions. Examples are given for cases based on 0th to 3rd degree polynomial basis functions. In all calculations, a centered scheme is applied in the interior, while an upwind matching scheme is employed at material interfaces and the Engquist-Majda non-reflecting boundary condition is implemented at the numerical outer boundaries. The staggered leapfrog scheme and the Runge-Kutta methods are utilized for the time integration. Excellent agreements are found between the numerical and analytical solutions.

THREE-DIMENSIONAL CALCULATIONS USING IMPEDANCE MATRIX LOCALIZATION

Francis X. Canning*
Rockwell Science Center
Thousand Oaks, CA 91360

Erik Rosen
SFA Inc.
Landover, MD

Luise Schuetz Couchman
Naval Research Laboratory
Washington, DC.

The Impedance Matrix Localization (IML) method is used to solve the wave equation (i. e. the Helmholtz equation) in three-dimensions. The problem considered is a scalar field with specified derivative (Neuman condition) on a surface. This corresponds, e.g., to acoustic scattering by a rigid body.

Directional expansion functions are used on a two-dimensional surface. The calculation of matrix elements must be done so that the cost of integrating over these functions is small. The matrix **A** contains values of the Green's function. **W** contains the products of weights of a quadrature formula and values of the taper function part of the expansion functions. The oscillating part of the expansion functions will be contained in a matrix **F**. The moment method matrix **T'** is then calculated as:

$$\mathbf{T}' = \mathbf{F} (\mathbf{W} \mathbf{A} \mathbf{W}^t) \mathbf{F}^t$$

A further efficiency comes from giving **F** many more rows than columns and zeroing certain elements of **T'** giving **T** (**F**. X. Canning, Radio Science, 29, 993-1008, 1994). Actually, these matrix elements are not even calculated to reduce the cost of the multiplication by **F**. The integral equation used in **A** has currents which only radiate to the exterior so that **T** is banded and sparse within that band. Sparse LU decomposition then efficiently solves the matrix problem.

Confirming The Invariance Of The Measured Equation Of Invariance

**By Kenneth K. Mei* and Yaowu Liu
Department of Electronic Engineering
City University of Hong Kong**

Abstract

Since the first presentation of the concept of the Measured Equation of Invariance (MEI) by Mei et al.(IEEE AP-S International Symposium, Chicago, 1992) many researchers have tested the concept and obtained good results, and a few have raised doubts about the validity of the basic postulate that the linear relations of the neighboring nodal field values at the terminating surface are invariant to incident fields, (Jevtic and Lee, IEEE Trans. AP Vol.42, No.8,pp.1097-1105, Aug.1994). In this paper it is shown that Jevtic and Lee's analysis is incorrect and their computations showing the deterioration of the results using MEI at high frequencies is actually caused by numerical errors in finding the MEI coefficients and not because of the failure of the postulate of invariance. When the mesh terminating surface is brought close to the object surface, typically two discretization steps away, the demand on the accuracy of the MEI coefficient increases. Single precision arithmetics and quadratic finite difference are only good for low frequencies. For high frequency problems it is necessary to use double precision and higher order finite difference. Although we assert that "Invariance to incident fields" is not equal to "Invariance to the Metron sets", it is satisfying to show that if discretization errors are minimized by using higher order approximation and double precision arithmetics, one can actually make the solutions practically independent of the choice of Metron sets. So, the postulate of invariance is confirmed.

Finite-Difference Analysis of Circular Dielectric-Loaded Waveguides

Jenn-Ming Guan[†] and Da-Chiang Chang^{*}

^{*} Private China Junior College of Technology, Taipei, Taiwan

[†] Department of Electrical Engineering, National Tsinghua University, Hsinchu, Taiwan

Dielectric-loaded waveguides of circular symmetry are commonly used in many microwave systems. The general configurations which can be analyzed in present investigation are shown in Fig. 1. with the piecewise-continuous dielectric constant distributions $\epsilon(r)$. The whole structures are assumed to be lossless. The matrix eigenvalue problems resulting from the finite-difference method to the governing differential equations are solved by the modified simultaneous iteration with the Chebyshev acceleration method (C. C. Su & J. M. Guan, IEEE MTT, to appear). This algorithm for sparse matrix eigenproblems involves no operations corresponding to matrix inversions. As a result, very fine discretizations associated with finite-difference method can be done and hence accurate results can be obtained efficiently. The complex modes in this lossless waveguide can also be treated by the present approach if they exist. Compared to the standard approach by solving the complicated characteristic equations (H. Lin & K. A. Zaki, IEEE MAG, 2950-2952, 1989), the present finite-difference method is more convenient especially when multilayer structures are considered.

Using the two transverse magnetic fields (C. C. Su, IEEE MTT, 328-332, 1986), the governing equations for the guided modes with the azimuthal dependence $e^{-jm\theta}$ are :

$$\Psi'(r) + \frac{1}{r}\Psi(r) + \left[\epsilon(r)k_0^2 + \gamma^2 - \frac{(1+m^2)}{r^2} \right] \Psi(r) - \frac{2m}{r^2} \Phi(r) - \frac{\epsilon'(r)}{\epsilon(r)} \left[\Psi'(r) + \frac{\Psi(r)}{r} + \frac{m}{r} \Phi(r) \right] = 0 \quad (1a)$$

$$\Phi'(r) + \frac{1}{r}\Phi(r) + \left[\epsilon(r)k_0^2 + \gamma^2 - \frac{(1+m^2)}{r^2} \right] \Phi(r) - \frac{2m}{r^2} \Psi(r) = 0, \quad (1b)$$

where $\Psi = H_z$, $\Phi = jH_r$, and the propagation constant $\gamma = \alpha + j\beta$. The associated boundary conditions at the permittivity discontinuity are the continuity condition of the fields H_z and E_z by using the divergent and curl equations of the magnetic field, respectively. For the azimuthally invariant modes ($m=0$), Ψ and Φ are uncoupled. Hence, (1a) and (1b) are the governing equations for the TM and TE modes, respectively. A standard matrix eigenvalue problem can be obtained by applying the finite-difference method to the equations (1). The numerical results for the dispersion characteristics of the first ten modes with $m=2$ are shown in Fig. 2. with $a=0$, $b=0.4$ in, $c=0.6$ in, $\epsilon(a < r < b) = 35.59$, and $\epsilon(b < r < c) = 1$. These results are in good agreement with those in the literature (C. Chen & K. A. Zaki, IEEE MTT, 1455-1457, 1988).

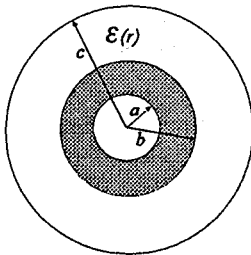


Fig. 1

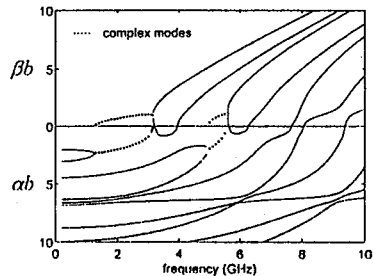


Fig. 2

Implementation of an Infinite Ground Plane in a 2-D TLM Network

John B. Erwin and Stuart M. Wentworth*

Department of Electrical Engineering

200 Broun Hall, Auburn University, Alabama 36849-5201

We investigate the scattering from a conducting cavity mounted in an infinite ground plane using the two-dimensional TLM method. To obtain the echowidth, the scattered fields along a virtual boundary surrounding the scatterer are determined. These scattered fields can be represented by the electric and magnetic currents that are integrated over a closed surface to determine the far field pattern. However, the equivalence principle shows that only the currents present in the aperture are needed to calculate the far field. Therefore, the closed loop integration simplifies to an integral over the aperture because the currents are zero elsewhere. In implementing TLM to solve this problem, the challenge lies in simulation of an infinite-appearing ground plane with a finite size mesh. We address how the incident plane wave can be simulated, and how the boundaries can be manipulated to make the ground plane appear infinite.

In order to model an incident plane wave, we employ an injection technique which involves running two concurrent TLM networks. One network determines the incident fields with the scatterer omitted and magnetic walls to guide the incident wave. The other network includes the scatterer and truncates the mesh with absorbing boundaries. The total fields may be determined in this second network by injecting pulses from the incident fields case. Each time step, the pulse values at each port along the magnetic walls in the incident fields case are injected into the corresponding ports along the absorbing walls in the total fields case. These injections allow the plane wave to appear non-attenuating. In the present work we employ wide-band absorbing boundaries (R. L. Higdon, "Numerical Absorbing Boundary Conditions for the Wave Equation," *Math. Computation*, Vol. 49, No. 179, pp. 65-90, July 1987) based on perfect absorption of waves at two incident angles.

Our approach to modeling an infinite ground plane in a finite TLM mesh is to employ a similar pulse injection technique to maintain the integrity of the plane wave reflected from the ground plane. For a normally incident plane wave, the incident fields and the fields scattered from the ground plane may be maintained along the boundary by using magnetic boundaries. However, if an element is mounted in the ground plane, then the magnetic walls would interfere with waves scattered from this element. An absorbing boundary is required to prevent re-scattering.

Our problem therefore requires simulation of both an incident plane wave and a plane wave reflected from an infinite ground plane while simultaneously absorbing the fields scattered from the cavity. To solve this problem, pulses are injected along the mesh borders which maintains the integrity of both plane waves. These pulses are determined directly from a one-dimensional string of nodes which represents a ground plane in free space, due to symmetry. These pulses inherently give the effects of an infinite ground plane, while the TLM mesh may be truncated with a finite ground plane consisting of only a few nodes. Echowidth results are presented which verify this approach.

HIGH-FREQUENCY ASYMPTOTIC REDUCTION OF THE FAST MULTIPOLE METHOD

Robert J. Burkholder* and Do-Hoon Kwon
The Ohio State University ElectroScience Laboratory
Department of Electrical Engineering
1320 Kinnear Road, Columbus, Ohio 43212

The fast multipole method (FMM) has been demonstrated to be very useful for increasing the efficiency of iterative solutions for large-scale electromagnetic integral equation problems (R. Coifman, V. Rokhlin, & S. Wandzura, *IEEE AP Magazine*, 35(3), 7-12, 1993). A straight-forward implementation of the method reduces the operational count of a matrix-vector multiplication from $O(N^2)$ to $O(N^{3/2})$ for large N (where N is the number of unknowns). Multistage recursive nesting of the FMM algorithm further reduces the count to $O(N^{4/3})$, $O(N^{5/4})$,...; however, nesting algorithms greatly increase the complexity of the implementation for realistic problems. Wagner and Chew (*IEEE APS Symposium Digest*, 427-430, 1994) showed that an operational count of $O(N^{4/3})$ could be achieved without nesting by making use of the directional property of the FMM translation operator T . In the FMM, subsectional basis functions are divided locally into groups and the interactions between groups are found using a multipole expansion with a translation theorem. It was shown that T can be evaluated in closed form for groups which are separated by far-field distances, resulting in a sinc function centered around the line connecting the two groups. This allows the plane waves in the multipole expansion to be filtered out by a windowing function if they propagate in directions away from the main beam of the sinc function. The operational count is reduced because the number of plane wave interactions between groups is reduced for far-field spacings.

In this paper, T is evaluated asymptotically for electrically large geometries yielding a uniform expression which is valid for all spacings between groups and is not limited to only far-field spacings. The expression may be used to efficiently compute T , which would otherwise require computing a finite sum of Hankel functions, but it is more valuable for giving physical insight into the directive properties of the translation operator. It clearly indicates the plane wave interactions which must be included between two given groups, and defines the width of the windowing function for excluding plane waves which propagate away from the line connecting the groups. As one would expect, more plane waves need to be included for closer spacings between groups. The derivation will be for the 2-D case, but the same approach may be applied to 3-D. Numerical results will be presented to demonstrate the accuracy and operational count of the asymptotically reduced FMM.

Resource Management in Time-Domain Maxwell Solvers

A. H. Mohammadian†, W. F. Hall, and V. Shankar

Rockwell International Science Center
1049 Camino Dos Rios
Thousand Oaks, CA 91360

This paper proposes some techniques for explicit time-domain Maxwell solvers (FVTD, FDTD, TLM, etc.) to reduce memory requirement for computing radar cross section (RCS) of large objects such as aircraft. Also, convergence criteria for both time-harmonic and pulse excitations are discussed to ensure the convergence of the numerical solution to a level desired by the user without having to guess the number of time marching steps before hand. These techniques have been implemented in our FVTD vector code (RCS3D) and parallel code (RCSMPP). Variations of these techniques might be appropriate for other explicit time-domain solvers.

Real life objects often have a plane of symmetry. Exploiting this feature reduces the size of the problem by a factor of two, which for an electrically large object results in huge memory savings. This way the frequency limit for RCS computation on a given platform can be doubled. This has already been worked out for method of moment codes. However, in the time-domain solvers these authors have not come across such a technique. We will present this technique by introducing the concept of "diffracted field" formulation for Maxwell's equations, when an object is over an "electric" ground plane ($\hat{n} \times \vec{E} = 0$) and a "magnetic" ground plane ($\hat{n} \times \vec{H} = 0$). Then, we will show how the computation for half of the object can lead to the RCS for the whole object for any arbitrary angle of incidence. We will also show how our technique can easily be generalized to more than one plane of symmetry.

Another technique to save memory is concurrent RCS computation. This involves evaluation of the RCS concurrent with the main solver for every time step instead of leaving RCS computation to the postprocessing stage. For example, for an object with one million surface cells, storage of $\hat{n} \times \vec{E}$, $\hat{n} \times \vec{H}$, and the surface coordinates requires close to 10 MW of additional memory. The proposed concurrent RCS computation eliminates this huge memory usage. All that is needed is the space to store the RCS at the desired directions and frequencies (if the excitation is a pulse).

Finally, an easy mechanism to check the convergence of the computation in terms of the final RCS results will be discussed. This convergence criterion will help save computation time, especially for problems where an apriori guess for the number of time steps based on the object size may not be good enough and may result in either under converged results or too much cpu usage.

$E_t - H_t$ FEM Modal Analysis of Transversely Periodic Waveguides

**Eric W. Lucas* and Thomas P. Fontana
Antenna/Apertures and Integrated Sensors Department
Westinghouse Electric Corporation
P.O. Box 746
Baltimore, Maryland 21203**

This presentation discusses the application of the variational vector finite element method to the eigenmode analysis of general uniform waveguides or transmission lines which are transversely arrayed in a singly or doubly infinite periodic lattice. The $E_t - H_t$ variational formulation follows that previously presented by the authors (E. W. Lucas and T. P. Fontana, IEEE AP/S Digest, 1994, T. P. Fontana and E. W. Lucas, IEEE AP/S Digest, 1994), however, with the additional inclusion of the generalized periodic boundary conditions (PBC's) over the unit-cell cross-section. The generalized PBC's include not only a constraint on the geometric periodicity of the structure but also the related "Floquet" or complex "phase-wall" constraint as well. For isotropic media (or in general reflection-symmetric media), one expects the modal spectrum to be bi-directional and the linear system self-adjoint with respect to the reaction (unconjugated) inner-product. The orthogonality properties of such modes follow from these concepts as is well known. However, the introduction of the generalized PBC's to the same bi-directional reflection symmetric system produces a (reaction) non-self-adjoint linear system whose adjoint corresponds to the appropriate dual waveguide. The generalized biorthogonality properties for such modes follow from these concepts. Other non-self-adjoint systems can arise for waveguides which include some types of non-reflection-symmetric media or general non-reciprocal media. The present formulation may be applied to periodic arrangements of such structures directly.

The authors have found use for such numerically generated periodic modes for the application of the modal BEM or "port" procedure in a 3D vector FEM periodic array formulation for phased-array antenna applications. (E. W. Lucas and T. P. Fontana, IEEE Trans. Antennas Propagat. [to appear Feb. 1995]).

DEGENERATION OF RECTANGULAR AND TRIANGULAR ROOFTOP FUNCTIONS IN THE DISCRETISATION OF PLANAR STRUCTURES

Jeannick Sercu* (IWT), Niels Faché** and Paul Lagasse*
*Department of Information Technology (INTEC), University of Ghent
Sint-Pietersnieuwstraat 41, 9000 Ghent, Belgium
** HP-Belgium, Lammerstraat 20, 9000 Ghent, Belgium

Abstract.

Over the past decade, the application of numerical field simulation techniques for the time-harmonic characterisation of planar scatterers and antennas in open media has broadened considerably. In many of these simulation techniques, the electromagnetic behaviour of the planar structure is governed by an integral equation in the unknown surface currents flowing on the planar metallization patterns. This integral equation is solved numerically by applying the method of moments. The planar structure is hereby subdivided or discretized into a mesh of rectangular and/or triangular cells. Subsectional basis functions defined over the cells of the mesh are used in the modelling of the surface current distribution. Due to the current continuity condition, the normal component of the discretised current need to be continuous across the boundaries of adjacent cells in the mesh. This follows from the observation that unphysical Dirac line charges have to be avoided, in order to have a physical acceptable numerical solution. The tangential component of the current however is allowed to jump across the intercell boundaries.

A set of basisfunctions for which these requirements are fulfilled are the vector-valued rooftop functions defined over a rectangular or triangular cell. Several researchers have reported the successful application of rectangular and triangular rooftop functions in the simulation of microstrip and slotline discontinuities and antennas. With each side of the cell, one rooftop function is associated, which models the normal component of the current flowing across the cell side. This function is constant along the corresponding side, and varies linearly to zero along the adjacent sides of the cell. Rooftop functions with rectangular support have only one component in the direction normal to the corresponding cell side. Rooftop functions with triangular support however also have a component tangential with the cell side. This component is necessary to obtain the continuity of the normal current component across the adjacent cell sides in the triangular cell.

In this paper, we consider the situation in which one of the cells in the mesh becomes very narrow or "degenerates". It follows that the contribution of the normal component decreases to zero. The tangential component however continues to contribute even in the limit of a triangular cell completely degenerated into a line segment. In this case, the tangential component is degenerated into a Dirac line current along the line segment. We have investigated the effect of degenerated triangular cells in the method of moment solution of microstrip discontinuities. It is well known in finite element analysis that almost degenerated triangular cells must be avoided, since they introduce mathematical instabilities in the solution process. The main conclusion of our study is that degenerated triangular cells in the method of moments do not affect the numerical results as long as the contributions of the tangential components of the vector-valued rooftop functions are taken into account accurately in the numerical solution process.

An Unstaggered, Colocated Scheme For Solving Maxwell's Equations in Curvilinear Coordinates

Ramakrishna Janaswamy^{1,*}

Yen Liu²

¹Code EC/Js, Naval Postgraduate School, Monterey, CA 93943

²NASA Ames Research Center, Moffet Field, CA 94035

Over the years, the Finite Difference Time Domain (FDTD) method has emerged as a powerful technique for modeling many electromagnetic problems. The basic FDTD algorithm was first described by Yee (*IEEE Trans. Antennas Propagat.*, (14), 302-307, 1966) and later refined by many authors. The method is based on a staggered central differencing in space and staggered leapfrog integration in time. This results in second order accuracy in both space and time. To be able to accurately model physical geometries, formulation in curvilinear coordinates is necessary. Generalization and practical implementation of Yee's algorithm to curvilinear coordinates was carried out by Fusco (*IEEE Trans. Antennas Propagat.*, (38), 76-88, 1990). However, because of the fact that the various field components are not defined at the same location, certain ambiguities and inaccuracies will result when Yee's algorithm is formulated in a curvilinear coordinate system. Furthermore, the advantages of a staggered grid over an unstaggered one would be lost as the size of the stencil is increased. To preserve the accuracy, the complete vector field must be defined at any spatial location.

In the present approach, we present an unstaggered, colocated scheme which removes the aforementioned difficulties of the FDTD method. The scheme was first described by Liu (*AIAA Paper* 93-0368, 1993) and is based on one-sided, antisymmetric differencing for the electric and magnetic field components for the spatial derivatives. The electric and magnetic field vectors are both defined at the same location. Because of these the scheme can be easily generalized to a curvilinear coordinate system with no ambiguities. We will consider both first and higher order differencing. Surprisingly, the results with first-order, antisymmetric differencing have the same order of accuracy as the Yee scheme. We will consider a two-dimensional version of the scheme and formulate the problem in a curvilinear coordinate system. Results will be presented for various test geometries to establish the power and convenience of the scheme.

Fast-Multipole-Method Solution of Two-Dimensional Conductor Geometries

Levent Gürel

Dept. of Electrical and Electronics Engineering

Bilkent University

Bilkent, Ankara, Turkey

Electromagnetic radiation and scattering problems involving two-dimensional arbitrary conductor geometries are formulated using integral-equation techniques and solved using a number of methods including the fast multipole method (FMM). The excitation can be either an incident field or a finite source. Both TE and TM polarizations are considered. The current induced on the conductor geometry is discretized to convert the integral equation into a matrix equation. Equivalently, the discretized current elements can be thought of as two-dimensional subscatterers (strips) put together to construct the desired geometry.

In order to compare the accuracy and the efficiency of the FMM solution, two reference solutions are obtained. First, a direct solution technique (e.g., Gaussian elimination) is employed to solve the resulting matrix equation. Then, the same matrix equation is solved by using an iterative scheme (e.g., CG or GMRES), in which every iteration involved a matrix-vector multiplication. Finally, in a third solution, the ordinary matrix-vector multiplication is replaced by FMM in the same iterative scheme. The FMM employed here uses diagonalized translation operators for the two-dimensional Helmholtz equation. [V. Rokhlin, "Rapid solution of integral equations of scattering theory in two dimensions," *J. Comput. Phys.*, vol. 86, no. 2, pp. 414-439, Feb. 1990.]

It will be shown that the FMM requires $O(N^{1.5})$ operations per iteration as opposed to the matrix-vector multiplication being an $O(N^2)$ operation per iteration and the direct solution having $O(N^3)$ computational complexity. In addition to the estimates of computational complexities and memory requirements of these methods, their actual performances will also be compared and discussed. Examples of several two-dimensional arbitrary conductor geometries will be used in these comparisons.

Boundary Conditions

<i>F. X. Canning and W. A. Davis</i>		Page
1:20	Numerical Absorbing Boundary Conditions for the Scalar and Vector Wave Equations <i>Bruno Stupfel, Commissariat a l'Ennergie Atomique, Raj Mittra, University of Illinois</i>	382
1:40	Relationship Between Generalized Impedance Boundary Conditions and Absorbing Boundary Conditions <i>J. L. Volakis*, T. B. A. Senior, S. Legault, University of Michigan</i>	383
2:00	Comparison of Some Absorbing Boundary Conditions for the FDTD-Method <i>J. De Moerloose*, M. A. Stuchly, University of Victoria</i>	384
2:20	A Numerical Absorbing Boundary Condition for 3D Edge-Based Finite Element Analysis of Very Low Frequency EM Fields <i>Amir Boag*, Israel Aircraft Industries, Raj Mittra, University of Illinois</i>	385
2:40	Complementary Operators: A Method to Annihilate Artificial Reflections Arising from the Truncation of the Computational Domain in the Solution of Partial Differential Equations <i>Omar M. Ramahi, Digital Equipment Corporation</i>	386
3:00	BREAK	
3:20	Solution Accuracy Limitations Due to Mesh Features and Boundary Conditions using Edge-based Finite Elements <i>Jay W. Parker*, Cinzia Zuffada, Jet Propulsion Laboratory</i>	387
3:40	Functional Boundary Conditions for Variational Principles in Electrostatics <i>W. A. Davis, Virginia Polytechnic Institute and State University</i>	388
4:00	Optimization of the Berenger PML for FD-TD Simulations <i>Christopher E. Reuter*, Rome Laboratory/ERST, Rose M. Joseph, Northwestern University, Daniel S. Katz, Cray Research, Inc., Eric T. Thiele, University of Colorado, Allen Taflove, Northwestern University</i>	389
4:20	Wideband Absorbing Boundary Condition for FD-TD Simulations of Waveguiding Structures in 3-D <i>Christopher E. Reuter*, Rome Laboratory/ERST, Rose M. Joseph, Northwestern University, Daniel S. Katz, Cray Research, Inc., Eric T. Thiele, University of Colorado, Allen Taflove, Northwestern University</i>	390

NUMERICAL ABSORBING BOUNDARY CONDITIONS FOR THE SCALAR AND VECTOR WAVE EQUATIONS

Bruno Stupfel[†] and Raj Mittra[§]

[†] Centre d'Études de Limeil-Valenton, Commissariat à l'Énergie Atomique.
94195 Villeneuve St Georges cedex, France.

[§] Electromagnetic Communication Laboratory, University of Illinois.
Urbana, IL 61801-2991

For the 2D Helmholtz equation, it has been shown (Stupfel and Mittra, URSI Symposium, 1994) that the following numerical absorbing boundary conditions (NABCs) for terminating a finite difference or a finite element mesh

$$\partial_n u(M_0) = \sum_{j=0}^{N-1} c_j u(M_j) \quad (1)$$

become analytically equivalent to many existing absorbing boundary conditions in the limit the mesh size h tends to zero. In (1), the coefficients c_j are computed by solving a linear system of equations derived by using test waves that may be either plane waves or those radiated by line sources. In addition, the numerical efficiency of these NABCs can be evaluated by using the reflection coefficient for plane and cylindrical waves incident upon an arbitrary boundary as an indicator. In this paper, we extend this procedure to the study of NABCs, that are derived herein for the 3D scalar and vector wave equations from the point of view of their numerical implementation in node- and edge-based FEM formulations, respectively.

First, we consider the 3D scalar wave equation for which we demonstrate, analytically, the following important results. For the particular cases where the boundary is either locally planar or spherical, and the c_j 's are determined by using plane waves or spherical waves, we show that the NABC given in (1) tends in the limit to the analytical ABCs as the distance h between the points M_j tends to 0. The numerical efficiencies of these NABCs are evaluated by computing the reflection coefficient for plane or spherical waves incident upon a planar outer boundary.

The same procedure is repeated for the vector wave equation

$$\nabla \times \nabla \times \underline{E} - k^2 \underline{E} = 0, \quad \nabla \cdot \underline{E} = 0$$

for which we define the NABC as

$$\underline{z} \times \nabla \times \underline{E} = \sum_{j=0}^{N-1} \left[c_j^{x1} \underline{x} \underline{t}_1(M_j) + c_j^{x2} \underline{x} \underline{t}_2(M_j) + c_j^{y1} \underline{y} \underline{t}_1(M_j) + c_j^{y2} \underline{y} \underline{t}_2(M_j) \right] \cdot \underline{E}(M_j)$$

with the following definitions: At a point M_0 situated on the boundary S , the orthonormal vectors $\underline{x} = \underline{t}_1(M_0)$, $\underline{y} = \underline{t}_2(M_0)$, $\underline{z} = \underline{n}(M_0)$ constitute a local reference frame. The vectors $\underline{t}_1(M)$, $\underline{t}_2(M)$ are the tangents to S along the principal lines of curvature defined at M , and $\underline{n}(M)$ is the outward normal to S at M .

Numerical results illustrating the use of the above NABCs are included.

RELATIONSHIP BETWEEN GENERALIZED IMPEDANCE BOUNDARY CONDITIONS AND ABSORBING BOUNDARY CONDITIONS

J.L. Volakis*, T.B.A. Senior and S. Legault
Radiation Laboratory
Electrical Engineering and Computer Science Dept.
University of Michigan
Ann Arbor, MI 48109-2122
volakis@engin.umich.edu senior@eecs.umich.edu

The generalized impedance boundary conditions (GIBCs) are improvements to the standard impedance or Leontovich boundary conditions and have recently received much attention (Senior and Volakis, IEE Press, 1995) because of their higher accuracy in simulating material layers and coatings. Mathematically, this is achieved by including higher order derivatives of the fields and the order of the GIBC is equal to the highest order field derivative included in the boundary condition.

So far, the GIBCs have been exclusively used for simulating material surfaces, and were thought to be independent of the absorbing boundary conditions (ABCs). The latter are, of course, of particular importance in finite element and finite difference simulations, where they are used for truncating the computational domain. In this paper, it will be shown (for the first time) that the GIBC formalism can incorporate the ABCs as a special case. Specifically, it will be shown that GIBCs derived for simulating dielectric surfaces can recover the usual two- and three-dimensional ABCs (Bayliss-Turkel, 1980; Webb and Kanellopoulos, 1989; Chatterjee and Volakis, 1993). This is achieved by letting the relative material parameters approach unity and by making the appropriate changes in surface curvature. Rytov's method (Rytov, 1940) is used for the derivation of the GIBCs and the advantage of this method is the inclusion of terms relating to the curvature of the simulated surface. The resulting ABCs include the same curvature terms and are therefore more general than those presently in the literature. Moreover, Rytov's method allows for a systematic procedure in deriving higher order ABCs which can be applied conformal to the scattering or radiating body.

COMPARISON OF SOME ABSORBING BOUNDARY CONDITIONS FOR THE FDTD-METHOD

J. De Moerloose* and M.A. Stuchly - Electrical and Computer Engineering Department, University of Victoria, Victoria, B.C., V8W 3P6, Canada.

The general purpose of our study is to point out the strengths and weaknesses of the different ABC's in specific frequency ranges and to set up a rule of thumb for the distance between the boundary and the structure under consideration.

A number of recently proposed ABC's, such as Berenger's Perfectly Matched Layer (J.P. Berenger, EUROEM symposium, Bordeaux France, 1994) and a so-called Semi-Global RBC (J. De Moerloose and D. De Zutter, APS Symposium, Seattle, 1994), have been claimed to outperform standard Mur 2nd order conditions. To proof these assessments, some of the following canonical problems have been evaluated :

- 1) reflection of a plane wave from an infinite boundary (PML)
- 2) pulse study /point source (PML, SGRBC)
- 3) scattering from a PEC square cylinder (PML, SGRBC)

Due to the superposition principle, the basic properties of a given ABC can be derived from its behaviour under plane wave incidence (type 1). This however assumes that the influence of corners and 2nd order reflections can be neglected (which ought to be the case if the ABC is truly efficient). In the plane wave experiment, the evanescent or inhomogeneous plane waves are often ignored despite their importance, especially for low frequency interaction problems. This has been already pointed out in [2], where use has been made of a special operator to absorb the evanescent wave part.

In this paper a thorough comparison between PML,SGRBC and Mur 2nd order ABC will be presented. Numerical experiments of type 1,2 and 3 will be performed over a wide frequency range, i.e. a few Hz to tens of GHz. The reflective behaviour in experiments of type 2 and 3 will be related to the basic results obtained from plane wave reflection (type 1).

The SGRBC and Mur 2nd order ABC explicitly assume a homogeneous surrounding space and as such are not suited to absorb dispersive wave-types. In the absence of such assumption, a fourth experiment is necessary to enable comparison of the dispersive behaviour of different ABC's. A parallel plate waveguide can be considered the simplest dispersive structure. This structure will be used as the basic experiment of type 4.

A Numerical Absorbing Boundary Condition for 3D Edge-Based Finite Element Analysis of Very Low Frequency EM Fields

Amir Boag*

Israel Aircraft Industries, Dept. 2464
Ben-Gurion Airport 70100, Israel

Raj Mittra‡

EM Communication Lab
University of Illinois, Urbana, IL

For open region problems, it is necessary to couple, explicitly, the FEM computational domain to the unbounded free space external to the mesh region. To satisfy the radiation condition in the numerically rigorous sense, the FEM solution can either be matched to a modal expansion, or be combined with the Boundary Element Method. These non-local boundary conditions satisfy the truncation conditions exactly, albeit at the expense of spoiling the sparsity of the matrices generated in these formulations. This has prompted many workers to search for local boundary conditions, e.g., those developed by Bayliss-Turkel and Engquist-Majda, that have relatively little effect on the sparsity of the FEM matrix. Both, of these absorbing boundary conditions (ABCs) work well for the propagating waves; however, their performance is usually less than satisfactory when treating the evanescent waves. Consequently, these ABCs require that the truncation boundary be removed far away from the outer boundary of the scatterer/antenna in order to diminish the evanescent content in the outgoing field impinging upon the boundary. At very low frequencies (ELF/VLF), receding the boundary to a distances which is a significant fraction of the wavelength leads to unrealistically large meshes. And yet, numerical experiments show that, when the solution domain is only a small fraction of the wavelength in size, the conventional ABCs make the boundaries behave almost as though they were perfect magnetic conductors.

The objectives of this paper are to explore ways that circumvent the aforementioned problems with the conventional ABCs at very low frequencies, and to carry out a systematic development of accurate, reliable and local type of absorbing boundary conditions for the three-dimensional edge-based formulations of the FEM. The method followed herein is based upon the Numerical Absorbing Boundary Condition (NABC) concept introduced earlier by the authors (Amir Boag, Alona Boag, Raj Mittra and Yehuda Leviatan, "A numerical absorbing boundary condition for finite difference and finite element analysis of open structures," *Microwave and Optical Technology Letters*, vol. 7, no. 9, pp. 395-398, June 20, 1994). It begins by posing the problem of deriving the NABC as that of determining a numerical relationship that links the value of the field along a boundary edge to those at a selected number of neighboring edges. The numerical relationship is derived by imposing the conditions that the equations must be satisfied to within a certain tolerance, by *all* of the *outgoing* wave components impinging upon the boundary from its interior. The number of adjacent boundary edges linked by the NABC is kept constant over the boundary, while the NABC coefficients are determined via a procedure based on the Singular Value Decomposition (SVD) algorithm. The number of edges involved in the NABC is first determined by using the criterion that the satisfaction of the outgoing field condition be at least as accurate as the satisfaction of the FEM equations at the internal edges (edges away from the boundary). The normalized error in the FEM equations for the interior edges is also used as a threshold in the SVD regularization of the equations for the NABC coefficients. Numerical examples that illustrate the derivation and application of the NABC are included in the paper.

Complementary Operators: A Method to Annihilate Artificial Reflections Arising from the Truncation of the Computational Domain in the Solution of Partial Differential Equations

Omar M. Ramahi
Digital Equipment Corporation
PK03-1/R11
129 Parker St.
Maynard, MA 01754

An absorbing boundary operation is developed to minimize the artificial reflections that arise when truncating the computational domain of an open-region scattering or radiation problems. Referred to as the Complementary Operators Method (COM), this technique is based on the use of two boundary operators that are complementary in their action. By solving the problem with each of the two operators independently, and then averaging the two solutions, the first order reflections that arise from the radiated (scattered) field as it impinges on the outer boundary can be effectively annihilated.

In this work, the COM technique is applied in conjunction with the Finite Difference Time Domain method to solve general scattering problems. While significantly reducing the magnitude of artificial reflections arising from purely traveling waves, the major distinguishing feature of this new technique, however, is its effectiveness in dealing with evanescent modes which traditionally have been a major challenge for Absorbing Boundary Conditions (ABCs) in general. To demonstrate this feature, a numerical experiment is conducted in which the radiated field consists of a single evanescent mode. Results will be presented showing in detail how the first artificial reflection of the mode can be eliminated without any advanced knowledge or estimate of the decay rate of the wave. Numerical results will also be presented for a host of two-dimensional and three-dimensional representative geometries to demonstrate that the COM technique provides highly accurate solutions even when the outer mesh-terminating boundary is brought very close to the radiation or scattering structure, thus resulting in significant savings in both computer memory and time.

In addition to the enhanced accuracy over previously derived ABCs, the COM technique offers an additional computational advantage. Since the application of COM requires two independent calculations, the solution procedure can be made to run on two separate processors making this technique well-suited for multiple-processor machines.

SOLUTION ACCURACY LIMITATIONS DUE TO MESH FEATURES AND BOUNDARY CONDITIONS USING EDGE-BASED FINITE ELEMENTS.

Jay W. Parker* and Cinzia Zuffada,
Jet Propulsion Laboratory, California Institute of Technology
Pasadena, California, USA 91109

Full-wave finite element solutions to electromagnetic scattering problems have accuracy limitations due to properties of the mesh and boundary conditions. While this is well known, users frequently encounter poor solutions without the ability to track down the source of error. This is due to the diversity of error sources, and the limited options available for mesh generation, diagnostics, and display. In particular, edge-element mesh accuracy issues are largely neglected in popular commercial mesh generator products.

Recognized pathologies include condition number limits when elements are too large, too small, or too distorted; problems with wave dispersion in large meshes; special field solution regions near singularity-producing geometry; and hypersensitive geometry/excitation, where the true solution is near a resonance. These are briefly reviewed with examples. Diagnostic and display techniques are used to identify accuracy-limiting features of meshes formed with various strategies in test cases of interest, including scattering from a conducting cube and a half-metal, half-permeable sphere. Because accuracy is also limited by wave-absorbing boundary condition approximation, we compare solution for an approximate condition with an integral equation coupled condition at the truncation surface. The object of this continuing work is identification of robust mesh requirements for initial generation and adaptation with appropriate diagnostics. Initial results and recommendations are presented.

FUNCTIONAL BOUNDARY CONDITIONS for VARIATIONAL PRINCIPLES in ELECTROSTATICS

W. A. Davis

The Bradley Department of Electrical Engineering
Virginia Polytechnic Institute and State University
Blacksburg, VA 24061-0111

In electrostatics and other variational forms, it is common to minimize the magnitude square of $\nabla\phi$ or other energy related forms over the volume. However, such a minimum neither takes into account the boundary conditions or the forcing function f . The forcing function problem is typically accounted for by adding twice the weighted forcing function to the functional [Boundary Value Problems of Mathematical Physics, Vol. 1, I. Stakgold, Macmillan, 1967] (this can also be developed in a Lagrangian sense). The problem of accounting for the boundary conditions still remains. In the finite-element method, it is common to use either fixed Dirichlet boundary conditions or to leave the boundary free, obtaining what are commonly called natural-boundary conditions. The solution implications of these natural-boundary conditions are not always clear, though they are typically found to be reasonable in a numerical sense. For a more fundamental understanding of these boundary effects and the proper relationship to the true problem, it is desirable to determine the impact of natural-boundary conditions (and what they are) on an analytical form of solution.

The application of the concepts of variational principles are extended in this paper to include the variation of appropriate boundary terms. This extension is accomplished in a Lagrangian form similar to the incorporation of the forcing term. This allows us to directly incorporate the boundary effects into the variational problem. The procedures for the Dirichlet and Neumann boundaries are considered for Laplace's and Poisson's equations with the classic results obtained for Dirichlet (forcing the functional values at the boundaries) and the natural boundary conditions resulting for the Neumann boundaries. More importantly, the paper provides a basis for extending variational methods to include boundary effects directly, thus providing a mechanism for other problems of interest where the use of fixed or natural boundaries may not be clear.

Optimization of the Berenger PML for FD-TD Simulations

Christopher E. Reuter*¹, Rose M. Joseph², Daniel S. Katz³, Eric T. Thiele⁴,
Allen Taflove²

¹Rome Laboratory/ERST, 525 Brooks Road, Griffiss AFB, NY 13441-4505

²Northwestern University, EECS Department, Evanston, IL 60208

³Cray Research, Inc., 222 N. Sepulveda Blvd, Ste. 1406, El Segundo, CA 90245

⁴University of Colorado, ECE Department, Boulder, CO 80309

Berenger (J.P. Berenger, *J. Comp. Phys.*, 114, pp. 185-200, 1994) recently introduced a novel absorbing boundary condition (ABC) for the FD-TD electromagnetic simulation technique. This ABC called the perfectly matched layer (PML) has shown dramatic improvement over the traditional analytical ABCs similar to that presented by Mur (G. Mur, *IEEE EMC*, pp. 377-382, 1981). In fact, we have shown a reduction in the local error caused by the PML of more than 40 dB as compared to standard second-order Mur ABCs (D.S. Katz, et al., *IEEE MGWL*, pp. 268-270, 1994).

It is desirable obtain the minimum reflection possible from the PML. Three parameters control the magnitude of the numerical reflections at grid-PML interfaces; 1) the PML thickness, 2) the theoretical reflection at normal incidence, $R(0)$, as defined by Berenger, and 3) the spatial profile of the conductivity within the PML. Berenger reported limited results for conductivity profiles having constant, linear, and parabolic distributions. Furthermore, since computer resources are limited, the above three parameters must be optimized to meet the required model fidelity and to enable solution of the problem within limits of the available computer system. A thicker PML generally reduces reflections but requires larger memory and longer cpu run time. Modification of the remaining two parameters has insignificant effect on the required memory and run time. However, the relationship between these two parameters and the magnitude of the reflection is not obvious and warrants investigation.

We have performed numerical experiments to determine the optimal values for these parameters while limiting computational requirements. This paper will discuss the results of these experiments for both 2-D and 3-D FD-TD simulations. All computations were performed on either a Cray Research Y-MP or C-90.

Wideband Absorbing Boundary Condition for FD-TD Simulations of Waveguiding Structures in 3-D

Christopher E. Reuter^{*1}, Rose M. Joseph², Daniel S. Katz³,
Eric T. Thiele⁴, and Allen Taflove²

¹Rome Laboratory/ERST, 525 Brooks Road, Griffiss AFB, NY 13441-4505

²Northwestern University, EECS Department, Evanston, IL 60208

³Cray Research, Inc., 222 N. Sepulveda Blvd, #1406, El Segundo, CA 90245

⁴University of Colorado, ECE Department, Boulder, CO 80309

The finite-difference time-domain (FD-TD) method is increasingly being used to model propagation of waves in microwave and optical circuits. Accurate termination of guided wave structures which extend beyond the FD-TD grid boundaries has been one outstanding problem for these models. Since propagation can be both dispersive and multi-modal, the grid termination chosen, typically an absorbing boundary condition, must be able to absorb field energy having arbitrary direction of propagation and group velocity. The termination algorithm must also be computationally efficient.

Previous approaches to this problem have included one-way wave equations, error-canceling super-absorbers, outgoing wave annihilators, and the Liao theory. Such terminations require *a priori* knowledge of the group velocity, and also may place restrictions on the bandwidth of the incident wave.

Here we examine the termination of waveguiding structures in three dimensions using the Perfectly Matched Layer (PML) boundary treatment (J.P. Berenger, J. Comp. Phys., 114, pp. 185-200, 1994). Previously, we have demonstrated the usefulness of this approach for waveguides in two dimensions. (C. E. Reuter, et al., Microwave and Guided Wave Letters, 4, pp. 344-346, 1994). Using PML absorbing material as a waveguide termination is straightforward, and does not require the propagating field energy to be characterized in advance. The approach is general, local in time and space, and extremely accurate over a wide range of group velocities. Results are presented for metal waveguides, microstrips, and dielectric optical guides in full three dimensions. Effects of varying the material properties of the guiding structures and the PML termination materials are also studied.

Special Session

Page

Transient Electromagnetic Wave Propagation in Dispersive Media

S. L. Dvorak

- 1:20 FDTD with Linear Dispersion: Simulations of the Interaction of 392
Optical Pulses with Realistic Metallic Gratings
Justin B. Judkins, Richard W. Ziolkowski, The University of Arizona*
- 1:40 Dispersive Media in FDTD Calculations 393
Raymond Luebbers, David Kelley, The Pennsylvania State University*
- 2:00 Radar-Type Transient EM Signals Scattered by Spherical 394
Anomalies in Dispersive Media and Performance Tests for
the Extended Born Approximation
Evert C. Slob, Delft University of Technology, Tarek M. Habashy,
Carlos Torres-Verdin, Schlumberger-Doll Research*
- 2:20 Exact, Closed-Form Field Expressions for Transient Plane Waves 395
Incident of Conductive Media (TM CASE)
*Hsueh-yuan Pao, Hughes Missile Systems Company, Steven L. Dvorak,
Donald G. Dudley, University of Arizona*
- 2:40 Asymptotic Description of Transient Electromagnetic Wave 396
Propagation in Lossy Dispersive Media
Kurt. E. Oughstun, University of Vermont

FDTD with Linear Dispersion: Simulations of the Interaction of Optical Pulses with Realistic Metallic Gratings

*Justin B. Judkins and Richard W. Ziolkowski **

Electromagnetics Laboratory
Department of Electrical and Computer Engineering
The University of Arizona
Tucson, AZ 85721

In order to follow the anticipated migration path for rewritable optical disks, preformat features on the disks (pits and grooves) will continue to decrease in size with respect to the wavelength of the read beam. To design and evaluate tracking formats for these future generation disks, accurate simulation of the head-media interface is necessary. It has been shown that scalar models and models that treat only perfectly conducting material are not adequate to describe the experimentally observed polarization dependence of push-pull tracking error signals for general design studies of optical storage disks. Other more detailed approaches have been attempted, but only for perfectly conducting and dielectric materials. However, an exact treatment of the problem that incorporates realistic grating geometries and real (absorbing) materials has not been presented.

In this paper, we present a finite-difference time-domain (FDTD) solution to the vector Maxwell's equations which includes linear, dispersive materials for the interaction of a two dimensional focused beam with a realistic model of a rewritable optical disk. This solution allows for arbitrary groove profiles and multi-layer coatings of complex refractive index media.

To cast this problem into an FDTD simulation, a small region of the disk where the beam interacts with the surface is discretized. Within this region, the media are characterized by complex refractive indices. For the case where the imaginary component of the refractive index is larger than the real component, which is the case for optical signals and realistic metals such as gold or silver, a dispersive polarization model must be utilized. We have incorporated a time domain Lorentz model into our FDTD solver to give the correct complex refractive index for the metal at a desired optical frequency. For the sake of efficiency, the numerical mesh is truncated within one wavelength of the surface of the disk. Both TE (perpendicular) polarization and the TM (parallel) polarizations are considered. The scattered field is sampled along an aperture parallel to the surface and a suitable free space transform is used to produce the final, far field distribution of the scattered intensity at the objective lens. The desired signals generated by the split detectors in a conventional push-pull tracking scheme are then generated from this data. A scan of one period of the disk profile is generated by incrementing the placement of the focused beam across the surface and recording the signals at each step. Simulated simulated track crossing signal (TCS), track error signal (TES), and differential track error signal (dTES) are calculated and compared with experimental results.

Our presentation will provide a brief review of this approach to modeling the propagation of pulses in linear dispersive media. It will be demonstrated that our 2D-FDTD/Lorentz-Dispersion simulator accurately describes the push-pull tracking error signals for TE and TM polarizations for a realistic groove geometries and thin-film stacks encountered with rewritable optical disks.

DISPERSIVE MEDIA IN FDTD CALCULATIONS

**Raymond Luebbers* and David Kelley
Department of Electrical Engineering
The Pennsylvania State University
University Park, PA 16802**

The Finite Difference Time Domain (FDTD) method has seen increasing application in the calculation of transient electromagnetic wave propagation. An extensive literature has emerged, which provides the FDTD practitioner with a wide variety of capabilities. These include improved absorbing boundaries, various methods for far zone transformation, inclusion of anisotropic materials, body-fitted non-Cartesian meshes, higher order accuracy, inclusion of non-linear materials, time domain predictors (to reduce the number of time steps needed), and many other tools. These allow application of FDTD to an extremely wide range electromagnetic calculations. One fast growing area of application is to materials with frequency-dependent constitutive parameters.

Within the past several years a number of approaches for including these dispersive materials in FDTD calculations of transient propagation in dispersive media have been developed. These include methods based on recursive convolution, auxiliary difference equations, auxiliary polarization equations, and Z transformation. In this presentation several of these will be discussed and compared. The comparisons will include ease of use, application to multiple poles, and accuracy.

Emphasis will be given to a new recursive convolution approach which provides second order accuracy by approximating the change of the electric and/or magnetic field with time as piecewise-linear, rather than piecewise-constant as in the original recursive convolution formulation. This increase in accuracy requires only a very modest increase in computation time and memory. Extension of this method to scattered field formulation will also be discussed.

Example applications to various media and geometries will be presented. These applications will include propagation through dispersive media, reflection from dispersive media, and interactions with dispersive media in three dimensions.

Radar-Type Transient EM Signals Scattered by Spherical Anomalies in Dispersive Media and Performance Tests for the Extended Born Approximation

Evert C. Slob*

Section of Applied Geophysics, Faculty of Mining and Petroleum Engineering
Centre for Technical Geoscience, Delft University of Technology
P.O. Box 5028, 2600 GA Delft, The Netherlands

Tarek M. Habashy and Carlos Torres-Verdín
Schlumberger-Doll Research, Old Quarry Road, Ridgefield, CT 06877-4108, USA

Extensive research effort has been directed toward the numerical modeling of electromagnetic wavefields in both the frequency and time domains. For three-dimensional scattering configurations little is available on exact transients. The analytical frequency-domain solution exists for the fields scattered by a homogeneous spherical anomaly generated by point dipoles embedded in a dissipative whole space but results have not been widely published. We have implemented the exact frequency-domain solution for this configuration for different frequencies and contrasts in the electric conductivity and permittivity as well as in the magnetic permeability. Transients are obtained by performing the inverse Fourier transform with a simple FFT. We study the effects on the scattered fields due to the different contrasts and frequency content of the source pulse. Such a solution provides a useful benchmark in the application of both the ground penetrating radar and the borehole radar. It also provides the framework for inversion of the radar response for mapping formation heterogeneities.

We also have investigated the performance of the recently developed extended Born approximation for integral equations, known as the Localized Non-linear (LN) approximation. Taking advantage of the localized behavior of the dyadic Green's function, the LN-approximation is obtained upon replacing the internal field at the scattering position by its value at the point of observation. In so doing, we obtain a closed-form expression for the internal field that allows a rapid computation of the external fields. The gradient-divergence term occurring in the integral equation is dominant in the LN-approximation and it accounts for the jump in the normal field component across interfaces of discontinuities. However, in axially symmetric problems the normal field component is zero in which case symmetry should be applied before the LN-approximation is made since the approximation does not preserve the symmetry. We show that these modifications to the extended Born approximation are reasonably accurate over a sufficiently wide range of frequencies. The approximation can in those situations be used to obtain transients over a wide window in time. Moreover, the extended Born approximation provides a straightforward methodology to account for multiple scattering among a collection of spheres, otherwise computationally laborious with integral equation techniques.

EXACT, CLOSED-FORM FIELD EXPRESSIONS
FOR TRANSIENT PLANE WAVES
INCIDENT ON CONDUCTIVE MEDIA (TM CASE)

Hsueh-yuan Pao
Hughes Missile Systems Company
P. O. Box 11337
Tucson, AZ 85734

Steven L. Dvorak and Donald G. Dudley
Department of Electrical and Computer Engineering
University of Arizona
Tucson, AZ 85721

There has recently been renewed interest in the interaction of transient electromagnetic pulses with lossy media because of applications in stealth technologies, remote sensing, measurement of the electrical properties of dielectric substrates, geophysical probing, and subsurface communications. The problem of transient plane wave incidence on a lossy half-space is a classic electromagnetics problem that has been investigated by a number of authors, e. g. D. G. Dudley et al., *J. Appl. Phys.*, 45, pp. 1171-1175, 1974, and T. M. Papazoglou, *J. Appl. Phys.*, 46, pp. 3333-3341, 1975. But exact, closed-form expressions for this problem are absent from the literature.

In this presentation, we discuss a novel closed-form solution for the canonical problem involving the transmission and reflection of a transient transverse magnetic (TM) plane wave obliquely incident on a lossy half space. In our model, we assume that a causal transient TM plane wave is incident at an arbitrary angle on a planar air/conductive interface. Starting with the equations for the reflected and transmitted waves in the Laplace domain, the corresponding time-domain expressions are represented as inverse Laplace transforms. We then demonstrate a method which allows for the analytical evaluation of the inverse Laplace transforms. We show that the inverse Laplace transforms satisfy second-order, non-homogeneous ordinary differential equations. The differential equations are solved analytically, yielding a closed-form canonical solutions involving incomplete Lipschitz-Hankel integral (ILHIs). The ILHIs are computed numerically using efficient convergent and asymptotic expansion in the same manner as one computes Bessel functions. The exact, closed-form expressions are verified by comparing with results obtained by standard numerical integration.

ASYMPTOTIC DESCRIPTION OF TRANSIENT ELECTROMAGNETIC WAVE PROPAGATION IN LOSSY DISPERSIVE MEDIA

Kurt E. Oughstun
College of Engineering & Mathematics
University of Vermont
Burlington, Vermont 05405-0156

ABSTRACT

The asymptotic description of ultrashort-ultrawideband electromagnetic plane wave pulse propagation in a lossy dispersive medium is presented for the important cases of a single resonance Lorentz model dielectric (describing resonance polarization phenomena from the far infrared through optical region of the spectrum) and the Rocard-Powles extension of a Debye model dielectric (describing orientational polarization phenomena from the static through microwave region of the electromagnetic spectrum). This well-defined mathematical approach correctly describes the interplay between absorption and dispersion in the mature dispersion regime where the field becomes locally quasimonochromatic with fixed frequency, wavelength, and attenuation in small regions of space that move with their own characteristic constant velocity. The resultant pulse distortion in the mature dispersion regime is shown to be primarily due to the precursor fields that are a characteristic of the dispersive medium. Observation of the temporal field evolution at a fixed propagation distance in the dispersive medium shows the transient character of the precursor fields associated with the propagated field due to an input unit step function modulated signal. However, these precursor fields penetrate the deepest into the lossy medium as they suffer the least attenuation in the dispersive medium, and so, in this sense, are the longest lived field in the medium. This then has a profound influence on the dynamical field evolution in a lossy dispersive medium. For a rectangular pulse envelope modulated signal, the propagated envelope degradation is due to interference between the leading and trailing edge precursors with the main signal contribution at the input carrier frequency. In addition, these precursor fields contain a significant proportion of the propagated electromagnetic field energy and so are critical to the problem of radiation dosimetry.

Theoretical Electromagnetics II

O. B. Kesler and E. V. Jull

Page

1:20	Slot Antenna on Perfectly Conducting Spheroid Coated with398 Homogeneous Materials <i>A. A. Sebak*, M. Zhang, University of Manitoba</i>
1:40	Simple Scattering Analysis of Finite Periodic Structure Boundaries ...399 <i>Jacob J. Kim, Oren B. Kesler*, Texas Instruments</i>
2:00	Off-Bragg Blazing with Rectangular Gratings: New Results400 <i>Wei Chen, D. G. Michelson, E. V. Jull*, University of British Columbia</i>
2:20	Quasi-addition Expression for Thin Spheroids401 <i>T. Do-Nhat*, R. H. MacPhie, University of Waterloo</i>
2:40	Deflection Angle of a Light Ray Due to the Effects of Both402 Gravitational and Electrostatic Fields of a Charged Body <i>T. Do-Nhat*, University of Waterloo</i>
3:00	BREAK
3:20	The Scattering of Waves by a Spheroidal Cavity-Backed Aperture403 <i>Elena D. Vinogradova, Institute of Radiophysics & Electronics of the National Academy of Sciences of the Ukraine</i>
3:40	Electromagnetic Wave Scattering by Wire Antennas with a Local404 Nonlinear Load at the Presence of Two Media <i>A. A. Gorbachev, T. M. Zaboronkova, S. P. Tarakankov, Radiophysical Research Institute</i>
4:00	Bistable Regime of Surface Magnetoplasmon-Polariton Modes405 Excitation in Kretschmann Configuration <i>K. N. Ostrikov*, N. A. Azarenkov, O. A. Osmayev, Kharkov State University & Scientific Centre for Physical Technologies</i>
4:20	Capabilities to Control Spurious Radiation of Antennas with406 Nonlinear Elements <i>Y. S. Shifrin*, A. I. Luchaninov, V. M. Shokalo, Kharkov State Technical University of Radio Electronics</i>
4:40	Analysis of Circular Dielectric Waveguide with Periodically407 Varying Cross-section by Effective Cross-section Approach <i>Protap Prammanick*, Abbas Mohannadi, The University of Saskatchewan</i>

Slot Antenna on Perfectly Conducting Spheroid Coated with Homogeneous Materials

A. A. Sebak* and M. Zhang

Department of Electrical and Computer Engineering, University of Manitoba

Winnipeg, Manitoba, Canada R3T 5V6

Slot antennas on conducting dielectric-coated objects have been under investigation over a long period of time. The main interests of this problem include the ability to provide a useful model for antennas mounted on an aircraft or a space shuttle, the need to understand the effect of the geometrical parameters on the behavior of an antenna, and verification of new developed numerical techniques.

In this paper we present an analytical solution to the radiation problem of asymmetrically excited narrow slot on a conducting spheroid coated with a homogeneous layer. The radiated and transmitted fields are first expanded in terms of spheroidal vector wave functions with unknown expansion coefficients. These unknown coefficients are determined by enforcing boundary conditions at the interface between the coating and free space regions and at the slotted spheroid.

The first application of the solution is to analyze the radiation characteristics of a rotational symmetric slot antenna. Further application is carried out for a rotational asymmetric slot antenna. Numerical results are obtained for the radiation patterns and conductance. The effect of some physical parameters on the radiation power has been also investigated. The accuracy of the solution has been attested by checking the boundary conditions and considering some special cases. When the spheroid approaches the spherical shape excited by either an asymmetric or a symmetric slot, the calculations agree well with the known results for a sphere(L. Shafai, *Canadian J. Phys.*, vol. 50, no. 23, 1972.). Our calculated results also show that, for certain coating thickness, some modes become resonant. This greatly enhances the radiated power and affects the radiation field.

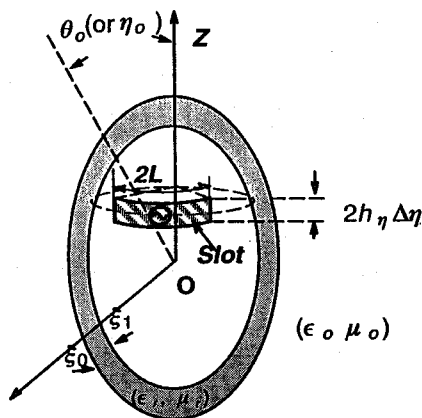


Fig.1 Geometry of the slotted coated prolate spheroid excited by a rotationally asymmetric slot.

SIMPLE SCATTERING ANALYSIS OF FINITE PERIODIC STRUCTURE BOUNDARIES

Jacob J. Kim and Oren B. Kesler*
Texas Instruments Incorporated
2501 W. University, M/S 8019
McKinney, Texas 75070

The problem of three dimensional(3-D) EM scattering by an arbitrary shaped finite conformal array or frequency selective surface has been investigated, with the primary objective of investigating the effect of edge shape of the finite periodic surface on its scattering characteristics. In the past, periodic structures such as phased arrays or frequency selective surfaces have been designed assuming that they were planar and infinite in extent due to the simplicity of the analysis, i.e., a single cell of the periodic structure needs to be considered via the use of Floquet's theorem. However, this assumption is not valid in practical applications, especially for finite conformal arrays in a curved surface. In recent years, the finite periodic array scattering problems have been addressed in the literature and the edge effects of truncated periodic arrays were analyzed by modeling each element individually. Although they are numerically rigorous solutions, their applications are limited to electrically small arrays or singly truncated periodic arrays due to limited computational resources.

This paper describes a practical EM analysis technique to predict 3-D scattering from a finite periodic structure on a planar/curved surface. First, an array aperture area is simulated with a surface impedance for every incident direction using the Periodic Moment Method(PMM) or other numerical solutions. Next the two dimensional(2-D) scattered field is computed from the impedance discontinuity between the array aperture area and the surrounding surface using 2-D Uniform Geometrical Theory of Diffraction(UTD) solutions. Alternately, the 2-D scattered field can be obtained by simple measurements of a planar test array model whose truncation is perpendicular to the incident plane wave direction. Then an efficient 2-D to 3-D conversion process, which is referred to as Uniform Field Integration Method(UFIM), is used to predict the 3-D scattering from an arbitrary shaped contour on a curved surface utilizing the 2-D scattered field. The UFIM is a similar approach as Equivalent Current Method(ECM), but is more versatile in that it can be used to evaluate 3-D EM scattering from many complex discontinuities whose solutions are not normally available in other analytical or numerical approaches.

A few test models with a finite surface impedance or conformal arrays on a planar surface were constructed and their scattering predictions were compared with actual 3-D measurements. All comparisons showed very good agreement.

Off-Bragg Blazing with Rectangular Gratings: New Results

Wei Chen, D.G. Michelson and E.V. Jull*
University of British Columbia
Department of Electrical Engineering
Vancouver, B.C., Canada V6T 1Z4

Perfect blazing to the $m=-1$ spectral order was once assumed to be possible only for Bragg angle incidence; i.e. for an angle $\vartheta_i = \sin^{-1}(\lambda/2d)$ from the normal to the grating surface, where d/λ is the grating period in wavelengths. The diffracted beam is then back in the direction of incidence, an inconvenience in most applications such as reflection grating multiplexers or demultiplexers and frequency scanned antennas. Off-Bragg blazing is preferable and now can be done with high efficiency. It has now been thoroughly and rigorously investigated numerically for TM polarization (magnetic field parallel to the grooves).

As a consequence of reciprocity off-Bragg blaze angles occur in pairs θ_1, θ_2 related by

$$\sin \theta_1 + \sin \theta_2 = \lambda/d,$$

a generalization of the Bragg condition ($\theta_1 = \theta_2$). In most applications maximum deviation ($|\theta_2 - \theta_1|$) is desirable and this is

$$\cos^{-1} \left(\frac{\lambda}{d} - 1 \right); \quad 0.5 < \frac{d}{\lambda} < 1.0$$

$$\sin^{-1} \left(\frac{2\lambda}{d} - 1 \right) - \sin^{-1} \left(1 - \frac{\lambda}{d} \right); \quad 1.0 < \frac{d}{\lambda} < 1.5$$

For TM polarization off-Bragg blazing has been found for every groove width to period ratio $0 < \frac{a}{d} < 1.0$ investigated, but the largest deviations and hence the most potentially useful designs were found for $0.5 < \frac{a}{d} < 0.6$. For these groove depths $0.1 < \frac{h}{\lambda} < 0.24$ gave off-Bragg blazing with maximum deviations for periods $0.9 < \frac{d}{\lambda} < 1.0$. Off-Bragg blazing occurs for wider and deeper grooves as well as narrower and shallower grooves but there is little suppression of specular reflection between the blaze angles, which limits the useful range of angles of incidence or the frequency bandwidth in applications of this technique.

Off-Bragg blazing of rectangular groove gratings was found here only for TM polarization. It has also been reported for sinusoidal and triangular gratings (M. Bredne and D. Maystre, *Optica Acta* 28, 1321-1327) but again only for TM polarization.

Quasi-addition expression for thin spheroids

T. Do-Nhat and R. H. MacPhie

Department of Electrical and Computer Engineering
University of Waterloo, Waterloo, Ontario, Canada N2L 3G1.

The addition expressions applied to incoming and outgoing waves for prolate spheroids developed by Sinha and MacPhie (Quart. Appl. Math. 38, 143-158, 1980) fail to converge rapidly near the surface of the convergent sphere of radius d , where d is center distance between two spheroids. Because of the slowly convergent problem, these addition theorems may not be used for the study of closely packed spheroids. In this paper, by using the coordinates transformation, the outgoing spheroidal wave of the first spheroidal coordinates system is transformed into a Fourier series of the second spheroidal one via the following relation (J. Dalmas & R. Deleuil, Opt. Acta 29, 1117-1131, 1982):

$$\psi_{mn}^{(4)} = S_{mn}(h, \eta) R_{mn}^{(4)}(h, \xi) e^{jm\phi} = \sum_{s=|m|}^{\infty} \sum_{|k|=|s-1|}^{\infty} j^{s-n} d_{s-m}^{mn} |(h) P_s^m(\cos\theta) h_s^{(2)}(hr) e^{jm\phi}. \quad (1)$$

For two prolate spheroids whose centers are on the same x axis, by using the geometrical transformation, the functions inside the summation can be expanded as Fourier series of the second spheroidal coordinates system as follows:

$$P_s^m(\cos\theta) = \sum_{\mu=-\infty}^{\infty} \sum_{\nu=-\infty}^{\infty} \sum_{|\mu|=|\nu|}^{\infty} \sum_{|k|=|l|}^{\infty} P_{k\mu, k'\nu}^{ms}(\tau_1', \tau_2') e^{j(\mu+\nu)\phi} \quad (2)$$

$$h_s^{(2)}(hr) = \sum_{\mu=-\infty}^{\infty} \sum_{\nu=-\infty}^{\infty} \sum_{|\mu|=|\nu|}^{\infty} \sum_{|k|=|l|}^{\infty} h_{k\mu, k'\nu}^s(\tau_1', \tau_2') e^{j(\mu+\nu)\phi} \quad (3)$$

$$e^{jm\phi} = \prod_{\mu=1}^{\infty} e^{j(-1)^{\mu-1} \frac{m}{\mu} \left(\frac{F'}{d}\right)^{\mu} \tau_1'^{\mu} \sin(\mu\phi)}, \quad F' \tau_1' \leq d, \quad (4)$$

where F' is the semi-focal distance of the second spheroid. The Fourier coefficients $P_{k\mu, k'\nu}^{ms}$ and $h_{k\mu, k'\nu}^s$ were found in the closed forms which depend on the variables of the second system $\tau_1' = (1-\eta'^2)^{1/2}(\xi^2-1)^{1/2}$, $\tau_2' = \eta'\xi'$. The expressions (2), (3) and (4) are valid everywhere as long as the spheroids' surfaces do not pass through their origin. By substituting (2), (3) and (4) into (1) the quasi-addition expression for thin spheroids can be found. In addition, for very thin spheroids ($\xi, \xi' \rightarrow 1$) only the leading terms of (2), (3) and (4) are needed. This quasi-addition expression can be used for the formulation of the quasi-addition spheroidal vector expressions. Finally, numerical results to be presented will show their convergent characteristics.

Deflection angle of a light ray due to the effects of both gravitational and electrostatic fields of a charged body

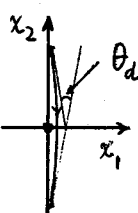
T. Do-Nhat

Department of Electrical and Computer Engineering
University of Waterloo, Waterloo, Ontario, Canada N2L 3G1.

In this paper the asymptotic expression of the deflection angle of a light ray influenced by a charged body (e.g. a charged blackhole) is derived by using the Reissner Nordström's metric (R.Adler, M.Bazin & M. Schiffer, Introduction to general relativity, Mc.Graw-Hill, 140, 1965). In the spherical coordinates system (r, θ, ϕ) centered at a charged body, the exact orbital non-linear differential equation of second order of $1/r(\phi)$ in the $\theta = \pi/2$ plane derived from the geodesic equation of motion, is given by

$$\frac{d^2}{d\phi^2} \left(\frac{1}{r} \right) + \frac{1}{r} = \frac{3a}{2} \left(\frac{1}{r} \right)^2 - 2b^2 \left(\frac{1}{r} \right)^3, \quad (1)$$

where $a = 2\kappa M/c^2$, $b^2/a = Q^2/(4\pi M c^2)$ with κ being the gravitational constant, c the light velocity in vacuum, M the mass of the body and Q its charge in the Heavyside-Lorentz unit. By using the perturbation method of Poincaré and Lindsted (H.Poincaré, les methodes nouvelles de la mecanique celeste, New York, Dover, II, 1957) applied to this non-linear differential equation, the orbital expression of $1/r$ of a light ray was found to be expressed as a simple Fourier series, from which the asymptotic formula of the deflection angle θ_d of a light ray was derived as follows:



$$\theta_d = \frac{4}{3}\epsilon + \left(\frac{5\pi}{12} - \frac{4}{9} - \frac{3\pi}{8}\gamma \right) \epsilon^2 + \left\{ \frac{122}{81} - \frac{10\pi}{36} + \left(-\frac{7}{3} + \frac{\pi}{4} \right) \gamma \right\} \epsilon^3 + \left\{ \frac{385\pi}{576} - \frac{130}{81} + \left(\frac{25}{9} - \frac{275\pi}{192} \right) \gamma + \frac{57\pi}{256} \gamma^2 \right\} \epsilon^4 + \dots \quad \gamma \leq \frac{32}{9\pi\epsilon}, \quad (2)$$

where $\epsilon = 3\kappa M/(c^2 R)$, and $\gamma = Q^2/(9\pi\kappa M^2)$ with R being the nearest distance to the charged body. It is noted that Einstein obtained the first term of (2), valid in weak gravitational fields. Finally, the deflection angle θ_d given by (2) unifies both gravitational and electrostatic effects due to a charged body. Numerical results to be presented show the convergent characteristics of (2) for various ϵ and γ .

THE SCATTERING OF WAVES BY A SPHEROIDAL CAVITY-BACKED APERTURE

Elena D. Vinogradova

Institute of Radiophysics & Electronics of the National Academy of Sciences of the Ukraine, 12, Ac. Proskura st., Kharkov, 310085, Ukraine
Phone: (7-0572)-44-85-43 Fax: (7-0572)-44-11-05
e-mail: yura@ire.kharkov.ua

It is well known that the rigorous methods investigating diffraction fields with an assured accuracy are adaptable only to the simplest nonclosed screens such as disks, strips, infinitely long slotted cylinders. As to three-dimensional screens, only for a sphere with a circular hole the effective algorithm for diffraction problems has recently been produced. Solution of these problems for three-dimensional screens is important for real waveguiding structures, resonators, mirror antennas.

Since coordinates of prolate ellipsoid of rotation allow to describe a great variety of reflecting surfaces, the investigation of diffraction problems for nonclosed spheroidal shells is very important. This problem in the rigorous statement for the scattering of concentrated electric type source field by a thin perfectly conducting spheroidal shell with a circular hole has been solved. The location of the vertical electric dipole along the antenna axis is arbitrary.

The problem is reduced to solving the infinite system of linear algebraic equations of the second kind for the scattered field Fourier coefficients. The method of solution is based on some variant of the regularization procedure when the Helmholtz operator is considered as superposition of the singular part (the Laplace operator) and the regular one, and the singular part is subjected to the inversion procedure. This procedure is closely connected with the Abel's integral transform technique.

The fast convergence of the method provides any desired computation accuracy and the following scattering characteristics as a frequency functions have been examined in detail: a) surface current density; b) the resistance of radiation; c) the energy accumulation inside and outside of the spheroidal resonant space, i.e. Q-factor. The far-field pattern of spheroidal antenna for different positions of incident source, the hole dimensions, values of "stretching" of spheroid and its wave dimensions have been investigated.

Computer data have been used for analysis of side lobes radiation blockade problem and examination of antenna properties of the system of interest.

ELECTROMAGNETIC WAVE SCATTERING BY WIRE ANTENNAS WITH A LOCAL NONLINEAR LOAD AT THE PRESENCE OF TWO MEDIA BOUNDARY

A. A. Gorbachev, T. M. Zaboronkova, S. P. Tarakankov

*Radiophysical Research Institute (NIRFI)
25 B. Pecherskaya st., Nizhny Novgorod, Russia*

Nonlinear effects in electromagnetic waves scattered by metallic constructions are caused by the presence of construction mechanical joints: screw joints of case panels, adjoining contacts of different metals at unit attachment points, etc. Nonlinear scattering gives rise a high level of interference in radio wave reception and may have as well a useful application, for example, in rescue operations under conditions of snow avalanches when special nonlinear scatterer-markers are used and in detection of hidden defects in industrial constructions. The present work is devoted to experimental and theoretical investigation of electromagnetic wave scattering by a single thin metallic circular antenna and a vibrator of arbitrary dimensions with nonlinear point load located near two media boundary. The current-voltage characteristic of the load nonlinear element for not so large values of voltage is described as $I = (u + \alpha u^2 + \beta u^3) / R_0$, where I is the current through the nonlinear element, u is the element voltage, R_0 is the initial resistance (at $u = 0$), α and β are nonlinear coefficients. As it is known, for a nonlinear contact of two metals via an oxide film the third harmonic is the most intensive and for a semiconductor element — the second one is.

The backscattered field on the second and the third harmonics has been measured at a special automated stand as dependent on: 1) the position of the nonlinear element at a fixed penetration depth of the antenna into a dielectric; 2) the penetration depth of the scatterer into a dielectric; 3) the polarization of the transmitting antenna; 4) the frequency of the incident field. This problem has been solved theoretically as well in the approximation of a weak nonlinearity. Analytical expressions have been obtained for current distribution in scatterers on higher harmonics as well as those for backscatter field components produced by these currents. Experimental and corresponding theoretical results are in a good agreement. The investigations made possible to discover some regularities in the higher harmonic backscattered field structure (the growth of a signal level as moving from the boundary within the near field zone with subsequent oscillations; the well known dependence of the oscillation period on the medium permittivity, operating frequency and scatterer sizes) which may be used in design of nonlinear markers for rescue systems.

BISTABLE REGIME OF SURFACE MAGNETOPLASMON-POLARITON MODES EXCITATION IN KRETSCHMANN CONFIGURATION

K.N.Ostrikov, N.A.Azarenkov, O.A.Osmayev

Kharkov State University and Scientific Centre
for Physical Technologies, Novgorodskaya str, 2, #93
310145, Kharkov, UKRAINE.

It is a common knowledge that traditional schemes of the attenuated total reflection method (ATRM) of excitation of surface waves (SW) provide significant field amplification which results in the nonlinear behaviour of the excited modes. The resulting amplitude dependent frequency shift of the SW modifies the excitation conditions by the ATRM. Therefore, an excited SW provides a backward influence on the excitation system. This backward influence is resulted in a bistable regime of the SW excitation in the studied structure. A planar slab of free-electron metal is sandwiched between an n-type semiconductor and a dielectric simulating the prism material in a prism coupler. The whole structure is immersed in an external magnetic field which is parallel to the interface. The excited strongly nonreciprocal surface magnetoplasmon-polariton modes propagate across an external magnetic field. These modes are caused by collective excitations in the semiconductor nonlinear medium. A plane TM wave is incident at the interface between the prism and a metal. In this geometry the resonant conditions of the SW excitation are derived. The possible nonlinear effects resulting in the SW nonlinear frequency shift are taken into account through the method of the weak nonlinearity with the formalism of the third order nonlinear susceptibilities. The variation of the input power leads to the fact that the system is triggered between the regimes of TR and ATR and vice versa under different values of the input power. The numerical results suggest about the realization of hysteretic dependence between input and output amplitudes and that this effect is realized under reasonably low values of the input power. This is due to the fact that the nonlinear effects are realized for slow waves under relatively low values of the amplitude and the realizing nonlinear response of the structure becomes high enough for the realization of the bistable regime.

CAPABILITIES TO CONTROL SPURIOUS RADIATION

Y.S.Shifrin*, A.I.Luchaninov, V.M.Shokalo
Kharkov State Technical University of Radio Electronics

The presence of either nonlinearities in antennas causes the spurious radiation (SR) emergence. In one cases the spurious radiation is a harmful one deteriorating, in particular, the radio engineering systems EMC. Accordingly, the necessity arises to decrease it. Such is, for example, SR of rectennas (antennas-rectifiers), of various types antennas owing to parasitic nonlinearities stipulated by their design, of active phased arrays under an adverse made of their operation.

In other cases the SR of antennas with nonlinear elements (ANE) is usefull and underlies device functioning. In such situations it is necessary to find means to amplify the needed frequency. As an example we can cite to the problems of radiation amplification of either harmonics of the main signal in the antennas- multipliers or in the systems of nonlinear radiolocation, where the signal on the harmonics frequency is used for the object location.

In any case the capabilities to control SR of the ANE are defined by the nonlinearity nature and by the parameters of the antenna scheme.

The paper consist of two parts.

The first part treats the rectenna SR. For the begining the SR characteristics of various separate rectenna receiving- rectifying element (RRE) are cited. The factors affecting "relative significance" of different harmonics in the radiated field are indicated: the flux density of power incident on the RRE; the radiator type; the rectification circuit; diodes and filters characteristics. The obtained results allow, in particular, to judge about the possibilities to decrease the SR of various RRE.

Further a method of the SR computation of the rectenna arrays with uniform and nonuniform radiation of their aperture is presented. The possibility to decrease the SR level of large rectennas through the arrangement of their aperture of different RRE are treated. The corresponding estimations are given.

The second part of the paper is devoted to the antennas-multipliers (AM). Here the problem of the desired harmonics amplification in the field radiated by the AM is the central one. The transformation factor (TF) - the relation of power re-radiated by the AM on the chosen harmonics frequency to the maximum power which the AM can extract from the free space on the main frequency - is accepted as the main parameter of the AM. The dependence of the TF on the radiator type, Schottky diode parameters, the input signal level is found.

It is shown that with the appropriate choice of the radiator parameters it is possible to obtain its optimal resistances on the base and on the desired harmonics frequencies. This ensures a high TF of the AM. The design of such an AM with the stripline radiator is offered.

The investigations results of large AM reflector arrays with a frequency doubling formed of such single AM are presented. The dependences of the TF of such arrays on dielectric permittivity and thickness of radiating structure substratum, power flow density of exciting, direction of its flow are given. The possibility to create AM arrays with the TF value no less than 80% with changing the exciting field parameters in sufficiently wide limits are set forth.

Analysis of Circular Dielectric Waveguide with Periodically Varying Cross-section by Effective Cross-section Approach

Protap Pramanick* and Abbas Mohammadi
 Department of Electrical Engineering, The university of Saskatchewan

There is an increasing demand for accurate and time efficient expressions for analyzing of optical structures. The effective cross-section approach is considered as a suitable method to analyze dielectric waveguides. The present article employs transmission matrix approach together with the effective cross-section approach to compute the axial wavenumber and phase shift of a penetrable circular dielectric waveguide with periodically varying cross-section.

The effective cross-section approach can be employed efficiently to analyze weakly guiding structures. According to this theory, the effective cross section for linearly polarized fibers can be obtained as a result of pushing the core walls outward at every point by an amount δn , where

$\delta n = 1 / \sqrt{k_0^2 (\epsilon_1 - \epsilon_2)}$. k_0 is the free space wavenumber. ϵ_1 and ϵ_2 are the dielectric constants of core and clad respectively. It can be shown that sufficiently far from cutoff, the propagation constant

$\beta_{\mu\nu}$ of a linearly polarized mode (LP $_{\mu\nu}$) obeys the relationship:

$$\beta_{\mu\nu}^2 = k_0^2 \epsilon_1 - k_{\mu\nu}^2$$

where $k_{\mu\nu}$ is the cutoff wavenumber of the TM $_{\mu\nu}$ mode of a hollow metallic circular waveguide with radius $r' = r + \delta n$. The excellent agreement of results of this method with classic literatures approve validity of this method (Fig.1).

More complex structures can be analyzed with employing transmission concept and effective cross-section approach. If the sinusoidally modulated circular dielectric waveguide is divided into a number of uniform sections in each section the effective cross section approach is employed, and finally all these sections are connect together based on transmission matrix approach, it can be shown that the propagation phase of the structure is given by $\beta_{\mu\nu} l = \text{Cos}((A_{11} + A_{22})/2)$. Where A_{11} and A_{22} are the two diagonal elements of the overall transmission matrix and l is length of the waveguide.

The phase shift and axial wavenumber of a penetrable circular dielectric waveguide with periodically varying cross-section have been computed efficiently with this method. The general wall corrugation has been considered with a period of corrugation equal to the mean radius of the circular waveguide. The real and imaginary parts of results of the present method have been shown in Fig.2. It has been found that there is very good agreement with full wave analysis(e.g. S.L.G. Lundqvist, T-MTT, 35, 282-287, 1987). The simplicity of theory, speed of computation and the ability to analyze complex structures are the main advantages of this new method.

Fig. 1

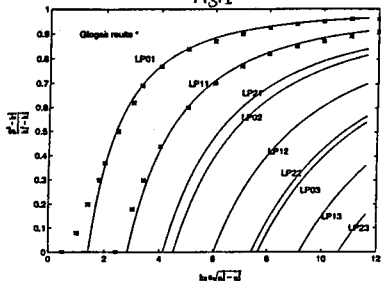
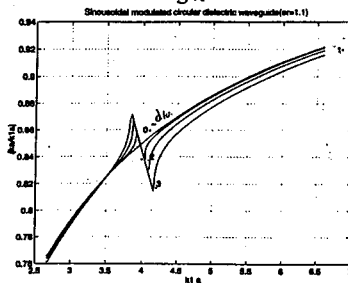


Fig. 2



THIS PAGE INTENTIONALLY LEFT BLANK.

Special Session

Transionospheric Propagation

L. M. Duncan and J. Goodman

Page

- 1:20 A Non-deterministic Transionospheric Transfer Function for a 410
Realistic Three-Dimensional Ionosphere
Marisa McCoy, John P. Basart, Iowa State University*
- 1:40 Effects of Ionospheric Scintillation on Differential Demodulation 411
of GPS Data
Roger A. Dana, Mission Research Corporation
- 2:00 Mid-Latitude Angle of Arrival Data for Resolved Ionospheric 412
Modes
W. M. Sherrill, Q. R. Black, B. Brown, Southwest Research Institute*
- 2:20 Synthetic Array Antenna and its Application to the Multipath 413
Propagation Environment
A. H. Abu Bakar, MARA Institute of Technology
- 2:40 The Scintillation Index in an Inhomogeneous (on Average) 414
Ionosphere with Random Large-Scale Irregularities
A. V. Kulizhsky, M. V. Tinin, Irkutsk State University
- 3:00 BREAK
- 3:20 Theoretical Modeling of the Chirp-Sonde Operation when 415
Diagnosing the HF Radio Channel
N. V. Ilyin, V. V. Khakhinov, V. I. Kurkin, V. E. Nosov,
S. N. Ponomarchuk, Institute of Solar-Terrestrial Physics*
- 3:40 The Harnessing of Complicated Signals for Measurements of 416
the Signal Distortions in the Ionospheric Channel
A. V. Medvedev, K. G. Ratovsky, Institute of Solar-Terrestrial Physics*
- 4:00 Applied Program Packages for Prediction and Current 417
Diagnostics of the HF Radio Channel
V. I. Kurkin, V. E. Nosov, S. N. Ponomarchuk, S. V. Pushkarev,
Institute of Solar-Terrestrial Physics*
- 4:20 Model-Emperical Study of the HF Propagation During 418
Magnetospheric Substorm
D. V. Blagoveshchensky, State Academy of Aerospace Instrumentation,
T. D. Borisova, Arctic and Antarctic Scientific Research Inst.*

A Non-deterministic Transionospheric Transfer Function for a Realistic Three-Dimensional Ionosphere

Marisa McCoy* and John P. Basart
Electrical and Computer Engineering Department
Iowa State University, Ames, IA, 50011

A non-deterministic ionospheric transfer function for realistic model atmospheres is being created. This transfer function will be applied to simulations of man-made interference sources to determine temporal, spectral, and spatial windows in the HF noise background for an orbiting radio-astronomy interferometer. By characterizing the ionosphere's behavior in the form of a transfer function, an analysis of the noise environment in space with respect to various ionospheric parameters, solar behavior, and interference source characteristics is possible.

Currently, no models exist for the HF noise background as seen from an orbiting radio astronomy payload. Breakthrough of signals from terrestrial sources would greatly increase the background noise of a receiver, making high resolution observations difficult at best. Past satellite observations have shown that noise levels tend to peak over developed areas, indicating that the man-made component of the background noise is non-negligible (Rush, Snyder, et. al., Radio Science, Vol. 15(6), 1127-1136, 1980). However, noise level predictions do not yet exist.

The total transfer function $T(\Theta, \Phi, \omega) = \hat{H}(\Theta, \Phi, \omega) \times H(\Theta, \Phi, \omega)$ contains both stochastic and deterministic parts. The deterministic transfer function $H(\Theta, \Phi, \omega)$ accounts for the refractive effects of the background ionization, which can be significant for signals in the 10-50 MHz range. This function is derived from ray tracing in a three-dimensional, realistic, inhomogeneous ionosphere (Argo, Delapp, Sutherland, Farrer, TRACKER Technical Manual, Los Alamos National Laboratory, 1994). The model ionospheres were generated by the ICED model. The primary components of the deterministic transfer function are the free space path loss (scaling as $1/r^2$), the ionospheric absorption (a function of particle collisions), and the iris effect of the ionosphere (a function of peak plasma frequency, source frequency, and ray launch angle). The stochastic transfer function $\hat{H}(\Theta, \Phi, \omega)$ is derived using the multiple phase screen (MPS) method (Knepp, Proc. IEEE, Vol. 71(6), 722-737, 1983) and finding the transmitted intensity of the wave at the receiver location. The MPS simulation inputs were derived from known irregularity characteristics. These simulations were intended to account for irregularity effects not normally incorporated into empirical ionospheric models. All transmitting 10-50 MHz sources were at 0 km altitude with the receiver at 20,000 km. The co-planar transmitters and receiver were located at the geographic equator. (Future work will include non-coplanar simulations).

We have found a strong sunspot number dependence on the overall transfer function. As the sunspot number decreased, the transfer function became more broadband and total losses decreased by more than 10 dB. In general, the total losses decreased with frequency until the "edges" of ionospheric transmission were reached. Then, the losses began to increase sharply with decreasing frequency until the ray did not penetrate the ionosphere.

EFFECTS OF IONOSPHERIC SCINTILLATION ON DIFFERENTIAL DEMODULATION OF GPS DATA

Roger A. Dana

Mission Research Corporation

735 State Street, P.O. Drawer 791

Santa Barbara, California 93102-0719

Global Positioning System (GPS) data are modulated on L-band carriers using coherent phase shift keying (PSK). Under benign propagation conditions it is possible and desirable to track the phase of the received signal. Accurate knowledge of received signal phase allows precise navigation and nearly error-free data demodulation. Furthermore, the GPS data format allows for the inherent $\pm\pi$ ambiguity in bi-phase tracking loops. However, in either naturally occurring or man-made L-band ionospheric scintillation, it may not be possible to accurately track the phase of the received signal. When the fading is slow, deep fades in the received signal are likely to produce phase-slips in the phase-lock tracking loop output, and when the fading is fast the phase tracking loop may not remain locked on the signal. Even when the phase tracking loop is able to maintain lock on the signal, frequent phase-slips in the tracking loop output significantly degrade PSK demodulation error rates.

Navigation can still be performed under disturbed propagation conditions, albeit with some degradation in accuracy, if the receiver can continue to demodulate GPS navigation data. One approach to developing a gracefully degrading GPS receiver is to use a frequency-lock loop when phase cannot be tracked. A simple solution to the problem of demodulating PSK data in scintillation, when phase tracking loops cannot maintain lock on the received signal but frequency can be tracked, is to use differential PSK (DPSK) demodulation. All that is required to reconstruct the correct GPS data using differential demodulation is a known data bit. For subsequent bits, the DPSK demodulated symbol metric is used to determine the bit polarity. Fortunately the GPS data contain many known bits, any one of which can be used as a reference.

In this talk the application of DPSK demodulation to GPS receivers is illustrated, and DPSK demodulation and word error rates for the GPS telemetry word (TLM), handover word (HOW), and navigation data are presented. These theoretical error rate curves are then compared to measured values taken during scintillation testing of a special GPS receiver that uses DPSK demodulation.

MID-LATITUDE ANGLE OF ARRIVAL DATA
FOR RESOLVED IONOSPHERIC MODES

W. M. Sherrill, *Q. R. Black, and B. Brown
Southwest Research Institute
6220 Culebra Road
P.O. Drawer 28510
San Antonio, Texas 78228-0510

A large database of mode resolved angle of arrival data has been collected based on 24-48 hour sequences of DF Ionograms for various paths from 55 km to 3500 km in range. The DF Sounding process generates angle of arrival data for resolved propagation modes by operating a multichannel frequency-slice DF processor in a FM-CW sounder receiving mode, in synchronization with a FM-CW sounder transmitter. Deployed cooperative as well as non-cooperative FM-CW sounder transmitters are used.

This paper addresses propagation over two particular paths with ranges of 1260 km and 3452 km respectively. We present received elevation angle vs frequency and time of day over 24 hour periods, for discrete, resolved propagation modes (1E, 1F2, 2F2, etc.). Also presented are corresponding azimuths as a function of frequency and time of day. These data are presented in a 3-dimensional graphical format which clearly shows the impact of the diurnal cycle as well as other processes (such as TID's) on each resolved mode. We compare the various resolved modes for degree of correlation in azimuth and elevation across modes (e.g. 1 hop vs 2 hop) over wide frequency ranges (MUF to LUF) at various times of day. Implications for the corresponding correlation of ionospheric refractive properties over frequency for each path are discussed.

We also provide the hourly standard deviation of azimuth as a function of time for each mode on each path.

Synthetic array antenna and its application to the multipath propagation environment

A. H. Abu Bakar
MARA Institute of Technology, Shah Alam, Malaysia

Introduction

Extensive study has been given to the array antenna system. Papers dealing with this general subject have appeared from time to time. However, some of the earliest papers on this subject have been published by Southworth and Foster, ^{1,2}, in 1930 and 1926 respectively. The actual date and person who first discussed the subject were not clearly known. This is due to the limited resources within the references that are made available. Anyway, work on the array system has been active way back in 1926's. In 1970 the presence of the computer initiated a new impetus to a wide application of the array system. From 1970, the research on the use of array antenna (or array sensors) such as in sonar, radar, radio communication and seismic systems has been active. Also, advanced techniques of array processing on the information gathered by the array sensors have been developed. Generally, the term sensor is used because sensor takes on variety of forms. In the case of radar, radio communication and radio astronomy, sensor are in the form of antennas. But however in sonar, seismology and medical imaging, the sensors used are hydrophones, geophones and ultrasonic probes. In all of these diverse applications, the sensors are designed to provide an interface between the environment in which the array is used and the signal processing part of the system. The physical manner in which this interface is established depends on the application of interest.

As the topic of this paper implies, array antenna is used as the interface between the multipath propagation environment and the instrumentation and signal processing part of the system. Fig.1 shows the layout of the synthetic array antenna position in relation to the multipath propagation environment, the measuring instruments and the signal processing unit. The practical array used in the experiment is the synthetic array. The single antenna element is positioned at any point over the measuring area by computer control. The scanning area has dimensions which are about $3\lambda \times 3\lambda$. The points at which measurements are made are selected on a regular grid. The spacing of the points has usually been set to 0.3λ . The total number of points is 100. The measurements are recorded on floppy disc in the field. At the base the data is then processed.

In this paper, the mathematical formulations of the system model and the signal processing required to retrieve the direction of arrival (DOA) of the multipath signals from the signals received by the array antenna are presented. The methods used to determine the DOA of signals are based on algorithms already developed. A fundamental theory of array antenna and the type of array antenna used in the experiment are reviewed. Also, its relationship to the multiple path signals model is examined.

Fig 2.0 shows typical performance of conventional beamforming technique compared to MUSIC using the measured data obtained by the synthetic array antenna.

The Scintillation Index in an Inhomogeneous (on Average) Ionosphere with Random Large-Scale Irregularities

A. V. Kulizhsky and M. V. Tinin
Applied Physics Institute, Irkutsk State University,
b. Gagarina-20, Irkutsk, 664003, Russia,

It is known that during the propagation of waves in ionosphere with random large-scale irregularities in the case of long propagation paths, strong fluctuations of the wave intensity be observed. In order to describe such phenomena in homogeneous (on average) ionosphere we can use a method of parabolic equation. The resulting equation for the fourth moment of field can be solved approximately by using, for example, the method of two-scale expansions. However, it is very difficult to apply this technique for the case of inhomogeneous (on average) ionosphere, especially whenever caustics are present in the background plasma. Nevertheless, such problems are of significant scientific and practical interest because real ionosphere are inhomogeneous, on average. Such is, especially the ionosphere for HF radio waves.

This report is devoted to the study of the scintillation index in a three-dimensionally inhomogeneous ionosphere with random large-scale irregularities. To solve the problem, we use the method of interference integral which permits the effects of background refraction and random irregularities to be taken into account correctly. We obtained the expressions for the scintillation index in both the illuminated zone and the neighbourhood of a simple caustic for an arbitrary irregularity spectrum and any smoothly-inhomogeneous background ionosphere. It is shown that these results generalize formulas for the scintillation index obtained for a homogeneous (on average) medium and the isotropic correlation function of irregularities (Kulizhsky A.V. and Tinin M.V. *Waves in Random Media* (1994) 149 - 165). On the basis of numerical calculations made with applications to the ionospheric propagation of HF radio waves, it is shown that the scintillation index on the caustic is close to unity and increases with increasing distance into the caustic shadow zone. In the illuminated zone, depending on propagation conditions, the behaviour of the scintillation index is different, both qualitatively and quantitatively and is largely determined by background refraction. Thus, if the field divergence is significant, then the scintillation index has a weakly-expressed zone of random focusings, and its value in that zone is only slightly larger than unity. The saturation zone, on the contrary, is clearly traceable, and here the value of scintillation index tends to unity. If background parameters are such that the field divergence is close to the divergence in a free space, then in this case the scintillation index has a well-defined zone of statistical focusing (values of index, depending on irregularity parameters, can be equal to five or more), while the saturation zone is traceable only at a very significant distance from the source.

THEORETICAL MODELING OF THE CHIRP-SONDE OPERATION WHEN DIAGNOSING THE HF RADIO CHANNEL

N. V. Ilyin, V. V. Khakhinov*, V. I. Kurkin,
V. E. Nosov, and S. N. Ponomarchuk
Institute of Solar-Terrestrial Physics,
Irkutsk 664033, P.O.Box 4026, Russia

In recent years, chirp-sondes have been gaining wide acceptance for diagnosing HF radio channels (Earl, G. F. and B. D. Ward, *Radio Sci.*, **22**, 275, 1987; Brynko, I. G. et al., *Adv. Space Res.*, **8**, (4)121, 1988). Until the present, however, there has been no clear idea of their potentialities and no data on correlative analysis of traditional pulsed sounding systems and chirp-sondes. This is attributable to the lack of theoretical analysis of the propagation of wideband chirp-signals in an ionospheric communication channel, with allowance made for the sonde's hardware performance and the operation of the pretreatment system for the received signal.

Based on the theory of linear systems this paper seeks to make a theoretical analysis of a generalized diagnostics scheme by the oblique-incidence sounding method using a continuous signal with a linear frequency modulation and pretreatment of the received signal by the frequency compression method. A dependence of the recorded spectrum level on group delays and carrier frequency of received sounding signals is obtained. It is shown that the result of processing of an individual time sample is mathematically equivalent to sounding the radio channel by a complex narrowband pulsed signal, whose group delays determine maxima on the recorded spectrum. The difference lies in the fact that in the course of a spectral analysis of a separate sample its carrier frequency changes by the amount of the operating range of the spectrum analyzer.

In the analysis, special attention is given to the absorption dispersion effect on the sounding signal shape distortion.

Expressions are obtained for estimating the resolving power and noise-immunity of a chirp-sonde, depending on its performance data.

By way of example we present the results of theoretical simulation of the chirp-sound operation for the Magadan-Irkutsk path of a length of 3000 km. A comparative analysis is made of the various sounding systems operating in the pulsed and continuous modes with composite signals and employing time or frequency compression.

The Harnessing of a Complicate Signals for Measurements of the Signal Distortions in the Ionospheric Channel

A. V. Medvedev and K. G. Ratovsky*

Institute of Solar-Terrestrial Physics, P. O. Box 4026, Irkutsk 664033, Russia

This paper is dedicated to the measurements problem of the signal distortion during vertical-incidence ionospheric soundings. Here we examine the distortion corresponding to the variability of the channel's amplitude-frequency characteristic (AFC) in the signal band. For an amplitude-modulated signal the distortion of this type implies the appearance of an additional quadrature component, whose amplitude is proportionate to the value of the AFC slope and whose shape corresponds to an derivative envelope of the emitted signal. The measurements of small signal distortion against a background of a noise generate a need for a synthesis of the signal optimized for this purpose. This paper gives an account of some possible approaches to solving this problem on the basis of the maximization of the energy of the derivative signal with a limited band, signal length and a limited peak power. The signals that decline sufficiently rapidly in time and have a spectrum grouped on signal band boundary were considered. The following types of signals are the subject of the paper:

1. the signals with ultimate partial energy in a given time interval with a given total energy and a limited frequency band (spheroidal functions);
2. the signals with ultimate instantaneous value of the derivative envelope at the specified conditions;
3. the empirically chosen signals with spectra grouped on signal band boundary.

The spectra and the time realizations of the model signals are given in paper. The efficiency of the chosen signals were tested by a numerical simulation. The values of following parameters of channel were specified: amplitude, phase, delay and AFC slope. As a part of the simulation process, the values of channel parameters were calculated by the method, which is given in the paper. As a result of the modeling effort, values of the determinated parameters errors for chosen signals were obtained. The dependencies of dispersions of the parameters on the noise dispersion for the chosen signals are given in the paper.

Applied Program Packages for Prediction and Current Diagnostics of the HF Radio Channel

V.I.Kurkin, V.E.Nosov, S.N.Ponomarchuk*, and S.V.Pushkarev
Institute of Solar-Terrestrial Physics, 664033, Irkutsk, P.O.Box 4026, Russia

Automated HF radio communication systems are designed to ensure the best conditions for transmitting information in the presence of a wide variety of interferences. Systems of such a kind must be adaptive, i.e. they are to be able to readjust parameters in accordance with the real state of the radio channel. Looking for effective algorithms for designing systems to ensure a maximum effective detection of the signal at the background of noise with an arbitrary law of distribution, requires conducting both theoretical and applied research. It is necessary to simulate the radio wave propagation process with proper account of the radio line hardware and data of current diagnostics. To achieve an effective control over radio communications, of important significance becomes the development of the system's information support. There is a need for an integral program envelope that would support databases, organize a network mode of operation and have an advanced graphics support for purposes of displaying information.

This paper presents, on a functional level, a description of applied program packages for prediction and current diagnostics of the radio channel based on algorithms for long-term prediction (V.I.Altynseva, N.V.Hyin et al. XXIII General Assembly of the International Union of Radio science (URSI). Abstracts, v. 1. Prague, 1990, p.108). and current diagnostics of radio wave propagation conditions (V.I.Kurkin, V.E.Nosov et al. Proceedings of International Symposium on Antennas and Propagation. Sapporo, Japan, 1992, p.1189-1192), as well as of a diagnostic system for ionospheric sounding by a continuous chirp-signal (I.G.Bryuko, I.A.Galkin et al. Adv. Space Res., 1989, v.8, No.4, p.(4)121-(4)124).

The configuration of diagnostic packages depends on the kind of the problem being solved. Long-term prediction operations imply calculating characteristics of HF radio signals of oblique-incidence and backscatter ionospheric sounding with specified technical parameters of the radio line.

Optimal operating frequencies of a communication radio line are chosen from results of vertical-, oblique-incidence and backscatter sounding of the ionospheric channel by a chirp-signal. Radio signal characteristics are calculated, experimental ionograms are processed using amplitude patterns, propagation modes are identified, and traces are constructed. Taking into account the energy relations between the signal level and the noise level, optimal operating frequencies are determined for different kinds of communication modems.

The core of automated information systems (AIS) is formed by a database (DB). Using DB ensures a uniform exchange between the various modules composing AIS. We have developed:

- DB for recording and storage of vertical-, oblique-incidence and backscatter ionospheric sounding ionograms;
- DB for storing results of ionogram processing;
- DB for geographical sites and codes of stations;
- DB for solar activity indices;
- DB for technical parameters of radio lines;
- DB for prediction results.

To record and store data in DB, use is being made of standard formats for primary and processed experimental data, as well as for results of calculation.

THIS PAGE INTENTIONALLY LEFT BLANK.

Rough Surfaces

G. S. Brown and Y. Kuga

Page

1:20	Analytical and Experimental Studies of Backscattering of 420 Electromagnetic Waves From High-Slope Rough Surfaces <i>Lynn Ailes-Sengers*, Akira Ishimaru, Yasuo Kuga, University of Washington</i>
1:40	An Improved Kirchhoff Approximation for the 421 Simulation of Electromagnetic Scattering from Rough Surfaces <i>Carlos Torres-Verdin*, Tarek M. Habashy, Schlumberger-Doll Research</i>
2:00	Scattering of a Gaussian Beam by Roughened Sinusoidal Surfaces 422 <i>David A. Kapp*, Gary S. Brown, Virginia Polytechnic Institute & State University</i>
2:20	Application of FDTD to Periodic Surface Scattering Problems 423 <i>B. Houshmand, Jet Propulsion Laboratory</i>
2:40	Transient Scattering from a Periodic Sea Surface 424 <i>A. Norman*, D. P. Nyquist, E. J. Rothwell, K. M. Chen, Michigan State University</i>
3:00	BREAK
3:20	Bistatic Scattering Characteristics of Surface Waves on Dielectric 425 Rough Surfaces <i>Hui Zhao, Yasuo Kuga*, Akira Ishimaru, University of Washington</i>
3:40	Monte Carlo Simulation of Electromagnetic Scattering From 426 Two-Dimensional Random Rough Surfaces <i>Robert L. Wagner*, Jiming Song, Weng Cho Chew, University of Illinois</i>
4:00	Electromagnetic Scattering From Slightly Rough Surfaces 427 With Inhomogeneous Dielectric Profile <i>Kamal Sarabandi, The University of Michigan</i>
4:20	Non-Coherent Scattering From a Plasma Slab with a Rough 428 Boundary <i>S. Shulga*, O. Bagatskaya, N. Zhuck, Kharkov State University</i>
4:40	Infrared Extinction of the Powder of Brass 70Cu/30An Modeled through Random Process <i>Hsing-Yi Chen*, I-Young Tarn, Yeou-Jou Hwang, Yuan-Ze Institute of Technology</i>

ANALYTICAL AND EXPERIMENTAL STUDIES OF BACKSCATTERING OF ELECTROMAGNETIC WAVES FROM HIGH-SLOPE ROUGH SURFACES

***Lynn Ailes-Sengers, Akira Ishimaru and Yasuo Kuga**

**Electromagnetics and Remote Sensing Laboratory
Department of Electrical Engineering
University of Washington
Seattle, WA 98195 USA**

Understanding electromagnetic wave scattering from very rough surfaces has practical applications to remote sensing of geophysical terrain, such as snow, soil and vegetation. This paper presents an analytical theory and experimental results for electromagnetic scattering in the back direction from two-dimensional, very rough, high slope, metallic and dielectric surfaces. These surfaces are defined as the surfaces whose rms slopes are of the order of unity and whose rms heights are of the order of a wavelength, and the second medium is lossy. This is the region where conventional Kirchhoff approximations and perturbation theories are not applicable. The theory is based on the first- and second-order Kirchhoff approximations with angular and propagation shadowing corrections. The second-order scattering includes the incident and scattering shadowing and the angular and propagation tapering shadowing. The second-order Kirchhoff approximations include the ladder and the cyclic terms, and the latter produces the enhanced backscattering for very rough surfaces. The vector theory is expressed in matrix form, and the second-order terms are given by four fold integrals which are evaluated approximately giving double integrals.

The theoretical results were compared with controlled, laboratory, millimeter-wave experiments showing good agreement over a range of surface characteristics and incident angles. The surfaces were fabricated by a computer-numerical-controlled milling machine, using Gaussian surface correlation functions. The dielectric material used was 3% Agar-Agar in water. At the experimental frequencies of 75-100GHz, the permittivity of this material was approximately that of water and therefore very lossy.

The analytical results for co- and cross-polarized cross sections were compared with experimental data for the cases of rms height equal to 1 wavelength and correlation distance equal to 1.4, 2, 3 and 4 wavelengths at 100GHz. The first-order scattering was dominant for correlation distances equal to 3 and 4 wavelengths, but as the slope increased with correlation distances equal to 1.4 and 2 wavelengths, the second-order scattering became comparable to the first-order scattering. The results showed that the peaks for first- and second-order scattering occur at different locations with the first-order peak corresponding to the rms slope of the rough surface.

An Improved Kirchoff Approximation for the Simulation of Electromagnetic Scattering from Rough Surfaces

Carlos Torres-Verdín* and Tarek M. Habashy
Schlumberger-Doll Research, Old Quarry Road, Ridgefield, CT 06877

We present a new nonlinear approximation for electromagnetic scattering arising from the excitation of rough surfaces. The approximation is based on the frequency-domain integral equation that describes surface scattering in terms of the Green function, the scattering potential and their normal derivatives. Common practice in rough surface scattering problems has been to replace the scattering potential and its normal derivative along the surface by the corresponding values of the incident potential. This popular approach, referred to as the Kirchoff approximation, is rendered accurate only when the roughness of the surface is small compared to the wavelength of the incident field. Further improvements on the Kirchoff approximation consists of developing an iterative Neumann series expansion to describe and update the values of the scattering potential and of its normal derivative along the surface. Although this latter strategy may in some cases help improve the accuracy of the scattering potential, the convergence of the series may be seriously degraded when the surface exhibits large undulations.

Drawing from our experience with a new nonlinear approximation for volume EM scattering (Habashy et. al., *J. Geophys. Res.*, 98, 1759-1775, 1993, and Torres-Verdín and Habashy, *Radio Sci.* 29, 1051-1079, 1994), we have developed an approximation for surface scattering that is as fast as the Kirchoff approximation but much more accurate. The key steps toward the derivation of our approximation are: (1) The surface integral equation is specialized for surface points such that, at a particular observation point, the Green function and its normal derivative become singular, (2) we then isolate the first-order contribution to the integral from the singularity around the observation point and neglect the remaining part of the integration, (3) this leads to an explicit solution for the surface potential that can be easily calculated in an analytical fashion, and (4) the scattering potential outside the surface is then derived from the surface potential values determined according to step (3). This procedure is closely related to boundary integral equation methods except that the new approximation does not require the inversion of a full complex matrix equal in size to the number of segmentations used to describe the scattering surface.

Benchmark examples are shown which compare the accuracy and speed of the new approximation against finite-difference, boundary integral, and Kirchoff simulations.

Scattering of a Gaussian Beam by Roughened Sinusoidal Surfaces

David A. Kapp* and Gary S. Brown

Bradley Department of Electrical Engineering, Virginia Polytechnic Institute & SU

To gain insight into the rough surface scattering problem, we have investigated the surface current induced on various one dimensional perfect electric conducting sinusoidal and roughened sinusoidal profiles by a Gaussian beam. The effects on the current distribution and the scattered field of a two scale sinusoidal surface (a linear superposition of two sinusoids) is also studied and several features which may have important implications in understanding the low grazing angle scattering problem are noted.

In considering the scattered fields from a sinusoidal surface, we have found that when the period is such that a Bragg diffracted order propagates horizontally large scale diffraction is exhibited well outside the illumination zone defined by the incident Gaussian beam. Interestingly, we have found that this effect is only exhibited for TE polarization (\vec{E} parallel to the surface) and not for TM polarization. We have traced this dependence to the fact that the current near the peaks of the sinusoid, in the TM case, points horizontally toward or away from an adjacent peak. Thus, an observer situated on a peak will not measure the scattered field from current near the adjacent peak. Furthermore, an observer situated near but not at a peak will only "see" a projection of the current at the adjacent peak. Since the scattered field resulting from this projected current is small in the TM case, peak to peak diffraction does not occur. In the TE case, however, peak to peak diffraction does occur due to the misalignment of the normal near the peak and the magnetic field scattered from an adjacent peak. The diffraction effect giving rise to a non-zero field outside the illumination zone is only exhibited in the forward direction (away from the source) and not in the backward scattering direction (toward the source).

When a second sinusoid with a smaller amplitude and period is added to the first sinusoid, the same large scale diffraction effects mentioned above are exhibited in the backward scattering direction outside the illumination zone. The effect in the backward scattering direction is a sensitive function of the period of the large scale and small scale periods. We have found that when the large scale period is such that it generates a Bragg diffracted order in the horizontal direction (low grazing angle backward direction), *in the absence of the small scale sinusoid*, this diffraction effect exists for TE polarization but not for TM. However, the result in the TE case appears to be more pronounced when the period of the small scale sinusoid is such that it would produce a Bragg diffraction order in the backscatter direction *in the absence of the large scale sinusoid*. We have also noticed that the scattered field in the low grazing angle backward scattering direction is a very sensitive function of the secondary sinusoid, and its presence can drastically effect the scattered field in this region. This paper will focus on these and other aspects of the problem, including a study on the effect of neglecting either forward or backward scattered waves on the surface and the interaction area of the scattered fields on the surface. Implications of these studies for the low grazing angle scattering problem will be discussed.

APPLICATION OF FDTD TO PERIODIC SURFACE SCATTERING PROBLEMS

B. Houshmand

Jet Propulsion Laboratory
California Institute of Technology
4800 Oak Grove Drive
Pasadena California 91109-8099

This paper presents the application of the Finite Difference Time Domain Method (FDTD) to scattering from periodic surfaces. This approach introduces a number of numerical inaccuracies due to numerical dispersion, reflections from the absorbing boundaries, and surface representation. The purpose of this work is to estimate the contribution of these numerical errors as a function of the incident angle. Here perfect electric conducting surfaces are considered, and a stair-casing approach is used for surface representation. In this work, a periodic absorbing boundary condition (ABC) is used in the directions of periodicity, and the Liao's 3rd order in the remaining directions. The latter boundary condition performs well for a wide range of incident angles. The FDTD algorithm employed here is based on the scattered field, and the excitation by an obliquely incident plane wave is implemented by enforcing the boundary condition on the scattering surface. This formulation eliminates the need to segment the computation domain into total and scattered field regions. In addition the absorbing boundary conditions operate only on the scattered field. The application of the periodic boundary condition simplifies the field representation of the scattered field. The scattered field is described by a discrete number of space harmonics in the computation domain where only a finite number are propagating. Such a representation allows the implementation of an exact ABC which can replace the Liao's ABC after the steady state is reached. Application of this algorithm to a flat perfectly conducting plate produced accurate results from normal incidence to the grazing angle of 89.0°. The observed scattered field across the surface deviated from the exact solution by a maximum of 3° in phase for the range of incidence angles as a result of numerical dispersion. In this paper the above algorithm will be applied to a number of periodic surfaces such as sinusoidal and grating structures, and the numerical performance will be evaluated against the frequency domain methods.

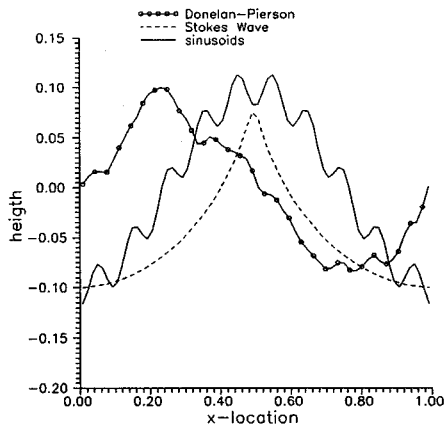
Transient Scattering from a Periodic Sea Surface.

A. Norman*, D.P. Nyquist, E.J. Rothwell and K.M. Chen
Department of Electrical Engineering
Michigan State University
East Lansing, MI 48824

An Integral Equation formulation for the scattering from a general periodic two-dimensional surface has been developed in the frequency domain. An application for this method is the frequency domain synthesis of transient scattering from a periodic sea surface. Utilizing the periodic Green's function, the problem can be reduced to solving for the surface fields over one period of the sea surface. The scattered fields can subsequently be found once again using the periodic Green's function. A Method of Moments type solution is obtained for the surface fields with Galerkin's method employed with pulse basis functions. The transient scattered fields are synthesized from the frequency domain results, this implies a large bandwidth with a relatively small frequency step size is needed to properly and accurately obtain the correct time domain results.

For highly oscillatory, or for very rough sea surfaces, the convergence of the periodic Green's function is extremely slow when the testing and observation points are close in height. The convergence problem is compounded by the large number of frequency points needed, thereby making the numerics intractable. This convergence problem has been addressed by various authors [Singh and Singh, etc]. Their techniques have proven to greatly improve the convergence rate of the periodic Green's function, and have been employed for this problem.

Results have been obtained for many sea surfaces, ranging from simple sinusoids, to a Stoke's wave and also a realization of the Donelan-Pierson sea spectrum (see figure). In addition to the various sea models used, a comparison of differing sea water models has been examined. The sea water models to be compared are a perfectly conducting model, an imperfectly conducting model ($\epsilon_r=80$, $\sigma=4$ S/m), and the more realistic (frequency dependent) Debye sea water model.



Bistatic Scattering Characteristics of Surface Waves on Dielectric Rough Surfaces

Hui Zhao, Yasuo Kuga^{*} and Akira Ishimaru

Department of Electrical Engineering,
University of Washington
Seattle, WA 98195 USA

Tel:(206)543-0478, Fax: (206)543-6185

E-mail: kuga@ee.washington.edu

Recently, experimental studies on backscattering enhancement from surface waves, also known as polaritons, have been reported [West and O'Donnell, 1994]. In these experiments the surface plasmon, which is a type of polariton caused by the negative real dielectric constant, was excited using a rough metal surface. Because of the difficulty of fabricating Gaussian rough surfaces with $h \ll \lambda$ and $l < \lambda$ at the optical wavelength, surfaces were made using a Gaussian random process written into the surface through randomly-phased Fourier components. In the microwave and millimeter-wave regions, it is well known that the surface waves can be excited using a thin dielectric layer placed on a metallic surface. If the rough profile is imprinted on the dielectric surface, backscattering enhancement due to polaritons may become observable.

In this paper, we will present the experimental investigation of bistatic scattering arising from the excitation of surface waves or polaritons on a dielectric surface with a highly one-dimensional random roughness at millimeter-wave frequencies. Surfaces with a Gaussian height distribution and a Gaussian correlation function with rms height $h=0.2\lambda$, correlation length $l=0.2\lambda$, and $h=0.2\lambda$, $l=0.4\lambda$ at 100 GHz are fabricated on machinable plastics with a dielectric constant of $\epsilon_r=1.41$. The flat side of the dielectric surface is then attached to a metal plate to support the surface waves. The thickness of the dielectric rough surface is controlled so that only few TE and TM modes are excited. When the surface is illuminated by the millimeter-wave source, surface waves are generated on the surface. The existence of the surface waves was verified by comparing the scattering characteristics of a rough surface with a bottom conducting plate to those of a rough surface without a conducting plate. By sweeping the frequency from 80 to 105 GHz, the excitation of different TE and TM modes is studied.

Monte Carlo Simulation of Electromagnetic Scattering From Two-Dimensional Random Rough Surfaces

ROBERT L. WAGNER*, JIMING SONG, AND WENG CHO CHEW
ELECTROMAGNETICS LABORATORY
DEPARTMENT OF ELECTRICAL AND COMPUTER ENGINEERING
UNIVERSITY OF ILLINOIS
URBANA, IL 61801

In this paper, we will present numerical results for the scattering of a vector electromagnetic beam from a two-dimensional randomly rough conducting surface. This problem has been difficult to solve numerically, because of the large computational cost involved. For instance, to model a portion of a rough surface only ten wavelengths on a side using a method of moments (MOM) approach would require solving a dense matrix equation with around $N = 20,000$ surface current unknowns. Direct solution of this matrix equation requires $O(N^3)$ computer operations, while an iterative solution has a cost of $O(N^2)$ operations per iteration, the cost of a dense matrix-vector multiply. Furthermore, to carry out a Monte Carlo simulation requires solving such a problem many times in order to obtain the desired scattering statistics. Clearly, a highly efficient computational procedure is required to obtain meaningful results.

In our approach to the problem, we begin by discretizing the electric field integral equation using the MOM with a parametric quadratic surface description. The fast multipole method (FMM) may then be applied to reduce the cost of a matrix-vector multiply from $O(N^2)$ to $O(N^{1.5})$, where N is the number of surface current unknowns, thus speeding the iterative solution of the MOM matrix equation. This technique has already been used for the computation of 3-D electromagnetic scattering from arbitrary conducting objects (Song and Chew, *Micro. Opt. Tech. Lett.*, 7, 760-765, Nov. 1994). By adapting this method to the specialized geometry of a rough surface, we further reduce the computational complexity of a matrix-vector multiply to $O(N \log N)$, making it possible to solve sizable rough surface problems. We will discuss the technique used, and present numerical results.

Electromagnetic Scattering From Slightly Rough Surfaces With Inhomogeneous Dielectric Profile

Kamal Sarabandi

Radiation Laboratory

Department of Electrical Engineering and Computer Science

The University of Michigan, Ann Arbor, MI 48109-2122

Tel : (313) 936-1575

Email: saraband@eecs.umich.edu

Remote sensing of soil moisture using microwave sensors require accurate and realistic scattering models for rough soil surfaces. In the past much effort has been devoted to the development of scattering models for either perfectly conducting or homogeneous rough surfaces. In practice, however, the permittivity of most soil surfaces is nonuniform, particularly in depth, for which analytical solution does not exist. The variations in the permittivity of a soil medium can easily be related to its soil moisture profile and soil type using the existing empirical models. In this paper analytical expressions for the bistatic scattering coefficients of soil surfaces with slightly rough interface and stratified permittivity profile are derived. The scattering formulation is based on a new approach where the perturbation expansion of the volumetric polarization current instead of the tangential fields is used to obtain the scattered field. Basically, the top rough layer is replaced with an equivalent polarization current and using the volumetric integral equation in conjunction with the dyadic Green's function of the remaining stratified half-space medium the scattering problem is formulated. First order analytical scattering solution is obtained for soil surfaces with arbitrary moisture profiles. The validity of the solution is verified, in two dimension, by comparing the analytical results with those obtained from a numerical solution for a periodic surface. Also the theoretical results are compared with the backscatter measurements of rough surfaces with known dielectric profile and roughness statistics.

NON-COHERENT SCATTERING FROM A PLASMA SLAB WITH A ROUGH BOUNDARY

S. Shulga^{*}, O. Bagatskaya, and N. Zhuck

Chair of Theoretical Radiophysics, Kharkov State University,
Svobody Sq., 4, Kharkov 310077, Ukraine

This report is a response to practical needs in the field of plasma diagnostics and remote sensing, which in theoretical terms reduce to the problem of calculating the electromagnetic scattering from a plane-layered plasma slab with the statistical roughness on its boundary. Detailed investigations of wave scattering from discrete layered structures made of isotropic material and having a slight roughness on its outer boundary have been considered earlier, e.g., by Zhuck, Shulga and Yarovoy [Soviet J. Comm. Techn. Electronics 36(3), 131 (1991)]. We have made use of the model that is more general than earlier models in the following respects:

- (a) it takes account of the electrical gyrotropy of the medium inside the slab typical of magnetized plasmas,
- (b) the piecewise-constant as well as the smooth variation of permittivity is allowed.

For calculational simplicity, the study is limited to the case in which the symmetry axis of the medium coincides with the direction of stratification. We solve the problem of plane wave diffraction from the aforementioned slab with a slightly rough boundary via a boundary transference procedure and a small perturbation technique. The quantities of interest, i.e. the bi-static scattering cross sections are expressible through the spectral density of roughness and the parameters referring to a regular slab, namely the limiting values of the elements of the permittivity tensor at the plane boundary and the Fresnel reflection coefficients for this boundary. These coefficients are representable in terms of proper solutions to a system of two coupled one-dimensional wave equations with respect to potential functions which determine the electromagnetic field inside anisotropic regions [Zhuck, Int.J. Electron. 75(1), 141 (1993)]. These equations are solved numerically via finite-difference method. For the case of statistically isotropic roughness, we present the results of computer analysis of the backscattering cross sections as functions of the geometric characteristics of surface perturbations, the electrophysical parameters of the slab and the viewing angle.

Author Index*

Author	Page	Author	Page
A			
Abdeen, M. A.	124	Barnhart, D.	260
Aberegg, K. R.	186	Baron, J. E.	168
Aberle, J. T.	36	Basart, J. P.	410
Abou-Jaoude, R.	24	Beck, F. B.	91, 113
Abramovitz, I.	131	Belkebir, K.	232
Abud Filho, E.	6	Benhabiles, B.	75
Adamenko, A. A.	58	Berrie, J.	183
Adekola, S. A.	148	Berry, M. H.	130
Aguirre, G.	215	Betts, G. E.	132
Ailes-Sengers, L.	420	Biro, O.	83
Al-Kanhal, M.	47	Birtcher, C. R.	127
Al-Rizzo, H. M.	189	Black, Q. R.	412
Alexopoulos, N. G.	153, 193	Blanc-Castillo, F.	96, 97
Alhargan, F. A.	217	Blanc-Feraud, L.	233, 344
Ali, M.	72	Blaunstein, N.	291, 314
Altman, Z.	300	Blood, D. W.	145
Anderson, J.	257	Boag, A.	385
Andrejev, A. A.	316	Bochkarev, G. S.	291
Andrenko, A. S.	252	Boerner, W.-M.	348
Andreyev, G. A.	316	Bogy, D.	155
Andronov, I. V.	196	Bolomey, J. C.	57, 234
Antar, Y. M. M.	69	Borselli, L.	154
Antilla, G. E.	182	Bouche, D.	300
Antipovsky, S. V.	165	Boumis, M.	142, 146
Anukhin, I. P.	76	Branco, M. G. C.	6
Arai, H.	318	Brown, B.	412
Aresu, A.	141	Brown, G. S.	104, 419, 422
Arvas, E.	47	Budaev, B.	155, 156
Asari, E.	321, 326	Bulka, Y. V.	58
Ashrafi, S.	317	Bunting, C. F.	87, 178
Asi, A.	208, 259	Burke, A. R.	317
Auclair, P. F.	110	Burkholder, R. J.	192, 375
Awada, K. A.	122	C	
Azarenkov, N. A.	12, 405	Cangellaris, A. C.	205, 215
B			
Bagatskaya, O.	428	Canning, F. X.	351, 353, 371, 381
Bakar, A. H. A.	413	Caputa, K.	72, 126
Baracco, I.	216	Car, D. D.	225
Barbaliscia, F.	142, 146	Casey, J. P.	30
Bardi, I.	83	Castaneda, J. A.	153, 193
Barlaud, M.	233, 344	Castillo, S. P.	39, 221
		Cendes, Z.	81, 92, 112
		Censor, D.	128

*Session Chairpersons also included, corresponding page numbers italicized

Author	Page
Chan, A. K.	33, 354
Chan, K. L.	217
Chang, C. W.	199
Chang, D. C.	103
Chang, D.-C.	373
Chang, H. C.	138
Chang, K.	35
Charkina, O.	54
Chaturvedi, P.	261
Cheah, S. Y.	29
Chen, C.-C.	266
Chen, H.-Y.	319
Chen, J.	197
Chen, K. M.	119, 120, 199, 267, 424
Chen, W.	209, 400
Chen, W.-Y.	66
Chew, W. C.	237, 301, 338, 343, 346, 347, 426
Chou, H. T.	16
Christodoulou, C. G.	275, 276, 277
Chuang, C. W.	192
Chui, C. K.	354
Coccioli, R.	191
Cockrell, C. R.	91, 113
Couchman, L. S.	371
Cown, B. J.	57, 155
Cryan, M.	73
Cuhaci, M.	366
Cwik, T.	67, 82, 85, 219, 220, 224

D

da Silva, L. C.	6
Dai, Y.	267
Damaskos, N. J.	151
Dana, R. A.	411
Daneshvar, K.	362
Das, P. C.	309
Davidson, A. M.	256
Davies, D.	134
Davis, R. M.	31
Davis, R.	27
Davis, W. A.	87, 178, 381, 388
Dawson, T. W.	126
De Loach, B. C.	365
De Moerloose, J.	384
De Zutter, D.	147
DeAguiila, H.	39

Author	Page
Dearholt, W.	221
Demarest, K.	261
Deshpande, M. D.	91, 113
Djuth, F. T.	287, 290
Do-Nhat, T.	109, 401, 402
Dobromyslov, V. S.	13
Dolshykov, V. V.	32
Douglas, M. G.	22
Drewniak, J. L.	37, 41, 176, 177, 321, 322
Duchene, B.	235
Dudley, D. G.	105, 395
Duncan, L. M.	409
Dunn, D. B.	121
Dvorak, S. L.	15, 18, 391, 395
Dycziej-Edlinger, R.	83, 339

E

Edwards, R. N.	137
Eidson, J. C.	312, 313
El-Sayed, A.	125
El-Sharawy, E.-B.	127
Elissalt, J. M.	232
Engheta, N.	243, 245, 246
Erwin, J. B.	374
Esman, R. D.	133
Esselle, K. P.	28
Estrada, J. P.	57

F

Fache, N.	378
Fang, J.	336
Fante, R. L.	21, 31
Fiddy, M. A.	229, 238
Fidel, B.	173
Fijany, A.	227
Fionda, E.	143, 146
Flechsig, D. E.	131
Flood, K. M.	51
Flykt, M.	241
Fontana, T. P.	85, 93, 377
Foster, J. C.	289
Fox, M. D.	128
Franchois, A.	234
Frankel, M. Y.	133
Fujimoto, H.	364
Fukao, S.	166

G

Garai, J. R. M. 180
 Garcia-Castillo, L. E. 96, 97
 Gedney, S. D. 223, 334
 Geffrin, J. M. 232
 Geleoc, M. 234
 Gelius, L.-J. 236
 Gerace, G. C. 26, 110, 121
 Geyer, R. G. 204
 Gilmore, S. W. 312
 Gobin, V. 187
 Gogoi, A. 250
 Goldberg, L. S. 102
 Gong, J. 280
 Goodman, J. 409
 Gorbachev, A. A. 404
 Gordon, R. K. 34
 Gordon, W. B. 164
 Gorev, P. V. 327, 329
 Goswami, J. C. 354
 Gothard, G. K. 302, 303
 Goto, K. 195
 Goutzoulis, A. 134
 Goverdhanam, K. 361
 Graglia, R. D. 77, 84
 Gravrok, R. 260
 Gray, D. 181
 Green, A. D. 4
 Groves, K. M. 289
 Guan, J.-M. 373
 Guella, T. P. 31
 Gupta, C. D. 250, 309
 Gurel, L. 380
 Gustavsson, M. 5

H

Habashy, T. M. 111, 343, 345,
 394, 421
 Hadi, M. F. 175
 Hagness, S. C. 359
 Hales, L. 362
 Hall, P. S. 73
 Hall, W. F. 376
 Hamid, M. 71
 Han, F. 40
 Hansen, J. P. 265, 270
 Hartery, F. 167

Hellberg, R. 20
 Henderson, J. H. 306
 Herd, J. S. 202
 Hernandez-Gil, J.-F. 95
 Heyman, E. 17, 171, 173
 Hickey, K. 167
 Hockanson, D. M. 41
 Holmes, W. S. 201
 Hoorfar, A. 284
 Horenian, M. 272, 323, 324
 Houshmand, B. 423
 Hrycak, P. 134
 Hu, X. 249
 Huang, Y. 120
 Huang, Z. 261
 Hubing, T. H. 41, 322
 Hussein, Z. A. 55, 56
 Hwang, Y.-J. 319

I

Ilavarasan, P. 120
 Ilyin, N. V. 415
 Inan, S. 349
 Ishihara, T. 195
 Ishii, J. 364
 Ishimaru, A. 99, 100, 420, 425
 Iskander, M. F. 106
 Ittipiboon, A. 69, 366

J

Jackson, D. R. 122, 153, 247
 Jaggard, D. L. 43, 51, 244
 Jakoby, R. 141
 Jamnejad, V. 67, 82, 220, 369
 Janaswamy, R. 255, 258, 379
 Jang, S. 128
 Jarry, P. 7
 Jean, M. 116
 Jennings, N. 299
 Jensen, M. A. 227
 Jin, J. M. 279, 338
 Joachimowicz, N. 234
 Johnson, A. 134
 Joisel, A. 234
 Joseph, R. M. 333, 359, 389, 390
 Judah, S. R. 217
 Judkins, J. B. 392

Author	Page
Jull, E. V.	397, 400
Juntunen, J.	44
Jussaume, D. E.	49

K

Kaklamani, D. I.	308
Kalfon, A. D.	179
Kalinichev, V. I.	13
Kamzolov, S. K.	169
Kanevsky, M. B.	170
Kang, Y.	94
Kapoor, R.	269
Kapp, D. A.	422
Karaev, V. Y.	170
Karam, M. A.	115
Karle, T.	211
Kastner, R.	17, 173
Katehi, L. P. B.	357, 361
Katz, D. S.	220, 224, 333, 361, 389, 390
Kazama, Y.	285
Ke, G.	320
Keam, R. B.	4, 201
Keller, M. G.	69
Kelley, D.	393
Kempel, L. C.	36, 183
Kesler, M. P.	360
Kesler, O. B.	397, 399
Khaikin, V.	62, 63
Khakhinov, V. V.	415
Khan, R.	27
Kiang, J.-F.	212, 307
Kim, J. J.	399
Kim, K. T.	248
King, A. S.	94, 226
King, R. W. P.	123
Kingsland, D.	339
Kipp, R.	183
Kleinman, R. E.	229, 231, 233, 344
Klotz, P. H.	179
Koh, W. J.	251
Komatsu, Y.	60
Kontorovich, V.	323, 324
Kostenko, P. Y.	58
Kotulski, J. D.	225
Kouloulias, V.	308
Kouyoumjian, R. G.	240

Author	Page
Kouznetsov, V. L.	169
Krjukov, A. V.	13
Krupka, J.	204
Kuga, Y.	419, 420, 425
Kulizhsky, A. V.	414
Kunasani, S. R.	356
Kung, C.-Y.	212, 307, 356
Kurkin, V. I.	415, 417
Kustom, R. L.	94
Kwon, D.-H.	375

L

Lacava, J. C. S.	52
Lacour, P.	75
Lagasse, P.	378
Lam, W.-H.	315
Lansing, F.	223
Larry, T. L.	135
Laxpati, S. R.	214
Leblebicioglu, K.	349
Lee, C. S.	213
Lee, H.-M.	108
Lee, J.-F.	34
Lee, J. F.	262, 339
Lee, K. H.	214
Lee, K.-F.	209
Lee, R. Q.	209
Lee, R.	339
Lee, S. W.	183, 279
Legault, S.	383
Lesselier, D.	235
Levin, M.	314
Li, H.-J.	273
Liechty, R. B.	137
Lin, Y.-C.	161
Lindell, I. V.	43, 45
Ling, H.	33
Liu, Yen	258, 370, 379
Liu, Yaowu	372
Lobel, P.	233, 344
Loughry, T.	39
LoVetri, J.	256
Lozhechko, V. V.	254
Lu, C. C.	237, 346, 347
Lu, J. W.	181
Lucas, E. W.	1, 93, 377
Luchaninov, A. I.	406

Author	Page
Luebbbers, R. J.	393
Lukin, V. V.	76
Lumini, F.	52
Lusted, K.	226
Lyandres, V.	323, 324

M

Ma, Y. C.	182
Maci, S.	154
MacPhie, R. H.	107, 109, 401
Maeda, Y.	60
Maekawa, Y.	166
Mahajan, M. B.	207
Maloney, J. G.	360
Manara, G.	191, 240
Manuar, O.	244
Marhefka, R. J.	251
Markey, B. J.	358
Marsh, A.	308
Marteau, S.	3
Martellucci, A.	141, 142, 143
Martin, A.	365
Martinez, J.	221
Marx, E.	149, 150, 239
Masukura, K.	166
McCoy, M.	410
McGahan, R. V.	229, 238
Medvedev, A. V.	416
Meeks, D. N.	278
Megalinsky, V. R.	165
Mei, K. K.	369, 372
Meyers, J. P.	110
Michelson, D. G.	400
Michielsen, B. L.	3, 187
Michielssen, E.	301
Miller, B. C.	137
Mittra, R.	219, 222, 293, 294, 299, 300, 331, 335, 340, 382, 385
Mix, J.	260
Mockapetris, L.	114
Moellers, J.	129, 134
Mohammadian, A. H.	376
Mohannadi, A.	407
Moheb, H.	283
Molinet, F. A.	348
Mongia, R. K.	69
Montbriand, L. E.	288

Author	Page
Morita, N.	285, 286
Morris, J. B.	238
Mortazawi, A.	365
Mowete, A. I.	148
Mrozowski, M.	264
Mur, G.	79
Murakami, T.	363
Murakawa, K.	60
Murphy, J.	299
Musclow, T.	210

N

Nalbandian, V.	213
Nandhakumar, N.	269
Nashashibi, A.	162
Nedelec, J.-C.	78
Nepa, P.	240
Nevels, R. D.	351, 354
Neves, J.	139, 140
Ngai, H.-O.	315
Nguyen, B. T.	263
Nguyen, C.	356
Ni, S.	279
Nikoskinen, K.	241
Noguchi, Y.	364
Norman, A.	120, 271, 424
Nosov, V. E.	415, 417
Nunnally, W. C.	137
Nyquist, D. P.	199, 267, 271, 424

O

O'Donnell, F. J.	132
O'Keefe, S.	181
Odendaal, J. W.	117
Oh, D.	222
Okoniewski, M.	22, 257, 264
Oliner, A. A.	243, 247
Oliver, M. B.	69
Orazi, R. J.	130
Osipov, A. V.	157
Osmayev, O. A.	12, 405
Ostner, H.	247
Ostrikov, K. N.	12, 405
Otto, G. P.	346
Oughstun, K. E.	396
Ozdemir, S. K.	368
Ozdemir, T.	89, 183

P

Pan, G. 10, 355, 367
 Pantic-Tanner, Z. 90
 Pao, H.-Y. 395
 Papiernik, A. 75, 216
 Pappert, S. A. 130
 Paraboni, A. 141
 Parker, J. W. 387
 Pasik, M. 215
 Pathak, P. H. 15, 16, 190, 192
 Patterson, J. 224
 Paul, A. 282
 Paul, D. K. 358
 Paynter, F. 266
 Pechenin, V. V. 316
 Pekar, M. 24
 Pekel, U. 340
 Pellet, M. 75
 Pelosi, G. 185, 191
 Perrotta, A. 284
 Peters, L. 265, 266
 Peterson, A. F. ... 77, 80, 84, 90, 185, 186
 Philbrick, C. R. 145
 Picard, D. 57
 Pichot, C. 75, 216, 233, 344
 Piette, M. 19, 268, 344
 Piket-May, M. 175, 260
 Plumb, R. G. 261
 Pommet, D. A. 238
 Ponomarchuk, S. N. 415, 417
 Pospelov, B. B. 328
 Power, D. 167
 Prammanick, P. 407
 Prather, W. D. 38
 Preis, K. 83
 Primak, S. 272, 323, 324
 Pushkarev, S. V. 417
 Putnam, J. M. 225

Q

Qian, J. 199
 Quinn, J. M. 289

R

Rahman, M. A. 203
 Rahmat-Samii, Y. 227, 293, 295
 Ramahi, O. M. 386

Rao, S. M. 70, 297, 302, 303, 306
 Rappaport, C. M. 119, 121, 341
 Ratovsky, K. G. 416
 Ray, K. G. 132
 Razdan, R. 358
 Reddy, C. J. 91, 113
 Rengarajan, S. R. 65, 68
 Reuter, C. E. 333, 389, 390
 Riad, S. M. 197, 203
 Richter, K. R. 83
 Robinette, L. K. 137
 Rocha, A. 140
 Roden, A. 334
 Rodriguez, J. V. 289
 Roe, P. L. 263
 Rojas, R. G. 147
 Roscoe, D. J. 69, 208, 366
 Rosen, E. 371
 Rossi, L. 154
 Rothwell, E. J. 267, 271, 424
 Rousseau, P. R. 16, 190
 Roy, T. 304
 Rui, X. 320

S

Sacks, Z. 262
 Saed, M. A. 200, 281
 Salama, I. M. 203
 Salazar-Palma, M. 95, 96, 97
 Samant, A. R. 46
 Samokhin, A. B. 118
 Sancer, M. I. 182
 Sandler, S. S. 123
 Sanford, J. 5
 Saoudy, S. A. 27, 167
 Sarabandi, K. 159, 161, 162, 163, 427
 Sarkar, T. K. 1, 211, 304
 Savage, J. S. 90
 Sayan, G. T. 349
 Scheff, K. 270
 Scholl, J. 353
 Schweicheir, E. 19, 268
 Schwering, F. 66, 213
 Scott, W. R. 88
 Scotto, M. 216
 Sebak, A. A. 398
 Senior, T. B. A. 152, 383

Author	Page
Sercu, J.	378
Shafai, L.	35, 188, 205, 208, 259, 283, 366
Shahid, M.	282
Shaker, J.	188
Shankar, V.	376
Shaw, J. D.	322
Sherrill, W. M.	412
Shestopalov, Y. V.	254
Shi, H.	176, 177
Shifrin, Y. S.	32, 406
Shirley, B. L.	360
Shlivinski, A.	17
Shokalo, V. M.	406
Shulga, S.	54, 428
ShUPIatsky, A. B.	165
Shur, M.	357
Sihvola, A.	44
Simons, N. R. S.	256
Simovski, C. R.	53
Simpson, R. A.	159, 168
Singh, S.	49
Siqueira, P.	163
Sletten, M.	270
Slob, E. C.	394
Smith, G. S.	360
Smith, W. T.	29
Sochava, A. A.	53
Solbach, K.	74
Somers, G. A.	325
Sohg, J.	426
Song, J. J.	94
Sonoi, Y.	166
Speciale, R. A.	8, 9
Spreckic-Zugec, T.	276
Stamnes, J. J.	236
Steinert, L. A.	61
Steinhardt, A. O.	325
Steyskal, H.	21, 25
Stogryn, A.	115
Streit, R. L.	30
Strickland, P.	210
Stuchly, M. A.	22, 124, 125, 126, 384
Stuchly, S. S.	65, 72, 257
Stupfel, B.	382
Suadoni, M. T.	191
Suda, T.	285

Author	Page
Sun, C. K.	130
Sun, D.	112
Sundberg, M.	5
Svezhentsev, A. Y.	11
Swaminathan, Ma.	304
Swann, C. J.	135

T

Taflove, A.	333, 359, 389, 390
Tan, J.	10, 367
Tanner, D. R.	90
Tarakankov, S. P.	404
Telikepalli, R.	210
Tentzeris, E.	361
Tertuliano, H.	7
Terzuoli, A. J.	26, 110, 121
Thiel, D. V.	181
Thiele, E.	333, 389, 390
Thomas, K.	260
Tiberio, R.	154
Tillery, J. K.	23
Tinin, M. V.	414
Torres-Verdin, C.	107, 111, 394, 421
Toyoda, S.	363
Tran, T.	317
Tranquilla, J. M.	189
Tretyakov, S. A.	53
Triolo, A.	66
Trivedi, A. C.	250, 309
Trzaska, H.	59
Turhan-Sayan, G.	368
Turk, K. W.	136
Tyler, G. L.	168

U

Ufimtsev, P. Y.	153, 193, 194
Uslenghi, P. L. E.	50, 149, 151, 239
Uzunoglu, N. K.	308

V

van den Berg, P. M.	231
van Jaarsveld, P. A.	117
Van Doren, . P.	41, 322
VanBlaricum, M. L.	129, 135
Vanzura, E. J.	198
Varadarajan, V.	222, 299

Author	Page
Veihl, J. C.	335
Vinogradova, E. D.	403
Viola, M. S.	305
Vishvakarma, B. R.	207
Volakis, J. L.	89, 183, 275, 280, 283
Vorst, A. V.	19, 268

W

Wada, K.	364
Wagner, R. L.	426
Wahid, P. F.	277, 278
Wallace, C. B.	38
Wallinga, G.	271
Walton, E. K.	24
Wang, G.	352
Wang, J. J. H.	23
Wang, Y.-D.	273
Warren, G. S.	88
Webber, G. E.	101
Webster, A. R.	139, 144
Webster, J. C.	311
Wedberg, T. C.	236
Weil, C. M.	198
Welch, L. R.	128
Wentworth, S. M.	70, 374
Westwater, E. R.	143, 311
Wheless, W. P.	37, 38
Whites, K. W.	46, 48
Whitman, G. M.	66
Williams, J. T.	122
Wilton, D. R.	77, 80, 84, 122, 297
Wittwer, D. C.	337
Wolf, E.	345
Wolstenholme, D. J.	26

Author	Page
Wong, T.	249
Wong, T. T.	94
Wu, Z.	336

X

Xu, X.-B.	171, 174
----------------	----------

Y

Yamane, H.	60
Yang, X.	174
Yanovsky, F. J.	350
Yatsik, V. V.	253
Yee, K. S.	331
Yevstafiev, V. V.	292
York, D. J.	360
York, R. A.	138
Yuan, X.	92, 112

Z

Zaboronkova, T. M.	404
Zaitsev, A. Y.	328
Zapata, J.	180
Zarroug, A.	73
Zhang, L.	40
Zhang, M.	398
Zhao, H.	425
Zhou, J.	94
Zhou, W.	277
Zhuck, N. P.	428
Ziolkowski, R. W.	18, 173, 255, 337, 392
Zomp, J.	134
Zuffada, C.	67, 82, 220, 387

1996 IEEE AP-S INTERNATIONAL SYMPOSIUM
AND USNC/URSI RADIO SCIENCE MEETING
Baltimore, Maryland
July 21 -26, 1996

The 1996 AP-S International Symposium sponsored by the IEEE Antennas and Propagation society and URSI (International Union of Radio Science) meeting sponsored by USNC Commissions A, B, C, D, E, F, and K will be held at the Hyatt Regency Hotel in Baltimore, Maryland, July 21 - 26 1996. The technical sessions, workshops and short courses will be coordinated among the two symposia to provide a comprehensive, well-balanced program. Industrial exhibits will be open from July 22 - 25, 1996.

- General information may be obtained from:

Jon Moellers, Steering Committee Chair
Westinghouse Electric Corporation
P.O. Box 746, M/S 55
Baltimore, MD 21203
tel: (410) 993-6774, fax (410) 993-7432
e-mail: jonm 21042@aol.com

- IEEE AP-S technical program inquiries should be directed to:

Joseph Frank
IEEE-APS Technical Program Committee Chair
c/o Ms. Libby Croston
The Johns Hopkins University, Applied Physics Laboratory
Johns Hopkins Road
Laurel, MD 20723-6099
tel: (301) 953-5225, fax: (301) 953-6123

- URSI inquiries may be directed to:

Julius Goldhirsh
URSI Technical Program Committee Chair
c/o Ms. Libby Croston
The Johns Hopkins University, Applied Physics Laboratory
Johns Hopkins Road
Laurel, MD 20723-6099
tel: (301) 953-5225, fax: (301) 953-6123
e-mail: julius_goldhirsh@aplmail.jhuapl.edu

- Potential exhibitors may obtain detailed information from:

Bruce Jenkins
Exhibits/Industrial Relations Chair
Electronics Resources, Inc.
10921 Rawley Road
New Market, MD 21774-6205
tel: (301) 865-3771, fax: (301) 865-3080

